PROTEOMIC AND SYSTEMS BIOLOGY ANALYSIS OF THE RESPONSE OF MONOCYTES TO INFECTION BY *COXIELLA BURNETII* AND EXPOSURE TO INNATE IMMUNE ADJUVANTS

by

Matthew Richard Shipman

A dissertation submitted in partial fulfillment
of the requirements for the degree

of

Doctor of Philosophy

in

Biochemistry

MONTANA STATE UNIVERSITY
Bozeman, Montana

May 2010

APPROVAL

of a dissertation submitted by

Matthew Richard Shipman

This dissertation has been read by each member of the dissertation committee and has been found to be satisfactory regarding content, English usage, format, citation, bibliographic style, and consistency, and is ready for submission to the Division of Graduate Education.

Dr Edward A. Dratz

Approved for the Department Chemistry/Biochemistry

Dr. David Singel

Approved for the Division of Graduate Education

Dr. Carl A. Fox

STATEMENT OF PERMISSION TO USE

In presenting this dissertation in partial fulfillment of the requirements for a doctoral degree at Montana State University, I agree that the Library shall make it available to borrowers under rules of the Library. I further agree that copying of this dissertation is allowable only for scholarly purposes, consistent with “fair use” as prescribed in the U.S. Copyright Law. Requests for extensive copying or reproduction of this dissertation should be referred to ProQuest Information and Learning, 300 North Zeeb Road, Ann Arbor, Michigan 48106, to whom I have granted “the exclusive right to reproduce and distribute my dissertation in and from microform along with the non-exclusive right to reproduce and distribute my abstract in any format in whole or in part.”

Matthew Richard Shipman

May 2010

TABLE OF CONTENTS

TABLE OF CONTENTS-CONTINUED

LIST OF TABLES

LIST OF FIGURES

LIST OF FIGURES-CONTINUED

Figure Page

LIST OF FIGURES-CONTINUED

Figure Page

LIST OF FIGURES-CONTINUED

Figure Page

LIST OF FIGURES-CONTINUED

Figure Page

LIST OF FIGURES-CONTINUED

LIST OF FIGURES-CONTINUED

ABSTRACT

Coxiella burnetii is an obligate intracellular pathogen that infects human monocytes, specifically inhabiting the phagolysosome. *C. burnetii* is a potential bioterror agent and is classified by the National Institute for Allergies and Infectious Diseases (NIAID) as a category B pathogen. This bacterium is remarkably infectious, requiring as little as one bacterium to cause infection. We used phase II *C. burnetii*, an avirulent laboratory strain that acts as a model for wild type phase I strains. Our research was directed towards a deeper understanding of the monocyte proteome in response to a) infection by phase II *C. burnetii*, and b) exposure to immune adjuvants known to increase monocyte resistance to infection by *C. burnetii*.

Monomac I cells were infected with phase II *C. burnetii* and aliquots were taken at 24, 48, and 96 hours postinfection. Experiments with immune adjuvants that increase monocyte killing of *C. burnetii*, involved Monomac I cells treated with Securinine, *E. coli* lipopolysaccharide (LPS), and monophosphoryl lipid A (MPL). Securinine is a $GABA_A$ receptor antagonist that is being developed at Montana State University for biodefense purposes, and triggers an innate immune response that differs from classic Toll-like receptor (TLR) stimulation of innate immunity represented by LPS and MPL.

We employed multiplex 2D gel electrophoresis (m2DE) using ZDyes, a new generation of covalent fluorescent protein dyes being developed at Montana State University, coupled with MS/MS analysis and bioinformatics to determine the proteome changes in Monomac I cells in response to the conditions described above, and to develop a preliminary mechanistic model using a systems biology approach to account for the observed changes and propose multiple testable hypotheses to focus downstream research efforts.

We also tested the effects on Monomac I cells infected with phase II *C. burnetii* +/- Securinine. We observed a high proportion of cell death in the + Securinine samples, using a dosage of Securinine higher than the optimal effective dosage. The information derived from this experiment will be useful in monitoring the tendency towards cell death in Securinine treated samples both from *C. burnetii* infected monocytes and other cell types (e.g. neurons) that contain $GABA_A$ receptors.

CHAPTER 1

INTRODUCTION

Coxiella burnetii

This project is devoted to better understanding of the host-pathogen response monocytes and *C. burnetii*, and how monocytes respond to stimulation with innate immune adjuvants. This information might be used to combat other pathogenic bacteria. *C. burnetii* is an obligate intracellular pathogen, and the causative agent of Q fever [7-15]. Obligate intracellular pathogens are metabolically inactive outside of the host cell, and must inhabit a host cell for the metabolically active/replicative phase of their life cycle. In the case of *C. burnetii*, the bacterium inhabits the monocyte phagolysosome in humans during its metabolically active phase and during replication. *C. burnetii* is a remarkably infective organism, requiring as little as one bacterium to cause infection (ID_{50}=1-10) [12,16-18]. Initially misclassified as a *Rickettsia* family member, *C. burnetii* has recently been reclassified as a member of the γ-proteobacterium clade and been shown to be most closely related, genetically, to *Legionella pneumophila* rather than *Rickettsia* species [10,12,17]. See figure 1 for a phylogenetic tree relating *C. burnetii* to other bacteria. The complete genome sequence for *C. burnetii* is available, providing a basis for proteomic analyses and for sequence comparisons between various strains of *C. burnetii*, as well as with other species [17,19].

Although *C. burnetii* can infect a number of cell lines *in vitro*, it's only known target *in vivo* is monocytes/macrophages [10]. It is also readily aerosolized, and environmentally persistent. As many as half of all *C. burnetii* infections are cleared by humans asymptomatically [18]. The remainder of infected individuals primarily contract the acute form of the disease, and display high fever, chills, sweats, vomiting, and diarrhea, among other symptoms. A smaller number of symptomatic individuals will contract the chronic form of the disease, which is much more likely to result in fatalities [18], as described below. Generally the acute form of Q fever is debilitating rather than fatal.

Prognosis for acute Q fever is greatly improved upon administration of antibiotics, although the bacterium can persist *in vivo* despite years of continuous antibiotic treatment [14,18,20]. One reason that improved detection and treatment of Q fever is important is that the bacterium can hide in reservoir within the body. Thus a person who apparently clears acute Q fever can reacquire the chronic form of the disease up to 20 years following initial infection, and it has been suggested by Marmion et al, (2005) that the reservoir for *C. burnetii* following Q fever infection is the bone marrow [10,12,13,18,21]. Chronic Q fever cases can >65% fatal, as one of the main complications is endocarditis, which damages the heart valves [12,18]. It has been proposed that slight genetic differences between various phase I *C. burnetii* strains may in fact account for the observation that some strains predominantly produce either the acute or the chronic form of Q fever [19]. In a recent study by Helbig, et al, (2005), a

group of patients displaying post Q fever fatigue syndrome,(QFS) a chronic fatigue state that can persist in some patients following Q fever clearance, that patients displaying QFS had a higher expression of the gene HLA-DRB 1*11 allele that is associated with reduced expression of IFN-γ and IL-2 in peripheral blood monocytes [22]. It is thus possible that the genetic background of infected individuals predisposes them in some way towards developing a chronic infection [22].

Infection with Q fever is often considered an occupational hazard, particularly for those who work in farming, slaughterhouses, and even veterinary care. Q-vax is an effective vaccine against *C. burnetii,* but rigorous testing of recipients for antibodies to *C. burnetii* from a prior exposure is essential prior to being vaccinated [23]. Previously acquired immunity to Q fever, either through natural infection or prior Q-vax administration, can cause a severe adverse reaction to a subsequent Q-vax inoculation [23]. Recall that many Q fever infections clear asymptomatically, and there are likely to be many people with a natural immunity to Q fever that are not aware of it. Other forms of *C. burnetii* vaccines have been used and/or proposed, but to date there is no generally accepted vaccine [10]. This makes studies involving preventative measures or potential treatments important for controlling or preventing the acquisition of Q fever infections.

Because *C. burnetii* can be readily aerosolized and weaponized, it makes a potential bioweapon and is considered a bioterror threat [9,11,12,17]. Indeed, this organism is known to have been weaponized by the U.S. Army and is believed to have

been weaponized by the USSR [9,20]. *C. burnetii* is prevalent worldwide, and there is significant concern that a terrorist organization such as al Qaeda or a rogue nation such as North Korea or Iran could develop a bioweapon containing this organism. In addition, the likely failure of the USSR to dismantle and/or secure its bioweapons stockpiles [15,24] may allow a resourceful organization/nation to either buy what they want from unscrupulous scientists or even enter a facility (e.g. a late night break in) and take what they want.

There are two primary types of *C. burnetii*, phase I and phase II. Phase I is the virulent wild-type form that causes infection in humans, while phase II is a laboratory form considered to be avirulent, and therefore much safer to work with [7,8,25,26]. *C. burnetii* is known to evade host defense mechanisms, but it appears that phase II is not able to completely inhibit host cell defenses, as evidenced by its inability to cause prolonged infections. Phase II *C. burnetii* can enter the host cell more readily than phase I, but phase II is unable to prevent various cellular defenses from eventually eliminating the bacterium over the long term [26,27]. Specifically, Phase II infections are partially controlled by macrophages, but an adaptive immune response is apparently required to completely clear the infection (detailed below). It has been demonstrated that phase I infections can prevent the delivery of lysosomal hydrolases to the phagolysosome, while a phase II infection cannot [27]. It must be noted that there are wide variations in susceptibility to infection and rate of *C. burnetii* replication depending

on the macrophage strain (from a particular *in vitro* cell line or freshly isolated peripheral monocytes / macrophages *in vivo*) [28,29].

Bacteria posses a number of virulence factors, molecules that are secreted or bound to the bacterial cell surface such as the lipopolysaccharide (LPS) coat of the bacterium that enable infection of the host and to evade host defenses. The best known virulence factor in various strains of *C. burnetii* is the LPS coat, despite reports that *C. burnetii* LPS is significantly less endotoxic than *E. coli* or other bacterial LPSs [30,31]. The phase II strain is propagated by repeatedly passing phase I *C. burnetii* through embryonated chicken eggs, anywhere from eight passages [32] up to ninety-four passages [7]. Loss of virenose and dihydrohydroxystreptose from *C. burnetii* LPS indicates conversion to phase II [7,17,33]. The loss of these two sugars on *C. burnetii*'s LPS coat is due to loss of the ability to produce them at the genetic level [32]. The transition between phase I and II is analogous to a smooth-to-rough transition seen in other organisms such as *Salmonella typhimurium* with the rough mutant being much less virulent than the smooth [7,8,13,25,26].

Other virulence factors for *C. burnetii* that have been proposed include acid phosphatase, catalase, and superoxide dismutase [13,34,35]. Acid phosphatase, used to cleave phosphates from compounds during digestion under acidic conditions, is found in *C. burnetii*, with activities reported to be among the highest of any known organism

Figure 1A

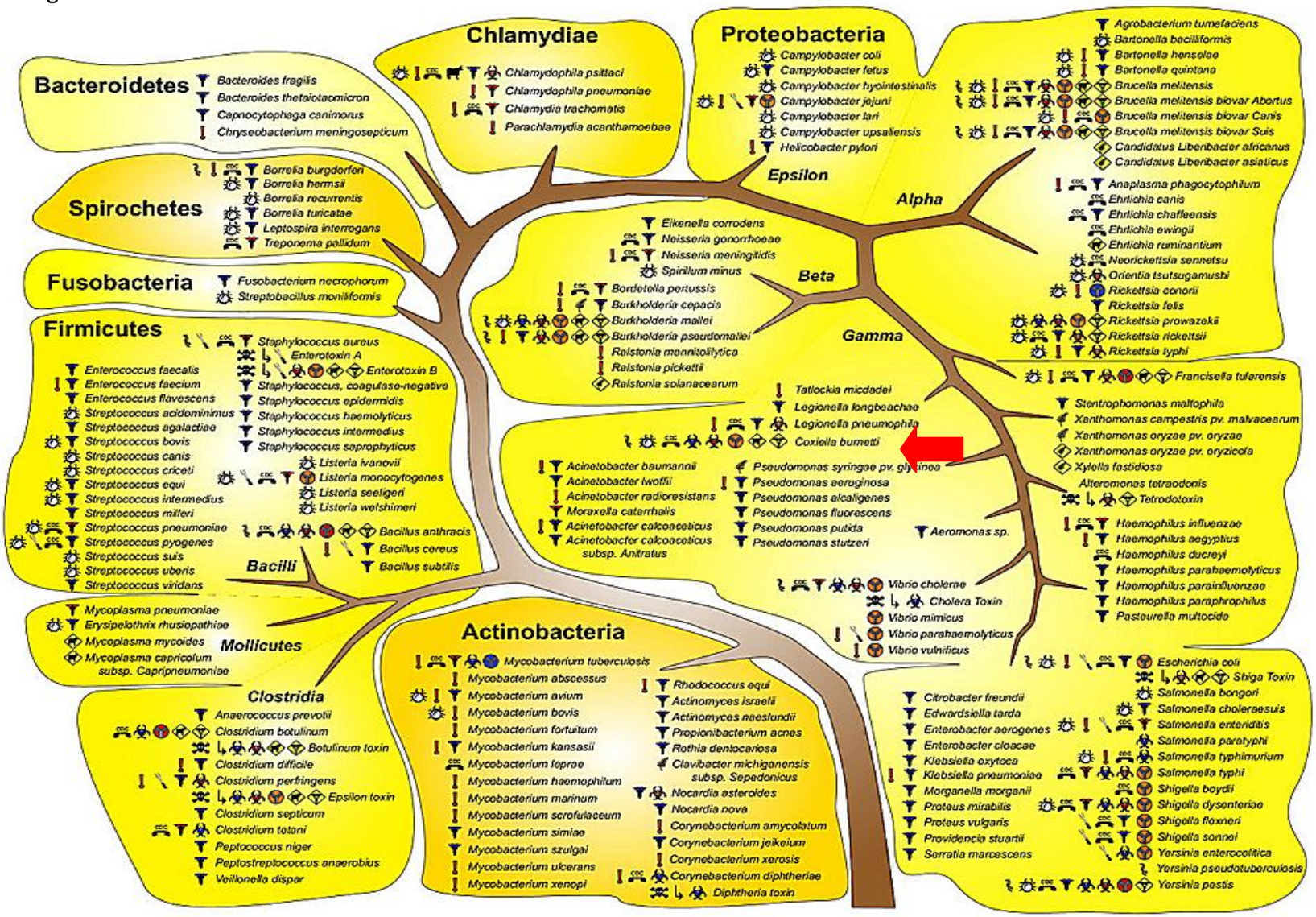
Bacteroidetes
Bacteroides fragilis
Bacteroides thetaiotaomicron
Capnocytophaga canimorus
Chryseobacterium meningosepticum
Chlamydiae
Chlamydophila psittaci
Chlamydophila pneumoniae
Chlamydia trachomatis
Parachlamydia acanthamoebae
Proteobacteria
Epsilon
Campylobacter coli
Campylobacter fetus
Campylobacter hyointestinalis
Campylobacter jejuni
Campylobacter lari
Campylobacter upsaliensis
Helicobacter pylori
Alpha
Agrobacterium tumefaciens
Bartonella bacilliformis
Bartonella henselae
Bartonella quintana
Brucella melitensis
Brucella melitensis biovar Abortus
Brucella melitensis biovar Canis
Brucella melitensis biovar Suis
Candidatus Liberibacter africanus
Candidatus Liberibacter asiaticus
Anaplasma phagocytophilum
Ehrlichia canis
Ehrlichia chaffeensis
Ehrlichia ewingii
Ehrlichia ruminantium
Neorickettsia sennetsu
Orientia tsutsugamushi
Rickettsia conorii
Rickettsia felis
Rickettsia prowazekii
Rickettsia rickettsii
Rickettsia typhi
Spirochetes
Borrelia burgdorferi
Borrelia hermsii
Borrelia recurrentis
Borrelia turicatae
Leptospira interrogans
Treponema pallidum
Beta
Eikenella corrodens
Neisseria gonorrhoeae
Neisseria meningitidis
Spirillum minus
Bordetella pertussis
Burkholderia cepacia
Burkholderia mallei
Burkholderia pseudomallei
Ralstonia mannitolilytica
Ralstonia pickettii
Ralstonia solanacearum
Fusobacteria
Fusobacterium necrophorum
Streptobacillus moniliformis
Gamma
Francisella tularensis
Firmicutes
Staphylococcus aureus
Enterotoxin A
Enterotoxin B
Staphylococcus, coagulase-negative
Staphylococcus epidermidis
Staphylococcus haemolyticus
Staphylococcus intermedius
Staphylococcus saprophyticus
Enterococcus faecalis
Enterococcus faecium
Enterococcus flavescens
Streptococcus acidominimus
Streptococcus agalactiae
Streptococcus bovis
Streptococcus canis
Streptococcus criceti
Streptococcus equi
Streptococcus intermedius
Streptococcus milleri
Streptococcus pneumoniae
Streptococcus pyogenes
Streptococcus suis
Streptococcus uberis
Streptococcus viridans
Listeria ivanovii
Listeria monocytogenes
Listeria seeligeri
Listeria welshimeri
Bacillus anthracis
Bacillus cereus
Bacillus subtilis
Bacilli
Tatlockia micdadei
Legionella longbeachae
Legionella pneumophila
Coxiella burnetii
Acinetobacter baumannii
Acinetobacter lwoffii
Acinetobacter radioresistans
Moraxella catarrhalis
Acinetobacter calcoaceticus
Acinetobacter calcoaceticus subsp. Anitratus
Pseudomonas syringae pv. glycinea
Pseudomonas aeruginosa
Pseudomonas alcaligenes
Pseudomonas fluorescens
Pseudomonas putida
Pseudomonas stutzeri
Aeromonas sp.
Stentrophomonas maltophila
Xanthomonas campestris pv. malvacearum
Xanthomonas oryzae pv. oryzae
Xanthomonas oryzae pv. oryzicola
Xylella fastidiosa
Alteromonas tetraodonis
Tetrodotoxin
Haemophilus influenzae
Haemophilus aegyptius
Haemophilus ducreyi
Haemophilus parahaemolyticus
Haemophilus parainfluenzae
Haemophilus paraphrophilus
Pasteurella multocida
Vibrio cholerae
Cholera Toxin
Vibrio mimicus
Vibrio parahaemolyticus
Vibrio vulnificus
Mollicutes
Mycoplasma pneumoniae
Erysipelothrix rhusiopathiae
Mycoplasma mycoides
Mycoplasma capricolum subsp. Capripneumoniae
Actinobacteria
Mycobacterium tuberculosis
Mycobacterium abscessus
Mycobacterium avium
Mycobacterium bovis
Mycobacterium fortuitum
Mycobacterium kansasii
Mycobacterium leprae
Mycobacterium haemophilum
Mycobacterium marinum
Mycobacterium scrofulaceum
Mycobacterium simiae
Mycobacterium szulgai
Mycobacterium ulcerans
Mycobacterium xenopi
Rhodococcus equi
Actinomyces israelii
Actinomyces naeslundii
Propionibacterium acnes
Rothia dentocariosa
Clavibacter michiganensis subsp. Sepedonicus
Nocardia asteroides
Nocardia nova
Corynebacterium amycolatum
Corynebacterium jeikeium
Corynebacterium xerosis
Corynebacterium diphtheriae
Diphtheria toxin
Clostridia
Anaerococcus prevotii
Clostridium botulinum
Botulinum toxin
Clostridium difficile
Clostridium perfringens
Epsilon toxin
Clostridium septicum
Clostridium tetani
Peptococcus niger
Peptostreptococcus anaerobius
Veillonella dispar
Escherichia coli
Shiga Toxin
Salmonella bongori
Salmonella choleraesuis
Salmonella enteritidis
Salmonella paratyphi
Salmonella typhimurium
Salmonella typhi
Shigella boydii
Shigella dysenteriae
Shigella flexneri
Shigella sonnei
Yersinia enterocolitica
Yersinia pseudotuberculosis
Yersinia pestis
Citrobacter freundii
Edwardsiella tarda
Enterobacter aerogenes
Enterobacter cloacae
Klebsiella oxytoca
Klebsiella pneumoniae
Morganella morganii
Proteus mirabilis
Proteus vulgaris
Providencia stuartii
Serratia marcescens

Figure 1B

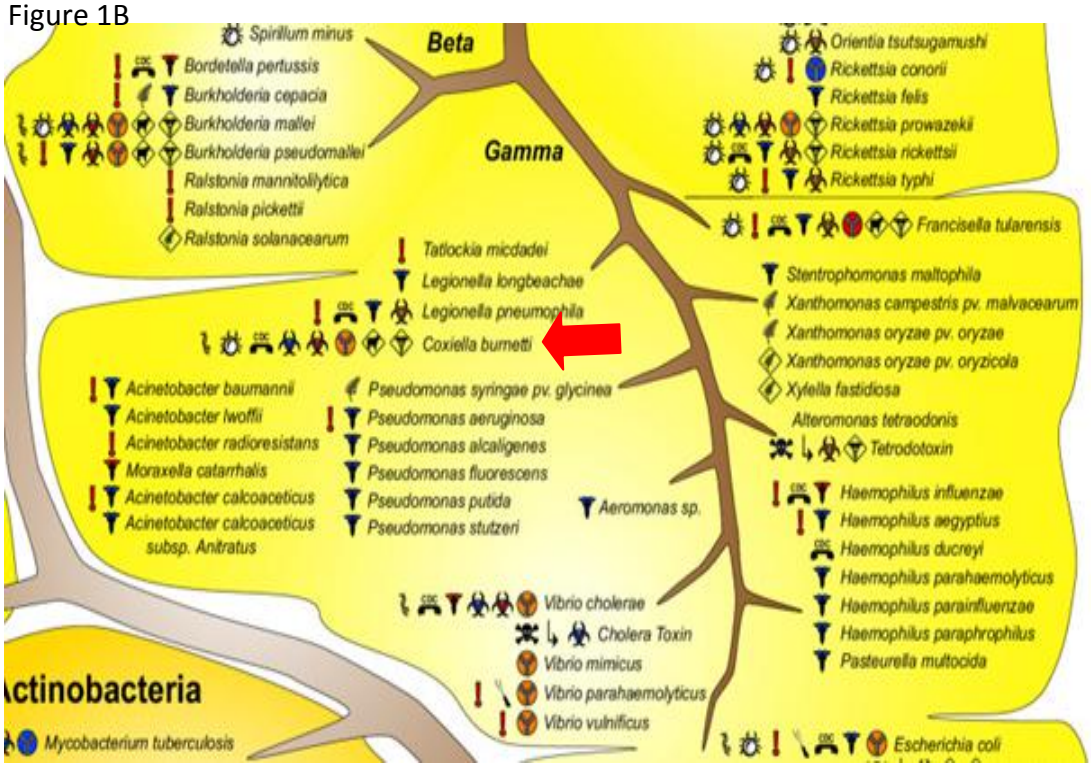

Figure 1A-B: Phylogenetic relationship between *C. burnetii* and other bacteria. The red arrows point to *C. burnetii*. A) (preceeding page) Bacterial phylogeny of various species important in medicine and/or biodefense. B) Enlargement of area closest to *C. burnetii*. The symbols next to *C. burnetii* indicate, from left to right, 1) potential for bioengineering, 2) zoonotic agent, 3) CDC notifiable agent, 4) validated biocrime agent, 5) validated biological weapon, 6) NIAID category B priority pathogen, 7) USDA high consequence animal pathogen, 8) HHS select agent. Adapted from [6].

[34]. Acid phosphatase has been proposed as a possible means to control the respiratory burst and high superoxide levels that most macrophages exhibit upon infection, which *C. burnetii* is known to inhibit [34,36]. The acid phosphatase activity during infection, reported by Baca et al, 1993, has been shown to be bacterially rather than host derived [34]. Baca et al, 1993 worked on phase I *C. burnetii*, and there may be differences in acid phosphatase expression/activity between phase I and II strains [34].

The *C. burnetii* life cycle is known to have two distinct forms, the small cell variant (SCV) and the large cell variant (LCV). The SCV is spore-like and resistant to environmental stresses including heat, desiccation, chemical exposure, and sonication [33]. Upon entry of the cell by phagocytosis, the SCV form begins to be activated, likely due to exposure to the increasingly acidified phagosome and possibly by exposure to degradative phagosomal enzymes [10], although this process is incompletely understood.

In Vero cells (a cultured cell line derived from green monkey kidney epithelial cells) the SCV-LCV transition is well underway by 8 hours postinfection and complete by 16 hours postinfection [37]. The LCV form is significantly more fragile than the SCV form, but is also more metabolically active, and is replicative with an approximately 20 hour doubling time [10,12,13,15,17,38,39], although this can vary with the choice of the model infected system [28,29,40]. A large parasitophorous vacuole containing primarily LCV *C. burnetii* is present in Vero cells by 2 days postinfection [37]. A parasitophorous vacuole is any host cell vacuole inhabited by a bacterium, in the case of *C. burnetii*, this is the phagolysosome. The LCV form may be more active in maintaining the active infection within the organism, while the SCV form may be able to form a reservoir of *C. burnetii* within cells that enables the reemergence of a latent infection [33]. *C. burnetii* does not actively lyse the host cell.

There have been suggestions that the LCV form is a log-phase form, while the SCV is a stationary phase form of the bacterium, as it is the SCV form that persists

despite environmental stresses such as heat, and desiccation [33]. In Vero cells, the SCV form begins to reappear by 6 days postinfection [37], suggesting that the transition is at least partially tied to the availability of host cell nutrients to the bacteria, and supports the SCV as a stationary phase bacterial form. Although host cells are cultured in media supplying nutrients, there will come a point where the nutrient carrying capacity of the phagolysosome will be unable to supply the complete nutritional needs of an expanding population of bacterium. In other words it would be expected that beyond a certain point, metabolically active *C. burnetii* would begin to deplete available nutrients faster than the host cell can provide them.

Samoilis et al., (2007) [38] documented the proteome of phase II *C. burnetii* using 2D gel electrophoresis, and observed a number of proteins not found in a previous study of the proteome of phase I *C. burnetii* by Skultety et al., (2005) that utilized both 2D gels and shotgun mass spectrometry (MS) [41]. Skultety et al., (2005) identified a series of abundant spots present on a 2D gel, using MALDI-TOF MS analysis [41]. Samoilis et al., (2007) [38] noted that many of the proteins identified in their study were not identified in the study by Skultety [41] , and suggested that these differences may be due to expression differences between phase I and II strains. It is possible that the differences between phase I and phase II protein expression may help to explain observed differences in infectivity between phase I and II strains, but further study will be needed to evaluate this hypotheses. It should be noted that many of the differences

in protein expression discussed by Samoilis et al., (2007) may in fact be due to different and/or non-optimal staining conditions on the part of Skultety et al., (2005) [38,41].

Skultety noted >500 proteins spots on 2D gels using silver staining, while Samoilis found >600 using colloidal Coomassie blue [38,41]. This is not expected as silver is generally considered to be more sensitive (~0.5 ng detection limit) than Coomassie staining (~1-30 ng detection limits depending on formulation). Silver staining is not linear, whereas Coomassie is, and this could also account for differences in detection between the two reported datasets. In silver staining, the observed spot intensity does not necessarily equal amount of protein in the spot. In Coomassie blue staining, the observed spot intensity is directly proportional to the amount of protein in the spot. The reported differences in protein expression between the two studies, as discussed by Samoilis [38], do suggest that at least some of the differences in phase I and phase II biology are attributable to differences in protein expression, and might ultimately explain the observed differences in virulence and infectivity. This certainly includes differences in the LPS generating machinery documented by Hoover et al., (2002) (described above) [32], which were shown to be genetically distinct by Seshadri et al., (2003), who showed that phase II *C. burnetii* is unable to produce the LPS components virenose and dihydrohydroxystreptose [17].

In general, many of the proteins identified by Samoilis et al., (2007) [38] appeared to be related to pathogenesis and detoxification, while Skultety et al., (2005) identified many proteins related metabolism and other cellular processes [38,41]. Both

studies used a whole cell extract and it would have been beneficial to analyze soluble and membrane fractions separately as membrane proteins are often difficult to detect in whole cell lysates. 2D gel electrophoresis and shotgun LC MS/MS approaches to proteomics typically identify largely different proteins when applied to the same system, providing complimentary information. Thus, in addition to the staining differences noted above, it is difficult to compare phase I and phase II studies run on different platforms. A more direct comparison between phase I and II proteomes under consistent detection conditions would be very informative as to the protein expression differences between the two strain types. Further work would be needed to 1) elucidate these differences, on a consistent platform(s), and 2) to quantify differences in expression of proteins as this has never to our knowledge been attempted for phase I and phase II *C. burnetii*.

C. burnetii specifically inhabits the phagolysosome within monocytes, and it's primary carbon sources are likely to be amino acids and peptides obtained from the host [7,10,17]. This is consistent with the presence in the *C. burnetii* genome of 15 amino acid transporters and 3 peptide transporters as inferred Seshadri et al., (2003) during sequencing of the *C. burnetii* genome [17]. The acidic environment in the phagolysosome presents challenges to *C. burnetii*'s survival. Although most bacteria actively transport H^+ from inside the cell to the cell surface for the purposes of generating ATP and for driving transmembrane pumps, they must maintain a neutral to

slightly basic pH in the cytosol and they do not acidify the extracellular environment with anywhere near the concentration of H^+ present in the phagolysosme.

One predicted manner in which *C. burnetii* could overcome the acidity of the phagolysosome is to produce a large number of basic proteins to act as a proton sink and help offset the phagolysosome's acidic environment [17]. *C. burnetii* is predicted to contain 2183 genes [17]. It has been demonstrated in 2D gels that *C. burnetii* produces proteins over a wide pI range and, in the 2D gel images, the proteome does not appear to be particularly basic, although this can be difficult to determine from 2D gels alone [38,41]. In addition, these 2D gel studies [38,41] used whole cell lysates rather than examining membrane and cytosolic fractions separately which provide substantially better resolution (discussed above). It should also be pointed out that highly basic proteins tend to resolve poorly on 2D gels. Cytosolic *C. burnetii* proteins would not be predicted to have a basic pI as they would not need to offset a low environmental pH in the bacterial cytosol.

Comparison of theoretical protein pI distributions between *C. burnetii*, *Legionella pneumophila*, and *Rickettsia prowazekii* can be seen in figure 2, as calculated by www.jvirgel.de from their genome sequences. While *C. burnetii* does produce a slightly larger number of predicted basic proteins in the membrane fraction and the secreted fraction (indicated by the red dots and blue dots, respectively, in figure 2). However, on the whole the pI distribution is roughly equal between predicted basic and acidic

proteins, owing to the relatively equal predicted pI distribution for the cytosolic proteins (black dots in figure 2).

For *L. pneumophila*, there is a slight tendency towards acidic proteins, as seen in the theoretical pI distributions (in figure 2C and D), but the bacterium still produces a relatively high number of basic membrane proteins, and a strong tendency towards acidic soluble fraction proteins (figure 2D). *R. prowazekii* produces a slight tendency towards basic proteins, a significant fraction of which are membrane proteins. Secreted and soluble proteins in *R. prowazekii* are predicted to be approximately equally distributed between acidic and basic. *L. pneumophila* initially inhabits the phagosome upon engulfment, but quickly reprograms the phagosome to acquire characteristics of the endoplasmic reticulum, which is *L. pneumophila*'s habitat [42,43]. *R. prowazekii* also initially inhabits the phagosome upon engulfment, but then escapes from the phagosome and inhabits the cytoplasm [44].

C. burnetii infection (phase I or phase II) typically triggers a Th1-type T cell adaptive immune response [45]. A lack of T cells in SCID mice was reported by Andoh et al., (2005) to allow a phase II infection to persist in these mice *in vivo* [29]. This supports observations that while innate immune cells by themselves can partially suppress *C. burnetii* infections, even a phase II infection requires a functional T cell response for complete clearance [28,29,40]. The requirement for both an adaptive and an innate immune response also explains why phase II *C. burnetii* can be used *in vitro* in purified cell lines devoid of adaptive immune cells, enabling the phase II bacteria to survive.

Many obligate intracellular pathogens have relatively small genomes, and have a tendency towards a phenomenon known as genome reduction [46], whereby the bacterial genome progressively loses metabolic capabilities, and becomes reliant on the host cell for metabolic survival. This phenomenon may be a result of increased adaptation of the bacteria to the host, and may have led to the origin of mitochondria from an endocytosed *Rickettsial* species, believed to be closely related to *Rickettsia prowazekii* [44,46,47]. A recent comparison of several species of obligate intracellular pathogens with the *E. coli* genome revealed that the intracellular pathogens had a reduction in genes for metabolic pathways related to carbohydrate transport and metabolism, as well as a decrease in the rate of gene rearrangement [46].

Obligate intracellular pathogens also tend to lose regulatory elements and structural genes [48]. The intracellular environment is relatively constant and may contribute to a weak selection pressure to retain functional bacterial genes that are complimented by the host genome/proteome. There is little pressure to retain a functional copy of a gene that can be complimented by the host cell, as opposed to a gene critical to bacterial function, that would be under evolutionary pressure to remain functional. A lack of genetic recombination, particularly in asexually reproducing populations, can lead to the accumulation of major deleterious mutations, as genetic variance becomes limited. As a bacterium becomes increasingly dependent on the host cell, more and more genetic function is surrendered to the host genome, as a function of weak selection pressure to prevent the accumulation of mildly deleterious mutations and a lack of

Figure 2A

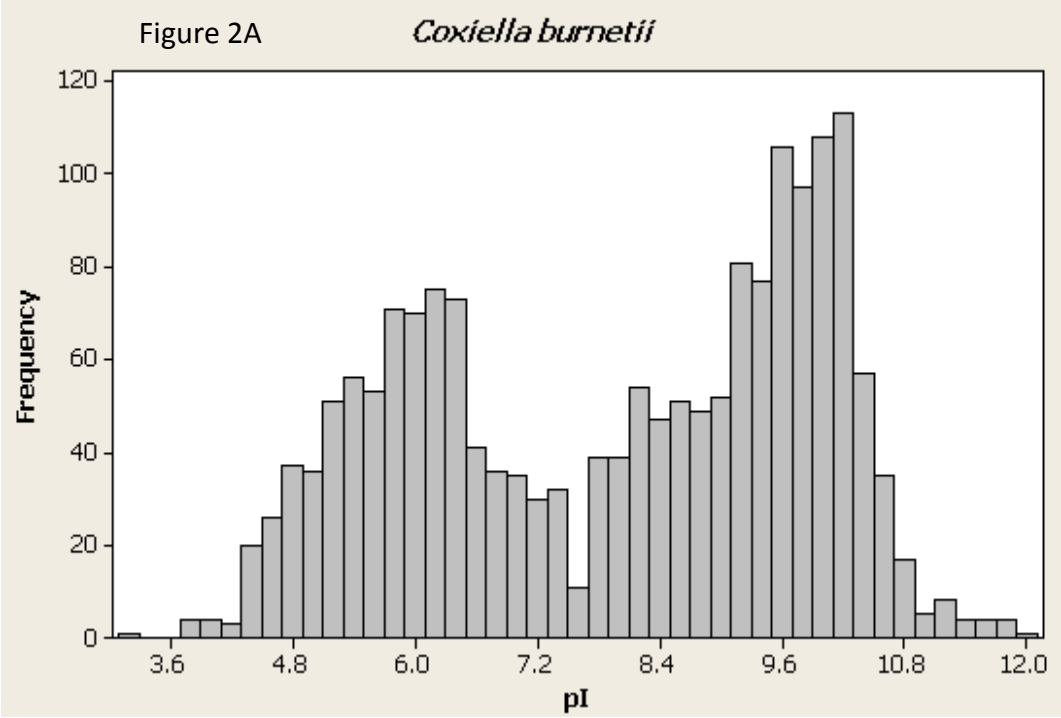

Figure 2B

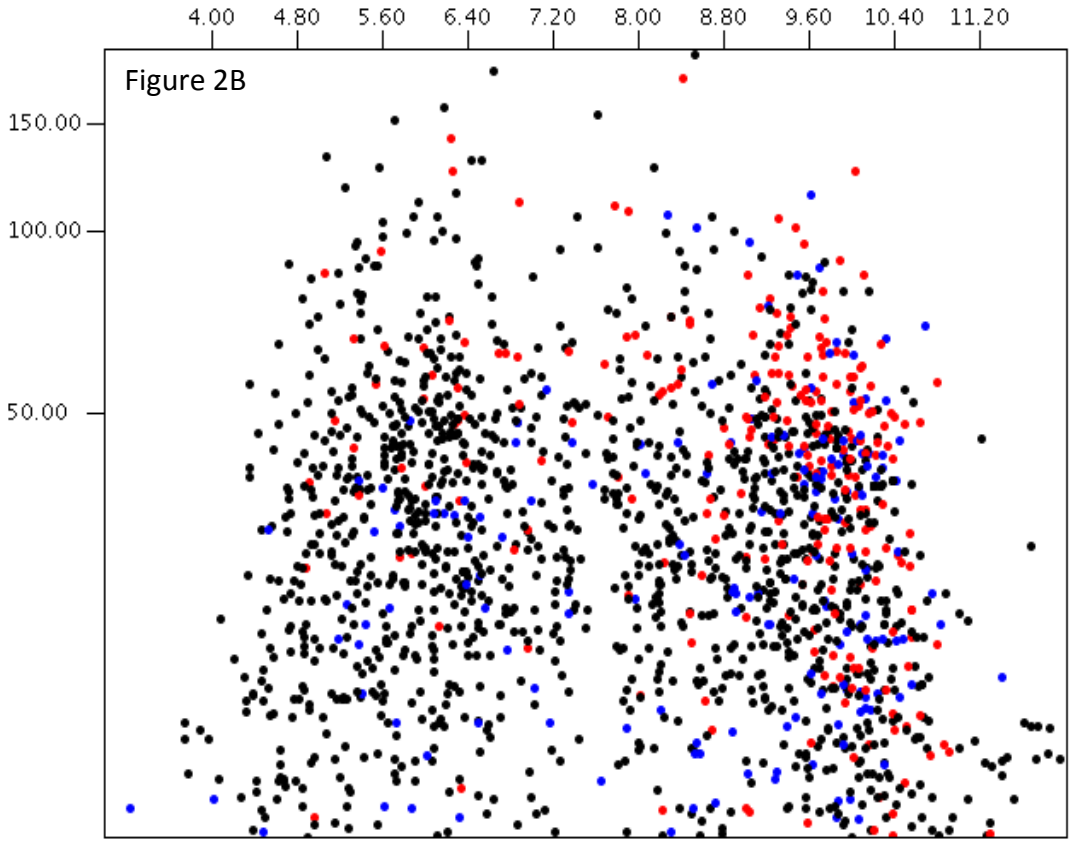

Figure 2C

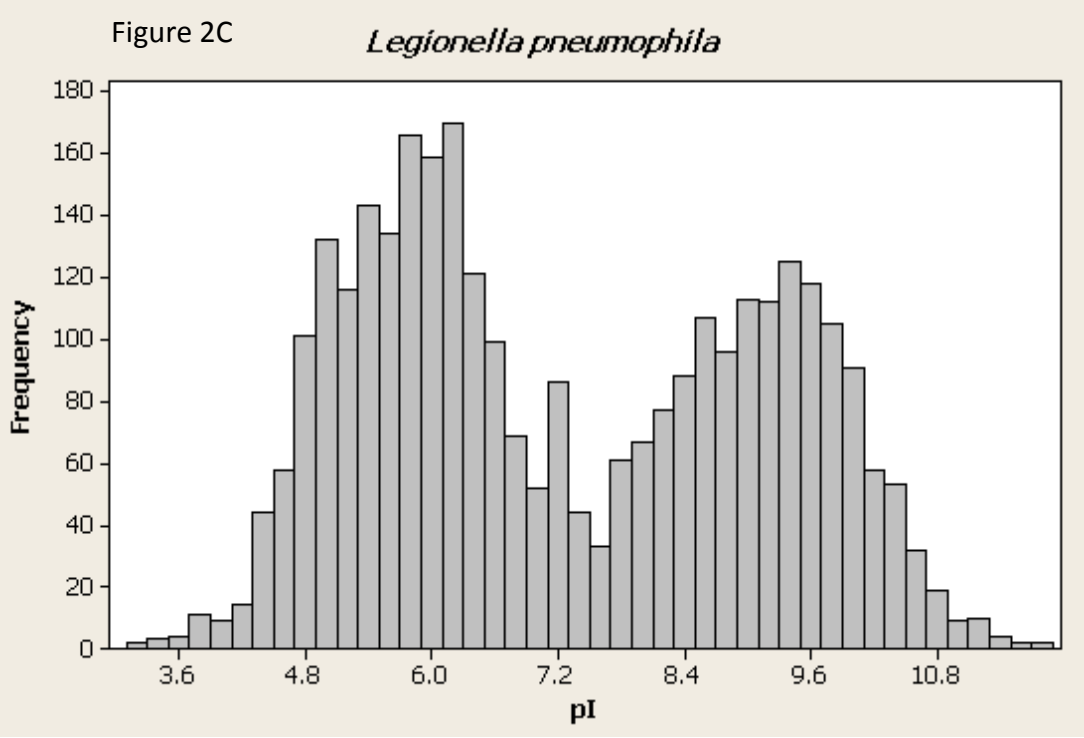
Legionella pneumophila
Frequency
0
20
40
60
80
100
120
140
160
180
3.6
4.8
6.0
7.2
8.4
9.6
10.8
pI

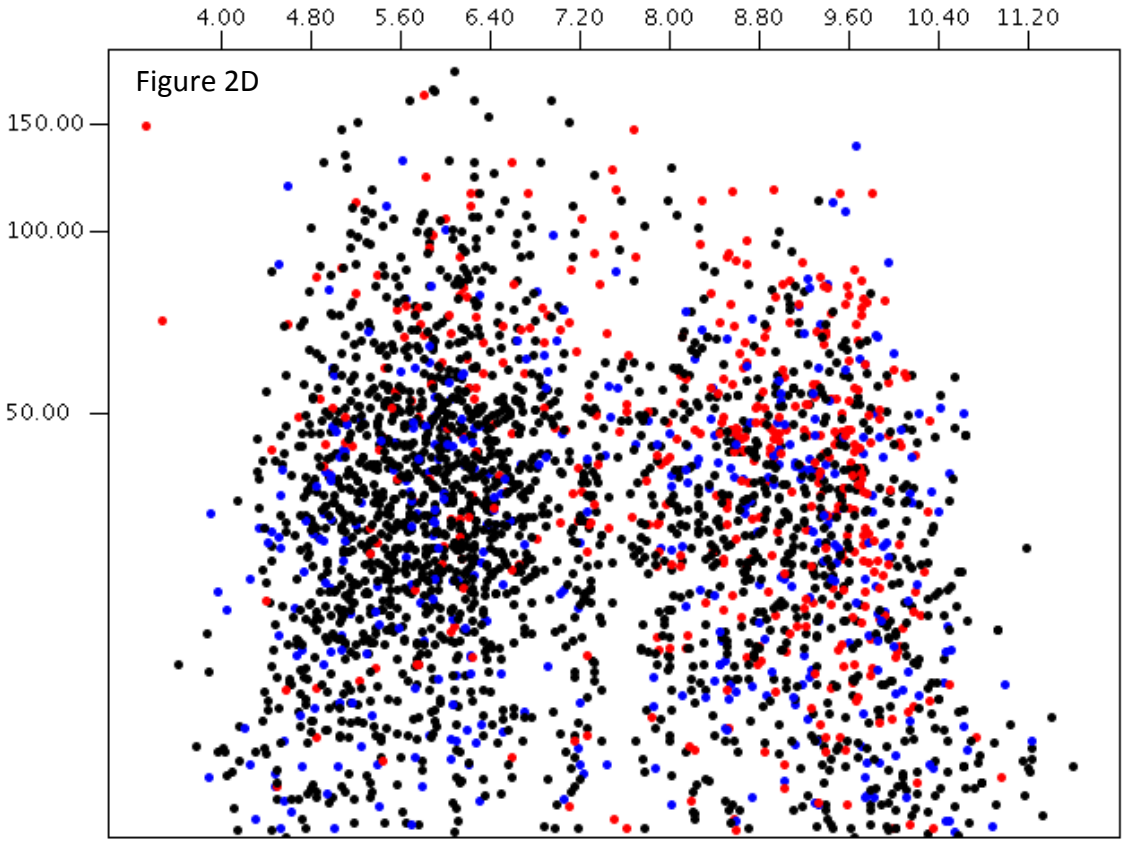
Figure 2D
4.00
4.80
5.60
6.40
7.20
8.00
8.80
9.60
10.40
11.20
150.00
100.00
50.00

Figure 2E

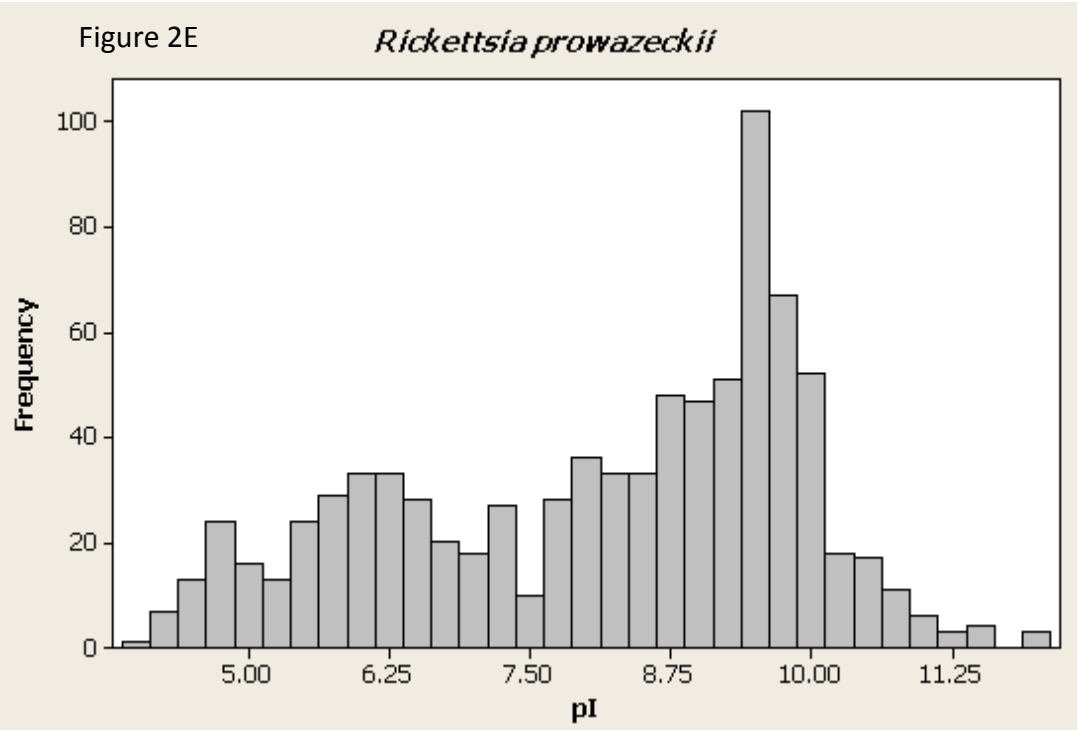
Rickettsia prowazeckii
Frequency
0
20
40
60
80
100
5.00
6.25
7.50
8.75
10.00
11.25
pI

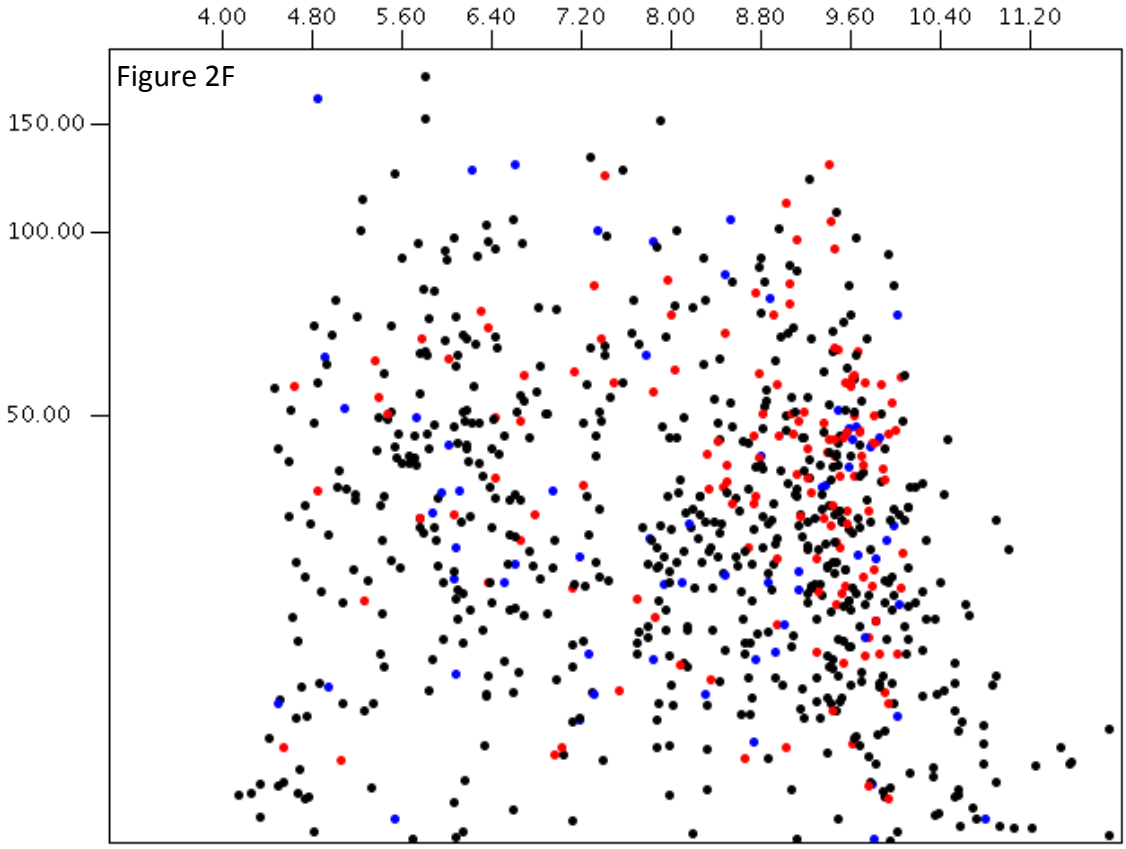
Figure 2F
4.00
4.80
5.60
6.40
7.20
8.00
8.80
9.60
10.40
11.20
150.00
100.00
50.00

Figure 2 A-F: (preceeding pages). Theoretical pI distribution and predicted 2D gels for *C. burnetii, L. pneumophila*, and *R. prowazeckii*. Dot plots are derived from www.jvirgel.de and are calculated from the genome sequences for these organisms. The theoretical pI data from the dot plots was exported to Minitab to create the histograms in A, C, and E. The slight differences observed between the dot plots and the histograms are the result of binning by Minitab. In B, D, and F black dots are soluble, blue are secreted, and red are membrane proteins.

opportunity for genetic recombination with the wild type genome [49]. Many obligate intracellular pathogens that have undergone genome reduction lose bacterial amino acid biosynthesis pathways, and become dependent on the host cell [50]. Most free living bacteria are capable of synthesizing all of their amino acids. Inhabiting the environment in the phagolysosome should provide a ready supply of host-cell derived peptides and amino acids for the bacterium. *C. burnetii* contains many intact metabolic pathways, but lacks a number of key amino acid synthesis enzymes, implying a dependence on the host cell for amino acids [17]. *C. burnetii* is predicted to be auxotrophic for 11 amino acids, including tryptophan and lysine [17]. There are indications, from the presence of pseudogenes in the *C. burnetii* genome that genome reduction is occurring, but may have only recently begun [17]. Other obligate intracellular bacteria that have undergone genome reduction include *Rickettsia prowazekii*, and *Mycobacterium leprae*.

Infection by *C. burnetii* causes Q fever, a chronically debilitating, potentially fatal disease, as has been described above. Because of its remarkable infectivity, environmental persistence, and ready aerosolization, there is significant concern that *C.*

burnetii could be developed as a bioterror weapon. In addition to the public health threat posed by naturally occurring *C. burnetii* infections, there is a need to develop biodefense strategies to better contain and control a deliberate outbreak caused by a terrorist organization. To this end, a better understanding of how *C. burnetii* affects the monocytes it inhabits, as well as how various treatment options affect the immune response is desirable. Our work, detailed below, aimed to provide inroads into these areas by evaluating protein expression patterns in monocytes in response to *C. burnetii* and in response to immune adjuvants that help to control monocyte infection, and by compiling a preliminary systems model of the monocyte responses that could help to focus downstream research efforts.

Monocytes/Innate Immunity

Innate immune cells constitute the first response elements of the immune system [51], and monocytes represent an important member of the innate immune machinery. Other cell types that contribute to innate immunity include macrophages, dendritic cells, neutrophils, basophils, eosinophils, and mast cells. Many of these innate immune cells are formed in the bone marrow, and then at some point in their developmental cycle migrate to the bloodstream and/or tissues (depending on the cell). Rather than relying on specific antibody recognition of a particular pathogen, the cells of the innate immune system rely on “pattern recognition” receptors to identify common structural features of invading pathogens, such as LPS coatings, single strand nucleic

acids or flagellin (a major protein component of flagella). These components are essential to the microbes, are highly conserved and therefore unlikely to mutate in such a way that the pattern recognition receptors will not recognize them [52]. As such, innate immune cells constitute a first line of defense against pathogens.

Monocytes are professional phagocytic cells that exist in an alert state in the bloodstream, and mature/differentiate into macrophages and dendritic cells after encountering a pathogen or other immune stimulus [51]. Local cytokine/chemokine profiles regulate the path of monocyte differentiation into either dendritic cells or macrophages [53]. Macrophages and dendritic cells can migrate across the endothelium into the tissues to sites of active inflammation [53]. Macrophages and monocytes both act to engulf foreign matter (e.g. microbes) via phagocytosis and stimulate other immune (innate and adaptive) responses. Dendritic cells are professional antigen presenting cells that process antigens and display them at the cell surface to present antigens to other cells, particularly naïve T cells. Dendritic cells are often considered to be poorly endocytic, and may represent a more mature form of a macrophage that has switched from active phagocytosis to near full-time antigen presentation, to stimulate the adaptive immune response [54]. The line between macrophages and dendritic cells is blurry at best, distinguished by few molecular markers although the shape of the cells is different, and there may simply exist a continuum of cell types from monocytes to macrophages to dendritic cells that lacks clear molecular boundaries [54].

Monocytes rely on phagocytosis to attack microbes. The microbes are engulfed and then initiate a process involving various interconnected pathways related to inflammation, apoptosis, lysosomal maturation, and MHC antigen presentation among others, although it should be noted that monocyte antigen presentation capabilities are relatively poor compared to dendritic cells [52,55]. Surface antigens presented to T or B cells trigger an adaptive immune response [52]. Innate immune cells will also secrete various markers for inflammation and other proteins, such as Hsp60, to act as danger signals to other immune cells and shape the immune response.

It is noteworthy that not all phagocytosis events or all phagocyte receptors trigger an immune response, e.g. phagocytosis of food or other nutrients. For a phagocyte to trigger an immune response, specific phagocyte receptors e.g. the toll-like receptors (TLRs) (described below), must be activated e.g. by bacterial LPS [55]. Most often, the precise response is a function of the stimulation of several receptors and the integration of subsequent cellular responses. When *Coxiella burnetii* triggers TLR4 (a receptor which recognizes gram-negative bacteria), for example, phagocytosis ensues [56]. A normal response from the monocyte to microbial phagocytosis would be to initiate a respiratory burst producing reactive oxygen intermediates, but this appears to be blocked by *C. burnetii* secretion of acid phosphatase, although the precise mechanism is not known [34,36] Recently, it was demonstrated that *C. burnetii* inhibits the translocation of $p47^{phox}$ and $p67^{phox}$ to the membrane [36]. The $p47^{phox}$ and $p67^{phox}$ proteins are important components of the NADPH oxidase complex, and preventing

their translocation to the membrane is believed to be involved in the inhibition of superoxide and other ROS production during *C. burnetii* infection.

The production of superoxide is a common cellular response to infection. Superoxide is an oxygen radical that is mildly toxic to many cell types, including the phagocytic cell producing the superoxide. Superoxide is converted to hydrogen peroxide by superoxide dismutase, and hydrogen peroxide is more toxic to many cell types than superoxide itself. Hydrogen peroxide can also be converted to hypochlorous acid (bleach) by myeloperoxidase. Hypochlorous acid is extremely toxic to most cell types. In addition, if nitric oxide is also being produced as a response to the infection the combination of superoxide and nitric oxide can produce peroxynitrite ($ONOO^-$), that is a powerful oxidant and highly toxic to cells [57,58]. A recent report using Monomac I cells indicated that elevation of TNF-α levels applied exogenously increased the expression of NADPH oxidase genes as well as increasing superoxide production, primarily as a result of activation of the NF-κB response [59].

It should be noted that macrophages are significantly longer lived than many other innate immune cells (e.g. neutrophils), and they tend to produce a relatively smaller oxidative burst [59-61]. This smaller oxidative burst may contribute to the persistence of several bacterial species that inhabit macrophages (e.g. *C. burnetii*), particularly if those bacteria can alter production and/or stimulus of inflammation markers by exporting bacterial proteins or other effectors to the host cell. Macrophage respiratory bursts are significantly larger if primed by prior exposure to immune

stimulating agents (including immune adjuvants, inflammation markers, and LPS) via an incompletely understood mechanism [59-61].

It may be noteworthy that the nature of the stimulus for superoxide production has been reported to have an effect on the amount of reactive oxygen species [61]. As an example of differential oxidative stress, consider the response of Caco-2 cells to cyanobacterial toxins [62]. In a recent study by Puerto et al, (2009), it was demonstrated that cyanobacterial extracts containing microcystins (cyanobacterial toxins), as well as purified microcystins, induced consistently higher levels of reactive oxygen species (e.g. H_2O_2) production than cyanobacterial extracts devoid of microcystins [62]. It is also of note that ROS can stimulate NF-κB, and thus a possible feed-forward mechanism is present [59]. In the feed-forward mechanism, increased production of TNFα, which can activate NF-κB, will lead to increased production of superoxide which also stimulates NF-κB, potentially producing a lethal cycle resulting in a runaway inflammatory response [59].

There are many different microbial recognition receptors that can trigger phagocytosis, more than one of which can be activated simultaneously. These recognition receptors include complement receptors, Fcγ receptors, integrins, and lectins for example [55]. Stimulation of these receptors can trigger a variety of downstream responses, and need not be confined to recognition of the microbe, since local extracellular concentrations of cytokines and chemokines (released by the infected cell and/or neighboring cells) can also alter the tendency towards, or efficiency of,

phagocytosis. Chemokines are chemotaxis-inducing cytokines released by immune cells that usually function to trigger the migration of nearby cells to the site of the chemokine releasing cell. Cytokines are a broader class of protein compounds that modify immune function in an autocrine and/or paracrine manner and able to act on both the releasing cell and/or nearby cells attracted to the site of cytokine release.

The Toll-like receptors (TLRs) are a family of pattern recognition receptors common to innate immune cells. TLRs detect molecular features that are commonly found in microbes, such as LPS coats and that are also so essential to microbial function that they are at least somewhat conserved. Typically, the cytoplasmic domain of TLRs, which contains a signal transduction modulator, is highly conserved across TLRs. On the other hand, the extracellular pattern recognition region tends to evolve, likely due to the changing nature of microbial challenges over time [63,64]. Not all TLRs are cell surface expressed. TLR1, 2, and 4 are commonly found as cell surface proteins, but TLR3, 7, and 9 are only expressed in endosomes, and also require endosomal maturation to become active [65]. In other words, while some TLRs are always 'on' others are inducible based on specific signals.

TLRs can be recruited to phagosomes during phagocytosis and relative responses to different TLRs can be used to assess the nature of the ingested microbe and help determine cellular response(s) [55,65]. It has been demonstrated that immune response to phase I *C. burnetii* infection in monocytes requires the activation of both TLR2 and TLR4 [66]. Monocyte killing of *C. burnetii* does not seem to be affected by

TLR2/4 activation, but the inflammatory response requires the activation of both to be optimally effective [66].

TLR activation often causes recruitment of the adaptor protein MyD88 to the cell membrane, which can integrate signals from multiple TLRs and initiate a signaling cascade that ultimately triggers inflammation, via the activation of NF-κB. Stimulation of TLR4 by LPS, for example, will trigger monocyte maturation to dendritic cells, but does not require MyD88 [52,65]. The protein TIRAP is also implicated in regulating inflammation in response to TLR activation, for at least a subset of TLRs [67]. This suggests that there are multiple signaling pathways involved in the activation of monocytes and other immune cells.

The levels of TLR expression and activation seems to vary considerably with the cell type [52,68]. TLRs and other innate immunity pattern recognition receptors have been reported in adipocytes, and in adipocytes, LPS activation of TLR4 has been shown to upregulate expression of TLR2 [68]. Other tissues such as spleen, heart, and lungs also express TLRs, underscoring the widespread nature of innate immunity. In the case of adipocytes, LPS stimulation leads to an increase in expression of leptins, suggesting an intersection between immune function and energy balance during infection, as leptins are directly involved in energy homeostasis [68].

It is tempting to speculate that adipocytes act as a 'master integrator' of energy homeostasis that is essential for the most efficient immune function. In flies, it has been observed that the fat body, which serves as an energy storage mechanism, is the

primary coordinator of innate immunity [69]. In light of this observation in flies, it is tempting to further speculate on a common evolutionary ancestral cell for adipocytes and macrophages. This is supported by observations reported by Charriére et al., (2003) that the transcriptomic profiles of preadipocytes have more in common with macrophages than differentiated adipocytes in a microarray analysis [70]. It was further demonstrated that injection of preadipocytes into the peritoneal cavity of nude mice induced the preadipocytes to rapidly transdifferentiate into macrophages [70]. Although experimental investigation of these issues are beyond the scope of the present investigation, it could be of interest for future work that the interrelation of adipocyte responses and innate immunity may be highly important in the immune response.

Another response to infection is apoptosis of the immune cell. Neutrophils are continually undergoing apoptosis. Unactivated neutrophils have a lifespan of <1 day in circulating blood but can survive for several days following activation [71]. Some bacterial pathogens have developed a number of remarkable adaptations to either prevent host cell apoptosis to enhance their intracellular propagation or in some cases to induce apoptosis in immune cells to reduce the potential immune response (e.g. by reducing the neutrophil population), or alternatively to release active bacteria from intracellular sites of propagation. For example *Shigella* sp. bacteria have been shown to induce host cell apoptosis for the purposes of disseminating the bacterium to new host cells and thus enhance propagation [60]. *C. burnetii* on the other hand has been

reported to inhibit monocyte apoptosis by inhibition of caspase activation [72], which has the effect of maintaining *C. burnetii*'s intracellular habitat.

A final note on phagocytosis of pathogens by innate immune cells involves certain specialized types of pathogens. Some pathogens, such as *C. burnetii*, *Yersinia pestis*, or *Francisella tularemia* are able to use their own effectors to either modulate/direct their internalization. This includes the modification of the phagosome to suit the pathogens needs. An example of this is *Legionella pneumophila* directing the phagosome to develop qualities resembling the ER, which is the specific organelle that *L. pneumophila* inhabits [42,43]. *C. burnetii* causes or allows the phagosome to develop into a phagolysosome, maintaining the acidic pH that *C. burnetii* requires to be metabolically active. It is likely that lipid rafts are an integral part of phagocytosis, phagosome maturation, and subsequent cellular responses as flotillin, a marker for lipid rafts, has been identified as part of the phagosome membrane [73]. There are a number of phagosome-associated proteins such as Rab7 and vacuolar H^+-ATPase that are believed to be lipid raft associated [55,73]. Regulation of lipid raft composition is one possible means by which pathogens could reprogram phagosomal maturation.

Adjuvants

Immune adjuvants are small molecules that act to specifically boost/activate the innate immune system, but do not trigger an adaptive immune response like a vaccine is intended to do. Adjuvants do not result in the production of memory cells like a

vaccine, but can rather stimulate the innate immune system in a broad manner. We tested three adjuvants known to increase cell killing of *C. burnetii*. We chose this particular model system based on previously published work by Lubick et al. (2007), which made the interesting and unexpected observation that treatment of monocytes with the $GABA_A$ receptor antagonist Securinine enhanced monocyte killing of *C. burnetii* [74]. We intended *C. burnetii* infections to serve as a model system that we hope will provide a framework that might be beneficial to combating a wide variety of weaponizable organisms.

One traditional idea behind the use of immune adjuvants is to combine them with noninfectious antigenic species in a vaccine to stimulate a more robust total immune response. The traditional approach is applied with the intent that such a more robust response will enable the conveyance of a more effective immune response, requiring less vaccine per dose and/or fewer vaccination boosters [75]. Furthermore, in a broader context, adjuvants might be useful as a prompt prophylactic defense against possible exposure to infectious agents without the need for prior vaccination. For example, an adjuvant could be administered to troops or civilian first responders before sending them into known or suspected hot zones where infectious agents may have been released. If infectious agents were found to have been released, adjuvant therapy could also be administered to the general populace relatively quickly, even if no vaccine is available, thus limiting the spread of disease.

The adjuvant approach, if effective in settings of interest, will also convey immune resistance much faster than a vaccine, as the innate immune system reacts very quickly to stimuli, and does not require time to develop memory cells. The use of adjuvants has possible applications not only to combat or protect against a bioweapons release, but also as a preventative measure following natural disasters, where the spread of disease could become rampant. Administration of an adjuvant(s) would prime the innate immune system to more effectively resist/control infections in a disease exposed individual. Thus the adjuvant's effects could prevent people from getting the disease, and maintain their effectiveness in performing their duties.

We tested the well known adjuvants *E. coli* LPS, and MPL, a less toxic derivative of *E. coli* LPS (see figure 3). Both LPS and MPL are known to act via Toll-like receptors (TLRs), which is one of the classical pathways of innate immune recognition. LPS, although effective in boosting the innate immune response, can cause such a large inflammatory response as to be lethal, and thus it's clinical effectiveness is limited. MPL, derived from the lipid A region of *E. coli* LPS, is significantly less toxic than LPS, and is currently used clinically/near clinically in vaccines [75-77]. LPS can be beneficial as a model compound in elucidating the mechanisms of the response(s) to adjuvant action. We wished to compare the LPS and MPL responses with responses to Securinine, which apparently does not rely on the TLR signaling response pathway (discussed below) [74].

The adjuvant of primary interest in our study was Securinine, a $GABA_A$ receptor antagonist that was recently shown to increase cell killing of *C. burnetii* and has been

investigated at Montana State University for biodefense purposes [74]. Securinine is a small molecule plant alkaloid derived from the shrub *Securinega suffructicosa* [78]. Securinine was shown to be a specific $GABA_A$ receptor antagonist with an IC_{50} of ~50 uM and had little to no cross-reactivity with other types of neurotransmitter receptors using equilibrium binding assays [78]. Securinine was independently identified as an adjuvant at Montana State University from a library of 2,000 natural compounds that were screened for their ability to induce monocyte production of IL-8, and was shown to induce cell killing/resistance to *C. burnetii* infection [74].

Western blot data from the Jutila group has indicated that Securinine activates the p38 response pathway but not the NF-κB response pathway, that is characteristic of TLR responses (M. Jutila and K. Lubick, personal communication). The Jutila group also used a THP1-Blue-CD14/SEAP TLR 1-10 assay to test whether or not Securinine triggers the TLRs [74]. The THP1-Blue-CD14/SEAP TLR 1-10 assay uses stably transfected monocytes that secrete an embryonic alkaline phosphatase (SEAP) reporter upon TLR activation [79]. TLR activation is detected by the use of the Quanti-BlueTM medium (Invivogen) that turns blue in the presence of SEAP [79]. The THP1-Blue-CD14/SEAP TLR 1-10 assay indicated that Securinine does not activate TLRs [74].

NF-κB is a transcription factor that is sequestered in the cytoplasm until a signal (e.g. from activation of a TLR by LPS or MPL) is received that causes the inhibitory protein IκB to be phosphorylated, releasing NF-κB from inhibition [80]. NF-κB then migrates to the nucleus where it regulates the expression of inflammation-related genes

[80]. This action by NF-κB is a classic response to microbial stimulation of TLRs, including activation by LPS and MPL. The p38 pathway is a MAPK pathway that responds to a variety of environmental and inflammatory stimuli [81]. Activation of the p38 pathway results in an increase in inflammation and can result in cell death [81]. p38 itself is the final kinase in a MAPK pathway that, when activated by phosphorylation, can go on to interact with downstream effectors, inducing inflammation, among other responses. The observations that Securinine is not activating NF-κB is evidence that a different signaling pathway is being triggered by Securinine distinct from TLR activation.

Securinine specifically blocks the $GABA_A$ receptor, and is believed to directly inhibit GABA binding by blocking the GABA binding site on the $GABA_A$ receptor [78]. $GABA_A$ receptors have been shown to exist in monocytes [74,82,83]. The finding that $GABA_A$ receptors are present on an innate immune cells potentially has profound implications for immunology. $GABA_A$ receptors are the primary inhibitory receptors in the nervous system and this suggests the hypothesis that $GABA_A$ receptors in monocytes may act to negatively regulate the innate immune response (discussed below). GABA itself has been shown to be present in human plasma at levels comparable to those found in CNS synapses [84].

The exact subunit composition of $GABA_A$ receptors is critical to their detailed function [85,86]. Interestingly, in a recent study by Bjurstöm et al., (2008), $GABA_A$ receptors in activated T lymphocytes do not appear to have γ subunits, but resting T lymphocytes do [84]. $GABA_A$ receptors have been shown to inhibit inflammation in

CD4+ T cell activities and halt T cell proliferation at physiological levels of GABA [84,87-89]. This suggests differential functionality for $GABA_A$ receptors, depending on the activation state of T cells, and a similar situation might well occur in monocytes. Securinine thus appears to represent a new class of immuneadjuvant with potential applications as a prophylactic adjuvant and possibly as an immune stimulation drug for treatment of existing infections.

Systems Biology

Biological response pathways (e.g. signaling or metabolic) often integrate with a number of other pathways, operating within a complex web of pathways. Traditional reductionist approaches that seek to explain an isolated pathway by breaking it into its component parts often cannot produce a sufficiently deep mechanistic understanding to enable predictive behaviors [90,91]. This state of affairs has led to the emergence of the field of "systems biology" that seeks to develop testable models to explain the behavior of complex biological systems.

Systems biology can be defined broadly as the integration of large amounts of biological data from various sources to create one or more comprehensive models of a system to enable 1) visualization of the changes in the various working parts within a particular system (e.g. "heat map" data from changes in genes, proteins or metabolites in response to different biological conditions), 2) visualization of the known and/or predicted interaction(s) between those parts, and 3) creation of a mathematical model

of interaction paths from which testable predictions about the system can be made. This framework can also highlight areas where information is scarce, promoting the focused acquisition data that will help flesh out specific parts of the model(s). We have generated a first generation systems-level model to explain a portion of the responses of monocytes to infection by *C. burnetii*, and treatment with Securinine.

The biological data used to formulate systems biology models can include integrating information from one or more -omics investigations (e.g. genomic, transcriptomic, proteomic, and/or metabolomic studies), as well as more traditional investigations such as those performed on a particular protein to elucidate its functions or modification state under specific conditions [90-93]. The data can be generated by a researcher or team of researchers, found in available biological data repositories, and combined with information mined from the literature. The overall goal is to progress from a reductionist-style cataloging of isolated biomolecules and biomolecular interactions to an integration of available data into a global mechanistic model of a particular system(s) of interest. This systems approach promises to have the effect of making biology a more predictive science [94].

Of particular interest is the discovery of emergent properties from the models that would not be obvious by simply looking at the individual pieces [90,93]. Many types of systems biology models are scalable [92]. That is, they can encompass one set of data, e.g., the response of monocytes to infection by *C. burnetii* or attempt to integrate several datasets that are broader in scope e.g. the response of the human

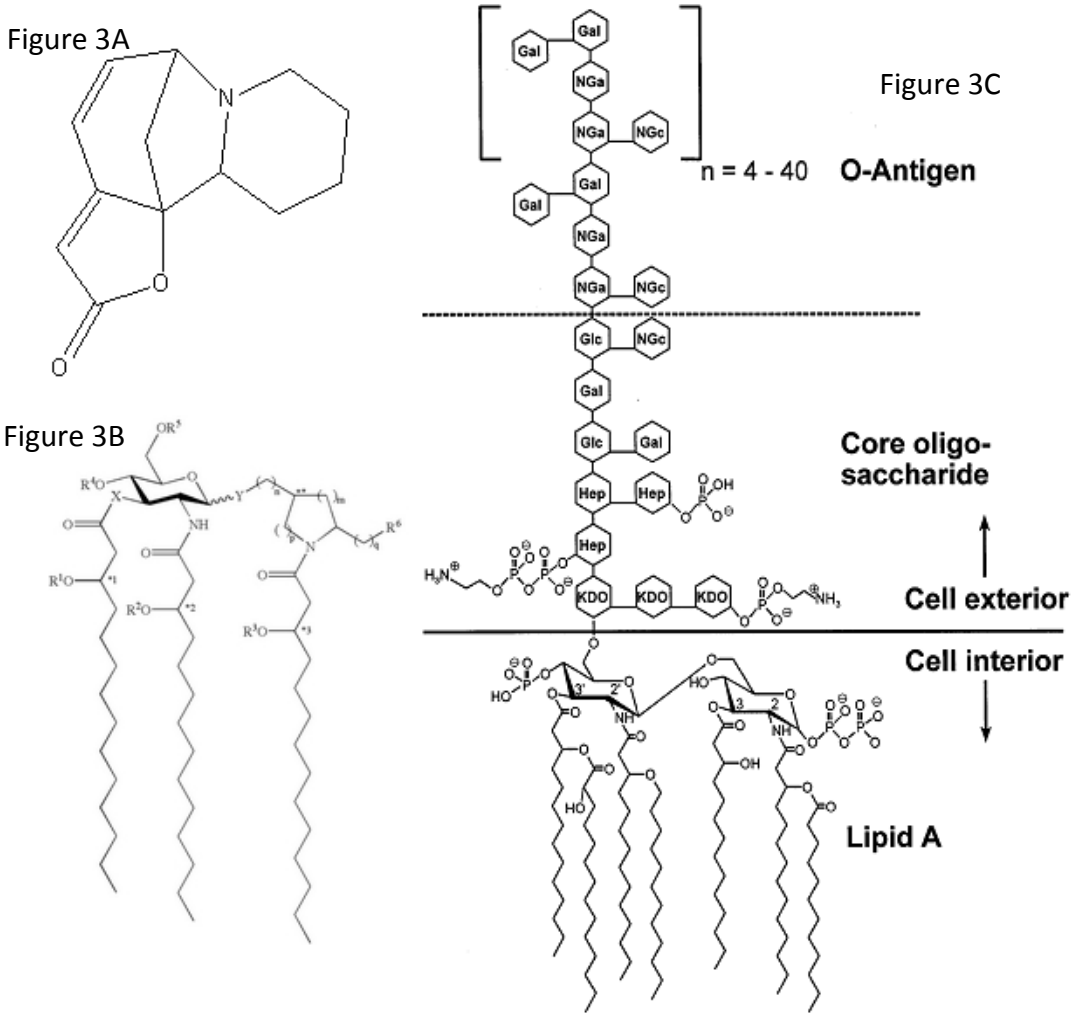

Figure 3: Adjuvant molecules investigated in this study. A) Securinine. B) MPL, adapted from [1]. C) LPS, adapted from [4].

immune system to infection by *C. burnetii* composed of data from monocytes, neutrophils, T cells, etc., any one dataset of which could comprise a systems model in its own right. For example, the immune response of T cells to *C. burnetti* could form the basis for a systems model, as could the response of monocytes to *C. burnetii* infection. Alternatively the individual T cell model and monocyte model of immune response to *C.*

burnetii infection could be integrated into a single, more comprehensive model of overall immune response to *C. burnetii* infection. While the individual models would detail the response within a single cell type, the more comprehensive model could help to elucidate interactions between various immune cell types.

Models can be qualitative, quantitative (e.g. modeling stoichiometry of a series of pathways) and /or explicitly mathematical (represented exclusively by a series of algorithms) [91,93]. Generation of models is often followed by testing, ideally of hypotheses generated by the model, as well as performing investigations into areas where data is scarce (e.g. adding metabolomic data to the model of the monocyte responses described below). Where there are indications from the model that expanded knowledge of a particular area (e.g. the metabolome) would enable a deeper understanding of the mechanics/dynamics of the system, downstream efforts could be focused to obtain the necessary data. Such additional information can then be used to revise the model as needed, repeating this process iteratively until a more predictive consensus model is reached [90,93].

The study of host-pathogen interactions has certainly begun to benefit from systems biology (see [90-93] for examples). The large public repository of data on this topic that can be mined to find interactions and integrating other relevant data can be a great benefit as a foundation for a systems level understanding. Examples of such data repositories include the Biodefense Proteomics Resource (http://www.proteomicsresource.org) and NCBI (www.ncbi.nlm.gov). One significant

impediment to the development of systems biology models is, ironically, the structure and organization of the data repositories. This is due to such factors as each database using different identifiers, and having multiple entries for a particular protein or gene sequence [95]. Multiple entries can arise, particularly in uncurated databases, when different research groups independently submit the same gene or protein sequence under different names, or the name of particular gene or protein changes over time.

Another impediment to generating systems level models is the ability to create visual representations of the model. Diagrams describing systems models become difficult to translate into a graphical model that can be easily understood, beyond a certain size [92]. The graphical representation must contain sufficient complexity to convey the concepts, interactions, and conclusions derived from the model, including the connections between the various model components, without containing so much information as to render it unreadable. Any given mapping of a model is inherently driven by the interests and focus of the investigators and is by its nature a somewhat subjective view based on the researchers' interpretation of their data and that published in the literature [92].

There are numerous examples of systems models developed for various aspects of immune function, a selection of which are described below. Transcriptomic data has been most commonly used to create systems models. Examples of this approach include Ravasi et al., (2007) and Nilsson et al., (2006), who used transcriptomic data to generate a systems model of macrophage activation [96,97]. Nilsson, et al., (2006) used

a series of mathematical and bioinformatics analyses of microarray data to study the time course of transcription factor regulation following LPS activation of macrophages [96]. Nilsson, et al., (2006) then used bioinformatics to predict the regulation of various targets of the transcription factors, to determine transcript dynamics in the LPS network, composed of connections active during the LPS response of macrophages [96]. This was followed by creation of a systems model demonstrating the interconnection of transcription factors and their various effectors. Three of the transcription factors most heavily involved in downstream regulation were further analyzed to determine the dynamics of their activities over the time course of their data [96].

Interestingly, when Nilsson et al., (2006) assembled their model, several emergent properties arose [96]. These emergent properties included potential new functions for previously described transcription factors ATF-3 and NRF-2, both of which are known to be activated by LPS stimulation of macrophages. Upon LPS stimulation, ATF-3 is activated and was suggested to stimulate the activation of Keap1, a negative regulator of NRF-2, following LPS activation. Keap1 activity peaked at 7 hours poststimulation and declined up to 24 hours. The time course of ATF-3/Keap1 action on NRF-2 was consistent with observations from the microarray data [96] NRF-2's functions include regulation of the oxidative response to infection (known) and a possible role in general modulation of inflammation (inferred emergent property) [96]. These proposed properties of ATF-3 and NRF-2 were not obvious from the data without the development of the model.

Ravasi et al., (2007) extended Nilsson et al., (2006) somewhat by discussing Nilsson's model in a broader context of macrophage activation [96,97]. One point made explicitly by Ravasi et al., (2007) is that a particular macrophage response can be digital (e.g. LPS activation), but the actual gene products involved in the macrophage response can have an analog response to the same stimulation [97]. In other words, individual genes in a macrophage activation response may have different thresholds of activation, due to a variety of factors e.g. epigenetic modifications, and etc. [97]. The individuality of gene activation in a particular response should be kept in mind when producing systems models as the factors governing activation of those genes could add important nuances to the model. Another important aspect of macrophage activation involves the emerging field of microRNAs, which have recently been shown to be able to regulate protein expression levels in cells [97]. Understanding the interaction of microRNAs with various macrophage activation programs (e.g. via LPS, MPL, or Securinine stimulation, or *C. burnetii* infection), could well be important to gaining a deeper mechanistic understanding of these systems, but this is beyond the scope of our investigation.

Proteomics data is also used for creating systems models. Recently, two models of phagosome formation in macrophages have been published [98,99]. These are especially relevant to studies involving obligate intracellular pathogens i.e. *C. burnetii*, *L., pneumophila*, etc., as these pathogens often hijack phagosomal maturation processes to create their intracellular environment. Trost et al., (2009) used a combination of 1D gels followed by shotgun proteomics to characterize phagosomal changes in macrophages

+/- treatment with IFN-γ, an important cytokine in macrophage immune responses [99]. Trost et al, (2009) also used TiO_2 enrichment of phosphopeptides to characterize IFN-γ-induced changes to the phagosomal phosphoproteome [99].

Trost et al., (2009) used their proteome data to construct a systems model of phagosome maturation. One interesting suggestion that arose from the model of Trost et al., (2009) is that there may be a calpain-mediated Ca^{2+} binding component involved in MHC antigen presentation due to phagosome maturation [99]. The model of Trost et al., (2009) indicates that calpain is being actively recruited to the early phagosome [99]. Trost et al., (2009) further suggest that regulation of the Src-family kinases may be involved in MHC-I antigen processing [99].

Rao et al., (2009) used data from a preliminary proteomic investigation to construct a systems model describing the differences in phagosomal maturation of macrophages in response to infection with different mycobacterial strains [98]. Rao et al., (2009) used a similar approach to Trost et al., (2009) to acquire their proteomics data (1D gels followed by shotgun analysis) [98,99]. Although very preliminary, Rao et al.,(2009) was able to use their model to support the hypothesis that phagosome maturation proceeds via a series of endosomal fusions [98]. The competing hypothesis is that the ER is a significant contributor to phagosome maturation, and the model in this study does not support this hypothesis, as very little ER protein was found in Rao et al., (2009) phagosome preparations [98].

The results described above demonstrate the utility in a systems approach to data analysis. Several emergent properties arose from the models (e.g. the functions of ATF-3, progress of endosomal maturation, and calpain involvement in MHC-I antigen processing), would not have been obvious from the datasets alone. The conclusions drawn from these models enabled the construction of a series of testable hypotheses that can be used to guide future work. We have also utilized this approach to describe a portion of the data presented below, and propose a number of testable hypotheses, as well as avenues for future research.

Bioweapons/Biodefense

What follows is a brief description of bioweapons and related issues from a historical perspective and demonstrates the relevance of research into *C. burnetii* and other potentially weaponizable organisms. The following discussion is derived from publically available source material only, no classified or otherwise secret information is known to be referenced in any description below[1]. Biological weapons are reported/believed to have been used throughout the history of human warfare. Known or suspected uses of bioweapons date to at least 300 B.C. [100]. Early instances of biowarfare stem from the purported use of dead and/or diseased bodies for the

[1] Note that this discussion is primarily concerned with biological organisms, not biologically derived toxins such as *Botulism* toxin, which are purified chemical products of biological organisms.

contamination of water or food supplies, rendering a besieged army unable to supply enough food and water to sustain itself [100]. It is also suspected, although not definitively proven, that Colonel Bouquet and Captain Eucyer of the British Royal Army, deliberately caused smallpox infected blankets to fall into the hands of Native Americans near Fort Pitt in 1763 during the French and Indian War [24,100].

It is often difficult to definitively establish a *bona fide* offensive use of a bioweapon as many purported attacks could be legitimately attributed to natural outbreaks [24,101]. In the case of Fort Pitt, it must be stated that naturally occurring (i.e. unintentional) smallpox outbreaks devastated native populations in North America. Many more Native Americans (in North, Central, and South America) are believed to have been felled by unintentionally introduced European diseases than were actually killed in direct combat, as the native populations had neither natural immunity to these diseases nor knowledge of how to treat them. Documentation from the time, in what is believed to be the two men's own handwriting, suggests that even if the smallpox outbreak near Fort Pitt was natural, there was the intent to release infected materials to the Native Americans for the purpose of devastating the local population [100].

Perhaps the most infamous group known to have developed and used bioweapons was imperial Japan's Unit 731 during WWII. Uses of bioweapons by Unit 731 against Chinese civilians and the Soviet army are documented [24], although there was no known large-scale battlefield use. The U.S. military is known to have conducted tests on both military and civilian populations during the Cold War. Perhaps the best

known civilian tests by the U.S. during the Cold War were conducted on a group of Seventh-Day Adventists. In a deal struck with the U.S. Army, the church provided conscientious objectors as volunteers for testing of biological weapons as part of Operation Whitecoat [20,102,103]. The 'Whitecoats', as they were known, worked as lab technicians at Fort Detrick, where they also volunteered to be deliberately infected with various nonlethal organisms for the purpose of testing vaccines and other developed medical countermeasures [20,102]. In exchange for offering themselves up as human guinea pigs, the Whitecoats were exempted from front-line military service [102].

Following World War II, the U.S. Army was tasked with developing a biological weapons program with three primary missions to develop 1) biological warfare agents, 2) means of delivery, and 3) appropriate countermeasures. Although missions 1 and 2 were relatively successful, mission 3 proved to be far less so [20]. Nonetheless, successes with mission 3 have eventually been developed, and have also led to important advances in both military and civilian medical care. The U.S. Army Medical Research Institute of Infectious Diseases (USAMRIID) was established in 1969 by the U.S. Army for the purpose of biodefense and arose from an earlier Army unit (U.S. Army Medical Unit) involved in the U.S. bioweapons program. USAMRIID successfully responded to a naturally occurring outbreak of Venezuelan equine encephalitis in the southern U.S. in 1971, and in 1977 provided vaccine for Rift Valley fever to Egypt during a natural outbreak there [104].

Despite attempts over the last century to prevent the development and use of bioweapons by international convention, enforcement has been difficult at best, and production of bioweapons by treaty signatories has proceeded despite violation of international law. The most recent treaty, the Biological Toxin and Weapons Convention, signed in 1972 and that took effect in 1975, is known to have been violated by both Iraq and the former Soviet Union [24]. In 1973, following the termination of the offensive portion of the U.S. program, much information was publically released. That same year, the U.S.S.R. began to modernize its bioweapons arsenal and founded Biopreparat, the large complex of Soviet labs dedicated to bioweapons and biotechnology research and development [20]. It is believed that release of previously secret U.S. documentation directly contributed to the modernization of the Soviet bioweapons arsenal [20]. The existence of Biopreparat was/is a direct violation of international law, and the current status of Biopreparat and/or its successors is not publically known. Following the first Gulf War, U.N. inspectors in Iraq uncovered evidence that Iraq was developing biological warfare agents prior to Operation Desert Storm [20]. To date, no international treaty has proven successful in preventing the development of biological weapons, in no small part because compliance provisions are generally weak and often have little enforcement provisions [105].

Perhaps the most visible figure calling for a robust U.S. biodefense strategy is Kanatjan Alibekov (a.k.a. Ken Alibek), a former First Deputy Director for Biopreparat who defected to the U.S. in 1992 [106]. Alibekov has reported extensively on the Soviet

bioweapons production activities. Additional information on Soviet/Russion bioweapons production has been provided by another defector, Vladimir Pasechnik [20]. Alibekov is controversial, and not without his critics, who argue that he inflates the true threat of biological weapons to further his own career in the U.S. (centered on biodefense and medical research). However, his knowledge from the inside of the Soviet bioweapon complex is unique and invaluable in determining the types of threats which are likely to exist and detailed knowledge of their likely production sites.

Recently, Cello et al., (2002) demonstrated the synthesis of poliovirus solely from published gene sequences, showing that it is not necessary to use extant organisms as starting materials to create biological weapons [107]. Although bacteria cannot (yet) be generated solely by replicating gene sequences, there has been rapid progress recently in the new field of synthetic biology towards the production of designer bacteria for peaceful purposes that could obviously be perverted to produce weapons. Perversion of this type, although not fully synthetic biology, includes the use of genetic engineering to modify specific traits of bacteria and other organisms. This was demonstrated by the Soviet production of anthrax with altered immunological properties to inhibit detection [101], which illustrates the potential for otherwise peaceful biotechnology to be converted to bioweapon production [101].

Despite the lethal potential of weaponized organisms, they appear to be of limited military use and currently are mainly of concern as bioterror agents [20,108]. Bioweapons pose as great a threat to the user as to the intended target, particularly

since it is often difficult to create vaccinations to weaponized organisms, including those designed to evade standard detection and treatments. When President Nixon terminated the U.S. offensive bioweapons program, numerous infectious agents had been created, but the U.S. was still lacking in medical countermeasures [20]. Furthermore, by 1969, the U.S. Army had concluded that biological weapons were not of significant strategic importance, and it was concluded that the use of bioweapons in an offensive capacity would rise to the level of a nuclear response [20,103]. In addition, many of the vaccines that were developed required either multiple inoculations and/or had potentially serious side effects [20]. The difficulty in making vaccines underscores the observation that it is far easier to develop a biological weapon than it is to develop medical countermeasures, making a terrorist organization unlikely to have the capability to develop both a bioweapon (relatively easy), and a viable vaccine (relatively difficult). Although the penchant for terrorist organizations to employ suicide bombers makes the development of countermeasures seem counterintuitive, a terrorist organization would likely want some manner of countermeasure to protect its high-value assets from an accidental release.

It has also been suggested, in light of the 2001 anthrax attacks in the U.S., that further restrictions be placed on the public dissemination of potentially sensitive research that could increase the risk of bioweapon proliferation [108]. This would include limiting the public dissemination of research that could be used in a dual use capacity or restricting their publication to classified peer-reviewed journals. Vetting of

personnel working with select agents would also include more extensive background investigation/monitoring of non-governmental personnel working with these organisms. Select agents are defined as biological agents and toxins posing severe threats to public health as well as the health of animals and plants [109] (see www.selectagents.gov for a complete listing). Currently, non-governmental researchers working with select agents must be cleared by passing a Security Risk Assessment (SRA), although this only catches people who have documented past transgressions (e.g. criminal history or known affiliation with terrorist groups) and does not rise to the level of a true security clearance [110]. Many federal agencies who work with select agents have a much more stringent level of clearance than the SRA, and also carry out frequent monitoring of researchers for drug use, financial liabilities, and in some cases psychological evaluations [110].

The reaction to further restrictions on the use of and publication on select agents is likely to be met with resistance from the academic community. It was suggested by Beck, (2003) that academic institutions can better self-regulate themselves than governmental institutions. However, this is naive at best, particularly in light of a report in 2007 by the Office of the Director of National Intelligence. Although details of the report are classified, publically available comments by authors of the report provided to Science [110], as well as the facts of the 2001 anthrax attacks, suggest that currently, a trained individual determined to release a bioweapon will succeed. This was recently bolstered by a report from the Commission on the Prevention of Weapons

of Mass Destruction Proliferation and Terrorism (CPWMDPT) chaired by Bob Graham and Jim Talent [111]. In the report by CPWMDPT, the U.S. was given a grade of F, the lowest possible grade, in the ability to recognize, respond to, recover from and/or prevent a bioweapons attack from inflicting mass casualties [111].

Although outright distrust of the infectious disease research community is likely to create more problems than it solves (possibly driving qualified researchers from the field, and thus limiting research capacity), reasonable restrictions such as background checks, as well as suitable monitoring of appropriate personnel is warranted [101]. Monitoring at governmental agencies is often in-house, and while it is not clear who would assume the role of monitoring civilian researchers, this would most likely fall to the FBI or the Department of Homeland Security.

The numerous documented failures of Soviet security (denied by the Soviets and later the Russians) at their bioweapons facility near Sverdlovsk have led to known/suspected releases of weaponized organisms into the surrounding populace [24,100]. This is cause for significant concern. The Aum Shinkinryo cult, best known for releasing Sarin gas on a Tokyo subway, was also researching bioweapons including *C. burnetii* [9,15]. These incidents underscore the need for continued research into *C. burnetii* and the means to protect against infection by *C. burnetii* and/or other infectious diseases as part of a broader biodefense strategy.

There are several considerations regarding the possible use of *C. burnetii* as a bioweapon. *C. burnetii* has advantages as a bioweapon in the sense that it is readily

available (worldwide endemic), easily aerosolized/weaponized, has a high infectivity/virulence, can be dispersed pneumatically, is stable for long-term storage, and is environmentally persistent. The fact that *C. burnetii* is primarily incapacitating in its known forms suggests that it would be most effective against a military target to demoralize and incapacitate a large number of personnel, in order to gain a tactical advantage. There are estimates that use of *C. burnetii* against troops could reduce effective manpower by up to 75% [15]. Against a civilian population, significant induction of fear could result from the use of *C. burnetii*.

Scope of Experiments Conducted

We have undertaken a series of proteomics level experiments with several objectives in mind. First, to better characterize the response of monocytes to infection with phase II *C. burnetii*, with the goal of generating a preliminary systems biology model to provide a foundation for future work. We attempted to detect *C. burnetii* proteins from infected monocyte samples by mass spectrometry and bioinformatics analysis (detailed below), but were not successful, likely owing to 1) a relatively low amount of bacterial protein compared to host cell protein amounts present at the time points we examined, and 2) the limited protein subfractionation carried out on our samples. It would be desirable in future studies to include the analysis of bacterial proteins in more simplified fractions.

Our second objective was to observe and compare the monocyte response to exposure by innate immune adjuvants, again with the goal of developing a model to inform and guide future experiments. We tested Securinine, a $GABA_A$ receptor antagonist that has been demonstrated to increase resistance to phase II *C. burnetii* infection [74], to document its effects on the proteome. Securinine represents a new class of immunomodulator acting through the $GABA_A$ receptors, which have been documented in immune cells and in particular have been demonstrated to be expressed in monocytes and T cells (M. Jutila, K. Lubick personal communication, [82-84,87,112]).

We also wished to compare Securinine to the well known TLR-mediated adjuvants LPS and MPL which also increase monocyte resistance to *C. burnetii* (detailed above). We had hoped that we would be able to tease apart the differences in the two types of innate immune regulation. Unfortunately, in hindsight, it became apparent during the course of this investigation we did not sample the TLR agonists within their optimal timeframe of their effects and/or did not utilize an optimal molarity for stimulation so this comparison, while intriguing based on available data, is incomplete and we were not able to accomplish this comparison as initially intended. We were able to make some comparisons between $GABA_A$ receptor-mediated and TLR-mediated responses however, which may help to guide future work.

Our final objective was to investigate the combined effects of Securinine exposure and infection by phase II *C. burnetii*. We were able to conclude that the combined action of Securinine + phase II *C. burnetii* infection induces monocyte

apoptosis, although at a Securinine dosage later determined to be higher than the optimal effective dosage for increased *C. burnetii* resistance. Apoptosis in this system is likely to be Ca^{2+} mediated, based on the differential regulation of a number of Ca^{2+} sensitive proteins, notably ERLIN2, which is important in regulating release of Ca^{2+} from the endoplasmic reticulum [113,114]. It would also appear that apoptosis in our samples is caspase-independent, based on the observation that NADH CoQ reductase is present at an observed pI and molecular weight suggesting it is intact (see figure20 below). NADH CoQ reductase is known to be cleaved during caspase mediated apoptosis [115].

The observation that caspases do not appear to be detectably active in our samples supports published observations that *C. burnetii* can inhibit caspase activation [72]. The model describing this dataset is of somewhat more limited utility than the models derived from the prior experiments, owing to the fact that Securinine dosages were subsequently found to be considerably higher than the optimal effective dosage for inducing monocyte resistance to *C. burnetii* (M. Jutila personal communication), and the fact that only two biological replicates were available (compared to three biological replicates for all previous work), therefore the results for this portion of the investigation were somewhat less statistically conclusive than the earlier experiments (*C. burnetii* time course of infection and adjuvant stimulation).

Overall, we developed a preliminary systems biology model integrating how many of the various components detected by our proteomic analyses appear to act and

interrelate with each other, based both on our observations and information derived from an extensive review of the literature. This model can serve as a useful starting point for future investigations. The pieces of this model have pointed to the desirability of characterizing changes in metabolites, lipids, and metal ions that result from the various stimuli tested. We suggest that examination of these factors will provide further information regarding proteins that change their functional status perhaps without changing their expression levels to an extent visible in a 2D gel (for example, in response to NAD^+/NADH ratios). NAD^+/NADH ratios (or ADP/ATP ratios) can have a significant allosteric regulatory impact on a number of key metabolic pathways. A prime example of this is the regulation of pyruvate dehydrogenase (PDH), which serves as a key regulatory site between fermentative and respiratory metabolism. PDH is inhibited when NAD^+/NADH or ADP/ATP ratios are low (i.e. NADH or ATP are relatively more abundant than NAD^+ or ADP respectively). This allosteric inhibition of PDH is at the level of protein function, it does not involve changes in the protein expression levels. PDH can also be regulated by covalent modification with phosphate, becoming inactive when phosphorylated and active when dephosphorylated.

Determining which metabolites change abundance in response to stimuli may allow us to infer which proteins are changing their functional status. For example, a sudden increase in the abundance of pyruvate, without a subsequent increase in acetyl CoA, lipids, or Krebs cycle intermediates, would indicate that the activity of PDH was being inhibited. A better understanding of the changes in metabolite, metal, and lipid

abundances, as well as testing of various pieces of the model, would enable the production of a more comprehensive model to more fully characterize the systems. Our results, described below, provide a foundation for a better understanding of the innate immune response, enabling a better understanding of *C. burnetii* infection and may be applicable to other obligate intracellular pathogens.

CHAPTER 2

METHODS

Cell Lysis

The Monomac I cells used in this investigation were grown, treated and/or infected by Mr. Kirk Lubick in the Dept. of Veterinary Molecular Biology (VTMB) at Montana State University in the lab of Dr. Mark Jutila in accordance with previously established protocols [74]. All infections were with phase II *C. burnetii*. Samples for protein analysis were received in 15 mL Falcon tubes, pelleted, stored on ice and transported to the Chemistry and Biochemistry Research Building (CBRB) at Montana State University for all subsequent experiments. Note that samples were not frozen upon receipt, and were not frozen during transit or prior to lysis.

Upon arrival at CBRB, cell samples (approximately $2x10^8$ cells) were centrifuged for5 minutes at 1000 xg, 4 °C using a Legend Sorvall Mach 1.6R centrifuge, and residual growth media was removed. The sample was not resuspended for this step. Each entire cell sample was processed. Excess growth media was removed and treated with either 70% ethanol or 10% bleach, as were all pipette tips and any tubes that came into contact with the samples. Note that the cell samples were received as wet pellets, with a very small amount of excess growth media present. The centrifugation step was performed so any residual growth media could be removed (typically ~100uL was recovered/tube). The entire cell sample (approx. $2x10^8$ cells) were resuspended to 4 mL

final volume (approx. $5x10^7$ cells/mL) using monocyte extraction buffer (MEB) (160 mM NaCl, 10 mM $MgCl_2 \cdot 6H_2O$, 1 mM Na_3VO_3, 5 mM NaF, 20 mM Tris pH 7.5, and 1 Roche Complete protease inhibitor cocktail tablet per 50 mL buffer) [34,116-120] mixed thoroughly and a small sample was withdrawn for cell counting.

The following lysis protocol was adapted from published protocols [34,38,121]. Control and experimental samples were lysed side-by-side on ice with a Dounce homogenizer (400 strokes/mL), followed by 4 rounds of 15x1seconds sonication on ice, a freeze thaw cycle to -80 °C with thawing on ice, followed by 2 rounds of 15x1 second sonication on ice. Sonication was performed using fifteen 1 second bursts with 1 second in between each burst. Between rounds of sonication, samples sat on ice for at least 1 minute. The sonicator was a Fisher Scientific Sonic Dismembranator model 100 on setting 3, using a Misonix Inc. ultrasonic converter and a microtip. Lysis was achieved at >98% as determined by cell counting in a hemacytometer comparing a sample from before lysis to one after lysis.

Samples were divided into four 1 mL aliquots and subjected to high speed centrifugation (45 minutes, 100,000 xg at 4 °C, using a Beckmann ultracentrifuge with a TL-55 rotor). The supernatant, representing the soluble fraction and primarily containing cytosolic proteins and the luminal contents of organelles, was transferred to 4x 1 mL microfuge tubes on ice. The pellet, constituting the membrane fraction containing the plasma and organellar membranes (e.g. nuclear, mitochondrial, etc.) was stored at -80 °C, until further processing [122-125].

The soluble protein fraction was subjected to precipitation with trichloroacetic acid (TCA) followed by an acetone cleanup. Briefly, freshly made 100% (w/v) ACS grade TCA (Fisher Scientific) (1g TCA diluted to 1 mL final volume using nanopure water) was added to a final concentration of 10% (v/v) in each of the 1 mL aliquots, vortexed briefly and incubated on ice for 1 hour. Precipitates were then pelleted at 6800 xg 4 °C in a Legend Sorvall Mach 1.6R centrifuge for 1 minute, and the supernatant was discarded. To each protein pellet was added 800 uL of -20 °C Optima grade acetone (Fisher Scientific) and the pellet was broken up by sonication and vortexing. The sonication apparatus was as above, used on power setting 2. The pellets were incubated overnight at -20 °C. The following morning the samples were centrifuged as above, the supernatant discarded and the pellet washed twice for 30 minutes (at -20 °C) with fresh acetone. Following the final wash, the supernatant was discarded and the pellet Speed-vac'd to dryness.

To each dried pellet of soluble fraction protein was added 200 uL of labeling buffer (7M urea, 2M thiourea, 30 mM Tris, 4% (w/v) CHAPS, 1 mM Na_3VO_3, 5 mM NaF, and 1 tablet Roche Complete protease inhibitor cocktail/50 mL buffer). The protein pellets were dissolved in labeling buffer and like pellets were pooled. From here the soluble fraction samples were either stored at -80 °C or continued on to the Bradford protein assay.

For membrane fractions, the lysed and frozen samples were thawed on ice and washed in 30 mM Tris pH 8.5 by sonication and vortexing to break up the membrane

pellet and suspend soluble fraction proteins. Sonication was as above on power setting 2. The washed samples were then centrifuged as above (100,000 xg for 45 minutes at 4 °C) and the supernatant discarded. The washed membrane pellets were resuspended by sonication and vortexing (as with washing step) in labeling buffer + 1% (w/v) ASB-14 [126-128] and either stored at -80 °C or were quantified by the Bradford protein assay.

Sample Preparation for Labeling and the Bradford Protein Assay

Samples were thawed and like aliquots combined into a single fraction if not done previously. An aliquot of labeling buffer was prepared by adding 4% (w/v) CHAPS and, if the sample was a membrane sample, 1% (w/v) ASB-14. Typically, 100 mL of labeling buffer was made at a time and aliquotted to ten 10 mL aliquots stored frozen at -80 °C until needed. Aliquots of labeling buffer were thawed to room temperature prior to further preparation and/or use. For a typical 10 mL aliquot of label buffer this was 0.4g CHAPS and (if necessary) 0.1g ASB-14. The pH of the label buffer was adjusted to pH 8.5 (target range 8.45-8.5) at room temperature. In the event that the maximum pH of the labeling buffer was overshot to by >0.05 pH units, the aliquot of labeling buffer was discarded and the pHing process started again. This was done to prevent the introduction of excess salt into the 1st dimension separation. Note that label buffer is the principle component of the final labeled protein solution, and substantial excess salt

here would have carried over to the 1st dimension, which may have caused problems with IEF separation. The sample was brought to pH at a later step (below).

For Bradford analysis the samples were brought to room temperature, and microfuge tubes (one per sample) were prepared as indicated for a single sample replicate in table 1 (799 uL nanopure water, 1 uL sample, and 200 uL Bradford reagent). The samples were vortexed well and allowed 15 minutes at room temperature to equilibrate. Then 200 uL of assay sample per assay vial was transferred to a 96 well plate and scanned on the Tecan Safire plate reader at 595 nm. The absorbance was used to approximate the concentration of the protein sample against average values from prior standard curves generated with BSA, . Label buffer was added as needed to adjust the protein concentration to ~10-15 ug/uL. This is a preliminary step, done to ensure that all samples would be at a concentration to enable them to fit within the standard curve range generated for this assay. The final protein concentration against a freshly made BSA standard curve took place after the sample pH had been adjusted.

After adjusting the concentration of the sample (if needed), the sample pH was adjusted to 8.4-8.5. The pH of the sample was adjusted in small increments, trying not to overshoot the mark so as to minimize the introduction of excess salts. A little overshoot was acceptable here as the salts were greatly diluted by the label buffer added to bring the sample to final volume following labeling.

Once the sample concentration and pH had been adjusted, the Bradford assay was set up as indicated in table 1. Note that three standard curves are used by this method, so the samples for the BSA curves were made three times. Also note that 5

Table 1 A-D(below, and following page): Bradford assay. Note that for each assay three BSA standard curves were made, and an average of the three was used to generate the working standard curve. A) Bradford assay setup, again note that three replicate curves were generated. B) Sample of the A595 scans for the Bradford assay. C) Sample working curve generated from the table in B. D) Sample of unknown [protein] calculations generated from working samples. The average was used to make calculations for labeling, etc.

Sample	uL dd-H_2O	uL BSA (2 mg/mL) or sample	uL Bradford reagent
BSA 0	800	0	200
BSA 1	799.5	0.5	200
BSA 2	799	1	200
BSA 5	797.5	2.5	200
BSA 10	795	5	200
BSA 20	790	10	200
BSA 25	787.5	12.5	200
Sample replicate 1	799	1	200
Sample replicate 2	799	1	200
Sample replicate 3	799	1	200
Sample replicate 4	799	1	200
Sample replicate 5	799	1	200

Table 1A

[BSA] ug/uL	A595	A595	A595	Average A595
0	0.3783	0.4104	0.446	0.4116
1	0.5019	0.4252	0.5091	0.4787
2	0.5057	0.4538	0.51	0.4898
5	0.6651	0.6003	0.6515	0.639
10	0.8383	0.76	0.8122	
20	1.0624	0.9861	1.0232	1.0239
25	1.1706	1.1089	1.1184	1.1326

Table 1B

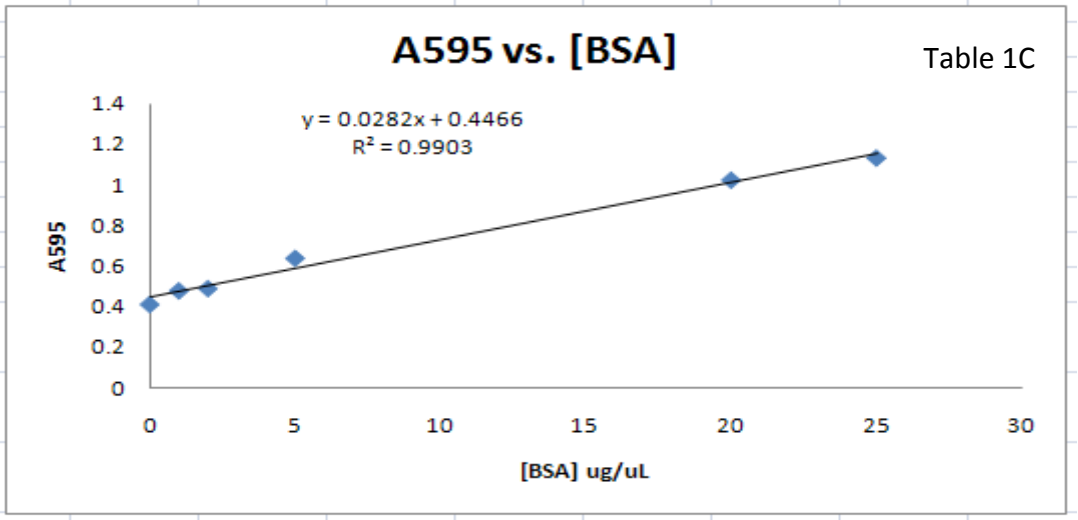

Table 1C

Sample	A595	[Protein] ug/uL		
Membrane control 24 hr. rep 1 Bradford vial 1	0.6513		Average	11.83422
Membrane control 24 hr. rep 1 Bradford vial 2	0.7276	9.964539007	Stdev	1.260801
Membrane control 24 hr. rep 1 Bradford vial 3	0.8008	12.56028369		
Membrane control 24 hr. rep 1 Bradford vial 4	0.8025	12.62056738		
Membrane control 24 hr. rep 1 Bradford vial 5	0.7904	12.19148936		
Membrane infect 24 hr. rep 2 Bradford vial 1	0.6475	7.124113475	Average	6.858156
Membrane infect 24 hr. rep 2 Bradford vial 2	0.6485	7.159574468	Stdev	0.33039
Membrane infect 24 hr. rep 2 Bradford vial 3	0.7835			
Membrane infect 24 hr. rep 2 Bradford vial 4	0.6334	6.624113475		
Membrane infect 24 hr. rep 2 Bradford vial 5	0.6306	6.524822695		

Table 1D

sample replicates were used for each sample to be tested. The samples were vortexed well, and allowed 15 minutes at room temperature to equilibrate. 200 uL per tube was transferred to a 96 well plate and scanned on the Tecan Safire microplate reader at 595 nm, using 3 flashes / read. The standard curve was prepared for sample measurements, by plotting an average of the A595 readings for the BSA standards, and a linear fit plotted (y=mx+b) to A595 vs. the BSA concentration. The equation for the line was determined and calculations were made accordingly ($Sample_{A595}$-b)/m, with an average of the sample readings calculated. A minimum of five concentration points were required to generate the working calibration curve. Seven experimental points were generated and up to two could be discarded to improve linearity. It was desirable, but not absolutely required, for the points to touch or nearly touch the trendline in the standard curve. If a minimum of five points on the standard curve could not be generated as such, the assay was rerun.

To assess the quality of the data, the average of the unknown sample A595 values +/- 10% of the average A595 value for that sample was calculated. A595 values that were < or > 10% of the average A595 for that sample could be discarded (up to 2 values/sample). In rare cases, a set of four A595 values that were nearly identical was used and the fifth was discarded even if it was within the 10% of the average A595. Each sample average was calculated with a minimum of 3 results. If this could not be achieved, the assay was rerun.

Labeling Reaction / Conditions for Multiplex 2DE

The labeling protocol described in this section refers to the use of the original prototype ZDyes and covers the datasets for the *C. burnetii* infection time course and monocyte exposure to Securinine, LPS and MPL. The final dataset, 96 hr *C. burnetii* infection +/- 50 uM Securinine utilized a different set of ZDyes and a different labeling procedure. The labeling protocol for the final dataset is detailed in a separate section (below). The infection time course and individual adjuvant exposures were conducted on 3-11NL isoelectric focusing strips. The final dataset was gathered using data from both 3-11NL and 4-7 isoelectric focusing strips (detailed in a separate section, below).

The following methods have been adapted from standard 2D-gel and 2D-DIGE protocols [129-131]. All steps were performed at room temperature, unless otherwise indicated, and used 24 cm immobilized pH gradient (IPG) strips pH 3-11NL. Following the Bradford assay, calculations were made as follows:

Control: volume to obtain 100 ug protein
Experimental: volume to obtain 100 ug protein
Pooled internal standard: 1/2 the volume of each of the above two samples (50 ug per sample).

Enough of each protein sample was aliquotted for three technical replicates in the 'forward labeling' condition and three in the 'reverse labeling' condition, for a total of six technical replicates per biological replicate (often referred to as dye swapping).

Forward labeling was always control sample labeled with ZGB, experimental with ZBB (1st generation ZDyes), and the pooled internal standard with Hbo277. For reverse labeling, control and experimental labeling was reversed. The samples were brought to 20 uL (5 mg/mL final concentration) with labeling buffer pH 8.5 containing the appropriate detergent(s) for each sample type. All samples were >5 mg/mL in their stock vials, and all were diluted to 5 mg/mL for labeling.

It should be noted that in the following discussions, 1X@RT and 5X@RT labelings refer only to the dye:protein ratios with the reaction performed at room temperature (RT). A 1X@0°C labeling (derived from the GE Healthcare CyDye labeling protocol) is 800 pmol dye/100ug of protein at pH 8.5 at 0 °C. Standard labelings in this investigation (1x@RT or 5X@RT), were performed at pH 8.5 at room temperature, typically 22-23 °C. A 1X@RT labeling therefore uses 800 pmol dye/100 ug of protein at pH 8.5 at RT, a 5X@RT labeling uses 4 nmol dye/100 ug of protein. Given the assumption that an organic reaction will approximately double in rate for every 10 °C increase in temperature, labeling a 1X@RT is approximately comparable to labeling 5X@0°C, and a 5X@RT is approximately comparable to 25X@0°C compared to the extent of reaction that would occur on ice at 0 °C.

The 5X@RT labeling has a further implication. A true 1X@0°C labeling (per GE protocol) is theoretically labeling ~1% of available lysines. There is likely a series of subpopulations of available lysines that can be divided based on various factors such as steric hindrance and electronic environment. Given that not all available lysines will

have a statistically equal chance to react (due to local steric hindrance and/or the electronic environment), the 5X@RT labeling is most likely increasing the probability that any given lysine will react, thus enlarging the available pool of lysines that can be labeled. This may have the effect of increasing signal (and thus number of proteins detected) in the gel by allowing more proteins to become functionally labeled, such that they can be detected above the detection limit. It is possible that more than one dye will label a given protein but this is not a serious problem since the dyes do not alter the pI of the protein, and the molecular weight of the dyes was not large enough to cause a significant shift in the second dimension for all but the smallest proteins (which have fewer lysines and likely will have fewer labelings). We did not observe a problem with molecular weight separations due to multiple labeling (predicted to cause vertical streaking).

For a 5X@RT labeling reaction, 4 nmol of dye per reaction (ZGB, Hbo277, or ZBB) was added at a dye stock concentration of 1 nmol/uL to a protein sample at 5 ug/uL. These dyes are synthesized in-house at Montana State University by Dr. Paul Grieco's research group and contain an NHS ester for linkage to lysines. Samples were vortexed well and centrifuged briefly to collect any drops of liquid at the bottom of the tube. Samples were allowed to react for 30 minutes in the dark. 5 uL of 10 mM lysine was then added to quench the protein labeling reaction, the samples were vortexed and centrifuged, as above. Samples were again centrifuged to pull liquid to the bottom of the tube. Quenched samples were allowed to incubate for 10 minutes in the dark. The

fractions were combined appropriately, 1 green + 1 red + 1 blue in appropriate labeling condition (all forward label or all reverse) and 8.44 uL of 1.1M DTT (20 mM final concentration), 2.25 uL of carrier ampholytes (0.5% final concentration) were added in labeling buffer to final volume of 450 uL final volume for a 24 cm strip followed by 3 uL of bromophenol blue solution. Samples were vortexed well and spun briefly by bringing an Eppendorf minispin plus tabletop microfuge with an Eppendorf F45-12-11 rotor up to 14000 rpm (max speed) before stopping.

The samples were loaded onto IEF strips via active rehydration using a Biorad Protean IEF cell at 50V, 20 °C for 14-16 hours, with a layer of mineral oil over the strip to prevent drying. To facilitate even loading of the strips, the sample was evenly distributed along the length of the tray between the electrodes before the strip was

Table 2: IEF voltage profile settings for Amersham IPGphor I, II, and III, and Biorad IEF.

Amersham IPGphor II and III		
Voltage (V)	Time/VHrs	Step/Gradient
500 V	825 VHrs	Step
1000V	2500 VHrs	Step
3000V	1 hr	Gradient
3000V	4500 VHrs	Step
8000V	1 hr	Gradient
8000V	12000 VHrs	Step
10000V	1 hr	Gradient
10000V	36000 VHrs	Step
500V	≤1 Hrs	Step/Hold

Amersham IPGphor I and Biorad IEF		
Voltage (V)	Time/VHrs	Step/Gradient
500 V	500 VHrs	Step
1000V	2000 VHrs	Step
3000V	1 hr	Gradient
3000V	4500 VHrs	Step
8000V	1 hr	Gradient
8000V	56000 VHrs	Step
500V	≤1 Hrs	Step/Hold

added. Note that wicks (Biorad electrode wicks part# 165-4071) were prewet with 8 uL of nanopure water and placed on the end of each strip to ensure proper contact with the tray electrodes and to help ensure that all of the sample stayed in contact with the gel, to ensure even loading. The following morning, (after loading 14-16 hours), the strips were distributed as needed to other IPGphor units such that only one type of sample was present on a given IPGphor. e.g. all of soluble fraction, biological replicate 1, reverse label strips were on one IPGphor, while the forward labeled strips from the same group were on a different IPGphor. IEF strips were run as shown in table 2.

The hold step at the completion of focusing was kept as short as possible. The strips were removed from the IEF cell within one hour of the completion of the high voltage step. Small differences in the initial 500V and 1000V steps were utilized in the IEF profiles to synchronize all of the IEF runs being completed within a narrow window of time. Typically the last set was finished within 1 hour of the first set. Strips were placed gel side up in a plastic strip holding tray (BioRad part#165-4043), wrapped in foil and stored at -80 °C until 2nd dimension separation.

2nd Dimension Gel Casting

2D gels were cast while the first dimension separation was in progress. Clean plates were selected from the low-fluorescent plate storage in the Dratz lab. Plates were wiped very thoroughly with 70% (v/v) ethanol and a lint-free cloth. If necessary, plates were rinsed with hot water and a gloved hand was used to remove particulates or

residue. Solutions (detailed below) were prepared based on the samples in 1st dimension strips. Gels were cast using 1.5mm spacer plates (plates with a 1.5 mm spacer affixed to the bottom plate) and the Amersham/GE Healthcare casting chamber (part# 80-6467-22). The 16% (v/v) acrylamide [0.3M Tris pH 8.8, 16% (v/v) bisacrylamide 37.5:1 (2.6% C), 19.8% (v/v) glycerol] was used for membrane samples (which contain 4% (w/v) CHAPS/1% (w/v) ASB-14) while the 18% (v/v) acrylamide solution [0.3M Tris pH 8.8, 18% (v/v) bisacrylamide 37.5:1 (2.6% C), 17.4% (v/v) glycerol] was used for soluble fraction samples (which contained 4% (w/v) CHAPS). It was observed that 18% (v/v) acrylamide was too high to permit mixed micelles [4% (w/v) CHAPS / 1% (w/v) ASB-14] to migrate off the gel, causing a large front (data not shown). Reducing to 16% (v/v) permitted the mixed micelles to run more efficiently through the entire gel, including running the front off of the gel, thus improving resolution in the low molecular weight region of the gel.

The acrylamide solutions were degassed for 25 minutes under a vacuum in a sonicator bath, starting with the higher % acrylamide solutions. After degassing, the stoppered flasks containing the gel solutions had the barb capped with parafilm and were stored at 4 °C until ready to pour the gels, as the vacuum flasks got very warm at the top during degassing, and heat transfer to the solutions would otherwise speed the polymerization process during casting potentially causing polymerization irregularities. The degassing was repeated for the 9.5% (v/v) acrylamide solution [0.3M Tris pH 8.8, 9.5% (v/v) bisacrylamide 37.5:1 (2.6% C)] and the flasks stored at 4 °C until ready to pour

the gels. Note that acrylamide solutions were allowed to reequilibrate to ~room temperature for ~20 minutes immediately prior to pouring the gels.

While degassing, the Amersham gel caster was set up with 13 gel cassettes, using plastic spacers and/or top plates to fill the remaining space in the caster. All gels contained a unique identifier containing first and last initial and a unique five digit number (e.g. MSxxxxx). All gel plates were wiped very thoroughly with 70% (v/v) ethanol and a lint-free cloth prior to layup.

Following layup, while solutions were cooling, two 1.1 mL aliquots of 10% (w/v) ammonium persulfate (APS) were prepared. Immediately prior to casting, the gradient maker was rinsed with 500 mL of nanopure water per chamber. 10% (w/v) APS and TEMED from stock containers was added to final concentrations of 0.016% (v/v) for APS and 0.016% (v/v) for TEMED for each acrylamide solution, and swirled gently to mix. After making sure the gradient high % acrylamide chamber stopcock was closed, the high %acrylamide solution was added to the upper chamber followed by the 9.5% (v/v) acrylamide to the lower chamber (which contained a magnetic stir bar to ensure proper mixing of the gradient). The gradient was established using a peristaltic pump and the gel solutions were pumped into the chamber until the solution just ran out of the end of the tubing. Immediately after starting the pump, the high %acrylamide stopcock was opened and the stir bar speed adjusted so that thorough mixing occurred at all levels of the low %acrylamide chamber. Casting continued until all of the acrylamide had been pumped into the casting chamber, including the solutions in the tubing.

Approximately 15-20 mL of displacement buffer [0.3M Tris pH 8.8, 50% (v/v) glycerol, with a trace of bromophenol blue] was added to the caster and the barb to the tubing line removed. Additional displacement buffer was added slowly until the top of the acrylamide just reached the top of the spacers in the gel plates. The displacement buffer remained just below the bottom of the gel plates. Each gel was gently covered with 3.5 mL of water-saturated butanol per gel, starting at one end of the gel and working towards the other. The top of the chamber was covered with plastic (either plastic spacer sheets for separating gel cassettes in the caster, or with Saran Wrap). The gels were allowed to polymerize overnight on the bench at room temperature.

The following morning, the caster was opened and each gel cassette rinsed with nanopure water. Gel cassettes were placed in 1x running buffer [0.1% (w/v) SDS, 0.192M glycine, and 0.025M Tris] in covered plastic containers (approx. 10"x12"x3.5"), and stored at 4 °C until ready to run the second dimension in the afternoon on the day the gels were removed from the caster. Each container had 1L of running buffer and six or seven gels (total of 13 gels). Prior to loading the gels, IPG strips were removed from the freezer, and reduced for 15 minutes in 7 mL/strip of 0.13M dithiothretol (DTT), diluted in equilibration buffer [6M urea, 4% (w/v) SDS, 30% (v/v) glycerol, 0.5M Tris pH 8.8] in the strip tray there were stored in, transferred to a fresh strip tray and then alkylated for 15 minutes in 7 mL/strip of 0.51M iodoacetamide (IAA) in equilibration buffer [129,130]. DTT and IAA solutions were freshly made immediately prior to using

them, and kept wrapped in foil to keep out the light. Reduction and alkylation was performed with gentle agitation on a rocker table.

IPG strips were loaded onto 2nd dimension gels under a layer of 0.5% (w/v) agarose / bromophenol blue (enough volume to cover the strip completely). Agarose was loaded and the strips were gently pushed through it to contact the 2nd dimension gel. This prevents the strip from sticking to the glass plates. Gel cassettes were placed into a Dalt II tank and run overnight in 1x running buffer at 16 °C while being covered with a black cloth. When gels were finished (indicated by the bromophenol blue front exiting the gel), they were removed from the tank. The gels were removed from the glass plates and placed in fix solution [10% (v/v) methanol/7% (v/v) acetic acid] for ~28 hrs. under a black cloth on a shaker table for the earlier sets of experiments.

Later experiments using 2nd generation ZDyes did not fix gels prior to scanning as described below. However, many of the glass plates have small visible scratches and/or dings due to repeated use. To prevent the possibility of microscratches or dings as well as residue on the plates from interfering with laser light passage (and thus possibly causing artifacts in the gel images) the unfixed gels were removed from the plates. Unfixed gels were removed from the plates and placed in 1L nanopure water in plastic containers (10"x12"x3.5") three gels/container. Fixed gels had to be removed from the glass in order to fix them.

The fix solution was carefully removed from the fixed gels as completely as possible, then replaced with 1-1.5 L of nanopure water and placed on the shaker table

for 1 hour under a black cloth. This wash was repeated once more by removing the water, adding fresh nanopure water (1-1.5 L), and then incubating overnight on the shaker table in the dark prior to scanning the following morning. In the later experiments (specifically the 96 hr infection +/- Securinine gels using 2nd generation ZDyes) the gels were scanned before fixing. All fix/wash steps were performed at room temperature.

Scanning

Following the overnight wash in nanopure water (detailed above), the gels were scanned on a Typhoon Trio gel scanner. The platen was cleaned prior to each gel being scanned by first wiping the surface with 20% (v/v) H_2O_2 using a clean Kimwipe. When the surface was dry, it was again wiped down with 95% (v/v) ethanol and a clean Kimwipe. After the ethanol, a final wipe down was performed with nanopure water, using a clean Kimwipe and any visible dust/lint was removed. Once the platen was clean, the gel was carefully placed on it after draining off most of the excess water. Gently and with wet, gloved fingers any air bubbles under the gel were removed as well as any small pieces of gel either on or under the gel being scanned.

For the first scan a PMT voltage was selected sufficient to cause a low level of pixel saturation. The PMT voltage was adjusted downward so that no saturation occurs within the analyzed region of the gel. Typically, a 30-50V reduction in PMT voltage was sufficient. Gels were scanned as close to saturation as possible, without actually

producing saturated pixels in the viewable/analyzable area of the gels. Once the PMT settings for the first gel in a series had been made they were usually sufficient for the remaining gels, although adjustments were occasionally needed. All gels were scanned at 200 um resolution and no gel was scanned using the 'Press gel' function of the scanner, as this increases the background in the gel image. Regions that were not going to be analyzed, the far left and right edges and the gel front, were allowed to saturate on the fluorescent scans, so long as saturation did not affect the analyzable region of the gel. Generally, the most highly abundant spots saturated shortly after the front (typically within 30-50 PMT volts), and before saturation became intense in nonanalyzed regions. Following a successful scan the gel was placed in nanopure water and the platen wiped off, as above, with clean Kimwipes.

Gel Analysis

Images were uploaded into the Progenesis software package (Nonlinear Dynamics). The Securinine soluble fraction images were analyzed using version 2, all remaining images were analyzed using version 3. For all analyses to be reported the internal standard gel image was not used in the analysis, for reasons to be described later, although the images were retained, and the control and experimental images were analyzed. In Progenesis, the software was set to the multiple dyes without DIGE structure setting. Gel images were labeled uniquely as follows:

MSxxxxx rep R FL/RL dye
where MSxxxxx is a unique gel I.D. number,
rep R indicates biological replicate (1,2, or 3)
FL/RL indicates whether the gel is forward or reverse labeled
dye indicates color of the dye (green or blue)

Other file names were allowed (particularly for rescanned images) so long as each gel image could be uniquely identified and it was clear which biological replicate, type of labeling and which color dye were being used. For all analyses, all control and experimental images for all biological replicates in a particular test condition were analyzed as one experiment (i.e. all control vs. all experimental). It was observed that Progenesis was very good at finding pairwise differences between individual biological replicates, but it was much more difficult for the software to find consistent changes over all three biological replicates, binned into a single group.

A reference image was chosen that had the best qualitative appearance, and spot separation. The area of interest (the portion of the gel being analyzed), was selected, effectively cropping off the edges of the images that did not contain well resolved spots. Gels were aligned first by manual alignment which involved manually placing landmarks to many of the most intense spots as well as some of the less intense spots, where possible (typically 60-100 manual landmarks). This was followed by automatic vector detection, by the software. The gel images were aligned automatically by Progenesis following manual/automatic vector detection. Alignment was manually validated and adjusted where needed for each gel. In manual validation of the alignment, the analyzable region of the gel was visually examined to look for

regions that were not well aligned. Where needed, additional manual landmarks were added and/or prior landmarks were removed and the alignment repeated.

As a test case, two sets of data (96 hr membrane fraction and 96 hr +/- Securinine membrane fraction) were selected for alignment by Progenesis using automatic vectors alone. No manual landmarks were used, and no manual adjustment of the autovectors was allowed. The data was otherwise analyzed as described. Using the 1st generation ZDyes, autovector (only) alignment very nearly replicated the original dataset using manual and autovectors (see figure 4). The 1st generation dyes found all but two of the original differentially expressed spots, as well as three additional spots in regions that would have benefitted from some manual adjustment. The 2nd generation ZDyes performed poorly in autovector alignment alone and only found approximately 1/3 of the original spots from the 96 hr +/- Securinine analysis using manual and automatic alignment.

It was observed in manual/automatic alignment that the 2nd generation ZDyes (1X@RT labeling) are significantly more difficult to align owing to a relatively higher background and lower signal to noise ratio than the 1st generation ZDyes (5X@RT labeling). The 1X@RT labeling used with the 2nd generation dyes also detected fewer aligned spot volumes in Progenesis than the 1st generation dyes. In the 1st generation ZDyes, soluble fraction gels found an average of ~1300 normalized spot volumes, and the membrane fraction gels found ~1150. The 2nd generation found ~1100 normalized

spot volumes in the soluble fraction (both 3-11NL and 4-7) and ~750 normalized spot volumes in membrane fraction gels (both 3-11NL and 4-7).

Following alignment and spot detection, regions of the gel that were too streaky or had a high background (usually at the extreme edge of the gel) were excluded. This covers regions that cannot be excluded effectively in cropping the gel without cutting out part of the analyzable area of the gel. This step removes spots from further consideration and they are not included in normalization or quantitation. In group setup in Progenesis, all control gels were grouped together, and all experimental gels were grouped together. It is at this point that image normalization and relative quantitation between control and experimental images occurs in the analysis. In the view results portion, every spot was manually examined to determine a) proper spot splitting, and b) ensure that the software had not selected an overly large spot area, thus requiring trimming. This evaluation included every detected spot, not just those that were a) statistically meaningful and/or b) differentially expressed. Note that it is possible for a spot to be differentially expressed but not statistically meaningful. It is generally beneficial to examine all of the aligned spot volumes detected by Progenesis as improper spot splitting can cause multiple spots to be selected in a single spot volume. Trimming these oversized volumes into individual spots will often enable the analyst to find an additional spot or two that is differentially expressed.

For the initial pass through the spots(all spots), a p-value of <0.05 was required to accept a difference in expression between experimental and control samples. At no

time did the fold change in expression play a part in decision making. Selected spots that were properly split (either manually or by the software) and had the appropriate p-value cutoff proceeded to Progenesis stats. Here the same p-value decision criteria, as well as a power score of $\geq$ 0.8 was required. For those spots passing this phase of statistical analysis, the data was exported to an Excel file.

The data was formatted in Excel for uploading into statistical packages. Spot number and normalized volume values were retained from the raw data. The data was then organized by spot number. For each spot, data was organized into control and experimental by biological replicate. Once spot data had been formatted, it was copied and pasted into its own file in SPSS v.16.

For nested ANOVA analysis [132] in SPSS, the data was pasted into the software, analyzed using syntax (see figure 5 for syntax and figure 6 for the structure of the data array), and the output data exported to Excel. In nested ANOVA analysis, the software creates an array that properly groups technical replicates within their respective biological replicate and experimental condition. Biological replicates are grouped according to control or experimental conditions and a two-way ANOVA is performed, generating the statistics of interest. For the final decision on the statistical significance

Figure 4A

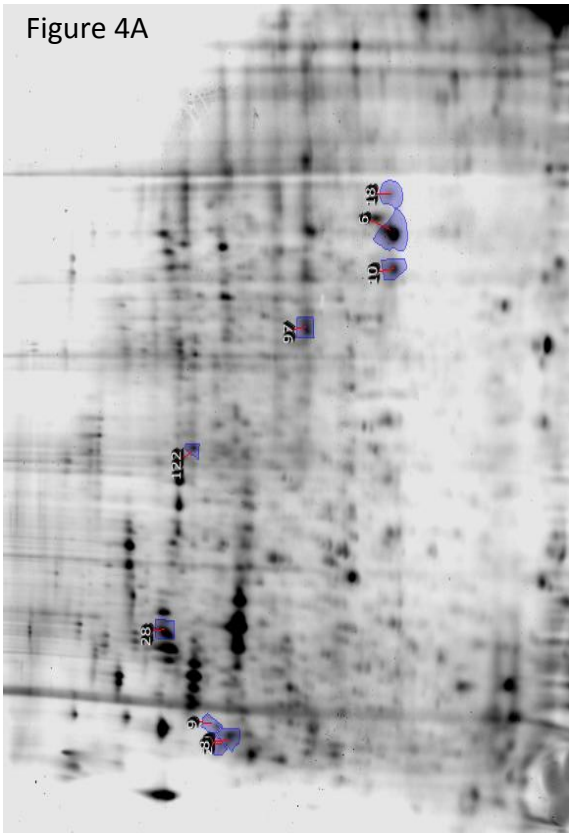

Figure 4B

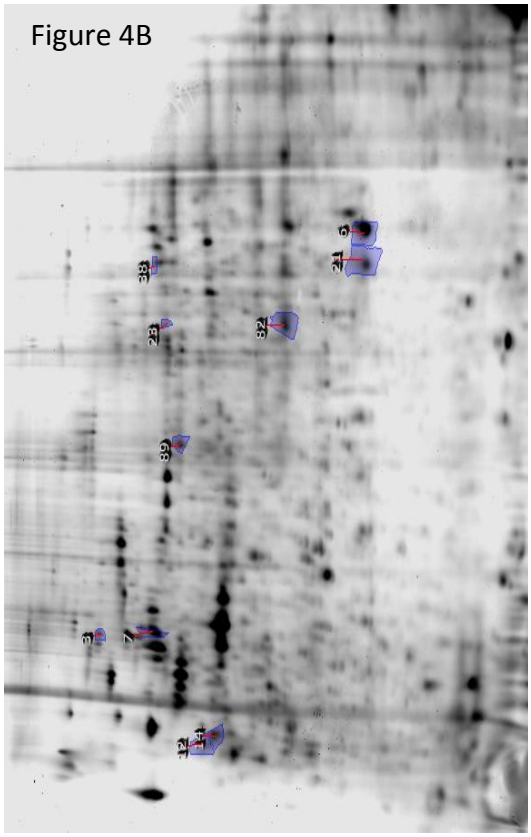

Figure 4C

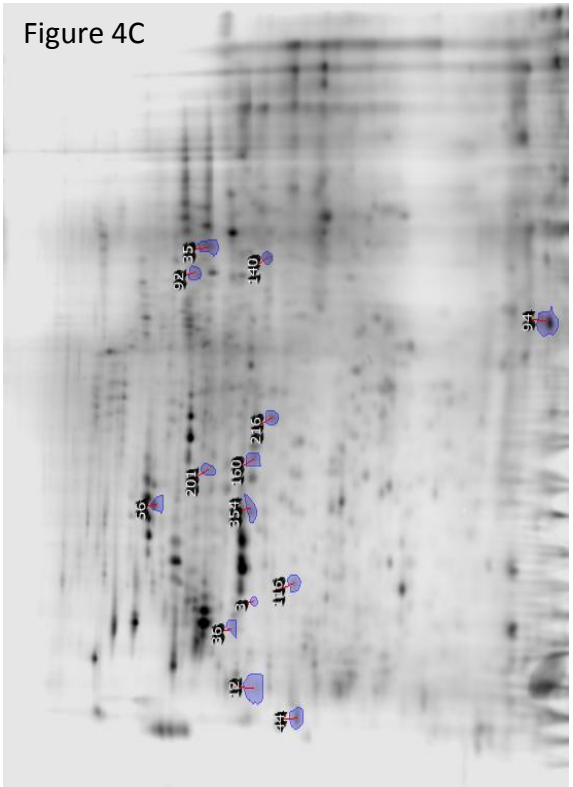

Figure 4D

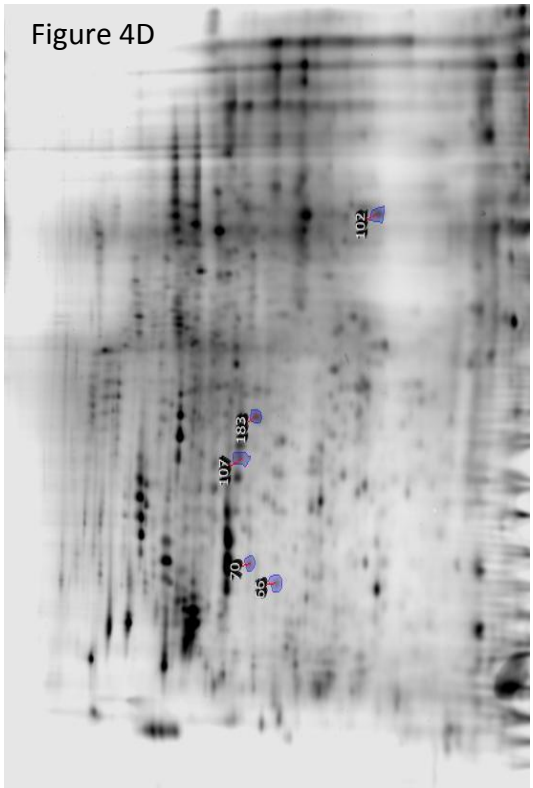

Figure 4A-D: (Previous page) Comparison between the 1st generation and 2nd generation ZDyes. Gels were analyzed using Progenesis and offline methods (described previously). A) Manual + automatic vector alignment on 96 hr membrane fraction data. B) Automatic vector alignment on 96 hr membrane fraction data. C) Manual + automatic vector alignment on 96 hr infect +/- 50 uM Securinine 3-11NL membrane fraction data. D) Automatic vector alignment on 96 hr infect +/- 50 uM Securinine 3-11NL membrane fraction data.

```
IF (Treatment=2) BiologicalReplicate = BiologicalReplicate+3 .
EXECUTE .
SAVE OUTFILE='C:\Documents and Settings\dratz\My Documents\Matts\Stats\Securinine soluble analysis\Spot 1\Spot 1_formatted for unianova.sav'
 /COMPRESSED.
UNIANOVA
  response  BY Treatment BiologicalReplicate
  /RANDOM = BiologicalReplicate
  /METHOD = SSTYPE(3)
  /INTERCEPT = INCLUDE
  /CRITERIA = ALPHA(.05)
  /PRINT = OPOWER
  /DESIGN = Treatment BiologicalReplicate(Treatment).
```

Figure 5: Sample SPSS v.16 syntax for nested ANOVA analysis. Provided by Tom Leuthner, SPSS technical support. Briefly, the first three lines, identify the data and establish an array that is saved in the SAVE OUTFILE step. The remainder of the code instructs the software as to the particulars of the nested ANOVA analysis (e.g. type three sums of squares [SSTYPE(3)] , ALPHA(.05)) and the additional outputs desired (e.g. PRINT=OPOWER which displays the observed power score along with the p-value already embedded in the output. Sum of squares is a method for determining the variance in a set of data, type three is the SPSS default. Alpha refers to the confidence interval. An alpha of 0.05 designates the 95% confidence interval.

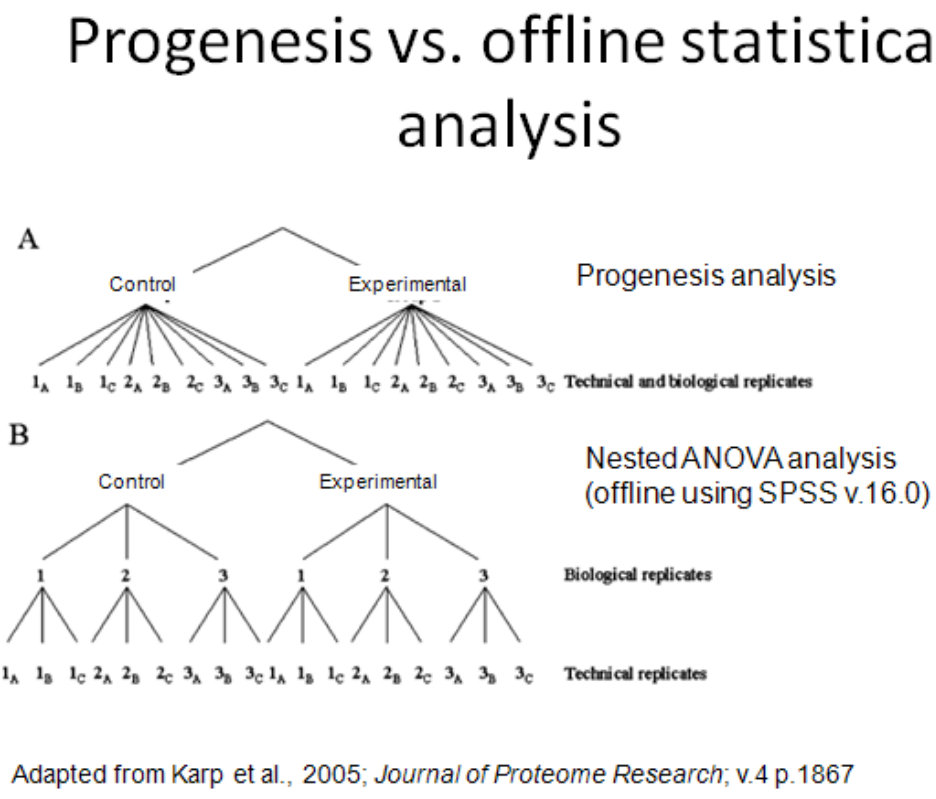

Figure 6: Comparison between the data structure in a) Progenesis, and b) the data structure of the nested ANOVA analysis. The offline designation in part b indicates that this analysis is not performed in Progenesis but rather in SPSS v. 16.

Briefly, in Progenesis analysis (A), all technical replicates are treated as independent biological replicates within a given treatment condition. The nested ANOVA analysis (B) groups the technical replicates for a particular biological replicate in a given treatment condition separately from other biological replicates in both treatment conditions. This is the 'Technical replicates' line in part B of the figure. Biological replicates are then grouped into control and experimental. Finally, a two-way ANOVA is performed on the data to generate a p-value and an observed power score. Protein spots that had both a p-value <0.05 and an observed power score >0.7 were accepted for MS identification. Reprinted with permission.

of a spot, the criteria used were: a p-value from thenested ANOVA where $p<0.05$ and an observed power score >0.7 . Both hard and electronic copies of the statistical analysis were retained. See appendix B for raw normalized spot volume data.

Coomassie Blue Staining/Spot Picking

Because 200-300 ug of protein were present in each gel, there was no need to run preparatory gels for spot picking. 300 ug of protein was loaded in every gel except those run for the soluble fraction of the 96 hr infection +/- 50 uM Securinine samples (ran 200 ug), where there was not enough protein to run 300 ug (due to probable apoptosis as detailed below). In the case of the 4-7 analysis from the 96 hr infection +/- 50 uM Securinine soluble and membrane fractions (detailed below), it was necessary to run a prep gel which was performed using 600 ug of protein / gel.

Gels selected for picking were placed in a glass container (13"x9"x2", a standard 3 qt. Pyrex© casserole dish) filled with 1 L of Blue Silver Coomassie blue [10% (v/v) phosphoric acid, 10% (w/v) NH_4SO_4, 0.12% (w/v) Coomassie Blue G-250, 20% (v/v) anhydrous methanol] [133] per 3 gels, covered with a tight fitting plastic lid and placed on a reciprocal shaker table. Gels were shaken very gently overnight, and the following morning the excess stain in the container was removed by vacuum aspiration as completely and gently as possible. Gels were rinsed twice with fresh nanopure water to remove excess Coomassie blue. The liquid was removed by vacuum aspiration each time. Vacuum removal minimized handling of the gels as they become more brittle than

usual during this step. Destaining was carried out using several changes of nanopure water and gently shaking the gels in each wash for 1 hour to overnight. Water washes were repeated until the gel background appeared to be gone. When the gels were sufficiently destained, they were ready to be picked. Destaining can also be performed in fix/destain [10% (v/v) methanol / 7% (v/v) acetic acid], but it was observed that while this is faster, it also leaves a higher background. For this reason, water was chosen as the destaining solution, even though it is significantly slower than destain [10% (v/v) methanol/7% (v/v) acetic acid].

A spot map was generated from Progenesis analysis, indicating the spots to be picked, and a unique identifier was defined for each spot, including the spot number on the gel, test condition, and soluble or membrane fraction. Care was exercised from this point forward to minimize keratin contamination as much as possible. The night prior to picking, a long sleeved lab coat was taken home, washed and dried thoroughly then immediately sealed in a plastic bag for transport. The lab coat was left in the bag until the time to handle the gels arrived. The work area was located in a positive air pressure, HEPA-filtered hood and the work area was first wiped down very thoroughly with 95% (v/v) ethanol. Gloves were changed frequently, especially in the event that a surface judged to be unclean was touched.

A large piece of glass to support the gels to be cut was cleaned very well with 95% (v/v) ethanol and was placed in the positive pressure HEPA-filtered hood over a light box. Eppendorf tubes from a box that was either unopened or had been opened in

the positive pressure HEPA filtered hood after wiping it down, were prepared by labeling them as indicated above. The tubes were rinsed with a small aliquot of 50% (v/v) acetonitrile, and then dried inverted on a clean Kimwipe in the positive air pressure, HEPA-filtered hood. Once the tubes were dry, the gels to be picked were placed one-by-one on the clean glass plate over the light box. Note that polarized sunglasses (Wiley X model WX Talon with smoke colored lenses) were very beneficial in both preventing dry eyes from the airflow from the hood, and helping to increase the contrast between gel spots and the background for fainter spots. A fresh scalpel blade, wiped with 95% (v/v) ethanol prior to using, was used to pick the appropriate pieces from the gels and placed the pieces in their designated tubes. The tubes remained closed except to add gel pieces or reagents. The scalpel blade was wiped with 95% (v/v) ethanol and a fresh Kimwipe between each gel piece. When all of the spots had been picked for the day, they were prepared for protein digestion. Typically three gels were picked for each test condition and like spots pooled in the same tube to maximize recovery.

In-gel Protein Digestion and MS Analysis

Gel pieces were macerated briefly with a clean pair of forceps to increase the surface area of the gel [134]. The forceps were wiped with 95% (v/v) ethanol before the first tube of gel pieces was macerated, as well as between each tube. Gel pieces were destained by covering them completely with 25 mM NH_4HCO_3/50% (v/v) acetonitrile.

The pieces were then vortexed for 10 minutes by fastening the tubes to a vortexer with a head capable of handling 12 samples at once and the tubes were centrifuged briefly to pellet the gel pieces and facilitate removal of the liquid by pipette. Gel pieces were washed until no longer visibly blue (typically 2-4 washes). Fresh 25 mM NH_4HCO_3/50% (v/v) acetonitrile was used for each wash. When all washes were complete, the gel pieces were dried completely in a Speed-vac.

Following drying, the gel pieces were rehydrated with Promega porcine modified trypsin solution [12.5 ng trypsin/uL in 25 mM NH_4HCO_3/10% (v/v) acetonitrile pH 8.0] [134,135]. The buffer pH was adjusted immediately prior to using for trypsin digestion if not already done when preparing stock trypsin. Trypsin was activated according to manufacturer's instructions using the 100 uL of the buffer included with the lyophilized trypsin (50 mM acetic acid), and incubated at 30 °C for 15 minutes. The trypsin solution was then diluted to a final volume with 1.8 mL of 25 mM NH_4HCO_3/10% (v/v) acetonitrile pH 8.0 (pH adjusted immediately prior to using this reagent). Enough trypsin to perform the digestion was retained, excess trypsin was aliquotted and immediately stored at -80 °C for future use. The gel pieces were covered with approx. three times their dry volume of trypsin solution. Gel pieces were rehydrated on ice for 30 minutes and any excess trypsin solution (the solution remaining after pieces had reswelled) was removed using a fresh pipette tip for each tube. The gel pieces were covered with 25 mM NH_4HCO_3/10% (v/v) acetonitrile pH 8.0 [134,135] the tube tops

were snapped shut and the tubes were incubated overnight at 37 °C in a Blue M single wall transite oven.

The following morning, the digests were centrifuged briefly in an Eppendorf Minispin Plus, as described above and 100 uL of nanopure water was added to each digest. The digests were then vortexed for 10 minutes and placed in a bath sonicator with sufficient water to cover ~2/3 of the tube depth for 5 minutes. Digests were transferred to fresh, appropriately labeled Eppendorf tubes and 20 uL of 50 % (v/v) acetonitrile/5% (v/v) formic acid was added to the peptide solution (not the gel pieces, see next step), leaving the gel pieces in the original tube for additional extraction.

Fresh 50% (v/v) acetonitrile/5% (v/v) formic acid was added to the gel pieces (enough to cover, typically ~50-100uL, depending on the amount of gel in the tube) and the pieces were vortexed and sonicated as before. The peptide solution was then combined with the first extract. This peptide extraction was repeated 2x more with fresh 50% (v/v) acetonitrile/5% (v/v) formic acid, with vortexing for 10 minutes (no further sonication) and combining with previous extracts. The peptide solutions were Speed-vac'd to <200 uL and transferred to labeled 0.6 mL tubes, being careful to not transfer gel pieces in the process, as these tend to clog the sample injection transfer line in the HPLC attached to the mass spectrometer used for analysis. Each new tube also had a mark indicating ~20 uL as a reference. The peptide extracts were then Speed-vac'd to $\leq$ 20 uL and 200 uL of fresh nanopure water was added to dilute the remaining organic solvents (acetonitrile and formic acid) to $\leq$5% of the final volume. The solutions

were then Speed-vac'd again to ~20 uL final volume and either stored at -80 °C or used immediately for MS analysis.

For MS analysis, the peptide extracts were transferred very carefully to fresh tubes (Agilent 250 uL polypropylene tubes part # 9301-0978, capped with Agilent snap cap PTFE with red silicon septa part# 5182-3458) appropriate for the autosampler on an Agilent XCT ultra mass spectrometer with an Agilent 1100 series HPLC. All digests were analyzed using an Agilent LC-chip with a 150 mm separation column (part# G4240-62002). All reagents used were HPLC grade. The sample loading mobile phase consisted of 95% (v/v) water/5% (v/v) acetonitrile/0.1% (v/v) formic acid and the elution phase was 5% (v/v) water/95% (v/v) acetonitrile/0.1% (v/v) formic acid. Data from completed runs were processed using the Bruker Daltonics Data Analysis software package (standard data analysis software for the XCT). The software was set to search for up to 1000 compounds with fragments qualified by amino acid mass differences. No requirement was set for the number of amino acid mass differences. This search output file was exported as a .mgf file and used to identify the peptides and proteins using the bioinformatics tools described below.

Bioinformatics

For bioinformatics analysis of the peptide data, four tools were used. Mascot (licensed in-house at Montana State University) [136], as well as X!Tandem, X!Hunter and X!Tandem P3 algorithms from www.thegpm.org [137-140]. All databases were

Homo sapiens. X!Tandem was used for the *C. burnetii* database only. Peptide analysis criteria were selected such that trypsin was allowed 1 missed cleavage and the parent ion mass tolerance was set to 0.8 Da. The NCBInr database was searched in Mascot with an MS/MS tolerance of 0.3 Da used along with cysteine carbamidomethylation deamidation, and methionine oxidation as variable modifications, and +2 and +3 ions were used for searching. For both X!Hunter and X!Tandem P3 searches all available human databases were searched and default parameters were used, with the exception that the parent mass tolerance was set to 0.8 Da. For X!Hunter only +2 charges were searched (see figure 7 for an example). In Mascot, the final protein score was calculated using the sum of all peptide scores that rose above significance ($p<0.05$, typically a peptide score of ~41), and was not taken from the actual protein score reported by the software.

Mascot is restricted in the number of posttranslational modifications that it can handle at one time, compared to the other tools, which are much more expansive in their capabilities for searching protein/peptide modifications. Every analysis in each tool was treated as an independent evaluation. In general, the top protein hit that met the selection criteria for the identified protein was the same across all tools, although in rare cases X!Hunter would identify another protein with an approximately equal score that matched observed pI and molecular weight. This is likely due to the differences in scoring algorithms between the various tools used. In these cases, the highest identification in both Mascot and P3 was selected. Mascot because it is a more

restricted search and less likely to spuriously find a peptide or protein hit due to increased potential protein/peptide modifications, and P3 looks for proteotypic peptides which should always or nearly always be present. It was noted in the results, when appropriate, where one tool had made another possible protein identification that could be significant. See appendix C for a list of all alternative hits. Increasing the potential number of available modifications could result in a peptide being spuriously identified if the modification is allowed to be present when in fact the modification is not actually there. Such an identification results from a case where the data is fit to the parameters of the algorithm. It is important to examine the peptides generated by the various algorithms in order to guard against this.

Protein identifications that were not keratin or trypsin, and were the highest ranked protein identification that most closely matched the approximate observed molecular weight and pI were accepted. The pI was allowed to vary so long as the observed molecular weight was closely approximated. The reason the pI was allowed to shift was that there can be posttranslational modifications on the protein that alter the observed pI but are not detected by bioinformatics searches. In the cases where low MW proteins were observed (e.g. the S100 proteins) the low MW protein was the highest ranked protein hit within the search tools. It was allowable to accept a hit of lower than the predicted molecular weight in cases (total of two hits in one dataset) where some sort of cleavage could reasonably be believed to be active (e.g. possible caspase or calpain mediated cleavage of vimentin which is known to occur during

apoptosis). In those cases, observed pI and molecular weight were expected to closely match that predicted for the cleavage product (as determined by a pI and MW calculator from www.expasy.org), and there must be significant overlap in the sequence coverage between tools with no valid peptides in the proposed cleaved region. It is not always possible to know that a caspase or another cutter is active, but there must be reason to suspect cleavage products could be possible (e.g. indications from the literature that such occurs or other prior experience with the system) in order to accept such a hit. The strength of the identifications is also a factor [e.g. Hsp60 identified as potentially cleaved had a Mascot score of 1044 (24% coverage), X!Hunter gave a score of -132 (26% coverage) and P3 gave a score of -84 (18% coverage)], and in both cases the identified (potentially cleaved) protein was the strongest hit.

All peptides in the accepted hits were manually validated for all search tools and a protein coverage map of accepted peptides was produced for each hit from each tool. This was achieved by examining the data for each identified peptide in the accepted protein hit, as described below. The different tools treat the MS data differently and usually gave slightly different list of peptides. Each tool give slightly different peptide lists likely due to treatment of modifications and/or mass tolerances (although we cannot be sure that these are the reasons) (see appendix A for coverage maps). A peptide was considered acceptable if a) the peptide E value (expect score) was <1, b) there was sufficient (~1/2 or greater peptide sequence) b- and/or y-ion sequence

coverage and c) a majority of the more intense peaks were matched in the MS/MS spectrum.

Figure 7A

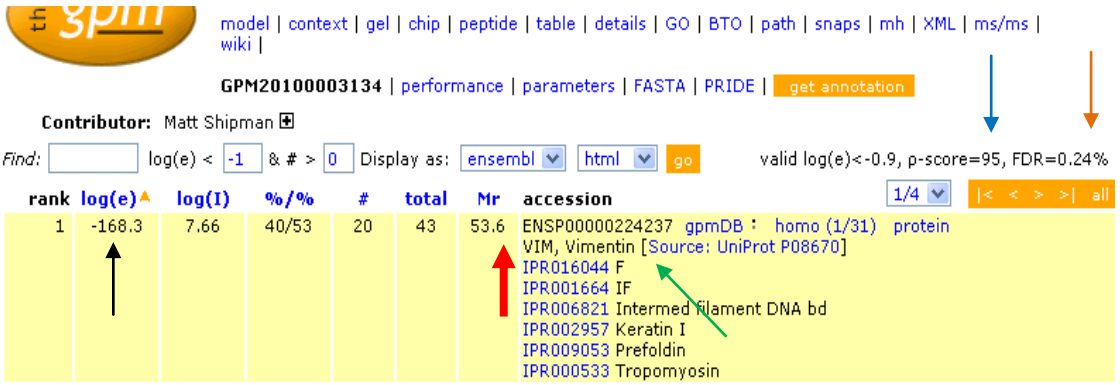

Figure 7B

Identified Peptides

spectrum	log(e)	log(I)	m+h	delta	z	sequence	n
303.1	-6.5	5.26	1208.616	-0.103	2	svdf^{87} SLADAINTEF K ^{97}ntrt	(270)
40.1	-6.3	6.11	1115.569	-0.096	2	tnek^{105} VELQELNDR ^{113}fany	(9178)
66.1	-6.2	5.61	1116.553	-0.100	2	tnek^{105} VELQELNDR ^{113}fany	(9178)
47.1	-6.1	5.71	1115.569	-0.156	2	tnek^{105} VELQELNDR ^{113}fany	(9178)
410.1	-5.2	5.19	1539.910	-0.098	2	qqnk^{130} ILLAELEQLK GQGK ^{143}srlg	(2340)
424.1	-4.0	5.25	1540.8945	-0.0018	2	qqnk^{130} ILLAELEQLK GQGK ^{143}srlg	(2340)
544.1	-6.4	6.94	1169.714	0.639	2	qqnk^{130} ILLAELEQLK ^{139}gqgk	(10175)
129.1	-6.8	5.56	1254.567	-0.014	2	gksr^{146} LGDLYEEEMR ^{155}elrr	(9288)
234.1	-6.8	5.61	1076.504	0.069	2	ever^{176} DNLAEDIMR ^{184}lrek	(6319)
39.1	-6.6	6.07	1092.499	-0.066	2	ever^{176} DNLAEDIMR ^{184}lrek	(6319)

Figure 7C

spectrum	log(e)	log(I)	m+h	delta	z	start	sequence	end	modifications
303.1	-6.5	5.26	1208.616	-0.103	2	87	SLADAINTEFK	97	
40.1	-6.3	6.11	1115.569	-0.096	2	105	VELQELNDR	113	
66.1	-6.2	5.61	1116.553	-0.1	2	105	VELQELNDR	113	Q [108] 0.984016
47.1	-6.1	5.71	1115.569	-0.156	2	105	VELQELNDR	113	
410.1	-5.2	5.19	1539.91	-0.098	2	130	ILLAELEQLKGQGK	143	
424.1	-4	5.25	1540.895	-0.0018	2	130	ILLAELEQLKGQGK	143	Q [137] 0.984016
544.1	-6.4	6.94	1169.714	0.639	2	130	ILLAELEQLK	139	
129.1	-6.8	5.56	1254.567	-0.014	2	146	LGDLYEEEMR	155	
234.1	-6.8	5.61	1076.504	0.069	2	176	DNLAEDIMR	184	
39.1	-6.6	6.07	1092.499	-0.066	2	176	DNLAEDIMR	184	M [183] 15.9949

Figure 7 A-C (preceding page): Sample bioinformatics data from X!Hunter for spot 3 from the Securinine treated soluble protein dataset. Search criteria were as described in methods. A) Sample output from X!Hunter displaying top hits, ρ-value (95) and FDR% (0.24%). The ρ-value(rho-value) is not a p-value. The ρ-value relates to the quality of the data in the protein identifications, with 0 being completely random and 100 being nonrandom. It is desirable for ρ-scores to be as close to 100 as possible. The colored arrows highlight pertinent information. The black arrow denotes the protein score. Note that score is the natural log (ln) of the expect score. The red arrow indicates protein molecular weight. The green arrow indicates the protein identification. The blue arrow indicates the ρ-score. The orange arrow indicates the FDR for this dataset. B) Peptide output from X!Hunter, note that highlighted residues are identified as posttranslational modifications by the algorithm. The black box outlines the peptide score. C) List of manually validated peptides from the X!Hunter output. Red indicates that the peptide is accepted as valid, with green indicating a posttranslational modification as determined by the algorithm.

It was observed that the search tools will often match peptides with relatively poor sequence coverage, that can still have a respectable peptide score (considered significant for a particular tool and having an E value <1). This is particularly true with larger peptides. For Mascot, E values of >1 are often identified as a 'first tier' peptide hit with a peptide score considered significant by Mascot, but these were eliminated from consideration due to the large E values.

It was also observed that +3 ions tended to have lower peptide scores, even when they have reasonable coverages, probably due to the greater complexity of the analysis i.e. both +1and +2 ions for b- and y-,(similar to the effects of increasing the size of the databases. Analysis of +3 or greater ions is akin to increasing the size of the database searched (e.g. all mammals vs. *Homo sapiens* alone). Increasing the size of

the search (via +3 or greater charges and/or the size of the database) increases the probability of a random match (false positive), and this will also have the effect of lowering protein/peptide scores, due to the increase in complexity of the Search. It should also be noted that the majority of the peptides in an identified protein had at least some sequence redundancy, that is to say that a given peptide sequence was often found in more than one identified compound from MS/MS analysis. A compound is defined as a particular MS/MS spectrum, and reflects the description given by the Bruker Data Analysis software package.

All MS/MS data from infected samples was searched against the *C. burnetii* databases in X!Tandem, using the parameters defined for the other X! tools as described above (default parameters with parent mass tolerance set to 0.8 Da). X!Tandem has a built in *C. burnetii* database, while the other tools do not. When *C. burnetii* and *H. sapiens* databases were searched simultaneously, the human protein was the better hit. As a result, all proteins in the gels detected as being differentially expressed are believed to be human.

96 Hr Infect +/- 50 uM Securinine

For this second experimental design, we utilized a 2nd generation pair of ZDyes code named BDRI227 and ZB-dipropyl (made in-house by Grieco lab) at 1X@RT labeling (see above for description of labeling conditions) at room temperature using 100 ug protein/channel. This Zdye set did not require gel fixing to remove unreacted Zdye

background before scanning. Labeling buffer was as described above with the exception that 30 mM bicine was substituted for Tris. Sample preparation, labeling, and strip loading proceeded as described above. In one membrane fraction set (3-11NL) the pooled internal standard was included in the run but was not analyzed for reasons

Table 3: IEF profiles for 96 hr infect +/- 50 uM Securinine experiment

3-11NL IEF GE Healthcare IPGphor II				4-7 IEF GE Healthcare IPGphor III		
Voltage (V)	Time/VHrs	Step/Gradient		Voltage (V)	Time/VHrs	Step/Gradient
500	2400 VHrs	Step		500	500 VHrs	Step
1000	5 Hrs	Gradient		1000	5 Hrs	Gradient
3000	1 Hr	Gradient		8000	3 Hrs	Gradient
3000	4500 VHrs	Step		8000	22,000 VHrs	Step
8000	1 Hr	Gradient		10000	1 Hr	Gradient
8000	12,000 VHrs	Step		10000	100,000 VHrs	Step
10000	1 Hr	Gradient		500	10 Hrs	Step/Hold
10000	36,000 VHrs	Step				
500	10 Hrs	Step/Hold				
3-11NL IEF GE Healthcare IPGphor I				4-7 IEF Biorad Protean IEF Cell		
Voltage	Time/VHrs	Step/Gradient		Voltage (V)	Time/VHrs	Step/Gradient
500	2000 VHrs	Step		500	500 VHrs	Step
1000	4 Hrs	Gradient		1000	3 Hrs	Gradient
3000	1 Hr	Gradient		8000	3 Hrs	Gradient
3000	4500 VHrs	Step		8000	130,000 VHrs	Step
8000	1 Hr	Gradient		500	10 Hrs	Step/Hold
8000	56,000 VHrs	Step				
500	10 Hrs	Step/Hold				

described below. The other membrane fraction (pH 4-7) also included 100 ug of unlabeled protein. The IEF profiles are listed in table 3. Also note that Securinine treatment is a posttreatment following infection and that the amount of Securinine used was 2X more that was used in the original Securinine analysis.

Note that for this 2nd experimental design, all other steps were performed as described above. The differences in the IEF profiles in table 3 reflect different IEF cells utilized in this separation. It was desirable to have all of the strips on different IEF cells in a given experiment finish within a similar timeframe. Because different IEF cells have different maximum voltages and because 3-11NL and 4-7 IEF strips are best performed using different final total volt-hours,minor modifications were made to the beginning of the run to help ensure strips on different IEF cells finished closely together. Total volt hours were similar between various runs with the same strip pH range. As with previous experiments, all strips for a biological replicate (all technical replicates e.g. in the forward label strips) were run simultaneously in the same IEF system. Reverse label from the same biological replicate were run on a separate IEF cell.

CHAPTER 3

RESULTS

Results of 2D Gel Analysis

It was determined in the course of our investigation that the pooled internal standard commonly used by 2D-DIGE investigators [131,141] causes what appears to be an artificial improvement in evaluation criterion, as has also been supported by an expert in the field [142]. This is most likely due either to a) direct correlation between the samples, or b) an artificial increase in the size of N by adding the internal standard images into the value of N and artificially increasing the degrees of freedom. Comparison of correlated data will tend to result in spuriously significant differences where no differences in fact exist [142-145]. Artificially increasing the size of N will artificially lower the calculated p-value. Neither condition is acceptable for a reliable statistical analysis. We discovered that there were a lot of false positives correlated with how we used the statistics in Progenesis to make decisions regarding statistical significance in differential protein expression (see table 4). The experiments were analyzed as two color channel control vs. experimental analysis only, the third color channel internal standard data was not used for either a) alignment or b) analysis.

We discovered in the course of the analysis that Progenesis was treating each image as an individual biological replicate, even though many of the images were "technical replicates" of the same biological sample. Since the technical replicates had

lower sample variance than the biological replicates Progenesis treating them equally could skew the statistical analysis of the results. Furthermore, acting as though there were more biological replicates than measured could incorrectly assign biological significance to changes in spot intensities that were not truly statistically significant. A better method was needed to separately account for both the technical and biological variation within our samples. To this end, we determined that the general linear model, specifically a nested ANOVA analysis [132] was an appropriate method. This was confirmed by consultation with SPSS technical support (Tom Leuthner, SPSS technical support, personal communication), who also provided the syntax outlined in the Methods section. SPSS is a widely used statistical analysis program. The nested ANOVA allowed us to determine both a p-value and an observed power score for each individual spot while properly accounting for both the technical and biological variation [132]. The general outline of the data structure being analyzed is shown in figure 6 (see above).

The results of the soluble fraction +/- Securinine analysis in Progenesis yielded 44 spots displaying a differential expression from +/-1.3 fold to +3.9 fold, with good statistics, meeting the above statistical selection criteria of $P<0.05$ and observed power >0.8 (see table 4 below). These values ($p<0.05$, power >0.8) are derived from Progenesis, and are not from the final nested ANOVA analysis. The results in table 4 were obtained from a total of 36 gel images (18 control and 18 Securinine stimulated with three gels in the 'forward label' and three in the ‘reverse label’ configuration). See figures 9-15 for all final Progenesis master images for the first experimental protocol.

Nested ANOVA data analysis groups or 'nests' technical replicates in their appropriate biological replicate which are further groups or 'nested' within the appropriate treatment condition prior to performing a two-way ANOVA (see figure 6). This approach provided a more rigorous statistical analysis of the results for the entire dataset, providing increased confidence in the statistically significant protein changes. MS identifications and bioinformatics data on the proteins identified are presented in tables 6-13.

Table 4: Sample statistical data obtained from Progenesis for +/- Securinine stimulation of Monomac I cells, soluble fraction prior to nested ANOVA analysis. The sign in the fold change column indicates the direction of change in the Securinine stimulated sample with respect to the unstimulated sample. ANOVA was calculated by Progenesis as were the q-values, and the power score. Final statistical data and bioinformatics data are found in tables 5-11 below.

S	Fold	ANOVA	Q-value	P
1	+3.9	1.89x10	2.57x10	1
2	+3.6	1.25x10	8.50x10	1
3	+3.4	1.02x10	1.09x10	1
4	+3	0.00010	0.00565	0.
5	+2.9	9.32x10	1.09x10	1
6	-2.9	2.06x10	3.50x10	1
7	-2.9	3.22x10	2.92x10	1
8	+2.9	3.01x10	1.39x10	1
9	+2.8	4.62x10	1.26x10	1
1	+2.6	9.25x10	0.00545	0.
1	+2.4	5.36x10	1.04x10	1
1	-2.3	9.54x10	1.09x10	1
1	+2.2	0.00010	0.00565	0.
1	+2.1	9.62x10	0.00545	0.
1	+2.1	3.11x10	1.06x10	1
1	+2.1	4.55x10	1.03x10	1
2	+2	1.17x10	1.14x10	1
2	-1.9	0.00366	0.080	0.
2	+1.9	2.79x10	0.00022	1
2	-1.9	0.00018	0.00874	0.
4	+1.8	0.00234	0.0636	0.
4	+1.7	0.00051	0.0208	0.
4	+1.6	0.00202	0.0585	0.
4	+1.6	0.00638	0.124	0.

Securinine, LPS, MPL and Infection Time Course

We analyzed gel data from adjuvant stimulated monocytes and the infection timecourse in the initial set of experiments (the later set of data infection +/- Securinine is described below). Soluble and membrane fractions were analyzed for all tested conditions. The infection time course took samples at 24, 48 and 96 hrs postinfection from Monomac I cells, infected at a 200:1 ratio with phase II *C. burnetii*. In all cases, the control cells were sham stimulated Monomac I cells cultured in parallel for each biological replicate. Adjuvant samples were stimulated with either 25 uM Securinine, or 5 ug/culture LPS or 5 ug/culture MPL and harvested at 24 hrs post treatment. Fractions that had differentially expressed spots are seen in tables 6-9 and figures 15-21.

The finding that not all fractions displayed differentially expressed spots was initially surprising. However, on further consideration proved less so. With regards to the infection time course, it is to be expected that the infection will take time to progress, and thus changes to the host cell proteome in response to infection will also take time to begin changing expression. The earliest proteome changes could well fall below the threshold of detection in these experiments. The first statistically significant changes in protein expression were detected at 48 hrs postinfection. As described in the introduction, while a given cellular response may be digital in nature, the individual gene responses are analog, and will each have different thresholds of activation. In the case of *C. burnetii* infection, there will be a certain threshold of various intracellular factors that determine whether a protein's expression increases or decreases in

response to infection. While the monocyte will respond to the infection (this is a digital response), each individual differentially expressed protein will have a different threshold of activation for up- or downregulation (this is an analog response). Once the threshold for a change in expression has been crossed, a certain amount of time must pass (48 hours in our dataset) before the change in expression is large enough to be detected in a gel in a statistically significant manner.

In the LPS and MPL adjuvant experiments (both of which stimulate Toll-like receptors), stimulation of the Toll-like receptors (TLRs) is a rapid response process and the samples may not have been harvested in a time frame that would enable optimal detection of proteome changes as discussed further below. It is also possible that the molarity of the LPS or MPL was sufficient to trigger a change in expression of inflammatory markers (e.g. IL-8, presumably having a low threshold of activation) but not sufficient to trigger widespread proteome changes (which would be predicted to require a higher threshold of activation). Also, the TLR response is primarily concerned with activation of the NF-κB response. NF-κB is a transcription factor and therefore is below our detection limits in a 2D gel. In addition, many of the downstream effectors activated by NF-κB are intended for export from the cell (e.g. inflammation markers) which are also invisible to our screen, as we did not evaluate the secretome.

We elected to run the gels from the first series of experiments using broad range (3-11NL) IEF strips due to funding and time constraints. This presented the best compromise between generating the data needed for the preliminary investigation

conducted, in the timeframe available, such that we were able to obtain the data presented within the grant support period. Broad range IEF can be thought of as akin to a low power magnification on a light microscope, as many of the broad details are visible, but some of the finer points that would be visible at higher magnification may be lost. Narrower range IEF (possibly including more extensive fractionation) can provide finer details, but at the cost of significantly increasing the number of gels that must be run. Increased numbers of gels would require a correspondingly longer analysis time and material/labor costs since two or more IEF strips are needed to cover the same pH range as a single broad range experiment. There is also a significant increase in the amount of protein required to perform the experiment, adding to the material and labor costs. We used both 3-11NL and 4-7 IEF strips for the 2nd experimental series (detailed below).

At 48 hours postinfection, the monocyte response to infection becomes slightly more detectable and by 96 hours there are many evident changes in protein expression. Adjuvants that stimulate the innate immune system and increase the monocyte clearance of *C. burnetii* were studied [74]. Securinine (25 uM Securinine for 24 hours), as well as LPS and MPL at 5 ug / culture also at 24 hours exposure, were studied. These exposures and timeframes were selected because they provide a similar level of IL-8 induction at 24 hours, and represent an attempt to normalize the exposures. Securinine stimulation gave a number of differentially expressed protein spots for analysis. LPS and MPL stimulation gave no differentially expressed proteins in the soluble fraction at 24

hours poststimulation. LPS stimulated membrane fraction samples showed one differentially expressed protein, MPL stimulated membrane fraction samples gave seven differentially expressed protein spots. Future experiments may well benefit from additional cellular subfractionation (e.g. organelle fractions), enabling deeper penetration into the proteome.

MPL is an LPS derivative that is effective as an adjuvant, but is nontoxic and is currently clinical to preclinical at least in vaccines produced by Glaxo Smith Kline ([77], M. Jutila, personal communication). The relatively low number of differentially expressed protein spots in the LPS and MPL samples is perhaps not surprising in hindsight, since these adjuvants stimulate inflammation via the toll-like receptor (TLR) pathway. The TLR pathway creates a rapid and fairly transient response. Securinine would appear to have a slower response time. At 24 hours of stimulation, it is quite possible that we simply took our LPS and MPL aliquots too late to see significant changes with the detection sensitivity employed [146]. Recent observations by Pabst et al., (2008) suggest the notion that we may not have captured the optimal time window to detect protein changes in the TLR pathway [146]. Securinine acts through the $GABA_A$ receptor [74,78,82,83], and appears to have a much different effect on the monocyte proteome, compared to stimulation by LPS and MPL.

Differentially expressed spots from the infection time course and adjuvant stimulation studies were picked for MS analysis as described above. Samples were digested with trypsin and run on the XCT ultra ion trap mass spectrometer with

ChipCube attachment, using an LCChip with a 150 mm C_{18} separation column (Agilent part # G4240-62002). The data was subjected to bioinformatics analysis as described above using Mascot, X!Hunter and X!Tandem P3 as described above. For the infected samples, X!Tandem was also searched for *C. burnetii* proteins, as it has databases containing the completed genomic sequences for several strains of the bacterium, which the other bioinformatics tools do not.

In no case was a *C. burnetii* protein observed to outscore a human protein on the X!Tandem searches (in any set of experiments). Only one significant bacterial protein was identified, GroEL, a protein homologous to human Hsp60. GroEL was identified in a Hsp60 spot, suggesting that this identification may be spurious and dependent on the homology between the two proteins. Based on the selection criteria defined above, human Hsp60 is considered to be the correct protein identification. When compared head to head, (searching against *C. burnetii* databases and human databases simultaneously in X!Tandem) human Hsp60 was the better identification. Although *C. burnetii* proteins must certainly be present in our infected samples, we did not have the sensitivity and resolution to adequately detect them with the protocols employed.

Several of the digested spots in the table were measured a second time in the mass spectrometer with a higher amount of peptide in an attempt to improve sequence coverage, and this information was incorporated into the table. We have noted that all of the MS/MS software analysis tools that we used gave substantially the same list of protein identifications, with similar, but slightly different, lists of peptides. In rare cases,

X!Hunter would find another protein of nearly equal protein score at or near the observed pI and molecular weight. Mascot and P3 gave the same top protein identifications and this was used to make the final protein identification selection, although it was noted in the conclusions below where X!Hunter made an alternative identification. Different tools also gave largely similar lists of peptides, generally differing in combinations of modifications to Asn and Gln (deamidation) and Met (oxidation) as well as nontraditional cleavage (cleaved N-terminally after Lys or Arg but not C-terminally, see table 5), and/or missed cleavages. Mascot is not able to handle more than three variable modifications at one time (this is a hard limit), and this limits Mascot's utility for identifying modified proteins since deamidation and oxidation must be included, as they are commonly found. The other tools have additional layers of database searching that include a much more expansive list of variable modifications.

In multilevel bioinformatics searches for identification of proteins/peptides from MS/MS data, there is usually an initial, relatively stringent search through the MS/MS data followed by one or more passes through the data with more relaxed standards. For example, in the X!Tandem P3 algorithm, the initial pass searches only for proteotypic peptides (peptides that are always or nearly always present for a given protein) to identify the protein(s) in question [138]. This is followed by searching the entire sequence(s) of an identified protein(s) against the MS/MS data to improve sequence coverage, and to examine the data for a wider array of possible posttranslational modifications [138].

With regards to the tools used, Mascot in particular functioned best as a more restricted search using only carbamidomethylation (on cysteines), deamidations, and methionine oxidation, as variable modifications. Although we are generating carbamidomethylation as a fixed modification during 2D gel preparation, Mascot does not handle this modification as a fixed condition very well, and this is potentially due to a bug in the programming (observed in both the in-house version and the online version). We determined this during searches using cysteine carbamidomethylation as a fixed variable in Mascot, and observed that carbamidomethylated peptides were poorly represented by Mascot, where these peptides would be detected by the other tools but not by Mascot. When we set cysteine carbamidomethylation to variable in Mascot, the software found the same carbamidomethylated peptides as the other tools. In addition, there is evidence that the alkylation with iodoacetamide does not proceed to completion [147], making it more properly a variable rather than a fixed modification.

We note that in our samples, using several different bioinformatics tools, all detected cysteines were found to be carbamidomethylated. Because carbamidomethylation often does not go to completion [147] and is therefore most properly treated as a variable modification, it could be argued that Mascot is correct in only identifying this modification as variable rather than fixed. However, if Mascot is set to find carbamidomethylation, it should find it in peptides where it exists, regardless of

Table 5: Sample lists of peptides found by the Mascot, X!Hunter and P3 bioinformatics tools. Red lettering indicates a peptide accepted per criteria outlined above, green lettering indicates an identified posttranslational modification. The blue box indicates a nontraditional cleavage product. R.GHLQIAACPNQD. is a tryptic peptide (preceeded by R) that does not have a K or R on the C terminus. Notice that the peptides identified are substantially similar, but contain complimentary information.

Mascot peptide list	X!Hunter peptide list	X!Tandem P3 peptide list
DFGSFDK	LLEAIKR	GELLEAIK
GELLEAIK	LLEAIKR	GELLEAIKR
GELLEAIK	LLEAIKR	DFGSFDKFK
RDFGSFDK	LLEAIKR	DFGSFDKFK
NVRPDYLK	GELLEAIK	DVTAQIALQPALK
NVRPDYLK	GELLEAIK	DVTAQIALQPALK
GELLEAIKR	GELLEAIKR	GDVTAQIALQPALK
GELLEAIKR	NVRPDYLK	GDVTAQIALQPALK
GELLEAIKR	VINWENVTER	GDVTAQIALQPALK
GELLEAIKR	GHLQIAACPNQD	GDVTAQIALQPALK
DFGSFDKFK	GDVTAQIALQPALK	GDVTAQIALQPALK
DFGSFDKFK	GDVTAQIALQPALK	GHLQIAACPNQDPL
GDVTAQIALQPALK	GDVTAQIALQPALK	AIWNVINWENVTER
GDVTAQIALQPALK	GDVTAQIALQPALK	AIWNVINWENVTER
GDVTAQIALQPALK	GDVTAQIALQPALK	HHAAYVNNLNVTEEK
GDVTAQIALQPALK	AIWNVINWENVTER	HHAAYVNNLNVTEEK
HHAAYVNNLNVTEEK	AIWNVINWENVTER	GHLQIAACPNQDPLQG
HHAAYVNNLNVTEEK	AIWNVINWENVTER	
HHAAYVNNLNVTEEK	AIWNVINWENVTER	
FNGGGHINHSIFWTNLSPNGGGEPK	AIWNVINWENVTER	
	AIWNVINWENVTER	

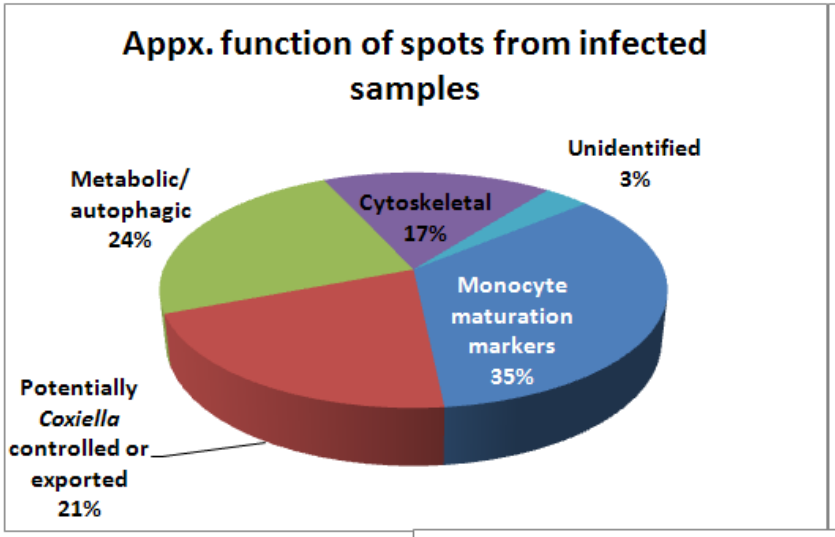

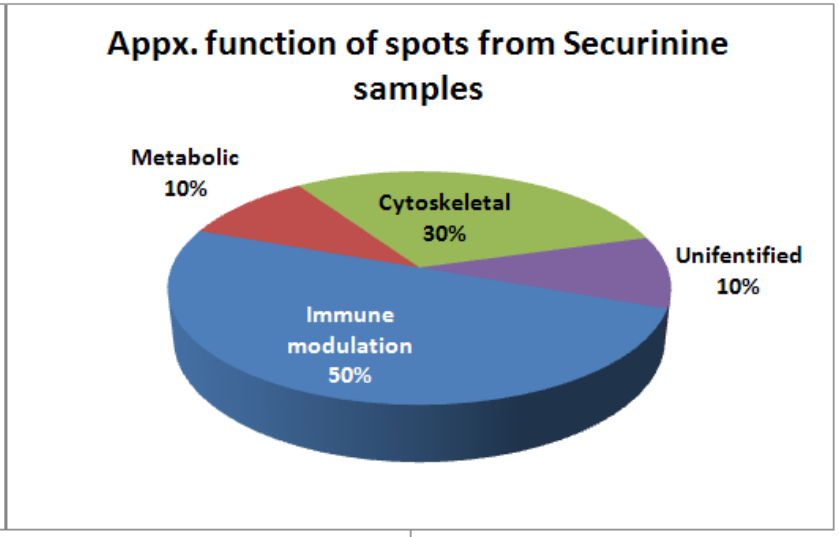

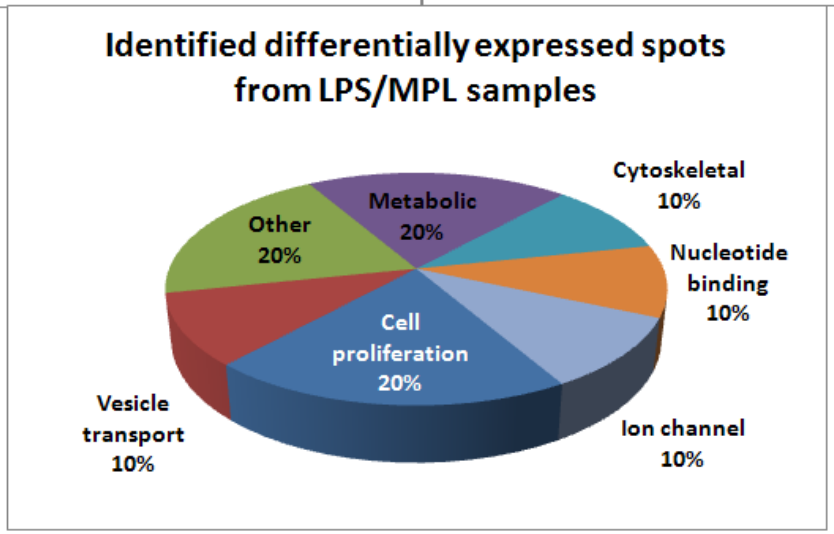

Figure 8: Graphical representation of the functional distribution of identified proteins in the infected, Securinine, LPS and MPL samples.

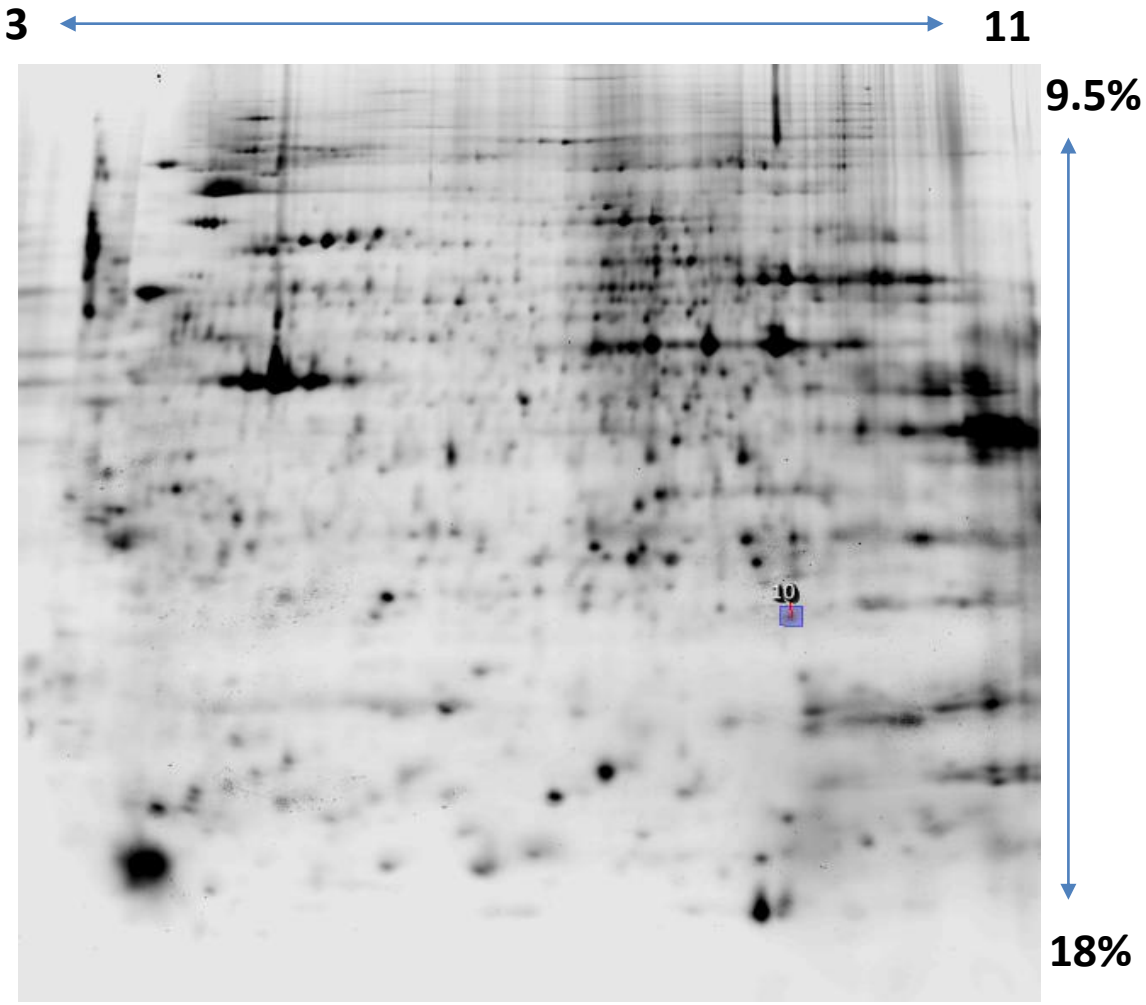

Figure 9: 48 hr postinfection soluble fraction analysis. Final Progenesis master image following gel image analysis and offline statistical analysis. Analysis was carried out for 3 biological replicates with 6 technical replicates for biological replicates 1 and 2 and 5 technical replicates for biological replicate 3. Technical replicates included reciprocal labeling, as described above.

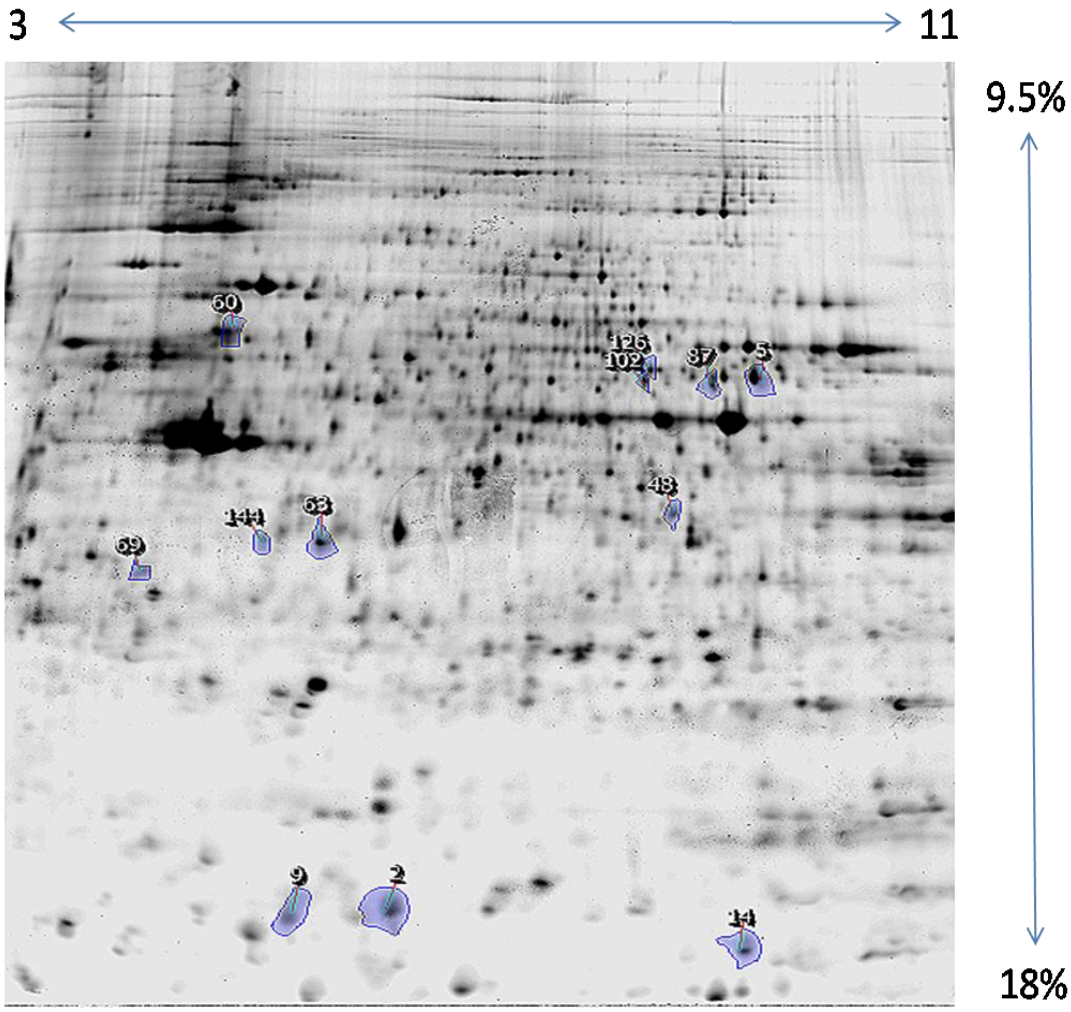

Figure 10: 96 hr postinfection soluble fraction. Final Progenesis master image following image analysis and offline statistical analysis. Analysis included 3 biological replicates, with 6 technical replicates per biological replicate, including reciprocal labeling.

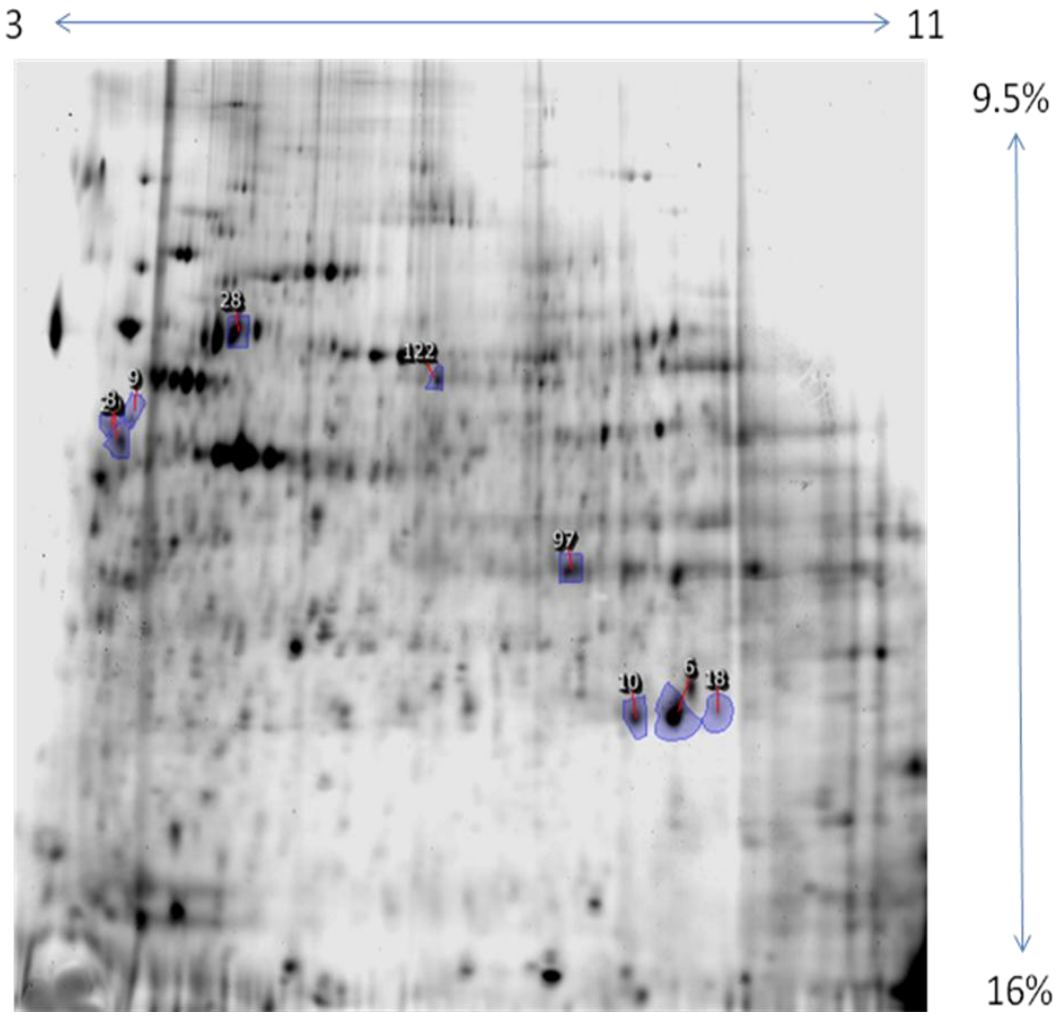

Figure 11: 96 hr postinfection membrane fraction. Final Progenesis master image following image analysis and offline statistical analysis. Analysis was for 3 biological replicates including 6 technical replicates per biological replicate with reciprocal labeling.

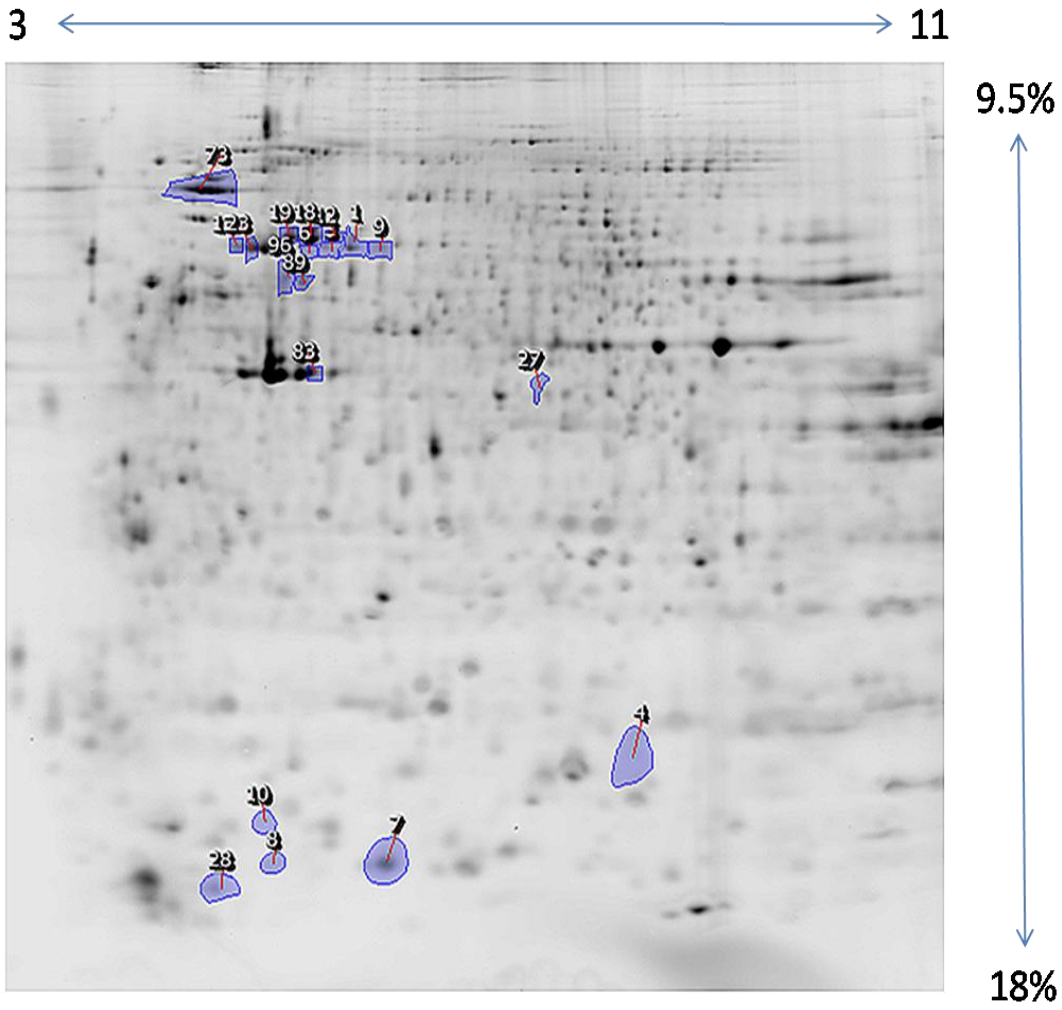

Figure 12: Securinine soluble fraction. Final Progenesis master image following image analysis and offline statistical analysis. Analysis of 3 biological replicates, with 6 technical replicates each including reciprocal labeling.

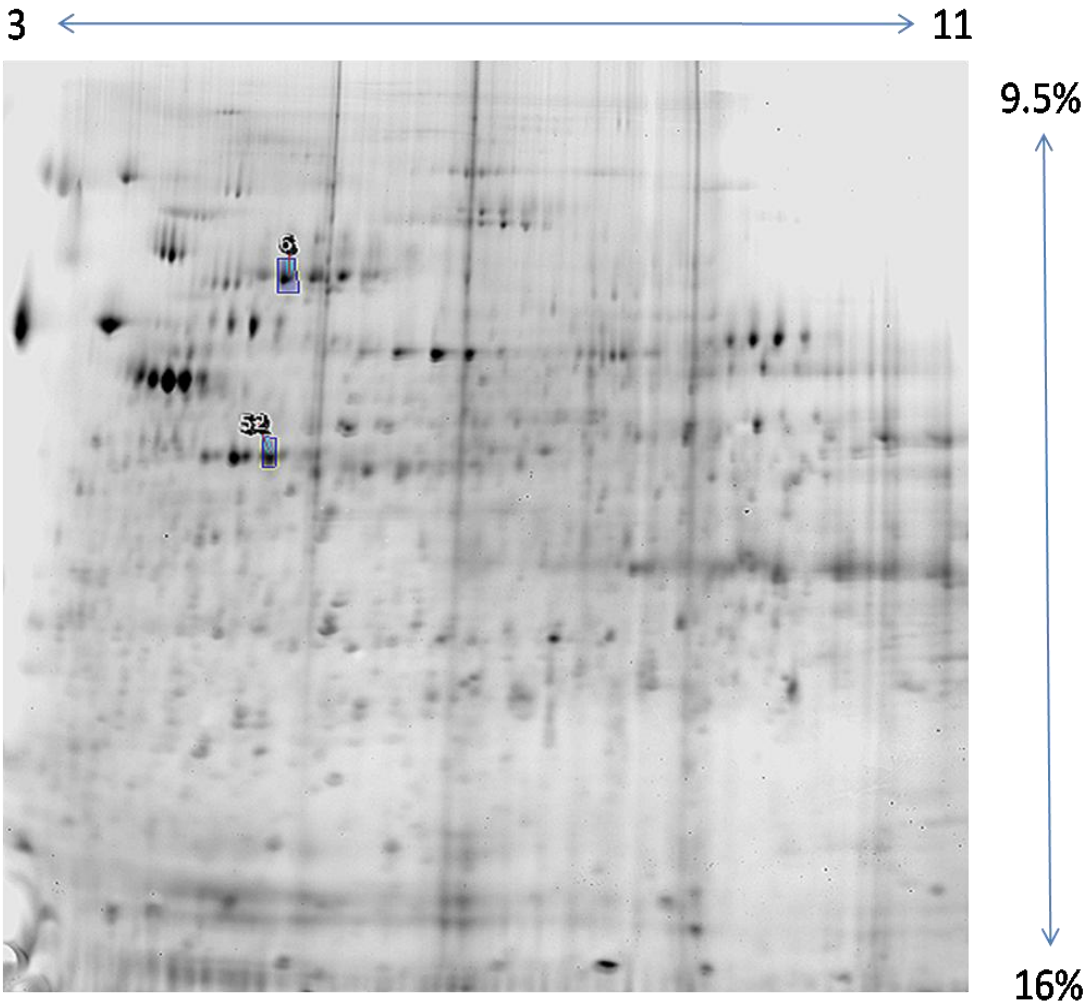

Figure 13: Securinine membrane fraction. Final Progenesis master image following image analysis and offline statistical analysis. Analysis includes 3 biological replicates with 5 technical replicates for biological replicate 1 and 6 each for biological replicates 2 and 3 with reciprocal labeling.

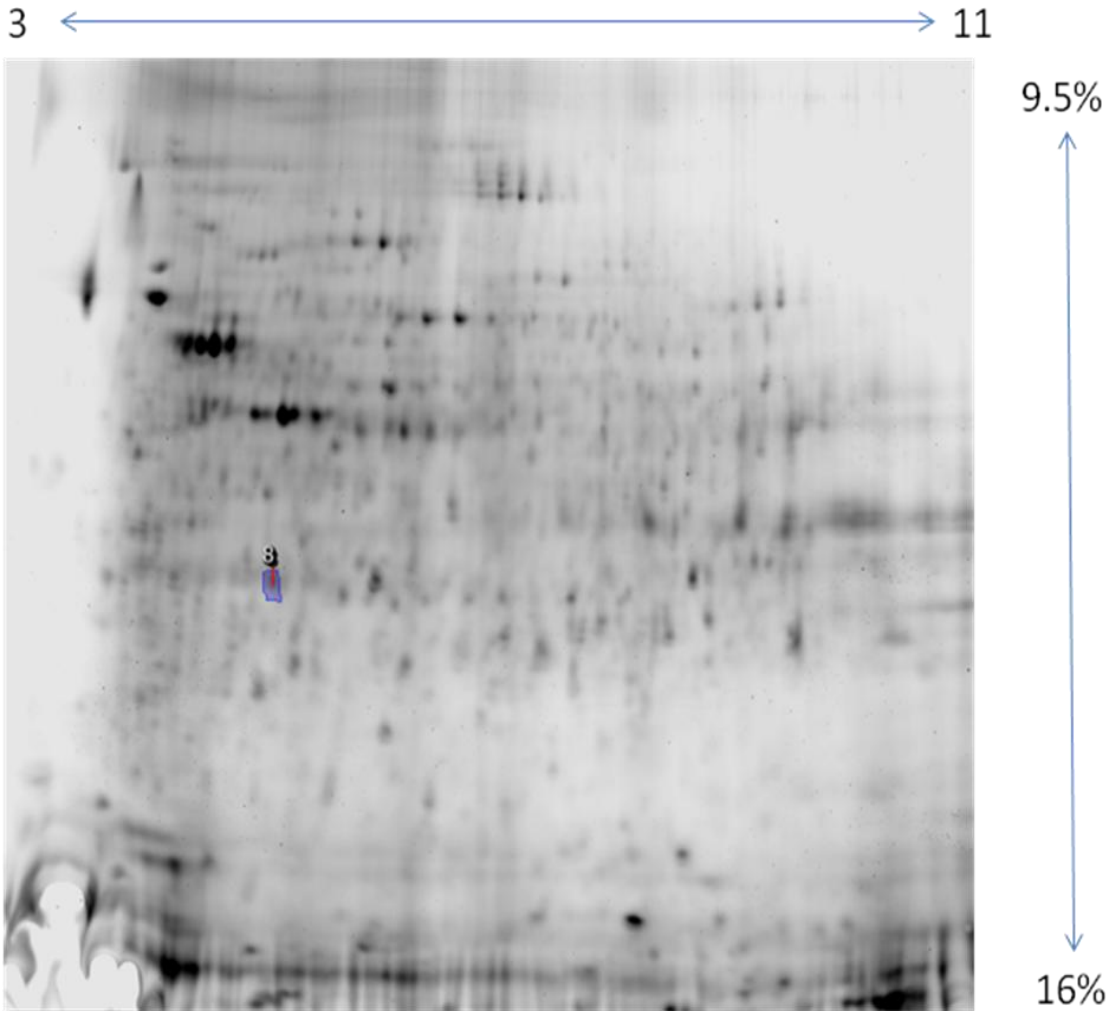

Figure 14: LPS membrane fraction. Final Progenesis master image following image analysis and offline statistical analysis. Analysis includes 3 biological replicates, with 6 technical replicates each including reciprocal labeling.

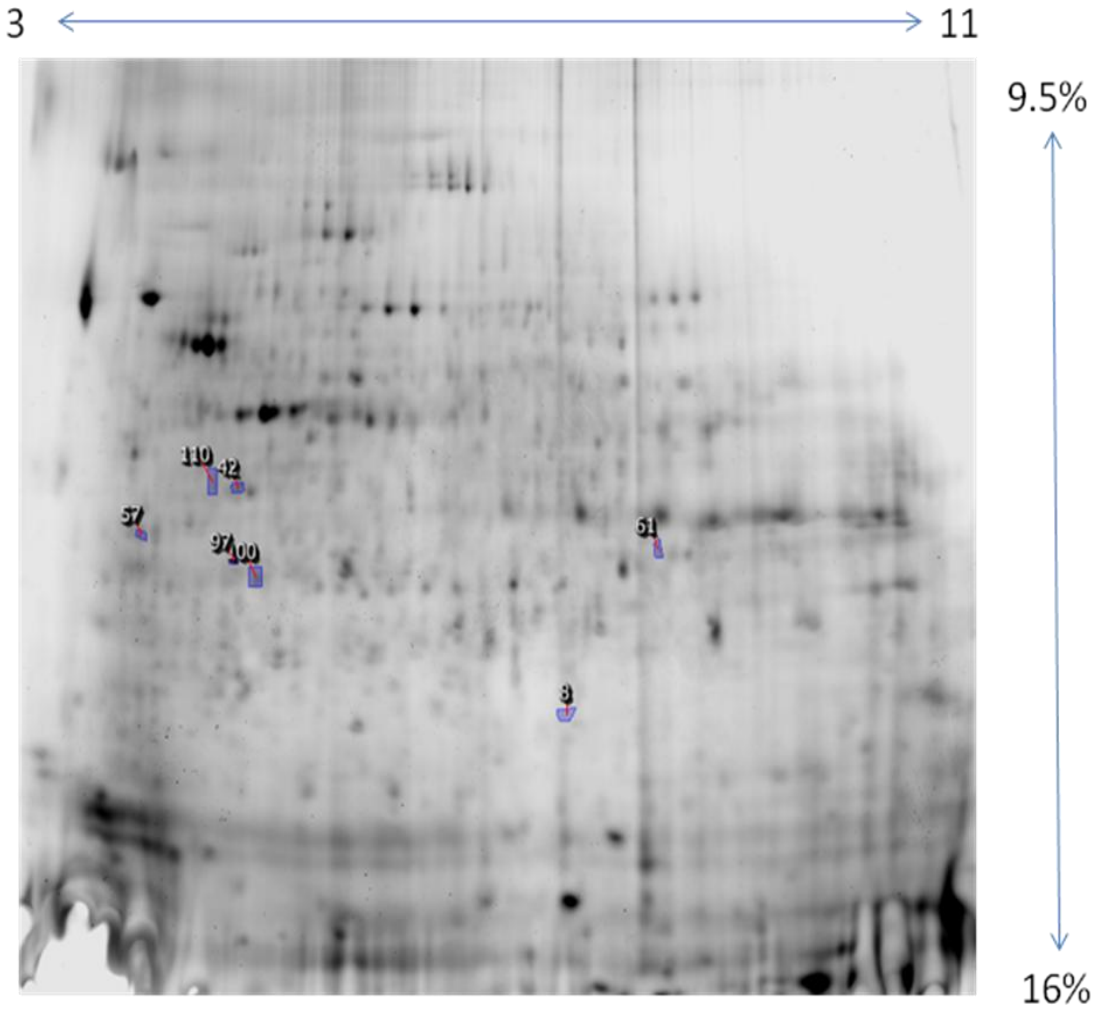

Figure 15: MPL membrane fraction. Final Progenesis master image following image analysis and offline statistical analysis. Analysis includes 3 biological replicates, with 6 technical replicates including reciprocal labeling.

Table 6: Statistical summary and bioinformatics data for regulated proteins in the 48 hr infection soluble fraction and 96 hr infection soluble fraction samples.

Test condition	Spot #	Fold change	Nested ANOVA p-value	Nested ANOVA power score	ID	Mascot score	Mascot # unique peptides	Mascot % coverage	Mascot NCBI accession #	X!Hunter score	X!Hunter # unique peptides	X!Hunter % coverage	X!Hunter FDR (%)	X!Hunter Uniprot accession #	P3 Score	P3 # unique peptides	P3 % coverage	P3 FDR (%)	P3 Uniprot accession #
48 hr sol	10	2.1	0.0101	0.921	Mn containing superoxide dismutase isoform A	519	4	23.4	30841309	-43.6	6	24.8	0.22	P04179	-31.1	5	23.0	1.07	P04179
96 hr sol	2	4.1	0.00257	0.998	S100 Ca binding protein A9	212	3	31.6	4506773	-40.7	4	28.9	0.02	P06702]	-17.4	3	31.6	0.95	P06702
	5	3	0.0147	0.861	Visfatin/PBEF	767	10	30.3	5031977	-59.7	7	15.5	0.37	P43490	-67.4	10	18.5	1.23	P43490
	9	2.7	0.0097	0.927	S100 Ca binding protein A9	239	4	44.7	4506773	-40.1	4	30.7	0.20	P06702	-28.2	4	30.7	1.00	P06702
	14	2.6	0.0156	0.85	S100 Ca binding protein A8	771	7	48.4	21614544	-31.2	5	34.4	0.41	P05109	-33.5	7	39.8	1.17	P05109
	48	1.7	0.018	0.82	Transaldolase 1	456	7	21.1	5803187	-56.1	7	19.3	0.46	P37837	-43.8	7	16.6	1.18	P37837
	60	1.6	0.0154	0.853	Chaperonin/Hsp60	722	12	26.2	31542947	-85.1	10	17.5	0.23	P10809	-118.9	12	21.5	1.10	P10809
	63	1.6	0.00465	0.985	Cytosolic inorganic pyrophosphatase	589	7	33.8	4583153	-84.1	9	30.8	0.34	Q15181	-96.1	9	24.2	1.12	Q15181
	69	1.6	0.01736	0.829	microtubule associated protein EB1	490	8	31.7	6912494	-86.4	8	27.6	0.24	Q15691	-71.9	9	19.8	1.46	Q15691
	87	1.5	0.0172	0.831	Fascin 1	421	8	22.2	4507115	-87.4	9	20.5	0.21	Q16658	-61.3	9	17.6	1.20	Q16658
	102	1.5	C	0.763	leucine aminopeptidase 3	857	8	20.9	37588925	-83.4	13	24.9	0.27	P28838	-103.4	21	30.1	1.20	P28838
	126	1.4	0.0127	0.887	leucine aminopeptidase 3	828	12	28.3	37588925	-84.9	12	24.3	0.22	P28838	-131.7	16	26.6	0.79	P28838
	144	1.3	0.00031	1	pyrophosphatase 1	278	5	33.8	4583153	-71.1	8	30.8	0.32	Q15181	-76.2	11	30.8	0.99	Q15181

Table 7: Statistical summary and bioinformatics data for regulated proteins identified in the 96 hr infection membrane fraction samples.

Test condition	Spot #	Fold change	Nested ANOVA p-value	Nested ANOVA power score	ID	Mascot score	Mascot # unique peptides	Mascot % coverage	Mascot NCBI accession #	X!Hunter score	X!Hunter # unique peptides	X!Hunter % coverage	X!Hunter FDR (%)	X!Hunter Uniprot accession #	P3 Score	P3 # unique peptides	P3 % coverage	P3 FDR (%)	P3 Uniprot accession #
96 hr mem	6	3.1	0.00914	0.934	Mg-containing superoxide dismutase	397	3	22.1	30841303	-77.9	13	32.4	0.32	P04179	-58.4	10	34.2	1.42	P04179
	8	2.4	0.00837	0.944	vimentin	1761	21	35.0	37852	-168.3	28	41.6	0.24	P08670	-149.1	24	32.4	0.63	P08670
	9	2.4	0.01044	0.917	vimentin	1146	13	21.9	37852	-148.2	22	35.0	0.18	P08670	-149.5	19	28.1	0.97	P08670
	10	2.3	0.00061	1	Rab7GTP	560	6	51.6	34147513	-44.6	7	30.9	0.32	P51149	-73.7	6	29.5	1.05	P51149
	18	-2	0.00404	0.99	Rab7GDP	240	4	30.7	34147513	-44.3	5	31.9	0.37	P51149	-35.2	4	27.1	1.29	P51149
	20	1.9	0.00572	0.975	vimentin	1048	14	32.2	37852	-137.4	19	44.4	0.46	P08670	-101.6	15	24.9	1.18	P08670
	28	1.6	0.01952	0.803	Chaperonin/Hsp60 (same protein)	1316	15	32.8	31542947	-127.2	10	30.7	0.32	P10809	-190.7	19	28.4	0.78	P10809
	97	-1.3	0.01187	0.898	Enoyl CoA hydratase 1	1591	12	29.5	70995211	-47.0	5	23.2	0.36	Q13011	-93.8	19	33.2	0.79	Q13011
	122	1.2	0.01408	0.869	Aldehyde dehydrogenase 2	1250	14	27.3	25777732	-117.1	20	32.5	0.15	P05091	-156.7	31	38.7	1.01	P05091

Table 8: Statistical summary and bioinformatics data for regulated proteins identified in the Securinine soluble fraction samples.

Test condition	Spot #	Fold change	Nested ANOVA p-value	Nested ANOVA power score	ID	Mascot score	Mascot # unique peptides	Mascot % coverage	Mascot NCBI accession #	X!Hunter score	X!Hunter # unique peptides	X!Hunter % coverage	X!Hunter FDR (%)	X!Hunter Uniprot accession #	P3 Score	P3 # unique peptides	P3 % coverage	P3 FDR (%)	P3 Uniprot accession #
Sec sol	1	3.9	0.0033	0.994	Hsp70 protein 1	2039	25	23.4	62089222	-137.3	14	23.7	0.31	P08107	-154.5	20	28.0	1.20	P08107
	3	3.4	0.0028	0.997	Hsp70 protein 1	1121	16	28.7	188488	-74.4	9	17.2	0.42	P08107	-112.8	14	20.1	0.93	P08107
	4	3	0.0281	0.714	Fatty acid binding protein 5	425	6	49.7	4557581	-27.9	6	43.7	0.38	Q01469	-43.4	6	37.0	1.35%	Q01469
	5	2.9	0.0192	0.806	L-plastin	691	16	23.3	4504965	-76.5	11	19.9	0.83	P13796	-105.4	8	14.4	1.60	P13796
	7	-2.9	0.000195	1	S100 Ca binding protein A4	43	2	18.3	4506765	-8.8	2	18.8	0.41	P26447	not found	not found	not found	not found	
	8	-2.8	0.00751	0.955	unidentified														
	9	2.7	0.0107	0.913	Hsp70 protein 1	701	12	23.1	188488	-94.9	9	16.3	0.34	P11142	-114.4	13	20.1	1.30%	P08107
	10	2.7	0.0068	0.963	L-plastin	2433	32	43.6	4504965	-242.7	35	43.2	0.34	P13796	-238.7	34	43.9	1.14	P13796
	11	2.6	0.007702	0.951	Thioredoxin	120	2	28.6	3153859	-15.5	2	22.9	0.24	P10599	-10.8	2	22.9	1.36	P10599
	12	2.4	0.00249	0.998	Hsp70 protein 8 isoform 1	2263	30	30.2	5729877	-152.0	14	30.2	0.41	P11142	-161.4	28	26.3	1.14	P11142
	13	-2.3	0.000198	1	L-plastin	2390	35	43.6	4504965	-147.8	17	28.2	0.45	P13796	-206.9	29	34.1	1.5	P13796
	18	2.1	0.00118	1	Hsp70 protein 8 isoform 1	2768	34	36.4	5729877	-160.0	21	33.3	0.53	P11142	-188.0	30	31.1	1.15	P11142
	19	2.1	0.022	0.775	Hsp70 protein 8 isoform 1	3117	38	34.8	5729877	-186.0	27	30.5	0.55	P11142	-211.8	36	29.3	1.07	P11142
	23	-2	0.00899	0.936	L-plastin	1216	14	24.2	4504965	-89.3	9	18.8	0.47	P13796	-121.8	8	15.3	0.68	P13796
	27	1.9	0.0137	0.874	Ser/cys proteinase inhibitor	606	10	37.4	13489087	-73.7	9	20.6	0.32	P30740	-71.1	9	21.4	1.27	P30740
	28	-1.9	0.0161	0.844	unidentified														
	73	1.5	0.00304	0.996	Hsp90	3526	27	28.2	6807647	-247.4	40	28.0	0.18	P08238	-219.8	33	25.1	0.69	P08238
	83	1.5	0.0151	0.857	Actin	750	5	21.6	4501885	-153.8	24	42.7	0.31	P63261	-120.7	16	38.1	1.23	P63261
	89	1.5	0.0171	0.831	Chaperonin/Hsp60	1280	18	34.2	31542947	-84.9	12	22.7	0.31	P10809	-122.1	9	21.5	1.08	P10809
	96	1.4	0.0235	0.759	Inosine 5' monophosphate dehydrogenase	734	10	22.8	66933016	-70.9	7	18.1	0.37	P12268	-44.4	5	12.5	1.45	P12268

Table 9: Statistical summary and bioinformatics data for regulated proteins in the Securinine, LPS, and MPL membrane fraction samples.

Test condition	Spot #	Fold change	Nested ANOVA p-value	Nested ANOVA power score	ID	Mascot score	Mascot # unique peptides	Mascot % coverage	Mascot NCBI accession #	X!Hunter score	X!Hunter # unique peptides	X!Hunter % coverage	X!Hunter FDR (%)	X!Hunter Uniprot accession #	P3 Score	P3 # unique peptides	P3 % coverage	P3 FDR (%)	P3 Uniprot accession #
Sec mem	6	1.8	0.000914	1	Hsp70	531	24	28.0	5729877	-94.1	12	16.3	0.44	P11142	-122.8	19	23.4	1.54%	P11142
	52	-1.3	0.0271	0.723	Actin	436	14	30.0	4501887	-125.8	16	36.8	0.57	P63261	-62.3	12	29.6	1.42%	P63261
LPS mem	8	1.2	0.0084	0.944	ATP synthase H+ transporting F1 complex beta subunit (caspase 10 cleavage product)	234	8	13.5	89574029	-67.8	7	13.8	0.47	P06576	-51.6	5	12.1	1.45	P06576
MPL mem	8	1.7	0.0092	0.933	Rab2AGTP	91	2	12.3	4506365	-27.5	3	17.9	0.62	P61019	-15.2	3	17.9	1.84%	P61019
	42	1.5	0.0093	0.933	ATP synthase mitochondrial F1 complex β precursor	299	7	14.7	32189394	-33.1	2	5.5	0.63	P06576	-55.2	5	10.0	2.19	P06576
	57	1.4	0.0101	0.921	tropomyosin 3 isoform 2	199	7	26.3	24119203	-58.4	5	21.0	0.39	P06753	-26.6	3	12.9	2.01	P06753
	61	1.4	0.0094	0.931	Guanine nucleotide binding protein β polypeptide 2-like 1	289	9	30.5	5174447	-61.2	8	26.2	0.51	P63244	-64.4	8	26.2	1.47%	P63244
	97	1.3	0.0027	0.997	p64 Cl ion channel	211	3	17.9	895845	-35.7	3	16.2	0.17	O00299	-27.7	4	21.2	1.18%	O00299
	100	1.3	0.0285	0.711	Prohibitin	173	5	15.8	4505773	-15.2	2	7.4	0.23	P35232	-20.3	3	11.8	1.51%	P35232
	110	1.2	0.016	0.845	ATP synthase mitochondrial F1 complex β precursor	508	14	25.5	32189394	-81.1	6	16.1	0.42	P06576	-73.4	10	20.6	1.82%	P06576

whether or not it is set as a fixed or variable modification. Carbamidomethylation is considered a fixed/complete modification by the P3 search algorithm, with no option to make this modification variable.

The other bioinformatics tools (X!Hunter and P3) handle modifications more readily and we used them to try to identify any modifications that might be present, as well as for independent evaluation of Mascot protein identifications. The other tools used perform their searches differently. For example, X!Hunter searches MS data against an annotated spectral database, where the database spectra searched are from actual MS/MS runs on identified peptides in the database [139]. The X!Hunter method is similar in concept to the small molecule spectral databases in GC/MS analysis. Mascot, and X!Tandem search against spectra predicted from the genome sequence. The P3 search tool uses a different approach entirely. P3 recognizes that in a given protein digest, not all digested proteins have an equal chance of detection, as some are detected very easily (they are perhaps recovered better during processing, as well as 'flying' and fragmenting well) where other peptides from the same proteins are not so easily detected [138]. Those peptides that are always or nearly always confidently detected for a protein are termed proteotypic peptides, and it is by these proteotypic peptides that P3 identifies proteins [138]. P3 then searches the remaining MS/MS data against a sequence library for the identified protein to extract all of the nonproteotypic peptides from each protein present in the data [138].

We have prepared sequence coverage maps for each protein that result from the analysis by each tool (See appendix A). All peptide hits from the algorithms used in the analysis were manually examined, as indicated in methods for peptide acceptance criteria in the bioinformatics section. Generally, the same peptides were identified by each software tool, although there were some differences in the peptide lists (see table 5, above, for an example). These differences can be rationalized by nontraditional cleavages (invisible to Mascot), and how each algorithm treats the dataset, particularly with regard to potential modifications. See figure 8 for a graphical representation of the functional classifications of the identified proteins that we determined while surveying the literature in preparation for developing the models described later. The bins were developed from surveyed literature and were designed to reflect general classifications (e.g. metabolism-related proteins, cytoskeletal proteins, etc.).

96 Hr Infect +/- 50 uM Securinine

For this second experimental set, we utilized a second generation pair of ZDyes named BDRI227 (green) and ZB-dipropyl (blue) that did not require gel fixing before the scanning step. The first generation blue Zdye that we used gave a high fluorescent background artifact in the gel which could be removed by fixation. The second generation blue Zdye did not produce the artifact, and thus did not require fixation. Labeling proceeded at 1X@RT as described above, as did IEF strip loading. The pooled internal standard was not utilized in this series of experiments, as it had been

determined to cause statistical correlation (as described above). We ran all separations in this series on both 3-11NL and 4-7 IEF strips. Gels for this series of experiments are represented by their final Progenesis master images as seen in figures 16-19. Identifications were made by MS analysis as above.

Please note that this treatment condition is infection followed by treatment with Securinine. Securinine exposure levels, and the timing of Securinine treatment were not the same as in previous dataset. Because of these considerations, and because we were only able to use two biological replicates, which will reduce the robustness of the statistical calculations, this dataset was not modeled as extensively as previous datasets. Rather than create a comprehensive systems model for this dataset, we binned the data in likely function(s) of each protein and tabulated (see figure 20). Note that many of the proteins have more than one potential function, and the binned results indicate function(s) for the detected proteins that are likely to be active in this system based on a survey of the literature. In addition, the detected cell death (likely some form of apoptosis) appears to be affecting many systems in a manner that is not entirely consistent with previously observed results (Securinine alone and infection alone).

As an example, Hsp70 is detected in both Securinine stimulated samples and in the 96 hr +/- Securinine data. While this is probably due to the presence of Securinine, the upregulation of Hsp70 in 96 hr +/- Securinine does not occur to nearly the same extent in terms of the number of different isoforms as in samples stimulated with Securinine alone, suggesting that other factors are at work which we cannot tie to a

single source. In samples stimulated with Securinine alone, we saw seven Hsp70 isoforms differentially expressed, six of which were in the soluble fraction, and one in the membrane fraction. In 96 hr postinfection samples there is no detected change in Hsp70 expression. In 96 hr infection +/- Securinine, we see changes in Hsp70 expression only in the membrane fraction. We are unable to determine whether the reduction in number of Hsp70 detections in the soluble fraction is due, for example, to *C. burnetii* inhibiting expression changes, or the monocyte responding to infection+Securinine, or some combination of the two.

It was also observed that in the infection+Securinine samples, there was pronounced downregulation of MHC antigens, where there was no indication of any changes in the previous datasets. The observation that MHC antigens were downregulated in infection+Securinine samples suggests that in either Securinine alone or infection alone, we should have seen some indication that MHC antigens were upregulated. MHC antigens were not observed to up- or downregulated in either Securinine alone or infection alone datasets.

We observed cell death visually under the microscope in the infected+Securinine samples provided by Kirk Lubick, but not in the infected alone or Securinine alone samples (data not shown) and this was strongly supported by the measurements of protein content in the samples. Specifically, the yield of soluble fraction protein in the infected + Securinine samples was significantly lower than would have been expected (presumably soluble fraction proteins were lost to the growth media), but membrane

fraction protein yields were in the expected range (expectations based on analysis of protein levels in previous samples). Soluble protein yields from the 96 hr infection - Securinine were ~ 13 mg in the samples provided (~13-15 mg of soluble fraction protein from previous samples). In stark contrast, the soluble protein yields from 96 hr infection+Securinine were ~1.5 mg. Membrane yields from this second experimental set were in the 3-4 mg range, which is the range expected from previous samples (e.g. Securinine membrane fraction). Membranes from lysed and unlysed cells will pellet following high speed centrifugation, but soluble fraction proteins lost to the growth media due to apoptosis/cell death could not be recovered as this fraction was not collected.

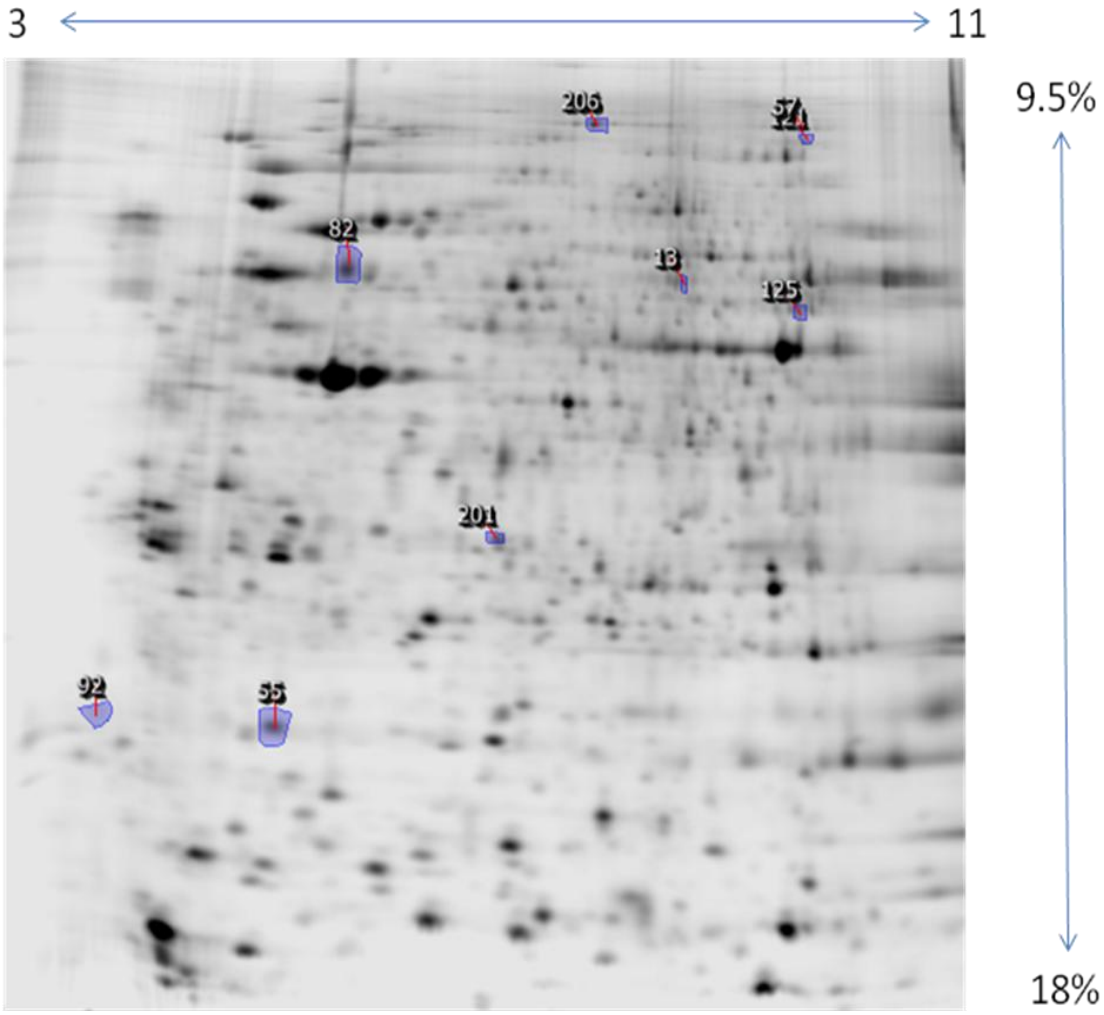

Figure 16: 96 hr infection +/- 50 uM Securinine 3-11NL soluble fraction. Final Progenesis master image following image analysis and offline statistical analysis. Analysis includes 2 biological replicates with 4 technical replicates in biological replicate 1 and 6 technical replicates in biological replicate 2, each with reciprocal labeling.

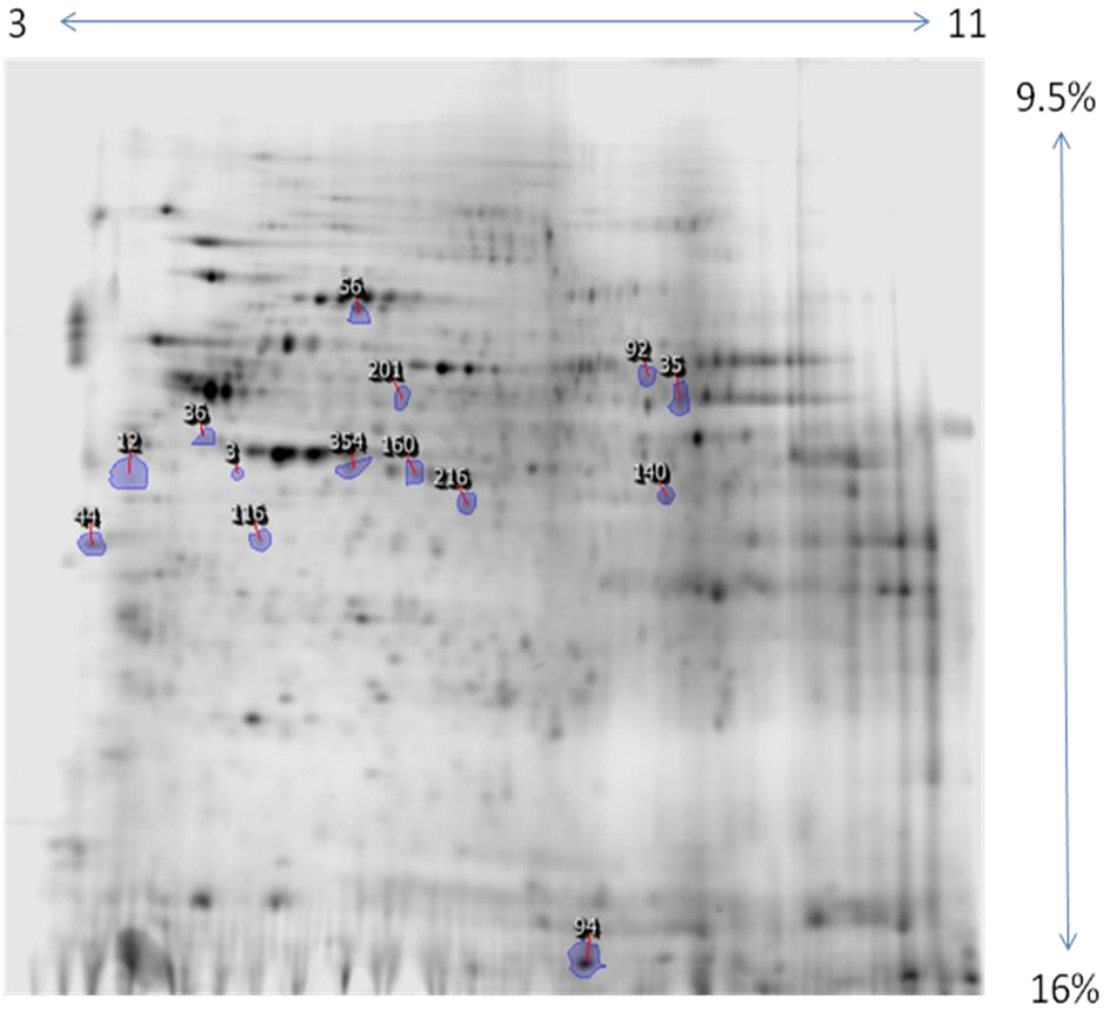

Figure 17: 96 hr infection +/- 50 uM Securinine 3-11NL membrane fraction. Final Progenesis master image following image analysis and offline statistical analysis. Analysis includes 2 biological replicates with 6 technical replicates, each with reciprocal labeling.

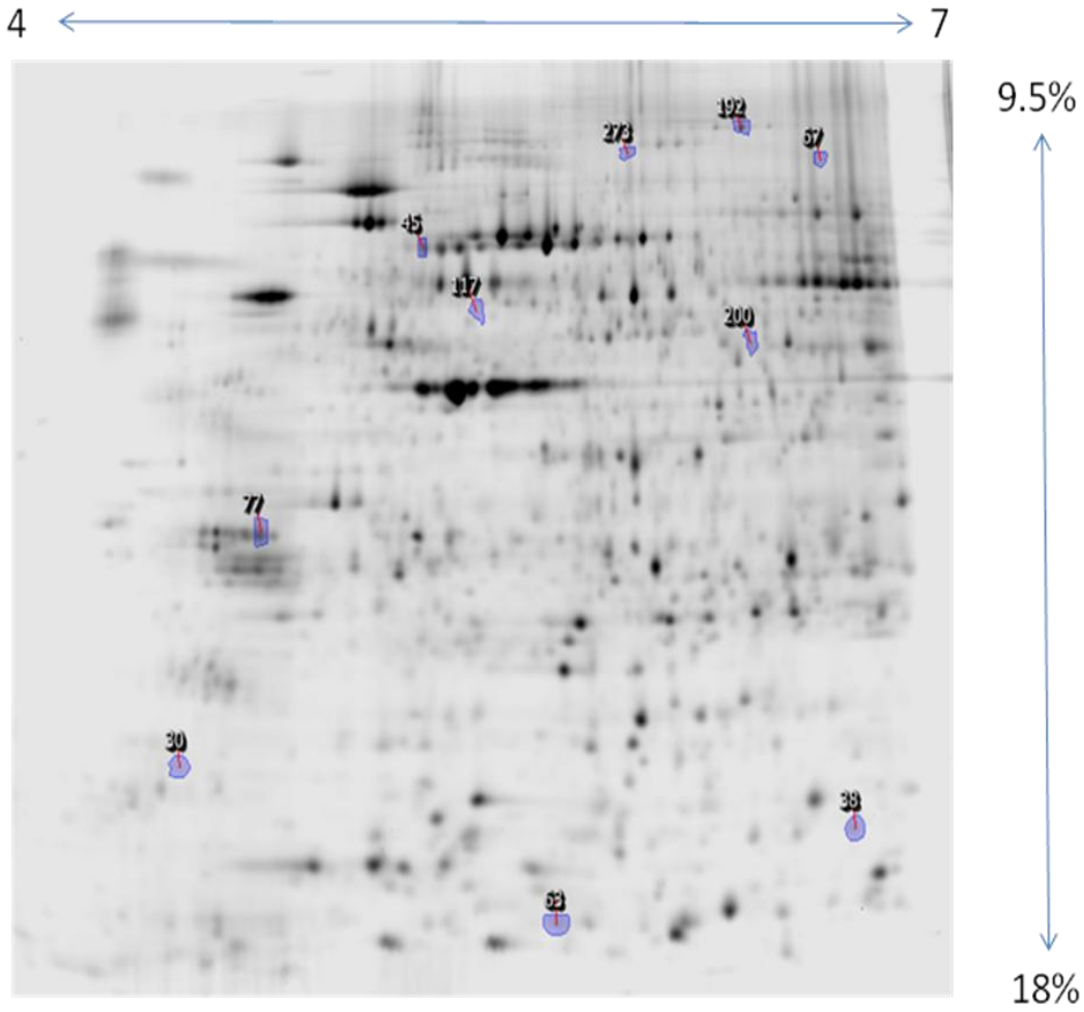

Figure 18: 96 hr infection +/- 50 uM Securinine 4-7 soluble fraction. Final Progenesis master image following image analysis and offline statistical analysis. Includes 2 biological replicates including 4 technical replicates for biological replicate 1 and 5 for biological replicate 2, with reciprocal labeling.

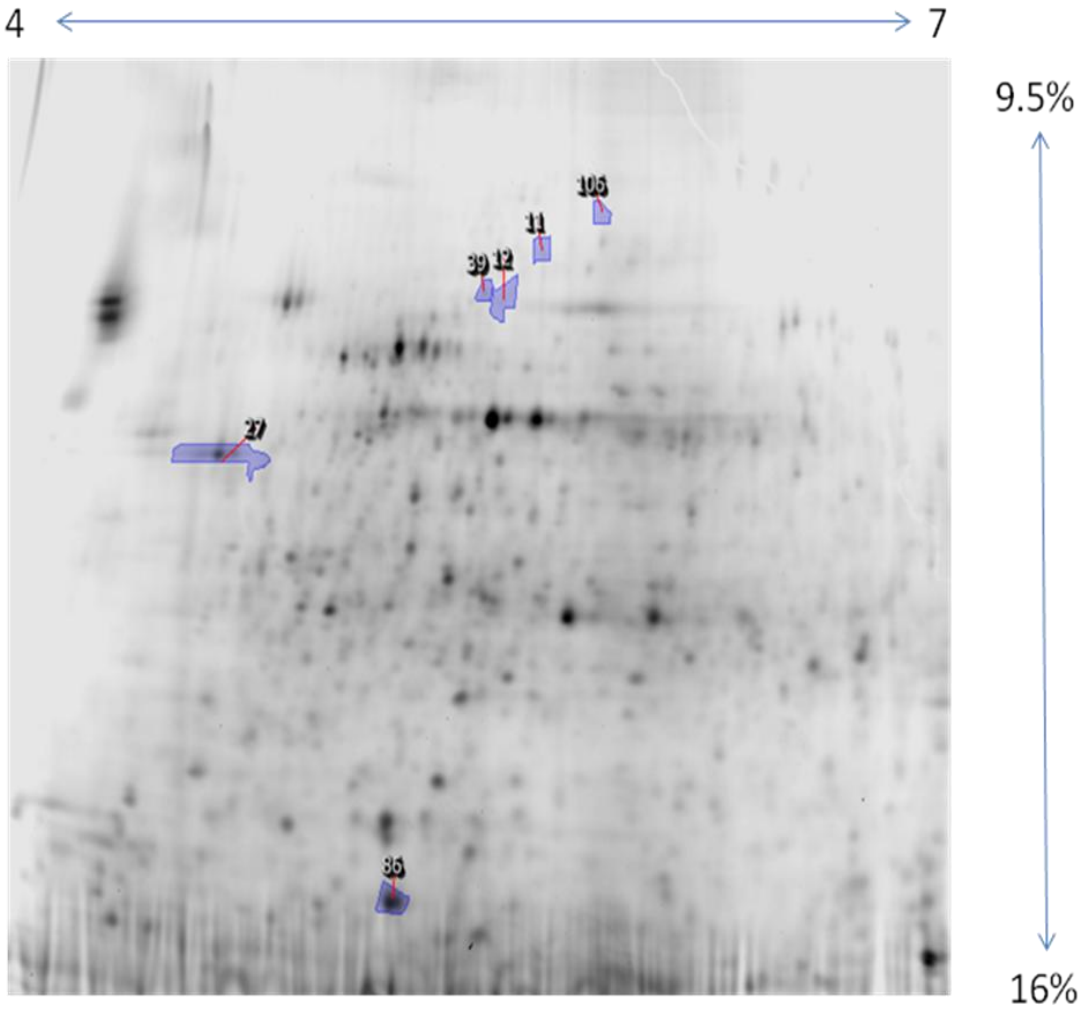

Figure 19: 96 hr infection +/- 50 uM Securinine 4-7 membrane fraction. Final Progenesis master image following image analysis and offline statistical analysis. Analysis includes 2 biological replicates with 5 technical replicates for biological replicate 1 and 6 for biological replicate 2, including reciprocal labeling.

Table 10: Statistical summary and bioinformatics data for regulated proteins in the 96 hr infection +/- 50 uM Securinine 3-11NL soluble fraction samples.

Test condition	Spot #	Fold change	Univariate GLM p-value	Univariate GLM power score	ID	Mascot score	Mascot unique peptides	Mascot % coverage	X!Hunter score	X!Hunter %FDR	X!Hunter # unique peptides	X!Hunter % coverage	P3 score	P3 FDR	P3 # unique peptides	P3 % coverage
3-11NL sol	13	3.9	0.0158	.953	chaperonin containing TCP1, subunit 6A isoform A	698	7	19.3	-80.1	0.45	10	15.8	-76.0	0.94	12	21.3
	55	-2.5	0.0376	.721	Eukaryotic translation initiation factor 5a	98	2	12.3	-40.9	0.46	5	40.0	u/i	u/i	u/i	u/i
	57	-2.5	0.0053	1.000	Eukaryotic translation elongation factor 2	401	6	9.9	-84.7	0.87	9	11.0	-101.7	1.48	9	12.1
	82	2.3	0.0313	.785	Hsp60/chaperonin	1417	15	31.8	-262.8	0.52	35	49.4	-146.7	1.16	22	35.3
	92	-2.2	0.0201	.909	Calmodulin	221	3	36.2	-35.3	0.51	3	24.8	-12.5	1.82	2	16.8
	121	-2	0.0274	.827	Staphylococcal nuclease domain containing protein 1	615	10	11.8	-112.2	0.67	15	16.8	-49.9	0.99	7	7.7
	125	2	0.0051	1.000	Glutamate dehydrogenase 1	1076	13	24.4	-178.1	0.39	24	35.1	-147.2	1.58	15	26.0
	200	-1.7	0.0372	.724	Proteasome activator subunit 1 isoform 1	690	8	36.1	-100.3	0.36	16	39.4	-88.0	1.17	13	36.1
	205	-1.7	0.0318	.779	vinculin isoform VCL	2096	27	20.5	-234.8	0.5	44	26.7	-243.8	1.26	51	23.5

Table 11: Statistical summary and bioinformatics data for regulated proteins in the 96 hr infection +/- 50 uM Securinine 3-11NL membrane fraction samples.

Test condition	Spot #	Fold change	Univariate GLM p-value	Univariate GLM power score	ID	Mascot score	Mascot unique peptides	Mascot % coverage	X!Hunter score	X!Hunter %FDR	X!Hunter # unique peptides	X!Hunter % coverage	P3 score	P3 FDR	P3 # unique peptides	P3 % coverage
3-11NL mem	3	-6.8	.034	.752	MHC class I histocompatibility antigen HLA alpha chain precursor	310	4	13.1	not found	not found	not found	not found	-40.8	1.44	4	12.7
	12	-5.3	.008	.998	Vimentin (cleaved under calpain	1855	26	43.1	-145.5	0.46	23	37.1	-128.0	1.31	14	27.7
	35	4	.022	.888	pyruvate kinase	460	7	18.1	-86.2	0.57	7	21.3	-61.2	0.73	7	16.8
	36	-3.9	.004	1.000	Hsp60 (cleavage induced by calpain)	1722	18	24.1	-132.4	0.60	19	26.2	-83.7	1.13	12	18.0
	44	3.6	.029	.815	Proliferating cell nuclear antigen	542	7	29.9	-57.3	0.65	11	29.9	-46.2	0.81	10	27.2
	56	3.4	.023	.873	Hsp70	1494	20	26.2	-154.6	0.55	14	24.1	-125.7	1.12	17	24.3
	92	2.8	.003	1.000	pyruvate kinase	347	6	14.7	-85.7	0.63	9	24.3	-49.1	1.23	6	16.0
	94	-2.8	.007	.999	β2 microglobin	not found*	not found*	not found*	-48.7	0.52	4	26.9	-11.0	1.86	4	26.9
	116	-2.5	.032	.776	N-ethylmaleimide-sensitive factor attachment protein, alpha	504	8	34.6	-96.9	0.55	10	41.7	-81.1	0.86	15	32.9
	140	2.4	.004	1.000	unidentified											
	160	-2.2	.003	1.000	MHC class 1 antigen	839	10	24.3	-49.3	0.46	6	16.7	-57.6	1.30	6	13.7
	201	-2	.015	.958	Alpha tubulin	227	3	12.2	-113.8	0.59	11	23.7	-68.5	1.13	9	23.1
	216	1.9	.018	.931	MHC class I histocompatibility antigen HLA alpha chain precursor	183	3	12.9	-32.3	0.74	3	10.2	-33.7	1.31	4	10.1
	354	-1.5	.035	.750	SPFH domain family, member 2 isoform 1	356	5	31.6	-28.2	0.62	2	6.8	-52.4	1.33	7	15.0

Table 12: Statistical summary and bioinformatics data for regulated proteins in teh 96 hr infection +/- 50 uM Securinine 4-7 soluble and 4-7 membrane fraction samples.

Test condition	Spot #	Fold change	Univariate GLM p-value	Univariate GLM power score	ID	Mascot score	Mascot unique peptides	Mascot % coverage	X!Hunter score	X!Hunter %FDR	X!Hunter # unique peptides	X!Hunter % coverage	P3 score	P3 FDR	P3 # unique peptides	P3 % coverage
4-7 sol	30	-3.8	0.0328	.769	myosin, light chain 6, alkali, smooth muscle and non-muscle isoform 1	268	5	24.5	-30.6	0.64	6	35.1	-26.0	1.74	5	24.5
	38	3.7	0.0007	1.000	peptidylprolyl isomerase A	189	3	23.0	-39.9	0.72	3	23.0	-13.7	0.31	2	16.4
	45	-3.6	0.0210	.900	L-plastin	786	12	25.8	-90.1	0.75	10	18.3	-98.1	1.19	7	14.8
	63	3.1	0.0126	.979	S100 Ca binding protein A11	134	2	25.7	-15.6	0.52	2	25.7	-14.4	0.79	2	25.7
	67	-3	0.0232	.875	programmed cell death 6 interacting protein	1968	24	22.3	-135.7	0.38	17	20.2	-165.5	1.31	26	22.1
	77	2.8	0.0009	1.000	tropomyosin 3 isoform 2	628	7	27.4	-101.4	0.67	13	35.5	-76.1	1.35	13	33.2
	117	-2.4	0.0295	.804	chaperonin	1378	15	25.8	-137.8	0.62	15	28.4	-79.9	1.41	10	25.8
	192	-1.9	0.0138	.970	vinculin isoform VCL	602	8	8.4	-68.4	0.73	8	8.7	-129.0	1.26	14	9.2
	200	-1.9	0.0184	.928	enolase 1	1151	15	40.0	-118.6	0.38	16	36.9	-83.6	1.87	12	28.8
	273	-1.7	0.0006	1.000	glycogen phosphorylase	190	3	7.7	-48.2	0.78	5	7.4	-49.4	1.91	4	5.4
4-7 mem	11	3.4	0.0020	1.000	Hsp70 protein 8 isoform 1	1902	21	27.6	-129.0	0.47	20	21.5	-197.0	1.57	29	32.2
	12	3.4	0.0193	.918	Hsp60	780	10	22.7	-80.0	0.40	12	18.3	-105.6	1.66	10	15.2
	27	-2.7	0.0368	.728	calreticulin precursor	458	3	10.8	-32.3	0.55	6	8.9	-36.0	0.88	8	10.8
	39	2.6	0.0153	.958	Hsp60	1545	15	25.7	-163.7	0.32	24	27.2	-157.2	1.26	24	29.1
	86	-2.1	0.0195	.916	beta-galactoside-binding lectin precursor	582	3	51.1	-70.2	0.5	14	64.4	-45.2	1.26	17	52.6
	106	2	0.0145	.964	NADH dehydrogenase (ubiquinone) Fe-S protein 1, 75 kDa (NADH-coenzyme Q reductase)	612	8	13.1	-112.8	0.56	14	21.0	-97.1	1.49	11	14.9

Figure 20

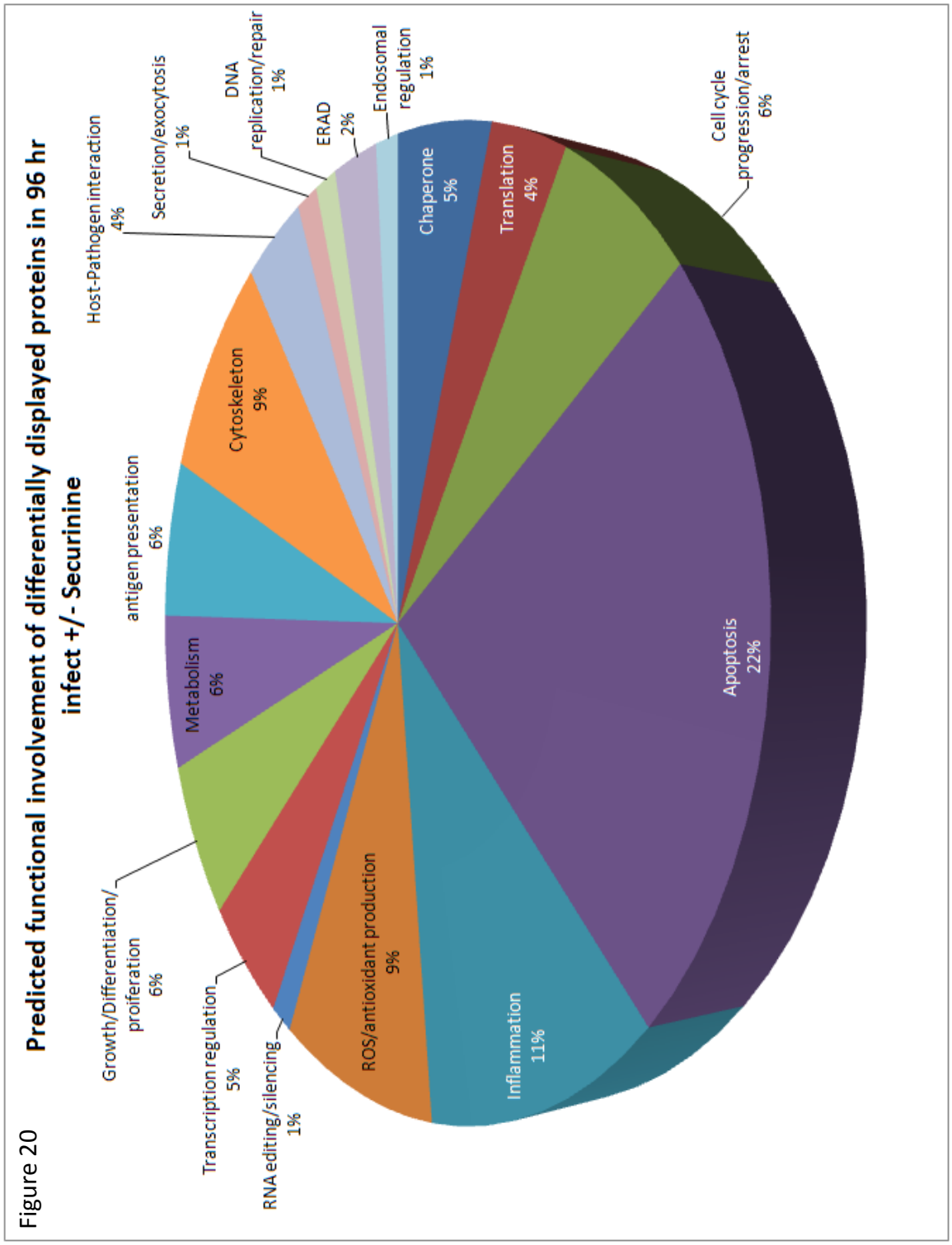
Predicted functional involvement of differentially displayed proteins in 96 hr infect +/- Securinine
Host-Pathogen interaction 4%
Secretion/exocytosis 1%
DNA replication/repair 1%
ERAD 2%
Endosomal regulation 1%
Chaperone 5%
Translation 4%
Cell cycle progression/arrest 6%
Apoptosis 22%
Inflammation 11%
ROS/antioxidant production 9%
RNA editing/silencing 1%
Transcription regulation 5%
Growth/Differentiation/ proiferation 6%
Metabolism 6%
antigen presentation 6%
Cytoskeleton 9%

Figure 20: (Previous page) Pie chart of binned protein functions from the 96 hr infection +/- 50 uM Securinine dataset based on a survey of the literature.. Chart depicts the literature identified functions and the approximate percentage of the dataset that a particular function represents, note that many proteins have more than one proposed function.

Table 13: Uniprot accession numbers and corresponding protein ID searched against DAVID and GOEAST

+/- Securinine	
Uniprot #	Protein ID
Q9NZL4	Hsp70 protein 1
Q53GZ6	Hsp70 protein 8
Q01469	FABP5
P13796	L-plastin
P26447	S100A4
P30740	SERPINB1
P10599	thioredoxin
P07900	Hsp90
P60709	beta actin
P10809	Hsp60
P20839	IMPDH

+/-Infected	
Uniprot #	Protein ID
P10809	Hsp60
Q6LEN1	MnSOD
P06702	S100A9
P43490	visfatin
P05109	S100A8
P37837	Transaldolase 1
Q15181	inorganic pyrophosphatase
Q15691	EB1
Q16658	fascin
P28838	LAP3
P08670	vimentin
P51149	Rab7
Q13011	ECH1
P05091	Aldh2

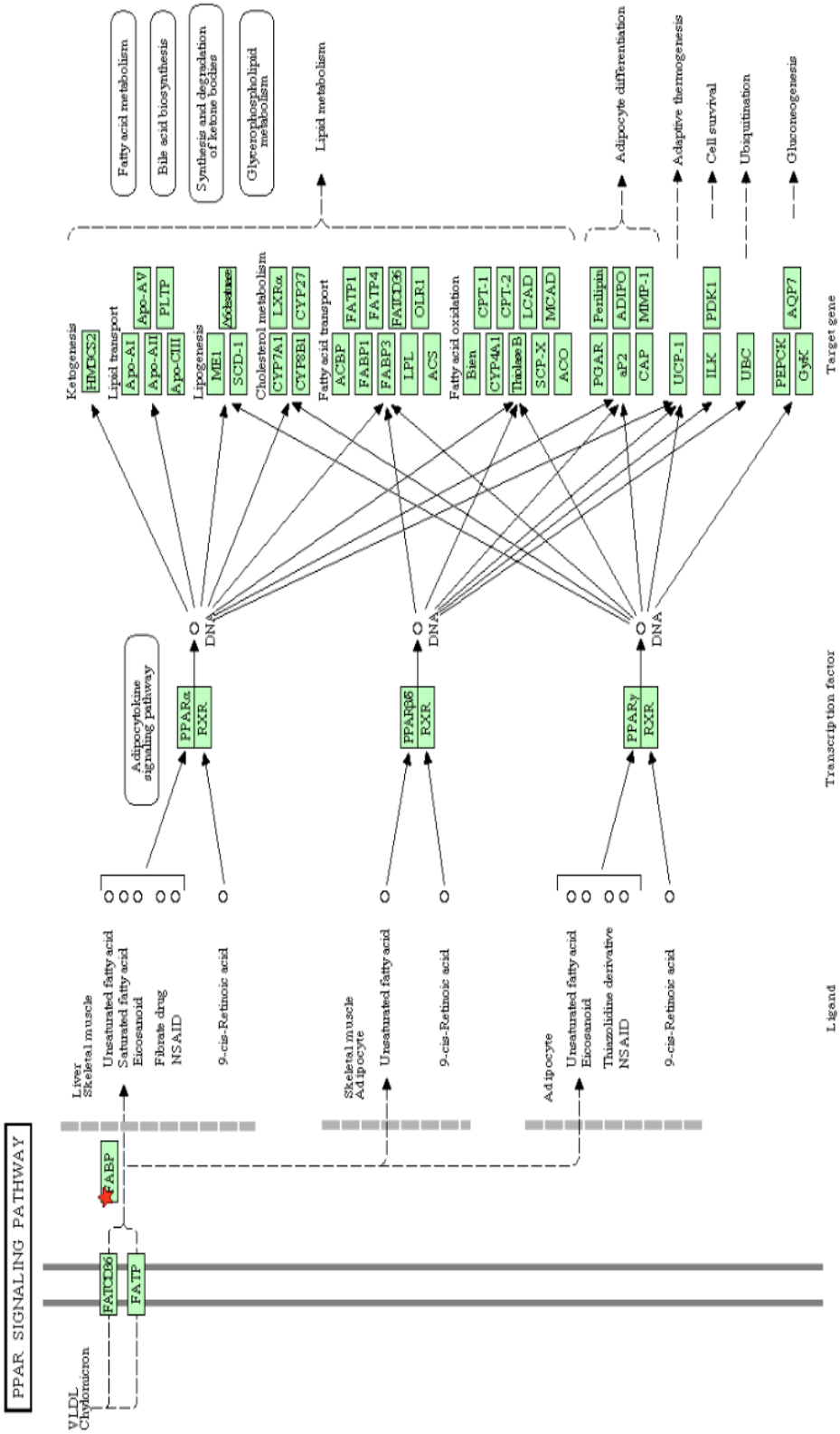

Figure 21: Pathway by KEGG (via DAVID) for Fatty acid binding protein 5 (FABP). FABP is highlighted by a red star. In this example, we see how FABP fits within the PPAR signaling pathway and some of the likely downstream functional effects, including cholesterol metabolism, lipid transport, and metabolic consequences.

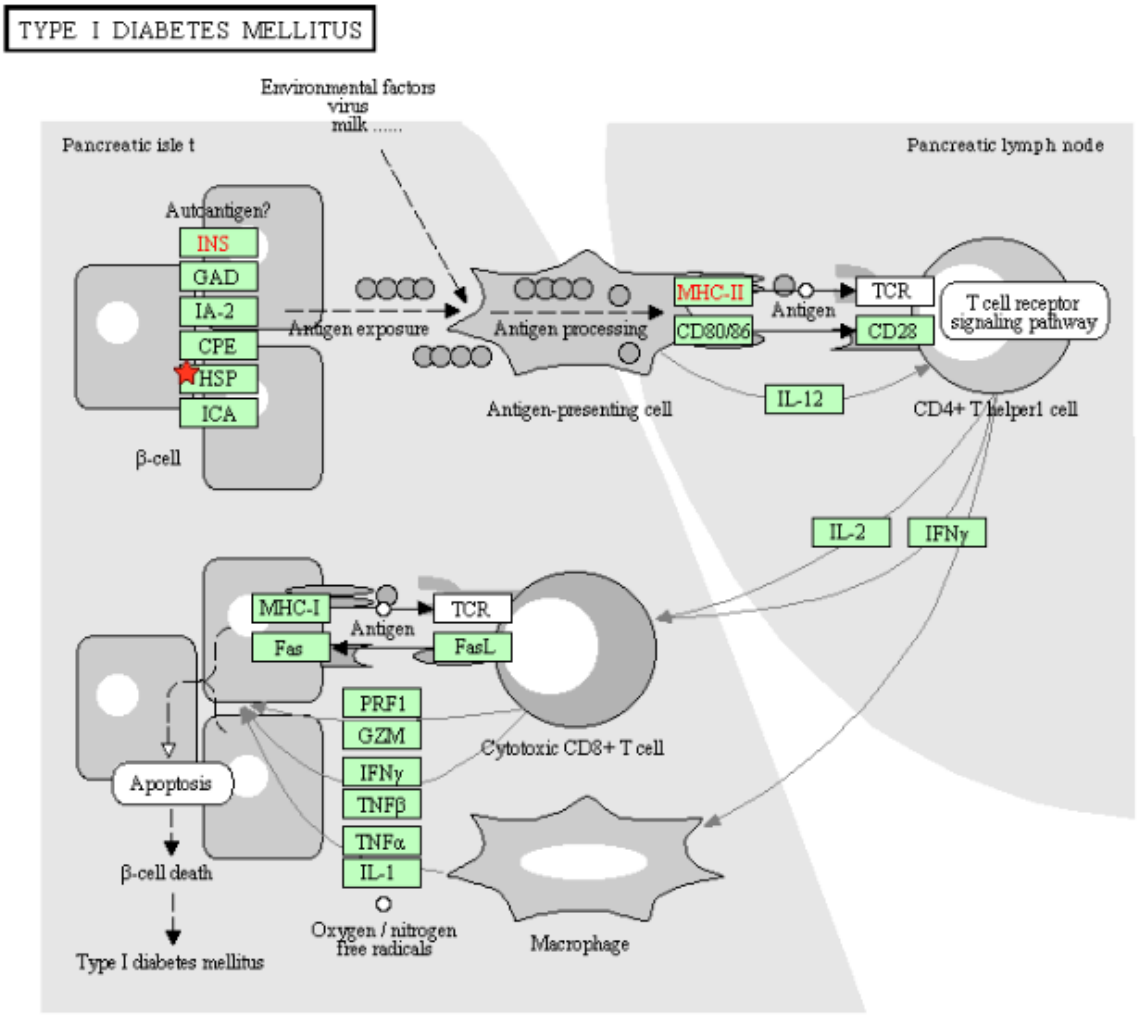

Figure 22: Pathway generated by KEGG (via DAVID) showing the role of Hsp60 in antigen processing. Hsp60 is indicated by the red star. Although taken from a diabetes example, the pathway does demonstrate how Hsp60 is involved in the activation of MHCII antigen presentation to T cells.

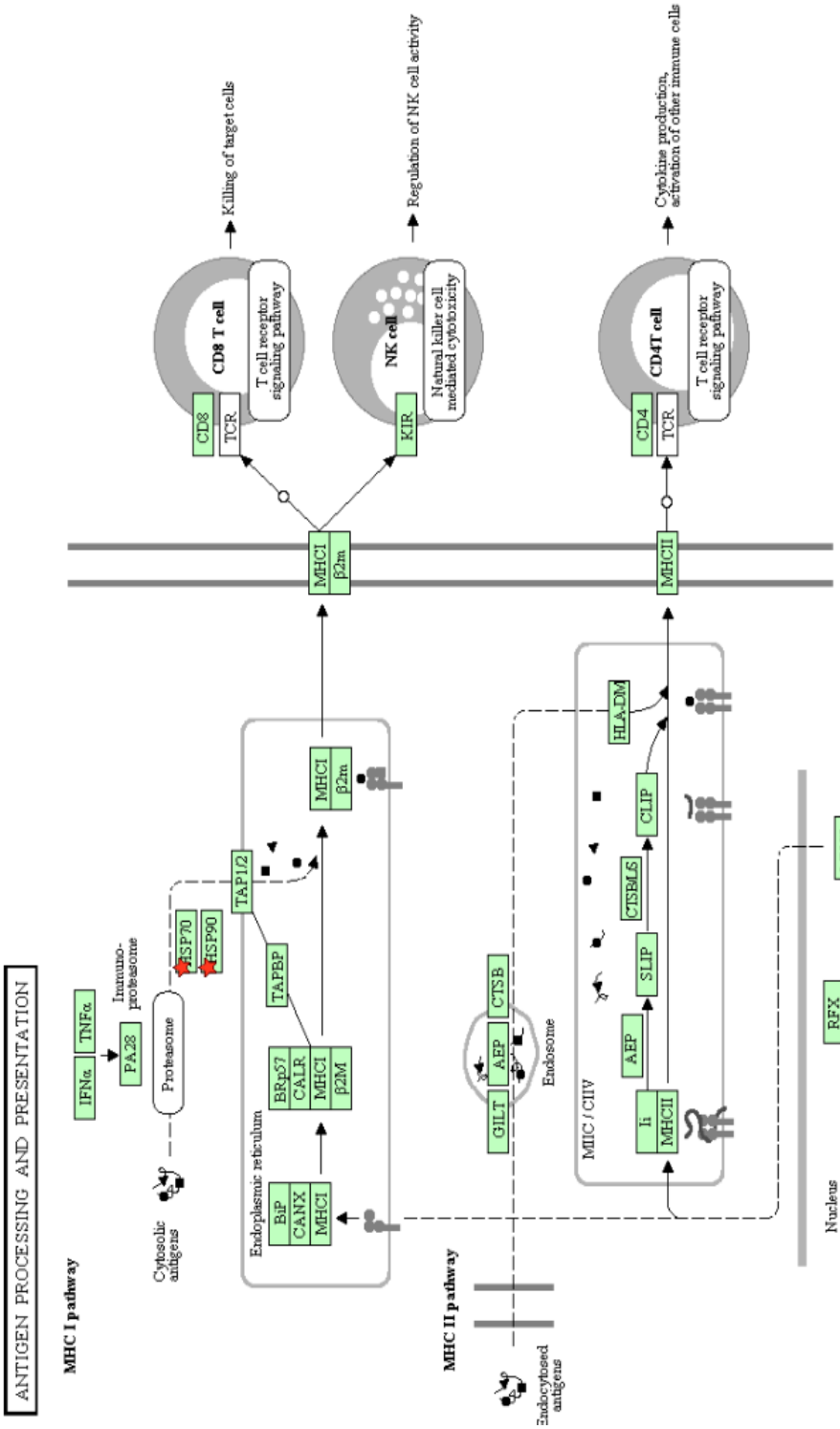

Figure 23: Pathway generated by KEGG (via DAVID) showing the involvement of Hsp70 and Hsp90 (red stars) in MHCI antigen presentation.

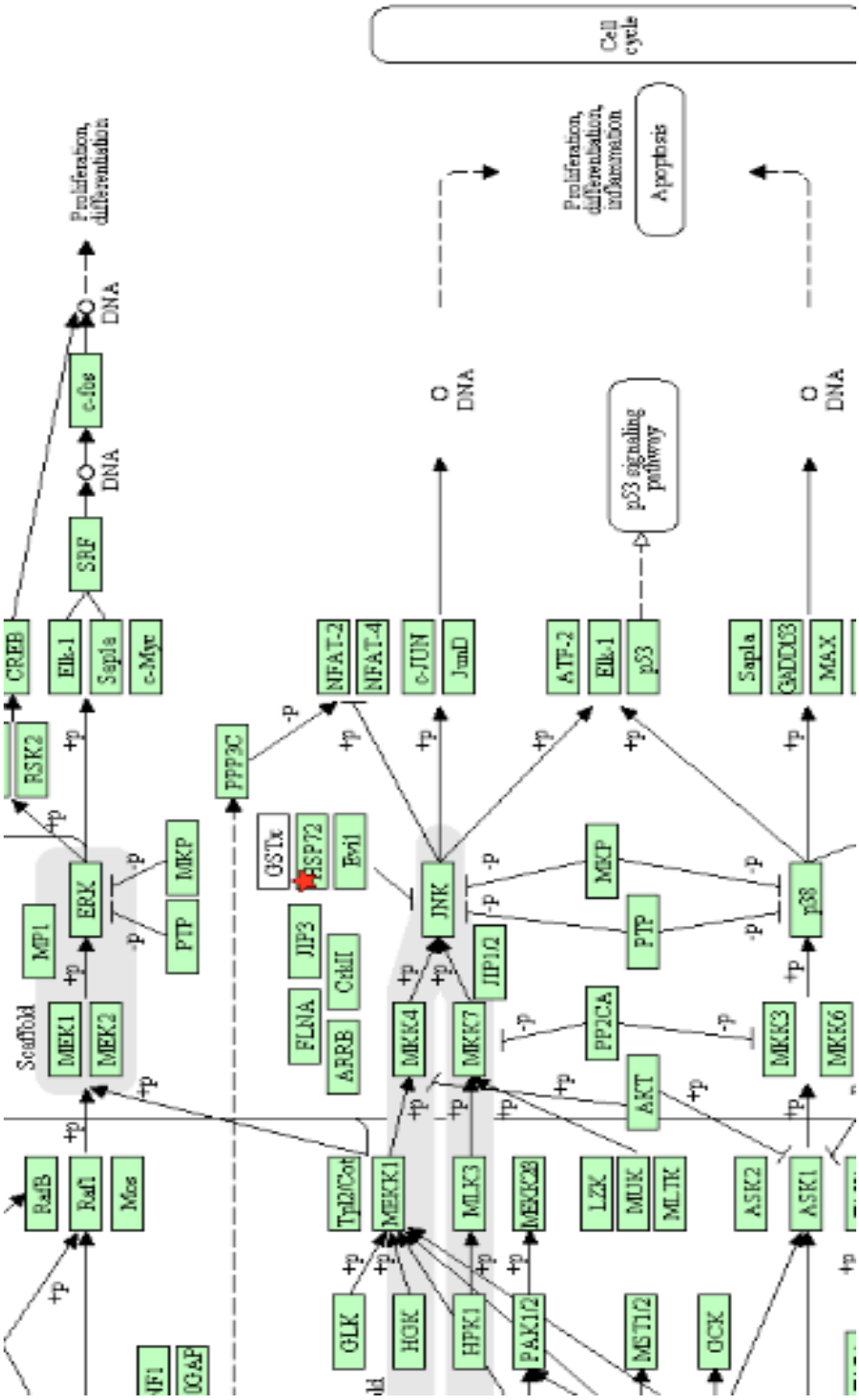

Figure 24: Detail of a pathway generated by KEGG (via DAVID) showing the role of Hsp70 (red star) in the inhibition of apoptosis by inhibiting Jnk signaling.

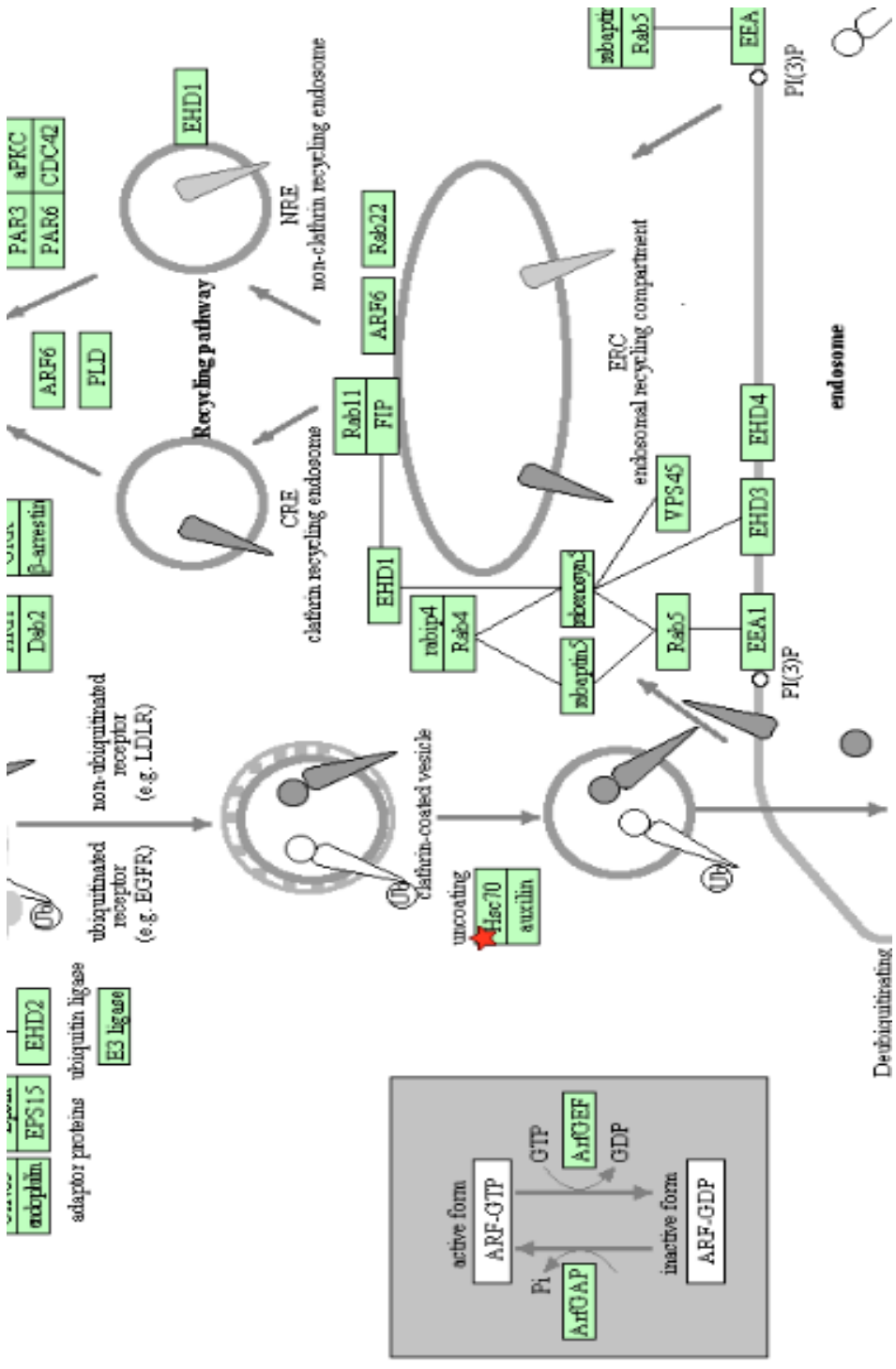

Figure 25: Detail from a pathway generated by KEGG (via DAVID), demonstrating the involvement of Hsp70 (red star) in the regulation of endocytosis.

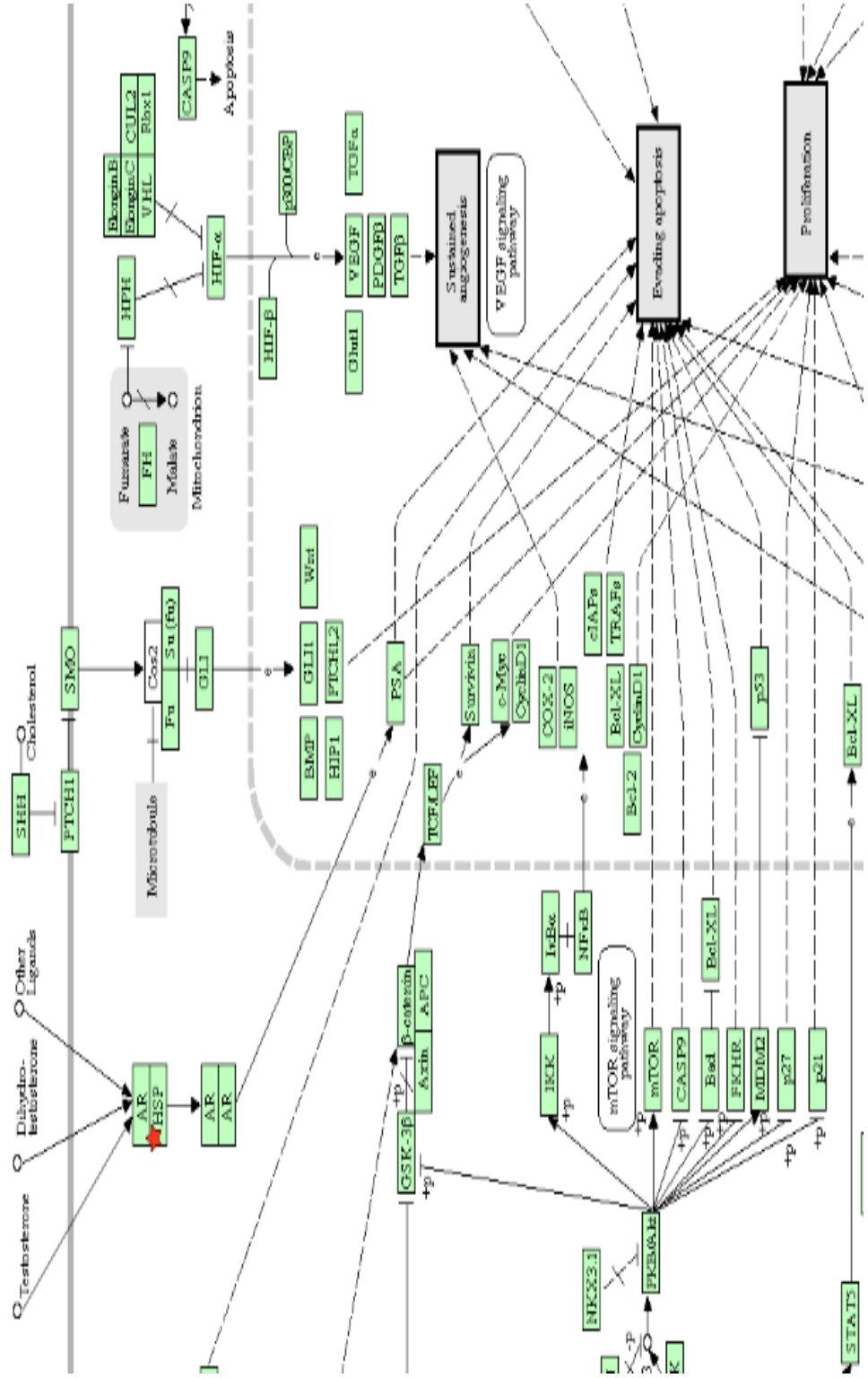

Figure 26: Detail of a pathway generated by KEGG (via DAVID) showing the role of Hsp90 (red star) in evading apoptosis and promoting cellular proliferation.

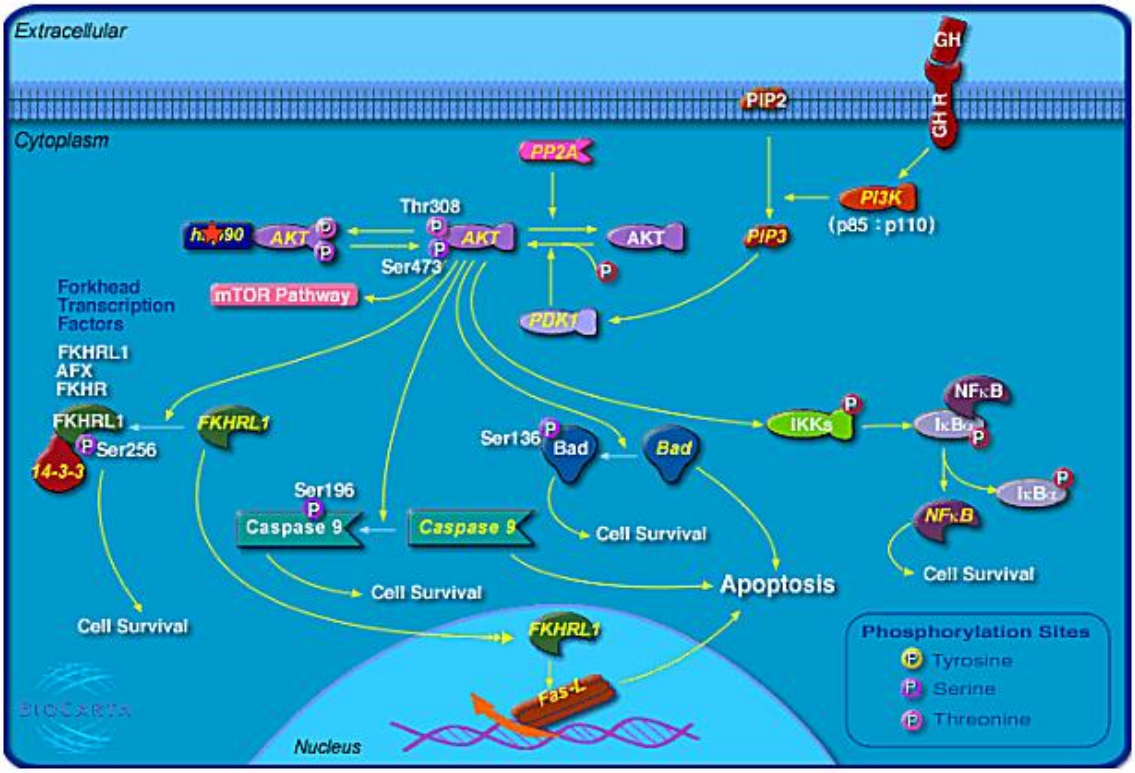

Figure 27: Pathway generated by DAVID showing one of Hsp90's (red star) client proteins, Akt and it's role in downstream signaling. Reprinted with permission from Biocarta, listed as AKT Signaling Pathway.

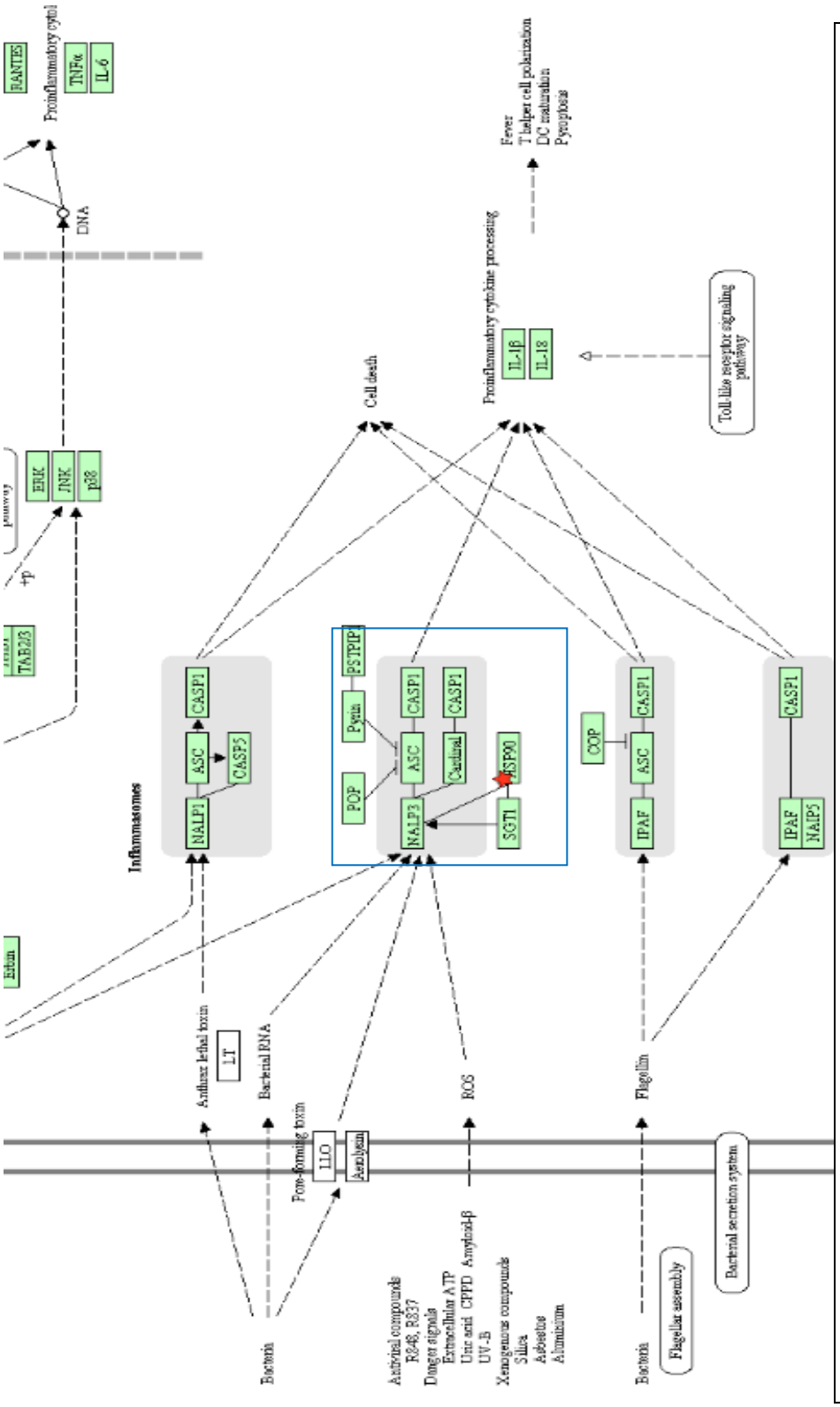

Figure 28: Detail from a pathway generated by KEGG (via DAVID) showing the role of Hsp90 in NOD-like receptor signaling (blue box). See figure 56 in the Hsp90 section of the discussion below for more details.

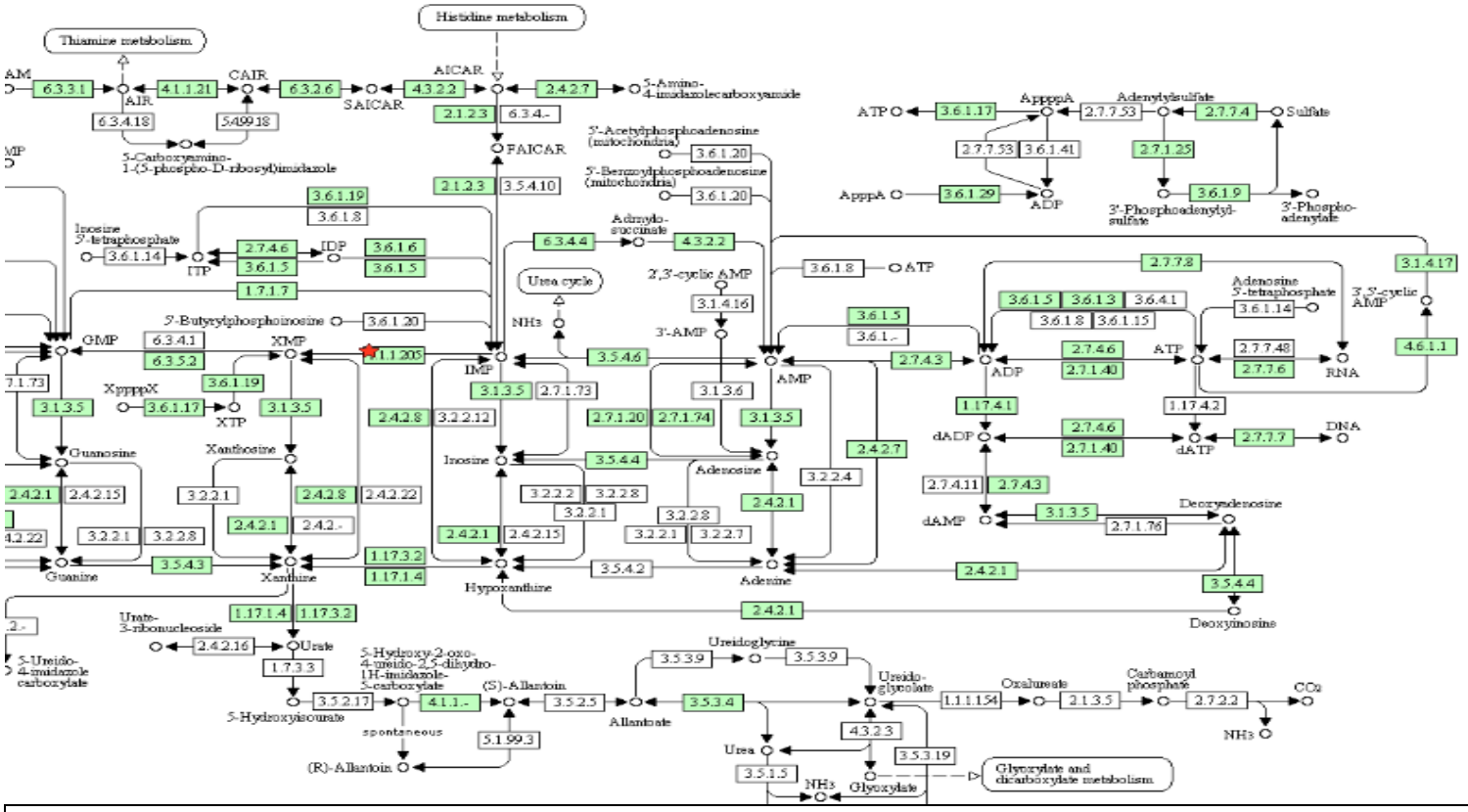

Figure 29: Detail from a pathway generated by KEGG (via) DAVID showing the various metabolic routes that can produce inosine-5'-monphosphate (IMP), and its processing by IMP dehydrogenase (IMPDH, red star) to xanthosine-5'-monophostate. The various protein numbers refer to enzyme (EC) numbers. Although this diagram does not cover the functional biological consequences (discussed below) of upregulated IMPDH it does give potential

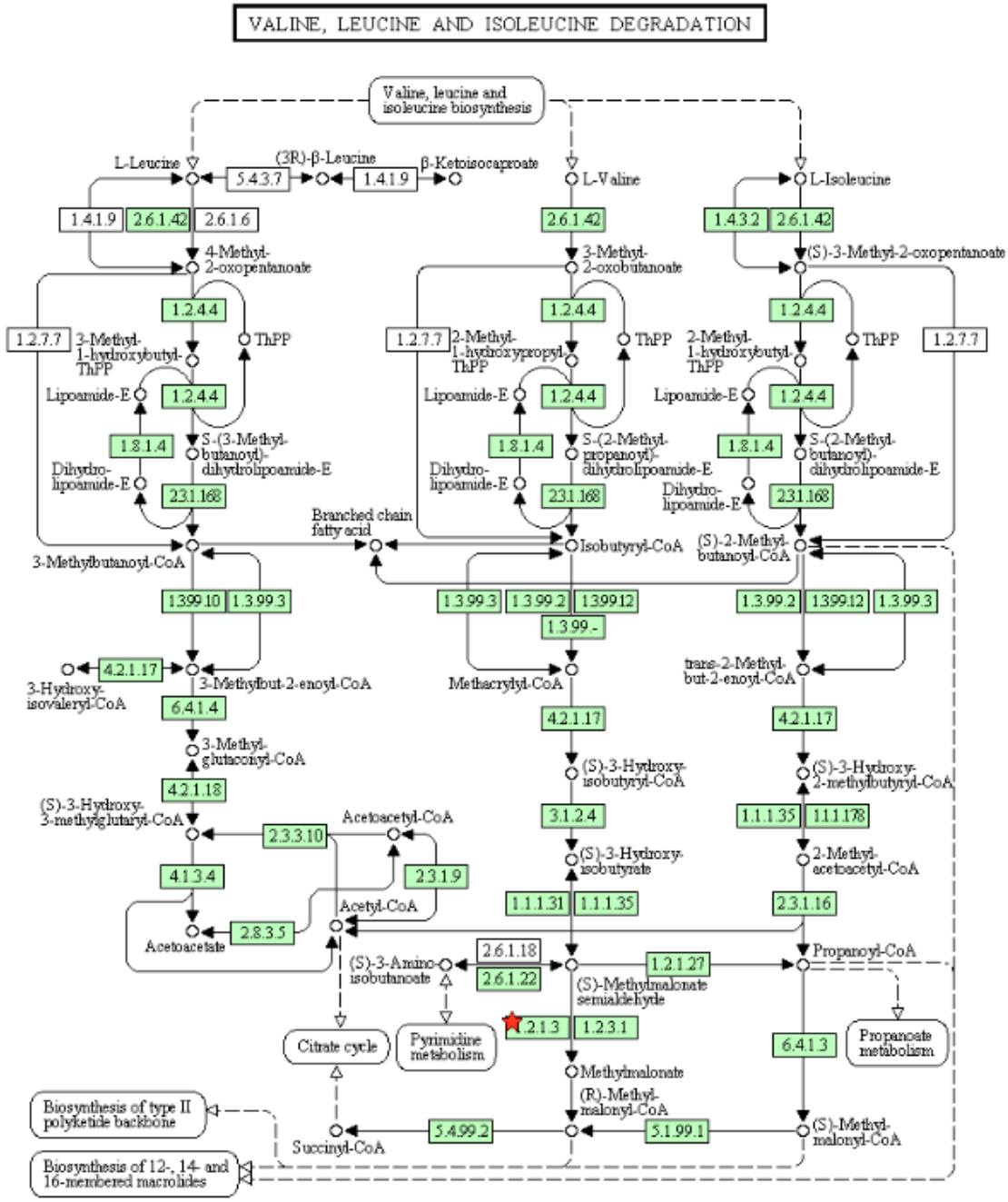

Figure 30: Pathway generated by KEGG (via DAVID) showing the role of Aldehyde dehydrogenase 2 (Aldh2, red star) in the amino acid degradation pathways for Val, Leu, Ile, suggesting metabolic products that could be monitored. The various protein numbers refer to enzyme (EC) numbers.

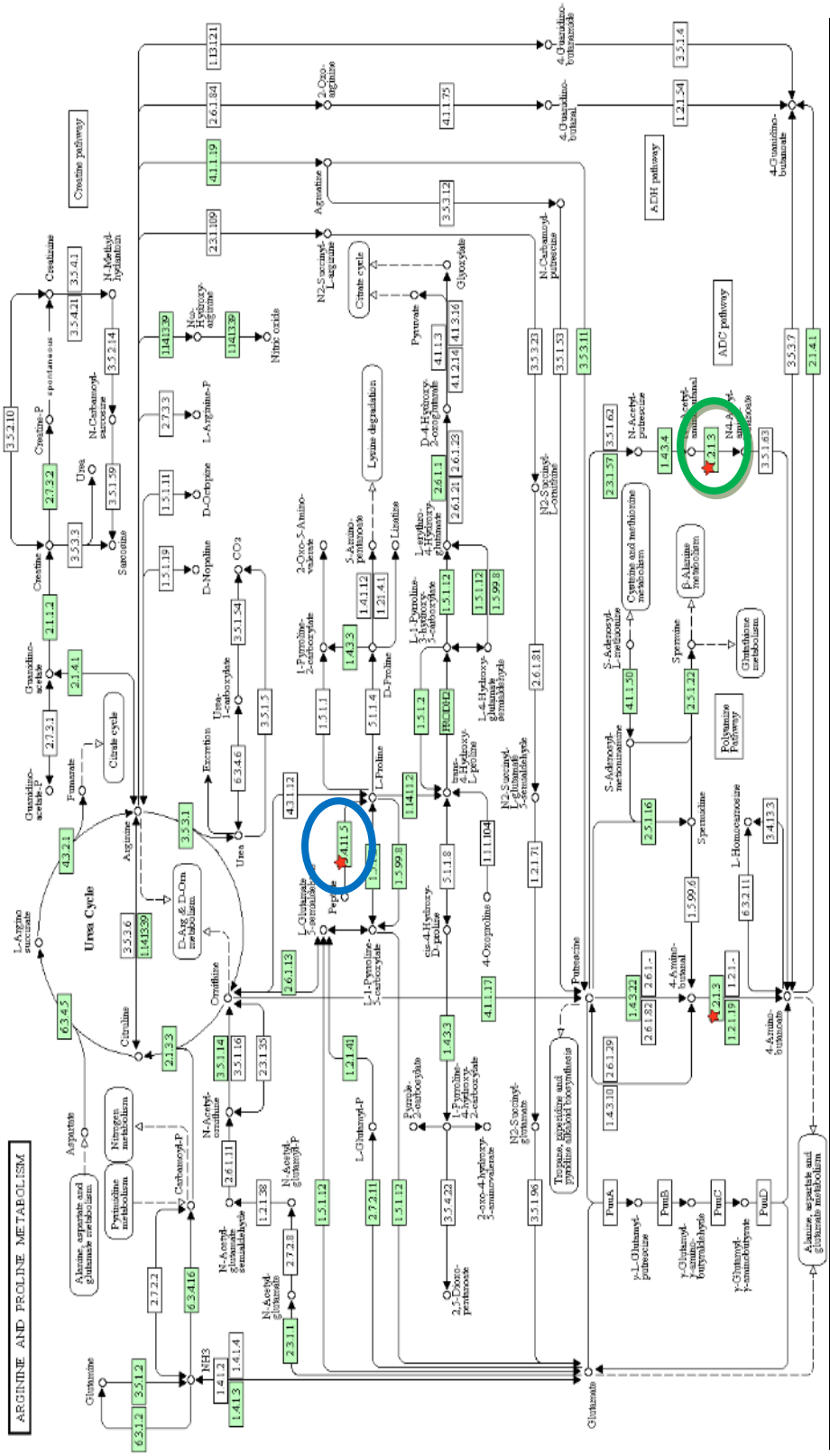

Figure 31: Pathway generated by KEGG (via DAVID) showing the role of Aldehyde dehydrogenase 2 (Aldh2, red stars in green circle) and Lap3 (red star in blue circle) in the amino acid metabolic pathways for Arg, and Pro suggesting metabolic products that could be monitored. The various protein numbers refer to enzyme (EC) numbers.

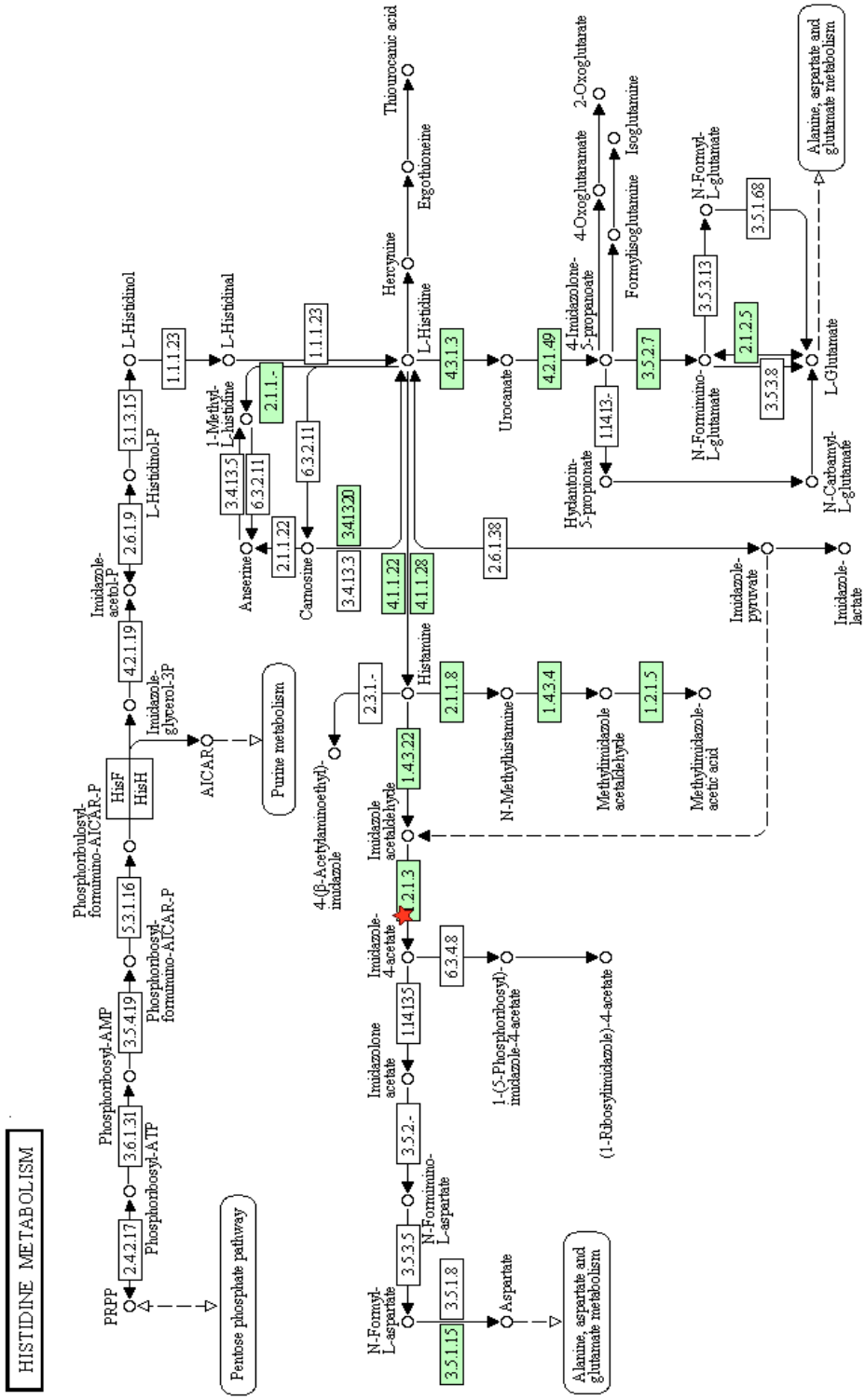

Figure 32: Pathway generated by Kegg (via DAVID) showing the role of Aldehyde dehydrogenase 2 (Aldh2, red star) in the amino acid metabolic pathway for His suggesting metabolic products to monitor. The various protein numbers refer to enzyme (EC) numbers.

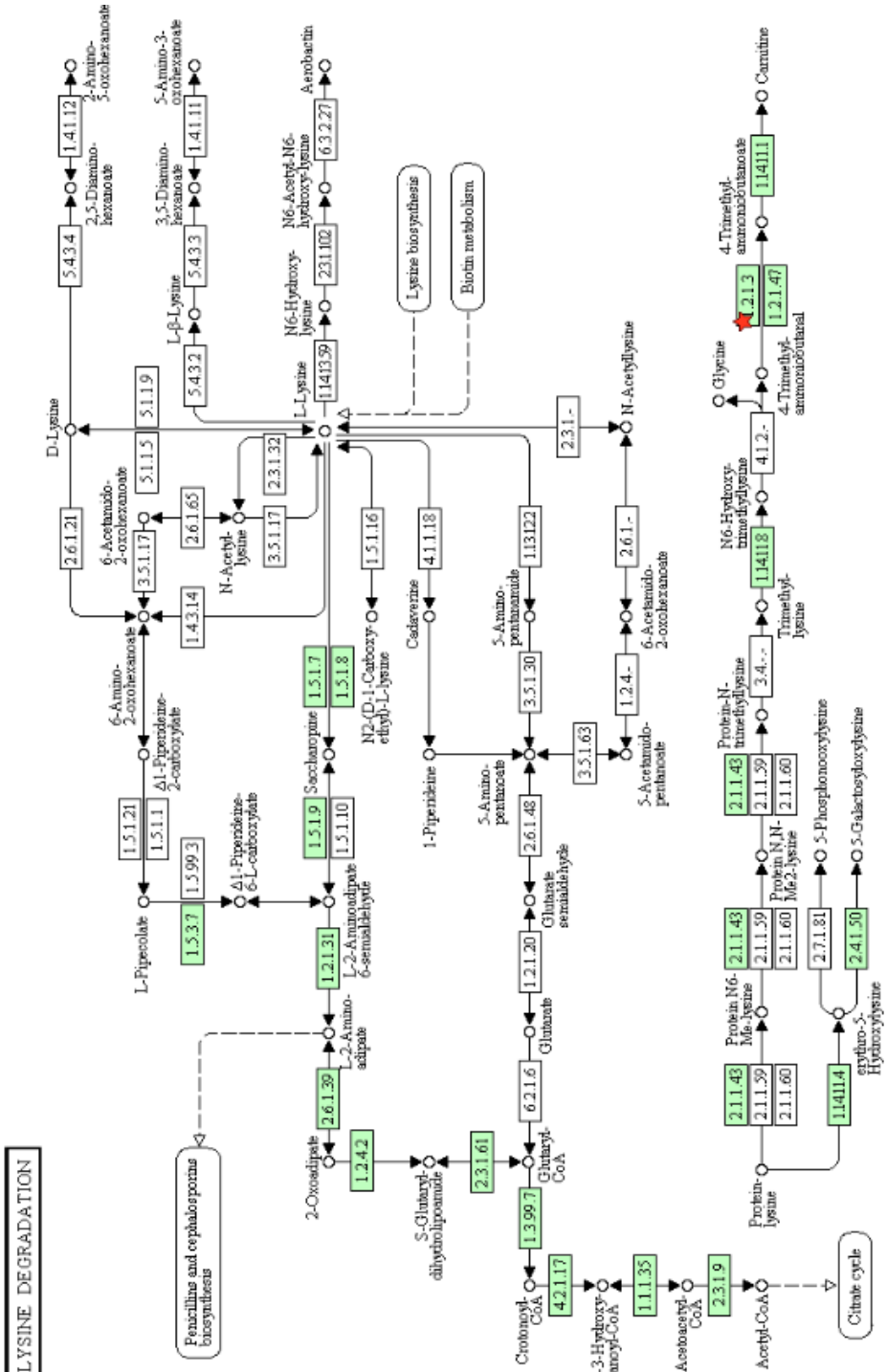

Figure 33: Pathway generated by KEGG (via DAVID) showing the role of Aldehyde dehydrogenase 2 (Aldh2, red star) in the amino acid degradation pathway for Lys, suggesting metabolic products to monitor. The various protein numbers refer to enzyme (EC) numbers.

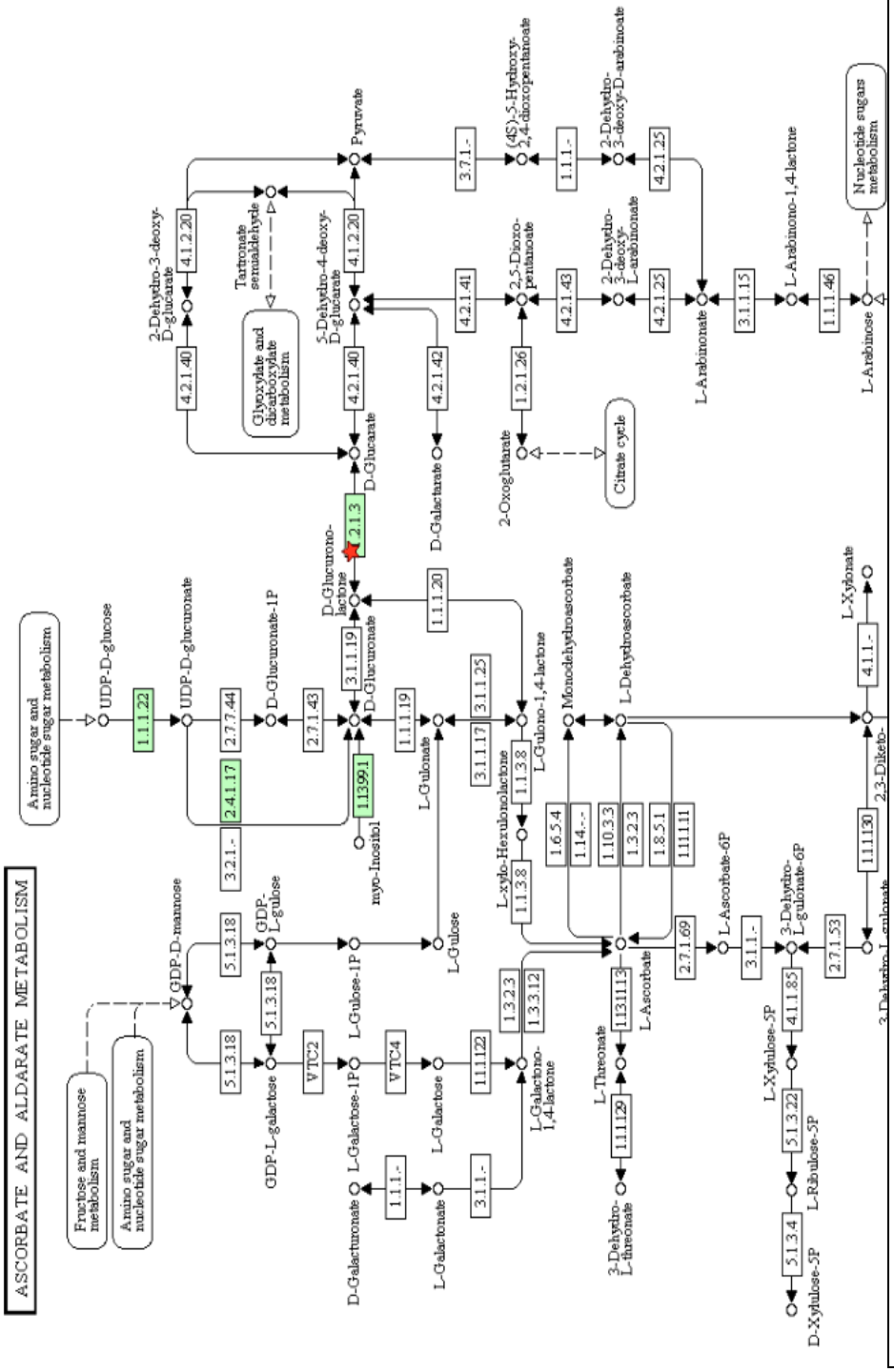

Figure 34: Detail of pathway generated by KEGG (via DAVID) showing the role of Aldehyde dehydrogenase 2 (Aldh2, red star) in the metabolic pathway for ascorbate and aldarate suggesting metabolic products to monitor. Aldarates are sugars where the functional groups on the first and last carbons are oxidized to carboxyls. The various protein numbers refer to enzyme (EC) numbers.

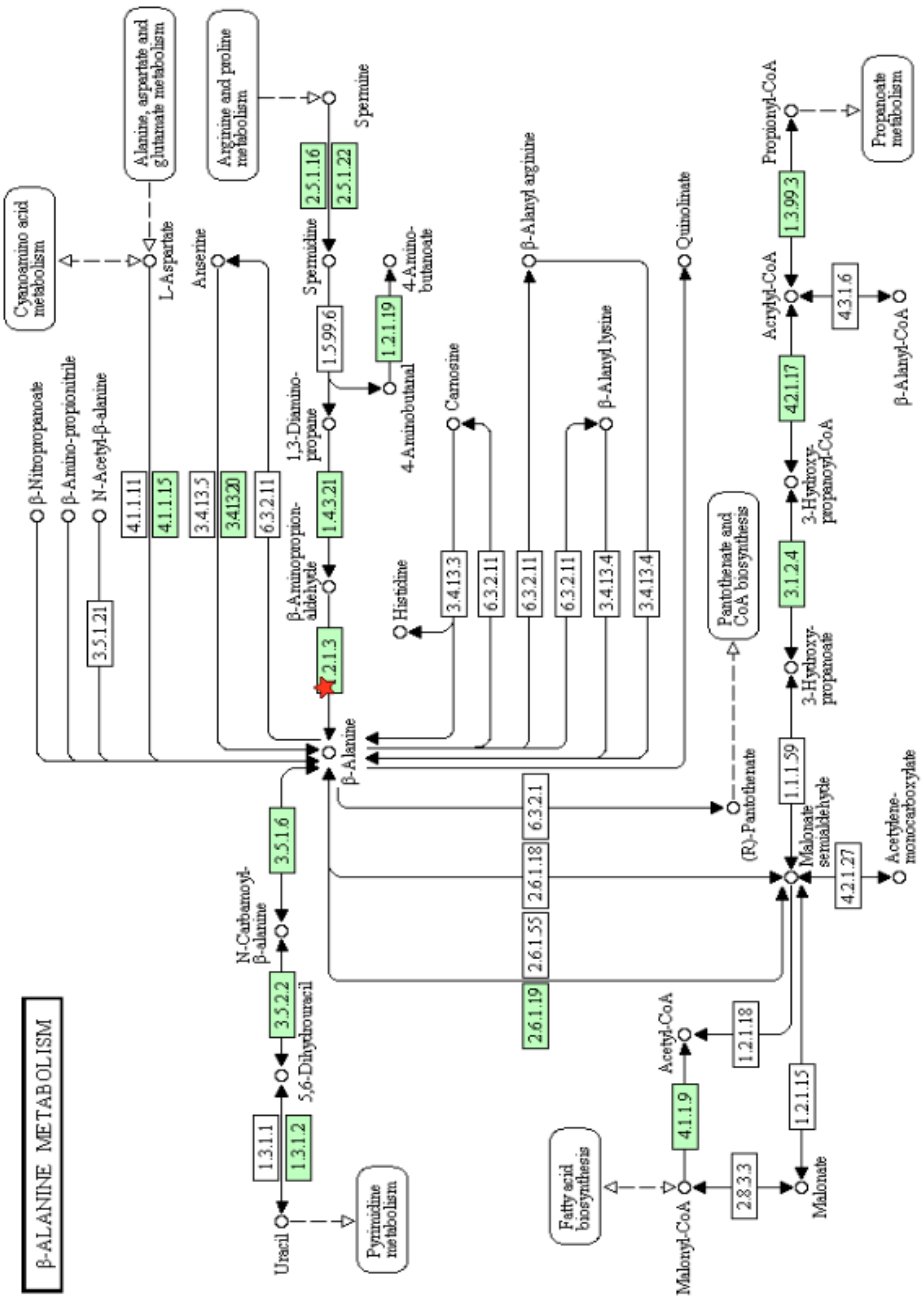

Figure 35: Pathway generated by KEGG (via DAVID) showing the role of Aldehyde dehydrogenase 2 (Aldh2, red star) in the metabolic pathway for β-Alanine, suggesting metabolic products to monitor. The various protein numbers refer to enzyme (EC) numbers.

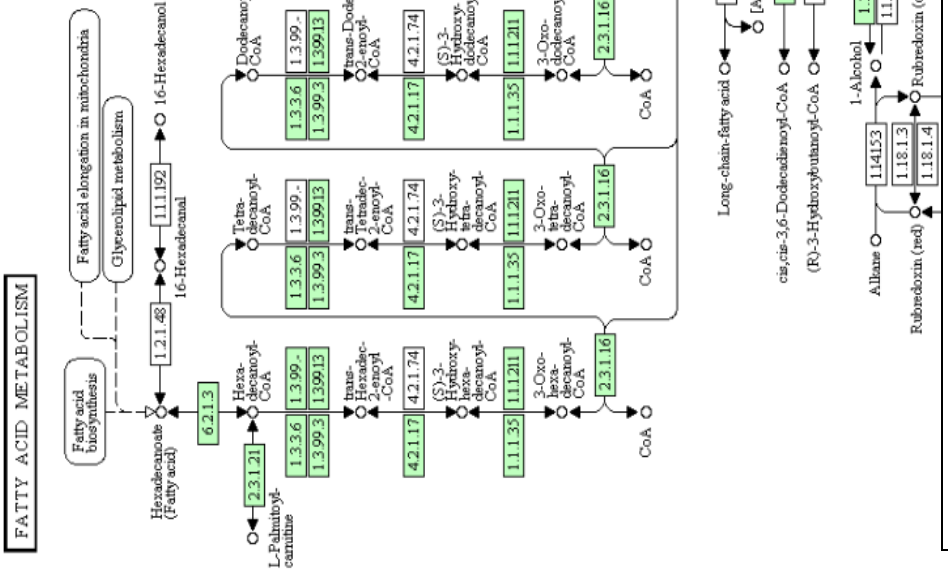

Figure 36: Pathway generated by KEGG (via DAVID) showing the role of Aldehyde dehydrogenase 2 (Aldh2, red star) in the metabolic pathway for fatty acids, suggesting metabolic products to monitor. The various protein numbers refer to enzyme (EC) numbers.

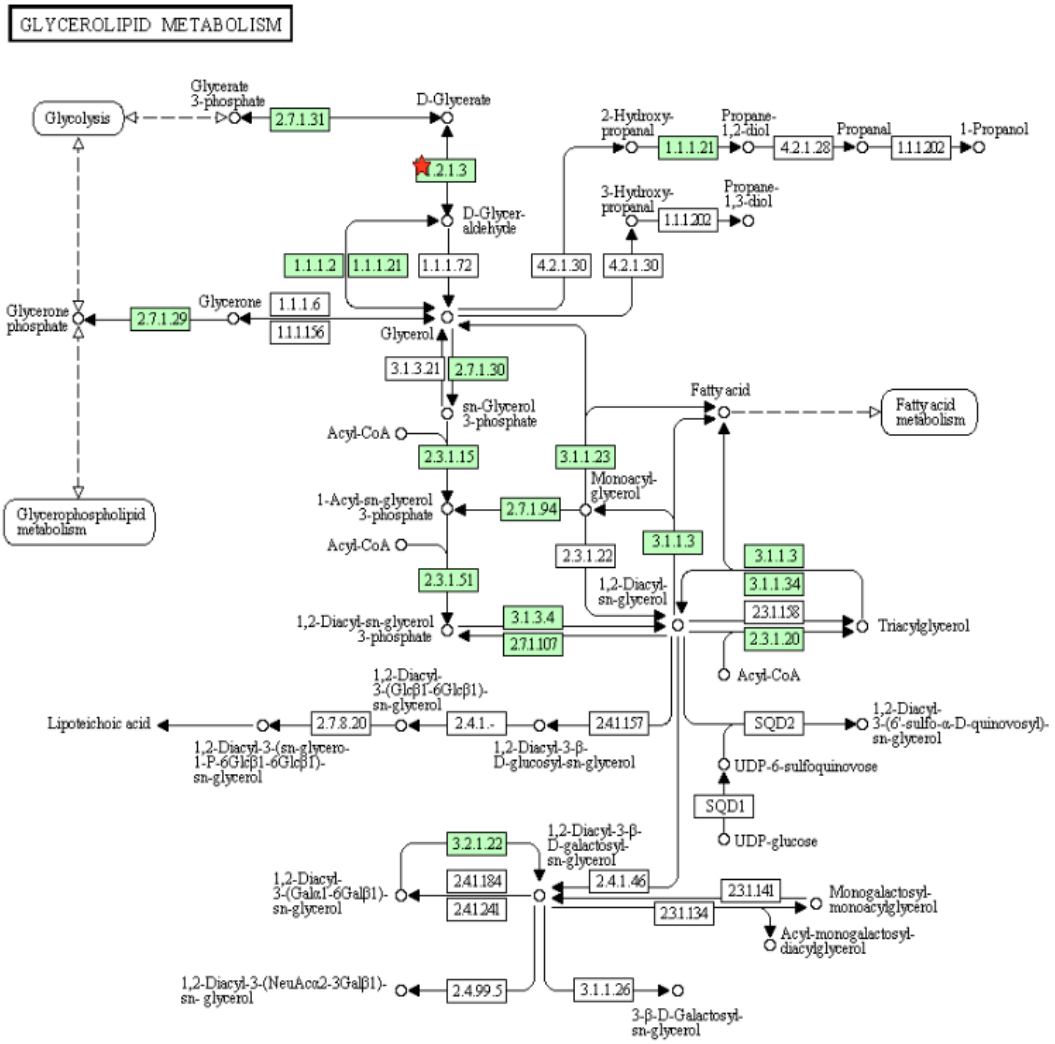

Figure 37: Pathway generated by KEGG (via DAVID) showing the role of Aldehyde dehydrogenase 2 (Aldh2, red star) in the metabolic pathway for glycerolipids, suggesting metabolic products to monitor. The various protein numbers refer to enzyme (EC) numbers.

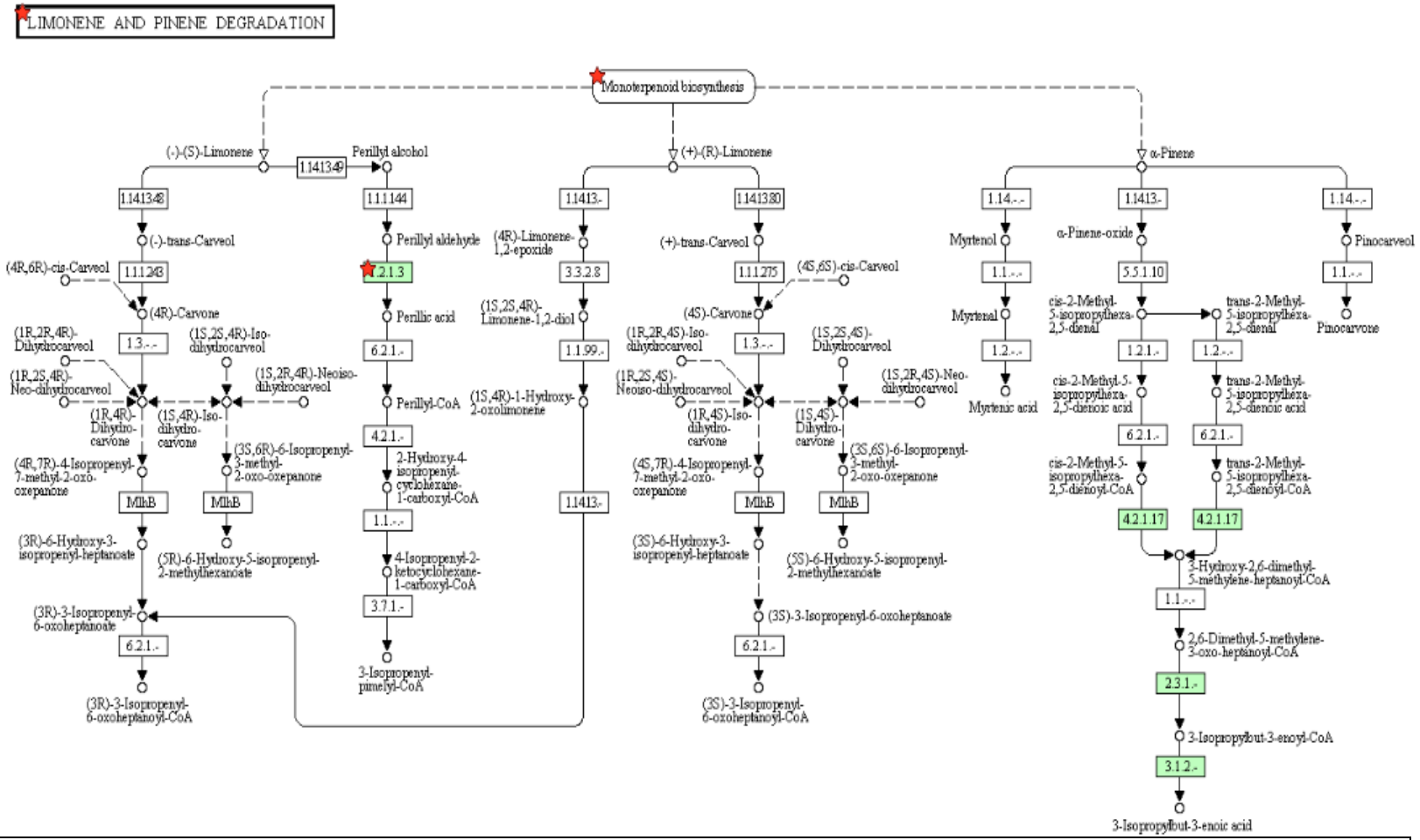

Figure 38: Pathway generated by KEGG (via DAVID) showing the role of Aldehyde dehydrogenase 2 (Aldh2, red star) in the metaboliic pathway for limonene suggesting metabolic products to monitor. The various protein numbers refer to enzyme (EC) numbers.

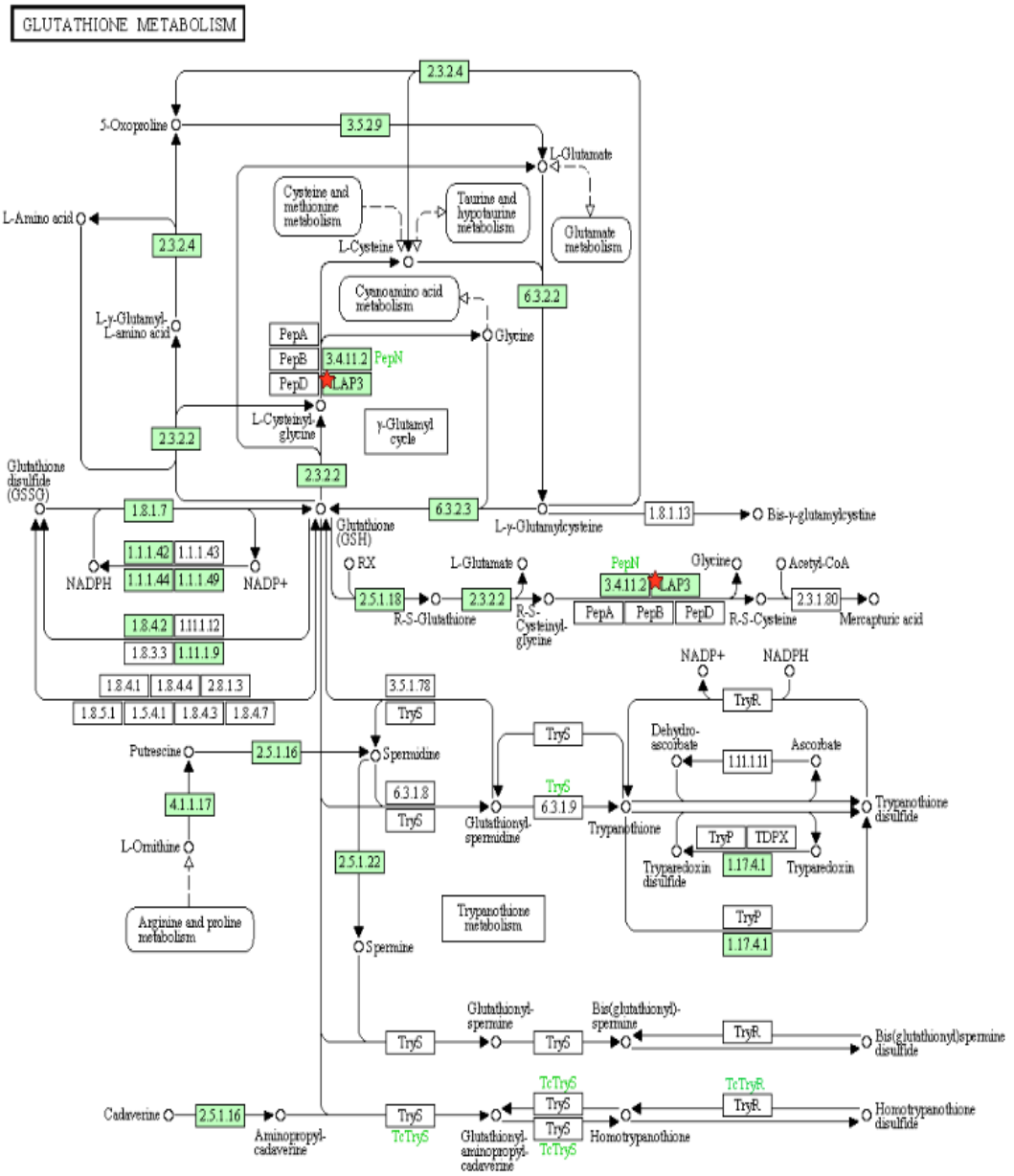

Figure 39: Pathway generated by KEGG (via DAVID) showing the role of leucine aminopeptidase 3 (Lap3, red star) in the metabolic pathway for glutathione, suggesting metabolic products to monitor. The various protein numbers refer to enzyme (EC) numbers.

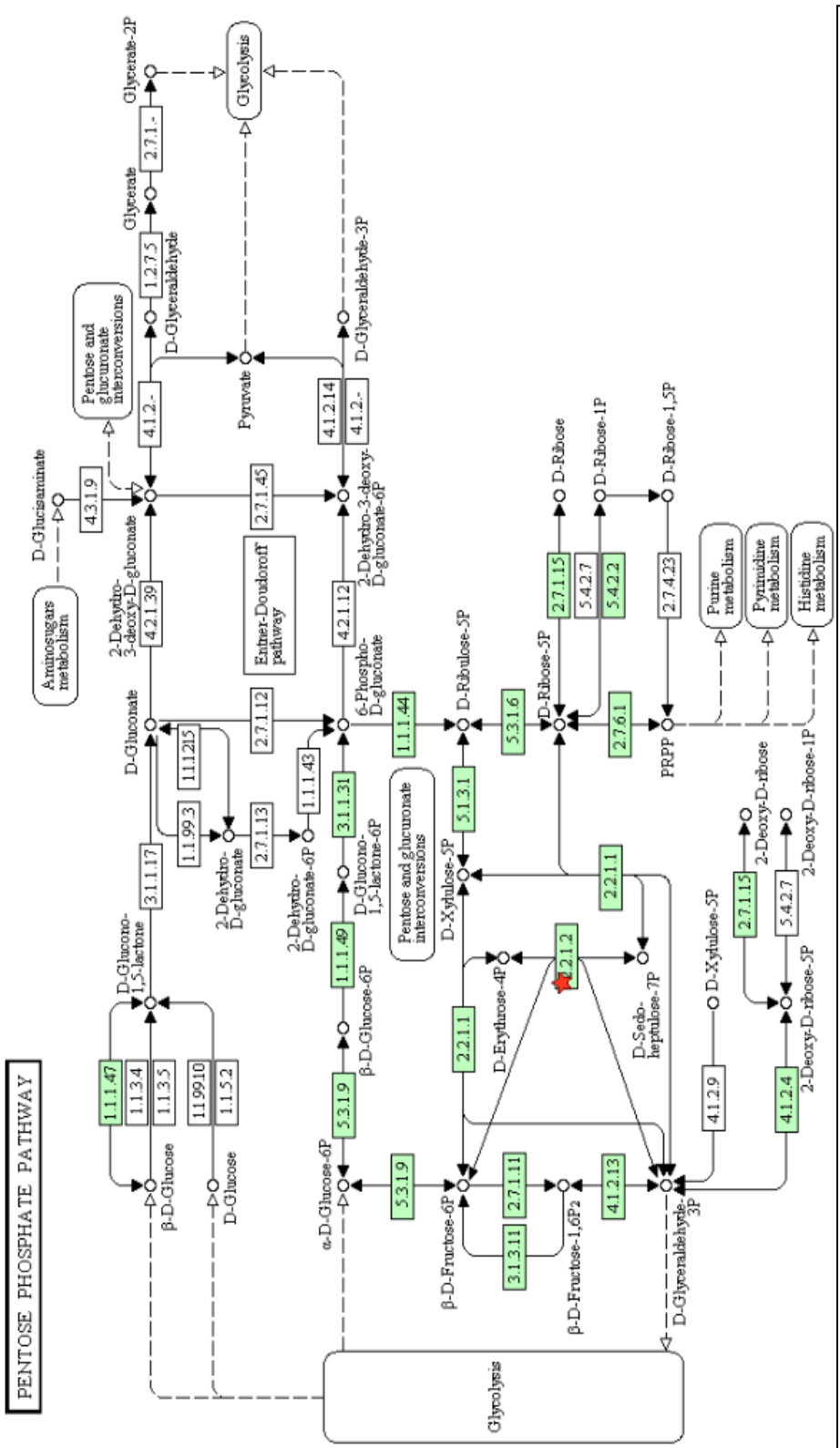

Figure 40: Pathway generated by KEGG (via DAVID) showing the role of transaldolase 1 (red star) in the pentose phosphate pathway, suggesting metabolic products to monitor during. The various protein numbers refer to enzyme (EC) numbers.

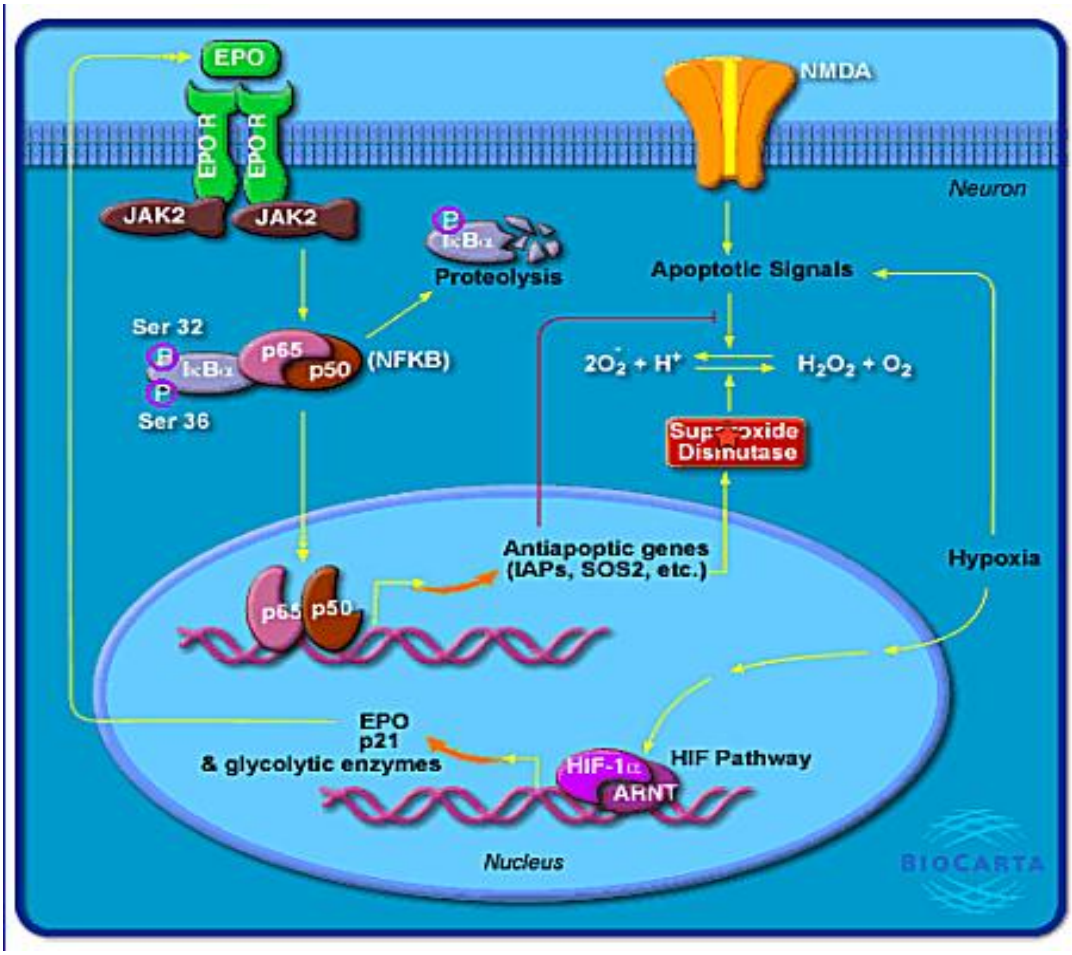

Figure 41: Pathway generated by DAVID showing the role of Mn superoxide dismutase (red star) in the regulation of reactive oxygen species generated by NF-κB activation. Reprinted with permission from Biocarta, listed as Erythropoietin Mediated Neuroprotection Through NF-κB.

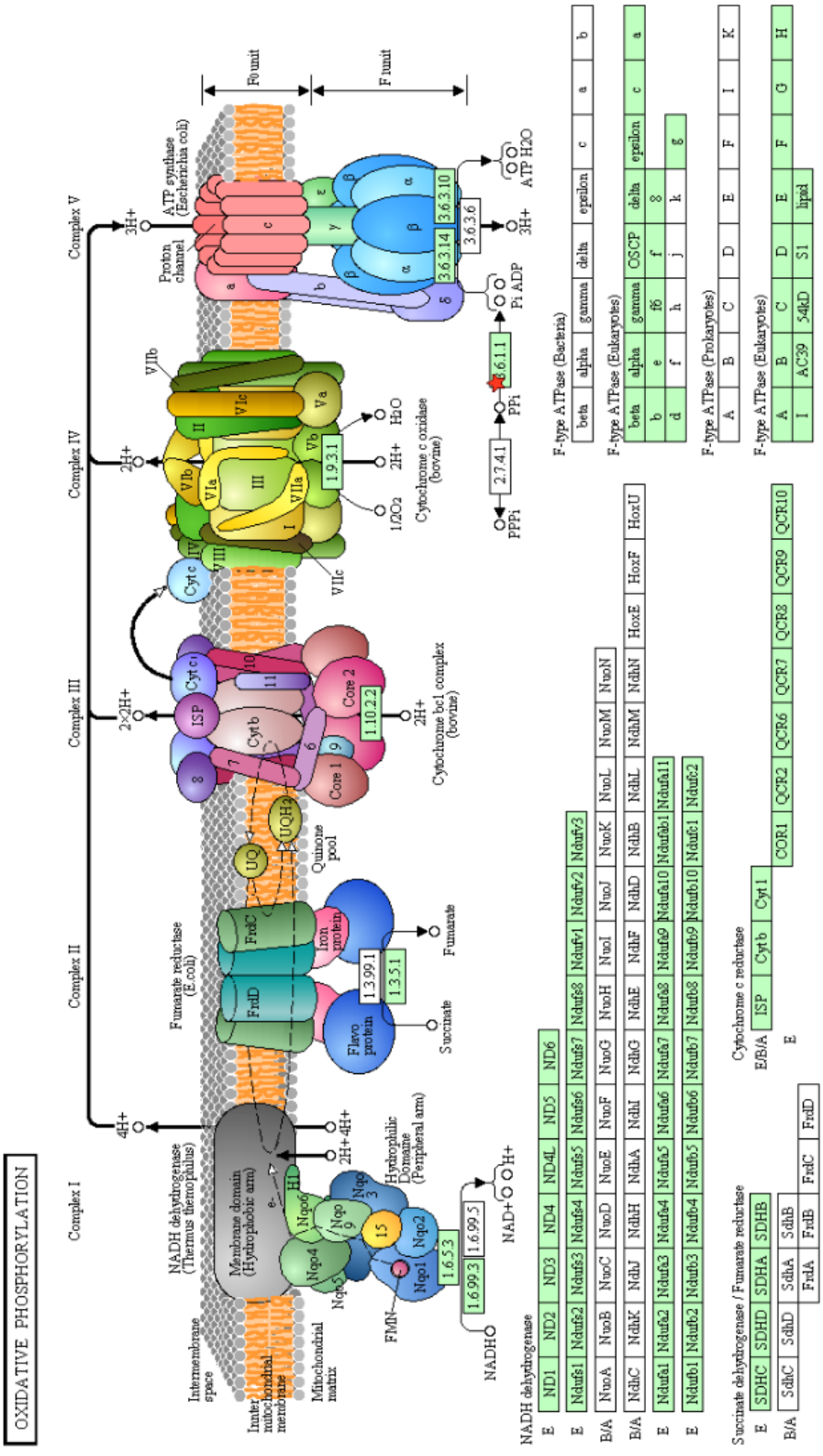

Figure 42: Pathway generated by KEGG (via DAVID) showing the role of inorganic pyrophosphatase (red star) in oxidative phosphorylation.

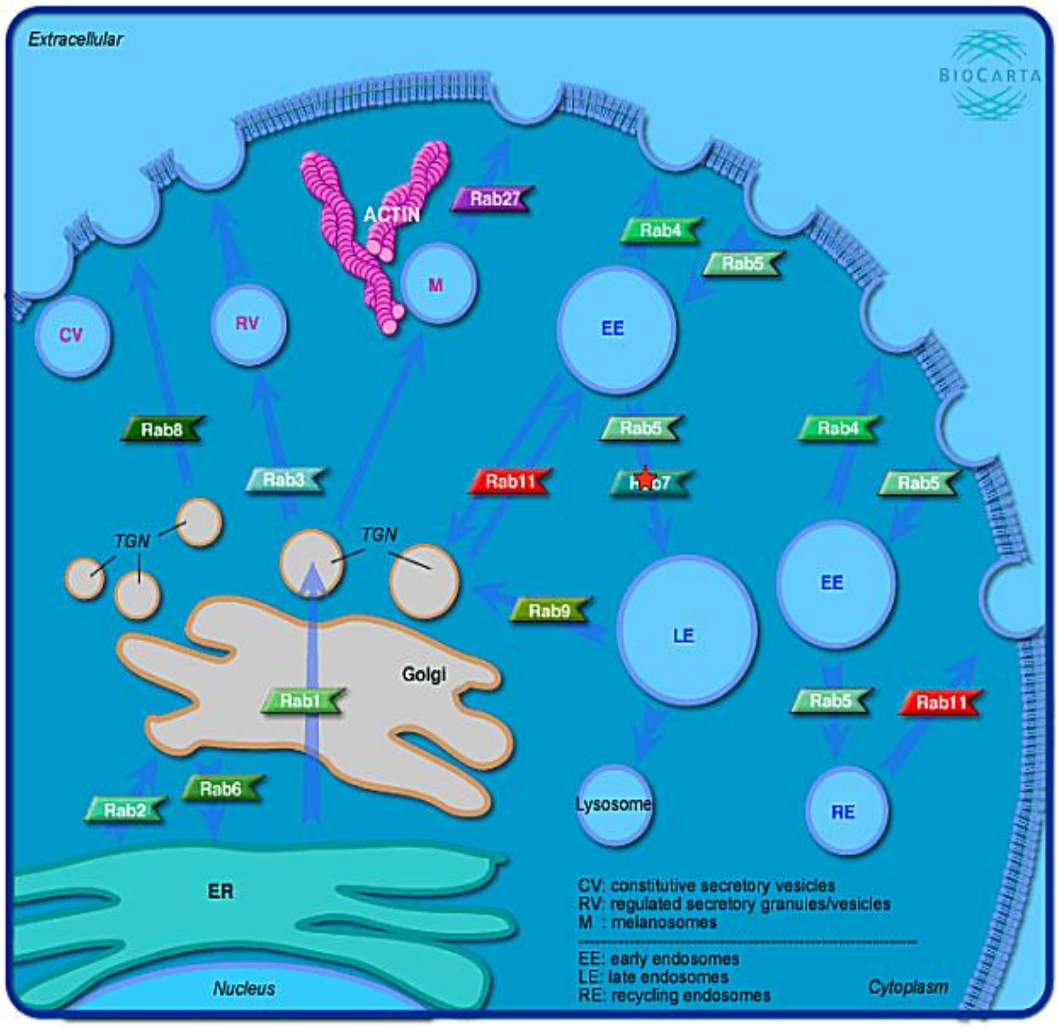

Figure 43: Pathway generated by KEGG (via DAVID) showing the role of Rab7 (red star) in phagosomal maturation. Reprinted with permission from Biocarta, listed as Rab GTPases Mark Targets In The Endocytotic Machinery.

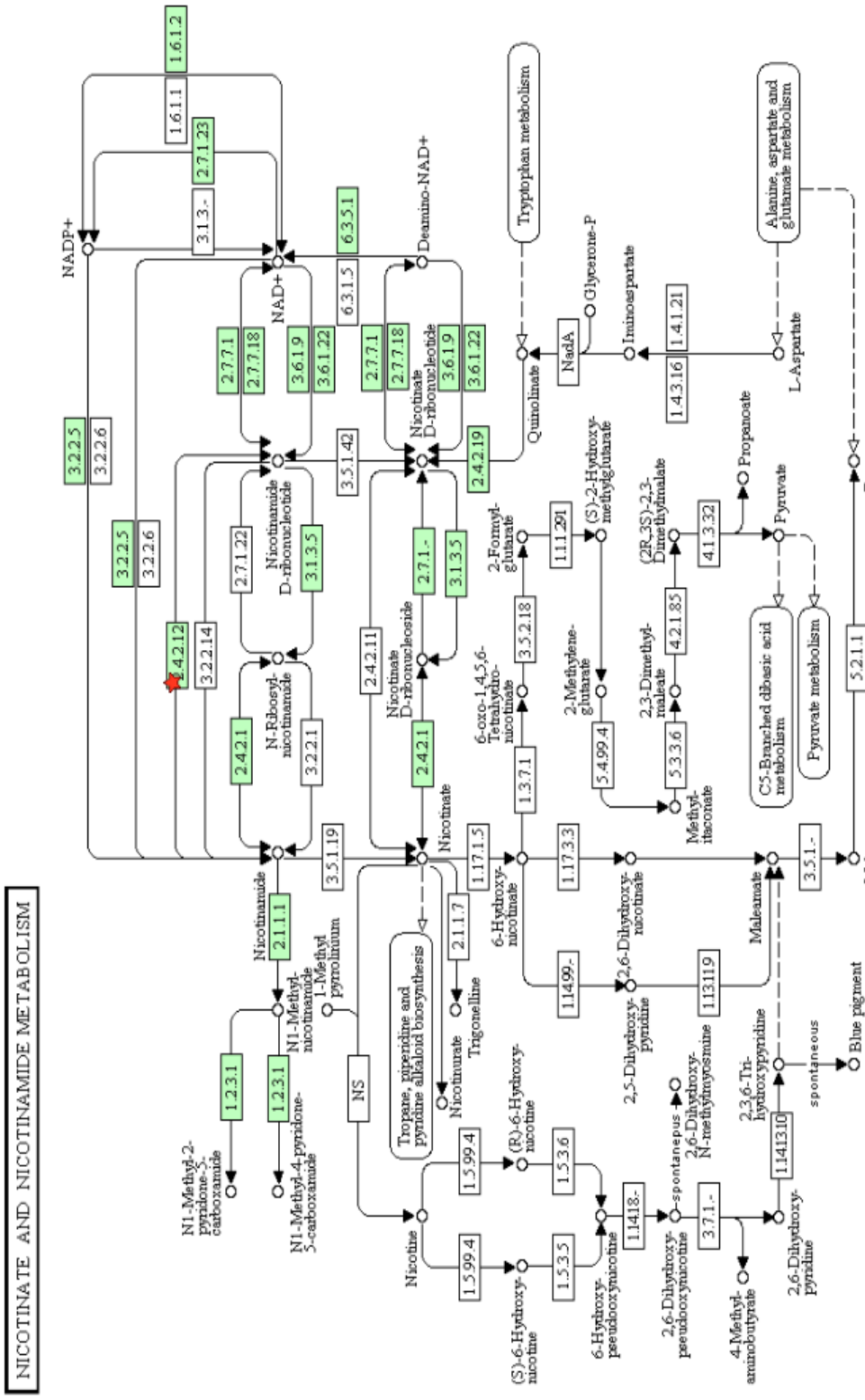

Figure 44: Pathway generated by KEGG (via DAVID) showing the role of visfatin (red star) in the metabolism of nicotinate and nicotinamide, suggesting metabolic products to monitor. The various protein numbers refer to enzyme (EC) numbers.

Figure 45A

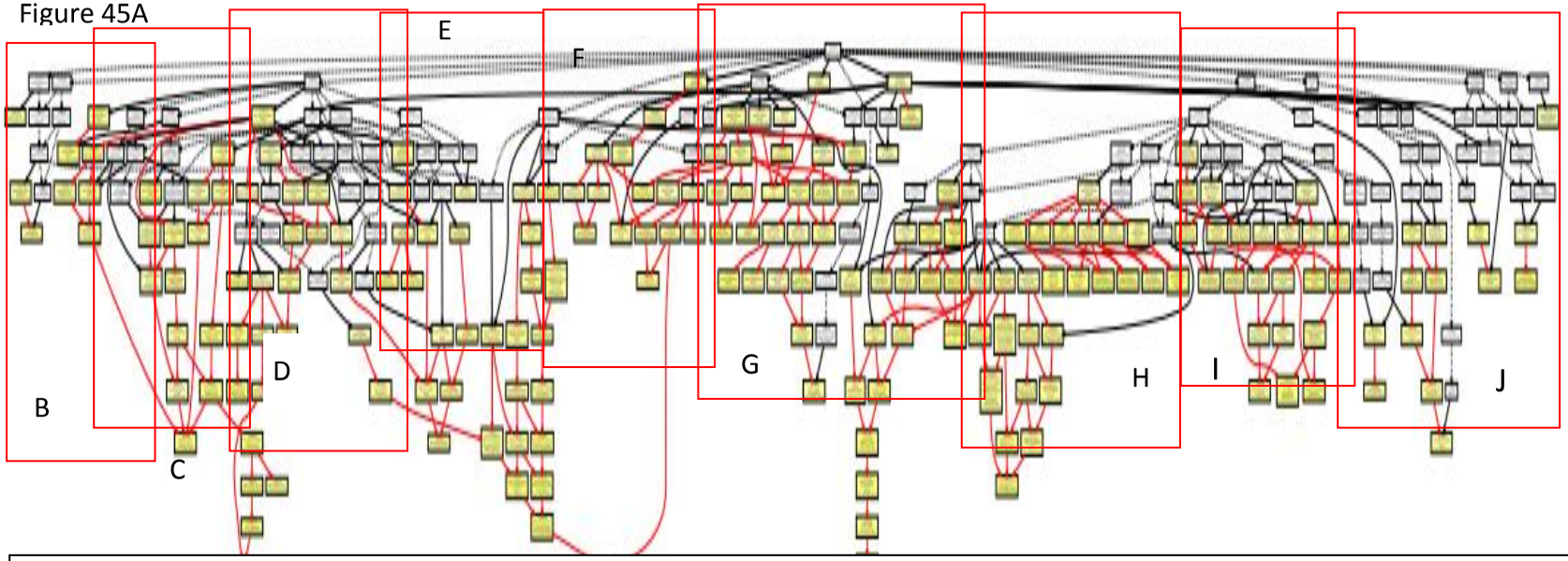

Figure 45 A-J: A) Overview of biological processes from the GOEAST software tool from the infected proteins. Boxes indicate approximate areas of greater detail in the following figures (B-J, following pages). In the following pages, yellow boxes indicate processes containing proteins that were determined to be significantly enriched with respect to the GO term in the analysis. The number at the top of the boxes is a GO ontology number, the next line describes the biological process , the bottom row of numbers n/13 where n is the number of proteins from the analysis that are assigned to the GO number at the top, followed by y/18596 where y is the number of gene IDs for a given GO number and 18596 is the total number of IDs in the entire GO dataset. The final number in parentheses indicates a p-value describing the significance of enrichment for the protein(s) associated with the GO number. White boxes do not have significant enrichment. Red arrows show connection between two enriched GO terms, black solid arrows show connection between an enriched and an unenriched term, and black dashed arrows show the connection between two unenriched terms. The word terms here refers to GO terms searched by GOEAST

Figure 45B

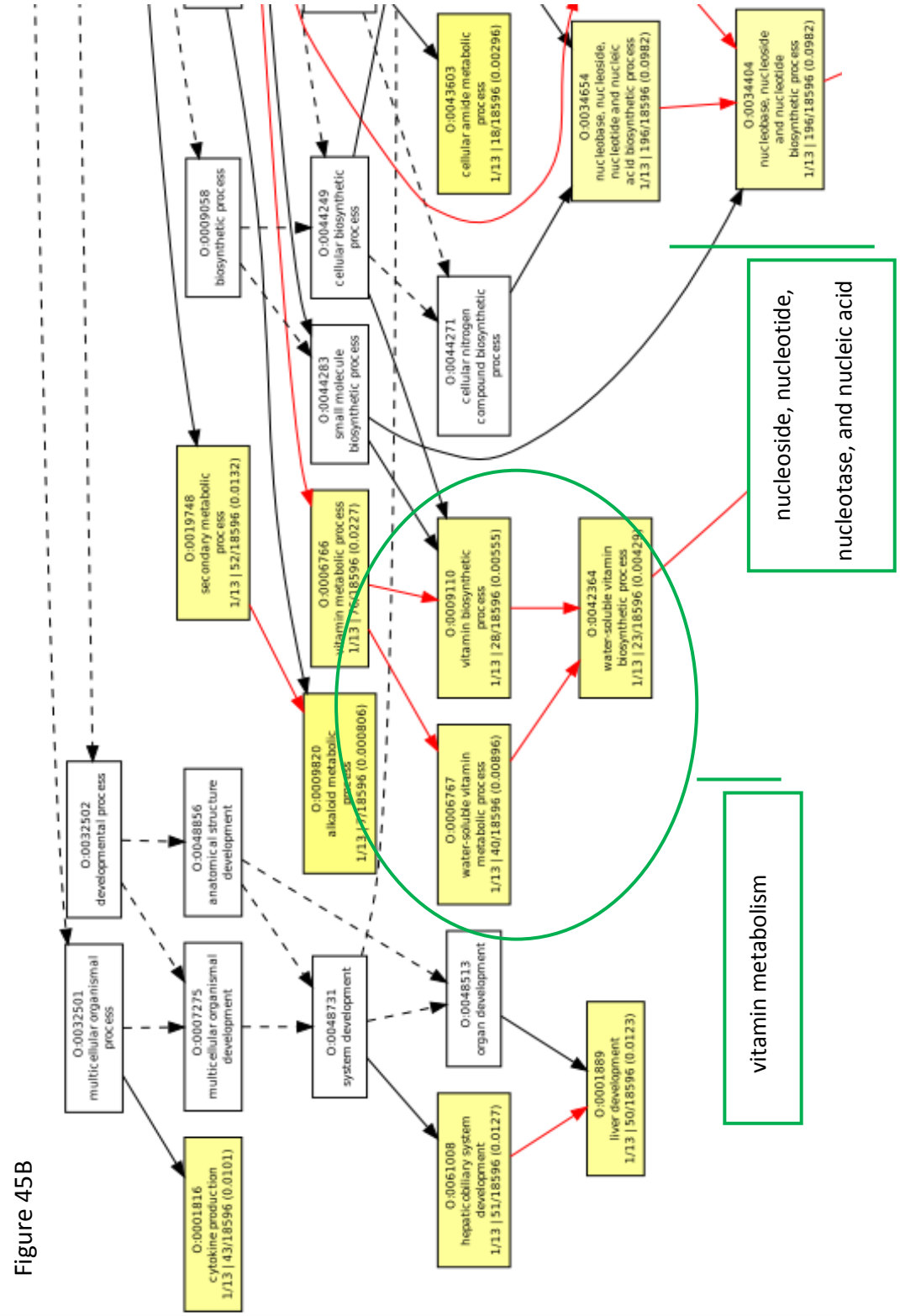
GO:0032501
multicellular organismal process
GO:0032502
developmental process
GO:0048856
anatomical structure development
GO:0007275
multicellular organismal development
GO:0048731
system development
GO:0048513
organ development
GO:0001816
cytokine production
1/13 | 43/18596 (0.0101)
GO:0061008
hepaticobiliary system development
1/13 | 51/18596 (0.0127)
GO:0001889
liver development
1/13 | 50/18596 (0.0123)
GO:0009820
alkaloid metabolic process
1/13 | 7/18596 (0.000806)
GO:0006767
water-soluble vitamin metabolic process
1/13 | 40/18596 (0.00896)
GO:0009110
vitamin biosynthetic process
1/13 | 28/18596 (0.00555)
GO:0042364
water-soluble vitamin biosynthetic process
1/13 | 23/18596 (0.00429)
GO:0006766
vitamin metabolic process
1/13 | 76/18596 (0.0227)
GO:0019748
secondary metabolic process
1/13 | 52/18596 (0.0132)
GO:0009058
biosynthetic process
GO:0044249
cellular biosynthetic process
GO:0044283
small molecule biosynthetic process
GO:0044271
cellular nitrogen compound biosynthetic process
GO:0043603
cellular amide metabolic process
1/13 | 18/18596 (0.00296)
GO:0034654
nucleobase, nucleoside, nucleotide and nucleic acid biosynthetic process
1/13 | 196/18596 (0.0982)
GO:0034404
nucleobase, nucleoside and nucleotide biosynthetic process
1/13 | 196/18596 (0.0982)
nucleoside, nucleotide,
nucleotase, and nucleic acid
vitamin metabolism

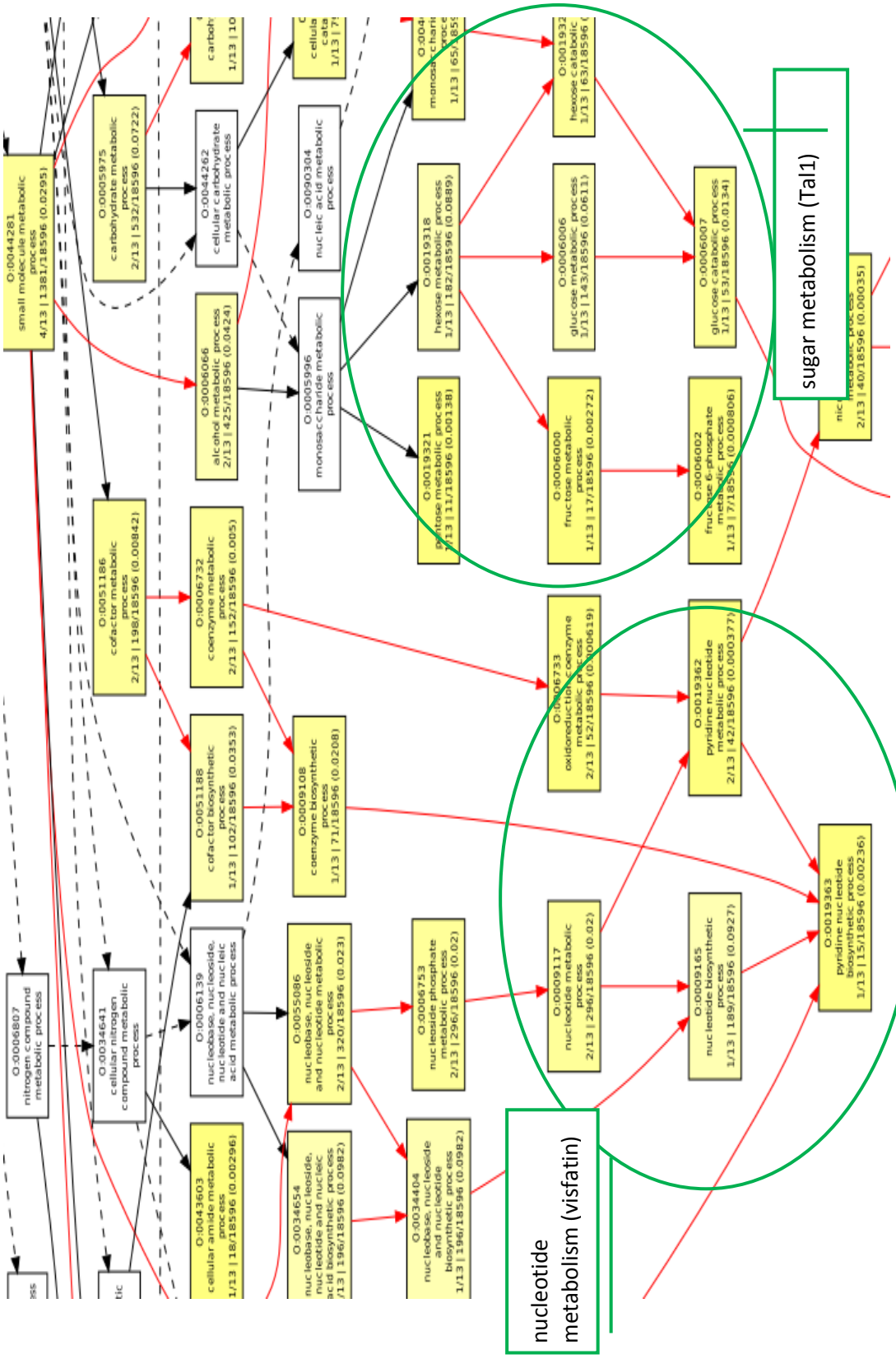

Figure 45C

Figure 45D

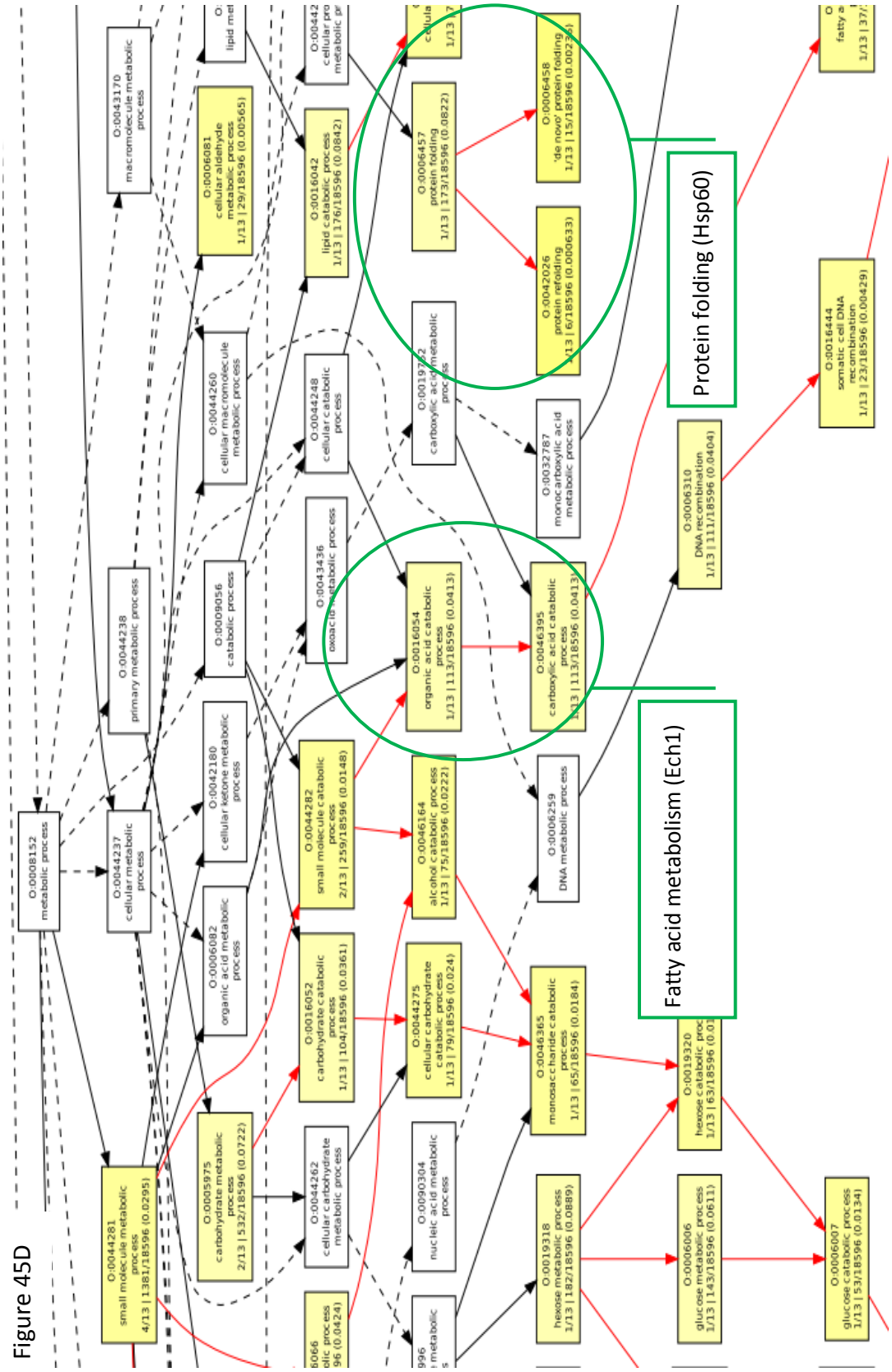

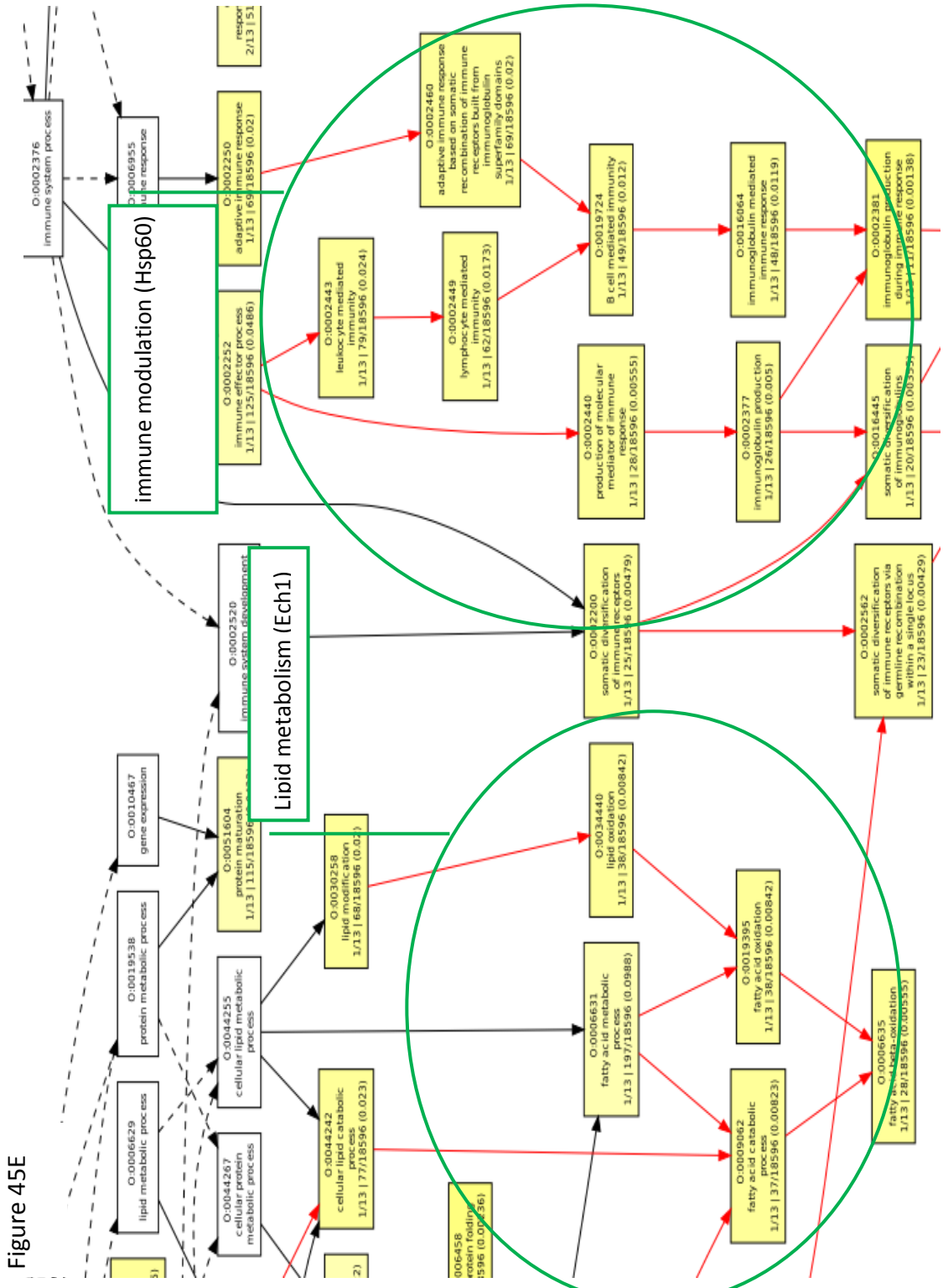
immune modulation (Hsp60)
Lipid metabolism (Ech1)
O:0002376
immune system process
O:0002250
adaptive immune response
1/13 | 69/18596 (0.02)
O:0002252
immune effector process
1/13 | 125/18596 (0.0486)
O:0002460
adaptive immune response based on somatic recombination of immune receptors built from immunoglobulin superfamily domains
1/13 | 69/18596 (0.02)
O:0002443
leukocyte mediated immunity
1/13 | 79/18596 (0.024)
O:0002449
lymphocyte mediated immunity
1/13 | 62/18596 (0.0173)
O:0019724
B cell mediated immunity
1/13 | 49/18596 (0.012)
O:0016064
immunoglobulin mediated immune response
1/13 | 48/18596 (0.0119)
O:0002381
immunoglobulin production during immune response
1/13 | 21/18596 (0.00138)
O:0002440
production of molecular mediator of immune response
1/13 | 28/18596 (0.00555)
O:0002377
immunoglobulin production
1/13 | 26/18596 (0.005)
O:0016445
somatic diversification of immunoglobulins
1/13 | 20/18596 (0.00355)
O:0002520
immune system development
O:0002200
somatic diversification of immune receptors
1/13 | 25/18596 (0.00479)
O:0002562
somatic diversification of immune receptors via germline recombination within a single locus
1/13 | 23/18596 (0.00429)
O:0051604
protein maturation
1/13 | 115/18596
O:0030258
lipid modification
1/13 | 68/18596 (0.0
O:0034440
lipid oxidation
1/13 | 38/18596 (0.00842)
O:0044255
cellular lipid metabolic process
O:0006631
fatty acid metabolic process
1/13 | 197/18596 (0.0988)
O:0019395
fatty acid oxidation
1/13 | 38/18596 (0.00842)
O:0044242
cellular lipid catabolic process
1/13 | 77/18596 (0.023)
O:0009062
fatty acid catabolic process
1/13 | 37/18596 (0.00823)
O:0006635
fatty acid beta-oxidation
1/13 | 28/18596 (0.00555)
O:0010467
gene expression
O:0019538
protein metabolic process
O:0006629
lipid metabolic process
O:0044267
cellular protein metabolic process

Figure 45E

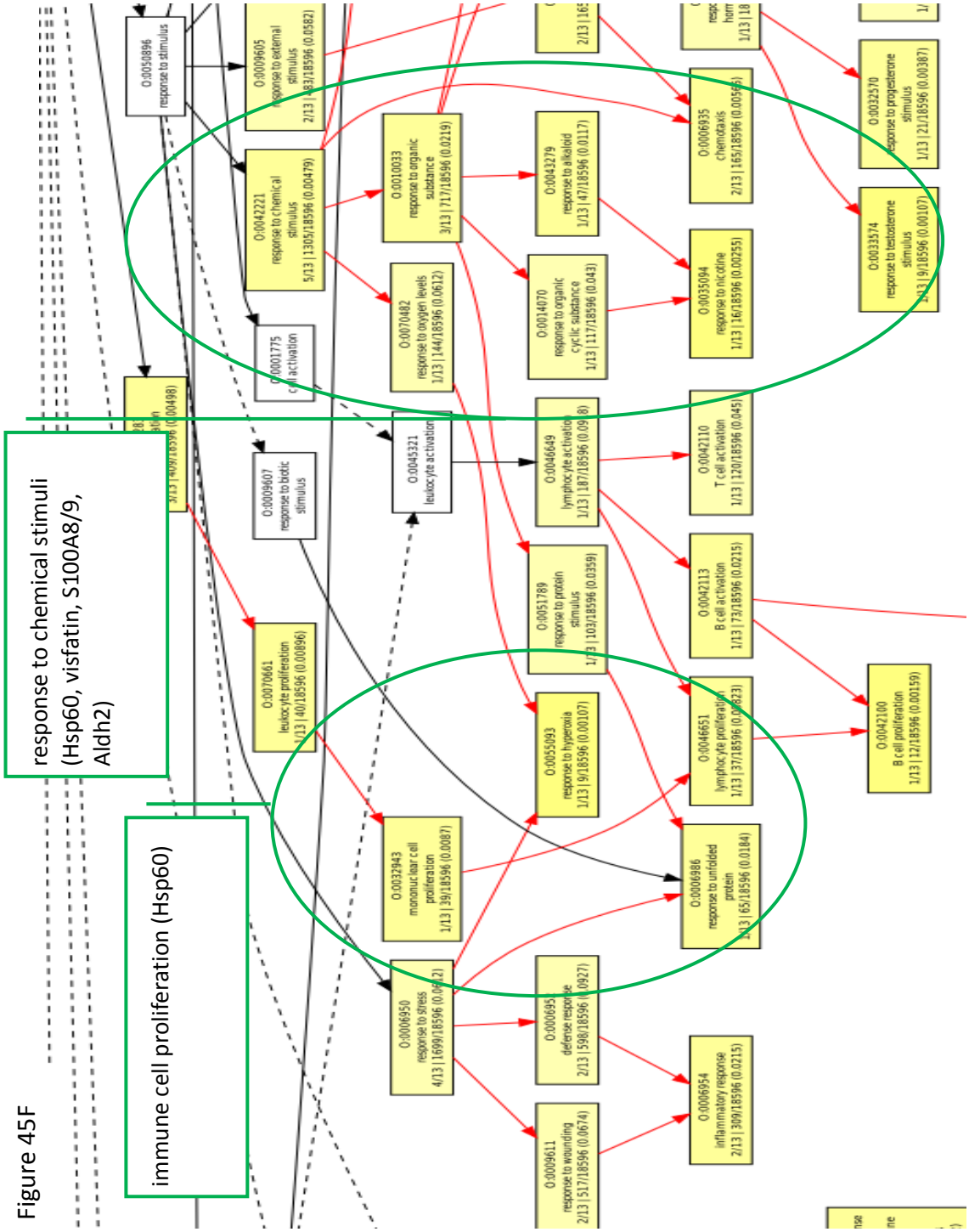
response to chemical stimuli (Hsp60, visfatin, S100A8/9, Aldh2)
immune cell proliferation (Hsp60)
O:0050896 response to stimulus
O:0009605 response to external stimulus 2/13 | 283/18596 (0.0582)
O:0042221 response to chemical stimulus 5/13 | 1305/18596 (0.00479)
O:0001775 cell activation
O:0009607 response to biotic stimulus
O:0070661 leukocyte proliferation 1/13 | 40/18596 (0.00896)
O:0032943 mononuclear cell proliferation 1/13 | 39/18596 (0.0087)
O:0006950 response to stress 4/13 | 1699/18596 (0.0472)
O:0009611 response to wounding 2/13 | 517/18596 (0.0674)
O:0006954 inflammatory response 2/13 | 309/18596 (0.0215)
O:0045321 leukocyte activation
O:0070482 response to oxygen levels 1/13 | 144/18596 (0.0612)
O:0010033 response to organic substance 3/13 | 717/18596 (0.0219)
O:0014070 response to organic cyclic substance 1/13 | 117/18596 (0.043)
O:0043279 response to alkaloid 1/13 | 47/18596 (0.0117)
O:0035094 response to nicotine 1/13 | 16/18596 (0.00255)
O:0006935 chemotaxis 2/13 | 165/18596 (0.00596)
O:0033574 response to testosterone stimulus 1/13 | 9/18596 (0.00107)
O:0032570 response to progesterone stimulus 1/13 | 21/18596 (0.00387)
O:0046649 lymphocyte activation 1/13 | 187/18596 (0.0198)
O:0051789 response to protein stimulus 1/13 | 103/18596 (0.0359)
O:0055093 response to hyperoxia 1/13 | 9/18596 (0.00107)
O:0042110 T cell activation 1/13 | 120/18596 (0.045)
O:0042113 B cell activation 1/13 | 73/18596 (0.0215)
O:0046651 lymphocyte proliferation 1/13 | 37/18596 (0.00923)
O:0042100 B cell proliferation 1/13 | 12/18596 (0.00159)
O:0006986 response to unfolded protein 1/13 | 65/18596 (0.0184)
O:0006955 immune response 2/13 | 598/18596 (0.0927)

Figure 45F

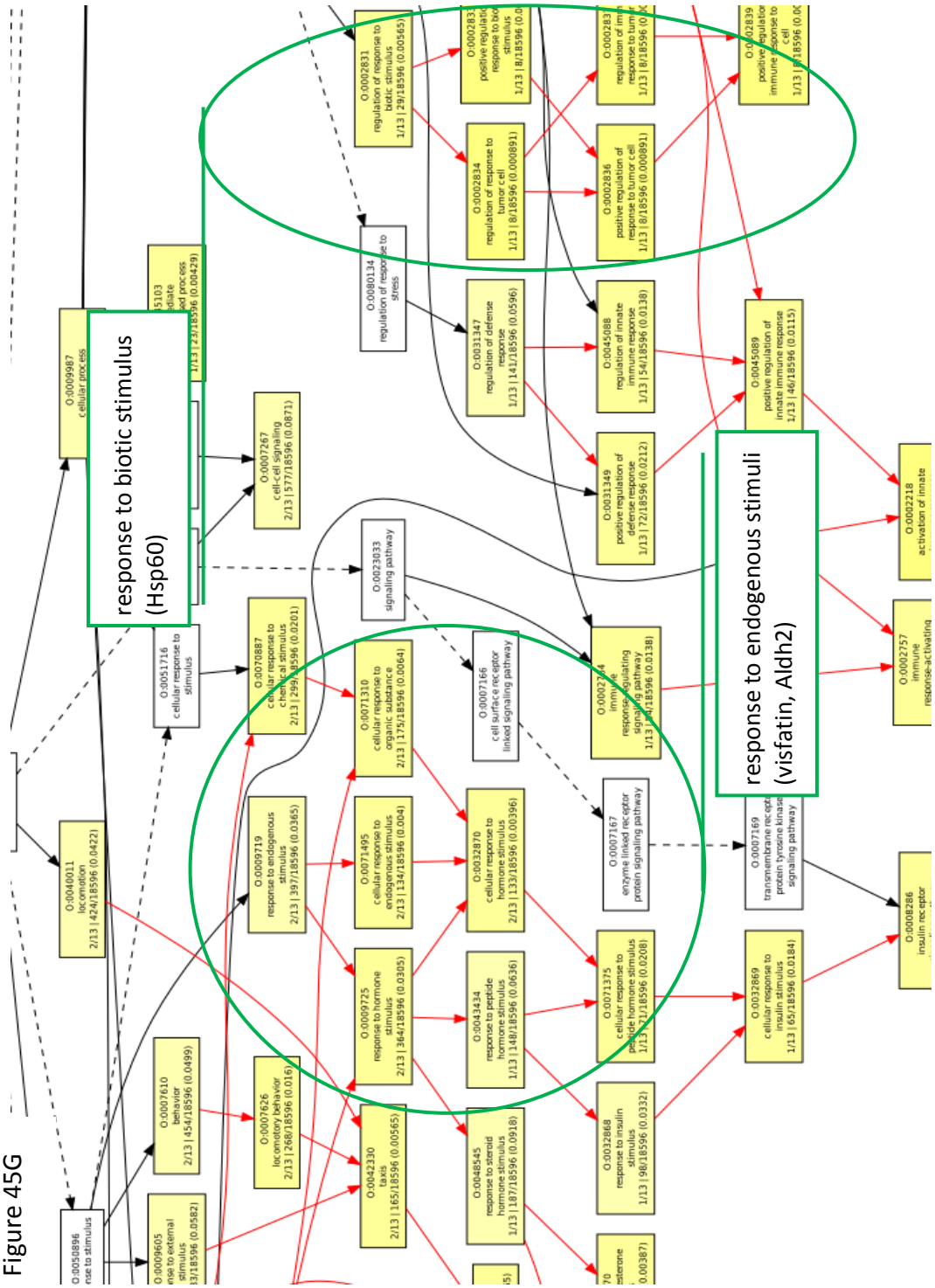
response to biotic stimulus
(Hsp60)
response to endogenous stimuli
(visfatin, Aldh2)

Figure 45G

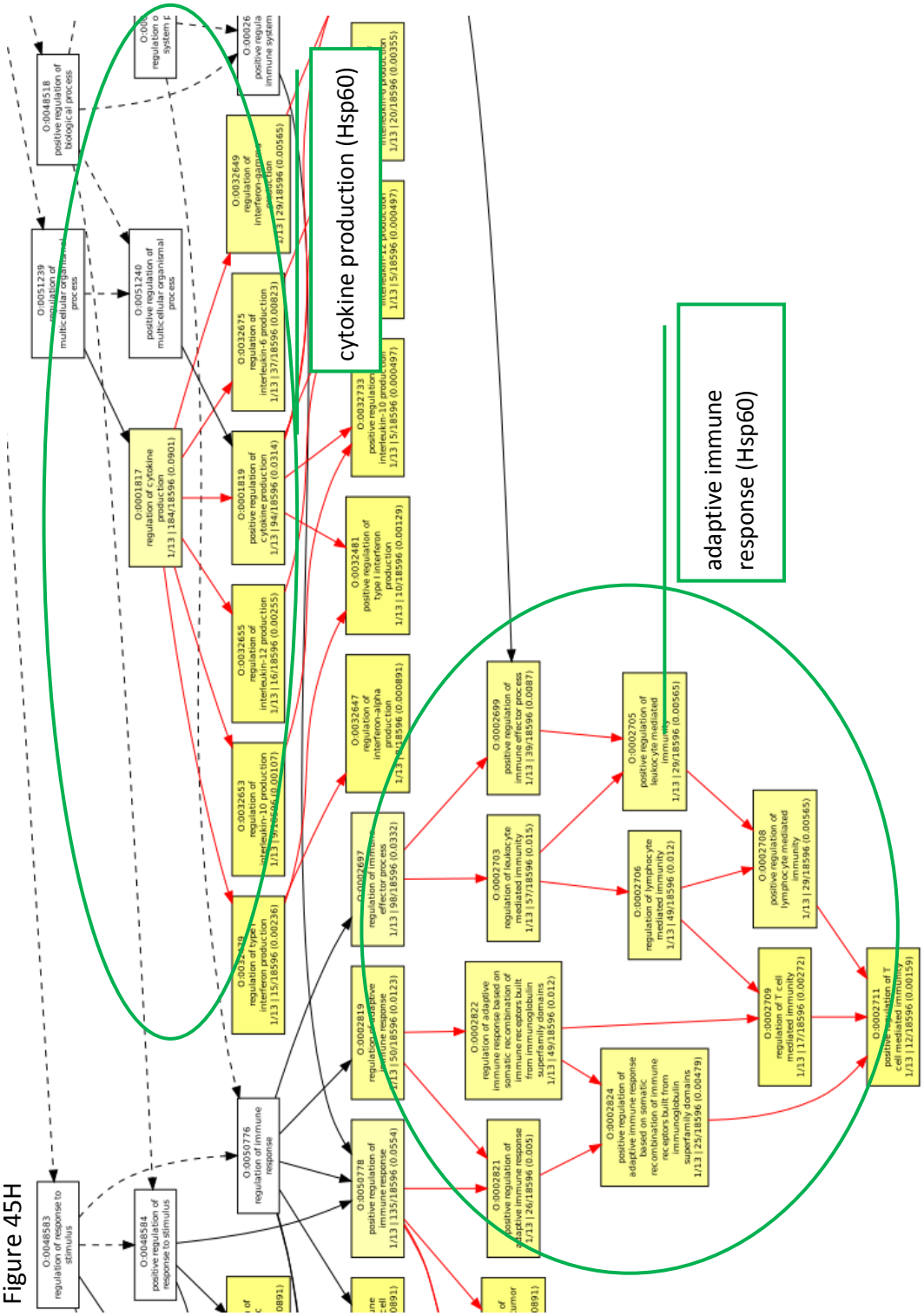
cytokine production (Hsp60)
adaptive immune response (Hsp60)
GO:0048583 regulation of response to stimulus
GO:0048584 positive regulation of response to stimulus
GO:0050776 regulation of immune response
GO:0050778 positive regulation of immune response
1/13 | 135/18596 (0.0554)
GO:0002819 regulation of adaptive immune response
1/13 | 50/18596 (0.0123)
GO:0002821 positive regulation of adaptive immune response
2/13 | 26/18596 (0.003)
GO:0002822 regulation of adaptive immune response based on somatic recombination of immune receptors built from immunoglobulin superfamily domains
1/13 | 49/18596 (0.012)
GO:0002824 positive regulation of adaptive immune response based on somatic recombination of immune receptors built from immunoglobulin superfamily domains
1/13 | 25/18596 (0.00479)
GO:0002697 regulation of immune effector process
1/13 | 98/18596 (0.0332)
GO:0002699 positive regulation of immune effector process
1/13 | 39/18596 (0.0087)
GO:0002703 regulation of leukocyte mediated immunity
1/13 | 57/18596 (0.015)
GO:0002705 positive regulation of leukocyte mediated immunity
1/13 | 29/18596 (0.00565)
GO:0002706 regulation of lymphocyte mediated immunity
1/13 | 49/18596 (0.012)
GO:0002708 positive regulation of lymphocyte mediated immunity
1/13 | 29/18596 (0.00565)
GO:0002709 regulation of T cell mediated immunity
1/13 | 17/18596 (0.00272)
GO:0002711 positive regulation of T cell mediated immunity
1/13 | 12/18596 (0.00159)
GO:0001817 regulation of cytokine production
1/13 | 184/18596 (0.0901)
GO:0001819 positive regulation of cytokine production
1/13 | 94/18596 (0.0314)
GO:0032675 regulation of interleukin-6 production
1/13 | 37/18596 (0.00823)
GO:0032649 regulation of interferon-gamma production
1/13 | 29/18596 (0.00565)
GO:0032733 positive regulation of interleukin-10 production
1/13 | 5/18596 (0.000497)
GO:0032655 regulation of interleukin-12 production
1/13 | 16/18596 (0.00255)
GO:0032653 regulation of interleukin-10 production
GO:0032481 positive regulation of type I interferon production
1/13 | 10/18596 (0.00129)
GO:0032647 regulation of interferon-alpha production
1/13 | 18596 (0.000891)
GO:0051239 regulation of multicellular organismal process
GO:0051240 positive regulation of multicellular organismal process
GO:0048518 positive regulation of biological process

Figure 45H

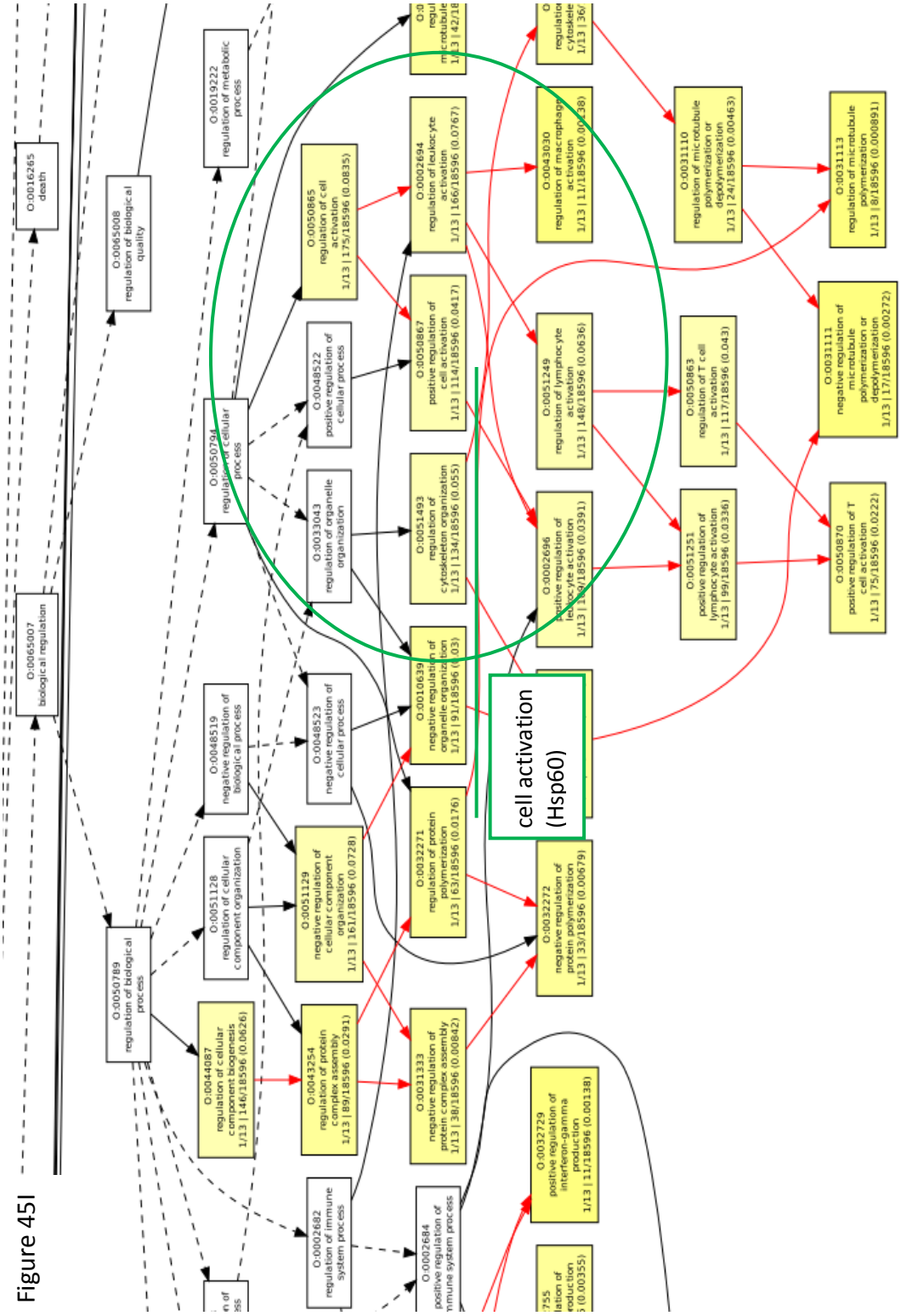

Figure 45I

Figure 45J

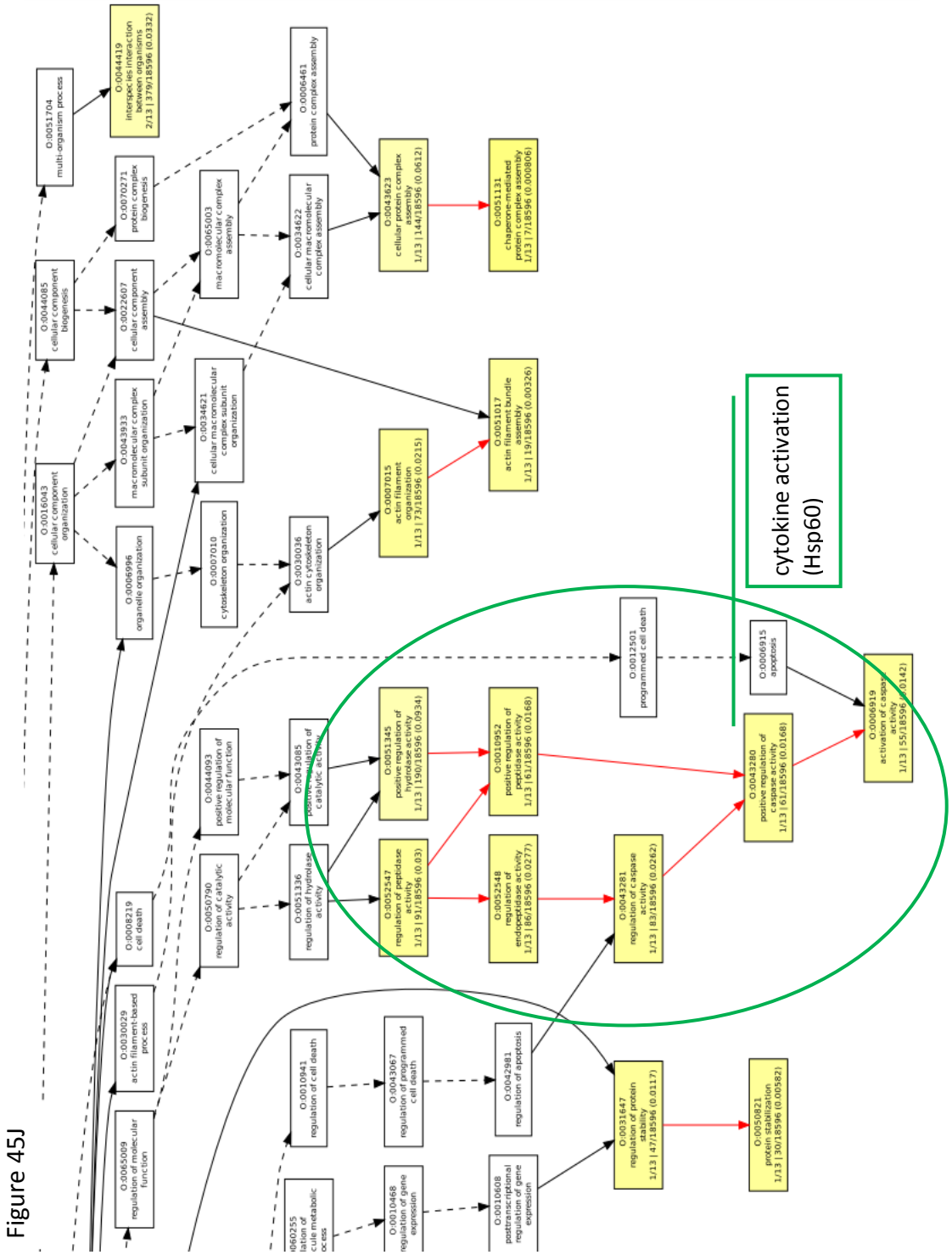
cytokine activation
(Hsp60)
O:0051704
multi-organism process
O:0044419
interspecies interaction
between organisms
2/13 | 379/18596 (0.0332)
O:0044085
cellular component
biogenesis
O:0016043
cellular component
organization
O:0006996
organelle organization
O:0007010
cytoskeleton organization
O:0030036
actin cytoskeleton
organization
O:0007015
actin filament
organization
1/13 | 73/18596 (0.0215)
O:0051017
actin filament bundle
assembly
1/13 | 19/18596 (0.00326)
O:0070271
protein complex
biogenesis
O:0022607
cellular component
assembly
O:0043933
macromolecular complex
subunit organization
O:0034621
cellular macromolecular
complex subunit
organization
O:0065003
macromolecular complex
assembly
O:0034622
cellular macromolecular
complex assembly
O:0006461
protein complex assembly
O:0043623
cellular protein complex
assembly
1/13 | 144/18596 (0.0612)
O:0051131
chaperone-mediated
protein complex assembly
1/13 | 7/18596 (0.000806)
O:0065009
regulation of molecular
function
O:0030029
actin filament-based
process
O:0008219
cell death
O:0050790
regulation of catalytic
activity
O:0044093
positive regulation of
molecular function
O:0051336
regulation of hydrolase
activity
O:0043085
positive regulation of
catalytic activity
O:0051345
positive regulation of
hydrolase activity
1/13 | 190/18596 (0.0934)
O:0052547
regulation of peptidase
activity
1/13 | 91/18596 (0.03)
O:0010952
positive regulation of
peptidase activity
1/13 | 61/18596 (0.0168)
O:0052548
regulation of
endopeptidase activity
1/13 | 86/18596 (0.0277)
O:0043281
regulation of caspase
activity
1/13 | 83/18596 (0.0262)
O:0043280
positive regulation of
caspase activity
1/13 | 61/18596 (0.0168)
O:0012501
programmed cell death
O:0006915
apoptosis
O:0006919
activation of caspase
activity
1/13 | 55/18596 (0.0142)
O:0010941
regulation of cell death
O:0043067
regulation of programmed
cell death
O:0042981
regulation of apoptosis
O:0031647
regulation of protein
stability
1/13 | 47/18596 (0.0117)
O:0050821
protein stabilization
1/13 | 30/18596 (0.00582)
O:0010468
regulation of gene
expression
O:0010608
posttranscriptional
regulation of gene
expression

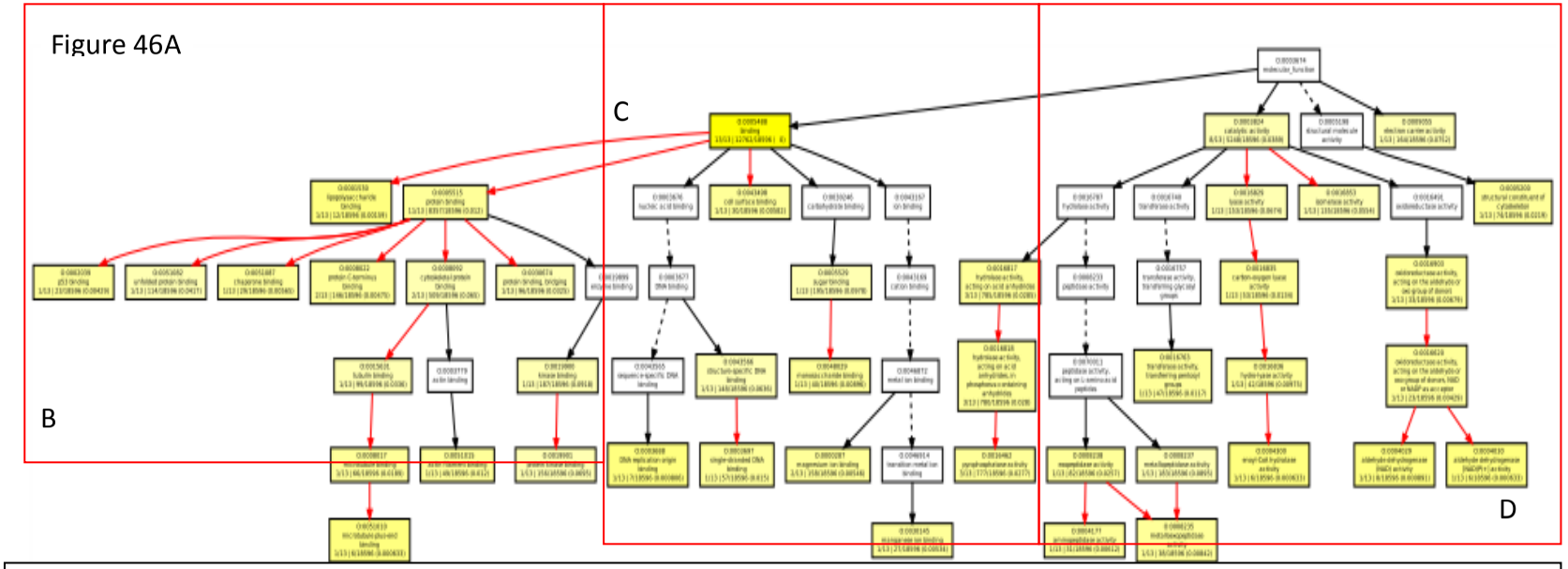

Figure 46 A-D: A) Overview of molecular processes from the GOEAST software tool from the infected proteins. Boxes indicate approximate areas of greater detail in the following figures (B-D, following pages). In the following pages, yellow boxes indicate processes containing proteins that were determined to be significantly enriched with respect to the GO term in the analysis. The number at the top of the boxes is a GO ontology number, the next line describes the biological process , the bottom row of numbers n/13 where n is the number of proteins from the analysis that are assigned to the GO number at the top, followed by y/18596 where y is the number of gene IDs for a given GO number and 18596 is the total number of IDs in the entire GO dataset. The final number in parentheses indicates a p-value describing the significance of enrichment for the protein(s) associated with the GO number. White boxes do not have significant enrichment. Red arrows show connection between two enriched GO terms, black solid arrows show connection between an enriched and an unenriched term, and black dashed arrows show the connection between two unenriched terms.

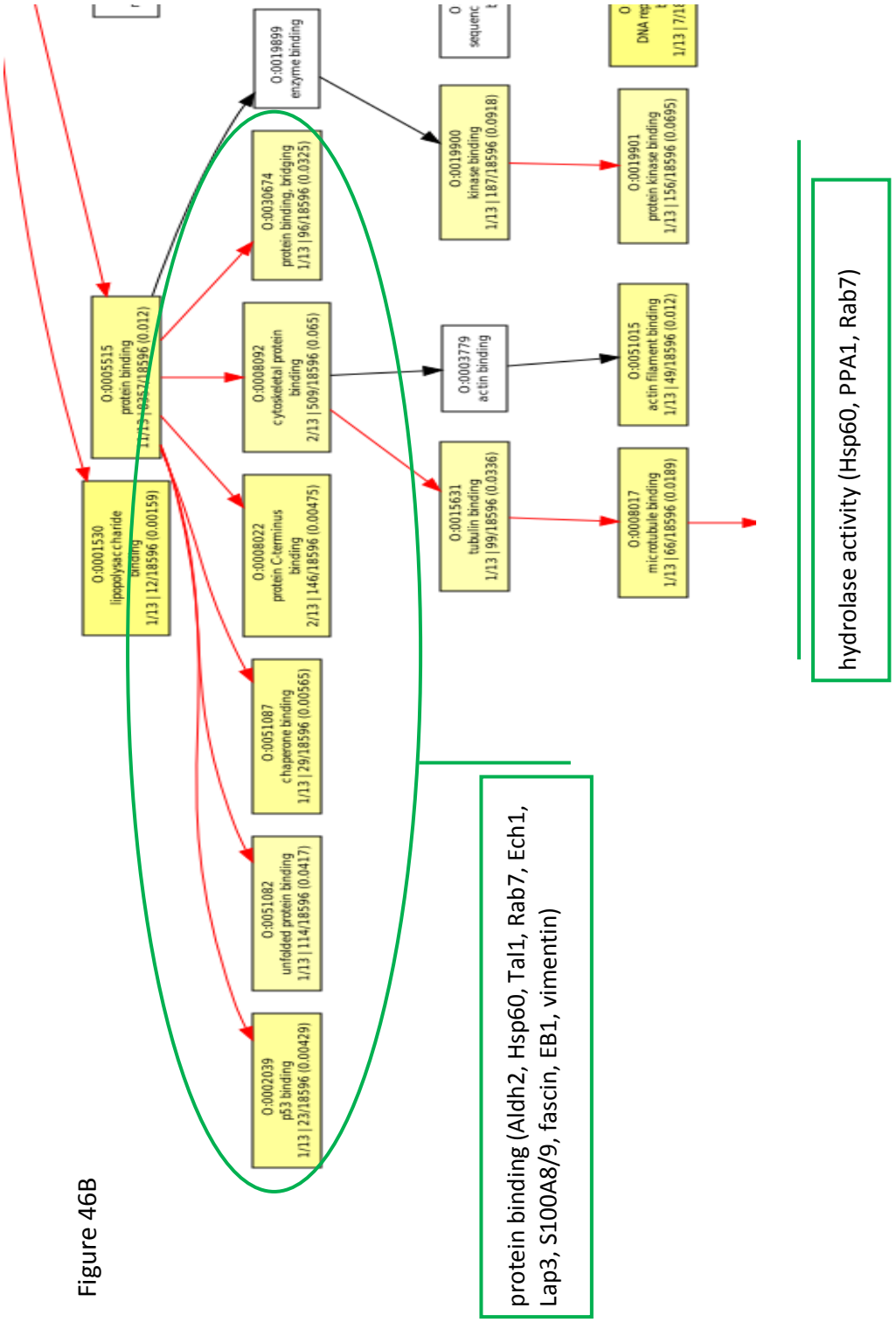
GO:0019899
enzyme binding
GO:0019900
kinase binding
1/13 | 187/18596 (0.0918)
GO:0019901
protein kinase binding
1/13 | 156/18596 (0.0695)
GO:0030674
protein binding, bridging
1/13 | 96/18596 (0.0325)
GO:0005515
protein binding
GO:0008092
cytoskeletal protein
binding
2/13 | 509/18596 (0.065)
GO:0003779
actin binding
GO:0051015
actin filament binding
1/13 | 49/18596 (0.012)
GO:0001530
lipopolysaccharide
binding
1/13 | 12/18596 (0.00159)
GO:0008022
protein C-terminus
binding
2/13 | 146/18596 (0.00475)
GO:0015631
tubulin binding
1/13 | 99/18596 (0.0336)
GO:0008017
microtubule binding
1/13 | 66/18596 (0.0189)
GO:0051087
chaperone binding
1/13 | 29/18596 (0.00565)
GO:0051082
unfolded protein binding
1/13 | 114/18596 (0.0417)
GO:0002039
p53 binding
1/13 | 23/18596 (0.00429)
protein binding (Aldh2, Hsp60, Tal1, Rab7, Ech1,
Lap3, S100A8/9, fascin, EB1, vimentin)
hydrolase activity (Hsp60, PPA1, Rab7)

Figure 46B

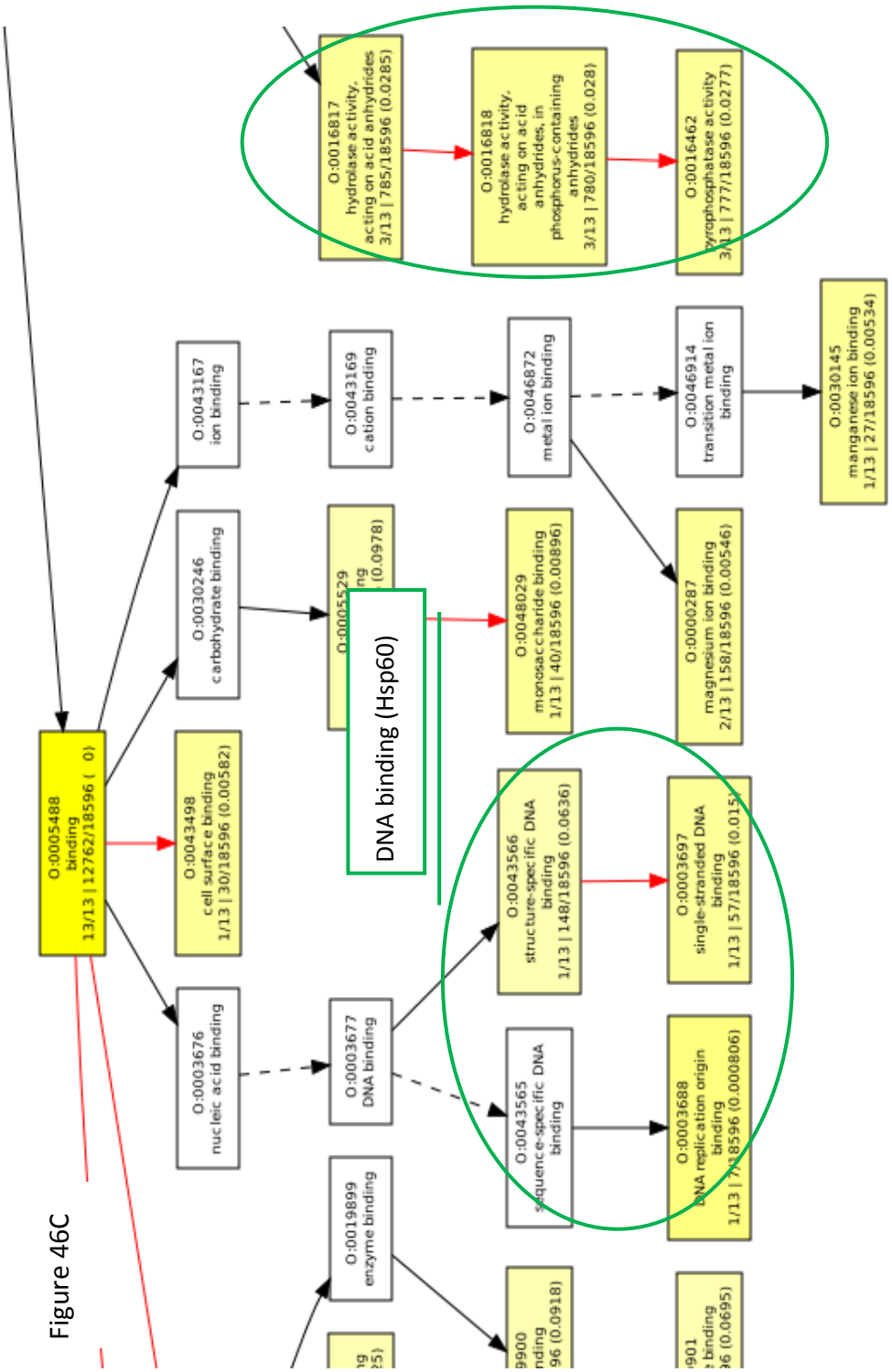
O:0005488
binding
13/13 | 12762/18596 (0)
O:0043167
ion binding
O:0030246
carbohydrate binding
O:0043498
cell surface binding
1/13 | 30/18596 (0.00582)
O:0003676
nucleic acid binding
O:0043169
cation binding
O:0005529
O:0048029
monosaccharide binding
1/13 | 40/18596 (0.00896)
O:0003677
DNA binding
O:0046872
metal ion binding
O:0046914
transition metal ion
binding
O:0030145
manganese ion binding
1/13 | 27/18596 (0.00534)
O:0000287
magnesium ion binding
2/13 | 158/18596 (0.00546)
O:0016817
hydrolase activity,
acting on acid anhydrides
3/13 | 785/18596 (0.0285)
O:0016818
hydrolase activity,
acting on acid
anhydrides, in
phosphorus-containing
anhydrides
3/13 | 780/18596 (0.028)
O:0016462
pyrophosphatase activity
3/13 | 777/18596 (0.0277)
DNA binding (Hsp60)
O:0043566
structure-specific DNA
binding
1/13 | 148/18596 (0.0636)
O:0003697
single-stranded DNA
binding
1/13 | 57/18596 (0.015
O:0043565
sequence-specific DNA
binding
O:0003688
DNA replication origin
binding
1/13 | 18596 (0.000806)
O:0019899
enzyme binding

Figure 46C

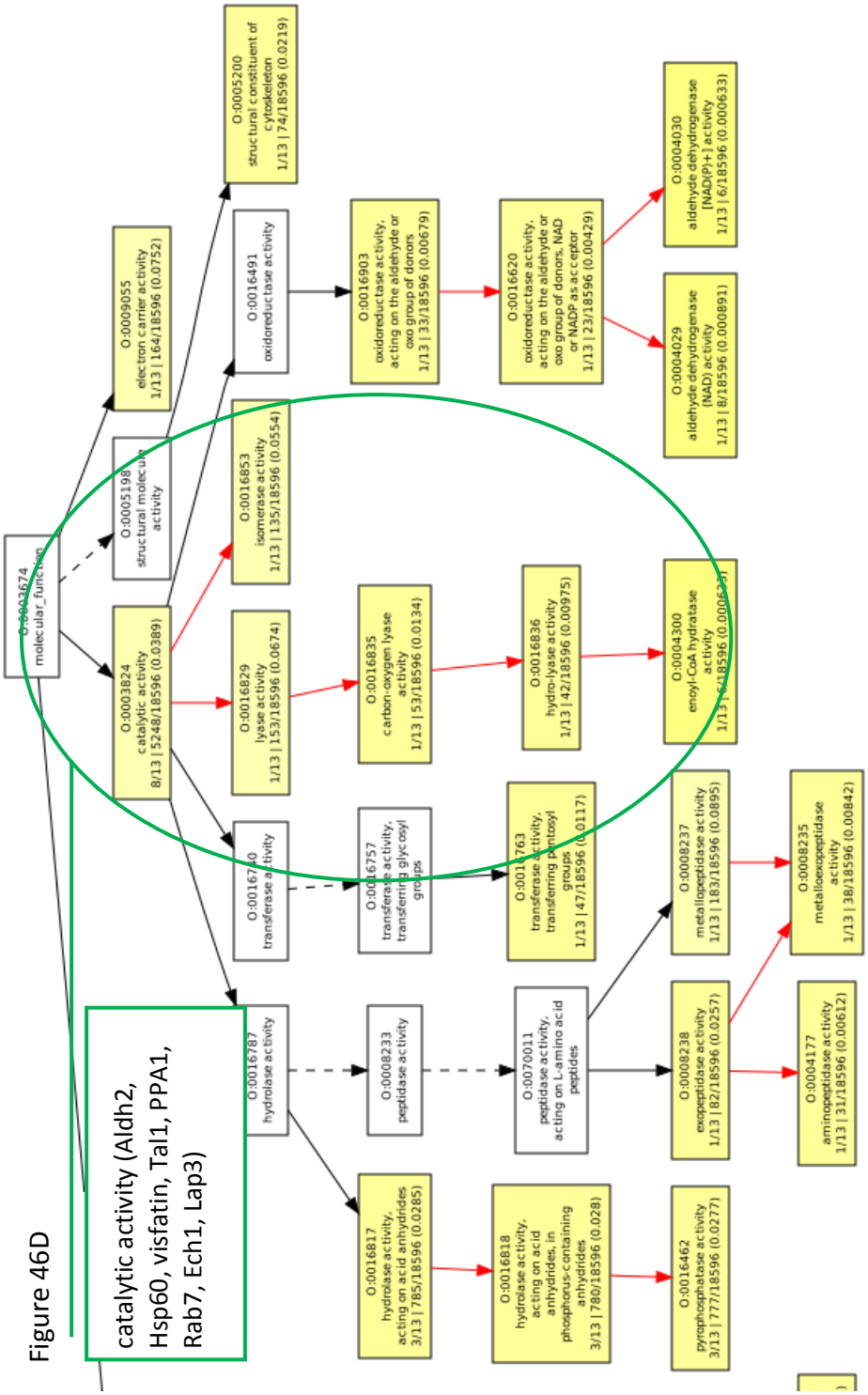
catalytic activity (Aldh2, Hsp60, visfatin, Tal1, PPA1, Rab7, Ech1, Lap3)
O:0005200 structural constituent of cytoskeleton 1/13 | 74/18596 (0.0219)
O:0009055 electron carrier activity 1/13 | 164/18596 (0.0752)
O:0005198 structural molecule activity
O:0016491 oxidoreductase activity
O:0016853 isomerase activity 1/13 | 135/18596 (0.0554)
O:0016903 oxidoreductase activity, acting on the aldehyde or oxo group of donors 1/13 | 33/18596 (0.00679)
O:0016620 oxidoreductase activity, acting on the aldehyde or oxo group of donors, NAD or NADP as acceptor 1/13 | 23/18596 (0.00429)
O:0004030 aldehyde dehydrogenase [NAD(P)+] activity 1/13 | 6/18596 (0.000633)
O:0004029 aldehyde dehydrogenase (NAD) activity 1/13 | 8/18596 (0.000891)
O:0003824 catalytic activity 8/13 | 5248/18596 (0.0389)
O:0016829 lyase activity 1/13 | 153/18596 (0.0674)
O:0016835 carbon-oxygen lyase activity 1/13 | 53/18596 (0.0134)
O:0016836 hydro-lyase activity 1/13 | 42/18596 (0.00975)
O:0004300 enoyl-CoA hydratase activity
O:0016757 transferase activity, transferring glycosyl groups
O:0016763 transferase activity, transferring pentosyl groups 1/13 | 47/18596 (0.0117)
O:0016787 hydrolase activity
O:0008233 peptidase activity
O:0070011 peptidase activity, acting on L-amino acid peptides
O:0008237 metallopeptidase activity 1/13 | 183/18596 (0.0895)
O:0008235 metalloexopeptidase activity 1/13 | 38/18596 (0.00842)
O:0008238 exopeptidase activity 1/13 | 82/18596 (0.0257)
O:0004177 aminopeptidase activity 1/13 | 31/18596 (0.00612)
O:0016817 hydrolase activity, acting on acid anhydrides 3/13 | 785/18596 (0.0285)
O:0016818 hydrolase activity, acting on acid anhydrides, in phosphorus-containing anhydrides 3/13 | 780/18596 (0.028)
O:0016462 pyrophosphatase activity 3/13 | 777/18596 (0.0277)

Figure 46D

Figure 47A

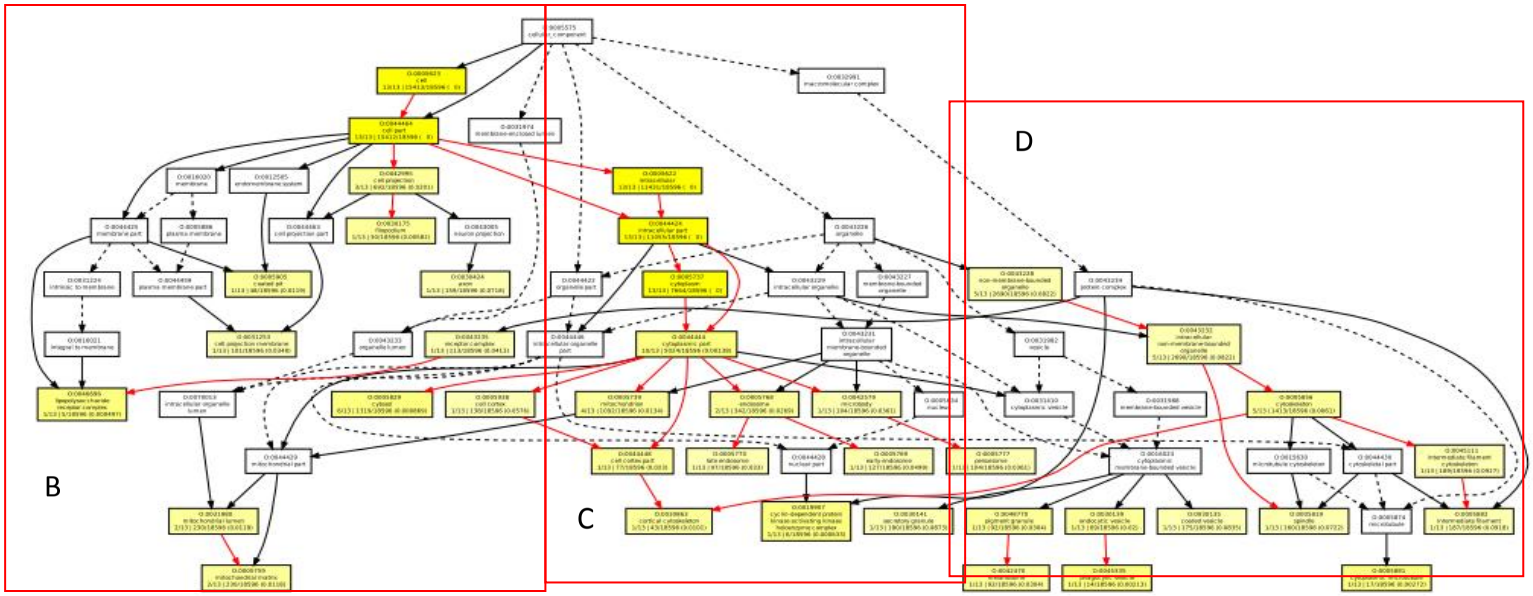

Figure 47 A-D: A) Overview of cellular compartments from the GOEAST software tool from the infected proteins. Boxes indicate approximate areas of greater detail in the following figures (B-D, following pages). In the following pages, yellow boxes indicate processes containing proteins that were determined to be significantly enriched with respect to the GO term in the analysis. The number at the top of the boxes is a GO ontology number, the next line describes the biological process , the bottom row of numbers n/13 where n is the number of proteins from the analysis that are assigned to the GO number at the top, followed by y/18596 where y is the number of gene IDs for a given GO number and 18596 is the total number of IDs in the entire GO dataset. The final number in parentheses indicates a p-value describing the significance of enrichment for the protein(s) associated with the GO number. White boxes do not have significant enrichment. Red arrows show connection between two enriched GO terms, black solid arrows show connection between an enriched and an unenriched term, and black dashed arrows show the connection between two unenriched terms.

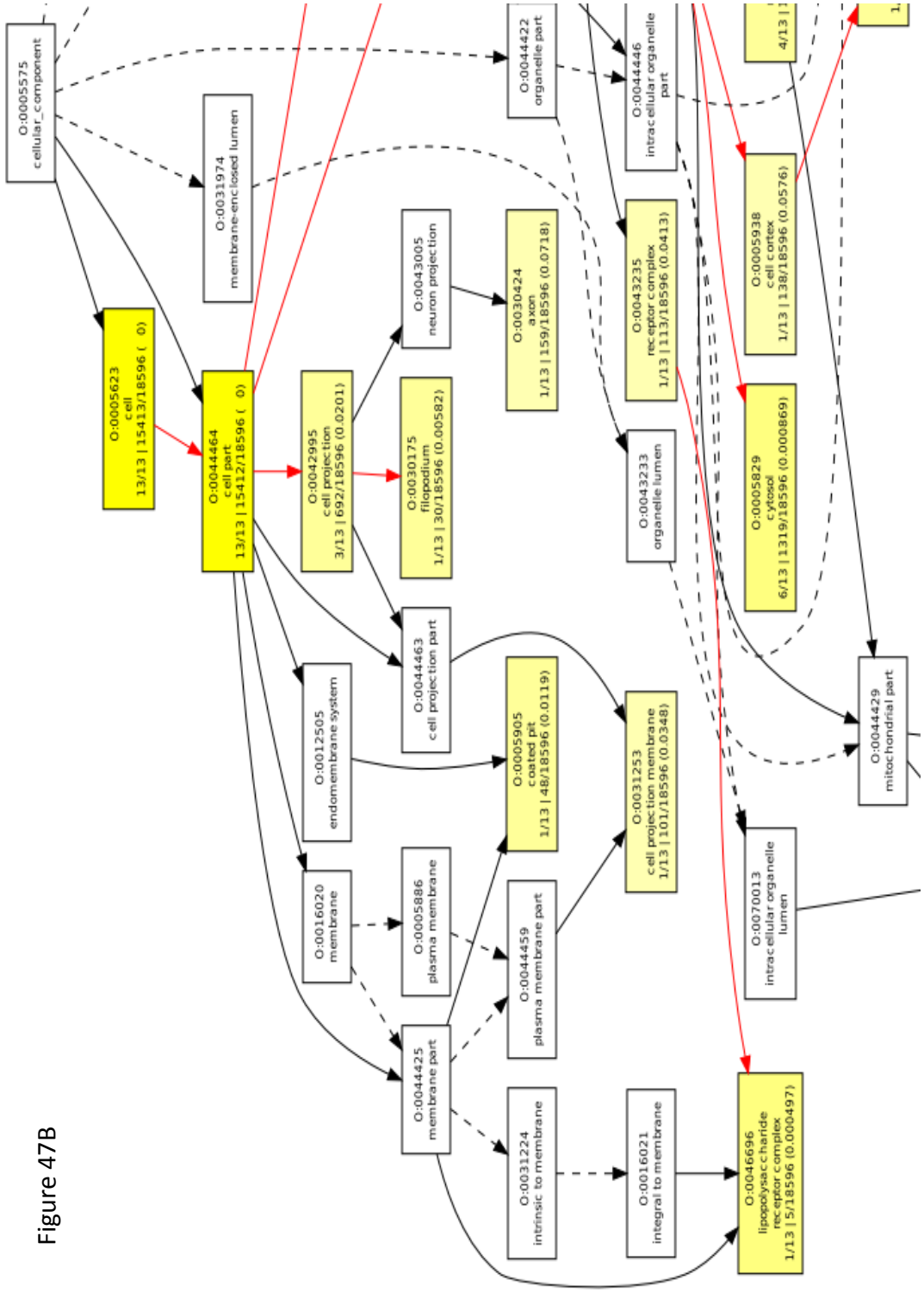
O:0005575
cellular_component
O:0031974
membrane-enclosed lumen
O:0044422
organelle part
O:0044446
intracellular organelle part
O:0005623
cell
13/13 | 15413/18596 (0)
O:0044464
cell part
13/13 | 15412/18596 (0)
O:0042995
cell projection
3/13 | 692/18596 (0.0201)
O:0043005
neuron projection
O:0030424
axon
1/13 | 159/18596 (0.0718)
O:0043235
receptor complex
1/13 | 113/18596 (0.0413)
O:0005938
cell cortex
1/13 | 138/18596 (0.0576)
O:0030175
filopodium
1/13 | 30/18596 (0.00582)
O:0043233
organelle lumen
O:0005829
cytosol
6/13 | 1319/18596 (0.000869)
O:0044463
cell projection part
O:0012505
endomembrane system
O:0005905
coated pit
1/13 | 48/18596 (0.0119)
O:0031253
cell projection membrane
1/13 | 101/18596 (0.0348)
O:0044429
mitochondrial part
O:0016020
membrane
O:0005886
plasma membrane
O:0044459
plasma membrane part
O:0070013
intracellular organelle lumen
O:0044425
membrane part
O:0031224
intrinsic to membrane
O:0016021
integral to membrane
O:0046696
lipopolysaccharide receptor complex
1/13 | 5/18596 (0.000497)

Figure 47B

Figure 47C

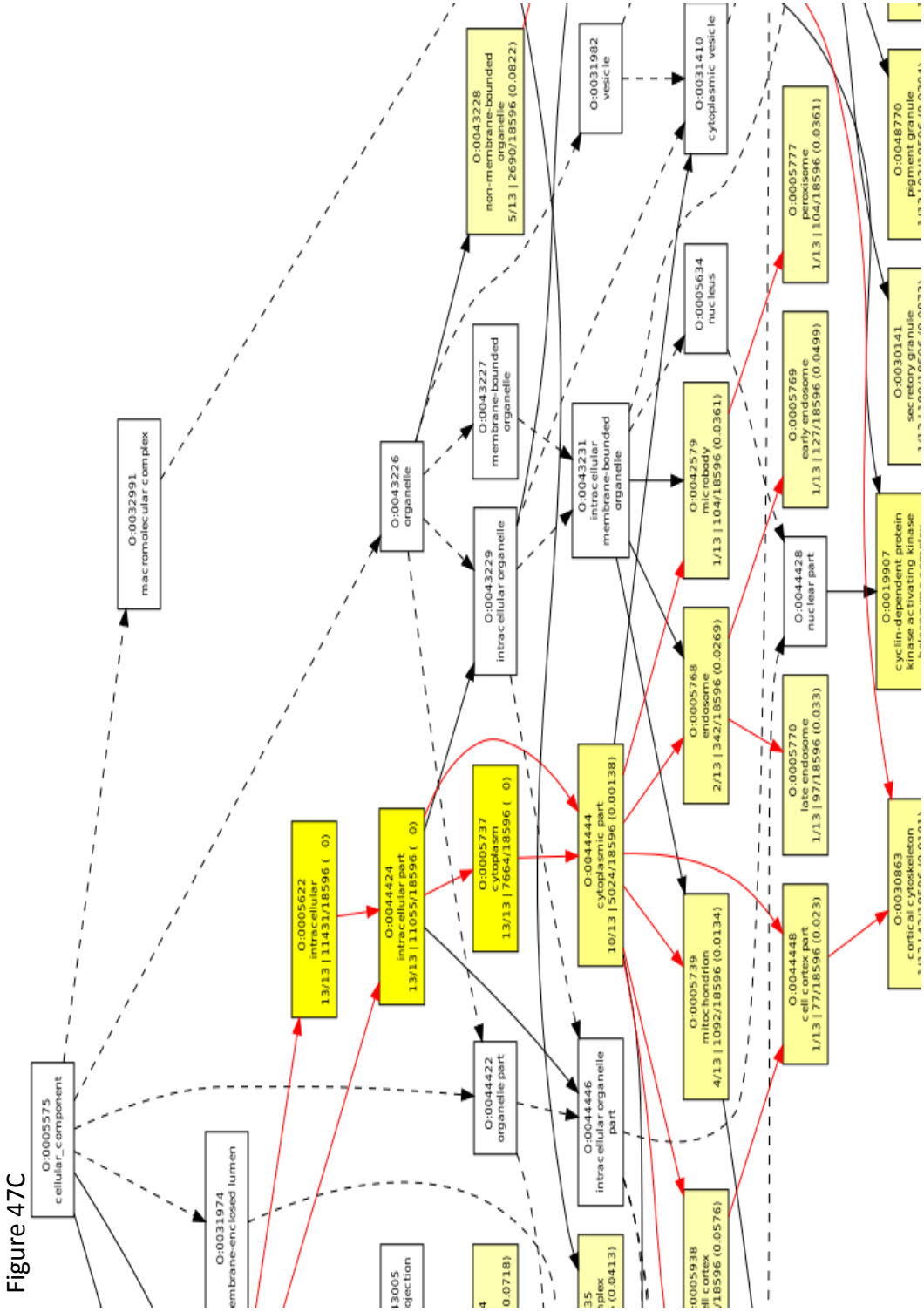
O:0005575
cellular_component
O:0032991
macromolecular complex
O:0031974
membrane-enclosed lumen
O:0005622
intracellular
13/13 | 11431/18596 (0)
O:0044424
intracellular part
13/13 | 11055/18596 (0)
O:0005737
cytoplasm
13/13 | 7664/18596 (0)
O:0043226
organelle
O:0043227
membrane-bounded organelle
O:0043228
non-membrane-bounded organelle
5/13 | 2690/18596 (0.0822)
O:0043229
intracellular organelle
O:0043231
intracellular membrane-bounded organelle
O:0031982
vesicle
O:0031410
cytoplasmic vesicle
O:0044422
organelle part
O:0044446
intracellular organelle part
O:0044444
cytoplasmic part
10/13 | 5024/18596 (0.00138)
O:0005634
nucleus
O:0042579
microbody
1/13 | 104/18596 (0.0361)
O:0005768
endosome
2/13 | 342/18596 (0.0269)
O:0005739
mitochondrion
4/13 | 1092/18596 (0.0134)
O:0005769
early endosome
1/13 | 127/18596 (0.0499)
O:0005777
peroxisome
1/13 | 104/18596 (0.0361)
O:0044428
nuclear part
O:0005770
late endosome
1/13 | 97/18596 (0.033)
O:0044448
cell cortex part
1/13 | 77/18596 (0.023)
O:0048770
pigment granule
O:0030141
secretory granule
O:0019907
cyclin-dependent protein kinase activating kinase
O:0030863
cortical cytoskeleton

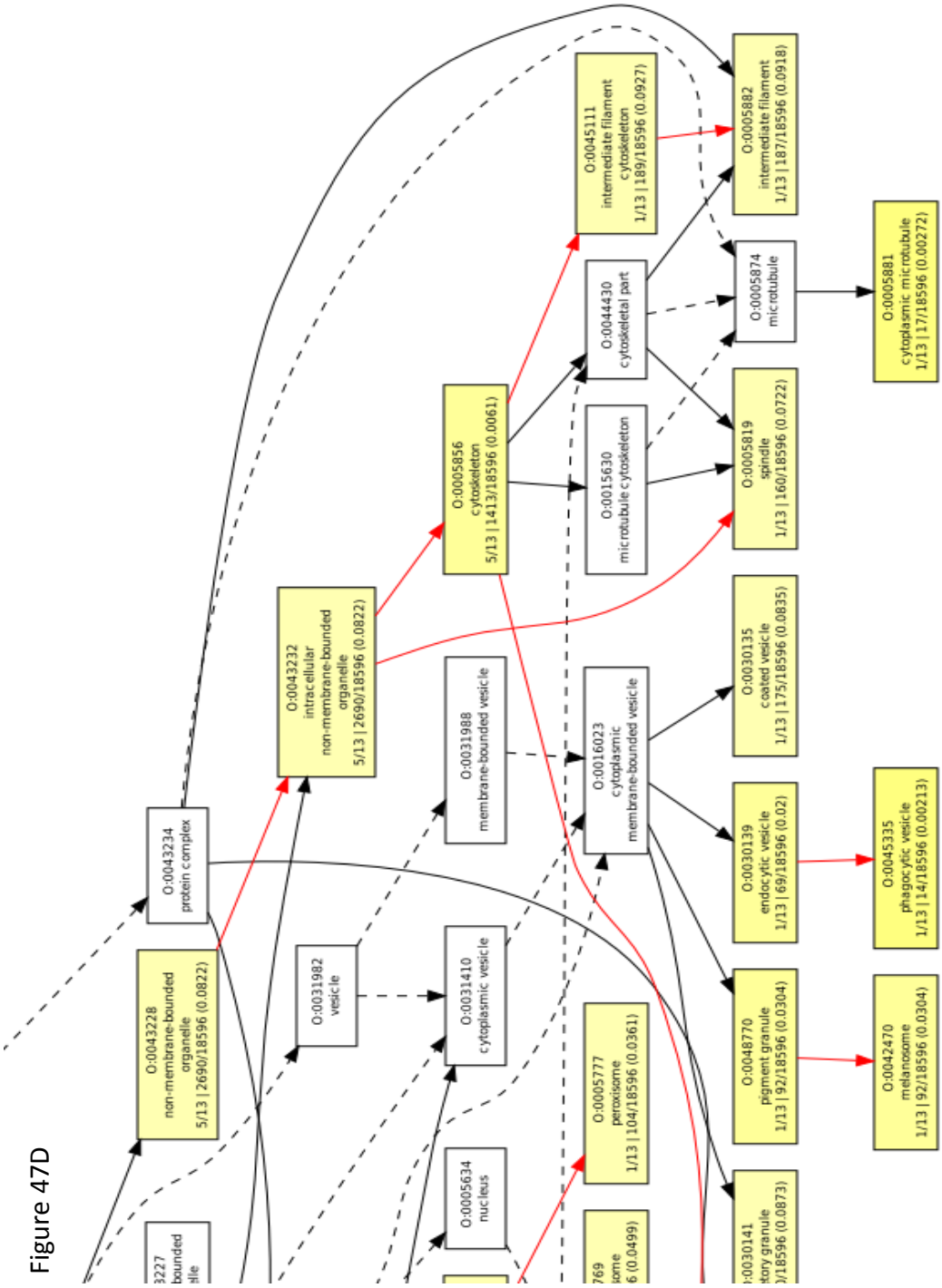
O:0043234
protein complex
O:0043228
non-membrane-bounded
organelle
5/13 | 2690/18596 (0.0822)
O:0031982
vesicle
O:0043232
intracellular
non-membrane-bounded
organelle
5/13 | 2690/18596 (0.0822)
O:0031410
cytoplasmic vesicle
O:0031988
membrane-bounded vesicle
O:0005634
nucleus
O:0005777
peroxisome
1/13 | 104/18596 (0.0361)
O:0016023
cytoplasmic
membrane-bounded vesicle
O:0005856
cytoskeleton
5/13 | 1413/18596 (0.0061)
O:0045111
intermediate filament
cytoskeleton
1/13 | 189/18596 (0.0927)
O:0044430
cytoskeletal part
O:0015630
microtubule cytoskeleton
O:0005882
intermediate filament
1/13 | 187/18596 (0.0918)
O:0005874
microtubule
O:0005819
spindle
1/13 | 160/18596 (0.0722)
O:0005881
cytoplasmic microtubule
1/13 | 17/18596 (0.00272)
O:0030135
coated vesicle
1/13 | 175/18596 (0.0835)
O:0030139
endocytic vesicle
1/13 | 69/18596 (0.02)
O:0045335
phagocytic vesicle
1/13 | 14/18596 (0.00213)
O:0048770
pigment granule
1/13 | 92/18596 (0.0304)
O:0042470
melanosome
1/13 | 92/18596 (0.0304)

Figure 47D

Figure 48A

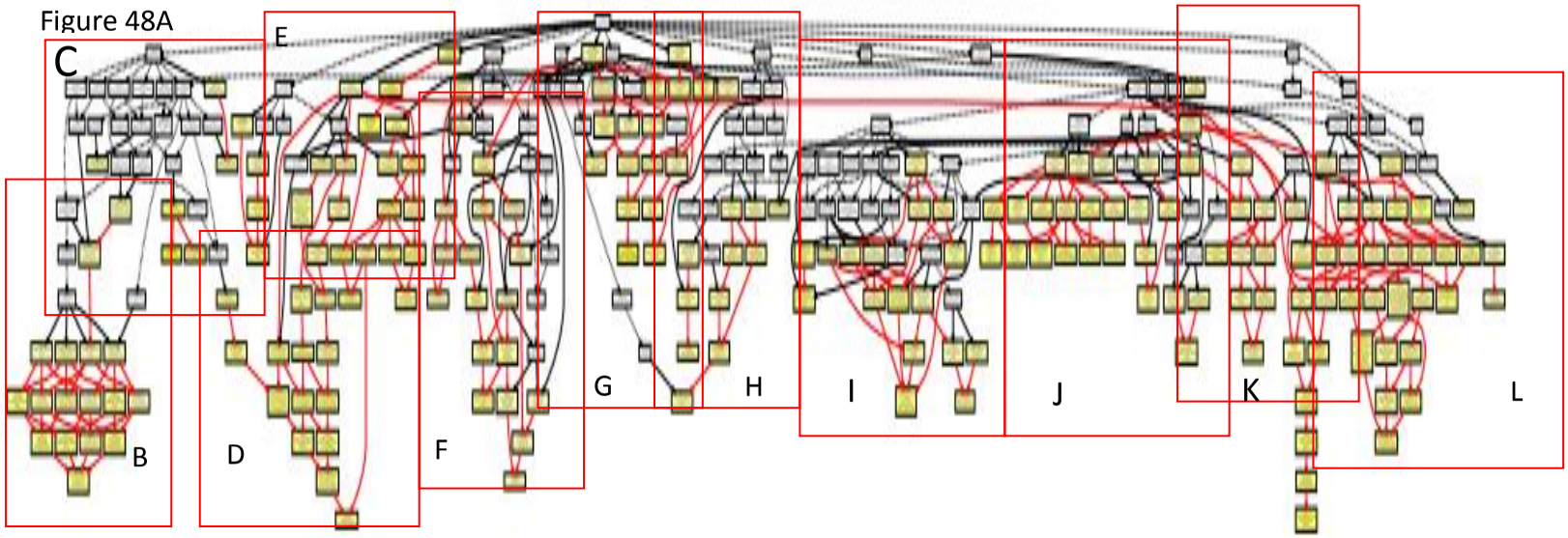

Figure 48 A-L: A) Overview of biological processes from the GOEAST software tool from the Securinine stimulated proteins. Boxes indicate approximate areas of greater detail in the following figures (B-L, following pages). In the following pages, yellow boxes indicate processes containing proteins that were determined to be significantly enriched with respect to the GO term in the analysis. The number at the top of the boxes is a GO ontology number, the next line describes the biological process , the bottom row of numbers n/10 where n is the number of proteins from the analysis that are assigned to the GO number at the top, followed by y/18596 where y is the number of gene IDs for a given GO number and 18596 is the total number of IDs in the entire GO dataset. The final number in parentheses indicates a p-value describing the significance of enrichment for the protein(s) associated with the GO number. White boxes do not have significant enrichment. Red arrows show connection between two enriched GO terms, black solid arrows show connection between an enriched and an unenriched term, and black dashed arrows show the connection between two unenriched terms.

Figure 48B

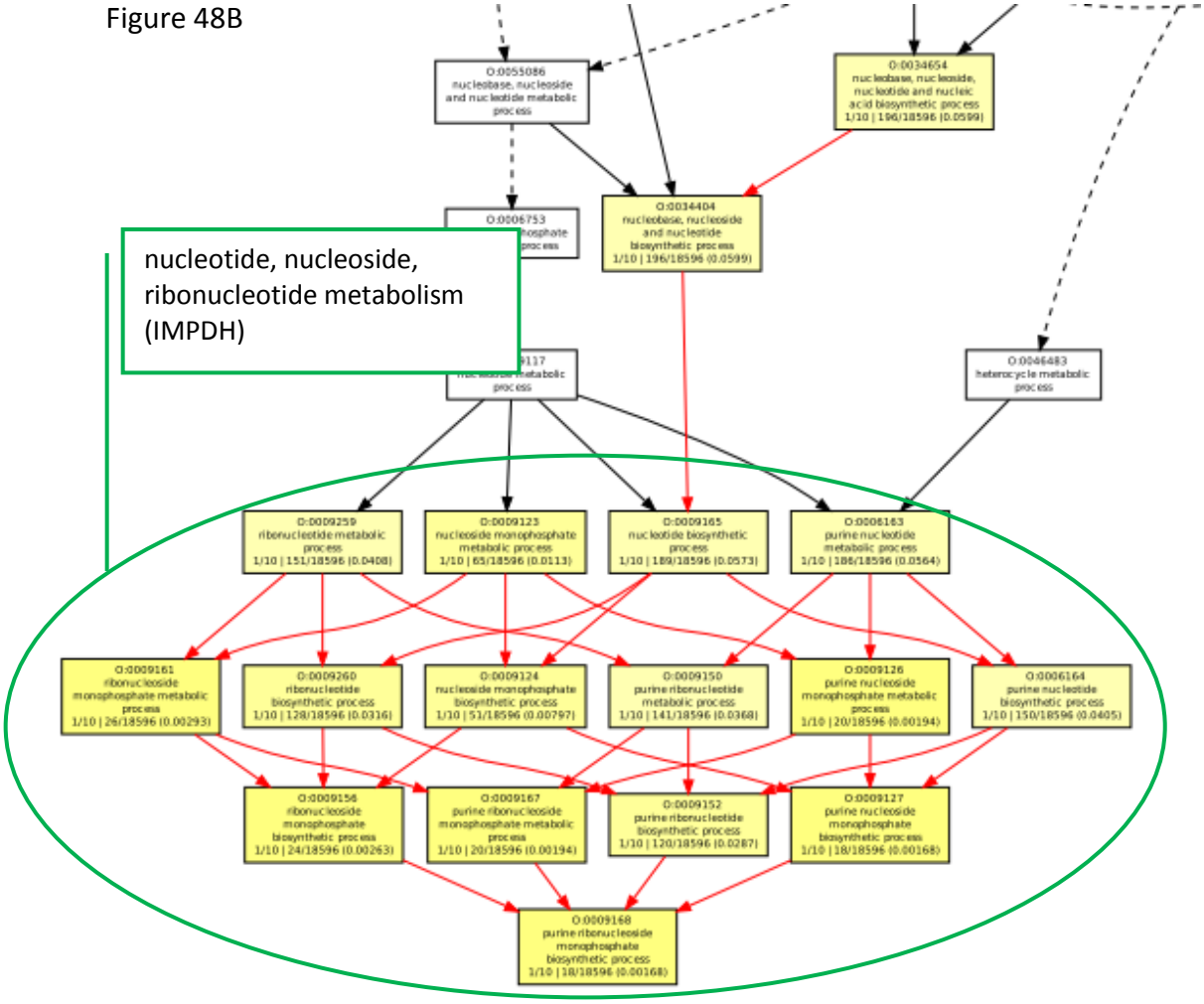
nucleotide, nucleoside, ribonucleotide metabolism (IMPDH)
O:0055086 nucleobase, nucleoside and nucleotide metabolic process
O:0034654 nucleobase, nucleoside, nucleotide and nucleic acid biosynthetic process 1/10 | 196/18596 (0.0599)
O:0034404 nucleobase, nucleoside and nucleotide biosynthetic process 1/10 | 196/18596 (0.0599)
O:0046483 heterocycle metabolic process
O:0009259 ribonucleotide metabolic process 1/10 | 151/18596 (0.0408)
O:0009123 nucleoside monophosphate metabolic process 1/10 | 65/18596 (0.0113)
O:0009165 nucleotide biosynthetic process 1/10 | 189/18596 (0.0573)
O:0006163 purine nucleotide metabolic process 1/10 | 186/18596 (0.0564)
O:0009161 ribonucleoside monophosphate metabolic process 1/10 | 26/18596 (0.00293)
O:0009260 ribonucleotide biosynthetic process 1/10 | 128/18596 (0.0316)
O:0009124 nucleoside monophosphate biosynthetic process 1/10 | 51/18596 (0.00797)
O:0009150 purine ribonucleotide metabolic process 1/10 | 141/18596 (0.0368)
O:0009126 purine nucleoside monophosphate metabolic process 1/10 | 20/18596 (0.00194)
O:0006164 purine nucleotide biosynthetic process 1/10 | 150/18596 (0.0405)
O:0009156 ribonucleoside monophosphate biosynthetic process 1/10 | 24/18596 (0.00263)
O:0009167 purine ribonucleoside monophosphate metabolic process 1/10 | 20/18596 (0.00194)
O:0009152 purine ribonucleotide biosynthetic process 1/10 | 120/18596 (0.0287)
O:0009127 purine nucleoside monophosphate biosynthetic process 1/10 | 18/18596 (0.00168)
O:0009168 purine ribonucleoside monophosphate biosynthetic process 1/10 | 18/18596 (0.00168)

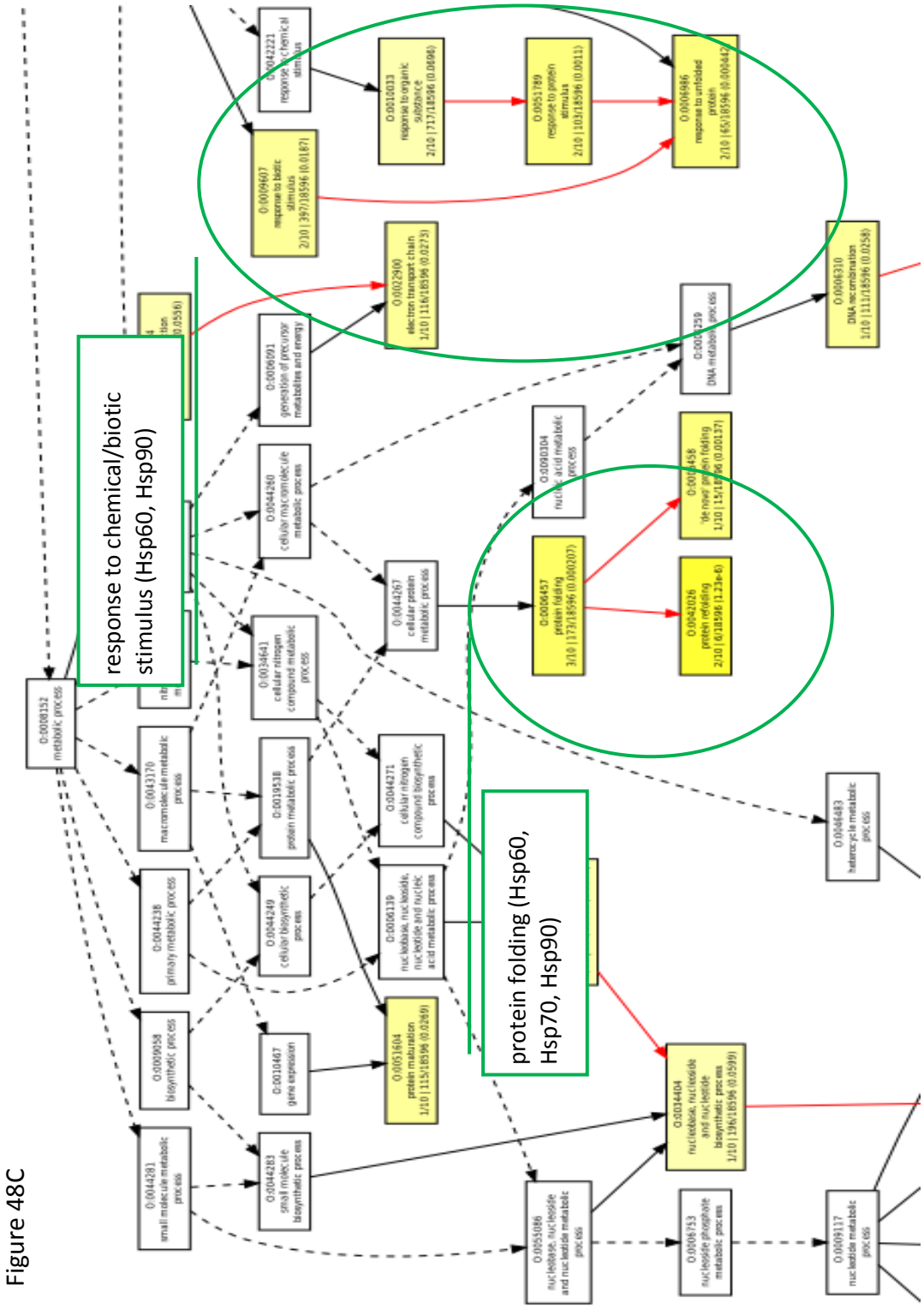
response to chemical/biotic stimulus (Hsp60, Hsp90)
protein folding (Hsp60, Hsp70, Hsp90)
GO:0006457 protein folding 3/10 | 173/18596 (0.080207)
GO:0042026 protein refolding 2/10 | 6/18596 (1.23e-6)
GO:0006986 response to unfolded protein 2/10 | 65/18596 (0.00044)
GO:0051789 response to protein stimulus 2/10 | 103/18596 (0.0011)
GO:0009607 response to biotic stimulus 2/10 | 397/18596 (0.0187)
GO:0042221 response to chemical stimulus
GO:0019538 protein metabolic process
GO:0044267 cellular protein metabolic process
GO:0044260 cellular macromolecule metabolic process
GO:0034641 cellular nitrogen compound metabolic process
GO:0044271 cellular nitrogen compound biosynthetic process
GO:0044238 primary metabolic process
GO:0044249 cellular biosynthetic process
GO:0009058 biosynthetic process
GO:0044281 small molecule metabolic process
GO:0044283 small molecule biosynthetic process
GO:0043170 macromolecule metabolic process
GO:0008152 metabolic process
GO:0006139 nucleobase, nucleoside, nucleotide and nucleic acid metabolic process
GO:0034404 nucleobase, nucleoside and nucleotide biosynthetic process
GO:0055086 nucleobase, nucleoside and nucleotide metabolic process
GO:0009117 nucleotide metabolic process
GO:0006259 DNA metabolic process
GO:0006310 DNA recombination
GO:0002790 electron transport chain
GO:0006091 generation of precursor metabolites and energy
GO:0010467 gene expression
GO:0051604 protein maturation
GO:0046483 heterocycle metabolic process
GO:0009165 nucleotide biosynthetic process
GO:0009135 nucleoside triphosphate biosynthetic process
GO:0009163 nucleoside biosynthetic process
GO:0009127 nucleoside monophosphate biosynthetic process
GO:0009123 nucleoside monophosphate metabolic process
GO:0009161 ribonucleoside monophosphate metabolic process
GO:0009142 nucleoside triphosphate metabolic process
GO:0009144 purine nucleoside triphosphate metabolic process
GO:0009199 ribonucleoside triphosphate metabolic process
GO:0009206 purine ribonucleoside triphosphate metabolic process
GO:0009201 ribonucleoside triphosphate biosynthetic process
GO:0009145 purine nucleoside triphosphate biosynthetic process
GO:0009152 purine ribonucleotide biosynthetic process
GO:0009260 ribonucleotide biosynthetic process
GO:0009156 ribonucleotide monophosphate biosynthetic process
GO:0009168 purine ribonucleoside monophosphate biosynthetic process
GO:0009126 purine nucleoside monophosphate metabolic process
GO:0009167 purine ribonucleoside monophosphate metabolic process
GO:0009150 purine ribonucleotide metabolic process
GO:0009259 ribonucleotide metabolic process
GO:0009128 purine nucleoside monophosphate biosynthetic process
GO:0009124 nucleoside monophosphate biosynthetic process
GO:0009154 purine ribonucleotide catabolic process
GO:0009261 ribonucleotide catabolic process
GO:0009164 nucleoside catabolic process
GO:0009166 nucleotide catabolic process
GO:0009146 purine nucleoside triphosphate catabolic process
GO:0009203 ribonucleoside triphosphate catabolic process
GO:0009207 purine ribonucleoside triphosphate catabolic process
GO:0009143 nucleoside triphosphate catabolic process
GO:0009200 deoxyribonucleoside triphosphate metabolic process
GO:0009146 purine nucleoside triphosphate catabolic process
GO:0009203 ribonucleoside triphosphate catabolic process
GO:0009207 purine ribonucleoside triphosphate catabolic process
GO:0009143 nucleoside triphosphate catabolic process
GO:0009200 deoxyribonucleoside triphosphate metabolic process

Figure 48C

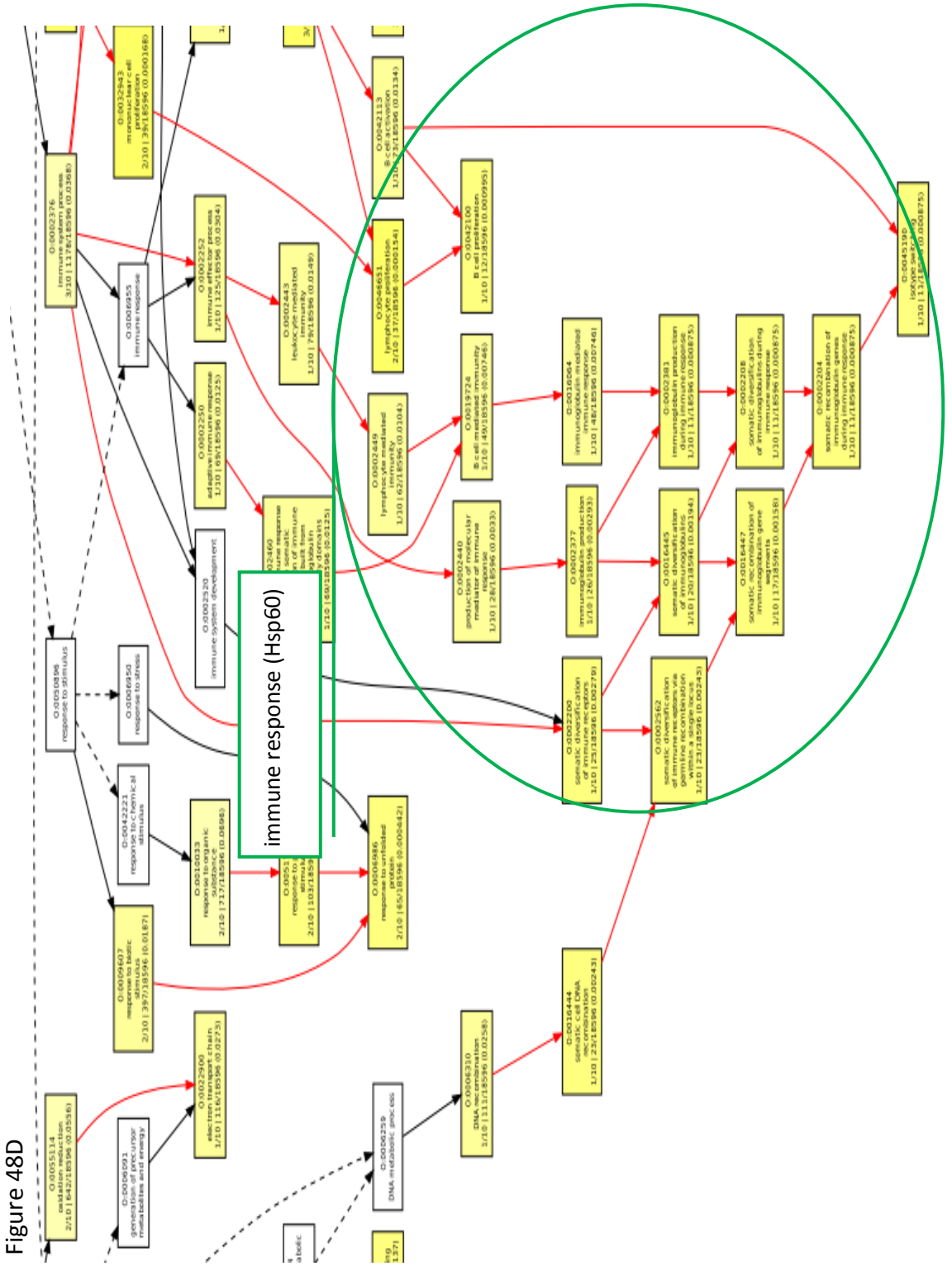

Figure 48D

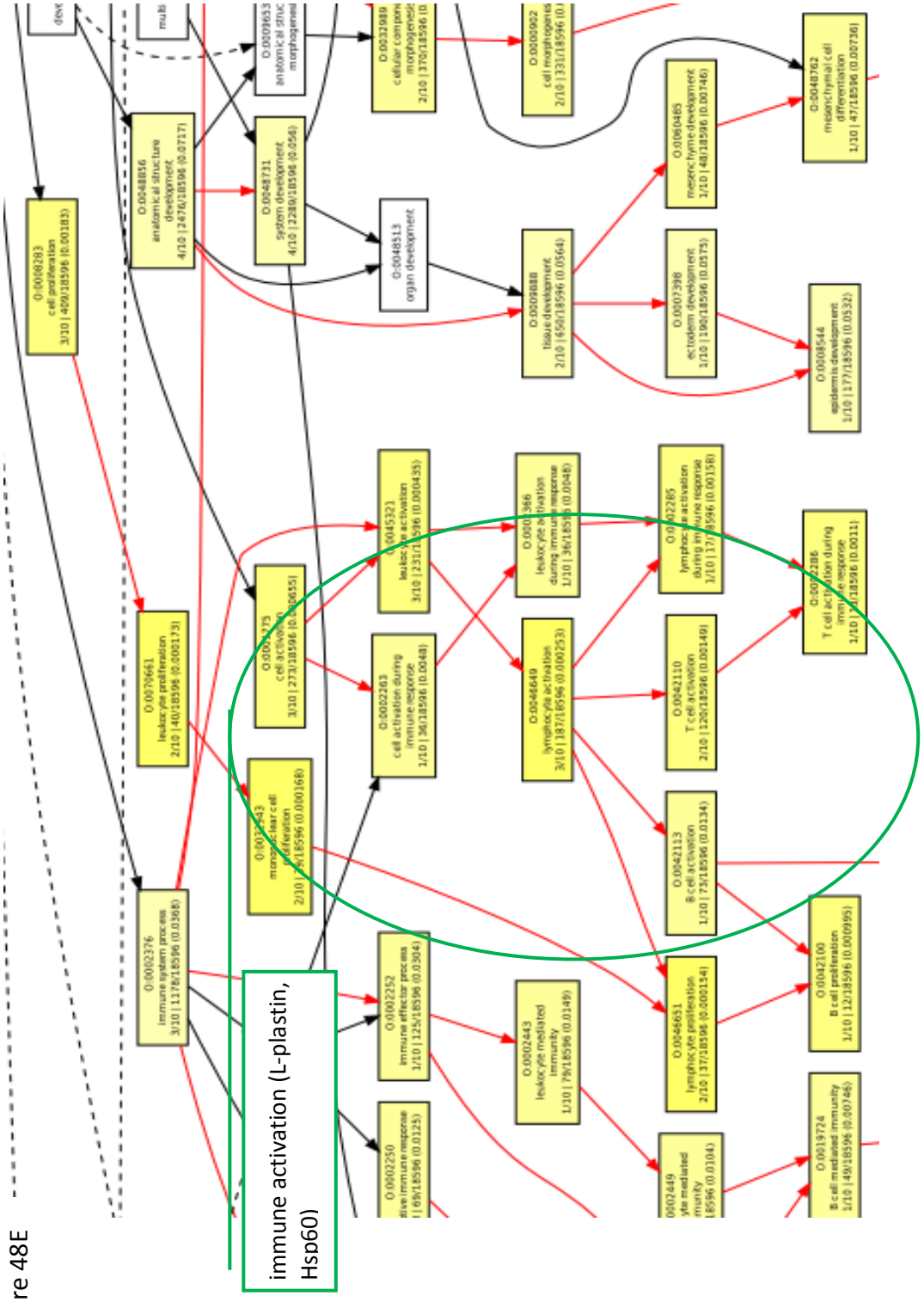

Figure 48E

Figure 48F

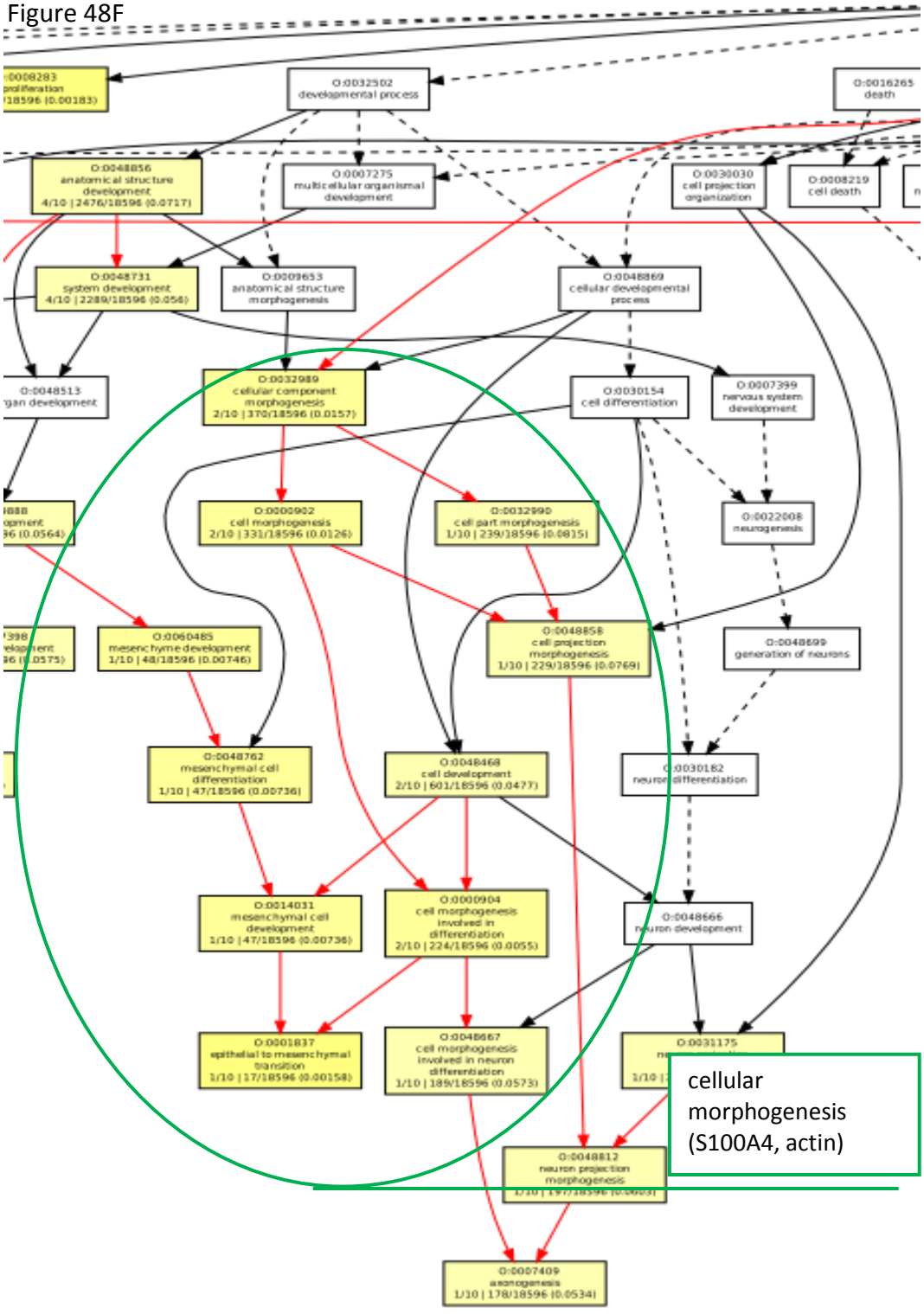
GO:0032502
developmental process
GO:0016265
death
GO:0048856
anatomical structure development
4/10 | 2476/18596 (0.0717)
GO:0007275
multicellular organismal development
GO:0030030
cell projection organization
GO:0008219
cell death
GO:0048731
system development
4/10 | 2289/18596 (0.056)
GO:0009653
anatomical structure morphogenesis
GO:0048869
cellular developmental process
GO:0048513
organ development
GO:0032989
cellular component morphogenesis
2/10 | 370/18596 (0.0157)
GO:0030154
cell differentiation
GO:0007399
nervous system development
GO:0000902
cell morphogenesis
2/10 | 331/18596 (0.0126)
GO:0032990
cell part morphogenesis
1/10 | 239/18596 (0.0815)
GO:0022008
neurogenesis
GO:0060485
mesenchyme development
1/10 | 48/18596 (0.00746)
GO:0048858
cell projection morphogenesis
1/10 | 229/18596 (0.0769)
GO:0048699
generation of neurons
GO:0048762
mesenchymal cell differentiation
1/10 | 47/18596 (0.00736)
GO:0048468
cell development
2/10 | 601/18596 (0.0477)
GO:0014031
mesenchymal cell development
1/10 | 47/18596 (0.00736)
GO:0000904
cell morphogenesis involved in differentiation
2/10 | 224/18596 (0.0055)
GO:0048666
neuron development
GO:0001837
epithelial to mesenchymal transition
1/10 | 17/18596 (0.00158)
GO:0048667
cell morphogenesis involved in neuron differentiation
1/10 | 189/18596 (0.0573)
GO:0048812
neuron projection morphogenesis
GO:0007409
axonogenesis
1/10 | 178/18596 (0.0534)
cellular morphogenesis (S100A4, actin)

Figure 48G

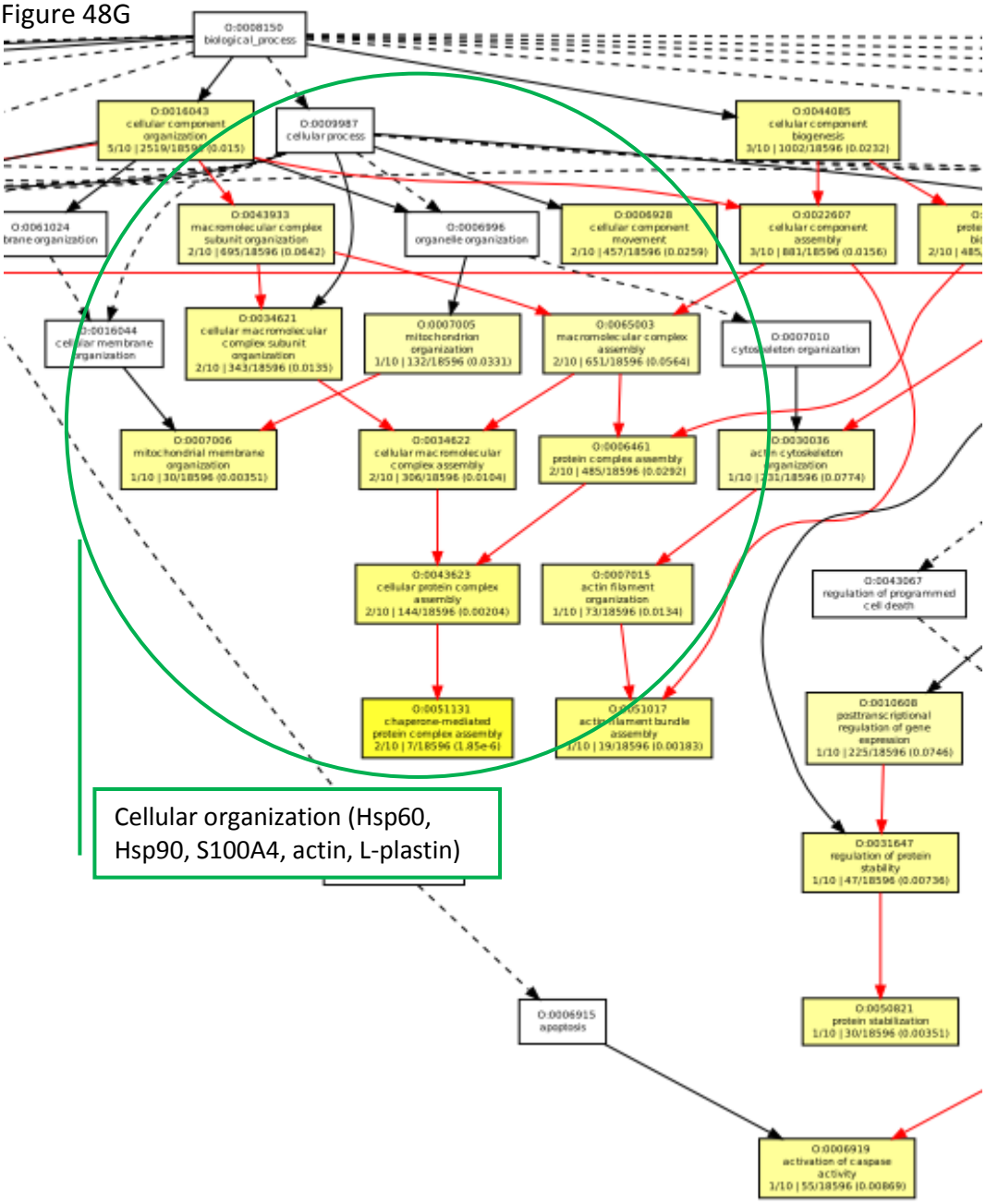

Figure 48H

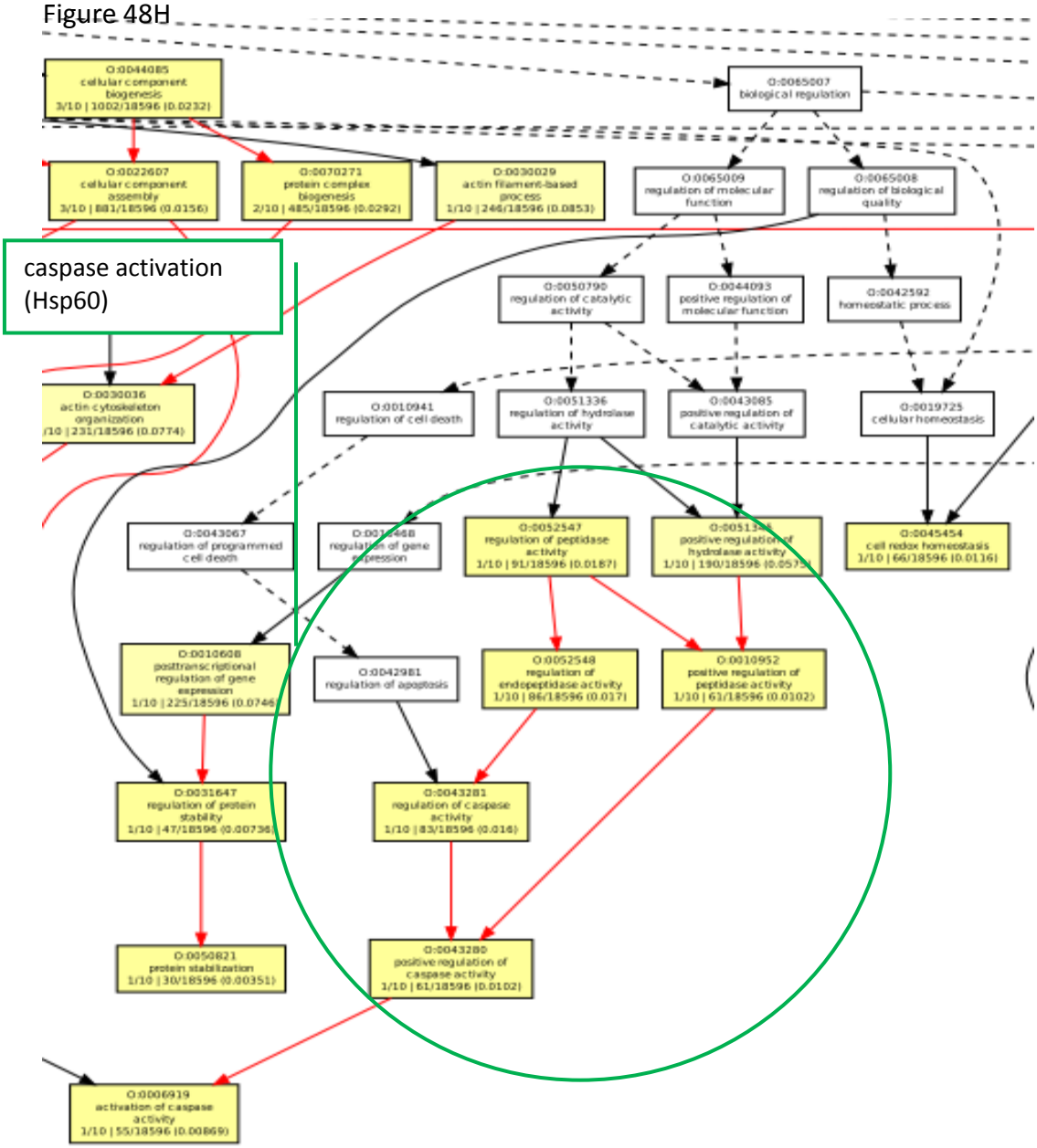
caspase activation
(Hsp60)
GO:0044085
cellular component
biogenesis
3/10 | 1002/18596 (0.0232)
GO:0065007
biological regulation
GO:0022607
cellular component
assembly
3/10 | 881/18596 (0.0156)
GO:0070271
protein complex
biogenesis
2/10 | 485/18596 (0.0292)
GO:0030029
actin filament-based
process
1/10 | 246/18596 (0.0853)
GO:0065009
regulation of molecular
function
GO:0065008
regulation of biological
quality
GO:0050790
regulation of catalytic
activity
GO:0044093
positive regulation of
molecular function
GO:0042592
homeostatic process
GO:0030036
actin cytoskeleton
organization
/10 | 231/18596 (0.0774)
GO:0010941
regulation of cell death
GO:0051336
regulation of hydrolase
activity
GO:0043085
positive regulation of
catalytic activity
GO:0019725
cellular homeostasis
GO:0043067
regulation of programmed
cell death
GO:0052547
regulation of peptidase
activity
1/10 | 91/18596 (0.0187)
GO:0045454
cell redox homeostasis
1/10 | 66/18596 (0.0116)
GO:0010608
posttranscriptional
regulation of gene
expression
1/10 | 225/18596 (0.0746)
GO:0042981
regulation of apoptosis
GO:0052548
regulation of
endopeptidase activity
1/10 | 86/18596 (0.017)
GO:0010952
positive regulation of
peptidase activity
1/10 | 61/18596 (0.0102)
GO:0031647
regulation of protein
stability
1/10 | 47/18596 (0.00736)
GO:0043281
regulation of caspase
activity
1/10 | 83/18596 (0.016)
GO:0050821
protein stabilization
1/10 | 30/18596 (0.00351)
GO:0043280
positive regulation of
caspase activity
1/10 | 61/18596 (0.0102)
GO:0006919
activation of caspase
activity
1/10 | 55/18596 (0.00869)

Figure 48I

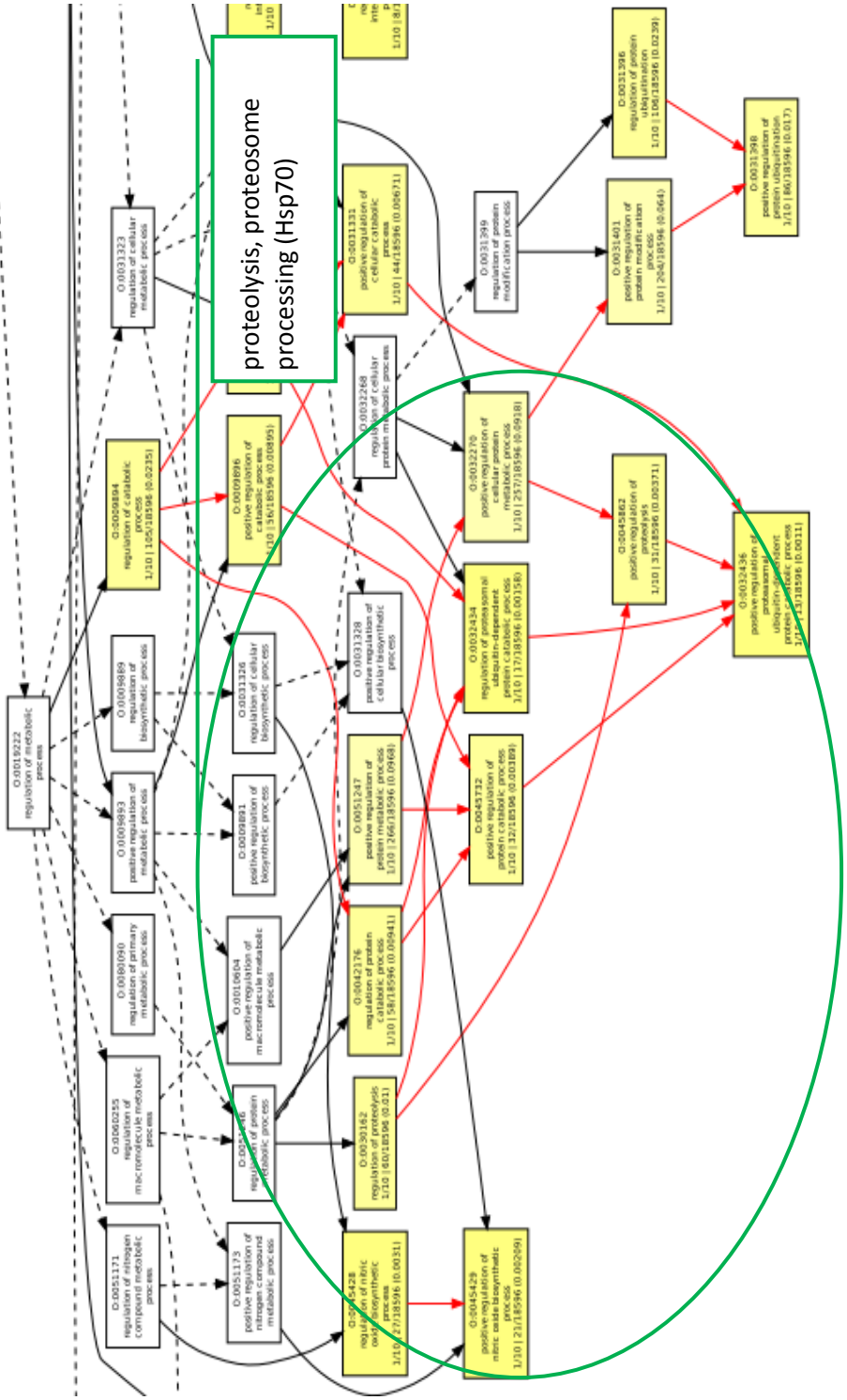

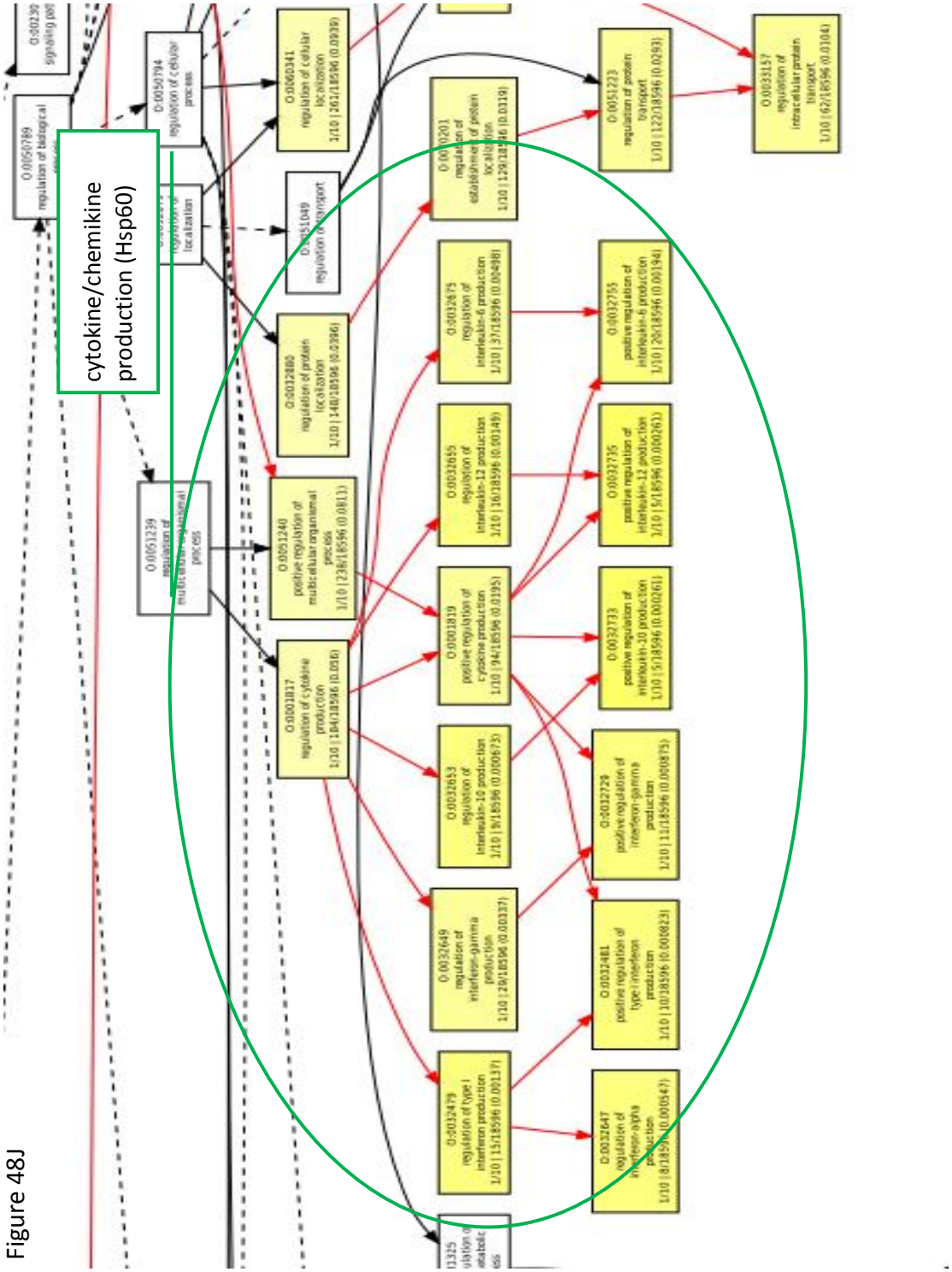

Figure 48J

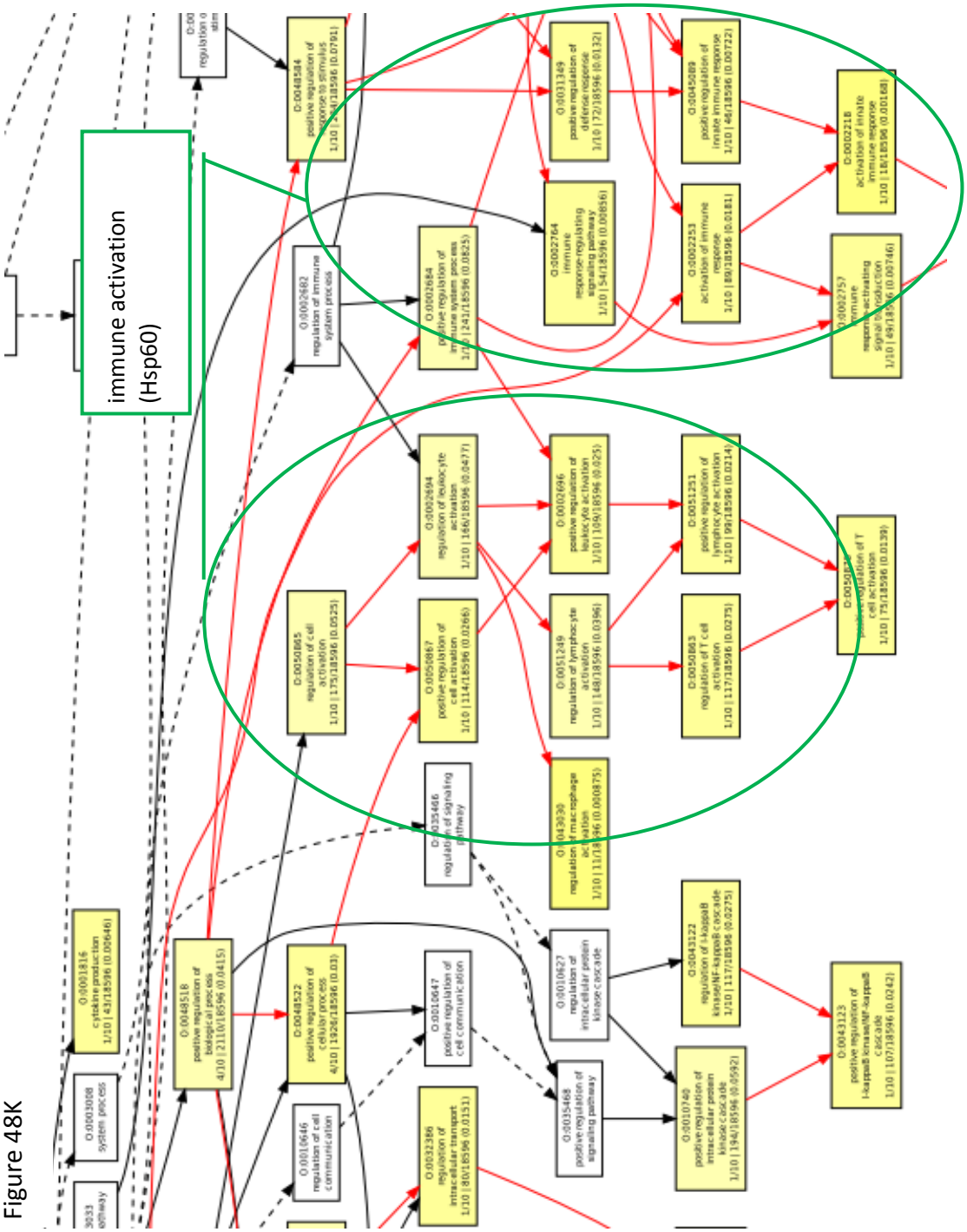

Figure 48K

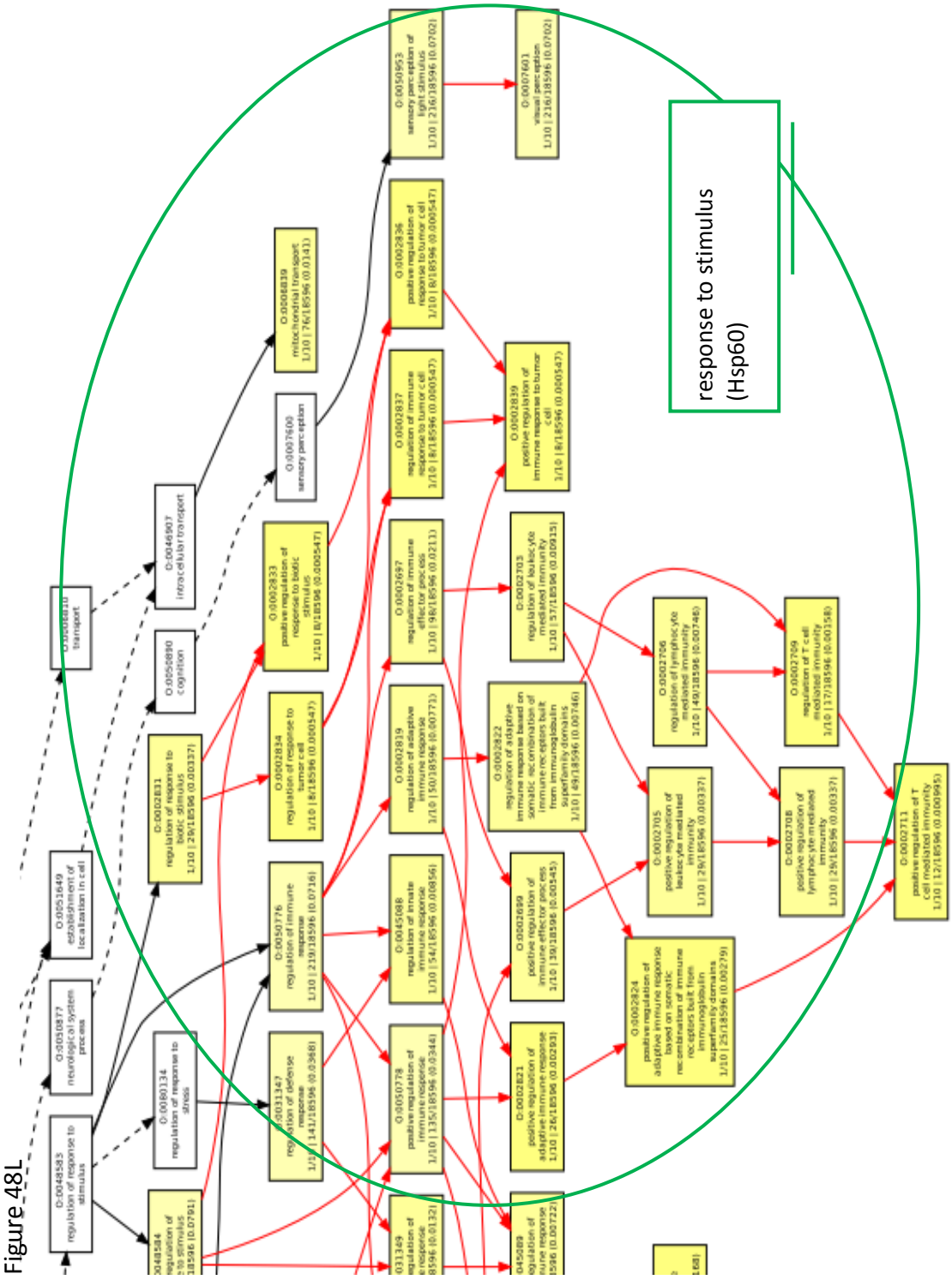

Figure 48L

Figure 49A

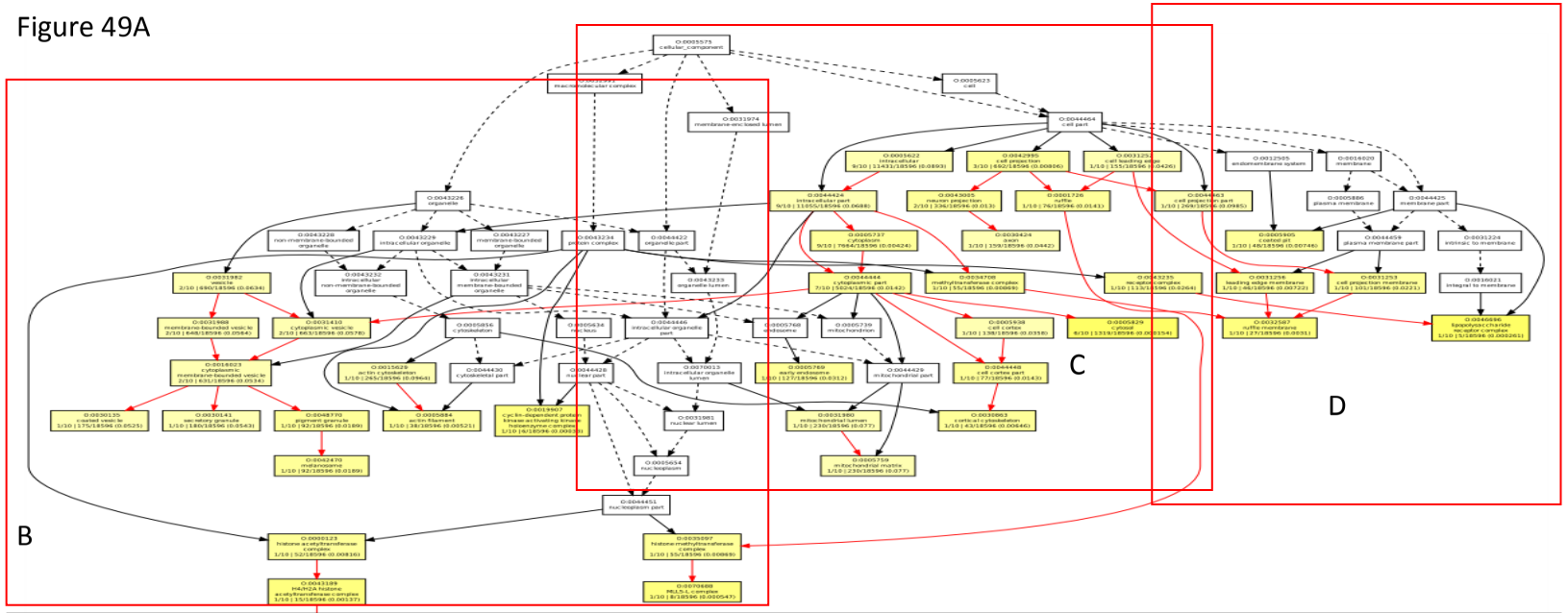

Figure 49 A-D: A) Overview of cellular component from the GOEAST software tool from the Securinine stimulated proteins. Boxes indicate approximate areas of greater detail in the following figures (B-D, following pages). In the following pages, yellow boxes indicate processes containing proteins that were determined to be significantly enriched with respect to the GO term in the analysis. The number at the top of the boxes is a GO ontology number, the next line describes the biological process , the bottom row of numbers n/10 where n is the number of proteins from the analysis that are assigned to the GO number at the top, followed by y/18596 where y is the number of gene IDs for a given GO number and 18596 is the total number of IDs in the entire GO dataset. The final number in parentheses indicates a p-value describing the significance of enrichment for the protein(s) associated with the GO number. White boxes do not have significant enrichment. Red arrows show connection between two enriched GO terms, black solid arrows show connection between an enriched and an unenriched term, and black dashed arrows show the connection between two unenriched terms.

Figure 49B

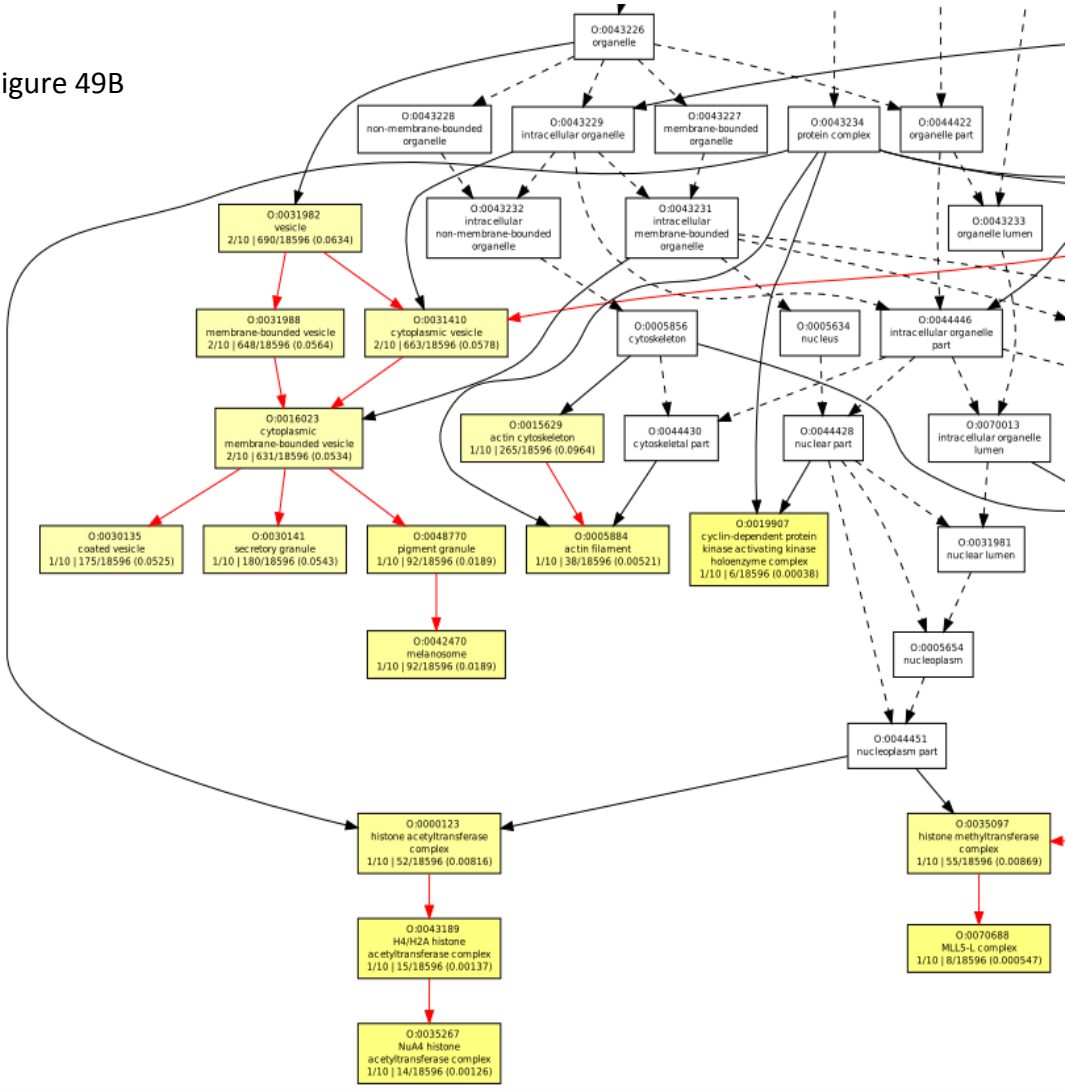
O:0043226
organelle
O:0043228
non-membrane-bounded
organelle
O:0043229
intracellular organelle
O:0043227
membrane-bounded
organelle
O:0043234
protein complex
O:0044422
organelle part
O:0031982
vesicle
2/10 | 690/18596 (0.0634)
O:0043232
intracellular
non-membrane-bounded
organelle
O:0043231
intracellular
membrane-bounded
organelle
O:0043233
organelle lumen
O:0031988
membrane-bounded vesicle
2/10 | 648/18596 (0.0564)
O:0031410
cytoplasmic vesicle
2/10 | 663/18596 (0.0578)
O:0005856
cytoskeleton
O:0005634
nucleus
O:0044446
intracellular organelle
part
O:0016023
cytoplasmic
membrane-bounded vesicle
2/10 | 631/18596 (0.0534)
O:0015629
actin cytoskeleton
1/10 | 265/18596 (0.0964)
O:0044430
cytoskeletal part
O:0044428
nuclear part
O:0070013
intracellular organelle
lumen
O:0030135
coated vesicle
1/10 | 175/18596 (0.0525)
O:0030141
secretory granule
1/10 | 180/18596 (0.0543)
O:0048770
pigment granule
1/10 | 92/18596 (0.0189)
O:0005884
actin filament
1/10 | 38/18596 (0.00521)
O:0019907
cyclin-dependent protein
kinase activating kinase
holoenzyme complex
1/10 | 6/18596 (0.00038)
O:0031981
nuclear lumen
O:0042470
melanosome
1/10 | 92/18596 (0.0189)
O:0005654
nucleoplasm
O:0044451
nucleoplasm part
O:0000123
histone acetyltransferase
complex
1/10 | 52/18596 (0.00816)
O:0035097
histone methyltransferase
complex
1/10 | 55/18596 (0.00869)
O:0043189
H4/H2A histone
acetyltransferase complex
1/10 | 15/18596 (0.00137)
O:0070688
MLL5-L complex
1/10 | 8/18596 (0.000547)
O:0035267
NuA4 histone
acetyltransferase complex
1/10 | 14/18596 (0.00126)

Figure 49C

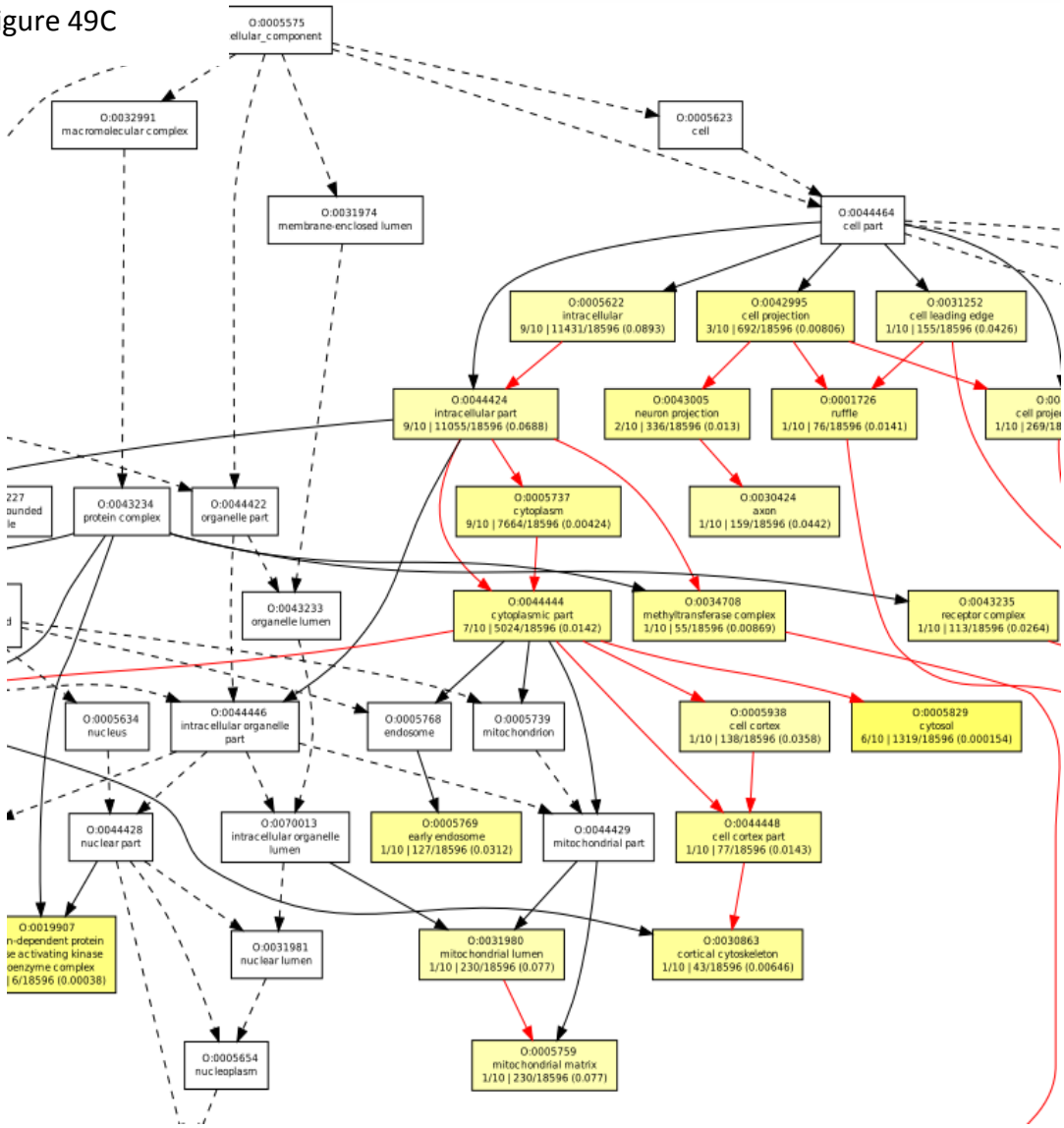
O:0005575
ellular_component
O:0032991
macromolecular complex
O:0005623
cell
O:0031974
membrane-enclosed lumen
O:0044464
cell part
O:0005622
intracellular
9/10 | 11431/18596 (0.0893)
O:0042995
cell projection
3/10 | 692/18596 (0.00806)
O:0031252
cell leading edge
1/10 | 155/18596 (0.0426)
O:0044424
intracellular part
9/10 | 11055/18596 (0.0688)
O:0043005
neuron projection
2/10 | 336/18596 (0.013)
O:0001726
ruffle
1/10 | 76/18596 (0.0141)
O:0043234
protein complex
O:0044422
organelle part
O:0005737
cytoplasm
9/10 | 7664/18596 (0.00424)
O:0030424
axon
1/10 | 159/18596 (0.0442)
O:0043233
organelle lumen
O:0044444
cytoplasmic part
7/10 | 5024/18596 (0.0142)
O:0034708
methyltransferase complex
1/10 | 55/18596 (0.00869)
O:0043235
receptor complex
1/10 | 113/18596 (0.0264)
O:0005634
nucleus
O:0044446
intracellular organelle part
O:0005768
endosome
O:0005739
mitochondrion
O:0005938
cell cortex
1/10 | 138/18596 (0.0358)
O:0005829
cytosol
6/10 | 1319/18596 (0.000154)
O:0044428
nuclear part
O:0070013
intracellular organelle lumen
O:0005769
early endosome
1/10 | 127/18596 (0.0312)
O:0044429
mitochondrial part
O:0044448
cell cortex part
1/10 | 77/18596 (0.0143)
O:0031981
nuclear lumen
O:0031980
mitochondrial lumen
1/10 | 230/18596 (0.077)
O:0030863
cortical cytoskeleton
1/10 | 43/18596 (0.00646)
O:0005654
nucleoplasm
O:0005759
mitochondrial matrix
1/10 | 230/18596 (0.077)

Figure 49D

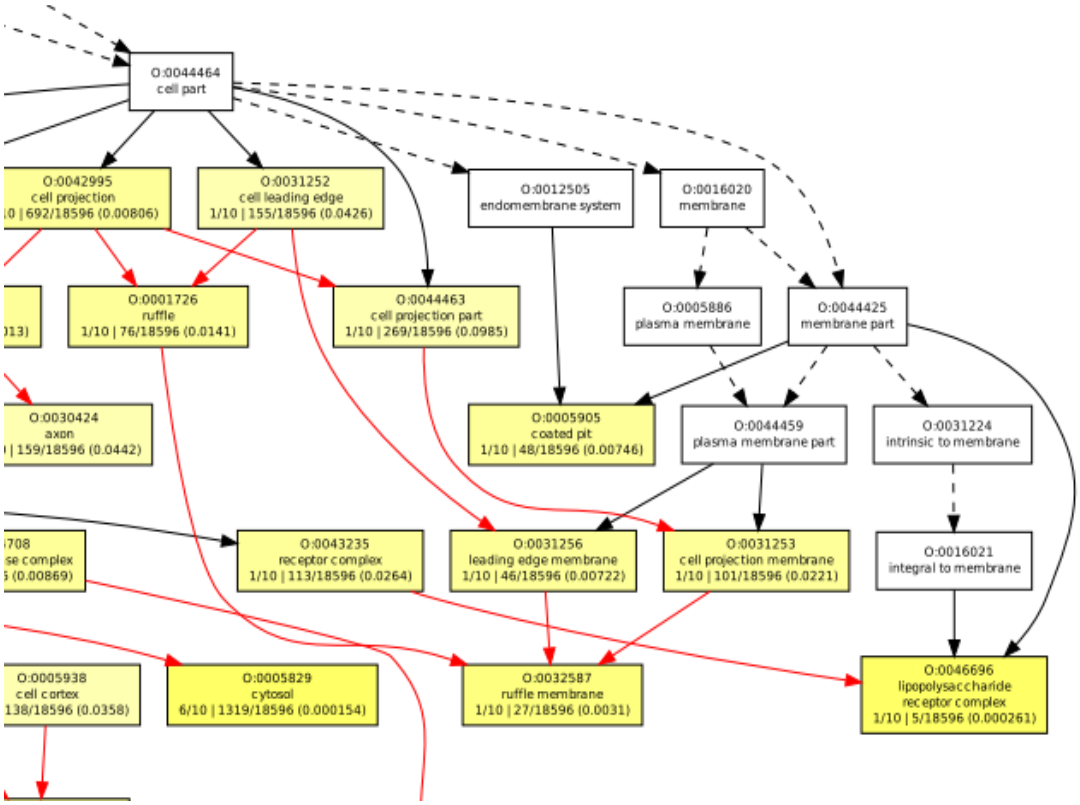
O:0044464
cell part
O:0042995
cell projection
692/18596 (0.00806)
O:0031252
cell leading edge
1/10 | 155/18596 (0.0426)
O:0012505
endomembrane system
O:0016020
membrane
O:0001726
ruffle
1/10 | 76/18596 (0.0141)
O:0044463
cell projection part
1/10 | 269/18596 (0.0985)
O:0005886
plasma membrane
O:0044425
membrane part
O:0030424
axon
159/18596 (0.0442)
O:0005905
coated pit
1/10 | 48/18596 (0.00746)
O:0044459
plasma membrane part
O:0031224
intrinsic to membrane
O:0043235
receptor complex
1/10 | 113/18596 (0.0264)
O:0031256
leading edge membrane
1/10 | 46/18596 (0.00722)
O:0031253
cell projection membrane
1/10 | 101/18596 (0.0221)
O:0016021
integral to membrane
O:0005938
cell cortex
138/18596 (0.0358)
O:0005829
cytosol
6/10 | 1319/18596 (0.000154)
O:0032587
ruffle membrane
1/10 | 27/18596 (0.0031)
O:0046696
lipopolysaccharide
receptor complex
1/10 | 5/18596 (0.000261)

Figure 50A

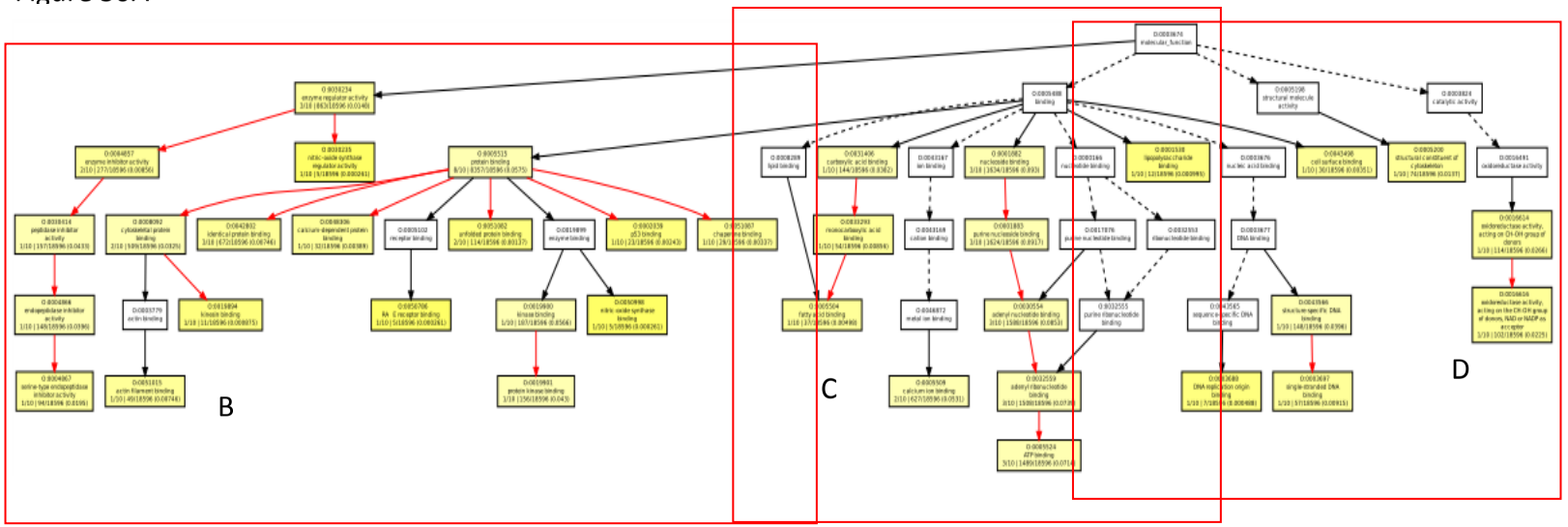

Figure 50 A-D: A) Overview of molecular component from the GOEAST software tool from the Securinine stimulated proteins. Boxes indicate approximate areas of greater detail in the following figures (B-D, following pages). In the following pages, yellow boxes indicate processes containing proteins that were determined to be significantly enriched with respect to the GO term in the analysis. The number at the top of the boxes is a GO ontology number, the next line describes the biological process , the bottom row of numbers n/10 where n is the number of proteins from the analysis that are assigned to the GO number at the top, followed by y/18596 where y is the number of gene IDs for a given GO number and 18596 is the total number of IDs in the entire GO dataset. The final number in parentheses indicates a p-value describing the significance of enrichment for the protein(s) associated with the GO number. White boxes do not have significant enrichment. Red arrows show connection between two enriched GO terms, black solid arrows show connection between an enriched and an unenriched term, and black dashed arrows show the connection between two unenriched terms.

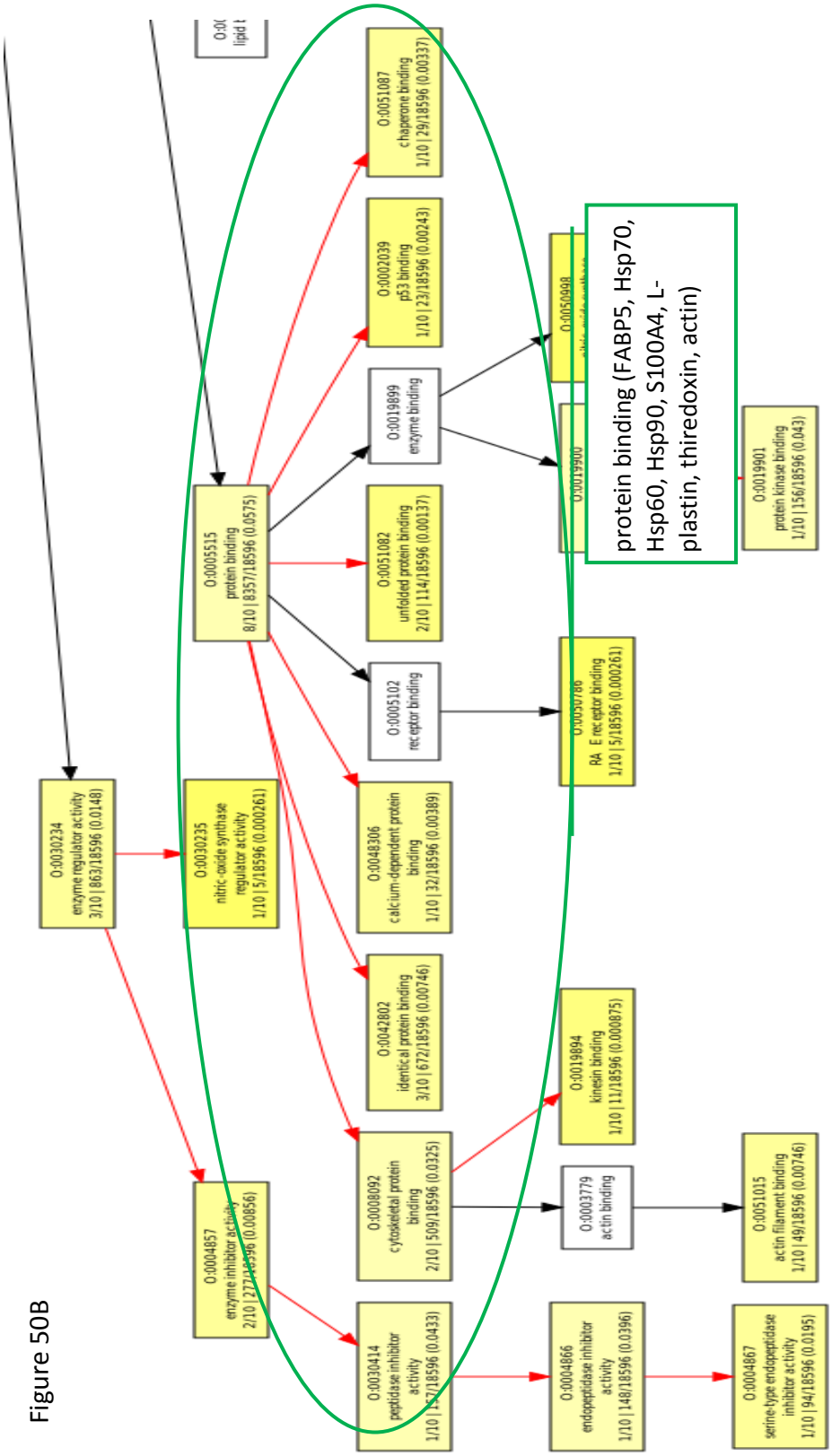
protein binding (FABP5, Hsp70, Hsp60, Hsp90, S100A4, L-plastin, thiredoxin, actin)

Figure 50B

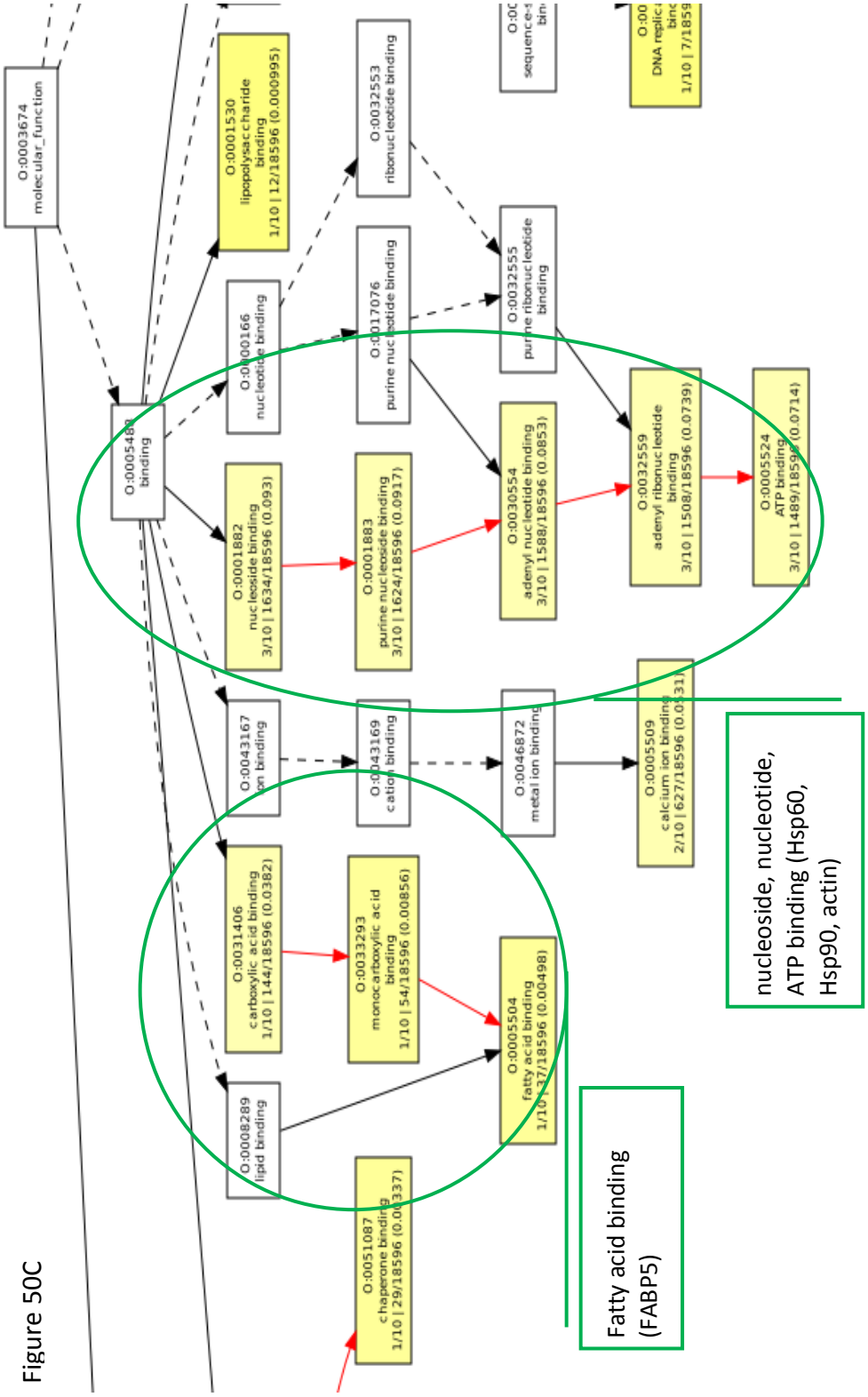
O:0003674
molecular_function
O:0005488
binding
O:0001530
lipopolysaccharide binding
1/10 | 12/18596 (0.000995)
O:0032553
ribonucleotide binding
O:0001882
nucleoside binding
3/10 | 1634/18596 (0.093)
O:0001883
purine nucleoside binding
3/10 | 1624/18596 (0.0917)
O:0030554
adenyl nucleotide binding
3/10 | 1588/18596 (0.0853)
O:0032559
adenyl ribonucleotide binding
3/10 | 1508/18596 (0.0739)
O:0005524
ATP binding
3/10 | 1489/18596 (0.0714)
O:0031406
carboxylic acid binding
1/10 | 144/18596 (0.0382)
O:0033293
monocarboxylic acid binding
1/10 | 54/18596 (0.00856)
O:0005504
fatty acid binding
1/10 | 37/18596 (0.00498)
O:0008289
lipid binding
O:0051087
chaperone binding
1/10 | 29/18596 (0.00337)
nucleoside, nucleotide, ATP binding (Hsp60, Hsp90, actin)
Fatty acid binding (FABP5)

Figure 50C

Figure 50D

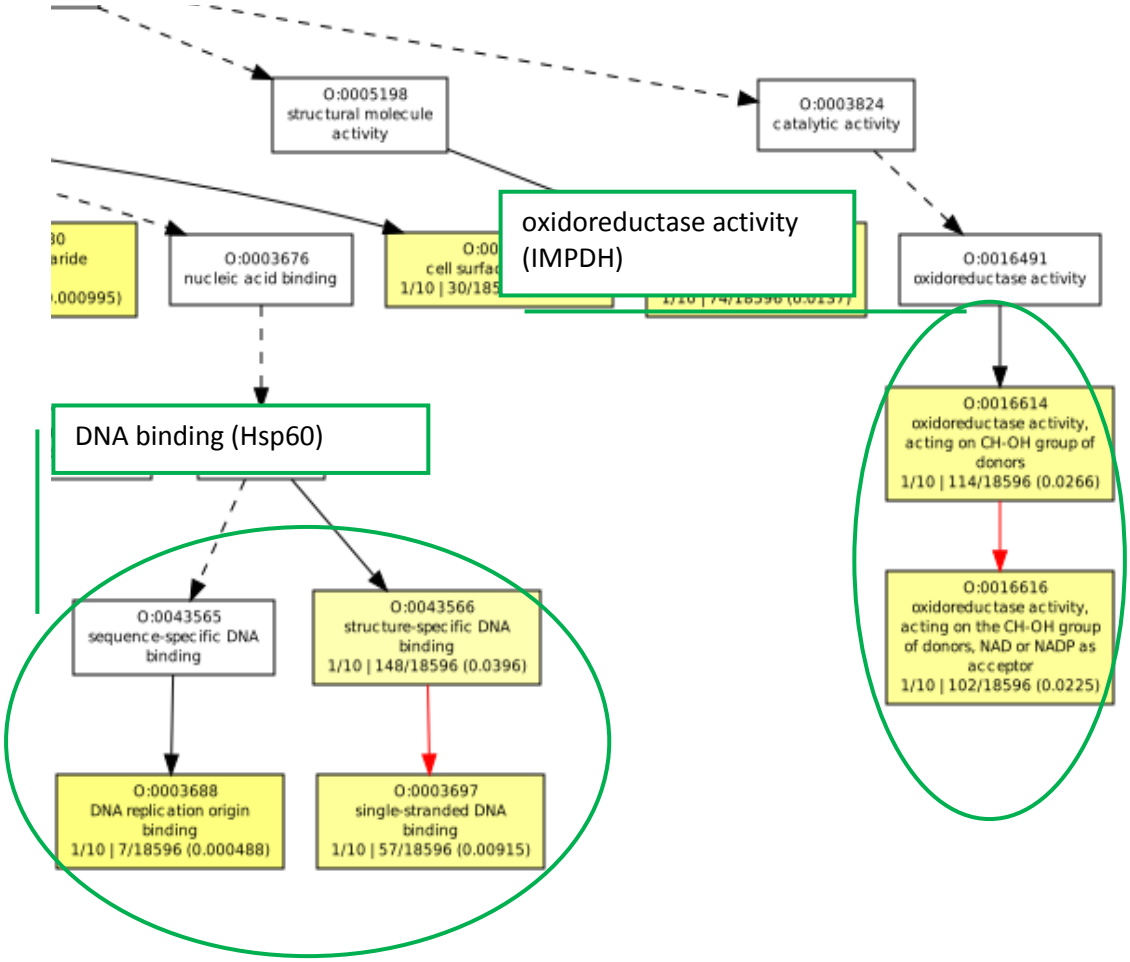
O:0005198
structural molecule activity
O:0003824
catalytic activity
oxidoreductase activity (IMPDH)
O:0003676
nucleic acid binding
O:0016491
oxidoreductase activity
DNA binding (Hsp60)
O:0016614
oxidoreductase activity, acting on CH-OH group of donors
1/10 | 114/18596 (0.0266)
O:0016616
oxidoreductase activity, acting on the CH-OH group of donors, NAD or NADP as acceptor
1/10 | 102/18596 (0.0225)
O:0043565
sequence-specific DNA binding
O:0043566
structure-specific DNA binding
1/10 | 148/18596 (0.0396)
O:0003688
DNA replication origin binding
1/10 | 7/18596 (0.000488)
O:0003697
single-stranded DNA binding
1/10 | 57/18596 (0.00915)

Automated Systems Biology Analysis Tools

In an effort to further extend our systems models we utilized the Database for Annotation, Visualization, and Integrated Discovery (DAVID) and Gene Ontology Enrichment Analysis Software Toolkit (GOEAST) [148-150]. We searched the databases using Uniprot accession numbers of the regulated proteins as indicated in table 13. Default parameters were used for both tools. Examples of the resulting outputs are shown in figures 21-50. Overall, the results of these analyses substantially confirm the results of the models we developed by manually searching the literature, and further extended them. The automated tools had more molecular details, particularly for likely protein-protein interactions and metabolic pathways.

CHAPTER 4

DISCUSSION

Securinine and Adjuvants

We have demonstrated a number of differentially expressed protein spots in monocytes in response to adjuvants and *C. burnetii* infection. In the following, we have taken a systems biology approach to attempt to better understand the data for Securinine stimulation and the time course of infection that utilizes relevant data from an extensive review of the literature. We focused on proteins and pathways that have been shown to interact with the differentially regulated proteins identified in our studies. This approach has enabled us to propose and better visualize pathways that are likely to be involved in the responses and to generate a testable model framework that may lead to a deeper understanding of the systems under study. The infected samples have demonstrated some of the potential interactions between the monocyte metabolism and *C. burnetii* metabolism/replication, that we anticipate may be valuable for guiding future experiments to further explore the host-pathogen interaction and adjuvant responses at work. First of all, it is clear that there are significant differences between the action of Securinine and the actions of LPS and MPL indicating very different pathways in immunological function between $GABA_A$ receptors and TLRs.

Our results, in conjunction with data provided by our collaborators Dr. Mark Jutila and Mr. Kirk Lubick, have enabled us to develop a preliminary model of

Securinine's action (see supplemental figure 1). This model is placed in a supplemental figure since the size of a readable image is too large to be accommodated within the regular text, due to thesis formatting requirements. Securinine has been shown to be a $GABA_A$ receptor antagonist and does not act through the Toll-like receptors [74]. GABA has been shown to be present in peripheral tissues [112], and in plasma [84] at levels comparable to those found in the central nervous system. Dr. Jutila and Mr. Lubick as well as others in the literature have demonstrated the presence of $GABA_A$ receptors in monocytes [82,83] although the exact subunit composition(s) has/have not yet been elucidated. Dr. Jutila and Mr. Lubick have demonstrated that Securinine is not acting through the TLRs [74], and that Securinine is triggering immune response pathways that are distinct from TLRs (data not shown, M. Jutila and K. Lubick personal communication).

GABA is present in the bloodstream at a concentration of approximately 100 nM (comparable to levels in the central nervous system, as mentioned above) and GABA has been reported to also regulate T lymphocytes [84]. Furthermore, it has been shown that GABA, applied exogenously, will inhibit LPS stimulation of macrophages in a dose-dependent manner [83]. GABA mediated dampening of the monocyte immune response through the $GABA_A$ receptor is likely to modulate the stimulation of the monocytes triggered by the Toll-like receptors (such as the stimulation elicited by LPS or MPL application) or other immune pattern recognition receptors, perhaps as a means of preventing runaway immune responses.

GABA's normal function is as an inhibitory neurotransmitter. We hypothesize that GABA in plasma acts on monocytes to dampen the immune response. Note that it is also possible that a monocyte specific $GABA_A$ agonist other than GABA is being produced/exported by the monocytes upon stimulation although we have no evidence for such an agonist and currently believe that GABA itself is the most likely signaling molecule. We propose that application of Securinine prevents the $GABA_A$ receptor-mediated inhibition of the monocyte immune response, increasing the effectiveness of the monocyte response and thus increasing the clearance of *C. burnetii*. It is not known whether *C. burnetii* has evolved the ability to actually trigger or attenuate the $GABA_A$ inhibition of immune function or whether the bacterium is passively benefiting from it. It would be beneficial to determine whether or not *C. burnetii* is actually able to directly affect monocyte $GABA_A$ receptors to modulate immune responses. There is no indication in our data as to whether *C. burnetii* is able to regulate GABA production. An evaluation of the metabolome would be beneficial to determining whether or not *C. burnetii* has any effect on GABA production by monocytes.

The systems biology model that we assembled to better understand the effects of the differentially expressed proteins, is detailed below. As mentioned previously, we do not appear to have sampled LPS and MPL stimulated samples in the optimal timeframe to detect changes in protein expression, or we may not have used an optimal molarity for stimulation. However, we do include a description of differentially expressed proteins detected in samples stimulated with LPS and MPL, but we were not

able to model these stimuli to the extent we did with Securinine. Supplementary figure 1 displays the inferred pathway diagram for the Securinine stimulus, including the interconnections proposed between the various proteins/functions. The text that follows contains functional descriptions of the proteins in question and protein-protein interactions described in the literature. The discussion also suggests experiments that would test some of the proposed relationships, to help deepen understanding of this system and expand the knowledge base to refine the model proposed for Securinine stimulus.

Hsp60

We observed an upregulation of Hsp60 in our 2D gels from Securinine stimulated soluble fraction samples. Hsp60 was also observed to be upregulated in both the soluble and membrane fractions of the infected samples (detailed below). A potentially cleaved Hsp60 was detected as differentially expressed in 96 hr infection + Securinine data, and this is discussed in more detail in the section below relating to the infection + Securinine dataset. Hsp60 is can be exported to the extracellular matrix to act on membrane receptors of immune cells [151]. Bacterial Hsp60 can analogs can also trigger immune responses, acting as 'danger signals'. For example, *Helicobacter pylori* Hsp60 stimulates the production of IL-8 [152,153], and when endogenous human Hsp60 is exported from the cell it also activates monocyte TNF-α production [154]. Macrophages that have phagocytosed invading particles secrete chemokines like IL-8 and TNF-α to attract other immune cells to the site of inflammation. The receptor(s)

involved in the binding/recognition of Hsp60 are yet to be completely resolved, and more than one receptor may be acted upon. It has been proposed that the receptors TLR2, TLR4, and the coreceptor CD14 are involved, although responses independent of these receptors have also been proposed [151,155-160].

A common concern with studies investigating Hsp60 (and other Hsps) is that the effects of Hsp60 on immune cells is similar to that induced by LPS, including activation of some of the proposed Hsp60 receptors . Activation of Hsp60 receptors is commonly assayed by detecting increases in the secretion of inflammatory markers. This immediately raises the question as to whether the observed responses are due to Hsp60 or rather to LPS contaminants, particularly where purified recombinant Hsp60 is used [161]. A fairly rigorous set of controls has been developed for this type of investigation that seems to conclusively indicate that LPS is not a factor in Hsp60 stimulation of immune responses. Briefly, addition of polymixin B, which specifically inhibits LPS, but not Hsp60, will abolish LPS stimulation but does not affect Hsp60 stimulation [153-157,160,162-170]. This suggests that LPS, although it could be a contaminant in some Hsp60 preparations, is not a significant contributor to Hsp60 stimulation of monocytes/macrophages. Other controls have noted that Hsp60 stimulation is abolished by heat treatment, and/or by treatment with proteinase K or trypsin, while LPS is insensitive to these treatments [154,157,168]. These controls also hold for Hsp70 and Hsp90, described in more detail below.

Hsp60 may also play a role in the regulation of adaptive immune responses, as it has been noted that in the presence of Hsp60, there is an increase in CD4+CD25+ inhibitory T-cell activity [160]. Hsp60 can insert into the membrane as part of the antigen presentation machinery of macrophages, and causes stimulus of a Th1 type T-cell adaptive response in infected samples [151,155-160,171]. In addition, exposure to Hsp60 seems to induce attenuation to later inflammatory stimuli, including LPS

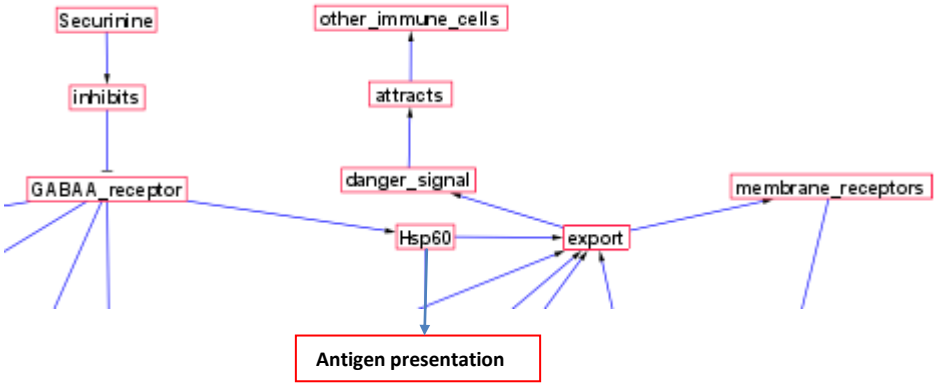

Figure 51: Detail from supplemental figure 1 related to Hsp60 function proposed in the model developed.

and additional Hsp60 [167]. This would suggest that while Hsp60 stimulates both the innate and adaptive immune responses, it may also serve as a feedback inhibitor to prevent a runaway immune/inflammatory response by desensitizing cells to prolonged inflammatory stimuli.

In response to stimulation with Securinine, upregulation of Hsp60 observed in the soluble fraction may have the following implications. First that the antigen presentation machinery is being primed. This is supported by reported observations

that Hsp60 is involved in antigen presentation to and stimulation of T cells, as discussed above [151,155-160,171]. Secondly, it would seem that the presence of Hsp60 is altering the cytokine profile in the cells (e.g. changes in the levels of TNF-α or IL-8), which can act in both an autocrine or paracrine manner to modulate and/or prime the innate immune response by the monocytes. This response should also help to activate the monocytes and possibly help regulate differentiation. Finally, as discussed above, it is possible that Hsp60 is being exported (not studied in our screen) to serve as a danger signal and help attract other immune cells.

Hsp70

We observed in Securinine treated samples that Hsp70 was strongly upregulated, appearing in a number of different isoforms (seven in all) in the soluble and membrane fractions. It has been reported that Hsp70 has an immunoprotective effect in monocytes, protecting them from their own apoptotic signals [172,173]. It has also been reported that Hsp70 may in fact be stimulating the production and export of inflammatory signals such as TNF-α and other cytokines [174-177], thus playing a role in modulating the inflammatory response. This cytokine modulation has been shown to involve both the NF-κB and p38 signaling pathways [178]. Supplemental figure 1 shows the various pathways we hypothesize to be affected by Hsp70, and to figure 52 to shows a simplified version of this diagram.

It has been reported that Hsp70 has an immunoprotective effect in monocytes, protecting them from their own apoptotic signals [172,173]. Analysis with DAVID revealed that this may be due to inhibition of Jnk signaling by Hsp70. Specifically, while the apoptotic machinery may be primed by Securinine exposure, Hsp70 may be protecting monocytes from apoptosis, until some other stimulus (e.g. *C. burnetii*

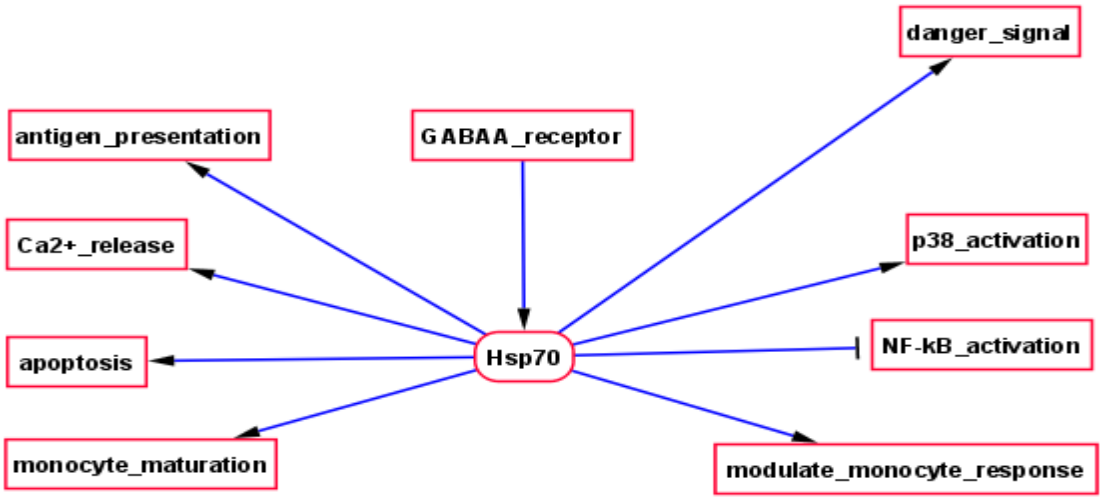

Figure 52: Simplified schematic of Hsp70 functions proposed in the model of Securinine response in this system. See supplemental figure 1 for greater detail.

infection) in conjunction with Securinine, pushes apoptosis to completion. The cells would thus be primed for apoptosis without actually undergoing apoptosis. It has also been reported that Hsp70 may in fact be stimulating the production and export of inflammatory signals such as TNF-α [174] thus playing a role in modulating the inflammatory response.

Previously reported results have indicated that Hsp70 can itself be secreted and act as a cytokine, potently activating both macrophage maturation and the immune system [175,176,179]. Export under these conditions would suggest that Hsp70 can act as a 'danger signal' to the immune system, in accordance with previous reports [174,179]. Wang et al., (2006) reported that Hsp70 will specifically bind to lipid rafts on the surface of macrophages [176], and Hsp70 was reported to increase phagocytosis in a dose-dependent manner [176]. There have also been indications that lipid rafts may be involved in Hsp70 secretion pathways [177,180,181] in addition to being involved Hsp70 recognition at the cell surface [180]. As an example, Hsp70 has been reported to preferentially associate with membrane lipid rafts following physiological stress in gut epithelial cells, and that disruption of lipid raft integrity will compromise this association [180], suggesting that a similar phenomenon may be occurring in our monocyte samples.

As described further below (in the Rab7 section of the infected model, below), lipid rafts emerge as having an important role in our models, and may provide an explanation for much of the biology in our tested systems. In the infected model, *C. burnetii* may be altering the composition of lipid rafts within monocytes as discussed in more detail below. This proposed alteration of lipid raft by *C. burnetii*, in particular the cholesterol and possibly the protein composition, may have implications for Hsp70 function in monocytes infected with the bacterium and exposed to Securinine. Specifically, the alterations to the composition of lipid rafts may make the macrophage

more or less susceptible to the effects of Hsp70. Hsp70 interaction with macrophage lipid rafts has been reported to facilitate antigen presentation to $CD4^+$ T-cells in an MHC-II-dependent manner [175,176,179] as well as activation of cognate T cells in an MHC-1-dependent manner [182].

The reported extracellular activities of Hsp70 are in keeping with the 'danger signal' hypothesis, in that Hsp70 released by a damaged/infected macrophage would alert other immune cells, priming them to help respond to the threat (e.g. a bacterium or particulate debris) at all levels of the immune system. We did not notice an increase in antigen presentation in Securinine stimulated samples, that would be represented by a lack of observed changes in MHC expression at the membrane. An increase in MHC expression at the membrane would be expected if antigen presentation activity had been increased. However, the lack of an antigen in Securinine stimulated samples will likely prevent upregulation of MHC from occurring, but Hsp70 could still be priming the cellular machinery controlling antigen presentation, enabling faster monocyte antigen presentation activity in the presence of Securinine.

As has been described with Hsp60 (above), there are a number of controls that have been used to demonstrate that the observed cellular responses to external Hsp70 are in fact due to the protein, and not due to contamination by LPS. This has been a concern [183,184], since it is believed that Hsp70 and LPS may share some receptors. It has been reported that, like Hsp60, Hsp70 can act through TLR2 and TLR4, triggering the IL-1 receptor signal pathway [185]. TLR4 is strongly implicated in recognition of LPS

from gram-negative bacteria. It has been suggested that the recently identified coreceptor TREM-1 synergizes with Toll-like receptors to mediate/modulate monocyte/macrophage responses to Hsp70 [178]. There have also been indications *in vivo* that the CD40 pathway and the CCR5 pathway are triggered by Hsp70 [175,186].

The identity of the Hsp70 receptor(s) has not been completely elucidated and, like Hsp60, may be at least somewhat dependant on cell type, and condition. Also, similar to Hsp60 (see above), at least some of Hsp70's effects transmitted through the Toll-like receptors may require the presence of specific co-receptors, and the coreceptor MD-2 has been reported to act in this fashion [185]. Both the MyD88 adapter protein and Traf6 have been shown to be required for Hsp70 action, suggesting that Hsp70 functions at least partially through TLR2/4 [185], although other pathways that are TLR2/4- and MyD88-independent cannot be ruled out. CD14 appears to synergize with TLR2/4 receptors to recognize Hsp70 [187]. Hsp70 can induce both IL-12p40 and ELAM-1 in a dose dependant manner, and may also interact with the CD91 receptor to trigger cellular responses, including the release of nitric oxide [175,179,185]. Different receptor complexes may require different thresholds of Hsp70 levels to trigger a response, and there is at least some evidence that the receptors' responses to stimulation by Hsp70 may differ with various receptors [161]. There appear to be multiple overlapping and redundant Hsp70 response pathways, and further work will be required to characterize this response more completely.

We find Hsp70 is upregulated in both our soluble and membrane fractions from Securinine stimulated samples. This suggests that at least some portion of the Hsp70 expression stimulated by the application of Securinine may be relocalized to the membrane, possibly as part of the antigen presentation machinery. It has been shown that subthreshold levels of Hsp70 in the extracellular environment can induce endotoxin tolerance by downregulating phosphorylation of the p65 subunit of NF-κB, and attenuating the degradation of IκBα by blocking the IKK pathway [188]. The induction of endotoxin tolerance by subthreshold levels of Hsp70 exposure may help explain why Securinine exposure appears to trigger the p38 pathway rather than the NF-κB pathway: namely that small amounts of Hsp70 are secreted upon Securinine exposure, thus inhibiting the activation of the NF-κB response as described above.

In keeping with this, Aneja et al., (2006) have reported that Hsp70 does not trigger the NF-κB response, and it has been reported that the cellular response to exogenous Hsp70 specifically mediates activation of the p38 pathway [176,186,188]. Activation of the p38 pathway by Hsp70 is at least partially mediated by Ca^{2+} release triggered by Hsp70 interaction with the CCR5 receptor transfected into HEK 293 cells [186], and we suggest that monitoring the Ca^{2+} flux in future experiments may prove informative as to the nature of p38 stimulus in Securinine stimulated monocytes. Flux in this discussion refers to dynamic changes in the subcellular localization of Ca^{2+} (e.g. release from the ER to the cytoplasm).

It has also been reported that Hsp70 acting through CCR5 may also act through the Erk1/2 pathway [186], but this cannot be confirmed from our data, due to detection limits. Overall, Hsp70 expression in Securinine stimulated monocytes is implicated in many aspects of the response, and may be the master regulator of the cellular response to Securinine exposure. As can be seen in supplemental figure 1 and figure 52, Hsp70 appears to be directly or indirectly involved in nearly every aspect of our proposed model for Securinine function. This was an emergent property of the model, and the apparent centrality of Hsp70 was not obvious until the model had been assembled.

One note on the several Hsp70 isoforms identified is that while Hsp70 is the best identification (per selection criteria detailed above), there were a two protein spots in the same region of the gel for which annexin was also listed as a high ranking identification. This is due to comigration of the two protein species, which we cannot resolve on broad range 2D gels that were used exclusively in the first set of experiments. The possible elevation of annexin in response to Securinine stimulation leads us to consider that what appear to be strong Hsp70 identifications in these two spots (implying immune modulation), could in fact be due to annexin, suggesting instead the induction of cell death. It was reported by Molina et al., (2007) that exposure of HEK cells to HIV resulted in upregulation of both Annexin V and Hsp70 in 2D gels [189]. We note that in samples stimulated with Securinine alone, there was no obvious morphological indication of apoptosis, although there could be some molecular indications not detected on our gels. This lack of observed apoptosis in samples

stimulated with Securinine alone is in stark contrast to Securinine + *C. burnetii* infected cells (discussed below) where indications of apoptosis were clearly present.

With respect to the Hsp70 identifications, the small number of protein spots that also potentially indicate changes in annexin expression levels could be the result of three mutually exclusive hypotheses. The first is that the expression levels of Hsp70 isoforms are changing expression, and annexin could simply be detected as a result of comigration. The two proteins are very similar in terms of pI and molecular weight and the presence of annexin could simply be a contaminating protein. The second possibility is that the differential expression observed in these spots is actually the result of annexin expression and that Hsp70 is sufficiently more abundant that it is overwhelming the annexin signal, in which case the Hsp70 would be the contaminate in those spots only. Finally, it is also possible that both species are changing expression and that comigration is preventing accurate elucidation of the fold change in both species. Further testing would be needed to evaluate which of these hypotheses is correct.

In Securinine stimulated samples, Hsp70 upregulation is most likely acting to 1) inhibit apoptosis, 2) activate maturation of the monocytes, 3) increase the rate of endocytosis, and 4) participate in antigen presentation to and activation of adaptive immunity. Also, we propose that Hsp70 is regulating the chemokine/cytokine profile as well as maturation of monocytes, and activation of the p38 pathway in accordance with previous reports [176,186]. This activation of the p38 response seems to occur without

stimulating further expression of p38 [186]. However, we cannot assess this in our data, as p38 expression is likely to have been below our limit of detection.

L-plastin

L-plastin is present in Securinine stimulated, soluble fraction samples in several isoforms which are both up- and down-regulated (see figure 53 and supplemental figure 1). L-plastin, an actin bundling protein has been shown to activate integrins when phosphorylated at Ser5 [190,191], and integrins can stimulate the p38 inflammation pathway [192]. We observed both up- and downregulation of L-plastin proteins in our 2D gels in a pattern suggesting changes in posttranslational modifications. Data provided by Dr. Jutila and Mr. Lubick has indicated that Securinine is stimulating the p38 inflammation pathway but not the NF-κB pathway, as indicated by Western blot data (M. Jutila, K. Lubick, personal communication).

Plastins comprise a class of actin bundling proteins [193-201] and L-plastin is found primarily in hematopoietic cells [193,195,197,198,201]. Integrins localize to focal adhesions, which are the primary sites of integrin stimulated actin polymerization [195,198]. L-plastin appears to be required for bactericidal pathways, as reported by Chen et al., (2003) who observed that L-plastin$^{-/-}$ mice were defective in killing *Staphylococcus aureus* [193]. Interestingly, L-plastin contains two EF-hand Ca^{2+} binding domains, the same type of Ca^{2+} binding motif found in S100A4, A8, A9, and A11 Ca^{2+} binding proteins (discussed below) [195,202]. This raises the intriguing possibility that L-

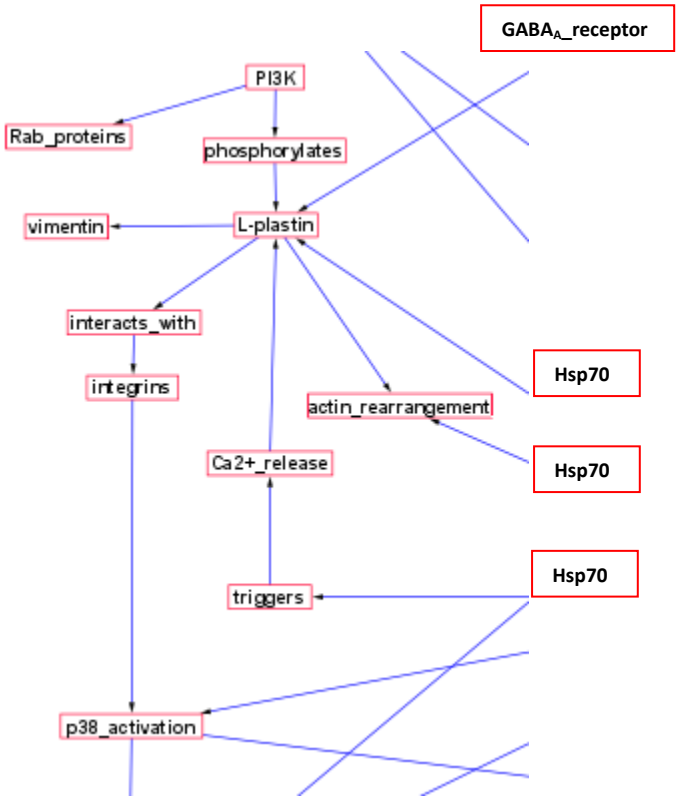

Figure 53: Detail of pathways in supplemental figure 1 related to L-plastin following stimulation of monocytes by Securinine exposure.

plastin, coupled with the downregulation of S100A4 that we observed, may be regulating the signaling/biology in Securinine stimulated monocytes in response to Ca^{2+} signals. Determining changes in cytoplasmic Ca^{2+} levels in our samples following stimulation was beyond the scope of our study, but doing so would be potentially informative. L-plastin can bind to F-actin [195,196,200], and this may have implications for F-actin bundling proteins in *C. burnetii* infected cells [203]. Particularly L-plastin

could modulate F-actin bundling rearrangements stimulated by *C. burnetii* infection (see model of response to infection below and supplemental figure 2). *In vitro*, Ca^{2+} binding inhibits actin bundling by L-plastin [198], suggesting that understanding the Ca^{2+} flux in our samples would be informative as to the actin bundling status of L-plastin.

L-plastin is unique among the plastin family in that it is regulated by phosphorylation [195], and phosphorylation of L-plastin has been shown to regulate at least some integrin-dependent functions [198]. L-plastin can be phosphorylated on Ser5 and Ser7, and there are indications that phosphorylation proceeds in the order of Ser5 followed by Ser7 [198,199]. Where phosphorylation at the Ser5 site appears to be

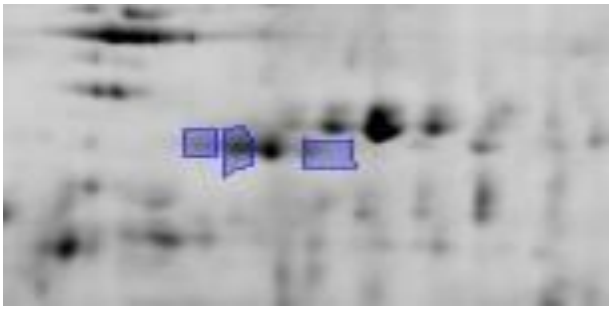

Figure 54: Detail of spots identified as L-plastin (spots are in the boxes). The number of proposed phosphorylations increases from right to left.

activating, a second phosphorylation at Ser7 seems to be inhibitory [199]. We were unable to detect the peptide containing Ser5 and Ser7 in our samples, but note that phosphorylated peptides can be difficult to detect in CID fragmentation. Oshizawa et al., (2003) demonstrated that singly phosphorylated L-plastin is involved in the activation of NADPH oxidase, a fundamental component of the oxidative burst response

to infection, and that phosphorylated L-plastin has a role in activating NADPH oxidase by modulating a molecule or molecules in the activation pathway [199].

Interestingly, work by Jones et al., (1998) suggests that PI_3K is directly involved in phosphorylation of L-plastin [198]. This is particularly relevant considering that PI_3K is involved in regulating Rab7 activities in phagolysosome formation (discussed below), and this immediately suggests an interaction between Securinine stimulation and formation of the phagolysosome during *C. burnetii* infection of monocytes. Jones et al., (1998) suggested that PKC could also be involved [198]. Further work will be needed to elucidate kinase/protein activities/interactions. Our gel data (see figure 54) suggest that the L-plastin identified spots are double phosphorylated L-plastin, singly phosphorylated L-plastin, and L-plastin. Although we were unable to directly identify phosphorylation in any of these species by MS analysis, the isoelectric point shifts of the different L-plastin species are consistent with this interpretation, and seem logical based on the available literature.

Integrin signaling through L-plastin stimulation is likely to be important as it can stimulate p38 signaling, which is upregulated in Securinine stimulated samples, as shown by Lubick and Jutila (personal communication). The observation by Chen et al., (2003), that L-plastin$^{-/-}$ mice were defective in killing *Staphylococcus aureus*, seems to stem from a lack of β2-integrin signaling [193]. In other words, L-plastin is not required for activation of β2-integrin, but L-plastin is required to help stabilize the signal giving rise to the respiratory burst that arises from activation of β2-integrin. The ability of L-

plastin to regulate the cytoskeleton is most likely how L-plastin is regulating β2-integin signaling, by creating conditions favorable to formation of an integrin signaling complex [193]. We do not know the activation status of integrins in our samples, but it is reasonable to suppose that activation of L-plastin is creating conditions favorable to integrin signaling, priming the cell for bactericidal activity.

It has been demonstrated that L-plastin interacts directly with subunits of vimentin during adhesion [194]. This is of interest as it suggests a point of interaction with the infected samples (which show an upregulation of vimentin, as detailed below), and a point at which Securinine stimulation might act on *C. burnetii* infection. Also of interest, as demonstrated by Correia, et al. (1999) [194], is that immunoprecipitation of L-plastin captures Hsp70, suggesting an interaction between the two proteins. Given that Hsp70 seems to have a strong immunomodulatory role in monocytes (described above), an interaction between Hsp70 and L-plastin may suggest a role for L-plastin in at least some portions of Hsp70-induced immune activity. Determining whether changes occur in the level of interaction between Hsp70 and L-plastin +/- Securinine stimulation would be quite informative.

It has been reported that L-plastin is involved in T cell activation and that L-plastin localizes to the immunological synapse, regardless of phosphorylation status [201]. The immunological synapse (IS) is a physical interface between an antigen presenting cell and a lymphocyte. The IS complex includes L-plastin, which may be regulating cytoskeletal rearrangements dictated by synapse formation [201]. This is of

interest in Securinine stimulated monocytes as it suggests that the observed upregulation of L-plastin could help to prime the antigen presentation machinery that is also stimulated by the heat-shock proteins.

In our Securinine stimulated samples, the two L-plastin isoforms that may be phosphorylated are strongly downregulated, ($\geq$2-fold) in response to 24 hours of Securinine stimulation (see figure 54). This suggests that L-plastin's phosphorylation-dependent activity may have been downregulated, and this may indicate a reduction in integrin-L-plastin related signaling, and/or a change in cytoskeleton dynamics. This observation is in keeping with the hypothesis that L-plastin is helping to prime the antigen presentation machinery at the IS, speeding processing of antigens upon their introduction (e.g. by *C. burnetii* infection) with subsequent upregulation of phosphorylated L-plastin.

Phosphorylation at Ser5 in L-plastin enhances actin bundling, while increasing the [Ca^{2+}] reduces L-plastin/actin bundling, even if Ser5 is phosphorylated [196,197]. Phosphorylation does not seem to be an absolute requirement for L-plastin's actin bundling ability, but phosphorylated L-plastin does have enhanced actin bundling capabilities [196]. As adhesion seems to be required for efficient phosphorylation [197], it is possible that the changes we observe in the expression of L-plastin isoforms reflect a lack of adhesion in the suspension cultures. Determining the changes in the phosphorylation of these two L-plastin isoforms at an earlier time point may help to

elucidate L-plastin-mediated pathway dynamics, particularly if one or more of these isoforms is upregulated at an earlier timepoint.

The possibility that L-plastin is responsible, at least in part, for regulating Ca^{2+}-mediated signaling suggests that the levels of Ca^{2+} and perhaps other metals through our system could be important to Securinine stimulation of monocytes. Although Ca^{2+} monitoring was beyond the scope of our investigation, observations from the literature indicate that Hsp70 not only interacts with L-plastin but also may be capable of altering the Ca^{2+} status of the cytoplasm [196]. Given that Ca^{2+} interferes with L-plastin's actin bundling activities, a more detailed knowledge of Ca^{2+} flux should prove informative as to L-plastin's ability to bundle actin and thus alter the cytoskeleton.

Hsp90

We observed an upregulation of Hsp90 in the soluble fraction of our Securinine stimulated samples (see figure 55). Hsp90 is one of the most abundant proteins in eukaryotic cells, comprising up to 2% of total cytosolic protein in unstressed cells [204-207]. Classified as a heat shock protein, Hsp90 possesses some chaperone functions that help to enhance protein folding [204-206,208-210]. Unlike other heat shock proteins Hsp90 seems to have a specific group of client proteins. The list of known client proteins includes a large number of transcription factors, kinases, and cell cycle regulators, leading to the hypothesis that Hsp90 is a chaperone regulating key proteins in signaling pathways [204-207,209]. Hsp90 is believed to maintain client proteins in an unfolded (and inactive), but activatable state allowing rapid response of the client

proteins to various signals upon which the unfolded, inactive client is released from Hsp90 and folds into its active state [205,206,211].

Hsp90 also requires a series of co-chaperones to form a complex that is able to actively refold proteins. These co-chaperones include Hsp70, Hip, Hop, Hsp40, and p23 [205-207]. Client proteins seem to first complex with Hsp70 and are then transferred to Hsp90, followed by dissociation of Hsp70 [211]. Failure to bind Hsp90 leads to client

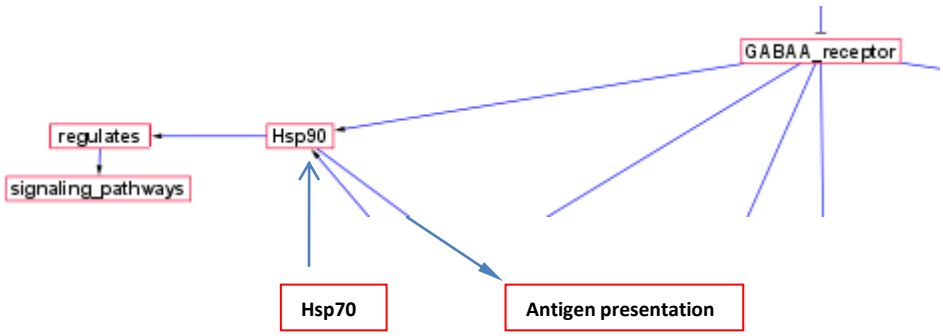

Figure 55: Detail of Hsp90 interactions from supplemental figure 1.

protein degradation [211]. The contributions of these co-chaperones complicates understanding of the functions of Hsp90. Given that both Hsp70 and Hsp90 are upregulated in our Securinine stimulated samples, this suggests that a number of signaling proteins could be sequestered by Hsp90, which might impact signaling pathways.

Due to the complexity of Hsp90 interactions it is difficult to draw specific conclusions about its function in Securinine stimulated monocytes. However, Hsp90 does seem to have some immune- specific functions that bear discussion. Monarch-1 is

a known Hsp90 client protein in the NOD-like receptor (NLR) protein family (previous family names include CATERPILLER or NACHT-LRR) [211]. NLR proteins are believed to be cytosolic pattern recognition receptors involved in innate immunity, in a similar manner to the Toll-like receptors found at the cell surface [212]. Failure to bind Hsp90 leads to degradation of Monarch-1 and inhibiting Hsp90 will prevent Monarch-1 from degrading NF-kB-inducing kinase (NIK) [211]. These results imply a role for Hsp90 in regulating inflammation via NF-κB. Given the observation that Securinine stimulation does not trigger the NF-κB pathway, it is possible that Hsp90 has a role in preventing the activation of NF-κB, possibly by failing to bind Monarch-1, or sequestering Monarch-1 and preventing its release. It was recently demonstrated that Jak1/2 are client proteins for Hsp90 and that without Hsp90, Stat1 activation is impaired [210]. Determining the activation status of relevant proteins might be informative, as many Hsp90 clients are likely to be below our detection limits and/or may be active but not changing their expression or isoform levels.

Hsp90 has been shown to be involved in LPS activation of macrophages by enabling LPS induction of NF-κB translocation to the nucleus [213], as well as activation of p38, Jnk, and ERK pathways [214], suggesting that Hsp90 has an important role in innate immune function in general. This is supported by another function of NLR proteins, namely their ability to activate caspases 1 and 5, via the formation of the inflammasome [215,216]. The inflammasome is a multiprotein signaling complex of >700 kDa whose purpose is to activate caspases 1 and 5 [2,215], and the inflammasome

is regulated by Hsp90 in both mammals and plants [216] (see figure 56). Hsp90 can inhibit caspase 1 and 5 activity by preventing its activation via the inflammasome [215]. Hsp90 binds to both the NACHT and LRR domains of NLR proteins [216]. As NLR proteins are involved in both inflammation and apoptosis [212], suggesting that Hsp90 is a key regulator of these functions.

Much work has also demonstrated that Hsp90 is involved in antigen presentation. Binder et al., (2001, 2005) demonstrated that peptides chaperoned by Hsp70 and Hsp90 were presented in an MHC class I-dependant manner much more efficiently than free cytosolic peptides [208,217]. It was also shown that loss of Hsp90 alone did not inhibit MHC I presentation, suggesting some redundancy with Hsp70 in this pathway, although this may be cell-line dependant [210,218].

The finding that both Hsp70 and 90 are lipid raft associable proteins has implications for our proposal that *C. burnetii* infection is actively modifying cellular lipid rafts (detailed below) and further supports the notion that better characterization of intracellular lipid rafts are important for understanding of immune function.

It is difficult to draw conclusions regarding the function of Hsp90 in Securinine stimulated cells due to the complexity of Hsp90's activities. However, some general conclusions can be drawn. First, Hsp90 would seem to have an important role in the activation of cells by Securinine stimulation, based on the nature of Hsp90 client proteins. Second, the observation that in our dataset Hsp70 is strongly

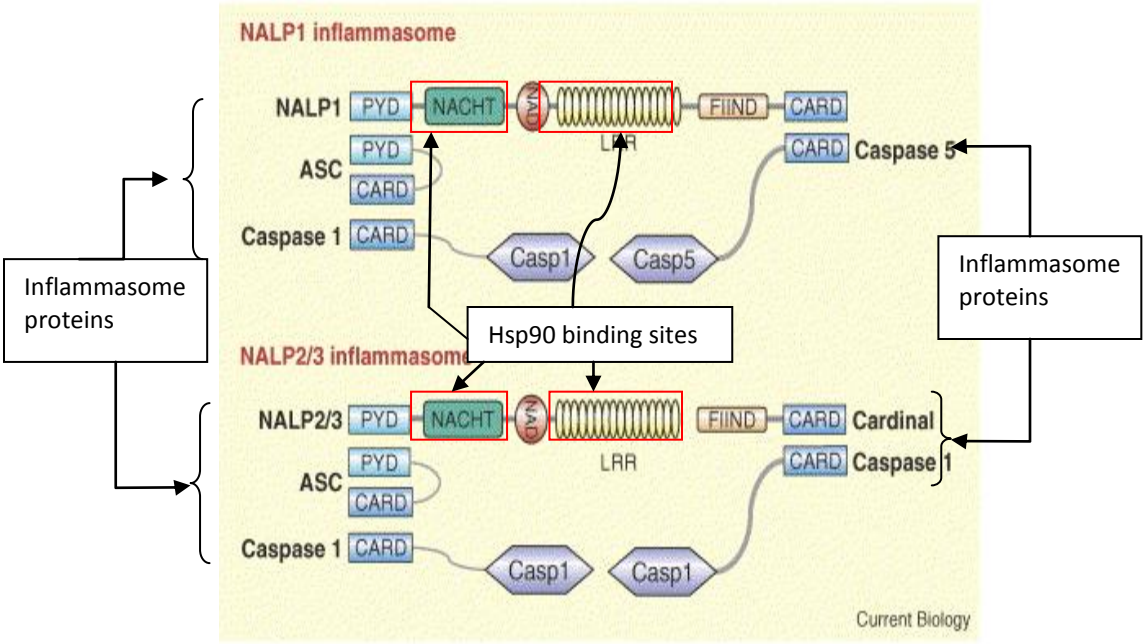

Figure 56: Schematic diagram of an inflammasome. Component proteins and Hsp90 binding sites are indicated. NACHT, NAD, LRR, PYD, CARD, and FIIND are protein domains. See figure 28 for details from DAVID. Adapted from [2], reprinted with permission.

upregulated by Securinine stimulation, and because Hsp70 is involved in delivery of client proteins to Hsp90 as described above, the upregulation of Hsp70 is potentially a factor in the response of Hsp90 client proteins to Securinine stimulation.

Perhaps a useful experiment would be to perform immunoprecipitations for Hsp90 and Hsp70 before and after Securinine stimulation. This would be followed by 1D and/or 2D-gel electrophoresis to separate and identify the Hsp90-bound proteins. This experiment has the potential to help identify which signaling pathways are involved in the induction of proteome changes caused by Securinine exposure. If a protein dissociates from Hsp90 following Securinine stimulation, it will appear as downregulation on a gel, and suggest that the protein has been released to either be

degraded by the proteasome or to perform a signaling function. Once such pathways have been identified they might be specifically targeted to gain a greater understanding of the signaling status within the cell in response to Securinine and thus better explain the response mechanism in this system. It would also be interesting to inhibit Hsp90 with geldanamycin or other Hsp90-specific inhibitor [205,218] +/- Securinine stimulation.

Serpin B1

Serpin B1 is upregulated ~2-fold in the soluble fraction of our Securinine stimulated samples, with a single isoform detected. Serpins are part of a superfamily of proteins that function in immunity. They act primarily as serine and cysteine protease inhibitors, and help prevent tissue damage and early cell death [219-224]. They are also involved in cell migration, phagocytosis, and cell killing of bacteria and viruses [219,221,224]. Clade B, with which we are concerned here, consists of predominantly intracellular proteins [221]. See figure 57 for a schematic summary of SerpinB1 interactions from supplemental figure 1.

SerpinB1, also referred to as Monocyte Neutrophil Elastase Inhibitor (MNEI) among other names, specifically targets elastase, cathepsin G and proteinase 3 [220,221,223,225,226]. SerpinB1 is efficient, acting as a suicide inhibitor at a stoichiometry of 1:1 [221,225,226]. Serpin B1 can also be exported via a nonclassical secretion pathway [227] to act extracellularly. It is not known if SerpinB1 was secreted

in our samples as we did not characterize the secretome, but it would be interesting to examine this.

It has been noted that Serpin B1 has a positive effect on bacterial clearance [219,221,228]. Serpin B1 does not directly affect bacterial growth per se [228], but seems to be acting in a more indirect manner. Specifically, it seems that Serpin B1 is acting as an inflammation modulator by limiting the damage done to host cell surface or other host proteins during inflammation, and thereby facilitating a stronger immune response by preventing degradation of immune active proteins [228]. Loss of Serpin B1 causes reduced effectiveness in the immune response, leading to bacterial spreading [219]. In this model, by reducing protein degradation and turnover, Serpin B1 allows for a prolonged, elevated immune response, thus increasing bacterial clearance.

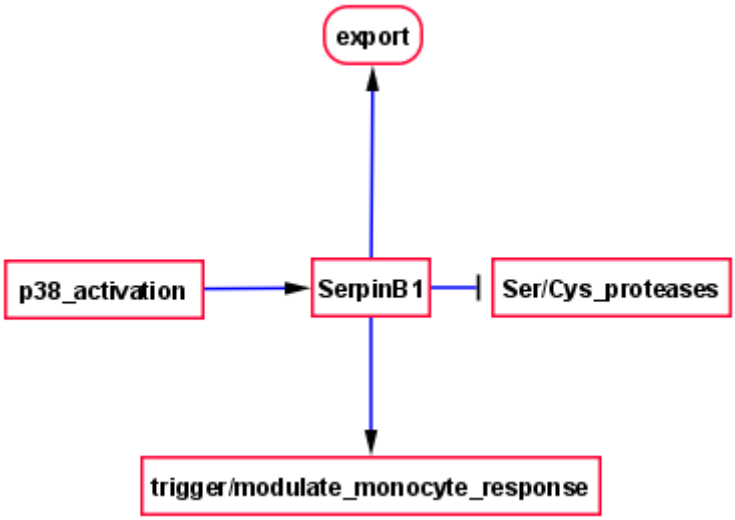

Figure 57: Schematic summary of Serpin B1 activation by p38 and downstream results of SerponB1 activation. See supplemental figure 1 for more details.

It has been observed that macrophage elastase (MMP-12) will cleave Serpin B1 [225]. Since we observed that Serpin B1 is upregulated this suggests that MMP-12 is not present, or not sufficiently active to overcome the upregulation of Serpin B1. Transcription of Serpin B1 is known to be regulated by NF-kB [226,227], suggesting that the some of the same proteins that regulate inflammation also regulate Serpin B1. It has been observed in our samples (Lubick, K and Jutila, M., personal communication), that Securinine is not activating NF-kB. This suggests that some other inflammation stimulator is controlling the upregulation of Serpin B1. Given that p38 signaling is upregulated in our samples (Lubick and Jutila, personal communication), we suggest that p38 can also upregulate Serpin B1 expression.

It seems reasonable to suppose that Serpin B1 is present in our samples in a protective capacity, since Serpin B1 has a positive effect on bacterial clearance [219]. This suggests that some or all of its target proteases are present either in the cytosol or exported, and that this expression is regulated by some form of inflammation signal other than NF-kB. It would be useful to determine the protein and metabolite composition secreted into the growth media +/- Securinine, as this might shed light on the signal(s) that triggered Serpin B1 upregulation. The observation that Securinine stimulation led to an increase in the expression of Serpin B1 expression levels suggests that this system may be regulated by the $GABA_A$ receptor.

Fatty Acid Binding Protein 5

We observed a nearly 3-fold upregulation of fatty acid binding protein 5 in the soluble fraction of Securinine stimulated samples (see figure 58 for a simplified diagram of the inferred interactions with FABP5, and see supplemental figure 1 for more details). Fatty acid binding proteins (FABPs) are lipid chaperones that sequester and distribute lipids in such a manner as to frequently regulate signaling and enzymatic activity [229]. The exact mechanisms of action by FABPs are not well understood, but FABP4 and FABP5 (often called aP2 and mal1 respectively) are present in adipocytes and macrophages and act in at least a partially redundant manner [229-231]. FABP5 is known to be upregulated in differentiated macrophages [232] , although it is found in many other tissues including epidermal cells, brain, kidney, and lung tissue [229,230,233]. The upregulation of FABP5 in Securinine stimulated samples may indicate that Securinine induces some level of monocyte maturation. FABP5 acts to coordinate metabolic and inflammatory activity in macrophages, and is a critical regulator of these responses [229,231,232,234].

FABP5 has attracted particular interest in diabetes research. It has been observed that the increase of FABP5 expression is correlated with decreases in insulin sensitivity and increases in inflammation [229,231-234]. Higher levels of FABP5 lead to a decrease in glucose uptake, even if insulin levels remain constant, demonstrating that in cases where FABP5 is upregulated, insulin sensitivity is reduced [229,231,232,234]. Changes in FABP5 may thus have significant implications for insulin sensitive signaling

pathways in Securinine stimulated cells. Insulin often acts to regulate many different metabolic and other pathways and may act in concert with other hormones [235].

A decrease in insulin sensitivity, even in the presence of unchanged levels of other hormones, is predicted to cause significant alterations in hormonally controlled pathways in macrophages. Insulin often acts as a negative regulator of hormonally controlled pathways, particularly those involving the use of cAMP as a second messenger. Insulin stimulation acts to increase the breakdown of cAMP, thus decreasing the initiation of hormonally stimulated signaling cascades. This response would not be obvious in our samples as hormone concentrations should be relatively low (see figure 59 for an example of hormonally regulated pathways). Experiments exploring the costimulation of Securinine +/- insulin could well be informative. The FABP4:5 ratio in resting macrophages has been measured as approximately 1:1 [232], although there may be some strain- or condition-specific influence on actual levels as ratios of 1:4 have also been reported. It would be useful to determine the FABP4:5 ratio in our system.

Also of interest is the observation that under conditions where expression of FABP5 increases, an increase in cholesterol esterification has also been reported [236]. Increased cholesterol esterification should reduce the amount of available cholesterol in the cell and could alter the cholesterol content of lipid rafts. The plasma membrane has a high concentration of cholesterol, up to 80% of total cellular

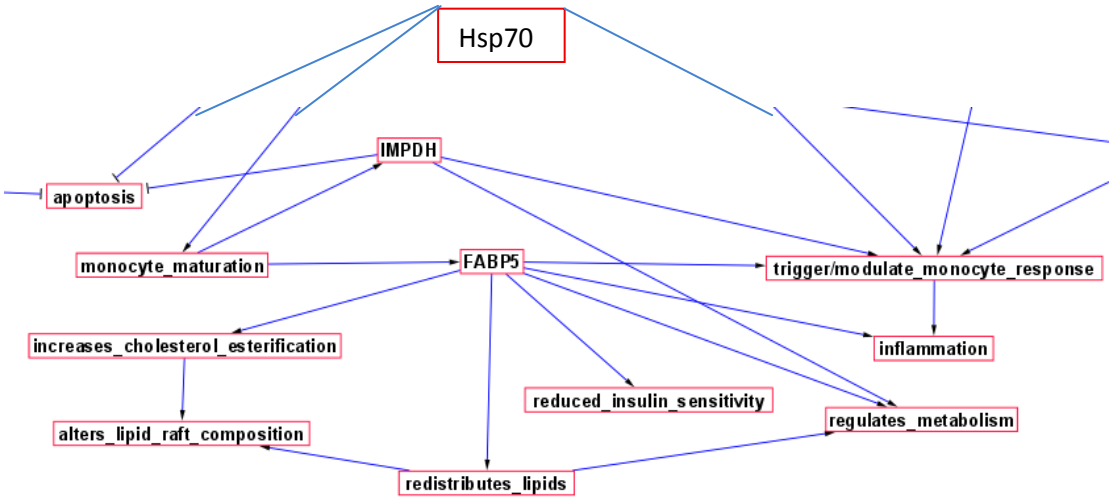

Figure 58: Local view of FABP5 and IMPDH (detailed below) showing hypothesized connections/activities.

cholesterol, and up to 40% of the plasma membrane lipid content is cholesterol [237]. The plasma membranemay be maintained in a state that small changes in cholesterol composition can have a large impact on membrane fluidity, as has been observed with model membranes [237]. In other words, even a modest change in the amount of cholesterol available for lipid rafts could have a large impact on both the composition and/or function of lipid rafts.

It is also possible that the observed increase in FABP5 in Securinine stimulated samples will alter lipid metabolism. FABP5 has been shown to interact with PPARβ/δ, a sensitive lipid receptor that, when activated, promotes fatty acid oxidation [238,239]. Specifically, FABP5 delivers ligands to PPARβ/δ [240]. If *C. burnetii* infection is altering the lipid metabolism in infected monocytes, as we have predicted, then a FABP5-

induced alteration, via Securinine stimulation, may affect *C. burnetii*'s ability to alter lipid metabolism.

Loss of FABP5 was shown to cause an increase in insulin sensitivity [231], and thus an increase in FABP5 would be predicted to cause a decrease in insulin sensitivity. This presumably would be independent of alterations to lipid rafts. It has been documented that an increase in FABP5 alters the lipid profile in macrophages to cause a reduction in short chain fatty acids and an increase in longer chain fatty acids [231,241]. This change in lipid profile is correlated with the level of insulin sensitivity. It was recently reported that the insulin stimulated phosphorylation of Akt was reduced in the presence of longer chain fatty acids, and stimulated in the presence of shorter chain fatty acids [231]. We would predict that in Securinine stimulated monocytes, levels of phosphorylated Akt would be reduced compared to unstimulated controls. What has become clear from examination of the potential network connections of FABP5 is that parallel investigations of lipidomic and metabolomic studies could well be important to increase our understanding of the changes in the biology of monocytes +/- Securinine. FABP5 appears to be a central player in regulation of the behavior of fatty acids and related proteins, as well as overall energy metabolism in macrophages. The upregulation of FABP5 has potential implications for the metabolic status of the cell, the effects of insulin on hormonally regulated pathways, and lipid raft compositions/activities, and generates numerous hypotheses to be tested in future work.

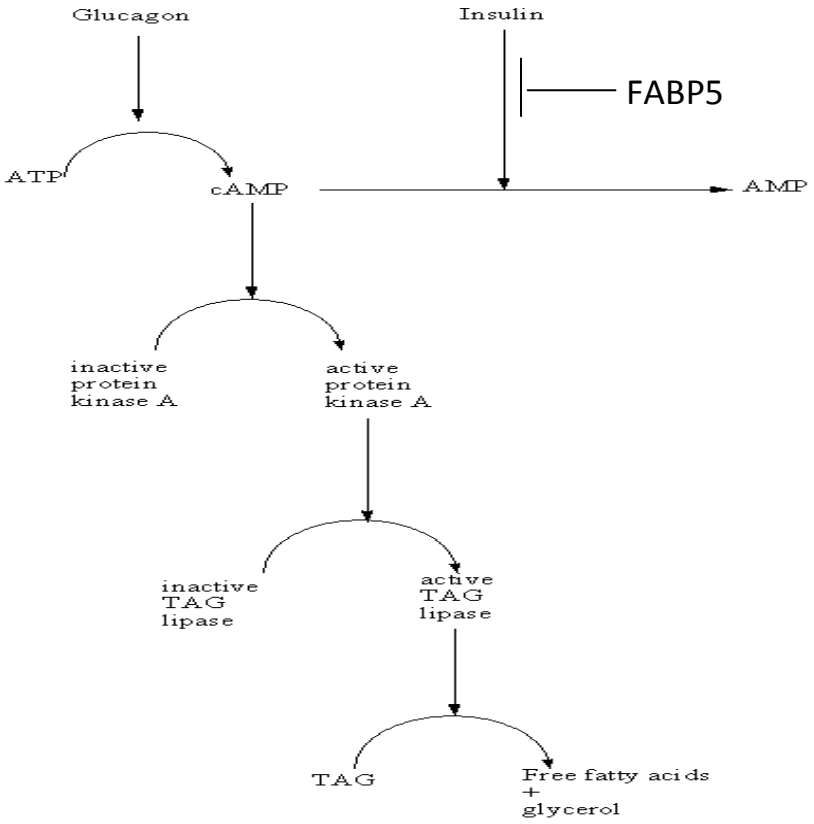

Figure 59: Example of the effects of insulin on hormonally regulated metabolic pathways. Here a hormone (e.g. glucagon or adrenaline) stimulates a receptor triggering the production of the second messenger cAMP. cAMP then initiates a signaling cascade that ultimately results in the activation of TAG lipase, causing the breakdown of triacylglycerol to free fatty acids. Insulin acts at the level of cAMP, causing cAMP to break down, thus blocking second messenger initiation of the signaling cascade. FABP5's reduction of insulin sensitivity is predicted to inhibit insulin inhibition of cAMP-mediated signal transduction, and thus would allow cAMP to stimulate the pathway in this diagram. It should be noted that we are not implying that TAG lipase is active in our system, this is merely an example of an insuling regulated enzyme cascade and potential FABP5 interaction with this cascade to illustrate a point.

Inosine-5'-monophosphate Dehydrogenase (IMPDH)

IMPDH was found to be upregulated in the soluble fraction of Securinine stimulated gels (see figure 58 above, in the FABP5 section, for a diagram of proposed IMPDH connections with Securinine stimulated activities). IMPDH catalyzes the NAD-dependant conversion of IMP to xanthosine 5' monophosphate, making it the key enzyme in GTP biosynthesis [242-250]. To date activities of IMPDH have largely been inferred from inhibition experiments using either mycophenolic acid or 3-hydrogenkwadaphnin, both of which specifically inhibit IMPDH [242-250]. Inhibition of IMPDH leads to post-G1 arrest apoptosis [247,248,250]. This is perhaps not so surprising, considering that loss of IMPDH activity will lead to loss of guanine nucleotide synthesis, and guanine nucleotides are essential for nucleic acid biosynthesis, as well as regulating energy storage and for a great many other regulatory mechanisms. This suggests that IMPDH may function in the inhibition of apoptosis. It has been shown that inhibiting IMPDH will reduce both growth and viability of cells [247].

It has been shown that activation of isolated peripheral blood monocytes using phorbol-12-myristate-13-acetate and either ionomycin or pokeweed mitogen causes an upregulation of IMPDH 24 mRNA hours after stimulation [251]. It was also suggested, that induction of IMPDH plays a role in cellular proliferation [251,252]. This implies that the upregulation of IMPDH following Securinine stimulation indicates either the cells are proliferating, or the cells are preparing for differentiation. It was demonstrated that IMPDH expression and activity were upregulated upon T cell activation [252], and

upregulation of IMPDH may be a general response to immune activation. There are two types of IMPDH reported, type I and type II. Both are inducible, albeit on different time courses [242,251]. We have not determined whether we are seeing type I or type II IMPDH upregulation in our samples.

Another reported function of IMPDH activity is its involvement in NO production and TNFα production [245]. Jonsson and Carlsten (2002) demonstrated that inhibition of IMPDH with the specific inhibitor mycophenolic acid, yielded a downregulation of both TNFα and NO [245]. This suggests a central role for IMPDH in cytokine production and/or regulation, and could well be a factor in cytokine regulation, specifically that increasing expression of IMPDH may induce an increase in the production and/or export of TNFα and NO in response to Securinine stimulation. It has also been reported that IMPDH is a factor in stimulation of the p38 pathway [246,249]. IMPDH is not the only factor that affects p38 activation, but could participate in the activation of p38 in Securinine stimulated samples observed by Dr. Jutila and Mr. Lubick. IMPDH also seems to downregulate ERK activation [246]. Quantifying the activity of IMPDH in our system (e.g. via [243]) could be informative as to the potential impact of IMPDH on the biology of monocytes, as would determining the activation state of ERK. We suggest that increased expression of IMPDH In Securinine stimulated samples is influencing the inflammatory response, as well as regulating p38 activation and monocyte differentiation. We also note that analysis with DAVID suggests a number of

metabolically related pathways that suggest possible targets for downstream metabolomic analyses see (figure 29).

Thioredoxin

Thioredoxin (Trx) was found to be upregulated in the soluble fraction of Securinine stimulated monocytes. Trx is a commonly observed intracellular redox enzyme, catalyzing dithiol-disulfide redox reactions, and acting as a proton donor [253-257]. Trx has antioxidant properties, protecting against oxidative stress, by reducing oxidized enzyme active sites (see figure 60) [254-256]. The active site of Trx must also be kept in a reduced state to maintain enzyme activity, using an NADPH- dependant mechanism catalyzed by the Trx reductase enzyme [253,258]. Trx activity has implications for a number of cellular mechanisms including signal transduction, inflammation, and apoptosis [253-257,259,260]. The majority of Trx functions depend on its reductase activity, making recycling of the active site by NADPH and thioredoxin reductase critical [253]. Trx acts both intracellularly and is exported to act extracellularly (see figures 60, and 61 for a summary of Trx activities and supplemental figure 1 for more detail) [253-257,259,260].

Trx is exported from the cell through a non-classical pathway, and can be secreted as a truncated, membrane-associated form (Trx80), that has been found at the cell surface of monocytes [253,254,259]. Both the full-length and truncated forms of Trx posses chemokine properties, and serve to attract other monocytes, T cells, and polymorphonuclear leukocytes [253,254,259]. Trx is unusual as a chemoattractant in

that it is not coupled to either a G protein or a chemokine receptor, unlike most known chemoattractant species, and sufficiently high levels of extracellular Trx can interfere with other chemokines [253]. The action of Trx in chemoattraction is likely due to its redox function maintaining the reduced state, and thus the actions of surface proteins that would otherwise be oxidized and inactivated by inflammation [254]. This suggests that the redox status of the extracellular environment is important in the regulation of certain cellular functions. It might be interesting to monitor changes in the extracellular redox status in our system, upon stimulation, perhaps by using redox sensitive indicators (e.g. an electrochromic dye such as Prussian blue).

The presence of Trx80 has been shown to stimulate $CD14^+$ monocyte maturation. Trx80 affects signaling cascades for p38, Jnk, and Erk and has proinflammatory actions, but does not seem to induce maturation of monocytes [259]. Subcellular localization in our samples places Trx in the soluble fraction, at an apparent molecular weight equal to the full-length form, but does not rule out secretion which would be invisible to our screen.

Trx has been implicated in regulation of NF-κB activity in the nucleus, which requires translocation of Trx from the cytoplasm [257]. Securinine does not activate NF-κB, and it is possible that Trx is prevented from entering the nucleus. Also, upregulation of Trx in the cytoplasm seems to prevent degradation of IκBα, thus inhibiting NF-κB activation [257]. We observe upregulation of Trx in the soluble fraction, which includes cytosolic proteins and may include some of the lumenal contents of organelles. As a

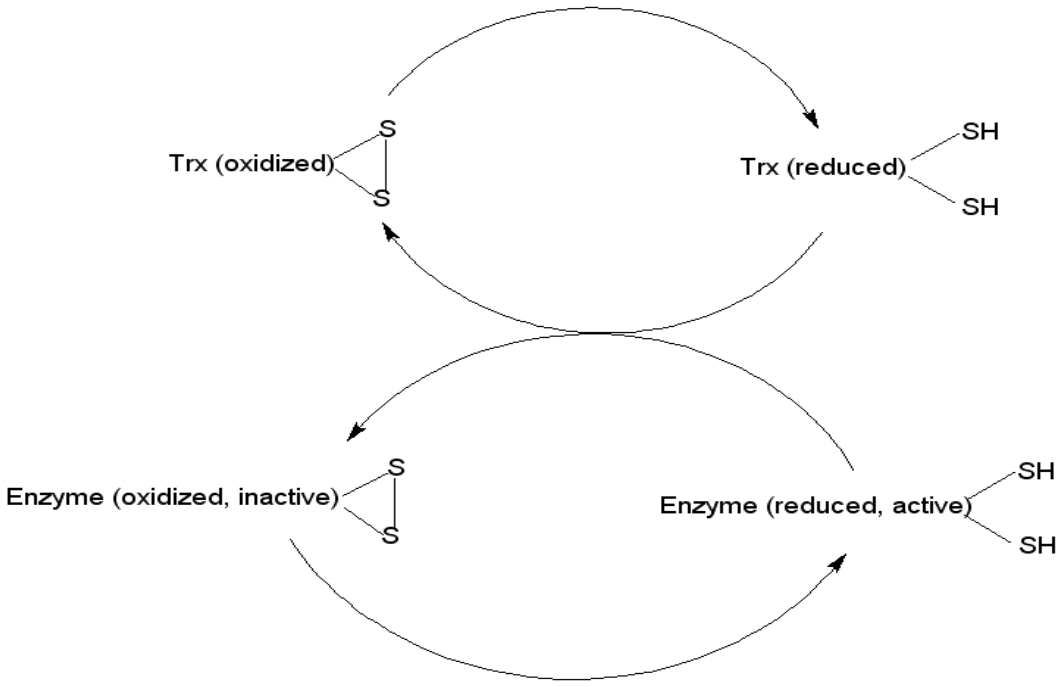

Figure 60: Schematic of Trx activity. Briefly, reduced Trx can donate electrons to an oxidized enzyme or other thiol site to produce the active, reduced form of the enzyme and the oxidized form of Trx.

result, we cannot distinguish nuclear lumenal Trx from cytosolic Trx. A fluorescently labeled Trx could be monitored microscopically to determine migration to the nucleus and determine if inhibition of Trx migration is involved in NF-κB suppression. It is also not entirely clear if Trx is directly interacting with NF-κB or with some other accessory protein that regulates NF-κB in the nucleus, suggesting that an antibody pull-down assay might shed light on this.

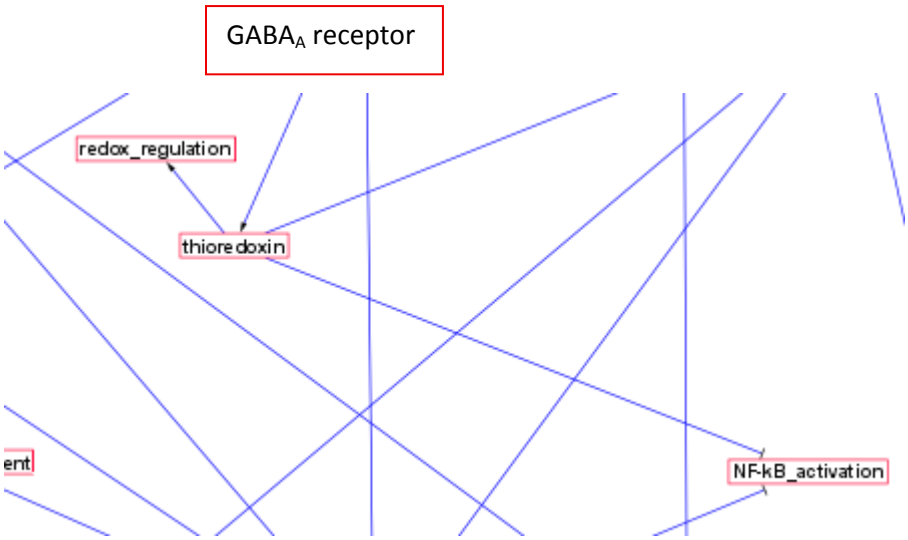

Figure 61: Summary of thioredoxin acivity from supplemental figure 1. Briefly, the GABAA receptor inhibition by Securinine leads to upregulation of thioredoxin, possibly as a result of oxidative stress. Thioredoxin upregulation is predicted to directly inhibit activation of NF-κB and also participate in the redox regulation of various proteins by protecting proteins from oxidation.

Trx involvement with signaling from the cytosol includes interaction with Ask1, an apoptosis inducing kinase [260]. This interaction depends on the redox status of Trx. When Trx is in the oxidized form, it dissociates from Ask1, thus freeing Ask1 to influence p38, Jnk, and contribute to TNFα-induced apoptosis [260]. In the reduced form, Trx binds to and inhibits Ask1 activity [260]. It would be useful to determine the redox status of Trx in our samples, in order to understand the precise role of Trx in Securinine stimulated monocytes. The ratio of the oxidized:reduced Trx species should provide an indication as to which form of Trx predominates and indicate which activities are most

likely to be occurring. It will also be informative to determine whether or not Trx is being exported. Our research group is in the process of creating multicolor ZDyes that are designed to reveal of disulfide states, as well as other thiol oxidation states of proteins, but these reagents were not available when we conducted our investigations.

S100A4

S100A4 was observed to be downregulated in the soluble fraction of Securinine stimulated samples. S100A4 is a member of the poorly described S100 Ca^{2+} binding family of proteins. The S100 proteins share a common Ca^{2+} binding motif [261]. A number of functions have been attributed to S100A4, including effects on cell motility, cytoskeletal rearrangements, signal cascades, cancer progression, apoptosis, and differentiation [262-270]. It has been observed that S100A4 is expressed in cells with high motility and that increased ectopic expression increases cell motility (see figure 62 and supplemental figure 1) [269].

S100 proteins have no known enzymatic function, but instead exert their influence by binding to other proteins and modifying their activity, following activation by Ca^{2+} binding [261,269]. S100A4 has been described as binding to target proteins such as p53 and inhibiting their phosphorylation [271]. Various other binding partners have been identified including F-actin, nonmuscle myosin heavy chain IIA, liprin β1, RAGE, annexins, and actin [263,265-268,270,272,273]. These binding partners support various functionalities related to the cytoskeleton, including motility, inflammation, and etc. S100A4 has also been shown to be secreted and to act extracellularly

[262,264,267,268,274]. Among the activities reported for extracellular S100A4 is activation of NF-κB through membrane receptors by inducing phosphorylation of IκBα, causing the degradation of IκBα, and subsequent release of NF-κB, as well as activation of the p38, ERK1/2, and Jnk pathways [262]. The observed downregulation of S100A4 is hypothesized to be inhibitory to NF-κB activation.

Downregulation of S100A4 would suggest that cell motility induced by S100A4 will be reduced, and that there will be alterations to the cytoskeleton. In addition, it would be expected that downregulation of S100A4 is related to inhibition of apoptosis. Another possibility is that the pronounced reduction in S100A4 expression in the

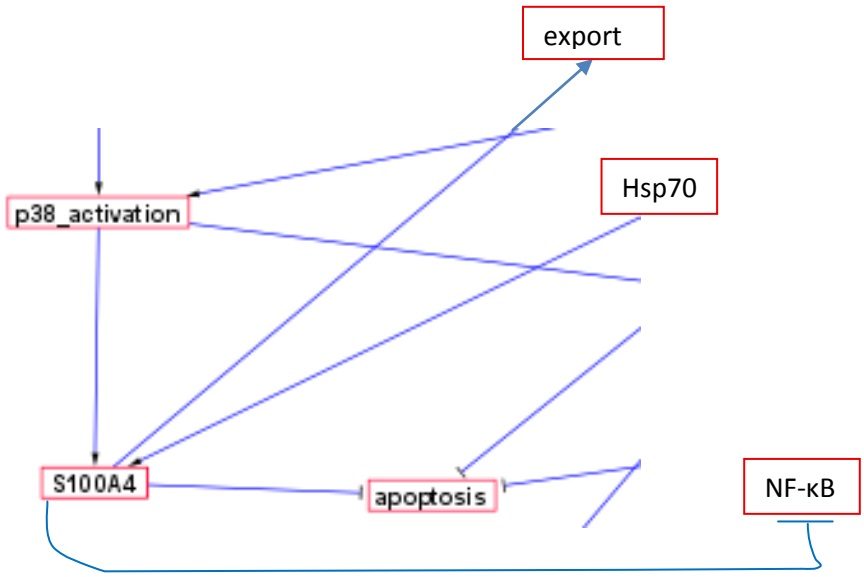

Figure 62: Proposed interactions involving S100A4. S100A4 can be activated by both Hsp70 and activated p38. S100A4 can also inhibit apoptosis, and can be exported to perform functions extracellularly. See supplemental figure 1 for more detail.

soluble fraction of our Securinine-stimulated samples is due to an increase in secretion. This is particularly relevant as it has been reported that Hsp70 can stimulate S100A4 secretion [274]. Given the elevated levels

of Hsp70 in our samples at both the soluble and membrane level, it seems likely that we are observing loss in S100A4 soluble fraction expression due to an increase in secretion. If secretion is occurring, then we would expect an impact on various signaling pathways such as p38. It would be useful to determine the changes in S100A4 in the media, as that should resolve whether we are seeing a true downregulation or enhanced secretion.

General Conclusions from Securinine Stimulation

A number of interesting proteins change expression in the Securinine stimulated samples. Of emergent interest is the strong upregulation of several Hsp70 isoforms. Although commonly thought of primarily as a protein folding chaperone, Hsp70 is hypothesized in our model to regulating a number of immune responses including modulation of inflammation, inhibition of apoptosis, and antigen presentation. Indications from the literature that Hsp70 interacts with other proteins found to be differentially expressed in our 2D gel data including L-plastin, Hsp90, Hsp60, and S100A4 leads to the hypothesis that Hsp70 is a regulator in the monocyte response to Securinine stimulation and possibly is a regulator of the monocyte immune response.

The proposed pathways for p38 activation by Securinine exposure (see figure 63) include two non-mutually exclusive optional pathways. The first is indirect activation of the p38 pathway, caused by inhibition of GABA binding to the $GABA_A$ receptor, which in turn causes the downstream activation of the p38 pathway through various mechanisms detailed above. The other possibility is direct stimulation of p38 by Securinine following diffusion of Securinine into the cell. Our data supports indirect activation of p38 due to inhibition of the $GABA_A$ receptor by Securinine exposure. However, at this time we cannot exclude the possibility that Securinine is also acting within the cell.

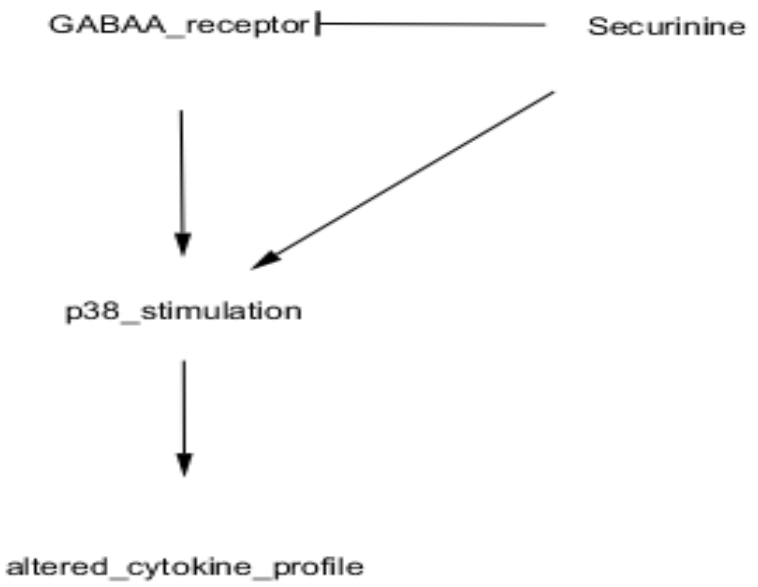

Figure 63: Possible pathways leading to activation of p38 in monocytes in response to Securinine exposure. One possibility is indirect p38 activation due to the downstream effects of Securinine inhibition of the $GABA_A$ receptor through e.g. Hsp70 etc., as described above. The other possibility is by direct Securinine stimulation of p38 upon diffusion of Securinine into the cell.

Although it is possible that p38 is being directly stimulated by Securinine, this seems unlikely for the following reasons. First, Securinine has been reported to bind directly to the GABA binding site of $GABA_A$ receptors [78,275]. Second, in order for Securinine to directly affect p38, it must enter the cell. While Securinine is of a size and charge where drug entry into the cell is possible, we suggest that stimulation of p38 through integrins stimulated by phosphorylated L-plastin and other factors (as proposed above in figure 63) is more likely. In this scenario, Securinine would only have to bind to the $GABA_A$ receptor and would indirectly trigger p38 activation through response pathway(s) controlled by the activation state of the $GABA_A$ receptor. Because the subunit composition of $GABA_A$ receptors is so critical to their biological function [84,86,112,276], it will be critical to determine the actual subunit composition(s) of the $GABA_A$ receptors expressed in monocytes. Subunit composition could be determined by purifying the intact receptor (e.g. by using antibody pull-downs), and identifying the subunits by MS analysis.

The presence of $GABA_A$ receptors and their proposed inhibitory effect on the monocyte immune response [82,84,87] allows us to extend our hypotheses to a more general model. There is a well known connection between stress and a depressed immune system. It is possible that GABA is being upregulated in response to chronic stress and, acting through the $GABA_A$ receptor in monocytes and possibly other immune cells, could be the cause of, or a significant contributor to stress-induced depression of the immune system. Development of this suggestion is beyond the scope of the

investigation reported here, but appears to be an attractive hypothesis based on the available data. $GABA_A$ receptor agonists and antagonists could be tested for their influence on the regulation of the immune response.

Analysis Using DAVID and GOEAST Software

Analysis using the DAVID (figures 21-29) and the GOEAST (figures 48-50) was undertaken following completion of our model, in order to evaluate the accuracy of our manually generated Securinine stimulated models using an automated approach. Data was input using Uniprot accession numbers for the regulated proteins (see table 13), and the default parameter settings were used for the evaluations. The results of the analyses substantially confirmed our original analysis using a manual approach, in addition to extending our original conclusions. DAVID in particular, was good for providing molecular targets (protein and metabolite) that can be used for more precisely testing various pieces of our models in downstream work. DAVID does not provide pathway data for all of our targets, but where this data exists it supports our manually constructed models. The GOEAST package provides complimentary data regarding protein biological and molecular functions as well as providing cellular localizations using the proteins provided, but does not provide metabolomic or other molecular data.

We note that no one approach (automated or manual) provided a completely comprehensive coverage for all of the variables, and the approaches used provide somewhat complimentary information. For example, DAVID provides quite a number of

metabolic pathways related to IMPDH, and various ways in which inosine-5'-monophosphate can be produced. This information will be valuable as a resource for planning derivitizations to use when designing metabolomic experiments. There is also a certain amount of information that is not likely to be relevant to our system using monocytes. For example, GOEAST makes potential links to axon grown for actin, which is a function not likely to be present in monocytes. This underscores the need to evaluate the output of automated systems analysis software packages to determine the relevance of the conclusions drawn from the software.

Conclusions from LPS/MPL Samples

LPS, derived from *E. coli*, can trigger a sufficiently strong immune response in innate immune cells to enhance clearance of *C. burnetii* or other infections. Unfortunately, the side effects of *E. coli* LPS are quite severe, thus limiting its clinical usefulness. Nonetheless, a knowledge of the proteome changes induced by LPS stimulation of monocytes could provide clues to designing better adjuvants and treatments. MPL is a derivative of LPS that triggers an innate immune response, but has much less severe effects than LPS, and MPL has recently been licensed in the U.S. (M. Jutila, Dr. S. Bavari personal communication, [77]). A comparison of the two responses at a proteome level could be useful in 1) identifying subsets of proteins that warrant further investigation, 2) identifying areas (e.g. the metabolome) where greater data coverage is needed, and 3) providing a basis for comparison with other treatment

stimuli e.g. Securinine. Both LPS and MPL are known to trigger a response through the classic toll-like receptor signaling pathway and to trigger NF-κB activation, as well as changes to the cytokine/chemokine profiles of the cell.

Two recent 2D gel analyses of LPS stimulated monocytes provide background for these experiments. Pabst et al., (2008) primed monocytes for 16 hours, finding 15 differentially expressed spots corresponding to 12 unique proteins [146]. Gadgil et al (2003), performed a similar series of experiments priming monocytes with LPS for 48 hours, finding 16 differentially expressed spots, 13 of which were unique protein spots [277]. Pabst et al., (2008) suggested that optimal monocyte priming may occur in the 30-60 hour range following stimulation with LPS [146]. We note that our stimulation was for 24 hours with LPS, in between the 16 hours of Pabst ,et al., (2008) and the 48 hours of Gadgil, et al., (2003) [146,277]. Pabst et al, (2008) observed that LPS stimulation caused a downregulation of ATP synthase precursor [146], ATP synthase precursor (LPS stimulation) and ATP synthase (MPL stimulated) were detected as upregulated in our samples. The differences observed between Pabst et al, (2008) and our samples could simply reflect differences in the timing of the experiments, and/or the cell lines used.

It is not clear why we observed only one differentially expressed protein in our experiments, in response to LPS stimulation, but we note that both of the cited studies were using freshly isolated primary monocytes, whereas we used cultured monocytes. This would seem to indicate a clear difference in the response time between primary

monocytes and the Monomac I cells we used, in addition to supporting the conclusion that we did not utilize an optimal LPS stimulation time for the Monomac I cells, and/or we did not have an optimal molarity of LPS (or MPL) in our samples. The cited studies provide clues that may be used to design better adjuvants for innate immune stimulation.

A small number of proteins were determined to be changing expression in the membrane fraction of both LPS and MPL stimulated samples in our data sets. LPS and MPL samples were stimulated for 24 hours as this time point gave similar IL-8 expression levels as Securinine stimulation. However, in addition to the time frame discussed above, LPS and MPL are likely to trigger fairly rapid responses, and many of the downstream effects are either a) transcription/signaling factors or b) secreted (e.g. cytokines). The relevant transcription and signaling factors were of insufficient copy number to be observed by the differential detection system we employed and we made no attempt to characterize the secretome.

Regarding the time frame, LPS and MPL-stimulated samples taken at different time points may have yielded more fruit, and future characterization of these stimuli should take this into account. We had intended to conduct a comprehensive comparison between LPS/MPL stimulation of TLRs and Securinine antagonism of the $GABA_A$ receptor. We were unable to perform such a comprehensive comparison due to the relatively small number of differentially expressed proteins detected. Nevertheless, some conclusions can be drawn from the expression changes, as detailed below.

Prohibitin

Prohibitin was observed to be upregulated in the membrane fraction of our MPL stimulated samples (see figure 64). Prohibitin is an abundant, highly conserved protein that has important, but as yet ill-defined cellular functions. One function of prohibitin seems to be in tumor suppression and general anti-proliferative activity [278-280]. Overexpression of prohibitin has been observed to cause growth arrest [278,279,281], while loss of prohibitin in epithelial cells leads to cellular aggregation [280]. It appears that the ERK pathway may be involved in cell cycle regulation via prohibitin expression [281]. Increasing prohibitin expression leads to an increase in ERK phosphorylation [280]. It should be noted that prohibitin's role in cell cycle progression has been challenged recently and the mechanisms involved are not fully understood [278].

In addition, prohibitin has been documented as being expressed in mitochondria, the nucleus, and at the cell surface, in addition to being found circulating in the blood [278,280,282,283]. Exogenous prohibitin can be translocated to the mitochondria and inhibit pyruvate carboxylase [283], suggesting that prohibitin may regulate metabolic processes under certain conditions. Prohibitin has been shown to enhance anaerobic metabolism in adipocytes [283]. This further suggests that measuring lipidome and metabolome profiles in our samples are likely to be quite informative.

Prohibitin appears to be a lipid raft associated protein in the plasma membrane [278,283-285]. It has been proposed that prohibitin may also be bound to the inner mitochondrial membrane and function as a chaperone similar to heat shock 60, acting

on respiratory chain subunits [278,279,282,283]. Indeed, prohibitin has been shown to bind directly to polypeptide chains of respiratory chain subunits [279]. Prohibitin association with lipid rafts is believed to occur at the plasma membrane rather than the mitochondria where lipid rafts are believed to be rare [278,285], although the scarcity of mitochondrial lipid rafts has recently been challenged [286-288]. It has been proposed that regions of the mitochondrial outer membrane that are rich in cardiolipin (a mitochondrial phospholipid), which appear during apoptosis, are in fact a raft-like mitochondrial lipid microdomain [288], and it is possible that prohibitin may associate with these raft-like domains.

Prohibitin may have a role in lymphocyte maturation/differentiation and modulation of inflammation [278], and it has been suggested that *Salmonella typhi* targets prohibitin to suppress early inflammation [281,282]. Theiss, et al., (2007) reported that increasing levels of prohibitin lead to an increase in GSH in epithelial cells, suggesting that prohibitin may play a role in protecting cells from oxidative damage [282]. Such effects could be monitored in our samples by measuring intracellular GSH:GSSG ratios. There are some indications that prohibitin may play a role in apoptosis [279,280,289]. Inhibition of apoptosis by prohibitin occurs at the membrane and involves a complex of proteins enriched in lipid rafts containing prohibitin, further implicating lipid rafts for prohibitin membrane localization [281]. Prohibitin could be a marker of monocyte maturation, as well as having a role in modulation of inflammatory compounds. *C. burnetii's* effect on the immune response could very well involve

inhibition of prohibitin, without causing a detectable change in expression (e.g. by altering the lipid raft composition such that prohibitin cannot bind). Prohibitin promises to be an interesting protein, but the overall lack of characterization hampers efforts to understand its role in our systems.

We do not know the exact localization of prohibitin in our samples. During the early phases of our investigation we attempted to perform organellar subfractionation, but the monocytes proved difficult to fractionate (data not shown), and therefore no further effort was made at subcellular fractionation beyond separating the samples into soluble or membrane fractions. It would be useful to know whether the observed increase in prohibitin expression in our samples is in the mitochondria, the nucleus, the plasma membrane or in some combination. The indications that prohibitin could be a lipid raft protein further suggests that a better understanding of the lipid raft compositions in our samples could well prove a fruitful avenue of research in the future. Future work involving monocytes that are deficient for prohibitin in response to MPL stimulation could prove very helpful in understanding prohibitin biology. The observation that prohibitin is required for Raf-related activation and potential involvement in ERK signaling [280,281], suggest a potentially important role for prohibitin in signal transduction in response to various stimuli. We also suggest that prohibitin may be stimulating an increase in the intracellular levels of GSH as a means to counteract the increase in oxidative species in the cell as a results of TLR stimulation by MPL.

It should be pointed out that macropain was also identified in the regulated prohibitin spot. Macropain and prohibitin have similar predicted pIs and molecular weights and may simply reflect comigration of these proteins. As prohibitin was the higher ranked protein in our bioinformatics searches it was chosen as the identified protein per stated acceptance criteria.

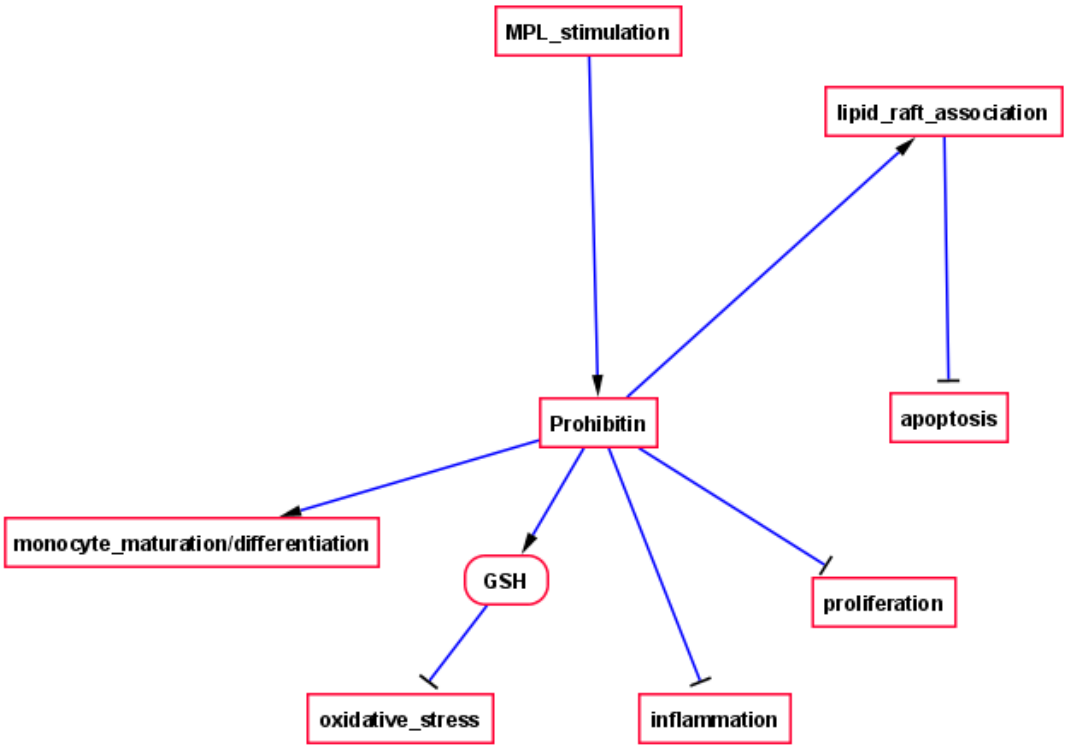

Figure 64: Schematic representation of the proposed functions for prohibitin in MPL-stimulated cells. Prohibitin is proposed to be inhibiting apoptosis through association with lipid rafts, and to inhibit oxidative stress (by increasing GSH expression), inflammation and cell proliferation in response to MPL stimulation. Prohibitin is also predicted to induce monocyte maturation and/or differentiation.

Rab2A

Rab2A is upregulated in the MPL stimulated membrane fractions. Rab2 proteins are involved in vesicular trafficking, especially retrograde transport between the Golgi and ER [290-293]. Retrograde transport between the Golgi and ER is part of the steady state maintenance and recycling mechanisms in the cell. Retrograde transport helps to maintain the flow of membranes between organelles, and to continuously recycle various proteins involved in secretory pathways to maintain those proteins in steady-state concentrations [294]. Rab2 specifically helps recruit the components necessary to initiate retrograde transport. These include interactions with glyceraldehyde-3-phosphate dehydrogenase (GAPDH) and atypical PKCι which, when complexed with Rab2, initiate recruitment of the motor protein dynein to tyrosinated microtubules of vesicular tubular clusters [293]. Tyrosination is the reversible addition of a C-terminal tyrosine residue [293]. Vesicular tubular clusters (VTCs) are an intermediate organellar compartment involved in the transport of secretory proteins between the ER and the Golgi [295]. VTCs are coated with either COPI proteins (retrograde transport, Golgi to ER) or COPII proteins (anterograde transport, ER to Golgi) [295].

Rab2 can specifically regulate the retrograde transport of certain membrane proteins [291]. At least some of the proteins Rab2 can regulate are involved in ERK1/2 signaling, and an increase in Rab2 activity increases retrograde transport thus preventing transport of these proteins to the plasma membrane [291]. Retrograde transport mediated by Rab2 could therefore be an important regulatory mechanism for

certain signaling pathways. An increase in Rab2 activity could correspond to an increase in the ratio of the GTP form of the protein:the GDP form of the protein similar to other Rab proteins (e.g. Rab7, described below). For Rab7, the GTP form is more closely associated with the membrane than the GDP form [296-298], and given that Rab2 is found in the membrane fraction, a similar phenomenon could be happening with Rab2.

Given the possibility that the MPL stimulated samples are desensitizing to the MPL stimulus, Rab2 is most likely involved in regulation of certain signaling proteins, and/or export products in our samples. Monitoring of fluorescently labeled Rab2 and known Rab2 targets in MPL and LPS stimulated cells would likely provide information as to the dynamics of anterograde/retrograde transport in monocytes during an innate immune response. In addition, the utilization of Rab2 mutants in either a constitutive GDP or GTP form may also prove informative as to the effects of the GDP and GTP forms of Rab2 on MPL stimulation of monocytes. Given that *C. burnetii* and other obligate intracellular pathogens hijack various vesicular processes, understanding of the role of Rab2 could yield insights into how this is done, and how it might be targeted to clinical effect.

ATP Synthase Mitochondrial F1 Complex β Precursor

ATP synthase mitochondrial F1 complex (referred to as F_1 ATPase in the following) was observed to be upregulated in the membrane fractions of both LPS and MPL stimulated samples. This is the only differentially expressed protein shared by both LPS and MPL stimulated samples under the conditions we investigated and was the only

differentially expressed protein we detected from LPS stimulated cells at 24 hours. F_1 ATPase is synthesized in a precursor form that is processed to give the final form of the protein. In MPL stimulated samples, the precursor form was observed, in LPS samples only the final processed form was observed. Given that the end result of stimulation by these two compounds is similar (detailed below), we had expected to see more overlap between the two test conditions, but this may simply reflect a poor choice of sampling times or molarity as described above [146].

It has been observed that at least some aspects of MPL and LPS stimulation occur on similar timescales when used for stimulation of TLRs [75]. Specifically, TRIF-dependent responses to TLR activation, e.g. upregulation of granulocyte colony stimulating factor and upregulation of IP-10, tend to respond on a similar time scale in both LPS and MPL stimulation although not always with the same magnitude of response [75]. TRIF, short for TIR domain-containing adaptor-inducing interferon β, is an adaptor protein activated by TLR activation and independent of the MyD88 adaptor protein response that is also triggered by TLR activation. A proteomic analysis of MPL stimulation of monocytes has not been attempted to our knowledge, so while some inflammatory markers may behave on a similar timescale in LPS and MPL stimulated samples, the relation of the protein expression dynamics between the two stimulating factors are not known.

The F_1 ATPase has been shown to occur in several locations in the cell. The best known location is in the mitochondrial inner membrane, where F_1 and F_0 subunits form the ATP generating machinery [299-301]. The upregulation of F_1 ATPase in our samples

could simply be a reflection of the need for increased production of aerobically generated ATP, suggesting that the cell's energy needs increased under MPL stimulation. However, it has also been shown that the βF_1 ATPase subunit is found on the cell surface, where it associates with lipid rafts [299,300,302-305]. Cell surface associated ecto F_1 ATPase may be a receptor for inflammatory signals, serve as a receptor for apolipoprotein and angiostatin, and even act as a target for cytotoxic immune cells [299,300,304].

It has been demonstrated that ecto ATP synthase at the cell surface is a target for angiostatin, and this interaction may have implications for proliferation and migration in endothelial cells [304]. It has also been shown that ecto F_1 ATP synthase may play a role in stimulating lymphocyte activity via binding of apolipoprotein and through a close association with MHC class I antigens [305]. Immunoprecipitation studies reveal that F_1 ATPase can be pulled down with MHC class I protein, suggesting a functional interaction [305]. This was further supported by confocal microscopic observations that MHC-I and ecto F1-ATP synthase colocalize in the membrane [305]. Apolipoprotein may compete with MHC-I for F_1 ATPase when levels of MHC-I at the plasma membrane are low, thus preventing the activation of lymphocytes [305].

We cannot determine whether the observed increase in F_1 ATP synthase in our samples is at the mitochondrial level because of the need for increased mitochondrial energy production or is located at the cell surface. Monitoring changes by fluorescent methods (e.g. using a fluorescent antibody or GFP construct on intact cells) should

distinguish changes in expression and/or subcellular localization following MPL or LPS stimulation. It would also be interesting to determine the concentration of ADP and ATP in the secretome, and whether or not these change in response to stimuli. ADP:ATP ratios were not assessed in our current screen.

p64 Chloride Channel

p64 is observed to be upregulated in the membrane fraction of the MPL stimulated samples. p64 is reported to be an intracellular chloride channel of the chloride intracellular (CLIC) family [306-308]. p64 may contribute to the chloride channel activity in the cells, in response to stimuli such as endotoxins. Two functions of chloride ion channels include providing counterions and to aid in the acidification of certain intracellular organelles by dissipating electrical potential, created by proton ATPases [309-311]. Counterion flow helps to offset the influx of positive charges such as H^+ or some other depolarizing cations. Other Cl^- channels such as Clc-3 are believed to have a role in secretory granules from pancreatic β cells and also function at some synapses in glutamate uptake and possibly exocytosis [311].

The exact role of p64 is not well defined in the literature, but p64 seems to localize primarily to intracellular membranes in the cell [306-308,310], and as p64 has been shown to be a binding partner for $p59^{fyn}$ [307]. Activation of p64 by $p59^{fyn}$ increases Cl^- channel activity in HeLa cells [307]. $p59^{fyn}$ is a nonmembrane Src receptor tyrosine kinase, that is involved in intracellular signaling [307], suggesting that activation of p64 by $p59^{fyn}$ tyrosine phosphorylation is involved in intracellular signaling. p64 is a

direct $p59^{fyn}$ target, and this implies that Cl^- levels mediated by p64 have an important role in various signaling events. Redhead et al., (1997) reported that p64 localization was consistent with a secretory pathway regulated by Ca^{2+} [310]. Clc-3 has been shown to be involved in activating NADPH oxidase [309], and that Clc-3 is a direct player in ROS generation. p64 may be playing a similar role in response to MPL treatment. Because Cl^- channels have been reported to regulate Ca^{2+}-mediated exocytosis [311,312], it seems feasible that p64 is involved in regulating exo- and/or endo-cytosis. Determining the localization of p64 and monitoring the changes in $[Cl^-]_i$ could well be important to understanding the role of p64 in MPL stimulated samples.

Guanine Nucleotide Binding Protein β Polypeptide 2-like 1/RACK1

RACK1 is upregulated in the membrane fraction of MPL stimulated samples. RACK1 is a widely distributed, and highly conserved protein [313,314]. Initially characterized as a scaffold protein for PKC, RACK1 is now believed to be central to many biological mechanisms [313-315]. Cells that overexpress RACK1 appear to have increased tyrosine phosphorylation levels a reduced growth rate, and increased cell spreading/migration [314,315]. Because RACK1 is a scaffold protein, it may exert its influence by shuttling binding partners to a particular location and/or providing specific protein complexes for particular binding partners. The RACK1-containing protein complexes determines the downstream activities regulated by RACK1 [315]. Determining the localization of RACK1 and which protein complexes are associated with it in our samples would be desirable.

RACK1 seems to be directly involved in signal transduction mediated by adenylyl cyclase, and is an integral part of the ribosomes in eukaryotes [314,316]. This immediately suggests that monitoring cAMP levels and associated targets may prove informative.

RACK1 has been implicated in immune function, specifically in cytokine and interferon receptor function, and RACK1 transcription is stimulated by activated NF-κB [313,314]. The action of RACK1 downstream of NF-κB appears to be involved in cell survival under certain conditions [313]. Various PKC's have been implicated in NF-κB activation in macrophages, and NF-κB regulates some of RACK1's binding partners [313]. This suggests that RACK1 may have a central role in regulating the innate immune response triggered by TLR signaling. It was recently reported that RACK1 forms a complex with β1 integrin and the insulin-like growth factor receptor, enabling RACK1 mediated cell migration [315]. It has also been shown in Jurkat T cells and HL60 neutrophils that RACK1 directly binds to Gβγ and inhibits chemotaxis [317]. Chen et al., (2008) further demonstrated that RACK1 binding directly inhibited the activity of $PI_3K\gamma$ [317]. As the PI_3K family is involved in Rab7 functions in formation of the phagolysosome, this suggests that RACK1 activity may be involved in *C. burnetii* infection, and this deserves further investigation. We did not observe a change in RACK1 expression in *C. burnetii* infected cells, but it is possible that RACK1 is changing its functional status in *C. burnetii* infected cells without a corresponding change in expression. It is also possible that RACK1 expression in *C. burnetii* infected cells is affected at later time points than we sampled.

Under certain conditions, RACK1 is phosphorylated, facilitating the formation of homodimers [318]. RACK1 facilitates delivery of HIF-1α to the proteasome by outcompeting Hsp90 for HIF-1α binding and recruiting elongin-C3 ubiquitin ligase to HIF-1α [318,319]. Calcineurin can dephosphorylate RACK1, preventing formation of a homodimer, in at least partially a Ca^{2+} dependant process [319]. Increases in cytosolic [Ca^{2+}] have been reported following TLR stimulation with LPS [320]. This underscores the need to understand the flux of metal ions between intracellular compartments, particularly Ca^{2+}, over time in response to MPL and also to other stimuli that we tested.

It has been shown that an age-related decline in RACK1 expression is coupled to a decline in PKC activity in monocytes and lymphocytes which is directly related to the age-related decline in immunity [321]. In a study by Corsini et al. (2005), it was shown that levels of the steroid DHEA influence expression of RACK1, indicating hormonal control over leukocyte activity [321]. Although not likely to be important in our system, the age-related decline in RACK1 levels has implications at the whole organism level, and suggests that MPL treatments will decline in effectiveness in older individuals and those with defective hormonal signaling. This may have implications for the use of MPL in vaccines particularly in older individuals or those with low levels of DHEA. Furthermore, the age-related decline in RACK1 expression may play a role in the reduction in immune function commonly associated with chronic stress, namely that cells are less responsive to endotoxins.

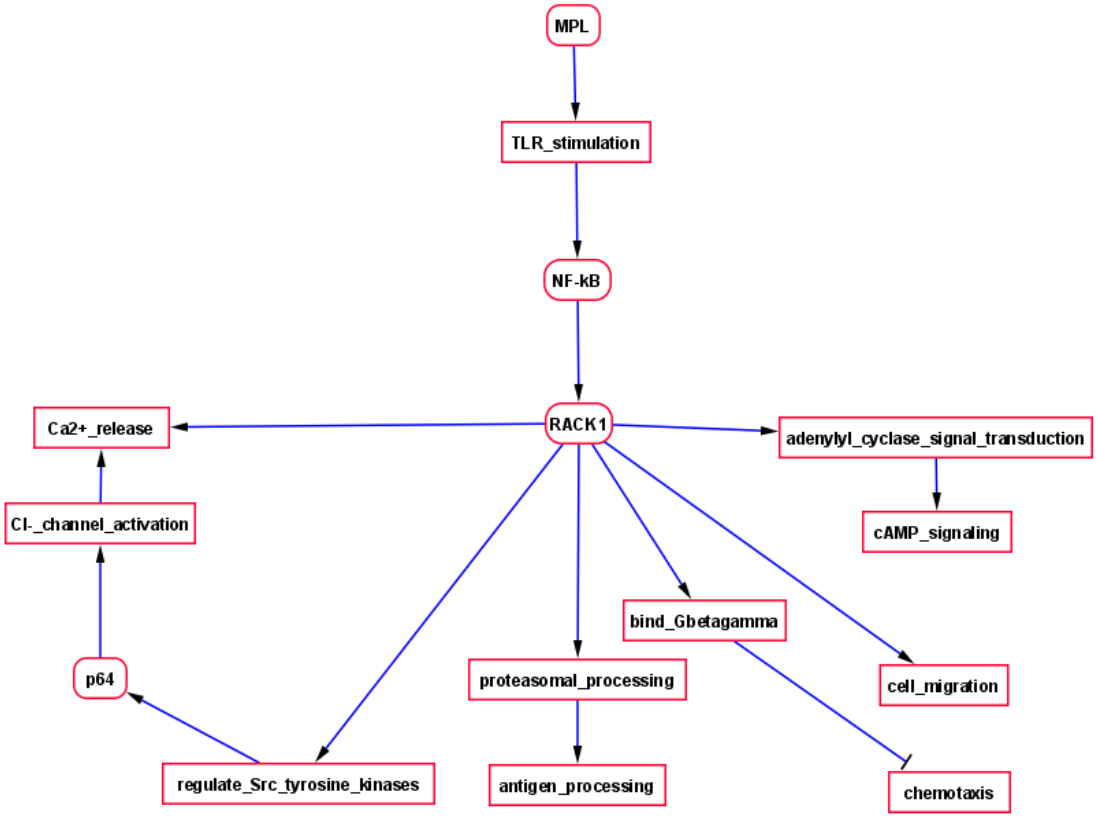

Figure 65: Proposed functions of RACK1 in response to MPL stimulation of TLRs. RACK1 is proposed to inhibit chemotaxis, as well as activating cell migration, cAMP signaling, and Ca^{2+} release either via direct stimulation and/or via activation of p64 through the Src tyrosine kinases.

RACK1 will associate preferentially with PKC, but also interacts with Src tyrosine kinases [314,316]. This is of interest as p64 also interacts with a Src kinase $p59^{fyn}$ (see above). It is possible that RACK1 is regulating the tyrosine phosphorylation status and therefore the activity of p64. Given that p64 is involved in Cl^- channel activity, that p64 can be regulated by Src tyrosine kinases, and that Cl^- ions can regulate Ca^{2+} signaling, it

follows that RACK1 may directly influence the ionic signaling mechanisms in monocytes, in response to MPL stimulation. It was recently demonstrated that inhibition of a Ca^{2+} dependant Cl^- channel CLCA1 can attenuate the LPS induced upregulation of mucins in human airway mucosa [322]. This suggests that the Ca^{2+} and Cl^- channel activities and the changes in the concentrations of these ions may be important in MPL and presumably LPS induced functions.

Of further interest in ionic signaling is that RACK1 binds to inositol 1,4,5-triphosphate receptors (IPRs) [323]. IPRs are directly involved in mediating Ca^{2+} signaling through their binding to inositol 1,4,5-triphosphate, which in turn signals Ca^{2+} release [323]. When RACK1 is bound to IPRs, the binding affinity for inositol 1,4,5-triphosphate is increased and this leads to the release of approximately 2x the levels of Ca^{2+} released in the absence of RACK1 [323].

The diversity of functions that have been reported for RACK1 are undoubtedly cell-specific in some cases. Nonetheless, we can conclude that RACK1 is potentially either regulating or being regulated by ionic signaling from Ca^{2+}. This may involve the p64 chloride ion channel as described above, and it is likely that Cl^- and Ca^{2+} as well as IPRs and inositol 1,4,5-triphosphate are involved in some aspects of the monocyte response to MPL stimulation via RACK1 related activities. Further, RACK1 expression is likely being regulated by NF-κB signaling which should be active in MPL stimulated samples. In addition, because RACK1 has been implicated in at least some proteasomal processing, it is possible that RACK1 may function in the proteasomal processing of MHC

class I antigens. Overall, RACK1 is likely to be a central protein that is affected in our MPL stimulated samples, and further investigation using knockdowns, and immunoprecipitations would likely prove to be fruitful in furthering our understanding of monocyte response to MPL in particular and endotoxins in general.

Tropomyosin 3 Isoform 2

Tropomyosin 3 isoform 2 was observed to be upregulated in the membrane fraction of MPL stimulated samples. Tropomyosins (Tm) are a group of actin binding proteins expressed in all eukaryotic cells [324]. They are best characterized in muscle, but have nonmuscle functions as well, including actin bundling, and actin filament function, possibly in a cell type specific manner [325,326]. Unfortunately, nonmuscle actions of Tms are poorly understood [325]. The various Tm isoforms are functionally distinct [325]. Tm2 and Tm3 are examples of this, playing different roles as components of actin stress fibers, and possibly both playing a role in cell spreading, but neither seems to directly affect cell attachment and motility [324-326]. It is also becoming clear that Tm isoforms are not homogenously distributed in the cell and instead localize to distinct regions [324-326]. McMichael et al., (2006) claim that macrophages do not express Tm3, but did not address monocytes or Monomac I cells [326]. Our data would seem to indicate that at least in Monomac 1 cells, Tm3 is indeed expressed in a monocyte and/or monocyte derived macrophages.

It is possible that increased expression of Tm3 isoform 2 (Tm3i2) in MPL stimulated samples is accompanied by changes in cytoskeletal dynamics. Gimona, et al.,

(1996) noted that increased expression of Tm3 in fibroblasts led to areas in the cell exhibiting actin disorganization [324]. It might well be informative to observe dynamic changes in Tm3i2 localization and cytoskeletal organization in response to MPL and LPS stimulation. Interestingly, Perez-Gracia et al. (2009), recently reported that oxidative stress in Alzheimer's disease caused a 40% increase in oxidatively damaged Tm3 isoform 2 protein [327], which happens to agree with the ~40% increase we observe in our samples. Although the agreement with Perez-Gracia is potentially coincidental, it does suggest that an increase in ROS in response to MPL stimulation could in fact be the source of our detected increase in expression, namely that Tm3i2 observed is in fact oxidized, and that this could be a marker of ROS induction/activity. Further experiments will be needed to test this.

Conclusions from *C. burnetii* Infected Monocytes (see supplemental figure 2)

Mn-containing Superoxide Dismutase (MnSOD)

We observed MsSOD being upregulated in the soluble fraction at 48 hrs postinfection and in the membrane fraction at 96 hrs postinfection (see figure 66 and supplemental figure 2). SODs are highly conserved proteins that convert the superoxide anion into H_2O_2. Bacteria contain one to three different types of SOD enzymes [328], and these contribute to the virulence of many human pathogens [329]. However, bioinformatics analysis establishes that we are observing human not bacterial MnSOD in

our experiments. Inflammatory signals, such as those caused by infection, trigger the production of reactive oxygen species (ROS) of which the superoxide anion is a primary example [330]. ROS produced by the innate immune system during response to infection can take part in the microbicidal process. MnSOD can also be upregulated by inflammation [330]. The levels of MnSOD present during an inflammatory condition can help to determine the ability of cells to resist the pathogenesis of that condition, e.g. in irritable bowel disorder (IBD), levels of MnSOD are often reduced [330].

C. burnetii does produce a superoxide dismutase, but it is more likely Fe rather than Mn based [35,38]. *C. burnetii*'s FeSOD is a potential virulence factor, and functions in suppression of the oxidative burst [35]. Infection by *C. burnetii* is known to produce a reduced respiratory burst and infected cells display a reduced production of superoxide anion [331,332]. Our results suggest that the MnSOD observed in our system is an early cellular response to the host cell respiratory burst and ROS activity, possibly regulated through cellular effectors by *C. burnetii*. Determination of the levels of superoxide anion and glutathione in response to *C. burnetii* infection over time might be helpful in determining whether the upregulation of MnSOD is strictly a host cell response to infection or is directed by *C. burnetii* via secretion of bacterial effectors to the host monocytes. *C. burnetii* is known to secrete proteins to host cells[332], and one or more of these proteins could be directing upregulation of MnSOD both for the purpose of reducing the effects of ROS and increasing the availability of glutathione. MnSOD has been reported to be stable to both heat and variations in pH [333]. Mitochondria

produce MnSOD to help control the redox state within the mitochondria during electron transport, as was reported by Wheeler, et al., (2001) [334]. Even modest levels of increase in the expression of MnSOD caused an ~50% reduction in ROS injury in the livers of rats fed ethanol, and that further increase to 3x the normal levels of MnSOD abolished ROS injury entirely [334].

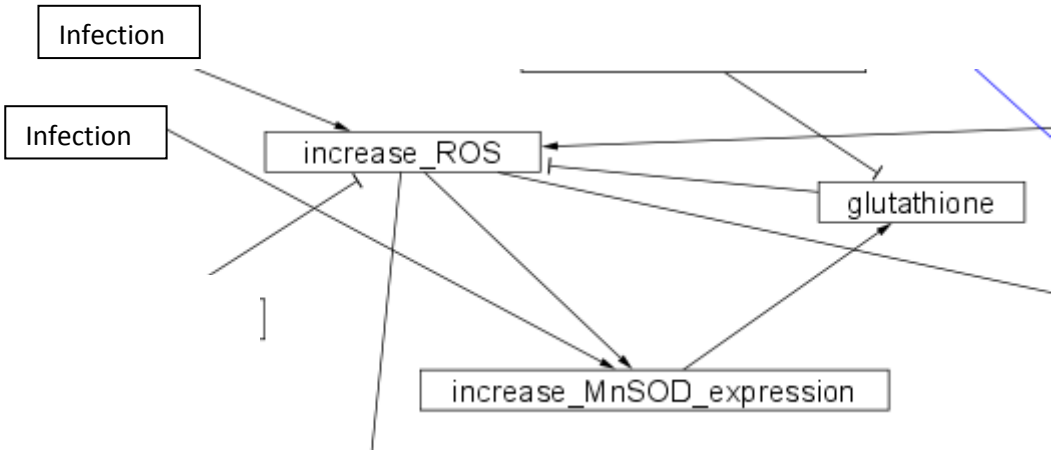

Figure 66: Schematic of MnSOD hypothesized actions. MnSOD is proposed to be an early acting response to increased ROS and/or infection. See supplemental figure 2 for more details.

The observation that the change in MnSOD expression altered its subcellular localization from cytosol to membrane between 48 and 96 hrs p.i. suggests that the site of maximum MnSOD activity was shifted. We cannot determine the precise organellar localization from our dataset, and further work would be needed to determine the

subcellular localization of MnSOD in the presence of *C. burnetii* as a function of time. Increasing the levels of MnSOD was reported by Wheeler et al. (2001) to cause an increase in the levels of glutathione, an important part of the ROS protection machinery in the cell [334]. MnSOD produces H_2O_2 from superoxide, and then glutathione is used by cells to convert H_2O_2 into water. Glutathione is a small molecule/peptide and is too low a molecular weight to be detected on a 2D gel.

Enoyl CoA Hydratase (ECH)

We observed ECH to be downregulated in the membrane fraction of 96 hr postinfection samples (see figure 67 and supplemental figure 2). ECH, an enzyme controlling the second step of fatty acid β-oxidation [335], is highly conserved, and plays a central role in fatty acid metabolism. A role for ECH as a response to infection is also beginning to emerge. Takahashi et al., (2007) reported that in human glioblastoma cells that were treated with siRNA to knockdown ECH expression (30-45% observed reduction), and subsequently infected with measles virus (MV), that MV replication was significantly impaired, in some cases nearly 100% [336]. Takahashi et al., (2007) extended their results to vesicular stomatitis virus and semliki forest virus, observing similar effects on the replication of these viruses [336]. Watari et al., (2001) had previously demonstrated a similar downregulation of ECH following infection, and further demonstrated that siRNA knockdown of ECH mRNA expression impaired the replication of MV in monkey kidney cells [337]. This suggests that ECH may often be

downregulated as a means to control pathogen replication within cells, as part of the innate immune response, possibly by reducing the availability of ATP and AcCoA.

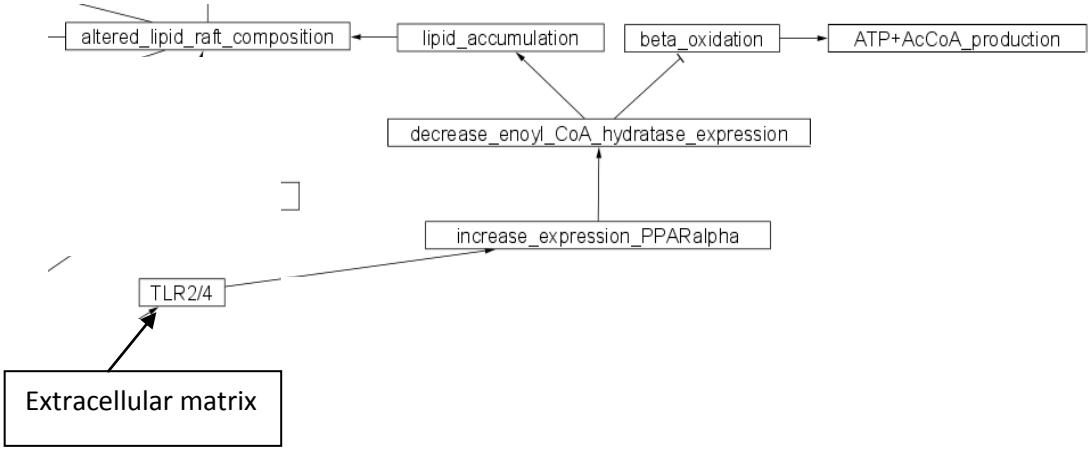

Figure 67: Summary of ECH regulation/activity. ECH is observed to be downregulated in infected monocytes. This is proposed to have the effect of reducing beta oxidation of fatty acids which may reduce the levels of available ATP and AcCoA. In addition, reduction of ECH expression should lead to an accumulation of lipids, which might alter the lipid raft compositions in the cell. The extracellular matrix component is any molecule that is present in the ECM and capalbe of triggering a TLR2/4 response. The Extracellular matrix component could be C. burnetii LPS or a secreted host cell protein such as Hsp60 which can also trigger TLRs, as described above. See supplemental figure 2 for more details.

In a recent study by Yokoyama et al, (2004) it was reported that an ~50% downregulation of ECH was observed in surgically removed hepatocellular carcinoma cells that were infected with hepatitis C virus [338]. Further, this downregulation was

observed in 70% of their tumor samples. Although the correlations in their data was a bit scattered (due to the nature of their samples and method of analysis), their results are in agreement with the knockdown data of Takahashi et al., (2007) [336] as well as with our own data. We see an ~15-20% reduction in ECH expression in *C. burnetii* infected monocytes at 96 hrs p.i.

In a recent gene expression study of hepatotoxic compounds on liver cells by Huang et al., (2004) it was observed that ECH mRNA levels were downregulated by up to 200% [339]. Although protein data was not provided, it seems clear that a response was occurring at the mitochondrial level. The data suggests that a mitochondrial-level response may be involved in a variety of cellular insults ranging from toxic compounds to tumors to infections, and alterations to metabolic pathways may be an overall defensive strategy that is not fully appreciated at this time. This situation argues that metabolomic and/or lipidomic studies could be informative if they are integrated with proteomic studies to obtain a more complete picture.

The response of mouse liver cells to LPS stimulation was recently reported to induce steatosis, the abnormal retention of lipids [340]. In particular, Ohhira et al., (2007) reported that LPS induced a reduction in the PPARα-related transcription regulation system, which includes ECH regulation, and observed an ~50% reduction in ECH mRNA expression in response to 2 hours of LPS stimulation [340]. This reduction increased slightly over at least 12 hours post-LPS stimulation.

We propose that a reduction in PPARα may be directly responsible for the reduction in ECH observed in our dataset. This would directly link *C. burnetii* LPS to the proposed reduction in β-oxidation as a result of infection, and is consistent with the reduction of ECH that we see in our system. In summary a decrease in ECH expression is predicted to reduce the amounts of available ATP and AcCoA, underscoring the desirability of lipidomic and metabolomic studies of this system. A further possibility is that *C. burnetii* may be taking advantage of the proposed buildup of lipids to alter the lipid composition of phagolysosome membranes, particularly with respect to lipid rafts containing Rab7 (see below) [341]. In addition, since we observed changes in Hsp60 that can trigger TLR2/4 (see below) and may also be a part of this pathway, it is possible that secreted Hsp60 is acting on infected monocytes to trigger a downregulation in ECH1 expression.

Vimentin

Vimentin was observed to be upregulated in the membrane fraction 96 hr postinfection (see figure 68 and supplemental figure 2). Vimentin is an intermediate filament protein, and is highly abundant in monocytes [342,343]. Increased vimentin expression results from monocyte differentiation, and does not seem to be the cause [344,345]. It was also observed that vimentin was membrane associated in purified phagosomes [73]. Vimentin is secreted by activated macrophages [343], and both PKC and TNFα are independently involved in controlling vimentin secretion [343].

It was recently reported that exposure of THP-1 monocytes to oxidized low-density lipoproteins (oxLDL) or LDL caused a large and significant increase in vimentin expression [344,345]. Bouchard et al., (2004) demonstrated that an increase in IL-15 prevented caspase cleavage of vimentin in neutrophils [346]. It has been reported that vimentin has a number of rapidly turned over phosphorylation sites that alter the dynamics of filament assembly [344]. Our gels demonstrated three separate protein spots identified as vimentin (see figure 69). One of the spots (spot 20) may be cleaved by caspase activity, suggesting that the reported caspase inhibition by *C. burnetii* [72] may not be fully functional. We detected no phosphorylated peptides, but these can be difficult to detect in an ion trap mass spectrometer, using collision induced dissociation that was employed in our experiments.

Vimentin may be involved in the regulation of the ser/thr kinase RhoA-binding kinase α (ROK). ROK is involved in cytoskeletal arrangement [344,347]. Regulation of the phosphorylation state of vimentin, which determines assembly/disassembly mechanics, likely also determines the ROK activation state [347]. Although vimentin does not trigger monocyte differentiation [344,345], it was shown to be important for proliferation [344]. Loss of vimentin expression in BM2 cells suppressed proliferation, but had a minimal effect on morphology in this [344]. In the BM2 study, it was also shown that reducing vimentin levels reduced ROS production [344], in agreement with other studies [343]. The upregulation of vimentin suggests that the monocytes in our

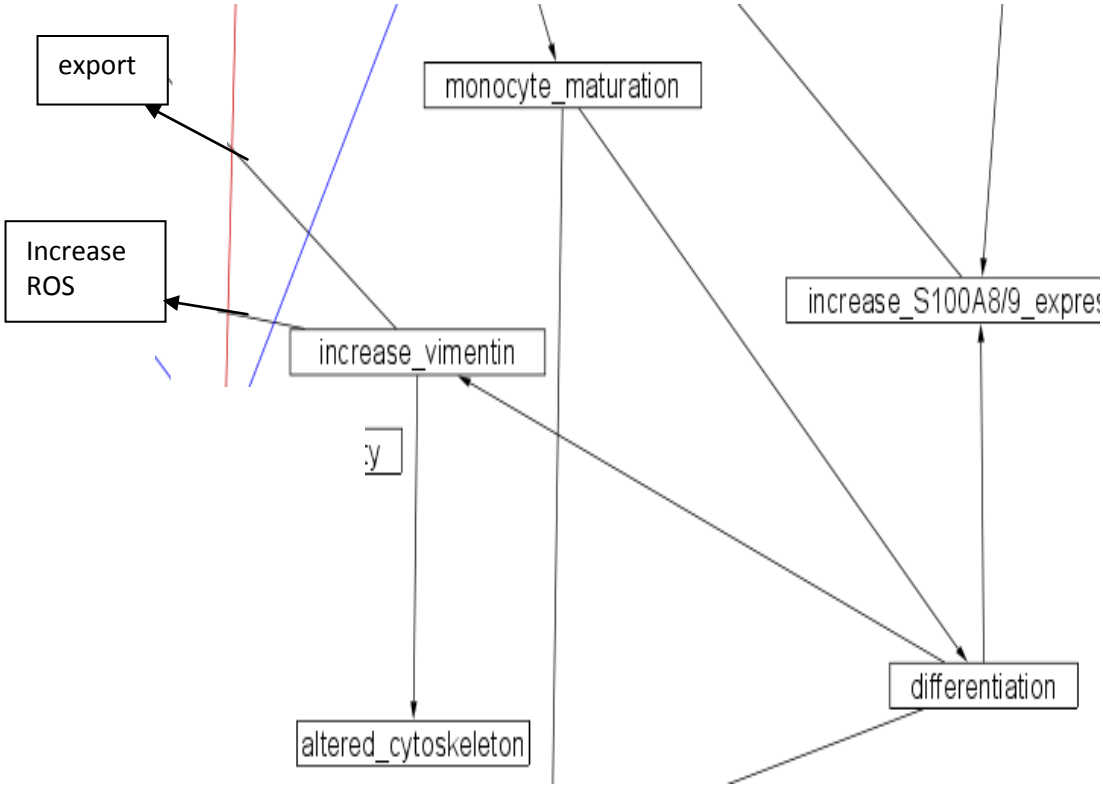

Figure 68: Summary of vimentin expression and proposed downstream effects. Elevation of vimentin is proposed to increase ROS, alter the cytoskeletal dynamics, and be exported from the cell. See supplemental figure 2 for more details.

study are in the process of differentiation. The differentiation status of the monocytes could be monitored with antibody-based detection of surface markers. The elevation of vimentin is in keeping with changes in expression that we observed in other monocyte maturation markers (e.g. S100 Ca^{2+} binding proteins A8/9, visfatin, etc.).

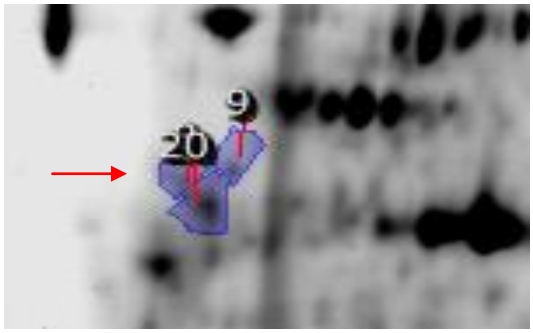

Figure 69: Spot cluster of identified vimentin protein isoforms. Spot 20 is potentially cleaved due to active caspases. The red arrow indicates spot 8 (obscured by spot 20).

It has been suggested that vimentin is associated with the phagosome membrane [73], which is in keeping with vimentin appearing in the membrane fraction of our samples, although we cannot definitively conclude it is the phagosome membrane. This association would be predicted to increase as a result of the upregulation of vimentin expression in response to *C. burnetii* infection. Several phosphorylations were demonstrated by Eriksson et al. (2004) to regulate the assembly and disassembly of vimentin fibers [347]. The separation pattern of the spots in our 2D gels suggests that spot 8 (see figure 69 above) is a full length copy that has added a phosphate. The vimentin assembly state is implicated in RhoA-binding kinase α's activation state [347], and we propose that vimentin may be regulating the cytoskeletal arrangement of the monocytes after *C. burnetii* infection. Vimentin regulation of

cytoskeletal dynamics could have implications for optimizing the cytoskeleton for autophagic vacuole delivery to the *C. burnetii* replicative vacuole, and the cellular localization of that vacuole.

Beneš, et al., (2006) showed that BM2 monocytic cells require vimentin for proliferation but not for maintaining their morphology. However, in the Beneš (2006) study, the cells were chemically induced to differentiate, whereas our cells were differentiated due to infection [344]. The situation in our cells may be more complex due to interactions between *C. burnetii* and the host cellular machinery. It was demonstrated by Beneš, et al., (2006), and by Zheng et al., (2005) that vimentin expression is upregulated by activated NF-κB. This is the likely cause of vimentin upregulation in our dataset having been stimulated by *C. burnetii* LPS and/or continued infection, although it is possible that Hsp60 could be triggering the upregulation (see below, and in the discussion for the Securinine stimulated model, for more details on Hsp60) [344,348].

In summary, we propose that the detection of upregulated vimentin in our samples has several implications. First, the upregulation of vimentin indicates that the monocytes have become activated and differentiation has been induced, possibly by the activation of NF-κB. Second, the presence of a possible vimentin cleavage product may indicate that the proposed *C. burnetii* inhibition of caspase activation [72] may not be complete. The upregulation of vimentin is proposed to increase the level of ROS present in the cells, either directly by action in the cytoplasm or as a result of

extracellular stimulation by secreted vimentin. Finally, the upregulation of vimentin may be altering the cytoskeleton of the infected cells. Further experimentation will be needed to test these hypotheses.

Aldehyde Dehydrogenase 2 (Aldh2)

We observed that Aldh2 is upregulated in the membrane fraction of 96 hr postinfection samples (see figure 70-72 and supplemental figure 2). Aldh2 catalyzes the conversion of aldehydes to carboxylic acids in mitochondria. Aldehydes can arise as a product of lipid oxidation, and Aldh2 appears to have a protective function under oxidative stress conditions, including response to reactive nitrogen species such as peroxynitrate and nitroglycerin [5,349,350] (see figures 71 and 72). Aldh2 contains a series of thiol groups that are subject to oxidation by ROS, which inactivates the protein [351]. Wenzel et al., (2007) demonstrated that Aldh2 was inhibited in a dose dependant manner by various oxidizing compounds [5]. Loss of Aldh2 results in a buildup of aldehyde species, which are potent oxidizing compounds, and have been reported to activate NADPH oxidases further increasing ROS production and ultimately increasing cell death [5].

It was demonstrated that lipoic acid, naturally abundant in mitochondria, can reduce oxidized Aldh2 back to its active state, while GSH cannot [5]. Microarray analysis of oxidative stress in *Schistosoma mansoni* demonstrated that oxidative conditions cause a large upregulation (up to 4-fold) in mRNA for Aldh2 [352], although we are

observing a much smaller protein upregulation in our samples (+1.2 fold upregulation) [343]. This observed expression difference could simply reflect a different time course of Aldh2 activation in our samples or may reflect the poor correlation between mRNA levels and protein expression levels, as noted by Griffin et al., (2002) [353]. The lower increase in Aldh2 in our samples vs. the *S. mansonii* mRNA samples may also possibly indicate that there is less oxidative stress in our samples than applied in the *S. mansonii* experiments. It was reported by Li et al., (2004) that overexpression of an Aldh2 transgene inhibited ROS induced caspase-3 mediated apoptosis [354]. Li et al., (2004) also noted a reduction in Erk1/2 activation and p38 activation in response to increased Aldh2 expression [354].

Lipoic acid provides an *in vivo* mechanism for reduction of oxidized Aldh2 thiols, to restore oxidized Aldh2's functionality [5]. A prediction that arises from our results is that oxidative stress in response to infection by *C. burnetii* could cause an increase in lipoic acid production, where lipoic acid acts in an antioxidant capacity by recycling Aldh2 to its active reduced state (see figure 71 for lipoic acid reduction mechanism). The prevalence in our dataset of changes in the expression of a number of metabolically active proteins suggests that a lipidomic and metabolomic study could prove informative.

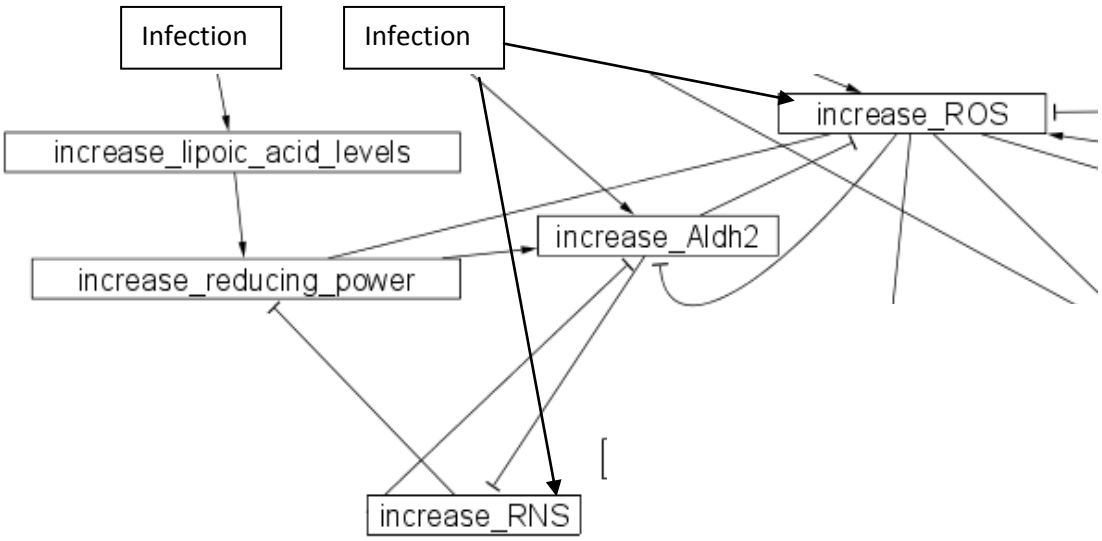

Figure 70: Proposed pathways for upregulation of Aldh2. Infection is proposed to cause both an increase in Aldh2 and lipoic acid. Lipoic acid helps to maintain Aldh2 in a reduced state, offsetting the inhibiting effects of ROS or RNS. ROS are likely to be upregulated as a response to infection, and RNS may also be upregulated.

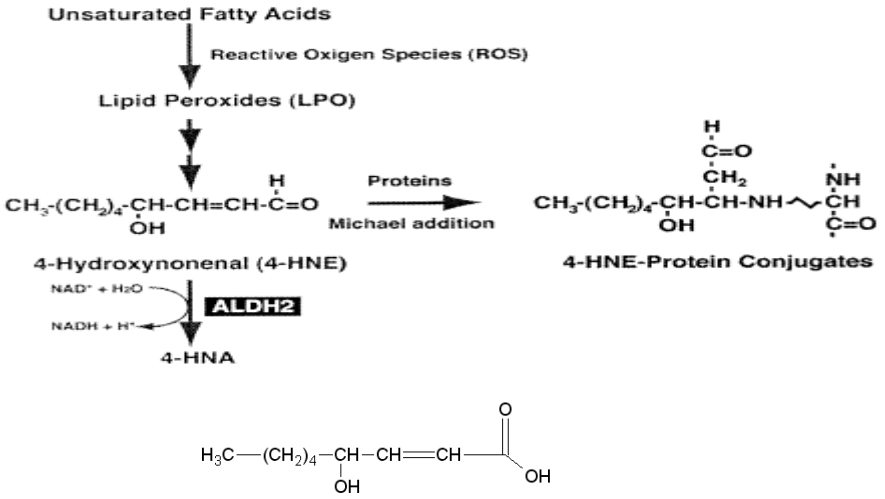

Figure 71: Example of Aldh2 removal of a harmful ROS species. In this example, ROS produce lipid peroxides and the production of aldehydes such as 4-HNE, which can damage proteins. Aldh2 reduces 4-HNE to 4-HNA (4-hydroxy-nonenoic acid), preventing protein damage. Figure adapted from [3].

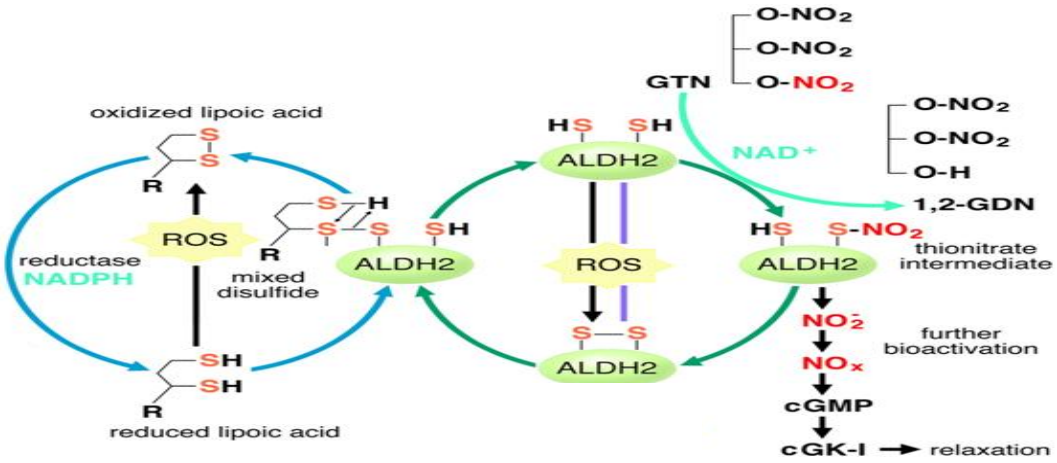

Figure 72: Aldh2 reduction of reactive nitrogen species and regeneration by lipoic acid. Aldh2 can act on RNS [such as nitroglycerine (GTN)] to produce free nitric oxide (NO_X) and oxidized Aldh2. Lipoic acid regenerates reduced Aldh2. ROS can inhibit both Aldh2 and regernation of reduced Aldh2. Adapted from [5]. 1,2-GDN = 1,2 glyceryl dinitrate.

In our *C. burnetii* infected samples Aldh2 is mildly upregulated and is proposed to be acting in an antioxidant capacity to protect the *C. burnetii* infected monocyte from products of ROS and RNS, arising as a result of infection. Of particular interest to this scenario is the proposal that lipoic acid may be upregulated to help maintain Aldh2 in an active, reduced state to enable the continuation of Aldh2's antioxidant functions. Monitoring and perturbing the GSH and lipoic acid levels in a cell in response to *C. burnetii* infection could prove informative.

S100 Ca^{2+} Binding Proteins A8/9 (S100A8/9)

S100A8 and A9 are strongly upregulated in the soluble fraction of 96 hr postinfection samples (see figure 73 and supplemental figure 2). These proteins are expressed in innate immune cells, including monocytes as either homo- or heterodimers [355], and serve as markers for macrophage differentiation [356]. Dimerization of S100A8/9 appears to be required for proper functioning, whether a homo- or heterodimer [357]. When functioning as a heterodimer, S100A8/9 has antimicrobial properties by chelating Zn^{2+}, inhibiting both bacterial adhesion to mucosal epithelium, and bacterial growth [355]. S100A8/9 complexes can appear at the cell surface shortly after leukocyte activation [357]. It was recently reported that S100A8/9 activity is required for recruitment/accumulation of monocytes/macrophages and neutrophils in *Streptococcal* infected lung tissue, suggesting a role in chemotaxis [355,358]. Raquil et al. (2008) reported that blockade of S100A8/9 strongly decreases recruitment of immune cells to the site of infection [355].

S100A8/9 is upregulated by 2.5-4 fold in our samples at 96 hrs p.i., suggesting a strong response by the monocytes to differentiate/mature in response to *C. burnetii* infection. We suggest that the presence of S100A8/9 indicates that the monocytes have detected and are responding to *C. burnetii* infection by differentiating into mature macrophages. These proteins may also be getting secreted to recruit more macrophages, but we currently have no evidence of this, as the secretome was not tested in our analysis.

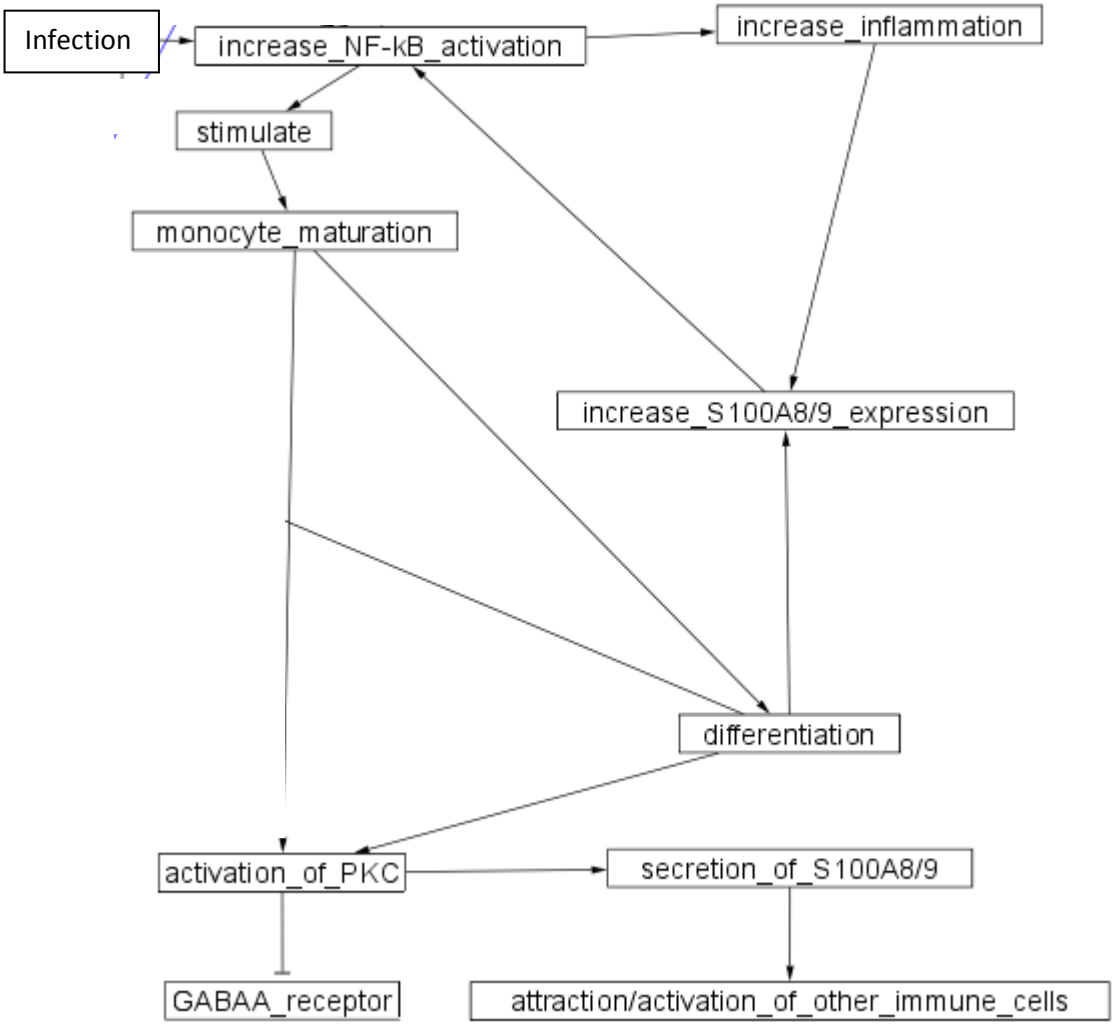

Figure 73: Schematic of S100A8/9 actions and relationships. It is proposed that monocyte maturation, stimulated by NF-κB activation leads to differentiation an increase in S100A8/9 expression, is predicted to cause an increase in NF-κB activation in a possible feed-forward mechanism. S100A8/9 upregulation is predicted to also lead to an increase in PKC activation which is predicted to cause an increase in S100A8/9 secretion to attract/activate immune cells. See supplemental figure 2 for more details.

It has been reported that secretion of S100A8/9 occurs in activated macrophages, consistent with the proteins being exported to signal the site of infection to other innate immune cells [355,356,359]. Secretion of S100A8/9 appears to occur following activation of protein kinase C (PKC) [356]. PKC activation is also followed by an increase in integrin affinity, which may increase monocyte recruitment [356]. In monocytes, elevated S100A8/9 increases NF-κB activation and therefore increases inflammation [355].

Recently it was shown by SAGE analysis that S100A8/9 mRNA is upregulated in squamous cell carcinomas, as well as other inflammatory conditions [358]. Wounds cause a rapid increase in S100A8/9 expression, before the appearance of inflammation, suggesting multiple pathways for activation of S100A8/9 [359]. The disappearance of S100A8/9 over time following wounding supports the idea that these are early acting proteins, and not part of a prolonged response [359].

The finding that S100A8/9 mRNA are upregulated during inflammation (both A8 and A9) or UV exposure (A9) [358] has implications for our model. The inflammation is of importance to our case, as it suggests that an increase in inflammation caused by the monocytes responding to *C. burnetii* infection may be the cause of the upregulation of S100A8/9. In other words, markers of inflammation secreted by infected monocytes can trigger cell surface receptors that help shape the monocyte response to infection. Also of note is the activation of PKC with respect to S100A8/9. When PKC is active, S100A8/9 is secreted [356]. We did not determine changes in S100A8/9 levels in the

secretome, but a significant upregulation of S100A8/9 following infection would suggest that PKC has become activated. When PKC is activated, the β-subunits of $GABA_A$ receptors are susceptible to phosphorylation, causing them to become inactivated [360]. It is possible that under normal circumstances, activated $GABA_A$ receptors cause an inhibition of S100A8/9 secretion as well as inhibiting differentiation of monocytes into macrophages. The observation that PKC activation is followed by secretion of S100A8/9 suggests that activation of PKC in our system, in response to infection, may cause phosphorylation of $GABA_A$ receptors, inactivating them, and subsequently releasing S100A8/9 from $GABA_A$ receptor inhibition. Inhibition of $GABA_A$ receptors could prove important in treating monocyte infections by certain organisms (e.g. as suggested by treatment with Securinine), and suggests that inactivation of $GABA_A$ receptors either by PKC phosphorylation and/or direct inactivation by antagonists (e.g. Securinine), may in fact be able to increase cell killing of *C. burnetii,* or other organisms in monocytes.

We hypothesize that in our samples, S100A8/9 upregulation indicates that the monocytes have begun to differentiate, and that the microbicidal properties of the S100A8/9 heterodimer are active. We further hypothesize that secretion of S100A8/9 may be regulated by the activation status of the monocyte GABAA receptors. The fact that we did not observe upregulation of S100A8/9 in Securinine stimulated samples could indicate that either Securinine influence on maturation/differentiation is not sufficient to stimulate S100A8/9 expression and/or Securinine stimulated monocytes

have differentiated beyond the point where S100A8/9 are upregulated. The finding that expression of S100A9 alone increases parasite load may simply apply to *Leishmania* infections. Further work will be needed to determine whether or not this phenomenon is applicable to *C. burnetii* infection. Recall that S100A8/9 are believed to be early acting proteins [359], and more mature macrophages may not display a significant upregulation of these proteins.

Rab7 GTP

We observe changes in two isoforms of Rab7 in the membrane fraction of 96 hr infected samples (see figure 74 and supplemental figure 2). The changes in two isoforms, one upregulated ~2-fold and one downregulated ~2-fold is suggestive, although not conclusive, that the GDP form has been downregulated, and the GTP form upregulated by a similar amount. Other posttranslational modifications could also account for the observed pattern in the 2D gel data.

The Rab7 protein is involved in maturation of phagosomes between the early maturation mediated by Rab5, and development into a fully mature phagolysosome, as determined by the presence of LAMP1/2 proteins and hydrolase delivery [361-363]. Rab7 appears as earlier endosomal markers, Rab5 and EEA1, are being downregulated from the maturing phagosome. The reduction in Rab5 and EEA1, as well as the appearance of Rab7, signals exit from the early/recycling endosomal stage and entry into the phagolysosomal maturation process. It is during this time that the maturing

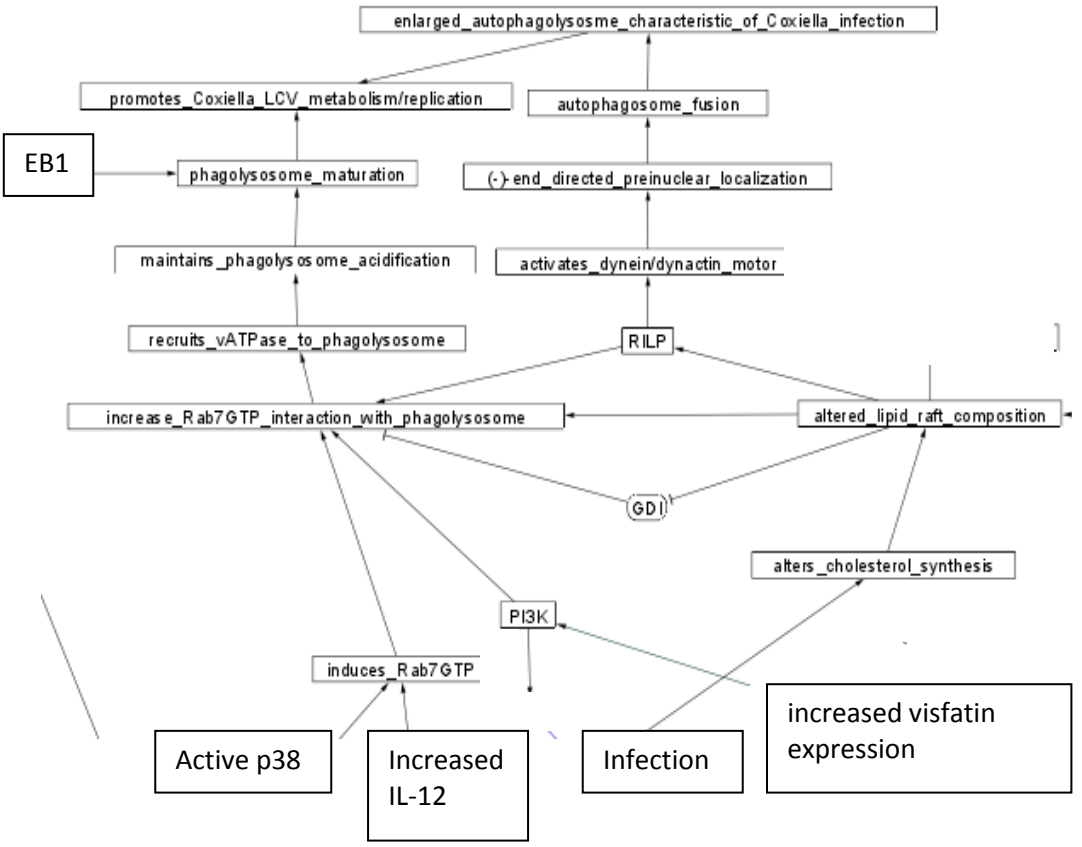

Figure 74: Summary of proposed functions related to changes in Rab7 expression during *C. burnetii* infection. We are hypothesizing that Rab7GTP is activated by *C. burnetii* infection, through several possible mechanisms including alterations to lipid raft composition, alterations to RILP and GDI function, activated p38, increased PI3K activity, and increases to IL-12 expression. Upregulation of Rab7GTP will have the effect of maintaining vATPase recruitment to the phagolysosome, and could contribute to the enlarged phagolysosome characteristic of *C. burnetii* infection. See supplemental figure 2 for more details.

phagosome goes from a pH of ~6 to ~5.5, on the way to the final phagolysosomal pH of ~4.5 [361-363]. The normal timeframe on this portion of maturation is <30 minutes varying with type of cell and ingested particle(s) [361-363]. Also, this point in the

phagosome maturation pathway represents a convergence between phagosome maturation and autophagosome delivery to the lysosome [364].

The Rab proteins are cycled on and off of the membrane by repeated cycles of binding and hydrolysis of GTP mediated by the protein GDI. It has been reported that Rab7GTP increases the size of phagolysosomes, as demonstrated by effects of the constitutively active Rab7GTP analog Rab7Q67L [296]. Phagosome maturation is normally accompanied by hydrolase delivery to the phagosome [73]. We failed to identify increases in the expression of in any hydrolases. In addition, hydrolases could have localized to the soluble fraction samples (following leakage from the phagolysosome during lysis), and may have simply been obscured by the more abundant soluble fraction proteins.

SNARE proteins are involved in the phagosome maturation process, but they can be somewhat promiscuous, being involved with several other cellular processes, making their functions difficult to definitively elucidate [361-363,365,366]. Results by Bucci et al., (2000) suggest that the presence of Rab7GTP directly controls close contact and aggregation of late endosomes during phagosome maturation, and they further propose that fusion of the membranes is mediated by various SNARE proteins, in a manner facilitated by Rab7GTP [296]. The spectrin family of proteins are believed to be involved in the perinuclear localization of mature phagolysosomes by bridging the Rab-interacting lysosomal protein (RILP) N-terminus

and the dynein/dynactin machinery [367]. Rab7 expression is clearly involved in the perinuclear localization of matured phagolysosomes, as demonstrated by Bucci, et al., (2000) [296]. Based on the localization of Rab7 in our samples, the predicted behavior of Rab7 in our system and the spot pattern observed in our gels, we suggest that it is the GTP form we are observing in spot 10 (+2.3-fold upregulated) and the GDP form in spot 18 (-2-fold downregulated). We note that there could be alternative explanations for our observations such as that spot 10 has a posttranslational modification that we are not detecting. It is also possible that the observed downregulation of spot 18 is due, not to a change in expression, but rather to a relocalization to the soluble fraction. The relatively low abundance of Rab7 when enriched in the membrane fraction would make it difficult for the protein to be found in the soluble fraction where membrane proteins often are not detected. These hypotheses will require further testing.

Rab7GTP, but not Rab7GDP, interacts with the C-terminus of RILP, which helps to lock Rab7 in the GTP-bound state [367,368]. Rab7GTP actively recruits RILP to the maturing phagosomal membrane, presumably late in maturation, as RILP colocalizes with LAMP1/2 proteins and Cathepsin D [368]. RILP stabilization of Rab7GTP [369] has implications for maintenance of vATPase expression and stimulation of acidification of the *C. burnetii* replicative vacuole. RILP stabilization of Rab7GTP could be important in maintaining vATPase recruitment and thus maintenance of the optimal pH for *C. burnetii* metabolism/replication.

The observation that loss of RILP will cause dispersal of lysosomes, even in the presence of constitutively active Rab7 (GTP form) [368], suggests that RILP is present and active in our samples, even though no change in RILP expression was observed in our samples. *C. burnetii* is predicted to be maintaining an interaction between Rab7GTP and RILP, or else the large replicative vacuole could not form or be maintained. The reported observations by Cantalupo et al., (2001) make no mention of the ratio of Rab7GTP:RILP necessary to maintain aggregation [368]. Targeted quantitation of RILP (e.g. by Western blot) in addition to experimental observation of the localization of Rab7GTP vacuoles and potential associated microtubule dynamics/motors over the course of *C. burnetii* infection would be required to elucidate the mechanism(s) involved in RILP/Rab7 interaction in *C. burnetii* infection.

The above discussion suggests that targeting the Rab7-RILP interaction in *C. burnetii* infected phagolysosomes/replicative vacuoles might be an effective form of treatment to at least slow the progression of the infection and allow adaptive immunity and/or an antibiotic or other treatment to clear/kill the bacterium. Disrupting the Rab7GTP-RILP interaction would be predicted to a) cause fission of the *C. burnetii* replicative vacuole, potentially increasing the concentration and therefore relative effect of hydrolases (in phase II, and possibly Crazy strain only as described by [27]), b) potentially cause the loss of vATPase, inhibiting the maintenance of the low pH necessary for *C. burnetii* replication/metabolism and c) disrupting the cholesterol accumulation, preventing lipid raft alteration.

The acquisition of vacuolar ATPase (vATPase), the protein responsible for acidification of the maturing phagolysosome, has been reported to be mediated by Rab7GTP [296]. In the study by Bucci et al., (2000), phagosomes overexpressing a DN-Rab7 construct (locked in the GDP form), showed a reduced phagolysosome acidification [296]. *C. burnetii* is an acidophile, requiring an acidic environment for at least some transport/synthesis of amino acids, nucleic acids, and proteins [332,370,371] and thus maintaining a functional vATPase at the phagolysosomal membrane, sufficient for maintaining lumenal pH levels.

Elevating Rab7GTP levels could be a means to enhance vATPase recruitment for metabolic and replicative purposes by *C. burnetii*. *Parachlamydia acanthamoebae* also requires a slightly acidic replicative environment, but regulates acquisition of vATPase to maintain a less acidic phagolysosomal lumen than fully mature lysosomes [372]. Controlling the rates of Rab7 GTP/GDP exchange appears to be a bacterial target for controlling the rates of vATPase acquisition. Alteration of Rab7GTP's function by *C. burnetii* appears to require bacterial protein synthesis, since exposure of *C. burnetii* infected cells to chloramphenicol (bacterial protein synthesis inhibitor), prevented formation of large *C. burnetii* replicative vacuoles [373]. This is likely due to a reduction in the ability of C. burnetii to upregulate the cholesterol generating machinery of the host cell which will indirectly impair Rab7GTP recruitment to the phagolysosomal membrane (detailed below).

It has been reported that lipid rafts or lipid raft-like domains are present not only at the cell membrane but also in internal membranes, including the ER, and the phagosome [374]. Li et al., (2003) observed that monocytes express flotillins in a lipid raft-like manner, and further that monocyte lipid rafts are similar in composition to those of T cells [374]. The results of Li et al., (2003) also suggest that both Rab7 and vATPase are lipid raft bound [374]. Rab7 binding to the phagolysosomal membrane has been shown to be sensitive to the cholesterol composition of the phagosome membrane, further supporting a lipid raft localization [341]. Specifically, when the cholesterol content of the phagosomal membrane increases, Rab7GTP recruitment increases [341]. This would make the composition of the lipid rafts an attractive target for *C. burnetii* modulation of Rab7 and vATPase expression, as detailed below.

Specifically, controlling the composition of lipid rafts in order to enhance the recruitment of Rab7GTP and thus vATPase, while at the same time impairing hydrolase delivery (see [27] for details of impaired hydrolase delivery), could be a means for *C. burnetii* to alter the monocyte phagolysosome to enhance bacterial replication. We suggest that *C. burnetii* is altering the monocyte phagolysosomal lipid raft composition to increase Rab7GTP recruitment and thus vATPase recruitment as well as to interfere with hydrolase delivery (see figure 75). Thus we predict that determining the alterations to lipid raft composition that is associated with *C. burnetii* infection could be informative.

Lebrand et al, (2002) reported that cholesterol can contribute to the regulation of Rab7 cycling [341]. Cholesterol accumulation in phagosomes was reported to selectively interfere with GDI, and that interference with GDI cycling reduced Rab7GDP and increased Rab7GTP [341]. *C. burnetii* infection has been shown to alter gene expression of key enzymes in the cholesterol biosynthesis pathway [375], although we point out that mRNA levels and corresponding protein levels are often not well correlated [353]. Furthermore, inhibition of cholesterol synthesis by statins inhibits *C. burnetii* replication [375], suggesting that it is necessary to produce new cholesterol

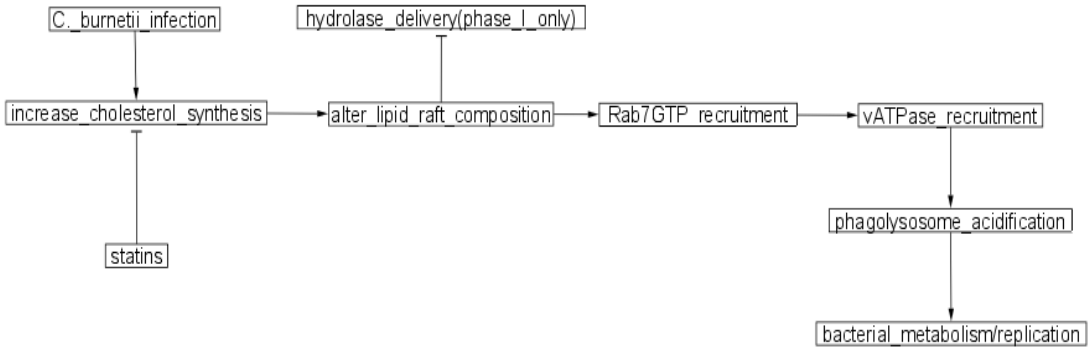

Figure 75: Model of proposed effects of lipid raft alteration by *C. burnetii* infection. *C. burnetii* increases cholesterol synthesis which will alter lipid raft composition. Altered lipid rafts will have the effect of increasing Rab7GTP recruitment, which will increase vATPase recruitment maintaining phagolysosomal acidification and thus promoting bacterial metabolism and replication. Altered lipid rafts are proposed to be the mechanism behind the reported impairment of hydrolase delivery in phase I (but not phase II) *C. burnetii* infections. Statins will inhibit the increase in cholesterol synthesis, and ultimately inhibit bacterial replication.

rather than simply redistribute it [376]. On the other hand, there is evidence that statins' primary benefit may be inhibition of NADPH oxidase due to inhibition of geranylgeranyl anchoring to the membrane [377,378], which would lower ROS production. A lower ROS response would benefit *C. burnetii* by reducing the ROS response to infection by the monocytes, and thus the inhibition of cholesterol formation, and not inhibition of NADPH oxidase is likely to be the major benefit to statin treatment of *C. burnetii* infections.

A model suggesting alterations to the lipid raft composition similar to our model was proposed by Voth and Heinzen (2007) where they suggest that *C. burnetii* replicative vacuoles see an increase in both flotillin protein (lipid raft marker) and Rab7 expression. It is likely that loss of cholesterol would alter the lipid raft composition, such that Rab7 is no longer locked into the GTP form, meaning that the vATPase recruitment would also be reduced. Reduction of vATPase recruitment would raise the pH of the *C. burnetii*-containing vacuole, inhibiting metabolism and replication. Alkalinization of the phagolysosome to a pH of ~6 was shown to reduce bacterial viability [332,371]. *C. burneti*i's secretion systems may be involved in regulating Rab5 and Rab7 proteins [376,379].

Rab7 is involved in the development of autophagic vacuoles in a manner analogous to phagosome maturation [297]. The convergence of phagosome maturation and autophagosome delivery of various cellular components strongly suggests the reason that *C. burnetii* inhabits this particular niche. Our Rab7 expression data and the

literature suggest that *C. burnetii* inhabits an autophagolysosome composed of autophagic vacuoles fused with a matured phagolysosome. The maturation of the phagosome to a phagolysosome is necessary to generate and maintain the acidification that is required by *C. burnetii* for metabolism and replication, as well as expression of the LAMP 1/2 proteins required by autophagic vacuoles for delivery to the lysosomes [297,380]. In addition, autophagic fusion delivers necessary nutrients, particularly peptides and amino acids which *C. burnetii* cannot make [17]. Simply put, *C. burnetii* may accelerate the formation of an autophagolysosome early in its maturation process to lay the groundwork for metabolic and replicative functions. It was reported by Vitelli et al., (1997) that constitutive expression of Rab7GTP causes an increase in the size of phagolysosomes, and that the reported increase in size of the phagolysosome due to the presence of Rab7GTP, could simply be due to an increase in Rab7GTP-medicated autophagosome delivery [296,381]. This suggests a mechanism by which *C. burnetii* replicative vacuoles (mature phagolysosomes) are able to grow to such large sizes.

We expected that with phase II *C. burnetii*, we would see an increase in hydrolase delivery [27,371]. We did not observe evidence for such delivery but the hydrolases would be predicted to partition to the soluble fraction, and could simply be too dilute to detect in the soluble fraction. It is possible that the bacterium may be causing a slower timetable of hydrolase delivery to the phagolysosome, which would also lower apparent hydrolase abundance. In the case of lipid raft alteration, we predict that phase II *C. burnetii* is altering the lipid raft composition to a different extent than

phase I strains. Phase II *C. burnetii* does not inhibit delivery of hydrolases, where phase I does inhibit hydrolase delivery [27].

It was recently reported that IL-12 can stimulate an increase in Rab7GTP expression in a dose dependant manner, although we cannot confirm the presence of the GTP form of Rab7 in our samples [382]. It would be useful to determine the levels of IL-12 in our samples as this may give an indication as which form of Rab7 is likely to be present. If we see an increase in IL-12 expression following infection, that may indicate that the Rab7GTP form is upregulated. In a study by Bhattacharya et al., (2006) [382] it was reported that inhibition of p38 MAPK prevented IL-12 induction of Rab7 expression. *C. burnetii* downregulates p38 activation [72], but could act downstream of p38 to help increase Rab7GTP accumulation.

IL-12 expression induces phosphorylation of p38 [382], but p38 phosphorylation returns to baseline shortly after *C. burnetii* infection [72], further suggesting that multiple regulatory pathways are being regulated by *C. burnetii* to maintain infection. As indicated below in the section on samples from 96 hrs postinfection +/- Securinine, Securinine+infection resulted in increased cell death. The mechanism is likely due to Ca^{2+}-mediated, caspase-independent apoptosis. In light of these findings, we suggest that in the presence of infection, which should stimulate NF-κB, and Securinine, which appears to be stimulating p38, that sufficiently high levels of Securinine can push an infected cell towards apoptosis, overriding or at least overwhelming *C. burnetii*'s activation of Erk1/2 which would prevent apoptosis [72]. Ghigo, et al., (2004) also noted

that IL-10 is involved in regulation of hydrolase delivery to the phagolysosome [27]. In light of these findings, we suggest that monitoring levels of various cytokines/chemokines both *in vivo* and in the extracellular matrix would be informative to better understand the regulatory roles of various inflammation markers in *C. burnetii* infection. A better understanding of the inflammation markers as influenced by Securinine stimulation could be informative as to the means by which Securinine controls *C. burnetii* infection.

It seems clear from the literature that one survival strategy for intracellular pathogens is to alter the time course of Rab protein expression. *Leishmania donovani* has been shown to inhibit phagosome acquisition of Rab7 [383], and a similar strategy seems to be employed by *Salmonella typhimurium* [384]. We predict that locking Rab7GTP to the phagolysosome is important for *C. burnetii* maturation and survival. The exact mechanism used by *C. burnetii* to lock in Rab7GTP has yet to be determined. Evidence from the literature suggests that intracellular pathogens such as *Leishmania*, *Salmonella*, *Legionella*, and *Mycobacteria* are adept at modifying the phagosome to suit their particular metabolic/replicative needs [366]. The plethora of phagosomal proteins identified by Garin et al., (2001) [73] suggests that there are ample protein targets, in addition to the lipid raft composition, for *C. burnetii* to regulate phagolysosomal composition.

One final possibility to explain the alteration of Rab7 in our samples is the recent report describing Rab7b [298]. Yang et al., (2004) reported that Rab7b is a lysosomal

protein ~68% homologous to Rab7 and is expressed only in differentiating monocytes, possibly acting as a maturation marker [298]. Rab7b was further characterized to be a negative regulator of TLR4-induced cytokine activation, and expression of Rab7b downregulated activation of Erk 1/2 [385]. Bioinformatics analysis, however, does not support the presence of Rab7b in our samples, and furthermore, the functions of Rab7 described above and the behavior of *C. burnetii* replicative vacuoles, also suggest it is unlikely that Rab7b is being observed here.

Overall, we propose the following hypotheses to explain the changes in Rab7 in our samples. Recall that Rab7 is present in our sample in two proteins spots, one upregulated and one downregulated, in a manner suggesting the possibility that Rab7GDP is downregulated in the membrane fraction and Rab7GTP is upregulated in the membrane fraction. This could be due to an actual change in expression of the two isoforms or a redistribution between the soluble and membrane fractions. Secondly, maintaining Rab7 in the GTP form would seem to be essential to *C. burnetii* metabolic and replicative activities, particularly the delivery of autophagic vacuoles (presumably containing essential nutrients) and maintenance of the low pH necessary for *C. burnetii* LCV activities.

The *C. burnetii* replicative vacuole is most commonly referred to as a phagolysosome. However, the necessity of autophagic delivery to the *C. burnetii* replicative vacuole suggest that the nature of the replicative vacuole makes it more properly an autophagolysosome. It is likely that *C. burnetii* is employing some

mechanism to maintain Rab7GTP at the autophagolysosomal membrane and perhaps the most attractive hypothesis is that *C. burnetii* is directly regulating the composition of lipid rafts via upregulation of host cell cholesterol synthesis. Given that statins have been shown to inhibit *C. burnetii* infection [375,376], an interesting experiment to perform would be to monitor the response of *C. burnetii* infected monocytes to statins + Securinine or other adjuvants. Given that Securinine and statins can increase resistance to *C. burnetii* infection, it follows that the combination of the two may be synergistic and this could suggest new avenues of treatment for Q fever.

Leucine Aminopeptidase 3 (Lap3)

We observe Lap3 being upregulated in the soluble fraction at 96 hrs postinfection (see figure 76 and supplemental figure 2). Lap3 was originally characterized in yeast for its ability to detoxify bleomycin [386], but has recently begun to attract further interest. Lap3 was originally identified as both bleomycin hydrolase (Blh1), and Gal6 [329,387] and Lap3 has been shown to possess cysteine protease activity [386,388,389].

It was observed by Kagayama, et al., (2009) that under conditions of nitrogen starvation, Lap3 is specifically targeted to autophagosomes to be degraded [388]. This suggests that at 96 hours postinfection, the infected monocytes may have entered nitrogen starvation causing Lap3 phagosome [73]. We failed to identify increases in the expression of in any hydrolases. In addition, hydrolases could have localized to the

soluble fraction samples (following leakage from the phagolysosome during lysis), and may have simply been obscured by the more abundant soluble fraction proteins.

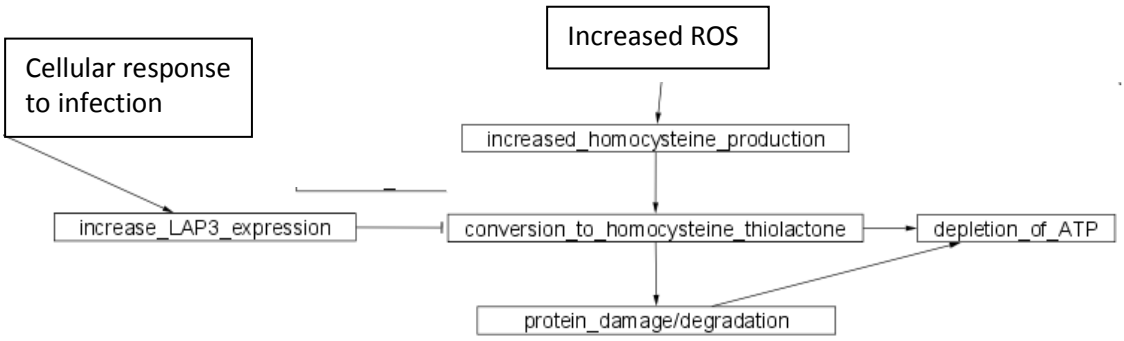

Figure 76: Summary of proposed Lap3 protection against homocysteine thiolactone. Lap3 is upregulated in response to infection by *C. burnetii*. Lap3 protects against ROS induced damage by preventing the formation of homocysteine thiolactone that tend to follow the ROS-induced elevation of homocysteine production. The Lap3-mediated inhibition of homocysteine thiolactone conversion is predicted to prevent depletion of ATP and also prevent damage to proteins by homocysteine thiolactone addition.

SNARE proteins are involved in the phagosome maturation process, but they can be somewhat promiscuous, being involved with several other cellular processes, making their functions difficult to definitively elucidate [361-363,365,366]. Results by Bucci et al., (2000) suggest that the presence of Rab7GTP directly controls close contact and aggregation of late endosomes during phagosome maturation, and they further propose that fusion of the membranes is mediated by various SNARE proteins, in a

manner facilitated by Rab7GTP [296]. The spectrin family of proteins are believed to be involved in the perinuclear localization of mature phagolysosomes by bridging the Rab-interacting lysosomal protein (RILP) N-terminus to have been localized to the autophagolysosome. The nitrogen availability in our samples is not known. However, if Lap3 were being targeted to autophagolysosomes as a result of nitrogen starvation, we would expect Lap3 expression to decrease. As such our data do not specifically indicate that Lap3 is being targeted to the autophagosome, although future experiments including subcellular fractionation would shed light on this.

A more likely possibility for Lap3 upregulation in our samples relates to the activation of monocytes. Activated monocytes produce ROS and have been shown to also produce homocysteine [390-392], a byproduct of methionine degradation [392,393]. Homocysteine production appears to be at least partially regulated by the NF-κB pathway, most likely via modulation of cytokine levels [392]. Homocysteine in high concentrations is toxic to cells, possibly through conversion of homocysteine to homocysteine thiolactone which can occur under cellular conditions [394]. The thiolactone conformation appears to detrimental due to 1) homocysteine thiolactone takes ATP to generate, needlessly dissipating energy reserves, 2) the thiolactone binds to the ϵ-amino group of lysines forming damaged proteins that 3) require further ATP/cellular resources to degrade via the unfolded protein response [387].

It should be noted that the exact mechanisms of homocysteine toxicity are incompletely understood, but have been observed to cause connective tissue and

vascular damage [394]. It was recently observed that Lap3 has a protective role under conditions of elevated homocysteine levels, apparently by hydrolysing homocysteine thiolactones [387]. We propose that elevated Lap3 levels in our infected samples are in fact a cellular response to elevated ROS production in activated monocytes responding to *C. burnetii* infection. Metabolomic studies to monitor homocysteine levels and other thiol metabolites, after infection with *C. burnetii* would be informative here, and monitoring metabolite levels following Securinine stimulation may also be enlightening.

Visfatin

Visfatin was observed to be upregulated in the soluble fraction at 96 hrs postinfection (see figure 77 and supplemental figure 2). Visfatin (a.k.a. pre-B cell colony enhancing factor a.k.a. nicotinamide phosphoribosyltransferase, a.k.a. NAMPT), is a highly conserved cytokine to which numerous functions have been ascribed in a variety of cells. Visfatin has been shown to be upregulated by various inflammatory markers e.g. IL-6, IL-8, LPS, and to be secreted by various cells during infection, including monocytes, lymphocytes and neutrophils but also amniotic epithelial cells, microvascular endothelium, and adipocytes [395-399]. Although bacteria do contain a homolog, bioinformatics searches indicate that the visfatin in our samples is of human origin.

Adya et al., (2009) have recently demonstrated that human endothelial cells upregulate mRNA expression for monocyte chemoattractant protein 1 (MCP1) in response to visfatin exposure in a dose-dependent manner [395]. Adya et al., (2009)

also demonstrated that activated PI_3K and NF-κB pathways are involved and necessary for MCP1 mRNA upregulation [395]. PI_3K is also involved in phagosome maturation and autophagic vacuole maturation [361,362,400,401], suggesting a possible interaction between the autophagolysosomal maturation, and the downstream effects of visfatin. PI_3K can also activate the Akt pathway [395] which is known to be involved in *C. burnetii*'s inhibition of apoptosis in infected monocytes [72].

In neutrophils, a cell type that is constitutively apoptotic and where apoptosis can be inhibited by LPS activation of TLRs, loss of visfatin expression abrogates LPS-induced inhibition of apoptosis [397]. Jia et al., (2004) further demonstrated that visfatin expression alone is sufficient to inhibit apoptosis in unstimulated neutrophils, that visfatin is secreted and its inhibition of apoptosis is at least partially due to its actions as a cytokine [397]. The antiapoptotic activities of visfatin were shown to be due to inhibition of caspase 3 and 8 activity, at least in part [397].

Visfatin mRNA expression levels can be modulated by several cellular factors. It was recently shown that blocking the nuclear translocation of activated NF-κB by the SN-50 inhibitor, caused a modest downregulation of visfatin mRNA in both WISH cells and primary amniotic epithelial cells [398]. In the same study, the general nuclear translocation blocker curcumin caused visfatin mRNA levels to drop below baseline [398]. Although mRNA and protein expression levels have notoriously poor correlations [353,402], the experiments of Kendal and Bryant-Greenwood (2007) do nonetheless

suggest that inflammation markers may in fact regulate the expression of visfatin and/or control its secretion [398].

In keeping with its proposed role as a cytokine and immunomodulator, visfatin has been shown to increase the expression of IL-1β, IL-1Ra, IL-6, IL-10, and TNFα, in a dose-dependent manner when incubated with isolated human peripheral blood monocytes [399,403]. Visfatin also stimulated secretion of IL-1β, IL-6, and TNFα dose-dependently in CD-14+ monocytes [399]. Visfatin upregulated monocyte cell surface expression of CD54, CD40 and CD80 in a study by Moschen et al, (2007) [399]. CD14+ monocytes, stimulated by visfatin and fixed with glutaraldehyde, have a stimulatory effect on T cell responses. p38 is of central importance here as inhibition of p38 resulted in near total loss of visfatin stimulatory effects and further demonstrated that visfatin can upregulate activity of NF-κB [399].

In the Moschen (2007) study, it was demonstrated that visfatin stimulation increases chemotaxis of CD14+ monocytes and CD19+ B cells in a dose-dependent manner [399]. These results further implicate visfatin in the inflammatory response to infection and in the recruitment of other immune cells. This extends the work of Kendal and Bryant-Greenwood (2007) and indicates that various cellular signals can modulate visfatin's expression and/or effects [398]. This was also observed by Brentano et al., (2007), who noted that IL-1β, TNFα, LPS and visfatin itself can stimulate expression of visfatin, and further noted that visfatin activates NF-κB and AP-1, which maintain inflammation, indicating a feed-forward mechanism [403].

Many of the proteins differentially expressed in our infected samples display connections to cellular energy metabolism, and visfatin is no exception. Visfatin is

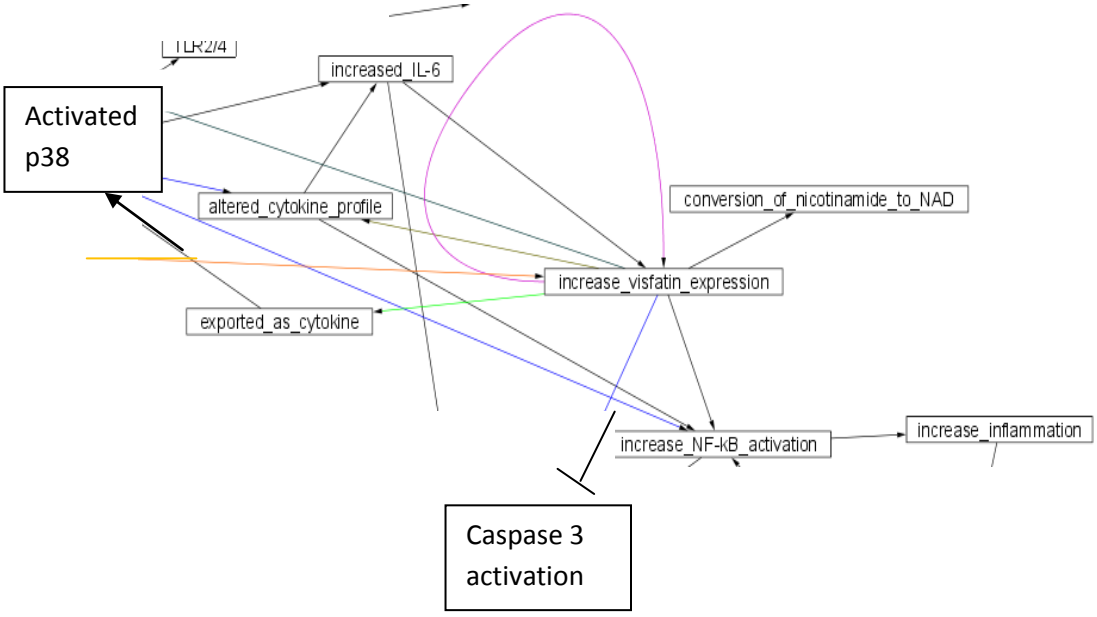

Figure 77: Summary of proposed visfatin interactions within *C. burnetii* infected monocytes at 96 hrs postinfection. Various effectors such as activated p38 and IL-6 can upregulate visfatin expression, and visfatin itself can also stimulate its own expression. Upregulated visfatin has a variety of downstream effects, including inhibition of caspase 3 activation, increased conversion of nicotinamide to NAD, and increasing NF-κB activation. Visfatin can also be exported as a cytokine to act in the extracellular environment.

involved in catalyzing the conversion of nictotinamide to NAD, an important electron carrier in metabolic reactions [396]. The inhibition of visfatin was shown to reduce the intracellular availability of NAD and reduced cytokine secretion of TNFα, as well as other

proinflammatory cytokines (e.g. IL-6) in a dose-dependent manner [396]. Busso et al., (2008) demonstrated these effects *in vivo* in mice, *in vitro* in mouse peritoneal cells and in isolated human peripheral blood monocytes [396]. These results further underscore the desirability of metabolomic studies in our system, in addition to characterization of the secretome. Visfatin appears to be involved in a general response to pathological conditions and the interactions between visfatin and its effectors may drive a feed-forward protective mechanism, that could later be modulated/downregulated or could lead to a chronic inflammatory state. Visfatin upregulation appears to be part of the monocyte response to infection, and activation of NF-κB, stimulated by the monocyte response to *C. burnetii* LPS (via TLR activation), may be involved.

The dose-dependent nature of visfatin expression as demonstrated by Moschen et al., (2007) suggests an interesting possibility regarding *C. burnetii* infections [399]. Phase I *C. burnetii* infections are much more difficult to clear than phase II infections, and it would be interesting to examine changes in visfatin expression in phase I infected monocytes, as it may be reduced in expression compared to phase II visfatin levels. Specifically, reduced levels of visfatin will reduce the secretion of inflammatory markers and activation of other immune cells, potentially resulting in a reduced immune response. We propose that the upregulation of visfatin in our samples indicates maturation by the monocytes, and alterations to the inflammatory profile which could activate other immune cells (e.g. neutrophils, lymphocytes, etc.) if those cells were

present. Our results further suggest that global analysis of the secretome from *C. burnetii* infected monocytes would be informative.

Transaldolase

We observed an upregulation of transaldolase in the soluble fraction of *C. burnetii* infected samples at 96 hrs postinfection (see figures 78, 79 and supplemental figure 2). Transaldolase is a key enzyme in the nonoxidative portion of the pentose phosphate pathway (PPP) [404,405]. It has been proposed that transaldolase is the rate limiting step for nonoxidative portion of PPP [404,406] and determines the rate of NADPH production needed for GSH reduction. The oxidative portion of PPP produces NADPH, the sole source of reducing power for glutathione (GSH) and thus the PPP is important for host defense against oxidative stress, and inflammation, among other functions [404-408]. GSH is a reactive oxygen scavenger, and maintaining GSH in a largely reduced state is critical for control of ROS production during aerobic metabolism or during enhanced ROS production. Transaldolase in conjunction with transketolase has been shown to contribute to regulation of the PPP via recycling of glucose-6-phosphate (see figure 78) [408] and also regulate mitochondrial transmemebrane potential ($\Delta\gamma_m$) through NADH/NAD^+ and NADPH/$NADP^+$ equilibria [404,406-408]. Upregulation of transalsolase has been shown to increase the $\Delta\gamma_m$, an event which precedes induction of apoptosis [409].

Loss of transaldolase activity in a diseased state can also have implications for NADPH levels, and loss of transaldolase was shown to have similar effects on glucose-6-phosphate and NADPH levels [408]. This is likely due to a reduced flux through the

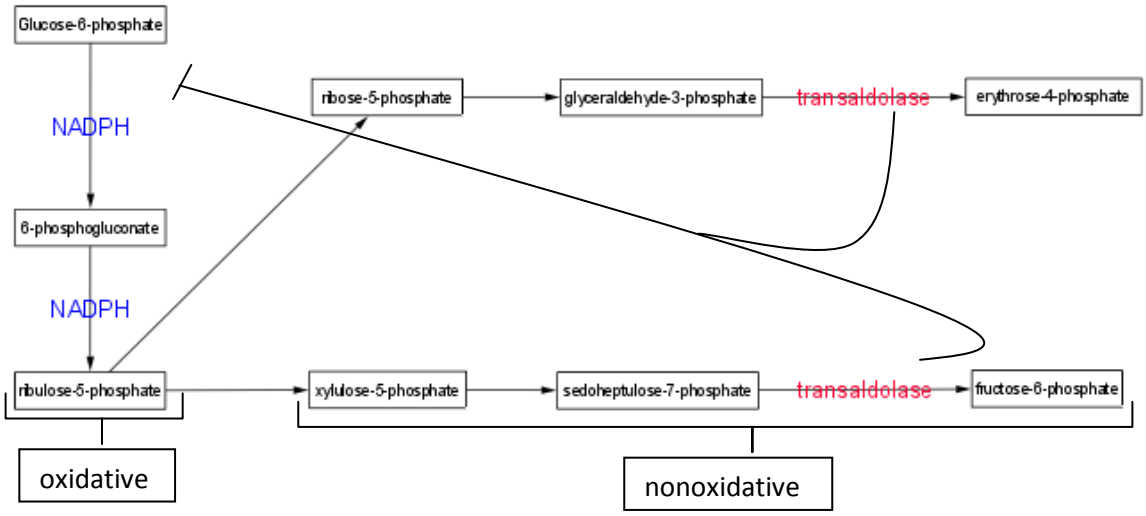

Figure 78: Summary of the pentose phosphate pathway (PPP) through transaldolase catalysis. The oxidative portion of the PPP is on the left, and NADPH producing steps are shown. The nonoxidative portion of the PPP is shown on the right. Normal levels of transaldolase will maintain a normal flux through the PPP, thus generating NADPH. However, overexpression of transaldolase will deplete available glucose-6-phosphate, which will reduce flux through the oxidative portion of this pathway, ultimately depleting levels of NADPH.

pathway leading to buildup of sedoheptulose-7-phosphate that prevents recycling and therefore depletion of glucose-6-phosphate and thus reduction of NADPH levels

[404,408,409]. It seems that some transaldolase is needed for PPP functioning, but there is a delicate balance to be maintained in order to generate sufficient levels of NADPH for GSH reduction.

It is of note that even in a situation where transaldolase is overexpressed, some NADPH and GSH remain, but their levels are greatly reduced, further suggesting at least some redundancy and regulation for the generation/regeneration of these compounds [404,409]. This implies that under conditions of increased transaldolase expression, at least some NADPH and GSH are present in the cell, but the amount of both will be

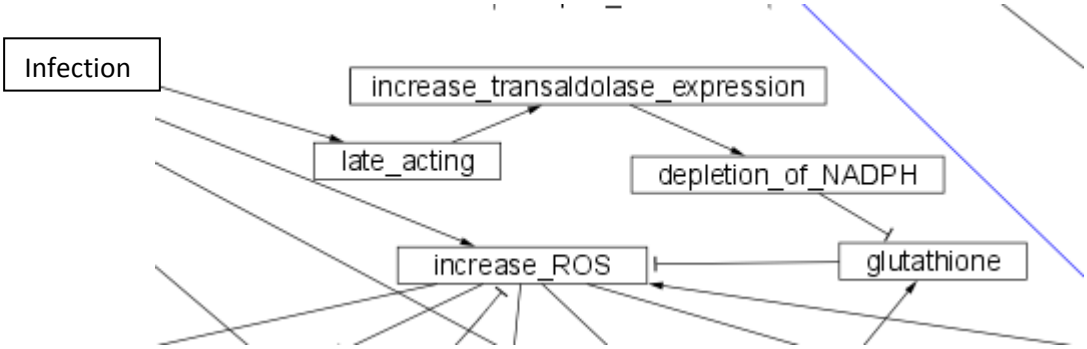

Figure 79: Summary of proposed effects of increased transaldolase expression. The increase in transaldolase expression seen in the soluble fraction of 96 hr postinfection samples is predicted to depletion of NADPH. Depletion of NADPH is predicted to reduce the availability of glutathione, a reactive oxygen scavenger, ultimately preventing glutathione inhibtion of ROS.

reduced due to the reduction in output from the oxidative phase of PPP, which is inhibited by elevated TAL [409]. G6P was found to be significantly depleted in cells overexpressing transaldolase [404,407], which could be related to transaldolase

inhibition of G6P dehydrogenase activity, namely by depleting G6P dehydrogenase's substrate. At elevated ROS levels, the level of available NADPH reducing capacity in the cell to maintain GSH is depleted, thus favoring the increase in ROS-induced apoptosis in cells overexpressing transaldolase.

It was reported that the transcription factor ZNF143 is primarily responsible for regulating transaldolase expression, although the AP-2α transcription factor may also be involved as a transcription inhibitor in a tissue specific manner [406]. Grossman et al., (2004) also suggest a protein half life of >4 days for transaldolase in their experiments [406]. This suggests that overexpression of transaldolase in our system may be a long-lasting effect increasing the susceptibility to ROS induced apoptosis in the infected monocytes. Specifically, the long half-life of transaldolase could inhibit PPP flux on a scale of days, leading to a potentially prolonged susceptibility to ROS-induced apoptosis. This prediction does not of course rule out that other cellular factors could accelerate transaldolase degradation in response to other stimuli.

We propose that the increase in transaldolase expression in our system is a cellular response to infection that would normally lead to apoptosis were *C. burnetii* not acting to prevent this. We further suggest that metabolomic studies would be very useful here to monitor the levels of glucose-6-phosphate (G6P), NADPH and GSH, as well as other relevant metabolites and the ROS levels in the mitochondria. The increased expression of transaldolase in our samples may be a priming mechanism to make the infected monocytes more susceptible to apoptosis as a response to infection,

and may help to explain increased bacterial clearance in the presence of Securinine via increased apoptosis, as well as clearance of phase II *C. burnetii*. Determining the mitochondrial potential ($\Delta\gamma_m$) as well as NADH/NAD^+ and NADPH/$NADP^+$ ratios and caspase 3 activity levels would also be informative as to the actual degree to which the *C. burnetii* infected monocytes are primed for apoptosis.

Microtubule-associated Protein EB1

We observed an upregulation of EB1 in the soluble fraction of 96 hr postinfection samples. EB1 was recently reported to regulate phagosome maturation [410], and to preserve microtubule (+) ends to enable transfer of the microtubules to other proteins e.g. Rab5 (a phagosome maturation marker) [411]. Rab5 requires a stabilized (+) end of a microtubule to become activated [410]. Briefly, following actin removal from the phagosome, Rab5 binds to EB1 microtubule (+) ends and becomes activated, which marks the beginning of phagosome maturation [410]. It is plausible that EB1 could be a *C. burnetii* target. With *C. burnetii*, it is possible that the actin coat removal of the phagosome is delayed and/or EB1 is inhibited thus delaying phagosome maturation. EB1 may also facilitate the formation of protein complexes, including a subset of the proteins involved in the dynein associated dynactin complex as part of EB1's involvement in microtubule-associated transport [411].

Bucci, et al (2000) observed that Rab7 is involved in directing the maturing phagosome to a perinuclear location through the RILP N-terminus [367] which would seem to be in direct contrast to the expression of EB1, a (+) end stabilizer. Perinuclear

localization requires (-) end stabilization, and is the default program during phagosome maturation [412]. Bucci et al., (2000) also noted the colocalization of Cathepsin D with perinuclear located phagolysosomes [296]. It is possible that this perinuclear localization is required for optimal delivery of hydrolases to the developing phagolysosome, and a more peripheral localization may inhibit optimal hydrolase delivery to the *C. burnetii* replicative vacuole.

Cytosolic Inorganic Pyrophosphatase/Pyrophosphatase 1 (PPA1)

We observed PPA1 to be upregulated in the soluble fraction of samples taken at 96 hrs postinfection. Bioinformatics analysis confirms that the PPA1 we observe is of human origin. Pyrophosphatases catalyze the conversion of pyrophosphates to inorganic phosphate which is important to cellular energy and phosphate metabolism [413]. Pyrophosphates are generated in a number of metabolic reactions, including activation of amino acids, and nucleic acid formation [413]. Pyrophosphatase is required during periods of active metabolism, particularly when synthesizing macromolecules including proteins, nucleic acids, and carbohydrates. It would make sense that PPA1 is being upregulated in monocytes after activation and during maturation, as this would be expected to increase the cells metabolic needs, but does not rule out that at least part of the PPA1 signal we observe is being regulated by *C. burnetii*. It was recently reported that PPA1 is upregulated in activated CD8+ T-lymphocytes [414], suggesting a function for PPA1 in immune responses. Bacterially derived PPA1 is essential for survival of *E. coli* and *Legionella pneumophila*. In *L.*

pneumophila infections, the bacterium upregulates PPA1 in response to the phagosomal microenvironment of monocytes [415,416], and *C. burnetii* may also generating its own PPA1 below the limits of our detection. The environmental activation observed in *L. pneumophila* may be a characteristic of γ-proteobacterial pathogens utilizing a dot/icm Type IV secretion system [415,417]. *C. burnetii* possesses a dot/icm system similar to *L. pneumophila*'s [417].

We propose that metabolic processes requiring pyrophosphates have been upregulated by the host cell, and that this is the source of stimulation for upregulating PPA1. Monitoring levels of pyrophosphate, as well as nucleic acid and protein synthesis, in response to infection with *C. burnetii* could prove informative here.

Chaperonin/Hsp60

We observed an upregulation of Hsp60 in the soluble fraction samples taken at 96 hrs postinfection (see figure 80 and supplemental figure 2). See the section on Securinine for more details on Hsp60. Hsp60 is the only protein upregulated in both Securinine stimulated and *C. burnetii* infected samples. Although not conclusive, this would seem to suggest a role for Hsp60 in immune function, as discussed above. We also observed a possible cleaved Hsp60 isoform in the infection + Securinine samples, as discussed below.

It is possible that some of the observed Hsp60 is being secreted to attract/regulate nearby immune cells, as described previously. Exactly how this is being

accomplished is still to be determined and there is a great deal of confusion in the literature regarding the mechanism of Hsp60 stimulation on diverse cell types. It is likely that the response(s) and possibly the receptors involved are cell-type dependant. Hsp60-induced desensitization of the monocyte immune response, detailed above in the Securinine section, may factor into the development of chronic infections, such as the chronic form of Q fever caused by *C. burnetii*. Specifically, desensitization of the monocyte by chronic Hsp60 exposure could reduce the long-term monocyte immune response, creating more favorable intracellular conditions to for the bacterium.

It has been shown that increased Hsp60 exposure increases activation of p38, NF-κB, and Erk, but not Jnk [153,157,163,170]. *C. burnetii* infection causes an increase in Akt and Erk1/2 activation, but a decrease in p38 activation [72]. This may suggest that Hsp60 expression/stimulation may benefit *C. burnetii* by increasing the activation of Erk1/2, but that *C. burnetii* is using some other means to specifically inhibit p38. A further possible Hsp60 function may be the response of ECH1 (detailed above). Hsp60 can be secreted, and because the response of TLRs to Hsp60 and LPS stimulation is so similar, it is possible that the decrease in ECH1 expression is at least partially regulated by Hsp60 stimulation of the monocytes. This would have further implications regarding the proposed lipid accumulation in response to *C. burnetii* infection, namely that Hsp60 is involved in altering the composition of lipid rafts via TLR-induced downregulation of ECH1. Additional work will be required to elucidate the possible interaction between Hsp60 and ECH1 expression.

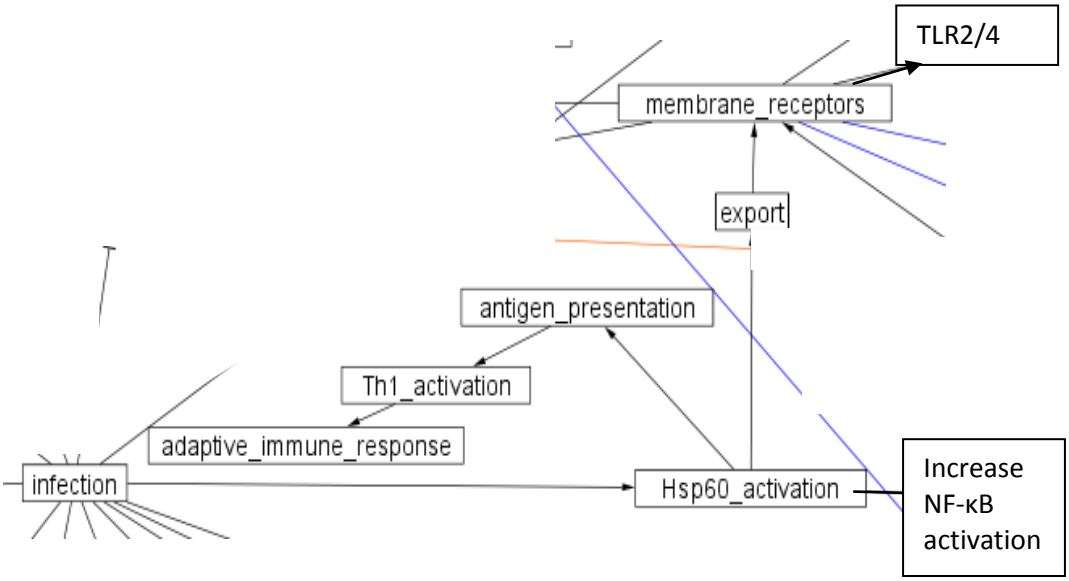

Figure 80: Summary of proposed functions of Hsp60 in C. burnetii infected samples. Briefly, infection triggers an upregulation of Hsp60 which can activate NF-κB. Hsp60 can also be exported/inserted into the membrane to either act on membrane receptors e.g. TLR2/4 and/or function in antigen presentation. See supplemental figure 2 for more details.

One interesting observation is that Hsp60 can bind LPS in an antigen presenting capacity, eliciting a response that is greater than either stimulus alone [159,166,418]. Although it seems to be generally accepted that stimulation of immune cells by Hsp60 alone is not due to LPS contamination, Hsp60 has been shown to bind LPS when coincubated together [159,166]. This may have implications for antigen presentation to T-cells, as well as potentially furtherstimulating the innate immune system to produce a more robust responses to infection. Specifically, Hsp60 presentation of LPS and other

antigens would act through presentation to professional antigen presenting cells/macrophages, thus lowering the threshold of microbe recognition and TLR signaling, to trigger/regulate Th1-mediated T-cell adaptive responses [151,155-160,171].

We propose that Hsp60 is a potentially important overall modulator of monocyte immune function. Specifically, we hypothesize that Hsp60 can activate NF-κB in C. burnetii infected cells, and thus altering the cytokine profile of the cell. Secreted Hsp60 is proposed to be involved in the observed downregulation of ECH1, which will reduce the availability of both ATP and AcCoA. Secreted Hsp60 could also act on other monocytes in culture to modulate their immune responses via interaction with cell surface receptors. Hsp60 is potentially involved in presentation of LPS to T cells, although we cannot directly test this in our system which contained no T cells. Further work will be needed to characterize the function(s) of upregulated Hsp60 in our system. We propose that monitoring the secretome would be informative here.

Analysis Using DAVID and GOEAST

As with Securinine, we evaluated our protein lists using DAVID (figures 31-45) and GOEAST (figure 46-48). Evaluations were performed as a check on our manual evaluation. Data was input using Uniprot accession numbers, and searched using the default parameters. As with Securinine, these analyses both confirmed and extended our original observations. DAVID again provided significant molecular detail, proteins and metabolites (particularly for Aldh2), providing targets for future evaluation and information that can be used to design metabolomics experiments. GOEAST provided

additional details regarding biological functions, cellular localizations and molecular functions for the proteins analyzed. As with Securinine, no one approach gave a completely comprehensive overview, and the analyses are at least somewhat complimentary in their findings. Also as with Securinine, not all of the proposed functions are necessarily relevant to our system requiring user evaluation.

Conclusions from 96 hr Infection +/- 50 uM Securinine

Many of the differentially expressed proteins identified from the second series of experiments have been assigned functions in apoptosis, inflammation, and ROS generation (figure 20), perhaps consistent with an immune response that leads to apoptotic cell death. It may be significant that many of the proteins observed in this dataset that are changing expression are Ca^{2+} mediated, which suggests alterations in the Ca^{2+} levels in the cell in response to infection + Securinine. In addition, we see downregulation of the glycolytic enzyme enolase 1, as well as the downregulation of glycogen phosphorylase which may inhibit glycolytic flux, although pyruvate kinase is upregulated suggesting that pyruvate is being generated in the infection + Securinine samples, possibly due to amino acid degradation. We note that pyruvate may act as an antioxidant [419-421].

Pyruvate can act as an antioxidant by directly neutralizing peroxides to their conjugate alcohols [422,423]. Pyruvate can also be converted to acetyl CoA (AcCoA) by the action of pyruvate dehydrogenase. AcCoA is a switching point in cellular

metabolism and can be converted into fatty acids to store energy or used in the Krebs cycle to make energy. The upregulation of pyruvate kinase may also reflect production of pyruvate, following conversion of oxaloacetate (OAA) to phosphoenolpyruvate (PEP) for antioxidant rather than energy generation purposes, which will reduce the availability of ATP. Conversion of PEP to pyruvate does generate 1 ATP per PEP, but this is not an efficient means of ATP generation and is not a normal route of ATP production in the cell.

It seems unlikely that oxaloacetate would be used to make phosphoenolpyruvate for purposes of energy generation, unless acetyl CoA is severely depleted, due to reduced glycolytic flux and reduced β-oxidation of fatty acids. Under these circumstances, conversion of OAA (a low abundance metabolite under normal conditions) to PEP is perhaps the only way to replenish AcCoA by producing it from pyruvate. This also suggests that ATP production may be impaired, due to reduced glycolytic flux, and reduced β-oxidation (due to reduction in ECH1 observed in 96 hr infected cells). These observations suggest that a better understanding of the metabolomic status of the cell is desirable.

The potential reduction in ATP production, and the observed downregulation of ERLIN2, which is an important inhibitor of ER Ca^{2+} release, suggests that Ca^{2+} is no longer being stored as effectively in the ER and has been released into the cytosol [113,114,424]. Specifically, ERLIN2 is an important part of a complex that targets

activated IP_3 receptors for ERAD degradation to control Ca^{2+} release [113,114]. Loss of ERLIN2 has been shown to increase Ca^{2+} release from the ER [113].

Ca^{2+} storage in the ER is an active transport process (up a Ca^{2+} concentration gradient) suggesting that loss or reduction of available ATP could reduce the efficiency of Ca^{2+} storage. The likely impairment of Ca^{2+} storage in the ER, as evidenced by loss of ERLIN2 and probable reduction in available ATP, suggests that Ca^{2+} has been released to the cytosol. Overall, the loss of cytoplasmic proteins from the samples and the cell count in infection+Securinine samples suggest that we are seeing cell death, most likely mediated by Ca^{2+} release from the ER. We did not see indications of this process in the samples for either infection alone or Securinine alone based on detected changes in protein expression. If indeed apoptosis is occurring, it is most likely caspase-independent [425], as discussed below.

Caspase-independent apoptosis is typically characterized by apoptosis inducing factor (AIF)-mediated type I chromatin condensation. [425]. AIF, ROS and Ca^{2+} can feed back on mitochondria causing damage and the release of death factors independent of caspase or other stimuli [424,425]. It has also been reported that NO can induce apoptosis in macrophages that is independent of caspases [426]. NO, as well as levels of NO modified proteins, and Ca^{2+} measurements are likely to be a valuable adjunct for future measurements. It is also possible that calpain proteases are activated by the inferred influx of Ca^{2+}, but are not changing their expression within our detection limits.

Calpains are dormant in the cytoplasm until activated by an increase in [Ca^{2+}] [425], [427].

Caspase-independent apoptosis is supported by the observation that NADH-CoQ reductase 75 kDa subunit is upregulated in infection+Securinine samples, and is found at a molecular weight that suggests it is intact. The NADH-CoQ reductase 75 kDa subunit contains a single caspase cleavage site that is cut during caspase-mediated apoptosis and that causes impaired function, including increased ROS generation and loss of mitochondrial transmembrane potential [115]. The observation that at least some manner of cleavage is occurring in the cytoplasm in relation to infection is supported by a differentially expressed protein identified as vimentin that appears at an apparent pI and mW suggesting cleavage. This protein appears to have been present in the 96 hr infection alone. The observation that this protein is strongly downregulated in infection + Securinine samples may simply reflect that cleaved protein has been targeted for degradation.

We also observe a differentially expressed protein in the infection + Securinine samples that is identified as Hsp60. This Hsp60 identification appears at an apparent pI and mW suggesting cleavage. Hsp60 cleavage was not observed in the first series of 96 hr infected samples, but it must be present at some level in the 96 hr infected samples from the second series of experiments, in order to be detected as downregulated in the infected+Securinine samples. The failure to detect cleaved Hsp60 in the first series of experiments may indicate that changes in this protein did not rise above the biological

noise in the system to be detected as a statistically meaningful differentially expressed protein. As mentioned with the vimentin cleavage product, the downregulation may simply indicate that the Hsp60 cleavage product has been targeted for degradation.

The potential presence of cleaved vimentin and Hsp60 suggests that some form of cytoplasmic protease is active. Calpain is known to be present in the cytoplasm and calpain mediated cell death is activated by increases in cytoplasmic Ca^{2+} levels [425]. Although it does affect the outer mitochondrial membrane proteins, calpain does not affect mitochondrial inner membrane proteins at least initially [425]. Given that Ca^{2+} is likely being released into the cytoplasm, where it could activate calpain, and that calpain can initiate caspase-independent apoptosis, we propose that our infected, Securinine-treated samples are undergoing Ca^{2+}-mediated, caspase-independent apoptosis.

Calpain can interact with calmodulin-dependent proteins, and given that we see a downregulation in calmodulin in the infection+Securinine samples, there may be functional changes in calmodulin-dependant proteins that are either changing expression levels below our detection limit, or changing activity levels without changing expression. Determination of the activation status of calpain and possibly caspases should be useful in understanding the biology of this system. Our research group is developing differential detection methods for changes in enzyme activities on 2D gels that should be applicable to this problem, but these new methods are not ready to be deployed as yet.

The observed upregulation of NADH-CoQ reductase 75 kDa subunit despite obvious cell death and potential cleavage of vimentin and Hsp60, would suggest that the electron transport chain may be relatively intact. However, the possible outer membrane permeabilization by calpain [425] and the possible loss of feed-ins to the Krebs cycle (specifically acetyl CoA from glycolysis and/or β-oxidation) may impair the formation of a H+ ion gradient needed to generate ATP. It is possible that amino acids could be broken down to generate Krebs cycle intermediates especially if OAA is being converted to PEP, but this will probably entail a decrease in reducing equivalents that feed into the electron transport chain. The loss of mitochondrial transmembrane potential has been shown to occur in the absence of activated caspases in necrotic T lymphocytes, and in proapoptotic SIV-infected macaque T cells, suggesting that loss of mitochondrial transmembrane potential is a central and irreversible step in caspase-independent cell death [72]. The expression patterns of several proteins would indicate apoptosis rather than necrosis. These include eukaryotic translation initiation factor 5A (downregulation), eukaryotic translation elongation factor 2 (downregulation), and S100A11 (upregulation, also a Ca^{2+} binding protein) since these changes have all been demonstrated to increase apoptosis [428,429].

Infection of macrophages by *L. pneumophila* has been reported to increase cytoplasmic Ca^{2+} levels [43]. It has also been shown that Mycobacterial species (M. *bovis* and *M. tuburculosis*) inhibit increases in intracellular Ca^{2+} levels, and exogenously increasing cellular Ca^{2+} will increase cell killing of mycobactrial species, due to increased

phagosomal acidification [430]. Increased Ca^{2+} levels are also part of macrophage maturation and phagosomal acidification [430]. While this would initially be beneficial to *C. burnetii*, there must be a tipping point beyond which calpains are activated. The loss of ERLIN2 and probable reduction in ATP levels suggests that cytoplasmic Ca^{2+} levels in the infected + Securinine samples are no longer regulated. Measurements will be required to determine the mitochondrial transmembrane potential in this situation, but it would be very beneficial in determining the role of the mitochondria in response to the stimuli in our samples. Lipidomic and metallomic studies coupled with metabolomic data to monitor various metabolic intermediates (e.g. Krebs cycle intermediates, NAD^+/NADH ratios, ADP/ATP ratios, etc.) as well as TUNEL assays should provide a clearer explanation of 1) the type of observed cell death, and 2) the pathway(s) that may be involved.

It was reported by Doerfler, et al., (2000) that the baculovirus p35 protein from *Autographa californica* nucleopolyhedrovirus inhibits caspase 3 activation and prevents spontaneous apoptosis in T lymphocytes [431]. A BLAST search of p35 against *C. burnetii* indicated a local homology to a *C. burnetii* ankyrin repeat protein (see figures 81-82). We note that the E value for the BLAST search is not conclusive. However, the BLAST search is at least suggestive, particularly given that a) comparison was between quite different organisms, and b) the number of ankyrin repeat proteins identified as top hits by the search. Alignment of the two proteins (p35 and the top *C. burnetii* ankyrin repeat protein in the list) revealed two sections of the two proteins (78 and 19

amino acids respectively) displaying an E value of 10^{-4} with ~30% homology (figured 81, 82). Seshadri, et al., (2003) documented an as yet uncharacterized 13-member family of ankyrin repeat proteins in the *C. burnetii* genome and these are implicated in pathogenesis [17]. The alignment of a *C. burnetii* ankyrin repeat protein with *A. californica* p35 protein suggests that these two proteins contain homologous regions that may be involved in caspase inhibition. This analysis does not examine the functional role or the homologous regions, it is merely suggesting. Although certainly not conclusive, it is possible that the ankyrin repeat proteins in *C. burnetii* are in some way responsible for the reported inhibition of caspase 3 activity [72], and this warrants further investigation.

Intriguingly, the observed upregulation of intact NADH CoQ reductase also suggests that the proposed caspase inhibition by *C. burnetii* [72] is functional even though the cells are dying. This is borne out by the observation that vinculin is downregulated. It was reported by Subauste et al., (2004), that loss of vinculin strongly inhibited caspase 3 and 9 activation, and vinculin could well be a *C. burnetii* target protein under these conditions [432]. As described above, the ankyrin repeat proteins in *C. burnetii* may be involved in the inhibition of caspase activation by interaction with vinculin, and protein interaction studies with these ankyrin repeat proteins and vinculin could prove informative.

We also observed that the expression of MHC antigens was largely downregulated (one isoform upregulated) in infection + Securinine samples, in addition

to downregulation of much of the proteasomal processing machinery needed to produce MHC antigens for presentation to the adaptive immune system. In the proteasomal processing machinery, we observe a downregulation of β2-microglobin (light chain of MHC I proteins), and proteasome activator subunit 1. Loss of these two proteins is predicted to inhibit antigen processing by the proteasome [433-437]. Because Hsp70 is present, and predicted to enhance antigen presentation (as described above), the downregulation of MHC presentation machinery may indicate that *C. burnetii* is able to inhibit antigen presentation, even when stimulated by Securinine treatment. We note that we did not observe proteasomal downregulation in either the infected alone or the Securinine alone experiments.

An examination of caspase and calpain activity/expression levels will be important to understand the biology observed in the infected + Securinine samples [438-450]. Numerous cytoskeleton interacting proteins are also altered suggesting that cytoskeletal dynamics are important in this system. There are also a number of lipid raft proteins present, such as ERLIN2, further indicating the desirability to understand lipid raft compositional changes in future measurements, in addition to determining metabolite, and lipid levels in the samples (as described above) to obtain additional mechanistic clues to the pathways active in this system.

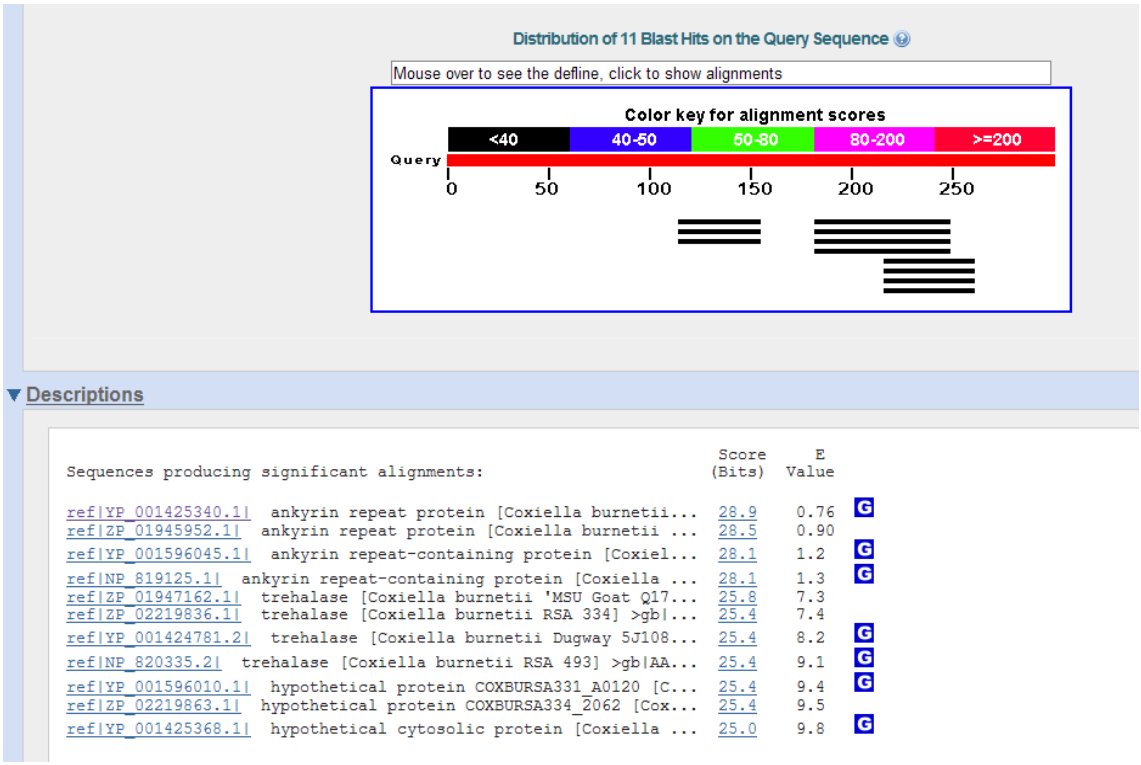

Figure 81: BLAST search results of *Autographa californica* nucleopolyhedrovirus p35 vs. *C. burnetii*. The top *C. burnetii* hit was further aligned with the p35 sequence (see figure 82 below).

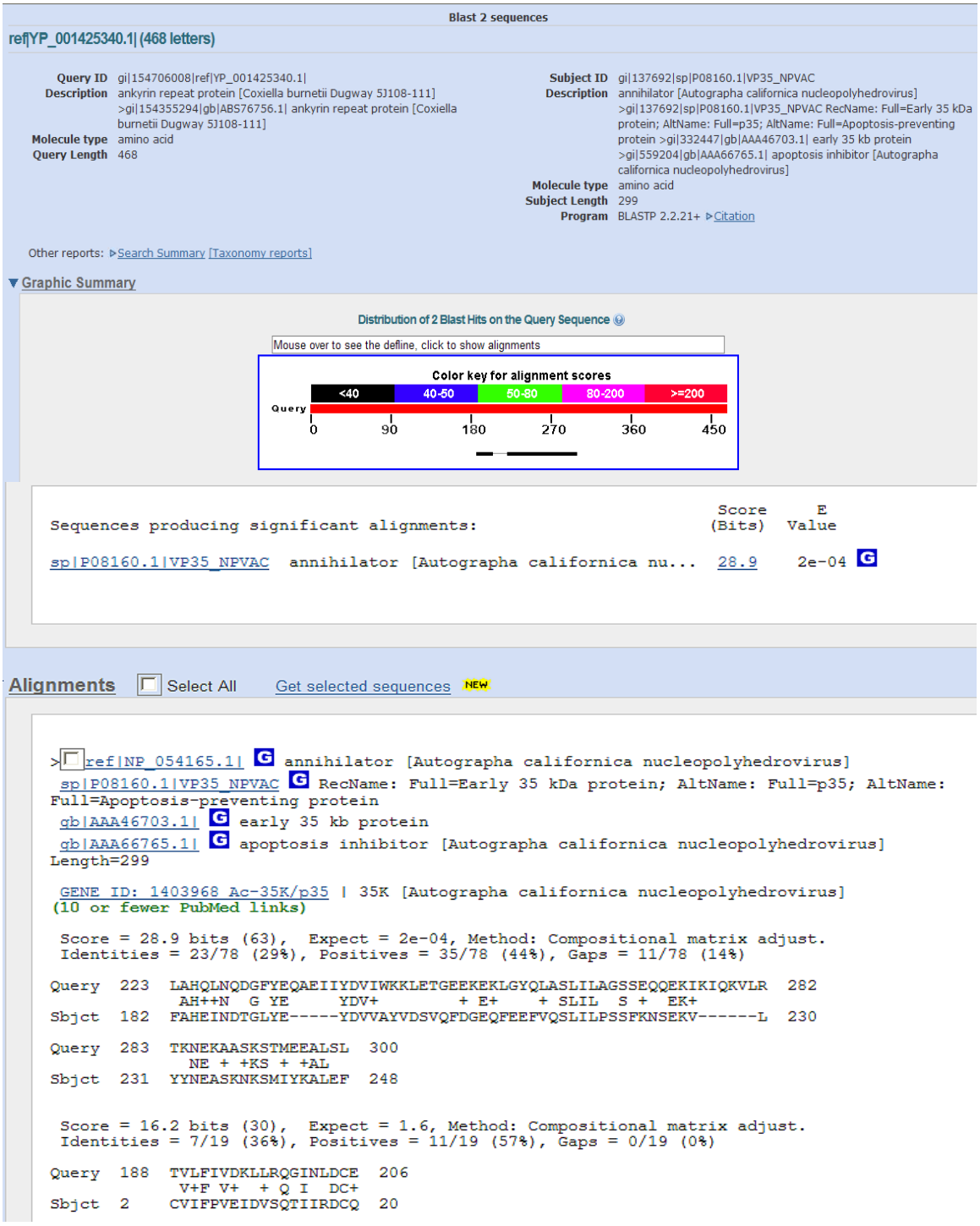

Figure 82: Alignment results from BLAST search. Indicates that a discrete region of the aligned *C. burnetii* ankyrin repeat protein has ~30% sequence similarity to a similar region in p35.

Overall Conclusions

Overall conclusions from the adjuvant studies (Securinine, LPS, and MPL stimulation) reveal that TLR stimulation/regulation by LPS and MPL differ significantly from the $GABA_A$ receptor mediated stimulation/regulation by Securinine in their modulation of the monocyte immune responses. Securinine stimulation triggered a strong response from the monocytes by upregulating various heat-shock proteins (Hsps 60, 70, and 90), all of which have been demonstrated to be centrally involved in the immune response at several levels. Whereas TLR stimulation triggers an NF-κB response, Securinine favors a p38-based response. Stimulation of Monomac I cells with Securinine appears to prime the monocytes for apoptosis, without actually stimulating apoptosis by itself. This is borne out by the observations a) that Securinine stimulated samples displayed no obvious morphological or biochemical signs of undergoing significant levels of apoptosis, and b) Securinine stimulation, in the presence of *C. burnetii* at 96 hrs postinfection, causes significant cell death, most likely a by caspase independent process that appears to be mediated by calpain, following the probable release of Ca^{2+} from the ER.

It is perhaps of concern that Securinine antagonism of $GABA_A$ receptors can lead to the induction of apoptosis under certain conditions, particularly given the rather ubiquitous presence of $GABA_A$ receptors in the nervous system. We do not know if Securinine can cross the blood-brain barrier, nor do we know the specific $GABA_A$ receptor subunit composition(s) that is/are sensitive to Securinine antagonism. It is

known that $GABA_A$ receptors are highly dependent on their subunit composition for detailed function and that changing this subunit composition renders a $GABA_A$ receptor more or less susceptible to stimuli [85,86,112,276,451-457]. Traditionally $GABA_A$ receptors are believed to contain 2α, 2β, and 1 of another type of subunit of which the γ2 subunit is probably the most common. It is this 5th subunit that is the most important for functionality and susceptibility to drug stimulation/inhibition. For example, the γ2 subunit is benzodiazapine sensitive but other subunits are not [451,458]. In addition, *C. burnetii* is not known to infect nervous tissue *in vivo*, and Securinine alone does not seem to initiate apoptosis. Therefore, the potential use of Securinine as an immune adjuvant is and/or as a potential therapeutic option for *C. burnetii* treatment is still plausible. Should damage to nervous tissue following Securinine exposure *in vivo* be demonstrated, this would invalidate the use of this compound as an immune adjuvant, since $GABA_A$ receptors are so common in the nervous system.

The presence in monocytes of a 5th subunit not known to be observed in neurons in abundance would indicate that apoptosis is not likely in neurons. However a common 5th subunit would be a concern. It is also possible that Securinine in its current form could serve as the basis for a family of similar compounds and that alterations to its structure might still enhance cell killing of *C. burnetii* without triggering apoptosis. The triggering of apoptosis by Securinine exposure does appear to be dose related (M. Jutila and K. Lubick, personal communication, data not shown) and there may be a

useful dosage below which apoptosis can be avoided, but still benefit monocyte clearance of *C. burnetii*.

There appear to be clear differences between the immune functions regulated by TLR recognition/stimulation triggered by LPS or MPL, and the immune functions regulated by the $GABA_A$ receptor in monocytes. Securinine alone appears to be activating an immune response while simultaneously priming the monocytes for apoptosis, even though apoptosis should be inhibited at least initially (e.g. by inhibition of apoptosis by Hsp70 or IMPDH). We noted no obvious signs of apoptosis in monocytes treated with either *C. burnetii* or Securinine alone, but did see obvious signs of cell death in combination at higher levels of Securinine, as detailed above. This suggests that either there is a dose dependency for Securinine induction of apoptosis or that the two stimuli in combination are enough to push the cells over the edge. It is also possible that both are true, i.e. that above a certain threshold of Securinine, infection with *C. burnetii* will accelerate or induce apoptosis.

Our initial experiments with Securinine were performed using 25 uM Securinine as the stimulus. In the infection+Securinine samples, 50 uM Securinine was used. 50 uM is the IC50 of Securinine [78]. It could be that Securinine at such a high level is too toxic for cells to handle. Data from the Jutila group supports this conclusion. Since we have performed these experiments they have determined that 12.5 uM Securinine is most effective dosage for enhancing monocyte cell killing of *C. burnetii* (K. Lubick, and M. Jutila, personal communication). It is also quite possible that simultaneous

stimulation of TLRs plus $GABA_A$ receptor inhibition could produce an effective immune response, using for example MPL and a reduced level of Securinine, that could be more productive than either alone in terms of clearance of *C. burnetii*.

In the 96 hr infection +/- 50 uM Securinine samples, we did not conclusively establish the type of cell death observed. Ca^{2+} release and ROS generation can influence any or all of the cell death possibilities and provides no outright clues as to the type. However, the number of differentially regulated proteins involved in some way in apoptosis and/or Ca^{2+} sensing suggests that it is this manner of cell death that was occurring. The presence of apparently intact NADH CoQ reductase would seem to indicate that caspases are not substantially active, and that we are observing caspase-independent apoptosis. Monitoring the activity levels of caspases and calpain could prove informative as to the type of cell death that is occurring.

This is intriguing given the observation that *C. burnetii* is able to actively inhibit the activation of caspases 3 and 9 [72]. Continued inhibition of caspases 3 and 9 despite Securinine exposure and an increase in *C. burnetii* cell killing by the monocytes suggests that either a) some *C. burnetii* machinery is able to remain functional in sufficiently high levels to influence the monocyte for a long time period even when the monocyte is actively dying, or b) the act of monocyte apoptosis and engulfment by other cell types, such as neutrophils, might actually be the mechanism by which Securinine enhances clearance of *C. burnetii* infections. Because we are using cultured monocytes, we could

not evaluate the interaction of Securinine stimulated monocytes with other immune cells.

Infection by *C. burnetii* has highlighted several areas of interest regarding the interaction of the bacterium with the monocyte. Our data, in conjunction with published literature, indicate a possible mechanism for the means that *C. burnetii* uses to hijack the phagosomal machinery and regulate hydrolase delivery. Specifically, the indication that *C. burnetii* infection stimulates the production of cholesterol and that *C. burnetii* replicative vacuoles contain flotillin [376], suggests that a portion of the host-pathogen response may be mediated by bacterially induced alterations to the composition of phagolysosomal lipid rafts. There are also indications (e.g. from ECH1, Aldh2, transaldolase and PPA1) that changes in the metabolome are important in the course of *C. burnetii* infection of monocytes.

With respect to future directions for this investigation, there are almost certainly alterations to the metabolome, lipidome and metallome occurring in our samples. There are indications that nonprotein biomolecules are important in various aspects of the responses detailed above: from IMPDH and various metabolic proteins e.g. pyruvate kinase (implicating the metabolome) FABP5 and ECH1 (implicating the lipidome), and S100 proteins, ERLIN2, and several others (implicating Ca^{2+} levels and possibly the metallome). Changes in small molecules, although not measured in our samples, are implied by the proteome changes, and warrant significant further investigation (see below). The likely alterations to the metabolic status within the cell

would be central to any host-pathogen interaction, particularly since *C. burnetii* is an obligate intracellular pathogen. It is also likely that the protein compositions of the cellular lipid rafts are being altered in addition to potential lipid modifications (as implied by Rab7 and ERLIN2, as well as Hsps and others). Given the likely importance of lipid rafts to various aspects of monocyte biology, as well as host-pathogen interactions and response to adjuvant, the composition of lipid rafts warrant further investigation.

A logical step, in addition to validation of various predictions above by traditional means (e.g. Western blots) would be to begin filling in various gaps in our current understanding. Specifically investigations into the metabolome, lipidome and metallome in infected and adjuvant treated cells would appear to be important as this information is not readily available in the literature. Lipidome and metabolome investigations have been performed in other systems, but such analyses are still quite new and have not yet been widely applied. Metallome data on a global scale is also rare, although it is relatively common to track individual metal ion levels, particularly Ca^{2+} and iron. Such information could be incorporated into the existing model, described above, both expanding and revising it.

Investigations into the metabolome, lipidome, and metallome should be relatively straightforward once extraction protocols have been established. The metabolome and lipidome samples can be run on a GC/MS using electron impact fragmentation in scanning ion mode (SIM), as this is a relatively rapid, sensitive, and quantitative analysis that can give absolute amounts if appropriate internal standards

and calibration curves are present. Derivitization of some classes of compounds would be required. Quantitation should be possible down to at least the low part per trillion (ppt) range. If SIM is not feasible e.g. due to a large number of ions present, scanning mode is also possible, and at least mid-ppt range quantitation should be possible. Complimentary data on the metabolome and lipidome should be obtainable using some form of HPLC-MS/MS analysis provided the method(s) chosen can provide sufficient fragmentation in order to identify the molecules (MW alone is not sufficient to identify metabolites and lipids). The metallome can be analyzed on ICP-MS for analysis and this is likely to be straightforward once extraction has been optimized.

Lipid raft isolation is a relatively well-established procedure although the definition of lipid rafts is not always agreed upon. Analysis of the lipid raft composition could be accomplished using 1D and 2D gel electrophoresis for isolated proteins and GC/MS techniques for lipids. This approach will be informative as to the changes that take place in response to the various stimuli discussed above and should either support or refute the proposed alterations to the lipid raft composition that are indicated by the current generation of the model (described above, and see supplemental figures 1 and 2).

A similar approach should be considered for analysis of the proteins and metabolites in the secretome which should be readily available by simply collecting and extracting the growth media. Small molecule extractions should be possible using extraction techniques established in the experiments outlined above. Protein extraction

will likely differ from those employed in the experiments previously detailed, and a TCA/acetone precipitation should suffice to extract secreted proteins from the growth media. A similar experiment for extraction of secretome proteins from *Clostridium acetobutylicum*, which relied on dialysis/ultrafiltration of the growth media, could provide a basis for a secretome protein extraction procedure [459]. Indications from our model are that the secretome may have an important part to play in the dynamics predicted by the current model. Particularly Hsp60, ATP/ADP ratios, as well as potentially secreted metabolites, inflammatory markers, lipids, etc. The metal composition of the secretome could also be informative and test nuances of the model.

The purpose of the proposed extensions to our existing studies would be to revise and expand the picture suggested in the first generation model detailed above, and might well provide sufficient data to produce a predictive mathematical algorithmic model that could be used to make testable predictions to perturbations in this system. Metabolome and lipidome data in addition to lipid raft studies will likely provide the most important contributions to the model, as indications from the current generation of the model are that lipids, metabolites, and lipid rafts have important roles in our system. The metallome and secretome are expected to provide nuances to the model. Such a second generation model could also have enough information that at least some portions of it will be directly applicable to providing a framework on which to model the behavior of other similar systems, at least so far as other obligate intracellular pathogens are concerned, and enable testable predictions about innate immunity in

general. Such models could well enable researchers to better understand both the innate immune response and more precisely refine adjuvant/treatment options not only for potential bioweapons, but also for infectious diseases as a whole.

The presence and apparent level of $GABA_A$ receptor involvement in monocyte immune functions may have implications beyond our study. In particular, considering the inhibitory nature of $GABA_A$ receptors in the nervous system, and the proposed inhibition of immune function by $GABA_A$ receptors, GABA stimulation of these receptors might be involved in stress-induced or depression-induced immune suppression. Although the relationship between $GABA_A$ receptors and immune suppression are beyond the scope of our investigation these are logical proposals based on the available literature and suggest that further investigation of this potential relationship would prove informative as to the effects of stress on the immune system.

Results from the automated systems biology analysis tools substantially supported the conclusions from our models, and further expanded them. Results from the automated analyses, although they do not cover every protein in our analysis, do provide some useful information. For example, the Hsp proteins (60, 70, and 90) are predicted by our model to be involved in antigen presentation based on our survey of the literature. DAVID in particular gave substantial molecular detail on the role of Hsp60 in MHCII antigen presentation (figure 22), as well as roles for Hsp70 and Hsp90 in MCHI antigen presentation (figure 24). In both cases (MHCI and MHCII presentation) , DAVID provided details for other proteins that are involved in both paths of antigen

presentation cooperating with the Hsps that serve to extend the information we provided in our manual analysis. GOEAST gave additional details regarding Hsp60's involvement in immune response signaling pathways (figure 48). DAVID also gave additional details about Hsp90's involvment in NOD-like receptor signaling (figure 28) beyond that predicted by our manually constructed models.

DAVID also provided details about various metabolic pathways such as those involved with IMPDH, Aldh2, Lap3, Tal1, and visfatin. Given the prior indications of our manually constructed model suggesting the involvement of various metabolites and lipids, the metabolic pathways highlighted by DAVID are expected to be of value as a guide to planning future metabolomic an lipidomic experiments. One of the biggest issues with metabolomic experiments is the need to chemically derivatize the samples in a variety of ways to optimize the visualization of groups of metabolites, as there is no one analytical method that will allow the visualization of all metabolites. The data provided by DAVID can be used to help plan the types of derivatizations that would best be utilized in metabolomics and/or lipidomics experiments. The data from DAVID can also inform enzymatic activity assays to monitor the flux capacities of specific metaboliic pathways once they have been identified.

The metabolite data from DAVID somewhat overlaps with the protein data from GOEAST . As an example, the metabolic data from IMPDH provided by DAVID fits well with the protein results from purine/nucleotide metabolism provided by GOEAST. The GOEAST data suggests that IMPDH is involved with metabolites related to

ribonucleotide metabolism, nucleoside metabolism, and nucleotide metabolism in addition to purine metabolism suggested by both our model and DAVID.

Overall, our manually constructed models are specifically oriented towards host-pathogen interactions in monocytes and the response to Securinine stimulation. Our interests informed the generation of these models. DAVID and GOEAST, which are more general in their approach, are geared towards more general cellular responses. As a result, there is information provided by DAVID and GOEAST that is not likely to be important to our systems. As an example, the Securinine data from GOEAST provides a section showing how actin is involved in neuronal growth. While interesting, neuronal growth is not likely to be important in monocytes. This observation underscores the pitfalls in relying solely on automated systems, and suggests that these automated systems are complimentary to a model constructed from targeted manual searches of the literature that will be much more targeted to and focused on the system(s) in question. The three approaches provided substantial support for each other's conclusions, as well as providing complimentary information that extends the models in useful ways. The sum total of the systems analyses should prove useful in designing future proteomic and metabolomic experiments, to test and refine the models.

REFERENCES CITED

1. http://www.ualberta.ca/~csps/JPPS10_3/MS_996/MS_996_clip_image003_0001.gif.

2. Petrilli V, Papin, S., and Tschopp, J. (2005) The inflammasome. Current Biology 15: R581.

3. Ohta S, Ohsawa, I., Kamino, K., Ando, F., and Shimokata, H. (2004) Mitochondrial ALDH2 deficiency as an oxidative stress. Annals of the NY Academy of Sciences 1011: 36-44.

4. http://www.freepatentsonline.com/6525028.html.

5. Wenzel P, Hink, U., Oelze, M., Schuppan, S., Schaeuble, K., Schildknecht, S., Ho, K.K., Weiner, H., Bachschmid, M., Münzel, T., and Daiber, A. (2007) Role of reduced lipoic acid in the redox regulation of mitochondrial aldehyde dehydrogenase (ALDH-2) activity. The Journal of Biological Chemistry 282: 792-799.

6. Ecker DJ, Sampath, R., Willett, P., Wyatt, J.R., Samant, V., Massier, C., Hall, T.A., Hari, K., McNeil, J.A., Büchen-Osmond, C., and Budowle, B. (2005) The microbial Rosetta Stone database: a compilation of global and emerging infectious microorganisms and bioterrorist threat agents. BMC Microbiology 5.

7. Hackstadt T, Peacock, M.G., Hitchcock, P.J., and Cole, R.L. (1985) Lipopolysaccharide variation in *Coxiella burnetii*: intrastrain heterogeneity in structure and antigenicity. Infection and Immunity 48: 359-365.

8. Hackstadt T (1988) Steric hindrance of antibody binding to surface proteins of *Coxiella burnetii* by phase I lipopolysaccharide. Infection and Immunity 56: 802-807.

9. Kagawa FT, Wehner, J.H., and Mohindra, V. (2003) Q fever as a biological weapon. Seminars in Respiratory Medicine 18: 183-195.

10. Maurin M, and Raoult, D. (1999) Q fever. Clinical Microbiology Reviews 12: 518-553.

11. Pappas G, Akritidis, N., and Tsianos, E.V. (2005) Attack scenarios with *Rickettsial* species: implications for response and management. Annals of the NY Academy of Sciences 1063: 451-458.

12. Parker NR, Barralet, J.H., and Bell, A.M. (2006) Q fever. The Lancet 367: 679-688.

13. Waag DM (2007) *Coxiella burnetii*: host and bacterial responses to infection. Vaccine 25: 7288-7295.

14. Karakousis PC, Trucksis, M., and Dumler, J.S. (2006) Chronic Q fever in the United States. Journal of Clinical Microbiology 44: 2283-2287.

15. Madariaga MG, Reazai, K., Trenholme, G.M., and Weinstein, R.A. (2003) Q fever: a biological weapon in your backyard. The Lancet Infectious Diseases 3: 709-721.

16. Hernychova L, Toman, R., Ciampor, F., Hubalek, M., Vackova, J., Macela, A., and Skultety, L. (2008) Detection and identification of *Coxiella burnetii* based on the mass spectrometric analyses of the extracted proteins. Analytical Chemistry 80: 7097-7104.

17. Seshadri R, Paulsen, I.T., Eisen, J.A., Read, T.D., Nelson, K.E., Nelson, W.C., Ward, N.L., Tettelin, H., Davidsen, T.M., Beanan, M.J., Deboy, R.T., Daugherty, S.C., Brinkac, L.M., Madupu, R., Dodson, R.J., Khouri, H.M., Lee, K.H., Carty, H.A., Scanlan, D., Heinzen, R.A., Thompson, H.A., Samuel, J.E., Fraser, C.M., and Heidelberg, J.F. (2003) Complete genome sequence of the Q-fever pathogen *Coxiella burnetii*. Proceedings of the National Academy of Sciences USA 100: 5455-5460.

18. http://www.cdc.gov/ncidod/dvrd/qfever/.

19. Beare PA, Samuel, J.E., Howe, D., Virtaneva, K., Porcella, S.F., and Heinzen, R.A. (2006) Genetic diversity of the Q fever agent, *Coxiella burnetii*, assessed by microarray-based whole genome comparisons. Journal of Bacteriology 188: 2309-2324.

20. Okutani SM (2007) Structuring Biodefense: Legacies and Current Policy Choices. Doctoral Dissertation, University of Maryland College Park.

21. Marmion BP, Storm, P.A., Ayres, J.G., Semendric, L., Mathews, L., Winslow, W., Turra, M., and Harris, R.J. (2005) Long-term persistence of *Coxiella burnetii* after acute primary Q fever. QJM 98: 7-20.

22. Helbig K, Harris, R., Ayres, J., Dunckley, H., Lloyd, A., Robson, J., and Marmion, B.P. (2005) Immune response genes in the post-Q-fever fatigue syndrome, Q fever endocarditis and uncomplicated acute primary Q fever. QJM 98: 565-574.

23. Channel BH Q-vax(R) Q Fever Vaccine Consumer Medicine Information.

24. Frischnecht F (2003) The history of biological warfare. EMBO Reports 4: S47-52.

25. Hackstadt T (1986) Antigenic variation in the phase I lipopolysaccharide of *Coxiella burnetii* isolates. Infection and Immunity 52: 337-340.

26. Moos A, and Hackstadt, T. (1987) Comparative virulence of intra- and interstrain lipopolysaccharide variants of *Coxiella burnetii* in the guinea pig model. Infection and Immunity 55: 1144-1150.

27. Ghigo E, Honstettre, A., Capo, C., Gorvel, J-P., Raoult, D., and Mege, J-L. (2004) Link between impaired maturation of phagosomes and defective *Coxiella burnetii* killing in patients with chronic Q fever. The Journal of Infectious Diseases 19: 1767-1772.

28. Zamboni DS, Mortara, R.A., Freymuller, E., and Rabionovitch, M. (2002) Mouse resident peritoneal macrophages partially control in vitro infection with *Coxiella burnetii* phase II. Microbes and Infection 4: 591-598.

29. Andoh M, Russell-Lodrigue, K.E., Zhang, G., and Samuel, J.E. (2005) Comparative virulence of phase I and phase II *Coxiella burnetii* in immunodeficient mice. Annals of the NY Academy of Sciences 1063: 167-170.

30. Amano K-i, and Williams, J.C. (1984) Chemical and immunological characterization of lipopolysaccharides from phase I and phase II *Coxiella burnetii*. Journal of Bacteriology 160: 994-1002.

31. Amano K-i, Williams, J.C., Missler, S.R., and Reinhold, V.N. (1987) Structure and biological relationships of *Coxiella burnetii* lipopolysaccharides. The Journal of Biological Chemistry 262: 4740-4747.

32. Hoover TA, Culp, D.W., Vodkin, M.H., Williams, J.C., and Thompson, H.A. (2002) Chromosomal DNA deletions explain phenotypic characteristics of two antigenic variants, phase II and RSA 514 (Crazy), of the *Coxiella burnetii* Nine Mile strain. Infection and Immunity 70: 6726-6733.

33. Heinzen RA, Hackstadt, T., and Samuel, J.E. (1999) Developmental biology of *Coxiella burnetii*. Trends in Microbiology 7: 149-154.

34. Baca OG, Roman, M.J., Glew, R.H., Christner, R.F., Buhler, J.E., and Aragon, A.S. (1993) Acid phosphatase activity in *Coxiella burnetii*. Infection and Immunity 61: 4232-4239.

35. Heinzen RA, Frazier, M.E., and Mallavia, L.P. (1992) *Coxiella burnetii* superoxide dismutase gene: cloning, sequencing, and expression in *Escherichia coli*. Infection and Immunity 60: 3414-3423.

36. Siemsen DW, Kirpotina, L.N., Jutila, M.A., and Quinn, M.T. (2009) Inhibition of the human neutrophil NADPH oxidase by *Coxiella burnetii*. Microbes and Infection 11: 671-679.

37. Coleman SA, Fischer, E.R., Howe, D., Mead, D.J., and Heinzen, R.A. (2004) Temporal analysis of *Coxiella burnetii* morphological differentiation. Journal of Bacteriology 186: 7344-7352.

38. Samoilis G, Psaroulake, A., Vougas, K., Tselentis, Y., and Tsiotis, G (2007) Analysis of whole cell lysate from the intercellular bacterium *Coxiella burnetii* using two gel-based protein separation techniques. Journal of Proteome Research 6: 3032-3041.

39. Samuel JE, Kiss, K., and Varghees, S. (2003) Molecular pathogenesis of *Coxiella burnetii* in a genomics era. Annals of the NY Academy of Sciences 990: 653-663.

40. Zamboni DS, and Rabinovitch, M. (2003) Nitric oxide partially controls *Coxiella burnetii* phase II infection in mouse primary macrophages. Infection and Immunity 71: 1225-1233.

41. Skultety L, Hernychova, L., Toman, R., Hubalek, M., Slaba, K., Zechovska, J., Stofanikova, V., Lenco, J., Stulik, J., and Macela, A. (2005) *Coxiella burnetii* whole cell lysate protein identification by mass spectrometry and tandem mass spectrometry. Annals of the NY Academy of Sciences 1063: 115-122.

42. Zusman T, Yerushalmi, G., and Segal, G. (2003) Functional similarities between the icm/dot pathogenesis systems of *Coxiella burnetii* and *Legionella pnuemophila*. Infection and Immunity 71: 3714-3723.

43. Wielang H, Hechtel, N., Faigle, M., and Neumeister, B. (2006) Efficient intracellular multiplication of *Legionella pneumophila* in human monocytes requires functional host cell L-type calcium channels. FEMS Immunology and Medical Microbiology 47: 296-301.

44. Andersson SGE, Zomorodipour, A., Andersson, J.O., Sicheritz-Pontén, T., Alsmark, U.C.M., Podowski, R.M., Näslund, A.K., Eriksson, A-S., Winkler, H.H., and Kurland, C.G. (1998) The genome sequence of *Rickettsia prowazekii* and the origin of mitochondria. Nature 396: 133-143.

45. Andoh M, Zhang, G., Russell-Lodrigue, K.E., Shive, H.R., Weeks, B.R., and Samuel, J.E. (2007) T cells are essential for bacterial clearance, and gamma interferon, tumor necrosis factor alpha, and B cells are crucial for disease development in *Coxiella burnetii* infection in mice. Infection and Immunity 75: 3245-3255.

46. Sakharkar KR, Dhar, P.K., and Chow, V.T.K. (2004) Genome reduction in prokaryotic obligatory intracellular parasites of humans: a comparative analysis. International Journal of Systematic and Evolutionary Microbiology 54: 1937-1941.

47. Andersson SGE, and Kurland, C.G. (1998) Reductive evolution of resident genomes. Trends in Microbiology 6: 263-268.

48. Wilcox JL, Dunbar, H.E., Wolfinger, R.D., and Moran, N.A. (2003) Consequences of reductive evolution for gene expression in an obligate endosymbiote. Molecular Microbiology 48: 1491-1500.

49. Stepkowski T, and Legocki, A.B. (2001) Reduction of bacterial genome size and expansion resulting from obligate intracellular lifestyle and adaptation to soil habitat. Acta Biochimica Polonica 48: 367-381.

50. Moran NA (2002) Microbial minimalism: genome reduction in bacterial pathogens. Cell 108: 583-586.

51. Janeway CA, Travers, P., Walport, M., and Shlomchik, M. (2001) Immunobiology: the immune system in health and disease: Garland Publishing.

52. Aderem A (2003) Phagocytosis and the inflammatory response. The Journal of Infectious Diseases 187: S340-345.

53. León B, and Ardavín, C. (2008) Monocyte-derived dendritic cells in innate and adaptive immunity. Immunology and Cell Biology 86: 320-324.

54. Hume DA (2006) The mononuclear phagocyte system. Current Opinion in Immunology 18: 49-53.

55. Underhill DM, and Ozinsky, A. (2002) Phagocytosis of microbes: complexity in action. Annual Review of Immunology 20: 825-852.

56. Ghigo E, Pretat, L., Desnues, B., Capo, D., Raoult, D., and Mege, J-L. (2009) Intracellular life of Coxiella burnetii in macrophages: an update. Annals of the NY Academy of Sciences 1166: 55-66.

57. Billack B (2006) Macrophage activation: role of Toll-like receptors, nitric oxide and nuclear factor kappa B. American Journal of Pharmaceutical Education 70.

58. Elkins KL, Cowley, S.C., and Bosio, C.M. (2007) Innate and adaptive immunity to *Francisella*. Annals of the NY Academy of Sciences 1105: 284-324.

59. Gauss KA, Nelson-Overton, L.K., Siemsen, D.W., Gao, Y., DeLeo, F.R., and Quinn, M.T. (2007) Role of NF-κB in transcriptional regulation of the phagocyte NADPH oxidase by tumor necrosis factor-α. Journal of Leukocyte Biology 82: 729-741.

60. DeLeo F (2004) Modulation of phagocyte apoptosis by bacterial pathogens. Apoptosis 9: 399-413.

61. Yagisawa M, Yuo, A., Yonemaru, M., Imajoh-Ohmi, S., Kanegasaki, S., Yazaki, Y., and Takaku, F. (1996) Superoxide release and NADPH oxidase components in mature human phagocytes: correlation between functional capacity and amount of functional proteins. Biochemical and Biophysical Research Communications 228: 510-516.

62. Puerto M, Pichardo, S., Jos, Á., Prieto, A.I., Sevilla, E., Frías, J.E., and Cameán, A.M. (2009) Differential oxidative stress responses to pur Microcystin-LR and Microcystin-containing and non-containing cyanobacterial crude extracts of Caco-2 cells. Toxicon epublication.

63. Trinchieri G, and Sher, A. (2007) Cooperation of Toll-like receptor signals in innate immune defense. Nature Reviews: Immunology 7: 179-190.

64. Rehli M (2002) Of mice and men: species variation of Toll-like receptor expression. TRENDS in Immunology 23: 375-378.

65. Takeda K, and Akira, S. (2005) Toll-like receptors in innate immunity. International Immunology 17: 1-14.

66. Meghari S, Honstettre, A., Lepidi, H., Ryffel, B., Raoult, D., and Mege-J-L. (2005) TLR2 is necessary to inflammatory response to *Coxiella burnetii* infection. Annals of the NY Academy of Sciences 1063: 161-166.

67. Horng T, Barton, G.M., Flavell, R.A., and Medzhitov, R. (2002) The adaptor protein TIRAP provides signaling specificity for Toll-like receptors. Nature 420: 329-333.

68. Lin Y, Lee, H., Berg, A.H., Lisanti, M.P., Shapiro, L., and Scherer, P.E. (2000) The lipopolysaccharide-activated Toll-like receptor (TLR)-4 induces synthesis of the closely

related receptor TLR-2 in adipocytes. The Journal of Biological Chemistry 275: 24255-24263.

69. Rajala MW, and Scherer, P.E. (2003) Minireview: the adipocyte-- at the crossroads of energy homeostasis, inflammation, and atherosclerosis. Endocrinology 144: 3765-3773.

70. Charriére G, Cousin, B., Arnaud, E., André, M., Bacou, F., Penicaud, L., and Casteilla, L. (2003) Preadipocyte conversion to macrophage. Evidence of plasticity. The Journal of Biological Chemistry 278: 9850-9855.

71. Elbim C, Katsikis, P.D., and Estaquier, J. (2009) Neutrophil apoptosis during viral infections. The Open Virology Journal 3: 52-59.

72. Voth DE, and Heinzen, R.A. (2009) Sustained activation of Akt and Erk 1/2 is required for *Coxiella burnetii* antiapoptotic activity. Infection and Immunity 77: 205-213.

73. Garin J, Diez, R., Kieffer, S., Dermine, J.F., Duclos, S., Gagnon, E., Sagoul, R., Rondeau, C., and Desjardins, M. (2001) The phagosome proteome: insight into phagosome functions. The Journal of Cell Biology 152: 165-180.

74. Lubick K, Radke, M., and Jutila, M. (2007) Securinine, a $GABA_A$ receptor antagonist, enhances macrophage clearance of phase II *C. burnetii*: comparison with TLR agonists. The Journal of Leukocyte Biology 82: 1062-1069.

75. Mata-Haro V, Cekic, C., Martin, M., Chilton, P.M., Casella, C.R., and Mitchell, T.C. (2007) The vaccine adjuvant monophosphoryl lipid A as a TRIF-based agonist of TLR4. Science 316: 1628-1632.

76. Casella CR, and Mitchell, T.C. (2008) Putting endotoxin to work for us: monophosphoryl lipid A as a safe and effective vaccine adjuvant. Cellular and Molecular Life Science 65: 3231-3240.

77. GlaxoSmithKline.

78. Beutler JA, Karbon, E.W., Brubaker, A.N., Malik, R., Curtis, D.R., and Enna, S.J. (1985) Securinine alkaloids: a new class of GABA receptor antagonist. Brain Research 330: 135-140.

79. www.invivogen.com/PDF/THP1-Blue-CD14v2_TDS.pdf.

80. Hagemann T, Biswas, S.K., Lawrence, T., Sica, A., and Lewis, C.E. (2009) Regulation of macrophage function in tumors: the multifaceted role of NF-{kappa}B. Blood 113: 3139-3146.

81. Coulthard LR, White, D.E., Jones, D.L., McDermott, M.F., and Burchill, S.A. (2009) p38(MAPK): stress responses from molecular mechanisms to therapeutics. TRENDS in Molecular Medicine 15: 369-379.

82. Alam S, Laughton, D.L., Walding, A., and Wolstenholme, A.J. (2006) Human peripheral blood mononuclear cells express $GABA_A$ receptor subunits. Molecular Immunology 43: 1432-1442.

83. Reyes-García MG, Hernández-Hernández, Fl., Hernádex-Téllez, B., and García-Tamayo, F. (2007) $GABA_A$ receptor subunits RNA expression in mice peritoneal macrophages modulate their IL-6/IL-12 production. Journal of Neuroimmunology 188: 64-68.

84. Bjurstöm H, Wang, J-Y., Ericsson, I., Bengtsson, M., Liu, Y., Kumar-Mendu, S., Issazadeh-Navikas, S., and Birnir, B. (2008) GABA, a natural immunomodulator of T lymphocytes. Journal of Neuroimmunology 205: 44-50.

85. Fritschy J-M, Johnson, D.K., Mohler, H., and Rudolph, U. (1998) Independent assembly and subcellular targeting of $GABA_A$-receptor subtypes demonstrated in mouse hippocampal and olfactory neurons *in vivo*. Neuroscience Letters 249: 99-102.

86. Chang Y, Wang, R., Barot, S., and Weiss, D.S. (1996) Stoichiometry of a recombinant $GABA_A$ receptor. The Journal of Neuroscience 16: 5415-5424.

87. Bergeret M, Khrestchatisky, M., Tremblay, E., Bernard, A., Gregoire, A., and Chany, C. (1998) GABA modulates cytotoxicity of immunocompetent cells expressing $GABA_A$ receptor subunits. Biomedicine and Pharmacotherapy 52: 214-219.

88. Song D-K, Suh, D-W., Huh, S-O., Jung, J-S., Ihn, B-M., Choi, I-G., Kim, Y-H. (1998) Central $GABA_A$ and $GABA_B$ receptor modulation of basal and stress-induced plasma interleukin-6 levels in mice. The Journal of Pharmacology and Experimental Therapeutics 287: 144-149.

89. Tian J, Lu, Y., Zhang, H., Chau, C.H., Dand, H.N., and Kaufman, D.L. (2004) γ-aminobutyric acid inhibits T cell autoimmunity and the development of inflammatory responses in a mouse type 1 diabetes model. the Journal of Immunology 173: 5298-5304.

90. Gardy JL, Lynn, D.J., Brinkman, F.S.L., and Hancock, R.E.W. (2009) Enabling a systems biology approach to immunology: focus on innate immunity. TRENDS in Immunology 30: 249-262.

91. Vodovotz Y, Csete, M., Bartels, J., Chang, S., and An, G. (2008) Translational systems biology in medicine. PLoS Computational Biology 4.

92. Raza S, Robertson, K.A., Lacaze, P.A., Page, D., Enright, A.J., Ghazal, P., and Freeman, T.C. (2008) A logic-based diagram of signaling pathways central to macrophage activation. BMC Systems Biology 2.

93. Zak DE, and Aderem, A. (2009) Systems biology of innate immunity. Immunological reviews 227: 264-282.

94. Wishart D Systems biology. Course lecture.

95. McGarvey PB, Huang, H., Mazumder, R., Zhang, J., Chen, Y., Zhang, C., Cammer, S., Will, R., Odle, M., Sobral, B., Moore, M., and Wu, C.H. (2009) Systems integration of biodefense omics data for analysis of pathogen-host interactions and identification of potential targets. PLoS One 4.

96. Nilsson R, Bajic, V.B., Suzuki, H., di Bernardo, D., Björkegren, J., Katayama, S., Reid, J.F., Sweet, M.J., Gariboldi, M., Carninci, P., Hayashizaki, Y., Hume, D.A., Tegner, J., and Ravasi, T. (2006) Transcriptional network dynamics in macrophage activation. Genomics 88: 133-142.

97. Ravasi T, Wells, C.A., and Hume, D.A. (2007) Systems biology of transcription control in macrophages. Bioessays 29: 1215-1226.

98. Rao PK, Singh, C.R., Jagannath, C., and Li, Q. (2009) A systems biology approach to study the phagosomal proteome modulated by mycobacterial infections. International Journal of Clinical and Experimental Medicine 2: 233-247.

99. Trost M, English, L., Lemieux, S., Courcelles, M., Desjardins, M., and Thibault, P. (2009) The phagosomal proteome in interferon-γ-activated macrophages. Immunity 30: 143-154.

100. Poupard JA, and Miller, L.A. (1992) History of biological warfare: catapults to capsomeres. Annals of the NY Academy of Sciences 666: 9-20.

101. van Aken J, and Hammond, E. (2003) Genetic engineering and biological weapons. EMBO Reports 4: S57-60.

102. http://news.bbc.co.uk/2/hi/programmes/file_on_4/4701196.stm.

103. Army USDot (1977) U.S. Army Activity in the U.S. Biological Warfare Program v.1 UNCLASSIFIED.

104. http://www.usamriid.army.mil/highlightspage.htm.

105. Walker JR (2003) Strengthening the BTWC. EMBO Reports 4: S61-S64.

106. http://en.wikipedia.org/wiki/Ken_Alibek.

107. Cello J, Paul, A.V., and Wimmer, E. (2002) Chemical synthesis of poliovirus cDNA: generation of infectious virus in the absence of natural template. Science 297: 1016-1018.

108. Beck V (2003) Advances in life sciences and bioterrorism. EMBO Reports 4: S53-56.

109. http://www.selectagents.gov/.

110. Bhattacharjee Y (2009) The Danger Within. Science 323: 1282-1283.

111. Graham B, and Talent J. (committee chairmen) (2010) Prevention of WMD proliferation and terrorism report card. none (government report).

112. Akinci MK, and Schofield, P.R. (1999) Widespread expression of $GABA_A$ receptor subunits in peripheral tissues. Neurocscience Research 35: 145-153.

113. Pearce MMP, Wormer, D.B., Wilkens, S., and Wojcikiewicz, R.J.H. (2009) An endoplasmic reticulum (ER) membrane complex composed of SPFH1 and SPFH2 mediates the ER-associated degradation of inositol 1,4,5-triphosphate receptors. 284 16.

114. Pearce MMP, Wang, Y., Kelley, G.G., and Wojcikiewicz, J.H. (2007) SPFH2 mediates the endoplasmic reticulum-associated degradation of inositol 1,4,5-triphosphate receptors and other substrates in mammalian cells. The Journal of Biological Chemistry 282: 20104-20115.

115. Ricci J-E, Muñoz-Pinedo, C., Fitzgerald, P., Bailly-Maitre, B., Perkins, G.A., Yadava, N., Scheffler, I.E., Ellisman, M.H., Green, D.R. (2004) Disruption of mitochondrial function during apoptosis is mediated by caspase cleavage of the p75 subunit of complex I of the electron transport chain. Cell 117: 773-786.

116. Dang PMS, A., Boussetta, T., Raad, J., Dewas, C., Kroviarski, Y., Hayem, G., Jensen, O.N., Gougerot-Pocidalo, M-A., and El-Benna, J. (2006) A specific p47phox-serine phosphorylated by convergent MAPKs mediates neutrophil NADPH oxidase priming at inflammatory sites. The Journal of Clinical Investigation 116: 2033-2043.

117. Greiner A, Lautwein, A., Overkleeft, H.S., Weber, E., and Driessen, C. (2003) Activity and subcellular distribution of cathepsins in primary human monocytes. Journal of Leukocyte Biology 73: 235-242.

118. Jiménez-Sainz MC, Murga, C., Kavelaars, A., Jurado-Pueyo, M., Krakstad, B.F., Heijnen, C.J., Mayor Jr., F., and Aragay, A.M. (2006) G protein-coupled receptor kinase 2 negatively regulates chemokine signaling at a level downstream from G protein subunits. Molecular Biology of the Cell 17: 25-31.

119. Lukashova V, Asselin, C., Krolewski, J.J., Rola-Pleszczynski, M., and Staňková, J. (2001) G protein independent activation of Tyk2 by the Platelet-Activating Factor receptor. The Journal of Biological Chemistry 276: 24113-24121.

120. Lukashova V, Chen, Z., Duhé, R.J., Rola-Pleszczynski, M., and Staňková, J. (2003) Janus Kinase 2 activation by the Platelet-Activating Factor receptor (PAFR): Roles of Tyk2 and PAFR C terminus. The Journal of Immunology 171: 3794-3800.

121. De Duve C, and Berthet, J. (1954) The use of differential centrifugation in the study of tissue enzymes. International Review of Cytology: 254-275.

122. Molloy MP (2000) Two-dimensional electrophoresis of membrane proteins using immobilized pH gradients. Analytical Biochemistry 280: 1-10.

123. Pedersen SK, Harry, J.L., Sebastian, L., Baker, J., Traini, M.D., McCarthy, J.T., Manoharan, A., Wilkins, M.R., Gooley, A.A., Righetti, P.G., Packer, N.H., Williams, K.L., and Herbert, B.R. (2003) Unseen proteome: mining below the tip of the iceberg to find low abundance and membrane proteins. Journal of Proteome Research 2: 303-311.

124. Righetti PG, Castagna, A., Antonioli, P., and Boschetti, E. (2005) Prefractionation techniques in proteome analysis: the mining tools of the third millennium. Electrophoresis 26: 279-319.

125. Santoni V, Kieffer, S., Desclaux, D., Masson, F., and Rabilloud, T. (2000) Membrane proteomics: use of additive main effects with multiplicative interaction model to classify plasma membrane proteins according to their solubility and electrophoretic properties. Electrophoresis 21: 3329-3344.

126. Twine SM, Mykytczujm N.C., Petit, M., Tremblay, T.L., Lanthier, P., Conlan, J.W., and Kelly, J.F. (2005) *Francisella tularensis* proteome: low levels of ASB-14 facilitate the visualization of membrane proteins in total protein extracts. Journal of Proteome Research 4: 1848-1854.

127. Twine SM, Petit, M.D., Shen, H., Mykytczuk, N.C.S., Kelly, J.F., and Conlan, J.W. (2006) Immunoproteomic analysis of the murine antibody response to successful and failed immunization with live anti-*Francisella* vaccines. Biochemical and Biophysical Research Communications 346: 999-1008.

128. Twine SM, Mykytczuk, N.C.S., Petit, M.D., Shen, H., Sjöstedt, A., Conlan, J.W., Kelly, J.F. (2006) *In vivo* proteomic analysis of the intracellular bacterial pathogen, *Francisella tularensis*, isolated from mouse spleen. Biochemical and Biophysical Research Communications 345: 1621-1633.

129. Australian Proteome Analysis F 2D Gel Manual.

130. Görg A (1998) Two-dimensional electrophoresis of proteins using immobilized pH gradients: A laboratory manual.

131. Healthcare GE Amersham CyDye DIGE Fluors (minimal dyes) for Ettan DIGE Product Booklet.

132. Karp NA, Spencer, M., Lindsay, H., O'Dell, K., and Lilley, K.S. (2005) Impact of replicate types on proteomic expression analysis. Journal of Proteome Research 4: 1867-1871.

133. Candiano G, Bruschi, M., Musante, L., Santucci, L., Ghiggeri, G.M., Carnemolla, B., Orecchia, P., Zardi, L., and Righetti, P.G. (2004) Blue silver: a very sensitive colloidal Coomassie G-250 staining for proteome analysis. Electrophoresis 25: 1327-1333.

134. Barry R (2003) Proteomic Analysis of *Sulfolobus solfataricus*, an Extremophilic *Archaeon*. Bozeman: Montana State University.

135. Han J, and Schey, K.L. (2004) Proteolysis and mass spectrometric analysis of an integral membrane: Aquaporin 0. Journal of Proteome Research 3: 807-812.

136. Perkins DN, Pappin, D.J.C., Creasy, D.M., and Cottrell, J.S. (1999) Probability-based protein identification by searching sequence databases using mass spectrometry data. Electrophoresis 20: 3551-3567.

137. Craig R, Cortens, J.P., and Beavis, R.C. (2004) Open source system for analyzing, validating, and storing protein identification data. Journal of Proteome Research 3: 1234-1242.

138. Craig R, Cortens, J.P., and Beavis, R.C. (2005) The use of proteotypic peptide libraries for protein identification. Rapid Communications in Mass Specrometry 19: 1844-1850.

139. Craig R, Cortens, J.P., Fenyo, D., and Beavis, R.C. (2006) Using annotated peptide mass spectrum libraries for protein identification. Journal of Proteome Research 5: 1843-1849.

140. Fenyo D, Phinney, B.S., and Beavis, R.C. (2007) Determining the overall merit of protein identification data sets: rho-diagrams and rho-scores. Journal of Proteome Research 6: 1997-2004.

141. Alban A, David, S.O., Bjorkesten, L., Andersson, C., Sloge, E., Lewis, S., and Currie, I. (2003) A novel experimental design for comparative two-dimensional gel analysis: two-dimensional difference gel electrophoresis incorporating a pooled internal standard. Proteomics 3: 36-44.

142. Karp NA, McCormick, P.S., Russell, M.R., and Lilley, K.S. (2007) Experimental and statistical considerations to avoid false conclusions in proteomics studies using differential in-gel electrophoresis. Molecular and Cellular Proteomics 6: 1354-1364.

143. Brett MT (2004) When is a correlation between non-independent variables "spurious"? Oikos 105: 647-656.

144. Hogg RV, and Craig, A.T. (1995) Introduction to Mathematical Statistics: Prentice Hall.

145. Johnson RA (1994) Miller & Freund's Probability & Statistics for Engineers: Prentice Hall.

146. Pabst MJ, Pabst, K.M., Handsman, D.B., Beranova-Giorgianni, S., and Giorgianni, F. (2008) Proteome of monocyte priming by lipopolysaccharide, including changes in interleukin-1 beta and leukocyte elastase inhibitor. Proteome Science 6.

147. Herbert B, GAlvani, M., Hamdan, M., Olivieri, E., MacCarthy, J., Pedersen, S., and Righetti, P.G. (2001) Reduction and alkylation of proteins in preparation of two-dimensional map analysis: Why, when, and how? Electrophoresis 22: 2046-2057.

148. Zheng Q, and Wang, X.J. (2008) GOEAST: a web-based software toolkit for Gene Ontology enrichment analysis. Nucleic Acids Research.

149. Huang DW, Sherman, B.T., Lempicki, R.A. (2009) Systematic and integrative analysis of large gene lists using DAVID bioinformatics resources. Nature Protocols 4: 44-57.

150. Dennis GJ, Sherman, B.T., Hosack, D.A., Yang, J., Gao, W., Lane, H.C., and Lempicki, R.A. (2003) DAVID: Database for annotation, visualization, and integrated discovery. Genome Biology 4: P3.

151. Breloer M, Dorner, B., Moré, S.H., Roderian, T., Fleischer, B., and von Bonin, A. (2001) Heat shock protein as "danger signals": eukaryotic Hsp60 enhances and accelerates antigen-specific IFN-ψ production in T cells. European Journal of Immunology 31: 2051-2059.

152. Lin SN, Ayada, K., Zhao, Y., Yokota, K., Takenaka, R., Okada, H., Kan, R., Hayashi, S., Mizuno, M., Hirai, Y., Fujinami, Y., Oguma, K. (2005) *Helicobacter pylori* heat-shock protein 60 induces production of the pro-inflammatory cytokine IL8 in monocytic cells. Journal of Medical Microbiology 54: 225-233.

153. Zhao Y, Yokota, K., Ayada, K., Yamamoto, Y., Okada, T., Shen, L., and Oguma, K. (2007) *Helicobacter pylori* heat-shock protein 60 induces interluekin-8 via a Toll-like receptor (TLR)2 and mitogen-activated protein (MAP) kinase pathway in human monocytes. Journal of Medical Microbiology 56: 154-164.

154. Kol A, Lichtman, A.H., Finberg, R.W., Libby, P., and Kurt-Jones, E.A. (2000) Cutting edge: heat shock protein (HSP) 60 activates the innate immune response: CD14 is an essential receptor for HSP60 activation of mononuclear cells. Journal of Immunology 164: 13-17.

155. Ausiello CM, Fedele, G., Palazzo, R., Spensieri, F., Ciervo, A., and Cassone, A. (2006) 60-kDa heat shock protein of *Chlamydia pneumoniae* promotes a T helper type 1 immune response through IL-12/IL-23 production in monocyte derived dendritic cells. Microbes and Infection 8: 714-720.

156. Chen W, Syldath, U., Bellmann, K., Burkart, V., and Kolb, H. (1999) Human 60-kDa heat-shock protein: a danger signal to the innate immune system. Journal of Immunology 162: 3212-3219.

157. Flóhe SB, Brüggemann, J., Lendemans, S., Nikulina, M., Meierhoff, G., Flóhe, S., and Kolb, H. (2003) Human heat shock protein 60 induces maturation of dendritic cells versus a Th1-promoting phenotype. The Journal of Immunology 170: 2340-2348.

158. Mertz AKH, Wu, P., Sturniolo, T., Stoll, D., Rudwaleit, M., Lauster, R., Braun, J., and Sieper, J. (2000) Multispecific $CD4^+$ T cell response to a singer 12-mer epitope of the immunodominant heat-shock protein 60 of *Yersinia enterocolitica* in *Yersinia*-triggered reactive arthritis: overlap with the B27-restricted CD8 epitope, functional properties, and epitope presentation by multiple DR alleles. The Journal of Immunology 164: 1529-1537.

159. Osterloh A, Kalinke, U., Weiss, S., Fleischer, B., and Breloer, M. (2007) Synergistic and differential modulation of immune responses by Hsp60 and lipopolysaccharide. The Journal of Biological Chemistry 282: 4669-4680.

160. Zanin-Zhorov A, Cahalon, L., Tal, G., Margalit, R., Lider, O., and Cohen, I.R. (2006) Heat shock protein 60 enhances $CD4^{+}CD25^{+}$ regulatory T cell function via innate TLR2 signaling. The Journal of Clinical Investigation 116: 2022-2032.

161. Pocklyey AG, Muthana, M., and Calderwood, S.K. (2008) The dual immunoregulatory roles of stress proteins. TRENDS in Biochemical Sciences 33: 71-79.

162. Bangen JM, Schade, F.U., and Flohé, S.B. (2007) Diverse regulatory activity of human heat shock proteins 60 and 70 on endotoxin-induced inflammation. Biochemical and Biophysical Research Communications 359: 709-715.

163. Gobert AP, Bambou, J-C., Werts, C., Balloy, V., Chignard, M., Moran, A.P., and Ferrero, R.L. (2004) *Helicobacter pylori* heat shock protein 60 mediates Interleukin-6 production by macrophages via a Toll-like receptor (TLR)-2-, TLR-4, and myeloid differentiation factor 88-independent mechanism. The Journal of Biological Chemistry 279: 245-250.

164. Habich C, Kempe, K., van der Zee, R., Burkart, V., and Kolb, H. (2003) Different heat shock protein 60 species share pro-inflammatory activity but not binding sites on macrophages. FEBS Letters 533: 105-109.

165. Habich C, and Burkart, V. (2007) Heat shock protein 60: regulatory role on innate immune cells. Cellular and Molecular Life Science 64: 742-751.

166. Habich C, Kempe, K., van der Zee, R., Rümenapf, R., Akiyama, H., Kolb, H., and Burkart, V. (2005) Heat shock protein 60: specific binding of lipopolysaccharide. The Journal of Immunology 174: 1298-1305.

167. Kilmartin B, and Reen, D.J. (2004) HSP60 induces self-tolerance to repeated HSP60 stimulation and cross-tolerance to other pro-inflammatory stimuli. European Journal of Immunology 34: 2041-2051.

168. Lehnardt S, Schott, E., Trimbuch, T., Laubisch, D., Krueger, C., Wulczyn, G., Nitsch, R., and Weber, J.R. (2008) A vicious cycle involving release of heat shock protein 60 from injured cells and activation of Toll-like receptor 4 mediates neurodegeneration in the CNS. The Journal of Neuroscience 28: 2320-2331.

169. Ohashi K, Burkart, V., Flohé, S., and Kolb, H. (2000) Cutting Edge: Heat shock protein 60 is a putative endogenous ligand of the Toll-like receptro-4 complex. The Journal of Immunology 164: 558-561.

170. Vabulas RM, Ahmad-Nejad, P., da Costa, C., Miethke, T., Kirschning, C.J., Hächer, H., and Wagner, H. (2001) Endocytosed HSP60s use Toll-like receptor 2 (TLR2) and TLR4 to

activate the Toll/Interleukin-1 receptor signaling pathway in innate immune cells. The Journal of Biological Chemistry 276: 31332-31339.

171. Flohé SB, Bangen, J.M., Flohé, S., Agrawal, H., Bergmann, K., and Schade, F.U. (2007) Origin of immunomodulation after soft tissue trauma: potential involvement of extracellular heat-shock proteins. Shock 27: 494-502.

172. Lang D, Hubrich, A., Dohle, F., Terstesse, M., Saleh, H., Schmidt, M., Pauels, H-G., and Heidenreich, S. (2000) Differential expression of heat shock protein 70 (hsp70) in human monocytes rendered apoptotic by IL-4 or serum deprivation. Journal of Leukocyte Biology 68: 729-736.

173. Li C-Y, Lee, J-S., Ko, Y-G., Kim, J-I., and Seo, J-S. (2000) Heat shock protein 70 inhibits apoptosis downstream of cytochrome c release and upstream of caspase-3 activation. The Journal of Biological Chemistry 275: 25665-25671.

174. Asea A, Kraeft, S-K., Kurt-Jones, E.A., Stevenson, M.A., Chen, L.B., Finberg, R.W., Koo, G.C., and Calderwood, S.K. (2000) HSP70 stimulates cytokine production through a CD14-dependant pathway, demonstrating its dual role as a chaperone and a cytokine. Nature Medicine 6: 435-442.

175. Wang Y, Whittall, T., McGowan, E., Younson, J., Kelly, C., Bergmeier, L.A., Singh, M., and Lehner, T. (2005) Identification of stimulating and inhibitory epitopes within the Heat Shock Protein 70 molecule that modulate cytokine production and maturation of dendritic cells. The Journal of Immunology 174: 3306-3316.

176. Wang R, Kovalchin, J.T., Muhlenkamp, P., and Chandawarkar, R.Y. (2006) Exogenous heat shock protein 70 binds macrophage lipid raft microdomain and stimulates phagocytosis, processing, and MHC-II presentation of antigens. Blood 107: 1636-1642.

177. Mortaz E, Redegeld, F.A., Nijkamp, F.P., Wong, H.R., Engels, F. (2006) Acetylsalicylic acid-induced release of Hsp70 from mast cells results in cell activation through TLR pathway. Experimental Hematology 34: 8-18.

178. el Mezayen R, el Gazzar, M., Seeds, M.C., McCall, C.E., Dreskin, S.C., and Nicolls, M.R. (2007) Endogenous signals released from necrotic cells augment inflammatory responses to bacterial endotoxin. Immunology Letters 111: 36-44.

179. Saba JA, McComb, M.E., Potts, D.L., Costello, C.E., and Amar, S. (2007) Proteomic mapping of stimulus-specific signaling pathways involved in THP-1 cells exposed to *Porphyromonas gingivalis* or its purified components. Journal of Proteome Research 6: 2211-2221.

180. Broquet AH, Thomas, G., Masliah, J., Trugnan, G., and Bachlet, M. (2003) Expression of the molecular chaperone Hsp70 in detergent-resistant microdomains correlates with its membrane delivery and release. The Journal of Biological Chemistry 278: 21601-21606.

181. Hunter-Lavin C, Davies, E.L., Bacelar, M.M.F.V.G., Marshall, M.J., Andrew, S.M., and Williams, J.H.H. (2004) Hsp70 release from peripheral blood mononuclear cells. Biochemical and Biophysical Research Communications 324: 511-517.

182. Panjwani NN, Popova, L., and Srivastava, P.K. (2002) Heat shock proteins gp96 and Hsp70 activate the release of nitric oxide by APCs. The Journal of Immunology 168: 2997-3003.

183. Gao B, and Tsan, M.F. (2003) Endotoxin contamination in recombinant human heat shock protein 70 (Hsp70) preparation is responsible for the induction of tumor necrosis factor alpha release by murine macrophages. The Journal of Biological Chemistry 278: 174-179.

184. Tsan MF, and Gao, B. (2004) Cytokine function of heat shock proteins. American Journal of Physiology Cellular Physiology 286: C739-744.

185. Vabulas RM, Ahmad-Nejad, P., Ghose, S., Kirschning, C.H., Issels, R.D., and Wagner, H. (2002) Hsp70 as endogenous stimulus of the Toll/Interleukin-1 Receptor signal pathway. The Journal of Biological Chemistry 277: 15107-15112.

186. Whittall T, Wang, Y., Younson, J., Kelly, C., Bergmeier, L., Peters, B., Singh, M., and Lehner, T. (2006) Interaction between the CCR5 chemokine receptors and microbial Hsp70. European Journal of Immunology 36: 2304-2314.

187. Sondermann H, Becker, T., Mayhew, M., Wieland, F., and Hartl, F-U. (2000) Characterization of a receptor for Heat Shock Protein 70 on macrophages and monocytes. Biological Chemistry 381: 1165-1174.

188. Aneja R, Odoms, K., Dunsmore, K., Shanley, T.P., and Wong, H.R. (2006) Extracellular heat shock protein-70 induces endotoxin tolerance in THP-1 cells. The Journal of Immunology 177: 7184-7192.

189. Molina L, Grimaldi, M., Robert-Hebmann, V., Espert, L., Varbanov, M., Devaux, C., Granier, C., and Biard-Piechaczyk, M. (2007) Proteomic analysis of the cellular responses induced in uninfected immune cells by cell-expressed X4 HIV-1 envelope. Proteomics 7: 3116-3130.

190. Wang J, and Brown, E.J. (1999) Immune complex-induced integrin activation and L-plastin phosphorylation require protein kinase A. The Journal of Biological Chemistry 274: 24349-24356.

191. Wang J, Chen, H., and Brown, E.J. (2001) L-plastin peptide activation of alpha(v)beta(3)-mediated adhesion requires integrin conformational change and actin filament disassembly. The Journal of Biological Chemistry 276: 14474-14481.

192. Mainiero F, Soriani, A., Strippoli, R., Jacobelli, J., Gismondi, A., Piccoli, M., Frati, L., and Santoni, A. (2000) RAC1/P38 MAPK signaling pathway controls β1 integrin-induced interleukin-8 production in human natural killer cells. Immunity 12: 7-16.

193. Chen H, Mocsai, A., Zhang, H., Ding, R-X., Morisake, J.H., White, M., Rothfork, J.M., Heiser, P., Colucci-Guyon, E., Lowell, C.A., Gresham, H.D., Allen, P.M., and Brown, E.J. (2003) Role for plastin in host defense distinguishes integrin signaling from cell adhesion spreading. Immunity 19: 95-104.

194. Correia I, Chu, D., Chou, Y-H., Goldman, R.D., and Matsudaira, P. (1999) Integrating the actin and vimentin cytoskeletons: adhesion-dependent formation of fimbrin-vimentin complexes in macrophages. The Journal of Cell Biology 146: 831-842.

195. Delanote V, Vandekerckhove, J., and Gettemans, J. (2005) Plastins: versatile modulators of actin organization in (patho)physiological cellular processes. Acta Pharmacologica Sinica 26: 769-779.

196. Janji B, Giganti, A., de Corte, V., Catillon, M., Bruyneel, E., Lentz, D., Plastino, J., Gettemans, J., and Friederich, E. (2006) Phosphorylation on Ser5 increases the F-actin-binding activity of L-plastin and promotes its targeting to sites of actin assembly in cells. Journal of Cell Science 119: 1947-1960.

197. Jones SL, and Brown, E.J. (1996) FcγRII-mediated adhesion and phagocytosis induce L-plastin phosphorylation in human neutrophils. The Journal of Biological Chemistry 271: 14623-14630.

198. Jones SL, Wang, J., Turck, C.W., and Brown, E.J. (1998) A role for the actin-bundling protein L-plastin in the regulation of leukocyte integrin function. Proceedings of the National Academy of Sciences USA 95: 9331-9336.

199. Oshizawa T, Yamaguchi, T., Suzuki, K., Yamamoto, Y., and Hayakawa, T. (2003) Possible involvement of optimally phosphorylated L-plastin in activation of superoxide-generating NADPH oxidase. Journal of Biochemistry 134: 827-834.

200. Samstag Y, Eibert, S.M., Klemke, M., and Wabnitz, G.H. (2003) Actin cytoskeletal dynamics in T lymphocyte activation and migration. Journal of Leukocyte Biology 73: 30-48.

201. Wabnitz GH, Köcher, Tl, Lohneis, P., Stober, C., Konstandin, M.H., Funk, B., Sester, U., Wilm, M., Klemke, M., and Samstag, Y. (2007) Costimulation induced phosphorylation of L-plastin facilitates surface transport of the T cell activation molecules CD69 and CD25. European Journal of Immunology 37: 649-662.

202. Liu F, Shinomiya, H., Kirikae, T., Hirata, H., and Asano, Y. (2004) Characterization of murine grancalcin specifically expressed in leukocytes and its possible role in host defense against bacterial infection. Bioscience, Biotechnology, and Biochemistry 68: 894-902.

203. Meconi S, Jacomo, V., Boquet, P., Raoult, D., Mege, J.L., and Capo. C (1998) *Coxiella burnetii* induces reorganization of the actin cytoskeleton in human monocytes. Infection and Immunity 66: 5527-5533.

204. Bishop SC, Burlison, J.A., and Blagg, B.S.J. (2007) Hsp90: A novel target for the disruption of multiple signaling cascades. Current Cancer Drug Targets 7: 369-388.

205. Buchner J (1999) Hsp90 & Co. - a holding for folding. TIBS 24: 136-141.

206. Picard D (2002) Heat-shock protein 90, a chaperone for folding and regulation. Cellular and Molecular Life Science 59: 1640-1648.

207. Pratt WB, and Toft, D.O. (2003) Regulation of signaling protein function and trafficking by the hsp90/hsp70-based chaperone machinery. Experimental Biology and Medicine 228: 111-133.

208. Binder RJ, and Srivastava, P.K. (2005) Peptides chaperoned by heat-shock proteins are a necessary and sufficient source of antigen in the cross-priming of $CD8^+$ T cells. Nature Immunology 6: 593-599.

209. Isaacs JS, Xu, W., and Neckers, L. (2003) Heat shock protein 90 as a molecular target for cancer therapeutics. Cancer Cell 3: 213-217.

210. Shang L, and Tomasi, T.B. (2006) The heat shock protein 90-CDC37 chaperone complex is required for signaling by Types I and II interferons. The Journal of Biological Chemistry 281: 1876-1884.

211. Arthur JC, Lich, J.D., Aziz, R.K., Kotb, M., and Ting, J.P-Y. (2007) Heat shock protein 90 associates with monarch-1 and regulates its ability to promote degradation of NF-κB-inducing kinase. The Journal of Immunology 179: 6291-6296.

212. Martinon F, and Tschopp, J. (2005) NLRs join the TLRs as innate sensors of pathogens. TRENDS in Immunology 26: 447-454.

213. Byrd CA, Bornmann, W., Erdjument-Bromage, H., Tempst, P., Pavletich, N., Rosen, N., Nathan, C.F., and Ding, A. (1999) Heat shock protein 90 mediates macrophage activation by Taxol and bacterial lipopolysaccharide. Proceedings of the National Academy of Sciences USA 96: 5645-5650.

214. Hsu HY, Wu, H.L., Tan, S.K., Li, V.P., Wang, W.T., Hsu, J., and Cheng, C.H. (2007) Geldanamycin interferes with the 90-kDa heat shock protein, affecting lipopolysaccharide-mediated interleukin-1 expression and apoptosis within macrophages. Molecular Pharmacology 71: 344-356.

215. Levin TC, Wickliffe, K.E., Leppla, S.H., and Moayeri, M. (2008) Heat shock inhibits caspase-1 activity while also preventing its inflammasome-mediated activation by anthrax lethal toxin. Cellular Microbiology 10: 2434-2446.

216. Mayor A, Martinon, F., de Smedt, T., Pétrilli, V., and Tschopp, J. (2007) A crucial function of Sgt1 and Hsp90 in inflammasome activity links mammalian and plant innate immune responses. Nature Immunology 8: 497-502.

217. Binder RJ, Blachere, N.E., and Srivastava, P.K. (2001) Heat shock protein-chaperoned peptides but not free peptides introduced into the cytosol are presented efficiently by Major Histocompatibility Complex I molecules. The Journal of Biological Chemistry 276: 17163-17171.

218. Rajagopal D, Bal, V., Mayor, S., George, A., and Rath, S. (2006) A role for Hsp90 molecular chaperone family in antigen presentation to T lymphocytes via Major Histocompatibility Complex Class II molecules. European Journal of Immunology 36: 828-841.

219. Benarafa C, Priebe, G.P., and Remold-O'Donnell, E. (2007) The neutrophil serine protease inhibitor serpinb1 preserves lung defense functions in *Pseudomonas aeruginosa* infection. The Journal of Experimental Medicine 204: 1901-1909.

220. Izuhara K, Ohta, S., Kanaji, S., Shiraishi, H., and Arima, K. (2008) Recent progress in understanding the diversity of the human ov-serpin/clade B serpin family. Cellular and Molecular Life Science 65: 2541-2553.

221. Managan MSJ, Kaiserman, D., and Bird, P.I. (2008) The role of serpins in vertebrate immunity. Tissue Antigens 72.

222. Silverman GA, Bird, P.I., Carrell, R.W., Church, F.C., Coughlin, P.B., Gettins, P.G.W., Irving, J.A., Lomas, D.A., Luke, C.J., Moyer, R.W., Pemberton, P.A., Remold-O'Donnell, E., Salvesen, G.S., Travis, J., and Whisstock, J.C. (2001) The serpins are an expanding superfamily of structurally similar but functionally diverse proteins. The Journal of Biological Chemistry 276: 33293-33296.

223. Benarafa C, Cooly, J., Zeng, W., Bird, P.I., and Remold-O'Donnell, E. (2002) Characterization of four murine homologs of the human ov-serpin Monocyte Neutrophil Elastase Inhibitor MNEI (SerpinB1). The Journal of Biological Chemistry 277: 42028-42033.

224. Tseng M-Y, Liu, S.Y., Chen, H-R., Wu, Y-J., Chiu, C-C., Chan, P-T., Chiang, W-F., Liu, Y-C., Lu, C-Y., Jou, Y-S., and Chen J., Y-F. (2009) Serine protease inhibitor (Serpin) B1 promotes oral cancer cell motility and is over-expressed in invasive oral squamous cell carcinoma. Oral Oncology: epublication ahead of print.

225. Cooley J, Takayama, T.K., Shapiro, S.D., Schechter, N.M., and Remold-O'Donnell, E. (2001) The serpin MNEI inhibits elastase-like and chymotrypsin-like serine proteases through efficient reactions at two active sites. Biochemistry 40: 15762-15770.

226. Zeng W, and Remold-O'Donnell, E. (2000) Human monocyte/neutrophil elastase inhibitor (MNEI) is regulated by PU.1/Spi1, Sp1, and NF-kB. Journal of Cellular Biochemistry 78: 519-532.

227. Yasumatsu R, Altiok, O., Benarafa, C., Yasumatsu, C., Bingol-Karakoc, G., Remold-O'Donnell, E., and Cataltepe, S. (2006) SerpinB1 upregulation is associated with in vivo complex formation of neutrophil elastase and cathepsin G in a baboon model of

bronchopulmonary dysplasia. American Journal of Physiology Lung, Cellular and Molecular Physiology 291: L619-627.

228. Woods DE, Cantin, A., Cooley, J., Kenney, D.M., and Remold-O'Donnell, E. (2005) Aerosol treatment with MNEI suppresses bacterial proliferation in a model of chronic *Pseudomonas aeruginosa* lung infection. Pediatric Pulmonology 39: 141-149.

229. Furuhashi M, and Hotamisligil, G.S. (2008) Fatty-acid binding proteins: role in metabolic diseases and potential as drug targets. Nature Reviews: Drug Discovery 7: 489-503.

230. Boord JB, Maeda, K., Makowski, L., Babaev, V.R., Fazio, S., Linton, M.F., Hotamisligil, G.S. (2004) Combined adipocyte-macrophage fatty acid-binding protein deficiency improves metabolism, atheroscelerosis, and survival in apolipoprotein E-deficient mice. Circulation 110: 1492-1498.

231. Maeda K, Cao, H., Kono, K., Gorgun, C.Z., Furuhashi, M., Uysal, K.T. Cao, Q., Atsumi, G., Malone, H., Krishnan, B., Minokoshi, Y., Kahn, B.B. Parker, R.A., and Hotamisligil, G.S. (2005) Adipocyte/macrophage fatty acid binding proteins control integrated metabolic responses in obesity and diabetes. Cell Metabolism 1: 107-119.

232. Maeda K, Uysal, K.T., Makowski, L., Görgün, C.Z., Atsumi, G., Parker, R.A., Brüning, J., Hertzel, A.V., Bernlohr, D.A., and Hotamisligil, G.S. (2003) Role of fatty acid binding protein mal1 in obesity and insulin resistance. Diabetes 52: 300-307.

233. Cao H, Maeda, K., Gorgun, C.Z., Kim, H-J., Park, S-Y., Shulman, G.I., Kim, J.S., and Hotamisligil, G.S. (2006) Regulation of metabolic responses by adipocyte/macrophage fatty acid-binding protens in leptin-deficient mice. Diabetes 55: 1915-1922.

234. Furuhashi M, Fucho, R., Görgün, C.Z., Tuncman, G., Cao, H., and Hotamisligil, G.S. (2008) Adipocyte/macrophage fatty acid-binding proteins contribute to metabolic deterioration through actions in both macrophages and adipocytes in mice. The Journal of Clinical Investigation 118: 2640-2650.

235. Garrett RH, and Grishamm C.M. (2005) Biochemistry: Thomsom Brooks/Cole.

236. Makowski L, Boord, J.B., Maeka, K., Babaev, V.R., Uysal, K.T., Morgan, M.A., Parker, R.A., Suttles, J., Fazio, S., Hotamisligil, G.S., and Linton, M.F. (2001) Lack of macrophage fatty-acid-binding protein aP2 protects mice deficient in apolipoprotein E against atherosclerosis. Nature Medicine 7: 699-705.

237. Maxfield FR, and Wüstner, D. (2002) Intracellular cholesterol transport. Journal of Clinical Investigation 110: 891-898.

238. Tan N-S, Shaw, N.S., Vinckenbosch, N., Liu, P., Yasmin, R., Desvergne, B., Wahli, W., and Noy, N. (2002) Selective cooperation between fatty acid binding proteins and peroxisome proliferator-activated receptors in regulating transcription. Molecular and Cellular Biology 22: 5114-5127.

239. Wang Y-X, Lee, C-H., Tiep, S., Yu, R.T., Ham, J., Kang, H., and Evans, R.E. (2003) Peroxisome-proliferator-activated receptor δ activates fat metabolism to prevent obesity. Cell 113: 159-170.

240. Berry DC, and Noy, N. (2007) Is PPARbeta/delta a retinoid receptor. PPAR Research.

241. Cao H, Gerhold, K., Mayers, J.R., Wiest, M.M., Watkins, S.M., and Hotamisligil, G.S. (2008) Identification of a lipokine, a lipid hormone linking adipose tissue to systemic metabolism. Cell 134: 933-944.

242. Carr SF, Papp, E., Wu, J.C., and Natsumeda, Y. (1993) Characterization of human type I and type II IMP dehydrogenase. The Journal of Biological Chemistry 268: 27286-27290.

243. Daxecker H, Raab, M., and Müller, M.M. (2002) Influence of mycophenolic acid on inosine 5'-monophosphate dehydrogenase activity in human peripheral blood mononuclear cells. Clinica Chimica Acta 318: 71-77.

244. Jonsson CA, and Carlsten, H. (2003) Mycophenolic acid inhibits inosin 5'-monophosphate dehydrogenase and suppresses immunoglobulin and cytokine production of B cells. International Immunopharcology 3: 31-37.

245. Jonsson CA, and Carlsten, H. (2002) Mycophenolic acid inhibits inosine 5'-monophosphate dehydrogenase and suppresses production of pro-inflammatory cytokines, nitric oxide, and LDH in macrophages. Cellular Immunology 216: 93-101.

246. Meshkini A, and Yazdanparast, R. (2008) Involvement of ERK/MAPK pathway in megakaryocytic differentiation of K562 cells induced by 3-hydogenkwadaphnin. Toxicology in Vitro 22: 1503-1510.

247. Moosavi MA, and Yazdanparast, R., (2008) Distinct MAPK signaling pathways, p21 up-regulation and caspase-mediated p21 cleavage establishes the fate of U937 cells exposed to 3-hydrogenkwadaphnin: differentiation *versus* apoptosis. Toxicology and Applied Pharmacology 230: 86-96.

248. Moosavi MA, Yazdanparast, R., Sanati, M.H., and Nejad, A.S. (2005) 3-hydrogenkwadaphnin targets inosine 5'-monophasphate dehydrogenase and triggers post-G1 arrest apoptosis in human leukemia cell lines. The International Journal of Biochemistry and Cell Biology 37: 2366-2379.

249. Shui H, Gao, P., Si, X., and Ding, G. (2009) Mycophenolic acid inhibits albumin-induced MCP-1 expression in renal tubular epithelial cells through the p38 MAPK pathway. Molecular Biology Reports epublication ahead of print.

250. Yazdanparast R, and Meshkini, A. (2009) 3-hydrogenkwadaphnine, a novel diterpene ester from *Dendrostellera lessertii*, its role in differentiation and apoptosis of KG1 cells. Phytomedicine 16: 206-214.

251. Jain J, Almquist, S.J., Ford, P.J., Shlyakhter, D., Wang, Y., Nimmesgern, E., and Germann, U.A. (2004) Regulation of inosine monophosphate dehydrogenase type I and type II isoforms in human lymphocytes. Biochemical Pharmacology 67: 767-776.

252. Dayton JS, Lindsten, T., Thompson, C.B., and Mitchell, B.S. (1994) Effects of human T lymphocyte activation on inosine monophosphate dehydrogenase expression. Journal of Immunology 152: 984-991.

253. Arnér ESJ, and Holmgren, A. (2000) Physiological functions of thioredoxin and thioredoxin reductase. European Journal of Biochemistry 267: 6102-6109.

254. Bertini R, Howard, O.M.Z., Dong, H-F., Oppenheim, J.J., Bizzarri, C., Sergi, R., Caselli, G., Pagliei, S. Romines, B., Wilshire, J.A., Mengozzi, M., Nakamura, H., Yodoi, J., Pekkari, K., Gurunath, R., Holmgren, A., Herzenberg, L.A., Herzenberg, L.A., and Ghezzi, P. (1999) Thioredoxin, a redox enzyme released in infection and inflammation, is a unique chemoattractant for neutrophils, monocytes, and T cells. The Journal of Experimental Medicine 189: 1783-1789.

255. Billiet L, Furman, C., Larigauderie, G., Copin, C., Brand, K., Fruchart, J-C., and Rouis, M. (2005) Extracellular human thioredoxin-1 inhibits lipopolysaccharide-induced interleukin-1β expression in human monocyte-derived macrophages. The Journal of Biological Chemistry 280: 40310-40318.

256. Go Y-M, Halvey, P.J., Hansen, J.M., Reed, M., Pohl, J., and Jones, D.P. (2007) Reactive aldehyde modification of thioredoxin-1 activates early steps of inflammation and cell adhesion. The American Journal of Pathology 171: 1670-1681.

257. Hirota K, Murata, M., Sachi, Y., Nakamura, H., Takeuchi, J., Mori, K., and Yodoi, J. (1999) Distinct roles of thioredoxin in the cytoplasm and in the nucleus. The Journal of Biological Chemistry 274: 27891-27897.

258. Williams Jr. CH (2000) Thioredoxin-thioredoxin reductase- a system that has come of age. European Journal of Biochemistry 267: 6101.

259. Pekkari K, Goodarzi, M.T., Scheynius, A., Holmgren, A., and Avila-Cariño, J. (2005) Truncated thioredoxin (Trx80) induces differentiation of human $CD14^{+}$ monocytes into a novel cell type (TAMs) via activation of the MAP kinases p38, ERK, and JNK. Blood 105: 1598-1605.

260. Saitoh M, Nishitoh, H., Fujii, M., Takeda, K., Toiume, K., Sawada, Y., Kawabata, M., Miyazono, K., and Ichijo, H. (1998) Mammalian thioredoxin is a direct inhibitor of apoptosis signal-regulating, kinase (ASK)1. The EMBO Journal 17: 2596-2606.

261. Zimmer DB, Sadosky, P.W., and Weber, D.J. (2003) Molecular mechanisms of S100-target protein interactions. Microscopy Research and Technique 60: 552-559.

262. Boye K, Grotterød, I., Aasheim, H-C., Hovig, E., and Mælandsmo, G.M. (2008) Activation of NF-kB by extracellular S100A4: analysis of signal transduction mechanisms and identification of target genes. International Journal of Cancer 123: 1301-1310.

263. Emberly ED, Murphy, L.C., and Watson, P.H. (2004) S100 proteins and their influence on pro-survival pathways in cancer. Biochemistry and Cell Biology 82: 508-515.

264. Hofmeister-Mueller V, Vetter-Kauczok, C.S., Ullrich, R., Meder, K., Lukanidin, E., Broecker, E-B., thor Strated, P., Andersen, M.H., Schrama, D., Becker, J.C. (2009) Immunogenicity of HLA-A1-restricted peptides derived from S100A4 (metastasin 1) in melanoma patients. Cancer Immunology and Immunotherapy 58: 1265-1273.

265. Kriajevska M, Fischer-Larsen, M., Moertz, E., Vorm, O., Tulchinsky, E., Grigorian, M., Ambartsumian, N., and Lukanidin, E. (2002) Liprin β1, a member of the family of LAR transmembane tyrosine phosphatase-interacting proteins, is a new target for the metatasis-associated protein S100A4 (Mts1). The Journal of Biological Chemistry 277: 5229-5235.

266. Mandinova AA, D., Schäfer, B.W., Spiess, M., Aebi, U., and Heizmann, C.W. (1998) Distinct subcellular localization of calcium binding S100 proteins in human smooth muscle cells and their relocation in response to rises in intracellular calcium. Journal of Cell Science 111: 2043-2054.

267. Novitskaya V, Grigorian, M., Kriajevska, M., Tarabykina, S., Bronstein, I., Berezin, V., Bock, E., and Lukanidin, E. (2000) Oligomeric forms of the metastasis-related Mts1 (S100A4) protein stimulate neuronal differentiation in cultures of rat hippocampal neurons. The Journal of Biological Chemistry 275: 41278-41286.

268. Pedersen KB, Andersen, K., Fodstad, Ø, and Mælandsmo, G. M. (2004) Sensitization of interferon-γ induced apoptosis in human osteosarcoma cells by extracellular S100A4. BMC Cancer 4: Article #52.

269. Tarabykina S, Griffiths, T.R.L., Tulchinsky, E., Mellon, J.K., Bronstein, I.B., and Kriajevska, M. (2007) Metastasis-associated protein S100A4: spotlight on its role in cell migration. Current Cancer Drug Targets 7: 217-228.

270. Watanabe Y, Usada, N., Minami, H., Morita, T., Tsugane, S-I., Ishikawa, R., Kohama, K., Tomida, Y., and Hidaka, H. (1993) Calvasculin, as a factor affecting the microfilament assemblies in rat fibroblasts transfected by *src* gene. FEBS Letters 324: 51-55.

271. Semov A, Moreno, M.J., Onichtchenko, A., Abulrob. A., Ball, M., Ekiel, I., Pietrzynski, G., Stanimirovic, D., and Alakhov, V. (2005) Metastasis-associated protein S100A4 induces angiogenesis through interaction with Annexin II and accelerated plasmin formation. The Journal of Biological Chemistry 280: 20833-20841.

272. Cui JF, Liu, Y.K., Zhang, L.J., Shen, H.L., Song, H.Y., Dai, Z., Yu, Y.L., Zhang, Y., Sun, R.X., Chen, J., Tang, Z.Y., and Yang, P.Y. (2006) Identification of metastasis candidate proteins

among HCC cell lines by comparative proteome and biological function analysis of S100A4 in metastasis *in vitro*. Proteomics 6: 5953-5961.

273. Rivard CJ, Brown, L.M., Aleida, N.E., Maunsbach, A.B., Pihakaski-Maunsbach, K., Andres-Hernando, A., Capasso, J.M., and Berl, T. (2007) Expression of the calcium binding protein S100A4 is markedly upregulated by osmotic stress and is involved in the renal osmoadaptive response. the Journal of Biological Chemistry 282: 6644-6652.

274. Dukhanina EA, Lukyanova, T.I., Romanova, E.A., Dukhanin, A.S., and Sashchenko, L.P. (2008) Comparative analysis of secretion of S100A4 metastatic marker by immune and tumor cells. Bulletin of Experimental Biology and Medicine 145: 78-80.

275. Honda T, Namiki, H., Kaneda, K., and Mizutani, H. (2004) First diastereoselective chiral synthesis of (-)-Securinine. Organic Letters 6: 87-89.

276. McKernan RM, and Whiting, P.J. (1996) Which $GABA_A$-receptor subtypes really occur in the brain? TRENDS in Neuroscience 19: 139-143.

277. Gadgil HS, Pabst, K.M., Giorgianni, F., Unstot, E.S., Desiderio, D.M., Beranova-Giorgianni, S., Gerling, I.C., and Pabst, M.J. (2003) Proteome of monocytes primed with lipopolysaccharide: analysis of the abundant proteins. Proteomics 3: 1767-1780.

278. Mishra S, Murphy, L.C., Nyomba, B.L.G., and Murphy, L.J. (2005) Prohibitin: a potential target for new therapeutics. TRENDS in Molecular Medicine 11: 192-197.

279. Nijtmans LGJ, de Jong, J., Sanz, M.A., Coates, P.J., Berden J.A., Back, J.W., Muijsers, A.O., van der Spek, H., and Grivell, L.A. (2000) Prohibitins act as a membrane-bound chaperone for the stabilization of mitochondrial proteins. The EMBO Journal 19: 2444-2451.

280. Rajalingam K, Wunder, C., Brinkmann, V., Churin, Y., Hekman, M., Sievers, C., Rapp. U.R., and Rudel, T. (2005) Prohibitin is required for Ras-induced Raf-MEK-ERK activation and epithelial cell migration. Nature Cell Biology 7: 837-843.

281. Sharma A, and Qadri, A. (2004) Vi polysaccharide of *Salmonella typhi* targets the prohibitin family of molecules in intestinal epithelial cells and suppresses early inflammatory responses. Proceedings of the National Academy of Sciences USA 101: 17492-17497.

282. Theiss AL, Idell, R.D., Srinivasan, S., Klapproth, J-M., Jones, D.P., Merlin, D., and Sitaraman, S.V. (2007) Prohibitin protects against oxidative stress in intestinal epithelial cells. The FASEB Journal 21: 197-206.

283. Vessal M, Mishra, S., Moulik, S., and Murphy, L.J. (2006) Prohibitin attenuates insulin-stimulated glucose and fatty acid oxidation in adipose tissue by inhibition of pyruvate carboxylase. The FEBS Journal 273: 568-576.

284. Browman DT, Resek, M.E., Zajchowski, L.D., and Robbins, S.M. (2006) Erlin-1 and erlin-2 are novel members of the prohibitin family of proteins that define lipid-raft-like domains of the ER. Journal of Cell Science 119: 3149-3160.

285. Kim K-B, Lee, J-W., Lee, C.S., Kim, B-W., Choo, H-J., Jung, S-Y., Chi, S-G., Soon, Y-S., Yoon, G., and Ko, Y-G. (2006) Oxidation-reduction respiratory chains and the ATP synthase complex are localized in detergent-resistant lipid rafts. Proteomics 6: 2444-2453.

286. Ciarlo L, Manganelli, V., Garofalo, T., Matarrese, P., Tinari, A., Misasi, R., Malorni, W., and Sorice, M. (2010) Association of fission proteins with mitochondrial raft-like domains. Cell Death and Differentiation: epublication ahead of print.

287. Garofalo T, Giammarioli, A.M., Misasi, R., Tinari, A., Manganelli, V., Gambardella, L., Pavan, A., Malorin, W., and Sorice, M. (2005) Lipid microdomains contribute to apoptosis-associated modifications of mitochondria in T cells. Cell Death and Differentiation 12: 1378-1389.

288. Sorice M, Manganelli, V., Matarrese, P., Tinari, A., Misasi, R., Malorni, W., and Garofalo, T. (2009) Cardiolipin-enriched raft-like microdomains are essential activating platforms for apoptotic signals on mitochondria. FEBS Letters 583: 2447-2450.

289. Barderas MG, Tuñón, J., Dardé, V.M., de la Cuesta, F., Jiménez-Nácher, J.J., Tarín, N., López-Bescós, L., Egido, J., and Vivanco, F. (2009) Atrovastatin modifies the protein profile of circulating human monocytes after an acute coronary syndrome. Proteomics 9: 1983-1993.

290. Ali BR, Wasmeier, C., Lamoreux, L., Strom, M., and Seabra, M.C. (2004) Multiple regions contribute to membrane targeting of Rab GTPases. Journal of Cell Science 117: 6401-6412.

291. Dong C, and Wu, G. (2007) Regulation of anterograde transport of adrenergic and angiotensin II receptors by Rab2 and Rab6 GTPases. Cellular Signalling 19: 2388-2399.

292. Tisdale EJ (1999) A rab2 mutant with impaired GTPase activity stimulates vesicle formation from pre-Golgi intermediates. Molecular Biology of the Cell 10: 1837-1849.

293. Tisdale EJ, Azizi, F., and Artalejo, C.R. (2009) Rab2 utilizes glyceraldehyde-3-phosphate dehydrogenase and protein kinase Cι to associate with microtubules and to recruit dynein. The Journal of Biological Chemistry 284: 5876-5884.

294. Girod A, Storrie, B., Simpson, J.C., Hohannes, L., Goud, B., Roberts, L.M., and Lord, J.M., Nilsson, T., and Pepperkok, R. (1999) Evidence for a COP-I-independent transport route from the Golgi complex to the endoplasmic reticulum. Nature Cell Biology 1: 423-430.

295. Marinez-Menarguez JA, Geuze, H.J., Slot, J.W., and Kumperman, J. (1999) Vesicular tubular clusters between the ER and Golgi mediate concentration of soluble secretory proteins by exclusion from COPI-coated vesicles. Cell 91: 81-90.

296. Bucci C, Thomsen, P., Nicoziani, P., McCarthy, J., and van Deurs, B. (2000) Rab7: A key to lysosome biogenesis. Molecular Biology of the Cell 11: 467-480.

297. Jäger S, Bucci, C., Tanida, I., Ueno, T., Kominami, E., Saftig, P., and Eskelinen, E-L. (2004) Role for Rab7 in maturation of late autophagic vacuoles. Journal of Cell Science 117: 4837-4838.

298. Yang M, Chen, T., Han, C. Li, N., Wan, T., and Cao, X. (2004) Rab7b, a novel lysosome-associated small GTPase, is involved in monocytic differentiation of human acute promyelocytic leukemia cells. Biochemical and Biophysical Research Communications 318: 792-799.

299. Burrell HE, Wlodarski, B., Foster, B.J., Buckley, K.A., Sharpe, G.R., Quayle, J.M., Simpson, A.W.M., and Gallagher, J.A. (2005) Human keratinocytes release ATP and utlize three mechanisms for nucleotide interconversion at the cell surface. The Journal of Biological Chemistry 280: 29667-29676.

300. Champagne E, Martinez, L.O., Collet, X., and Barbaras, R. (2006) Ecto-F_1F_0 ATP synthase/F_1 ATPase: metabolic and immunological functions. Current Opinion in Lipidology 17: 279-284.

301. Schnaufer A, Clark-Walker, G.D., Steinberg, A.G., and Stuart, K. (2005) The F1-ATP synthase complex in bloodstream stage trypanosomes has an unusual and essential function. The EMBO Journal 24: 4029-4040.

302. Bae T-J, Kim, M-S., Kim, J-W., Kim, B-W., Choo, H-J., Lee, J-W., Kim, K-B., Lee, C.S., Kim, J-H., Chang, S.Y., Kang, C-Y., Lee, S-W., and Ko, Y-G. (2004) Lipid raft proteome reveals ATP synthase complex in the cell surface. Proteomics 4: 3536-3548.

303. Moser TL, Stack, M.S., Asplin, I., Enghild, J.J., Højrup, P., Everitt, L., Hubchak, S., Schnaper, H.W., and Pizzo, S.V. (1999) Angiostatin binds ATP synthase on the surface of human endothelial cells. Proceedings of the National Academy of Sciences USA 96: 2811-2816.

304. Moser TL, Kenan, D.J., Ashley, T.A., Roy, J.A., Goodman, M.D., Misra, U.K., Cheek, D.J., and Pizzo, S.V. (2001) Endothelial cell surface F_1-F_0 ATP synthase is active in ATP synthesis and is inhibited by angiostatin. Proceedings of the National Academy of Sciences USA 98: 6656-6661.

305. Vantourout P, Martinez, L., O., Fabre, A., Collet, X., and Champagne, E. (2008) Ecto-F_1-Atpase and MHC class I close association on cell membranes. Molecular Immunology 45: 485-492.

306. Ashley RH (2003) Challenging accepted ion channel biology: p64 and the CLIC family of putative intracellular anion channel proteins. Molecular Membrane Biology 20: 1-11.

307. Edwards JC, and Kapadia, S. (2000) Regulation of the bovine kidney microsomal chloride channel p64 by $p59^{fyn}$, a Src family tyrosine kinase. The Journal of Biological Chemistry 275: 31826-31832.

308. Suginta W, Karoulias, N., Aitken, A., and Ashley, R.H. (2001) Chloride intracellular channel protein CLIC4 (p64H1) binds directly to brain dynamic I in a complex containing actin, tubulin, and 14-3-3 isoforms. Biochemical Journal 359: 55-64.

309. Moreland JG, Davis, A.P., Matsuda, J.J., Hook, J.S., Bailey, G., Nauseef, W.M., and Lamb, F.S. (2007) Endotoxin priming of neutrophils requires NADPH oxidase-generated oxidants and is regulated by the anion transporter Clc-3. The Journal of Biological Chemistry 282: 33958-33967.

310. Redhead C, Sullivan, S.K., Koseki, C., Fujiwara, K., and Edwards, J.C. (1997) Subcellular distribution and targeting of the intracellular chloride channel p64. Molecular Biology of the Cell 8: 691-704.

311. Thévenod F (2002) Ion channels in secretory granules of the pancreas and their role in exocytosis and release of secretory proteins. The American Journal of Physiology Cell Physiology 283: 651-672.

312. Shimamoto C, Umegaki, E., Katsu, K-i., Kato, M., Fujiwara, S., Kubota, T., and Nakahari, T. (2007) $[Cl^-]_i$ modulation of Ca^{2+}-regulated exocytosis in Ach-stimulated antral mucous cells of guinea pig. American Journal of Physiology Gastrointestinal and Liver Physiology 293: G824-837.

313. Choi D-S, Young, H., McMahon, T., Wang, D., and Messing, R.O. (2003) The mouse RACK1 gene is regulated by nuclear factor-κB and contributes to cell survival. Molecular Pharmacology 64: 1541-1548.

314. McCahill A, Warwicker, J., Bolger, G.B., Houslay, M.D., and Yarwood, S.J. (2002) The RACK1 scaffold protein: a dynamic cog in cell response mechanisms. Molecular Pharmacology 62: 1261-1273.

315. Keily PA, O'Gorman, D., Luong, K., Ron, R., and O'Connor, R. (2006) Insulin-like growth factor I controls a mutually exclusive association of RACK1 with proteins phosphatase 2A and β1 integin to promote cell migration Infection and Immunity 26: 4041-4051.

316. Sengupta J, Nilsson, J., Gursky, R., Spahn, C.M.T., Nissen, P., and Frank, J. (2004) Identification of the versatile scaffold protein RACK1 on the eukaryotic ribosome by cryo-EM. Nature Structural and Molecular Biology 11: 957-962.

317. Chen S, Lin, F., Shin, M.E., Wang, F., Shen, L., and Hamm, H.E. (2008) RACK1 regulates directional cell migration by acting on Gβγ at the interface with its effectors PLCβ and PI3Kγ. Molecular Biology of the Cell 19: 3909-3922.

318. Liu YV, and Semenza, G.L. (2007) RACK1 vs. Hsp90: Competition for HIF-1α degradation vs. stabilization. Cell Cycle 6: 656-659.

319. Liu YV, Hubbi, M.E., Pan, F., McDonald, K.R., Mansharamani, M., Cole, R.N., Liu, J.O., and Semenza, G.L. (2007) Calcineurin promotes hypoxia-inducible factor 1α expression by dephosphorylating RACK1 and blocking RACK1 dimerization. The Journal of Biological Chemistry 282: 37064-37073.

320. Aki D, Minoda, Y., Yoshida, H., Watanabe, S., Yoshida, R., Takaesu, G., Chinen, T., Inaba, T., Hikida, M., Kurosake, T., Saeki, K., Yoshimura, A. (2008) Peptidoglycan and lipopolysaccaride activate PLCy2, leading to enhanced cytokine production in macrophages and dendritic cells. Genes to Cells 13: 199-208.

321. Corsini E, Racchi, M., Sinforiani, E., Lucchi, L., Viviani, B., Rovati, G.E., Govoni, S., Galli, C.L., and Marinovich, M. (2005) Age-related decline in RACK-1 expression in human leukocytes is correlated to plasma levels of dehydroepiandrosterone. Journal of Leukocyte Biology 77: 247-256.

322. Hauber H-P, Goldmann, T., Vollmer, E., Wollenberg, B., Hung, H-L., Levitt, R.C., and Zabel, P. (2007) LPS-induced mucin expression in human sinus mucosa can be attenuated bh hCLCA inhibitors. Journal of Endotoxin Research 13: 109-116.

323. Patterson RL, van Rossum, D.B., Barrow, R.K., and Snyder, S.H. (2004) RACK1 binds to inositol 1,4,5-triphosphate receptors and mediates Ca^{2+} release. Proceedings of the National Academy of Sciences USA 101: 2328-2332.

324. Gimona M, Kazzaz, J.A., and Helfman, D.M. (1996) Forced expression of tropomyosin 2 or 3 in v-Ki-ras-transformed fibroblasts results in distinct phenotypic effects. Proceedings of the National Academy of Sciences USA 93: 9618-9623.

325. Gunning PW, Schevzov, G., Kee, A.J., and Hardeman, E.C. (2005) Tropomyosin isoforms: divining rods for actin cytoskeleton function. Trends in Cell Biology 15: 333-341.

326. McMichael BK, Kotadiya, P., Singh, T., Holliday, L.S., and Lee, B.S. (2006) Tropomyosin isoforms localize to distinct microfilament populations in osteoclasts. Bone 39: 694-705.

327. Perez-Gracia E, Blanco, R., Carmona, M., Carro, E., and Ferrer, I. (2009) Oxidative stress damage and oxidative stress responses in the choroid plexus in Alzheimer's disease. Acta Neuropathologica 118: 497-504.

328. Leclère V, Chotteau-Lelièvre, A., Gancel, F., Imbert, M., and Blondeau, R. (2001) Occurrence of two superoxide dismutases in *Aeromonas hydrophila*: molecular cloning and differential expression of the sodA and sodB genes. Microbiology and Molecular Biology Reviews 147: 3105-3111.

329. Yu J, Yu, X., and Liu, J. (2004) A thermostable manganese-containing superoxide dismutase from pathogen *Chlamydia pneumoniae*. FEBS Letters 562: 22-26.

330. Carroll IM, Andrus, J.M., Bruno-Bácena, J.M., Klaenhammer, T.R., Hassan, H.M., and Threadgill, D.S. (2007) Anti-inflammatory properties of *Lactobacillus gasseri*, expressing manganese superoxide dismutase using the interleukin 10-deficient mouse model of colitis. American Journal of Physiology Gastrointestinal and Liver Physiology 293: G729-738.

331. Baca OG, Li, Y.P., and Kumar, H. (1994) Survival of the Q fever agent *Coxiella burnetii* in the phagolysosome. Trends in Microbiology 2: 476-480.

332. Heinzen RA, Scidmore, M.A., Rockey, D.D., and Hackstadt, T. (1996) Differential interaction with endocytic and exocytic pathways distinguish vacuoles of *Coxiella burnetii* and *Chlamydia trachomatis*. Infection and Immunity 64: 796-809.

333. Werber MM, and Greenstein, L.A. (1991) Biochemical and stability properties of recombinant human MnSOD. Free Radical Research 12: 335-348.

334. Wheeler MD, Nakagami, M., Bradford, B.U., Uesugi, T., Mason, R.P., Connor, H.D., Dikalova, A., Kadiiska, M., and Thurman, R.G. (2001) Overexpression of manganese superoxide dismutase prevents alcohol-induced liver injury in the rat. The Journal of Biological Chemistry 276: 36664-36672.

335. Agnihotri G, and Liu, H-W. (2003) Enoyl-CoA hydratase: Reaction, mechanism, and inhibition. Bioorganic and Medicinal Chemistry 11: 9-20.

336. Takahashi M, Watari, E., Shinya, E., Shimizu, T., and Takahashi, H. (2007) Suppression of virus replication via down-modulation of mitochondrial short chain enoyl-CoA hydratase in human glioblastoma cells. Antiviral Research 75: 152-158.

337. Watari E, Shinya, E., Kurane, S., Tahahashi, H. (2001) Effects of cyclosporin A on cell fusion in a monkey kidney cell line persistently infected with measles virus. Intervirology 44: 209-214.

338. Yokoyama Y, Kuramitsu, Y., Takashima, M., Iizuka, N., Toda, T., Terai, S., Sakaida, I., Oka, M., Nakamura, K., and Okita, K. (2004) Proteomic profiling of proteins decreased in hapatocellular carcinoma from patients infected with hepatitis C. Proteomics 4: 2111-2116.

339. Huang Q, Jin, X., Gaillard, E.T., Knight, B.L., Pack, F.D., Stoltz, J.H., Jayadev, S., and Blanchard, K.T. (2004) Gene expression profiling reveals multiple toxicity endpoints induced by hepatotoxicants. Mutation Research 549: 147-168.

340. Ohhira M, Motomura, W., Fukuda, M., Yoshizaki, T., Takahashi, N., Tanno, S., Wakamiya, N., Kohgo, Y., Kumei, S., and Okumura, T. (2007) Lipopolysaccharide induces adipose differentiation-related protein expression and lipid accumulation in the liver through inhibition of fatty acid oxidation in mice. Journal of Gasteroenterology 42: 969-978.

341. Lebrand C, Corti, M., Goodson, H., Cosson, P., Cavalli, V., Mayran, N., Fauré, J., and Gruenberg, J. (2002) Later endosome motility depends on lipids via the small GTPase Rab7. The EMBO Journal 21: 1289-1300.

342. Kang JH, Kim, H.T., Choi, M-S., Lee, W.H., Huh, T-L., Park, Y.B., Moon, B.J., and Kwon, O-S. (2006) Proteome analysis of human monocytic THP-1 cells primed with oxidized low-density lipoproteins. Proteomics 6: 1261-1273.

343. Mor-Vaknin N, Punturieri, A., Sitwala, K., and Markovitz, D.M. (2003) Vimentin is secreted by activated macrophages. Nature Cell Biology 5: 59-63.

344. Beneš P, Macečková, V., Zdráhal, Z., Konečna, H., Zahradníčková, E., Mužík, J., and Šmarda, J. (2006) Role of vimentin in regulation of monocyte/macrophage differentiation. Differentiation 74: 265-276.

345. Tsuru A, Nakamura, N., Takayama, E., Suzuki, Y., Hirayoshi, K., and Nagata, K. (1990) Regulation of the expression of vimentin gene during the differentiation of mouse myeloid leukemia cells. The Journal of Cell Biology 110: 1655-1664.

346. Bouchard A, Ratthé, C., and Girard, D. (2004) Interleukin-15 delays human neutrophil apoptosis by intracellular events and not via extracellular factors: role of Mcl-1 and decreased activity of caspase-3 and caspase-8. Journal of Leukocyte Biology 75: 893-900.

347. Eriksson JE, He, T., Trejo-Skalli, A.V., Härmälä-Braskén, A-S., Hellman, J., Chou, Y-H., and Goldman, R.D. (2004) Specific in vivo phosporylation sites determine the assembly dynamics of vimentin intermediate filaments. Journal of Cell Science 117: 919-932.

348. Zheng M, Son, M-Y., Park, C, Park, J-I., Jo, E-K., Yoon, W-H., Park, S-K., Hwang, B-D., and Lim, K. (2005) Transcriptional repression of vimentin gene expression by pyrroline dithiocarbamate during 12-O-tetradecanoyl-phorbol-13-acetate-dependent differentiation of HL-60 cells. Oncology Reports 14: 713-717.

349. Baek HY, Lim, J.W., Kim, H., Kim, J.M., Kim, J.S., Jung, H.C., and Kim, K.H. (2004) Oxidative-stress-related proteome changes in *Helicobacter pylori*-infected human gastric mucosa. Biochemical Journal 379: 291-299.

350. Ohda S, Ohsawa, I., Kamino, K., Ando, F., and Shimokata, H. (2004) Mitochondrial ALDH2 deficiency as an oxidative stress. Annals of the NY Academy of Sciences 1011: 36-44.

351. Mollnau H, Wenzel, P., Oelze, M., Treiber, N., Pautz, A., Schulz, E., Schuhmacher, S., Reifenberg, K., Stalleicken, D., Scharffetter-Kochanek, K., Kleinert, H., Münzel, T., and Daiber, A. (2006) Mitochondrial oxidative stress and nitrate tolerance-comparison of nitroglycerin and pentaerithrityl tetranitrate in Mn-SOD +/- mice. BMC Cardiovascular Disorders 6: 44-53.

352. Aragon AD, Imani, R.A., Blackburn, V.R., and Cunningham, C. (2008) Microarray based analysis of temperature and oxidative stress induced messenger RNA in *Schistosoma mansoni*;. Molecular and Biochemical Parasitology 162: 134-141.

353. Griffen TJ, Gygi, S.P., Ideker, T., Rist, B., Eng, J., Hood, L., and Aebersold, R. (2002) Complementary profiling of gene expression at the transcriptome and proteome levels in *Saccharomyces cerevisiae*. Molecular and Cellular Proteomics 1: 323-333.

354. Li X-M, Patel, B.B., Blagoi, E.L., Patterson, M.D., Seeholzer, S.H., Zhang, T., Damle, S., Gao, Z., Boman, B., and Yeung, A.T. (2004) Analyzing alkaline proteins in human colon crypt proteome. Journal of Proteome Research 3: 821-833.

355. Raquil M-A, Anceriz, N., Rouleau, P., and Tessier, P.A. (2008) Blockade of antimicrobial proteins S100A8 and S100A9 inhibits phagocyte migration to the alveoli in *Streptococcal* pneumonia. The Journal of Immunology 180: 3366-3374.

356. Steinbrink K, Schönlau, F., Rescher, U., Henseleit, U., Vogel, T., Sorg, C., and Sunderkötter, C. (2000) Ineffective elimination of *Leishmania major* by inflammatory (MRP14-positive) subtype of monocytic cells. Immunobiology 202: 442-459.

357. Srikrishna G, Panneerselvam, K., Westphal, V., Abraham, V., Varki, A., and Freeze, H.H. (2001) Two proteins modulating transendothelial migration of leukocytes recognize novel carboxylated glycans on endothelial cells. The Journal of Immunology 166: 4678-4688.

358. Rundhaug JE, Hawkins, K.A., Pavone, A., Gaddis, S., Kil, H., Klein, R.D., Berton, T.R., McCauley, E., Johnson, D.G., Lubet, R.A., Fischer, S.M., and Aldaz, C.M. (2005) SAGE profiling of UV-induced mouse skin squamous cell carconomas, comparison with acute UV irradiation effects. Molecular Carcinogenesis 42: 40-52.

359. Thorey IS, Roth, J., Regenbogen, J., Halle, J-P., Bittner, M., Vogl, T., Kaesler, S., Bugnon, P., Reitmaier, B., Durka, S., Graf, A., Wöckner, M., Rieger, N., Konstantinow, A., Wolf, E., Goppelt, A., and Werner, S. (2001) The Ca^{2+}-binding proteins S100A8 and S100A9 are encoded by novel injury-regulated genes. The Journal of Biological Chemistry 276: 35818-35825.

360. Hinkle DJ, and Macdonald, R.L. (2003) Beta subunit phosphorylation selectively increases fast desensitization and prolongs deactivation of alpha1beta1gamma2L and alpha1beta3gamma2L GABA(A) receptor currents. Journal of Neuroscience 23: 11698-11710.

361. Vieira OV, Bothelho, R.J., Rameh, L., Brachmann, S.M., Matsuo, T., Davidson, H.W., Schreiber, A., Backer, J.M., Cantley, L.C., and Grinstein, S. (2001) Distinct roles of class I and class III phosphatidylinositol 3-kinases in phagosome formation and maturation. The Journal of Cell Biology 155: 19-25.

362. Vieira OV, Bucci, C., Harrison, R.E., Trimble, W.S., Lanzetti, L., Gruenberg, J., Schreiber, A.D., Stahl, P.D., and Grinstein, S. (2003) Modulation of Rab5 and Rab7 recruitment to phagosomes by phosphatidylinositol 3-kinase. Molecular and Cellular Biology 23: 2501-2514.

363. Vieira OV, Botelho, R.J., and Grinstein, S. (2002) Phagosome maturation: aging gracefully. Biochemical Journal 356: 689-704.

364. Feng Y, Press, B., and Wandinger-Ness, A. (1995) Rab7: An important regulator of late endocytic membrane traffic. The Journal of Cell Biology 131: 1435-1452.

365. Berón W, Alverez-Dominguez, C., Mayorga, L., and Stahl, P.D. (1995) Membrane trafficking along the phagocytic pathway. Trends in Cell Biology 5: 100-104.

366. Duclos S, and Desjardins, M. (2000) Subversion of a young phagosome: the survival strategies of intracellular pathogens. Cellular Microbiology 2: 365-377.

367. Jordens I, Fernandez-Borja, M., Marsman, M., Dusseljee, S., Janssen, L., Calafat, J., Janssen, H., Wubbolts, R., and Neefjes, J. (2001) The Rab7 effector protein RILP controls lysosomal transport by inducing the recruitment of dynein-dynactin motors. Current Biology 11: 1680-1685.

368. Cantalupo G, Alifano, P., Roberti, V., Bruni, C.B., and Bucci, C. (2001) Rab-interacting lysosomal protein (RILP): the Rab7 effector required by transport to lysosomes. The EMBO Journal 20: 686-693.

369. Harrison RE, Bucci, C., Vieira, O.V., Schroer, T.A., and Grinstein, S. (2003) Phagosomes fuse with late endosomes and/or lysosomes by extension of membrane protrusions along microtubules: Role of Rab7 and RILP. Molecular and Cellular Biology 23: 6494-6506.

370. Howe D, and Mallavia, L.P. (2000) *Coxiella burnetii* exhibits morphological change and delays phagolysosomal fusion after internalization by J774A.1 cells. Infection and Immunity 68: 3815-3821.

371. Ghigo E, Capo, C., Tung, C-H., Raoult, D., Gorvel, J-P., and Mege, J-L. (2002) Coxiella burnetii survival in THP-1 monocytes involves the impairment of phagosome maturation: IFN-γ mediates its restoration and bacterial killing. The Journal of Immunology 169: 4488-4495.

372. Greub G, Mege, J.L., Gorvel, J.P., Raoult, D, and Méresse, S. (2005) Intracellular trafficking of *Parachlamydia acanthamoebae*. Cellular Microbiology 7: 581-591.

373. Howe D, Melnicáková, J., Barák, I., and Heinzen, R.A. (2003) Maturation of the *Coxiella burnetii* parasitophorous vacuole requires bacterial protein synthesis but not replication. Cellular Microbiology 5: 469-480.

374. Li N, Mak, A., Richards, D.P., Naber, C., Keller, B.O., Li, L., and Shaw, A.R.E. (2003) Monocyte lipid rafts contain proteins implicated in vesicular trafficking and phagosome formation. Proteomics 3: 536-548.

375. Howe D, and Heinzen, R.A. (2006) *Coxiella burnetii* inhabits a cholesterol-rich vacuole and influences cellular cholesterol metabolism. Cellular Microbiology 8: 496-507.

376. Voth DE, and Heinzen, R.A. (2007) Lounging in a lysosome: the intracellular lifestyle of *Coxiella burnetii*. Cellular Microbiology 9: 829-840.

377. Adam O, and Laufs, U. (2008) Antioxidative eVects of statins. Archives of Toxicology 82: 885-892.

378. Liao JK, and Laufs, U. (2005) Pleiotropic effects of statins. Annual Review of Phamacology and Toxicology 45: 89-118.

379. Voth DE, and Heinzen, R.A. (2009) *Coxiella* type IV secretion and cellular microbiology. Current Opinion in Microbiology 12: 74-80.

380. Romano PS, Gutierrez, M.G., Berón, W., Rabinovitch, M., and Columbo, M.I. (2007) The autophagic pathway is actively modulated by phase II *Coxiella burnetii* to efficiently replicate in the host cell. Cellular Microbiology 9: 891-909.

381. Vitelli R, Santillo, M., Lattero, D., Chiariello, M., Bifulco, M., Bruni, C.B., and Bucci, C. (1997) Role of small GTPase Rab7 in the late endocytic pathway. The Journal of Biological Chemistry 272: 4391-4397.

382. Bhattacharya M, Ojha, N., Solanki, S., Mukhopadhyay, C.K., Madan, R., Patel, N., Krishnamurthy, G., Kumar, S., Basu, S.K., and Mukhopadhyay, A. (2006) IL-6 and IL-12 specifically regulate the expression of Rab5 and Rab7 via distinct signaling pathways. The EMBO Journal 25: 2878-2888.

383. Scianimanico S, Desrosiers, M., Dermine, J-F., Mérese, S., Descoteaux, A., and Desjardins, M. (1999) Impaired recruitment of the small GTPase Rab7 correlates with the inhibition of phagosome maturation by *Leishmania donovani* promastigotes. Cellular Microbiology 1: 19-32.

384. Amer AO, and Swanson, M.S. (2002) A phagosome of one's own: a microbial guide to life in the macrophage. Current Opinion in Microbiology 5: 56-61.

385. Wang Y, Chen, T., Han, C., He, D., Liu, H., An, H., Cai, Z., and Cao, X. (2007) Lysosome-associated small Rab GTPase Rab7b negatively regulates TLR4 signaling in macrophages by promoting lysosomal degradation of TLR4. Blood 110: 962-971.

386. Xu HE, and Johnston, S.A. (1994) Yeast bleomycin hydrolase is a DNA-binding cysteine protease. The Journal of Biological Chemistry 269: 2117-2183.

387. Zimny J, Sikora, M., Guranowski, A., and Jakubowski, H. (2006) Protective mechanisms against homocysteine toxicity: the role of bleomycin hydrolase. The Journal of Biological Chemistry 281: 22485-22492.

388. Kageyama T, Suzuki, K., and Ohsumi, Y. (2009) Lap3 is a selective target of autophagy in yeast, *Saccharomyces cerevisiae*. Biochemical and Biophysical Research Communications 378: 551-557.

389. Raisner RM, and Madhani, H.D. (2008) Genomewide screen for negative regulators of sirtuin activity in *Saccharomyces cerevisiae* reveals 40 loci and links to metabolism. Genetics 179: 1933-1944.

390. Garg S, Vitvitsky, V., Gendelman, H.E., and Banerjee, R. (2006) Monocyte differentiation, activation, and mycobacterial killing are linked to transsulfuration-dependent redox metabolism. The Journal of Biological Chemistry 281: 3872-3820.

391. Schini-Kerth VB (2009) Homocysteine, a proinflammatory and proatheroscleritic factor. Circulation Research 93: 271-273.

392. Schroecksnadel K, Frick, B., Winkler, C., Wirleitner, B., Schennach, H., and Fuchs, D. (2005) Asprin downregulates homocysteine formation in stimulated human peripheral blood mononuclear cells. Scandanavian Journal of Immunology 62: 155-160.

393. Schroecksnadel K, Frick, B., Wirleitner, B., Schennach, H., and Fuchs, D. (2003) Homocysteine accumulates in supernatents of stimulated human peripheral blood mononuclear cells. Clinical and Experimental Immunology 134: 53-56.

394. Toohey JI (2008) Homocysteine toxicity in connective tissue: theories, old and new. Connective Tissue Research 49: 57-61.

395. Adya R, Tan, B.K., Chen, J., and Randeva, H.S. (2009) Pre-B cell colony enhancing factor (PBEF)/visfatin induces secretion of MCP-1 in human endothelial cells: Role in visfatin-induced angiogenesis. Atherosclerosis epub ahead of print: epub ahead of print.

396. Busso N, Karababa, M., Nobile, M., Rolaz, A., van Gool, F., Galli, M., Leo, O., So, A., and de Smedt, T. (2008) Pharmacological inhibition of nicotinamide phosphoribosyltransferase/visfatin enzymatic activity identifies a new inflammatory pathway linked to NAD. PLoS One 3: e2267.

397. Jia SH, Li, Y., Parodo, J., Kapus, A., Fan, L., Rotstein, O.D., and Marshall, J.C. (2004) Pre-B cell colony-enhancing factor inhibits neutrophil apoptosis in experimental inflammation and clinical sepsis. The Journal of Clinical Investigation 113: 1318-1327.

398. Kendal CE, and Bryant-Greenwood, G.D. (2007) Pre-B cell colony-enhancing factor (PBEF/visfatin) gene expression is modulated by NF-kB and AP-1 in human amniotic epithelial cells. Placenta 28: 305-314.

399. Moschen AR, Kaser, A., Enrich, B., Mosheimer, B., Theurl, M., Niederegger, H., and Tilg, H. (2007) Visfatin, an adipocytokine with proinflammatory and immunomodulating properties. The Journal of Immunology 178: 1748-1758.

400. Fader CM, and Columbo, M.I. (2009) Autophagy and multivesicular bodies: two closely related partners. Cell Death and Differentiation 16: 70-78.

401. Mizushima N, Ohsumi, Y., and Yoshimori, T. (2002) Autophagosome formation in mammalian cells. Cell Structure and Function 27: 421-429.

402. Feder ME, and Walser, J-C. (2005) The biological limitations of transcriptomics in elucidating stress and stress responses. Journal of Evolutionary Biology 18: 901-910.

403. Brentano F, Schorr, O., Ospelt, C., Stanczyk, J., Gay, R.E., Gay, S., and Kyburz, D. (2007) Pre-B cell colony-enhancing factor/visfatin, a new marker of inflammation in rheumatoid arthritis with proinflammatory and matrix-degrading activities. Arthritis and Rheumatism 56: 2829-2839.

404. Banki K, Hutter, E., Columbo, E., Gonchoroff, N.J., and Perl, A. (1996) Glutathione levels and sensitivity to apoptosis are regulated by changes in transaldolase expression. The Journal of Biological Chemistry 271: 32994-33001.

405. Perl A (2007) The pathogenesis of transaldolase deficiency. IUBMB Life 59: 365-373.

406. Grossman CE, Qian, Y., Banki, K., and Perl, A. (2004) ZNF143 mediates basal and tissue-specific expression of human transaldolase. The Journal of Biological Chemistry 279: 12190-12205.

407. Banki K, Hutter, E., Gonchoroff, N.J., and Perl, A. (1998) Molecular ordering in HIV-induced apoptosis. The Journal of Biological Chemistry 273: 11944-11953.

408. Qian Y, Banerjee, S., Grossman, C.E., Amidon, W., Nagy, G., Barcza, M., Niland, B., Karp, D.R., Middleton, F.A., Banki, K., Perl, A. (2008) Transaldolase deficiency influences the pentose phosphate pathway, mitochondrial homoeostasis and apoptosis signal processing. Biochemical Journal 415: 123-134.

409. Banki K, Hutter, E., Gonchoroff, N.J., and Perl, A. (1999) Elevation of mitochondrial transmembrane potential and reactive oxygen intermediate levels are early events and occur independently from activation of caspases in Fas signaling. The Journal of Immunology 162: 1466-1479.

410. Kitano M, Nakaya, M., Nakamura, T., Nagata, S., and Matsuda, M. (2008) Imaging of Rab5 activity identifies essential regulators for phagosome maturation. Nature 453: 241-245.

411. Vaughan KT (2005) Microtubule plus ends, motors, and traffic of Golgi membranes. Biochimica et Biophysica Acta 1744: 316-324.

412. Blocker A, Severin, F.F., Burkhardt, J.K., Bingham, J.B., Yu, H., Olivo, J-C., Schroer, T.A., Hyman, A.A., and Griffiths, G. (1997) Molecular requirements for bi-directional movement in phagosomes along microtubules. The Journal of Cell Biology 137: 113-129.

413. Koike E, Toda, S., Yokoi, F., Izuhara, K., Koike, N., Itoh, K., Miyazaki, K., Sugihara, H. (2006) Expression of new human inorganic pyrophosphatase in thyroid diseases: its intimate association with hyperthyroidism. Biochemical and Biophysical Research Communications 341: 691-696.

414. Jung-Hui K, Chae, W.-J., Choi, J-M., Nam, H-W., Morio, T., Kim, Y-S., Jang, Y-S., Choi, K-Y., Yang, J-J., and Lee, S-K. (2006) Proteomic analysis of resting and activated $CD8^+$ T cells. Journal of Microbiology and Biotechnology 16: 911-920.

415. Abu Kwaik Y (1998) Induced expression of the Legionella pneumophila gene encoding a 20-kilodalton protein during intracellular infection. Infection and Immunity 66: 203-212.

416. Triccas JA, and Gicquel, B. (2001) Analysis of stress- and host cell-induced expression of the *Mycobacterium tuburculosis* inorganic pyrophosphatase. BMC Microbiology 1: epub.

417. Zamboni DS, McGrath, S., Rabionovitch, M., and Roy, C.R. (2003) *Coxiella burnetii* express type IV secretion system proteins that function similarly to components of the *Legionella pneumophila* Dot/Icm system. Molecular Microbiology 49: 965-976.

418. Gülden E, Mollérus, S., Brüggemann, J., Burkhart, V., and Habich, C. (2008) Heat shock protein 60 induces inflammatory mediators in mouse adipocytes. FEBS Letters 582: 2731-2736.

419. Dupont A, Chwastyniak, M., Beseme, O., Guihot, A-L., Drobecq, H., Amouyel, P., Pinet, F. (2008) Application of saturation dye 2D-DIGE proteomics to characterize proteins modulated by oxidized low density lipoprotein treatment of human macrophages. Journal of Proteome Research 7: 3572-3582.

420. Mercado-Lubo R, Leatham, M.P., Conway, T., and Cohen, P.S. (2009) *Salmonella enterica* serovar typhimurium mutants unable to convert malate to pyruvate and oxaloacetate are avirulent and immunogenic in BALC/c mice. Infection and Immunity 77: 1397-1405.

421. Miwa H, Fujii, J., Kanno, H., Taniguchi, N., and Aozasa, K. (2000) Pyruvate secreted by human lymphoid cell lines protects cells from hydrogen peroxide mediated cell death. Free Radical Research 33: 45-56.

422. Mallet RT, Squires, J.E., Bhatia, S., and Sun, J. (2002) Pyruvate restores contractile function and antioxidant defenses of hydrogen peroxide-challenged myocardium. Journal of Molecular and Cellular Cardiology 34: 1173-1184.

423. Arya DS, Bansal, P., Ojha, S.K., Nandave, M., Mohanty, I., and Gupta, S.K. (2006) Pyruvate provides cardioprotection in the experimental model of myocardial ischemic reperfusion injury. Life Sciences 79: 38-44.

424. Lemasters JJ, Theruvath, T.P., Zhong, Z., and Nieminen, A-L. (2009) Mitochondrial calcium and the permeability transition in cell death. Biochimica et Biophysica Acta 1787: 1395-1401.

425. Jäättelä M, and Tschopp, J. (2003) Caspase-independent cell death in T lymphocytes. Nature Immunology 4: 416-423.

426. Chiapello LS, Baronetti, J.L., Garro, A.P., Spesso, M.F., and Masih, D.T. (2008) *Cryptococcus neoformans* glucuronoxylaomannan induces macrophage apoptosis mediated by nitric oxide in a caspase-independent pathway. International Immunology 20: 1527-1541.

427. Wang KKW (2000) Calpain and caspase: can you tell the difference? TRENDS in Neuroscience 23: 20-26.

428. Uzzo RG, Dulin, N., Bloom, T., Bukowski, R., Finke, J.H., and Kolenko, V. (2001) Inhibition of NFκB induces caspase-independent cell death in human T lymphocytes. Biochemical and Biophysical Research Communications 287: 895-899.

429. Arnoult D, Petit, F., Leliévie, J.D., Locossier, D., Hance, A., Monceaux, V., Fang, R.H.T., Huntrel, B., Ameisen, J.C., and Estaquier, J. (2003) Caspase-dependent and -independent T-cell death pathways in pathogenic simian immunodeficiency virus infection: relationship to disease progression. Cell Death and Differentiation 10: 1240-1252.

430. Stober CB, Lamms, D.A., Li, C.M., Kumararatne, D.S., Lightman, S.T., and McArdle, C.A (2001) ATP-mediated killing of Mycobacterium bovis Bacille Calmette-Guerin within human macrophages is calcium dependent and associated with the acidification of Mycobacteria containing phagosomes. The Journal of Immunology 166: 6276-6286.

431. Doerfler P, Forbush, K.A., and Perlmutter, R.M. (2000) Caspase enzyme activity is not essential for apoptosis during thymocyte development. The Journal of Immunology 164: 4071-4079.

432. Subauste MC, Pertz, O., Adamson, E.D., Turner, C.E., Junger, S., Hahn, K.M. (2004) Vinculin modulation of paxillin-FAK interactions regulates ERK to control survival and motility. The Journal of Cell Biology 165: 371-381.

433. Bousquet-Dubouch M-P, Nguen, S., Bouyssié, D., Burlet-Schlitz, O., French, S.W., Monsarat, B., and Bardag-Gorce, F. (2009) Chronic ethanol feeding affects proteasome-interacting proteins. Proteomics 9: 3609-3622.

434. Mori M, Terui, Y., Ikeda, M., Tomizuka, H., Uwai, M., Kasahara, T., Kubota, N., Itoh, T., Mishima, Y., Douzono-Tanaka, M., Yamada, M., Shimamura, S., Kikuchi, J., Furukawa, Y., Ishizaka, Y., Ikeda, K., Mano, H., Ozawa, K., and Hatake, K. (1999) beta 2-microglobulin identified as an apoptosis-inducing factor and its characterization. Blood 94: 2744-2753.

435. Preckel T, Fung-Leung, W-P., Cai, Z., Vitiello, A., Salter-Cid, L., Winqvist, O., Wolfe, T.G., von Herrath, M., Angulo, A., Ghazal, P., Lee, J-D., Fourie, A.M., Wu, Y., Pang, J., Ngo, K.,

Peterson, P.A., Früh, K., and Yang, Y. (1999) Impaired immunoproteasome assembly and immune responses in PA28$^{-/-}$ mice. Science 286: 2162-2165.

436. Sijts A, Sun, Y., Janek, K., Kral, S., Paschen, A., Schadendorf, D., and Kloetzel, P-M. (2002) The role of the proteasome activator PA28 in MHC class I antigen presentation. Molecular Immunology 39: 165-169.

437. Wang M, Harhaji, L., Lamberth, K., Harndahl, M., Buus, S., Heegaard, N.H.H., Claesson, M.H., and Nissen, M.H. (2009) Modified human beta 2-microglobulin (desLys^{58}) displays decreased affinity for the heavy chain of MHC class I and induces nitric oxid production and apoptosis. Scandanavian Journal of Immunology 69: 203-212.

438. Bevec D, Klier, H., Holter, W., Tschachler, E., Valent, P., Lottspeich, F., Baumruker, T., and Hauber, J. (1994) Induced gene expression of the hypusine-containing protein eukaryotic initiation factor 5A in activated human T lymphocytes. Proceedings of the National Academy of Sciences USA 91: 10829-10833.

439. Cecil DL, Johnson, K., Rediske, J., Lotz, M., Schmidt, A.M., and Terkeltaub, R. (2005) Inflammation-induced chondrocyte hypertrophy is driven by receptor for advanced glycation end products. The Journal of Immunology 175: 8296-8302.

440. Chang N, Sutherland, C., Hesse, E., Winkfein, R., Wiehler, W.B., Pho, M., Veillette, C., Li, S., Wilson, D.P., Kiss, E., and Walsh, M.P. (2007) Identification of a novel interaction between the Ca^{2+}-binding protein S100A11 and the Ca^{2+}- and phospholipid-binding protein annexin A6. American Journal of Physiology Cellular Physiology 292: 1417-1430.

441. Gosslau A, Jao, D.L-E., Butler, R., Liu, A.Y-C., and Chen K.Y. (2009) Thermal killing of human colon cancer cells is associated with the loss of eukaryotic initiation factor 5A. Journal of Cellular Physiology 219: 485-493.

442. He H, Li, J., Weng, S., Li, M., and Yu, Y. (2009) S100A11: diverse functions and pathology corresponding to different target proteins. Cell Biochemistry and Biophysics epub ahead of print.

443. Hopkins MT, Lampi, Y., Wang, T-W., Liu, Z, and Thompson, J.E. (2008) Eukaryotic translation initiation factor 5A is involved in pathogen-induced cell death and development of disease symptoms in *Arabidopsis*. Plant Physiology 148: 479-489.

444. Ji WT, Wang, L., Lin, R.C., Huang, W.R., and Liu, H.J. (2009) Avian reovirus influences phosphorylation of several factors involved in host protein translation including eukaryotic translation elongation factor 2 (eEF2) in Vero cells. Biochemical and Biophysical Research Communications 384: 301-305.

445. Makino E, Sakaguchi, M., Iwatsuki, K., and Huh, N-h. (2004) Introduction of an N-terminal peptide of S100C/A11 into human cells induces apoptotic cell death. Journal of Molecular Medicine 82: 612-620.

446. Moore CC, Martin, E.N., Lee, G., Taylor, C., Dondero, R., Reznikov, L.L., Dinarello, C, Thompson, J., and Scheld, W.M. (2008) Eukaryotic translation initiation factor 5A small interference RNA-liposome complexes reduce inflammation and increase survival in murine models of severe sepsis and acute lung injury. The Journal of Infectious Diseases 198: 1407-1414.

447. Owsianowski E, Walter, D., Fahrenkrog, B. (2008) Negative regulation of apoptosis in yeast. Biochimica et Biophysica Acta 1783: 1303-1310.

448. Ryazanov AG (2002) Elongation factor-2 kinase and its newly discovered relatives. FEBS Letters 514: 26-29.

449. Zanelli CF, and Valentini, S.R. (2007) Is there a role for eIF5A in translation? Amino Acids 33: 351-358.

450. Zelivianski S, Liang, D., Chen, M., Mirkin, B.L., and Zhao, R.Y. (2006) Suppressive effect of elongation factor 2 on apoptosis induced by HIV-1 viral protein R. Apoptosis 11: 377-388.

451. Barnard EA, Skolnick, P., Olsen, R.W., Mohler, H., Sieghart, W., Biggio, G., Braestrup, C., Bateson, A.N., and Langer, S.Z. (1998) International Union of Pharmacology: XV: Subtypes of γ-aminobutyric acid$_A$ receptors: classification on the basis of subunit structure and receptor function. Pharmacological Reviews 50: 291-313.

452. Baumann SW, Baur, R., and Sigel, E. (2001) Subunit arrangement of γ-aminobutyric acid type A receptors. The Journal of Biological Chemistry 276: 36275-36280.

453. Connolly CN, Krishek, B.J., McDonald, B.J., Smart, T.G., and Moss, S.J. (1996) Assembly and cell surface expression of heteromeric and homomeric γ-aminobutyric acid type A receptors. The Journal of Biological Chemistry 271: 89-96.

454. Kash TL, Trudell, J.R., and Harrison, N.L. (2004) Structural elements involved in activation of the γ-aminobutyric acid type A (GABA$_A$) receptor. Biochemical Society Transactions 32.

455. Mody I (2005) Aspects of the homeostatic plasticity of GABA$_A$ receptor-mediated inhibition. Journal of Physiology 562: 37-46.

456. Tretter V, Ehya, N., Fuchs, K., and Sieghart, W. (1997) Stoichiometry and assembly of a recombinant GABA$_A$ receptor subtype. The Journal of Neuroscience 17: 2728-2737.

457. Wafford KA, Macaulay, A.J., Fradley, R., O'Meara, G.F., Reynolds, D.S., and Rosahl, T.W. (2004) Differentiating the role of γ-aminobutyric acid type A (GABA$_A$) receptor subtypes. Biochemical Society Transactions 32: 553-556.

458. Tehrani MHJ, and Barnes, E.M., Jr. (1997) Sequestration of γ-aminobutyric acid$_A$ receptors on clathrin-coated vesicles during chronic benzodiazepine administration *in vivo*. The Journal of Pharmacology and Experimental Therapeutics 283: 384-390.

459. Schwarz K, Fiedler, T., Fischer, R-J., and Bahl, H. (2007) A standard operating procedure (SOP) for the preparation of intra- and extracellular proteins of Clostridium acetobutylicum for proteome analysis. Journal of Microbiological Methods 68: 396-402.

APPENDICES

APPENDIX A

SEQUENCE COVERAGE MAPS

48 hr soluble fraction/spot 10/MnSOD/Mascot
MLSRAVCGTSRQLAPALGYLGSRQKHSLPDLPYDYGALEPHINAQIMQLHHSKHHAAYVNNLNVTEEKYQEA
LAKGDVTAQIALQPALKFNGGGHINHSIFWTNLSPNGGGEPKGELLEAIKRDFGSFDKFKEKLTAASVGVQGS
GWGWLGFNKQRGHLQIAACPNQDPLQGTTGLIPLLGIDVWEHAYYLQYKNVRPDYLKAIWNVINWENVTE
RYMACKK

48 hr soluble fraction/spot 10/MnSOD/X!Hunter
MLSRAVCGTSRQLAPALGYLGSRQKHSLPDLPYDYGALEPHINAQIMQLHHSKHHAAYVNNLNVTEEKYQEA
LAKGDVTAQIALQPALKFNGGGHINHSIFWTNLSPNGGGEPKGELLEAIKRDFGSFDKFKEKLTAASVGVQGS
GWGWLGFNKERGHLQIAACPNQDPLQGTTGLIPLLGIDVWEHAYYLQYKNVRPDYLKAIWNVINWENVTE
RYMACKK

48 hr soluble fraction/spot 10/MnSOD/X!Tandem P3
MLSRAVCGTSRQLAPALGYLGSRQKHSLPDLPYDYGALEPHINAQIMQLHHSKHHAAYVNNLNVTEEKYQEA
LAKGDVTAQIALQPALKFNGGGHINHSIFWTNLSPNGGGEPKGELLEAIKRDFGSFDKFKEKLTAASVGVQGS
GWGWLGFNKERGHLQIAACPNQDPLQGTTGLIPLLGIDVWEHAYYLQYKNVRPDYLKAIWNVINWENVTE
RYMACKK

96 hr soluble fraction/Spot 2/S100 Ca^{2+} binding protein A9/Mascot

MTCKMSQLERNIETIINTFHQYSVKLGHPDTLNQGEFKELVRKDLQNFLKKENKNEKVIEHIMEDLDTNA
DKQLSFEEFIMLMARLTWASHEKMHEGDEGPGHHHKPGLGEGTP

96 hr soluble fraction/Spot 2/S100 Ca^{2+} binding protein A9/X!Hunter

MTCKMSQLERNIETIINTFHQYSVKLGHPDTLNQGEFKELVRKDLQNFLKKENKNEKVIEHIMEDLDTNA
DKQLSFEEFIMLMARLTWASHEKMHEGDEGPGHHHKPGLGEGTP

96 hr soluble fraction/Spot 2/S100 Ca^{2+} binding protein A9/X!Tandem P3

MTCKMSQLERNIETIINTFHQYSVKLGHPDTLNQGEFKELVRKDLQNFLKKENKNEKVIEHIMEDLDTNA
DKQLSFEEFIMLMARLTWASHEKMHEGDEGPGHHHKPGLGEGTP

96 hr soluble fraction/Spot 5/Visfatin,PBEF/Mascot

MNPAAEAEFNILLATDSYKVTHYKQYPPNTSKVYSYFECREKKTENSKLRKVKYEETVFYGLQYILNKYLKGKVV
TKEKIQEAKDVYKEHFQDDVFNEKGWNYILEKYDGHLPIEIKAVPEGFVIPRGNVLFTVENTDPECYWLTNWIE
TILVQSWYPITVATNSREQKKILAKYLLETSGNLDGLEYKLHDFGYRGVSSQETAGIGASAHLVNFKGTDTVAG
LALIKKYYGTKDPVPGYSVPAAEHSTITAWGKDHEKDAFEHIVTQFSSVPVSVVSDSYDIYNACEKIWGEDLRH
LIVSRSTQAPLIIRPDSGNPLDTVLKVLEILGKKFPVTENSKGYKLLPPYLRVIQGDGVDINTLQEIVEGMKQKM
WSIENIAFGSGGGLLQKLTRDLLNCSFKCSYVVTNGLGINVFKDPVADPNKRSKKGRLSLHRTPAGNFVTLEEG
KGDLEEYGQDLLHTVFKNGKVTKSYSFDEIRKNAQLNIELEAAHH

96 hr soluble fraction/Spot 5/Visfatin,PBEF/X!Hunter

MNPAAEAEFNILLATDSYKVTHYKQYPPNTSKVYSYFECREKKTENSKLRKVKYEETVFYGLQYILNKYLKGKVV
TKEKIQEAKDVYKEHFQDDVFNEKGWNYILEKYDGHLPIEIKAVPEGFVIPRGNVLFTVENTDPECYWLTNWIE
TILVQSWYPITVATNSREQKKILAKYLLETSGNLDGLEYKLHDFGYRGVSSQETAGIGASAHLVNFKGTDTVAG
LALIKKYYGTKDPVPGYSVPAAEHSTITAWGKDHEKDAFEHIVTQFSSVPVSVVSDSYDIYNACEKIWGEDLRH
LIVSRSTQAPLIIRPDSGNPLDTVLKVLEILGKKFPVTENSKGYKLLPPYLRVIQGDGVDINTLQEIVEGMKQKM
WSIENIAFGSGGGLLQKLTRDLLNCSFKCSYVVTNGLGINVFKDPVADPNKRSKKGRLSLHRTPAGNFVTLEEG
KGDLEEYGQDLLHTVFKNGKVTKSYSFDEIRKNAQLNIELEAAHH

96 hr soluble fraction/Spot 5/Visfatin,PBEF/X!Hunter P3

MNPAAEAEFNILLATDSYKVTHYKQYPPNTSKVYSYFECREKKTENSKLRKVKYEETVFYGLQYILNKYLKGKVV
TKEKIQEAKDVYKEHFQDDVFNEKGWNYILEKYDGHLPIEIKAVPEGFVIPRGNVLFTVENTDPECYWLTNWIE
TILVQSWYPITVATNSREQKKILAKYLLETSGNLDGLEYKLHDFGYRGVSSQETAGIGASAHLVNFKGTDTVAG
LALIKKYYGTKDPVPGYSVPAAEHSTITAWGKDHEKDAFEHIVTQFSSVPVSVVSDSYDIYNACEKIWGEDLRH
LIVSRSTQAPLIIRPDSGNPLDTVLKVLEILGKKFPVTENSKGYKLLPPYLRVIQGDGVDINTLQEIVEGMKQKM
WSIENIAFGSGGGLLQKLTRDLLNCSFKCSYVVTNGLGINVFKDPVADPNKRSKKGRLSLHRTPAGNFVTLEEG
KGDLEEYGQDLLHTVFKNGKVTKSYSFDEIRKNAQLNIELEAAHH

96 hr soluble fraction/Spot 9/S100 Ca^{2+} binding protein A9/Mascot
MTCKMSQLERNIETIINTFHQYSVKLGHPDTLNQGEFKELVRKDLQNFLKKENKNEKVIEHIMEDLDTNADKQ
LSFEEFIMLMARLTWASHEKMHEGDEGPGHHHKPGLGEGTP

96 hr soluble fraction/Spot 9/S100 Ca^{2+} binding protein A9/X!Hunter
MLTELEKALNSIIDVYHKYSLIKGNFHAVYRDDLKKLLETECPQYIRKKGADVWFKELDINTDGAVNFQEFLILVI
KMGVAAHKKSHEESHKE

96 hr soluble fraction/Spot 9/S100 Ca^{2+} binding protein A9/X!Tandem P3
MLTELEKALNSIIDVYHKYSLIKGNFHAVYRDDLKKLLETECPQYIRKKGADVWFKELDINTDGAVNFQEFLILVI
KMGVAAHKKSHEESHKE

96 hr soluble fraction/Spot 14/S100 Ca^{2+} binding protein A8/Mascot
MLTELEKALNSIIDVYHKYSLIKGNFHAVYRDDLKKLLETECPQYIRKKGADVWFKELDINTDGAVNFQEFLILVI
KMGWQPTKKAMKKATKSS

96 hr soluble fraction/Spot 9/S100 Ca^{2+} binding protein A9/X!Hunter
MLTELEKALNSIIDVYHKYSLIKGNFHAVYRDDLKKLLETECPQYIRKKGADVWFKELDINTDGAVNFQEFL
ILVIKMGVAAHKKSHEESHKE

96 hr soluble fraction/Spot 9/S100 Ca^{2+} binding protein A9/X!Tandem P3
MLTELEKALNSIIDVYHKYSLIKGNFHAVYRDDLKKLLETECPQYIRKKGADVWFKELDINTDGAVNFQEFL
ILVIKMGVAAHKKSHEESHKE

96 hr soluble fraction/Spot 48/Transaldolase 1/Mascot
MSSSPVKRQRMESALDQLKQFTTVVADTGDFHAIDEYKPQDATTNPSLILAAAQMPAYQELVEEAIAYGRKL
GGSQEDQIKNAIDKLFVLFGAEILKKIPGRVSTEVDARLSFDKDAMVARARRLIELYKEAGISKDRILIKLSSTWE
GIQAGKELEEQHGIHCNMTLLFSFAQAVACAEAGVTLISPFVGRILDWHVANTDKKSYEPLEDPGVKSVTKIYN
YYKKFSYKTIVMGASFRNTGEIKALAGCDFLTISPKLLGELLQDNAKLVPVLSAKAAQASDLEKIHLDEKSFRWL
HNEDQMAVEKLSDGIRKFAADAVKLERMLTERMFNAENGK

96 hr soluble fraction/Spot 48/Transaldolase 1/X!Hunter
MSSSPVKRQRMESALDQLKQFTTVVADTGDFHAIDEYKPQDATTNPSLILAAAQMPAYQELVEEAIAYGRKL
GGSQEDQIKNAIDKLFVLFGAEILKKIPGRVSTEVDARLSFDKDAMVARARRLIELYKEAGISKDRILIKLSSTWE
GIQAGKELEEQHGIHCNMTLLFSFAQAVACAEAGVTLISPFVGRILDWHVANTDKKSYEPLEDPGVKSVTKIYN
YYKKFSYKTIVMGASFRNTGEIKALAGCDFLTISPKLLGELLQDNAKLVPVLSAKAAQASDLEKIHLDEKSFRWL
HNEDQMAVEKLSDGIRKFAADAVKLERMLTERMFNAENGK

96 hr soluble fraction/Spot 48/Transaldolase 1/X!Tandem P3
MSSSPVKRQRMESALDQLKQFTTVVADTGDFHAIDEYKPQDATTNPSLILAAAQMPAYQELVEEAIAYGRKL
GGSQEDQIKNAIDKLFVLFGAEILKKIPGRVSTEVDARLSFDKDAMVARARRLIELYKEAGISKDRILIKLSSTWE
GIQAGKELEEQHGIHCNMTLLFSFAQAVACAEAGVTLISPFVGRILDWHVANTDKKSYEPLEDPGVKSVTKIYN
YYKKFSYKTIVMGASFRNTGEIKALAGCDFLTISPKLLGELLQDNAKLVPVLSAKAAQASDLEKIHLDEKSFRWL
HNEDQMAVEKLSDGIRKFAADAVKLERMLTERMFNAENGK

96 hr soluble fraction/Spot 60/Hsp60/Mascot
MLRLPTVFRQMRPVSRVLAPHLTRAYAKDVKFGADARALMLQGVDLLADAVAVTMGPKGRTVIIEQSWGS
PKVTKDGVTVAKSIDLKDKYKNIGAKLVQDVANNTNEEAGDGTTTATVLARSIAKEGFEKISKGANPVEIRRGV
MLAVDAVIAELKKQSKPVTTPEEIAQVATISANGDKEIGNIISDAMKKVGRKGVITVKDGKTLNDELEIIEGMKF
DRGYISPYFINTSKGQKCEFQDAYVLLSEKKISSIQSIVPALEIANAHRKPLVIIAEDVDGEALSTLVLNRLKVGLQ
VVAVKAPGFGDNRKNQLKDMAIATGGAVFGEEGLTLNLEDVQPHDLGKVGEVIVTKDDAMLLKGKGDKAQI
EKRIQEIIEQLDVTTSEYEKEKLNERLAKLSDGVAVLKVGGTSDVEVNEKKDRVTDALNATRAAVEEGIVLGGG
CALLRCIPALDSLTPANEDQKIGIEIIKRTLKIPAMTIAKNAGVEGSLIVEKIMQSSSEVGYDAMAGDFVNMVEK
GIIDPTKVVRTALLDAAGVASLLTTAEVVVTEIPKEEKDPGMGAMGGMGGGMGGGMF

96 hr soluble fraction/Spot 60/Hsp60/X!Hunter
MLRLPTVFRQMRPVSRVLAPHLTRAYAKDVKFGADARALMLQGVDLLADAVAVTMGPKGRTVIIEQS
WGSPKVTKDGVTVAKSIDLKDKYKNIGAKLVQDVANNTNEEAGDGTTTATVLARSIAKEGFEKISKGANPVEI
RRGVMLAVDAVIAELKKQSKPVTTPEEIAQVATISANGDKEIGNIISDAMKKVGRKGVITVKDGKTLNDELEIIE
GMKFDRGYISPYFINTSKGQKCEFQDAYVLLSEKKISSIQSIVPALEIANAHRKPLVIIAEDVDGEALSTLVLNRLK
VGLQVVAVKAPGFGDNRKNQLKDMAIATGGAVFGEEGLTLNLEDVQPHDLGKVGEVIVTKDDAMLLKGKG
DKAQIEKRIQEIIEQLDVTTSEYEKEKLNERLAKLSDGVAVLKVGGTSDVEVNEKKDRVTDALNATRAAVEEGIV
LGGGCALLRCIPALDSLTPANEDQKIGIEIIKRTLKIPAMTIAKNAGVEGSLIVEKIMQSSSEVGYDAMAGDFVN
MVEKGIIDPTKVVRTALLAAGVASLLT TAEVVVTEIPKEEKDPGMGAMGGMGGGMGGGMF

96 hr soluble fraction/Spot 60/Hsp60/X!Tandem P3
MLRLPTVFRQMRPVSRVLAPHLTRAYAKDVKFGADARALMLQGVDLLADAVAVTMGPKGRTVIIEQS
WGSPKVTKDGVTVAKSIDLKDKYKNIGAKLVQDVANNTNEEAGDGTTTATVLARSIAKEGFEKISKGANPVEI
RRGVMLAVDAVIAELKKQSKPVTTPEEIAQVATISANGDKEIGNIISDAMKKVGRKGVITVKDGKTLNDELEIIE
GMKFDRGYISPYFINTSKGQKCEFQDAYVLLSEKKISSIQSIVPALEIANAHRKPLVIIAEDVDGEALSTLVLNRLK
VGLQVVAVKAPGFGDNRKNQLKDMAIATGGAVFGEEGLTLNLEDVQPHDLGKVGEVIVTKDDAMLLKGKG
DKAQIEKRIQEIIEQLDVTTSEYEKEKLNERLAKLSDGVAVLKVGGTSDVEVNEKKDRVTDALNATRAAVEEGIV
LGGGCALLRCIPALDSLTPANEDQKIGIEIIKRTLKIPAMTIAKNAGVEGSLIVEKIMQSSSEVGYDAMAGDFVN
MVEKGIIDPTKVVRTALLDAAGVASLLTTAEVVVTEIPKEEKDPGMGAMGGMGGGMGGGMF

96 hr soluble fraction/Spot 63/Inorganic pyrophosphatase/Mascot
STEERAAAFSLEYRVFLKNEKGQYISPFHDIPIYADKDVFHMVVEVPRWSNAKMEIATKDPLNPIKQDV
KKGKLRYVANLFPYKGYIWNYGAIPQTWEDPGHNDKHTGCCGDNDPIDVCEIGSKVCARGEIIGVKVLGILA
MIDEGETDWKVIAINVDDPDAANYNDINDVKRLKPGYLEATVDWFRRYKVPDGKPENEFAFNAEFKDKDFAI
DIIKSTHDHWKALVTKKTNGKGISCMNTTLSESPFKCDPDAARAIVDALPPPCESACTVPTDVDKWFHH

96 hr soluble fraction/Spot 63/Inorganic pyrophosphatase/X!Hunter
MSGFSTEERAAPFSLEYRVFLKNEKGQYISPFHDIPIYADKDVFHMVVEVPRWSNAKMEIATKDPLNPIKQDV
KKGKLRYVANLFPYKGYIWNYGAIPQTWEDPGHNDKHTGCCGDNDPIDVCEIGSKVCARGEIIGVKVLGILA
MIDEGETDWKVIAINVDDPDAANYNDINDVKRLKPGYLEATVDWFRRYKVPDGKPENEFAFNAEFKDKDFAI
DIIKSTHDHWKALVTKKTNGKGISCMNTTLSESPFKCDPDAARAIVDALPPPCESACTVPTDVDKWFHHQKN

96 hr soluble fraction/Spot 63/Inorganic pyrophosphatase/X!Tandem P3
MSGFSTEERAAPFSLEYRVFLKNEKGQYISPFHDIPIYADKDVFHMVVEVPRWSNAKMEIATKDPLNPIKQDV
KKGKLRYVANLFPYKGYIWNYGAIPQTWEDPGHNDKHTGCCGDNDPIDVCEIGSKVCARGEIIGVKVLGILA
MIDEGETDWKVIAINVDDPDAANYNDINDVKRLKPGYLEATVDWFRRYKVPDGKPENEFAFNAEFKDKDFAI
DIIKSTHDHWKALVTKKTNGKGISCMNTTLSESPFKCDPDAARAIVDALPPPCESACTVPTDVDKWFHHQKN

96 hr soluble fraction/Spot 69/EB1/Mascot

MAVNVYSTSVTSDNLSRHDMLAWINESLQLNLTKIEQLCSGAAYCQFMDMLFPGSIALKKVKFQAKLEHEYI
QNFKILQAGFKRMGVDKIIPVDKLVKGKFQDNFEFVQWFKKFFDANYDGKDYDPVAARQGQETAVAPSLVA
PALNKPKKPLTSSSAAPQRPISTQRTAAAPKAGPGVVRKNPGVGNGDDEAAELMQQVNVLKLTVEDLEKER
DFYFGKLRNIELICQENEGENDPVLQRIVDILYATDEGFVIPDEGGPQEEQEEY

96 hr soluble fraction/Spot 69/EB1/X!Hunter

MAVNVYSTSVTSDNLSRHDMLAWINESLQLNLTKIEQLCSGAAYCQFMDMLFPGSIALKKVKFQAKLEH
EYIQNFKILQAGFKRMGVDKIIPVDKLVKGKFQDNFEFVQWFKKFFDANYDGKDYDPVAARQGQETAVAPSL
VAPALNKPKKPLTSSSAAPQRPISTQRTAAAPKAGPGVVRKNPGVGNGDDEAAELMQQVNVLKLTVEDLEK
ERDFYFGKLRNIELICQENEGENDPVLQRIVDILYATDEGFVIPDEGGPQEEQEEY

96 hr soluble fraction/Spot 69/EB1/X!Tandem P3

MAVNVYSTSVTSDNLSRHDMLAWINESLQLNLTKIEQLCSGAAYCQFMDMLFPGSIALKKVKFQAKLEH
EYIQNFKILQAGFKRMGVDKIIPVDKLVKGKFQDNFEFVQWFKKFFDANYDGKDYDPVAARQGQETAVAPSL
VAPALNKPKKPLTSSSAAPQRPISTQRTAAAPKAGPGVVRKNPGVGNGDDEAAELMQQVNVLKLTVEDLEK
ERDFYFGKLRNIELICQENEGENDPVLQRIVDILYATDEGFVIPDEGGPQEEQEEY

96 hr soluble fraction/Spot 87/Fascin 1/Mascot

MTANGTAEAVQIQFGLINCGNKYLTAEAFGFKVNASASSLKKKQIWTLEQPPDEAGSAAVCLRSHLGRYL
AADKDGNVTCEREVPGPDCRFLIVAHDDGRWSLQSEAHRRYFGGTEDRLSCFAQTVSPAEKWSVHIAMHP
QVNIYSVTRKRYAHLSARPADEIAVDRDVPWGVDSLITLAFQDQRYSVQTADHRFLRHDGRLVARPEPATGY
TLEFRSGKVAFRDCEGRYLAPSGPSGTLKAGKATKVGKDELFALEQSCAQVVLQAANERNVSTRQGMDLSAN
QDEETDQETFQLEIDRDTKKCAFRTHTGKYWTLTATGGVQSTASSKNASCYFDIEWRDRRITLRASNGKFVTS
KKNGQLAASVETAGDSELFLMKLINRPIIVFRGEHGFIGCRKVTGTLDANRSSYDVFQLEFNDGAYNIKDSTGK
YWTVGSDSAVTSSGDTPVDFFFEFCDYNKVAIKVGGRYLKGDHAGVLKASAETVDPASLWEY

96 hr soluble fraction/Spot 87/Fascin 1/X!Hunter

MTANGTAEAVQIQFGLINCGNKYLTAEAFGFKVNASASSLKKKQIWTLEQPPDEAGSAAVCLRSHLGRYLAA
DKDGNVTCEREVPGPDCRFLIVAHDDGRWSLQSEAHRRYFGGTEDRLSCFAQTVSPAEKWSVHIAMHPQV
NIYSVTRKRYAHLSARPADEIAVDRDVPWGVDSLITLAFQDQRYSVQTADHRFLRHDGRLVARPEPATGYTLE
FRSGKVAFRDCEGRYLAPSGPSGTLKAGKATKVGKDELFALEQSCAQVVLQAANERNVSTRQGMDLSANQD
EETDQETFQLEIDRDTKKCAFRTHTGKYWTLTATGGVQSTASSKNASCYFDIEWRDRRITLRASNGKFVTSKK
NGQLAASVETAGDSELFLMKLINRPIIVFRGEHGFIGCRKVTGTLDANRSSYDVFQLEFNDGAYNIKDSTGKYW
TVGSDSAVTSSGDTPVDFFFEFCDYNKVAIKVGGRYLKGDHAGVLKASAETVDPASLWEY

96 hr soluble fraction/Spot 87/Fascin 1/X!Tandem P3

MTANGTAEAVQIQFGLINCGNKYLTAEAFGFKVNASASSLKKKQIWTLEQPPDEAGSAAVCLRSHLGRYLAA
DKDGNVTCEREVPGPDCRFLIVAHDDGRWSLQSEAHRRYFGGTEDRLSCFAQTVSPAEKWSVHIAMHPQV
NIYSVTRKRYAHLSARPADEIAVDRDVPWGVDSLITLAFQDQRYSVQTADHRFLRHDGRLVARPEPATGYTLE
FRSGKVAFRDCEGRYLAPSGPSGTLKAGKATKVGKDELFALEQSCAQVVLQAANERNVSTRQGMDLSANQD
EETDQETFQLEIDRDTKKCAFRTHTGKYWTLTATGGVQSTASSKNASCYFDIEWRDRRITLRASNGKFVTSKK
NGQLAASVETAGDSELFLMKLINRPIIVFRGEHGFIGCRKVTGTLDANRSSYDVFQLEFNDGAYNIKDSTGKYW
TVGSDSAVTSSGDTPVDFFFEFCDYNKVAIKVGGRYLKGDHAGVLKASAETVDPASLWEY

96 hr soluble fraction/Spot 102/Leucine aminopeptidase 3/Mascot

MFLLPLPAAGRVVVRRLAVVRSGSRSLSTADMTKGLVLGIYSKEKEDDVPQFTSAGENFDKLLAGKLRETLNI
SGPPLKAGKTRTFYGLHQDFPSVVLVGLGKKAAGIDEQENWHEGKENIRAAVAAGCRQIQDLELSSVEVDPC
GDAQAAAEGAVLGLYEYDDLKQKKKMAVSAKLYGSGDQEAWQKGVLFASGQNLARQLMETPANEMTPT
RFAEIIEKNLKSASSKTEVHIRPKSWIEEQAMGSFLSVAKGSDEPPVFLEIHYKGSPNANEPPLVFVGKGITFDS
GGISIKASANMDLMRADMGGAATICSAIVSAAKLNLPINIIGLAPLCENMPSGKANKPGDVVRAKNGKTIQ
VDNTDAEGRLILADALCYAHTFNPKVILNAATLTGAMDVALGSGATGVFTNSSWLWNKLFEASIETGDRVW
RMPLFEHYTRQVVDCQLADVNNIGKYRSAGACTAAAFLKEFVTHPKWAHLDIAGVMTNKDEVPYLRKGMT
GRPTRTLIEFLLRFSQDNA

96 hr soluble fraction/Spot 102/Leucine aminopeptidase 3/X!Hunter

MFLLPLPAAGRVVVRRLAVRRFGSRSLSTADMTKGLVLGIYSKEKEDDVPQFTSAGENFDKLLAGKLRETLNIS
GPPLKAGKTRTFYGLHQDFPSVVLVGLGKKAAGIDEQENWHEGKENIRAAVAAGCRQIQDLELSSVEVDPCG
DAQAAAEGAVLGLYEYDDLKQKKKMAVSAKLYGSGDQEAWQKGVLFASGQNLARQLMETPANEMTPTRF
AEIIEKNLKSASSKTEVHIRPKSWIEEQAMGSFLSVAKGSDEPPVFLEIHYKGSPNANEPPLVFVGKGITFDSGGI
SIKASANMDLMRADMGGAATICSAIVSAAKLNLPINIIGLAPLCENMPSGKANKPGDVVRAKNGKTIQVDNT
DAEGRLILADALCYAHTFNPKVILNAATLTGAMDVALGSGATGVFTNSSWLWNKLFEASIETGDRVWRMPLF
EHYTRQVVDCQLADVNNIGKYRSAGACTAAAFLKEFVTHPKWAHLDIAGVMTNKDEVPYLRKGMTGRPTRT
LIEFLLRFSQDNA

96 hr soluble fraction/Spot 102/Leucine aminopeptidase 3/X!Tandem P3

MFLLPLPAAGRVVVRRLAVRRFGSRSLSTADMTKGLVLGIYSKEKEDDVPQFTSAGENFDKLLAGKLRETLNIS
GPPLKAGKTRTFYGLHQDFPSVVLVGLGKKAAGIDEQENWHEGKENIRAAVAAGCRQIQDLELSSVEVDPCG
DAQAAAEGAVLGLYEYDDLKQKKKMAVSAKLYGSGDQEAWQKGVLFASGQNLARQLMETPANEMTPTRF
AEIIEKNLKSASSKTEVHIRPKSWIEEQAMGSFLSVAKGSDEPPVFLEIHYKGSPNANEPPLVFVGKGITFDSGGI
SIKASANMDLMRADMGGAATICSAIVSAAKLNLPINIIGLAPLCENMPSGKANKPGDVVRAKNGKTIQVDNT
DAEGRLILADALCYAHTFNPKVILNAATLTGAMDVALGSGATGVFTNSSWLWNKLFEASIETGDRVWRMPLF
EHYTRQVVDCQLADVNNIGKYRSAGACTAAAFLKEFVTHPKWAHLDIAGVMTNKDEVPYLRKGMTGRPTRT
LIEFLLRFSQDNA

96 hr soluble farction/Spot 126/Leucine aminopeptidase 3/Mascot

MFLLPLPAAGRVVVRRLAVVRSGSRSLSTADMTKGLVLGIYSKEKEDDVPQFTSAGENFDKLLG
KLRETLNISGPPLKAGKTRTFYGLHQDFPSVVLVGLGKKAAGIDEQENWHEGKENIRAAVAAGCRQI
QDLELSSVEVDPCGDAQAAAEGAVLGLYEYDDLKQKKKMAVSAKLYGSGDQEAWQKGVLFG
QNLARQLMETPANEMTPTRFAEIIEKNLKSASSKTEVHIRPKSWIEEQAMGSFLSVAKGSDEPF
LEIHYKGSPNANEPPLVFVGKGITFDSGGISIKASANMDLMRADMGGAATICSAIVSAAKLNLN
IIGLAPLCENMPSGKANKPGDVVRAKNGKTIQVDNTDAEGRLILADALCYAHTFNPKVILNAAT
LTGAMDVALGSGATGVFTNSSWLWNKLFEASIETGDRVWRMPLFEHYTRQVVDCQLADVN
NIGKYRSAGACTAAAFLKEFVTHPKWAHLDIAGVMTNKDEVPYLRKGMTGRPTRTLIEFLLRFS
QDNA

96 hr soluble farction/Spot 126/Leucine aminopeptidase 3/X!Hunter

MFLLPLPAAGRVVVRRLAVRRFGSRSLSTADMTKGLVLGIYSKEKEDDVPQFTSAGENFDKLLAGKLRETLNIS
GPPLKAGKTRTFYGLHQDFPSVVLVGLGKKAAGIDEQENWHEGKENIRAAVAAGCRQIQDLELSSVEVDPCG
DAQAAAEGAVLGLYEYDDLKQKKKMAVSAKLYGSGDQEAWQKGVLFASGQNLARQLMETPANEMTPTRF
AEIIEKNLKSASSKTEVHIRPKSWIEEQAMGSFLSVAKGSDEPPVFLEIHYKGSPNANEPPLVFVGKGITFDSGGI
SIKASANMDLMRADMGGAATICSAIVSAAKLNLPINIIGLAPLCENMPSGKANKPGDVVRAKNGKTIQVDNT
DAEGRLILADALCYAHTFNPKVILNAATLTGAMDVALGSGATGVFTNSSWLWNKLFEASIETGDRVWRMPLF
EHYTRQVVDCQLADVNNIGKYRSAGACTAAAFLKEFVTHPKWAHLDIAGVMTNKDEVPYLRKGMTGRPTRT
LIEFLLRFSQDNA

96 hr soluble farction/Spot 126/Leucine aminopeptidase 3/X!Tandem P3

MFLLPLPAAGRVVVRRLAVRRFGSRSLSTADMTKGLVLGIYSKEKEDDVPQFTSAGENFDKLLAGKLRETLNIS
GPPLKAGKTRTFYGLHQDFPSVVLVGLGKKAAGIDEQENWHEGKENIRAAVAAGCRQIQDLELSSVEVDPCG
DAQAAAEGAVLGLYEYDDLKQKKKMAVSAKLYGSGDQEAWQKGVLFASGQNLARQLMETPANEMTPTRF
AEIIEKNLKSASSKTEVHIRPKSWIEEQAMGSFLSVAKGSDEPPVFLEIHYKGSPNANEPPLVFVGKGITFDSGGI
SIKASANMDLMRADMGGAATICSAIVSAAKLNLPINIIGLAPLCENMPSGKANKPGDVVRAKNGKTIQVDNT
DAEGRLILADALCYAHTFNPKVILNAATLTGAMDVALGSGATGVFTNSSWLWNKLFEASIETGDRVWRMPLF
EHYTRQVVDCQLADVNNIGKYRSAGACTAAAFLKEFVTHPKWAHLDIAGVMTNKDEVPYLRKGMTGRPTRT
LIEFLLRFSQDNA

96 hr soluble fraction/Spot 144/Pyrophosphatase 1/Mascot
STEERAAAFSLEYRVFLKNEKGQYISPFHDIPIYADKDVFHMVVEVPRWSNAKMEIATKDP
LNPIKQDVKKGKLRYVANLFPYKGYIWNYGAIPQTWEDPGHNDKHTGCCGDNDPIDVCEIGSKVCAR
GEIIGVKVLGILAMIDEGETDWKVIAINVDDPDAANYNDINDVKRLKPGYLEATVDWFRRYKVP
DGKPENEFAFNAEFKDKDFAIDIIKSTHDHWKALVTKKTNGKGISCMNTTLSESPFKCDPDAAR
AIVDALPPPCESACTVPTDVDKWFHH

96 hr soluble fraction/Spot 144/Pyrophosphatase 1/X!Hunter
MSGFSTEERAAPFSLEYRVFLKNEKGQYISPFHDIPIYADKDVFHMVVEVPRWSNAKMEIATKDPLNPIKQDV
KKGKLRYVANLFPYKGYIWNYGAIPQTWEDPGHNDKHTGCCGDNDPIDVCEIGSKVCARGEIIGVKVLGILA
MIDEGETDWKVIAINVDDPDAANYNDINDVKRLKPGYLEATVDWFRRYKVPDGKPENEFAFNAEFKDKDFAI
DIIKSTHDHWKALVTKKTNGKGISCMNTTLSESPFKCDPDAARAIVDALPPPCESACTVPTDVDKWFHHQKN

96 hr soluble fraction/Spot 144/Pyrophosphatase 1/X!Tandem P3
MSGFSTEERAAPFSLEYRVFLKNEKGQYISPFHDIPIYADKDVFHMVVEVPRWSNAKMEIATKDPLNPIKQDV
KKGKLRYVANLFPYKGYIWNYGAIPQTWEDPGHNDKHTGCCGDNDPIDVCEIGSKVCARGEIIGVKVLGILA
MIDEGETDWKVIAINVDDPDAANYNDINDVKRLKPGYLEATVDWFRRYKVPDGKPENEFAFNAEFKDKDFAI
DIIKSTHDHWKALVTKKTNGKGISCMNTTLSESPFKCDPDAARAIVDALPPPCESACTVPTDVDKWFHHQKN

96 hr membrane fraction/Spot 6/MnSOD/Mascot

LSPAVCGTSRHLAPVLGYLGSRQKHSLPDLPYDYGALEPHINAQIMQLHHSKHHAAYVNNLNVTEEKYQEALAKGDVTAQIALQPALKFNGGGHINHSIFWTNLSPNGGGEPKGELLEAIKRDFGSFDKFKEKLTAASVGVQGSGWGWLGFNKERGHLQIAACPNQDPLQGTTGLIPLLGIDVWEHAYYLQYKNVRPDYLKAIWNVINWENVT

96 hr membrane fraction/Spot 6/MnSOD/X!Hunter

MLSRAVCGTSRQLAPALGYLGSRQKHSLPDLPYDYGALEPHINAQIMQLHHSKHHAAYVNNLNVTEEKYQEALAKGDVTAQIALQPALKFNGGGHINHSIFWTNLSPNGGGEPKGELLEAIKRDFGSFDKFKEKLTAASVGVQGSGWGWLGFNKERGHLQIAACPNQDPLQGTTGLIPLLGIDVWEHAYYLQYKNVRPDYLKAIWNVINWENVTERYMACKK

96 hr membrane fraction/Spot 6/MnSOD/X!Tandem P3

MLSRAVCGTSRQLAPALGYLGSRQKHSLPDLPYDYGALEPHINAQIMQLHHSKHHAAYVNNLNVTEEKYQEALAKGDVTAQIALQPALKFNGGGHINHSIFWTNLSPNGGGEPKGELLEAIKRDFGSFDKFKEKLTAASVGVQGSGWGWLGFNKERGHLQIAACPNQDPLQGTTGLIPLLGIDVWEHAYYLQYKNVRPDYLKAIWNVINWENVTERYMACKK

96 hr membrane fraction/Spot 8/Vimentin/Mascot

MSTRSVSSSSYRRMFGGPGTASRPSSSRSYVTTSTRTYSLGSALRPSTSRSLYASSPGGVYATRSSAVRLRS
SVPGVRLLQDSVDFSLADAINTEFKNTRTNEKVELQELNDRFANYIDKVRFLEQQNKILLAELEQLKGQGKSRL
GDLYEEEMRELRRQVDQLTNDKARVEVERDNLAEDIMRLREKLQEEMLQREEAENTLQSFRQDVDNASLAR
LDLERKVESLQEEIAFLKKLHEEEIQELQAQIQEQHVQIDVDVSKPDLTAALRDVRQQYESVAAKNLQEAEEWY
KSKFADLSEAANRNNDALRQAKQESTEYRRQVQSLTCEVDALKGTNESLERQMREMEENFAVEAANYQDTI
GRLQDEIQNMKEEMARHLREYQDLLNVKMALDIEIATYRKLLEGEESRISLPLPNFSSLNLRETNLDSLPLVDTH
SKRTFLIKTVETRDGQVINETSQHHDDLE

96 hr membrane fraction/Spot 8/Vimentin/X!Hunter

MSTRSVSSSSYRRMFGGPGTASRPSSSRSYVTTSTRTYSLGSALRPSTSRSLYASSPGGVYATRSSAVRLRSSVP
GVRLLQDSVDFSLADAINTEFKNTRTNEKVELQELNDRFANYIDKVRFLEQQNKILLAELEQLKGQGKSRLGDL
YEEEMRELRRQVDQLTNDKARVEVERDNLAEDIMRLREKLQEEMLQREEAENTLQSFRQDVDNASLARLDLE
RKVESLQEEIAFLKKLHEEEIQELQAQIQEQHVQIDVDVSKPDLTAALRDVRQQYESVAAKNLQEAEEWYKSKF
ADLSEAANRNNDALRQAKQESTEYRRQVQSLTCEVDALKGTNESLERQMREMEENFAVEAANYQDTIGRLQ
DEIQNMKEEMARHLREYQDLLNVKMALDIEIATYRKLLEGEESRISLPLPNFSSLNLRETNLDSLPLVDTHSKRT
LLIKTVETRDGQVINETSQHHDDLE

96 hr membrane fraction/Spot 8/Vimentin/X!Tandem P3

MSTRSVSSSSYRRMFGGPGTASRPSSSRSYVTTSTRTYSLGSALRPSTSRSLYASSPGGVYATRSSAVRLRS
SVPGVRLLQDSVDFSLADAINTEFKNTRTNEKVELQELNDRFANYIDKVRFLEQQNKILLAELEQLKGQGKSRL
GDLYEEEMRELRRQVDQLTNDKARVEVERDNLAEDIMRLREKLQEEMLQREEAENTLQSFRQDVDNASLAR
LDLERKVESLQEEIAFLKKLHEEEIQELQAQIQEQHVQIDVDVSKPDLTAALRDVRQQYESVAAKNLQEAEEWY
KSKFADLSEAANRNNDALRQAKQESTEYRRQVQSLTCEVDALKGTNESLERQMREMEENFAVEAANYQDTI
GRLQDEIQNMKEEMARHLREYQDLLNVKMALDIEIATYRKLLEGEESRISLPLPNFSSLNLRETNLDSLPLVDTH
SKRTLLIKTVETRDGQVINETSQHHDDLE

96 hr membrane fraction/Spot 9/Vimentin/Mascot

MSTRSVSSSSYRRMFGGPGTASRPSSSRSYVTTSTRTYSLGSALRPSTSRSLYASSPGGVYATRSSAVRLRS
SVPGVRLLQDSVDFSLADAINTEFKNTRTNEKVELQELNDRFANYIDKVRFLEQQNKILLAELEQLKGQGKSRL
GDLYEEEMRELRRQVDQLTNDKARVEVERDNLAEDIMRLREKLQEEMLQREEAENTLQSFRQDVDNASLAR
LDLERKVESLQEEIAFLKKLHEEEIQELQAQIQEQHVQIDVDVSKPDLTAALRDVRQQYESVAAKNLQEAEEWY
KSKFADLSEAANRNNDALRQAKQESTEYRRQVQSLTCEVDALKGTNESLERQMREMEENFAVEAANYQDTI
GRLQDEIQNMKEEMARHLREYQDLLNVKMALDIEIATYRKLLEGEESRISLPLPNFSSLNLRETNLDSLPLVDTH
SKRTFLIKTVETRDGQVINETSQHHDDLE

96 hr membrane fraction/Spot 9/Vimentin/X!Hunter

MSTRSVSSSSYRRMFGGPGTASRPSSSRSYVTTSTRTYSLGSALRPSTSRSLYASSPGGVYATRSSAVRLRSSVP
GVRLLQDSVDFSLADAINTEFKNTRTNEKVELQELNDRFANYIDKVRFLEQQNKILLAELEQLKGQGKSRLGDL
YEEEMRELRRQVDQLTNDKARVEVERDNLAEDIMRLREKLQEEMLQREEAENTLQSFRQDVDNASLARLDLE
RKVESLQEEIAFLKKLHEEEIQELQAQIQEQHVQIDVDVSKPDLTAALRDVRQQYESVAAKNLQEAEEWYKSKF
ADLSEAANRNNDALRQAKQESTEYRRQVQSLTCEVDALKGTNESLERQMREMEENFAVEAANYQDTIGRLQ
DEIQNMKEEMARHLREYQDLLNVKMALDIEIATYRKLLEGEESRISLPLPNFSSLNLRETNLDSLPLVDTHSKRT
LLIKTVETRDGQVINETSQHHDDLE

96 hr membrane fraction/Spot 9/Vimentin/X!Tandem P3

MSTRSVSSSSYRRMFGGPGTASRPSSSRSYVTTSTRTYSLGSALRPSTSRSLYASSPGGVYATRSSAVRLRS
SVPGVRLLQDSVDFSLADAINTEFKNTRTNEKVELQELNDRFANYIDKVRFLEQQNKILLAELEQLKGQGKSRL
GDLYEEEMRELRRQVDQLTNDKARVEVERDNLAEDIMRLREKLQEEMLQREEAENTLQSFRQDVDNASLAR
LDLERKVESLQEEIAFLKKLHEEEIQELQAQIQEQHVQIDVDVSKPDLTAALRDVRQQYESVAAKNLQEAEEWY
KSKFADLSEAANRNNDALRQAKQESTEYRRQVQSLTCEVDALKGTNESLERQMREMEENFAVEAANYQDTI
GRLQDEIQNMKEEMARHLREYQDLLNVKMALDIEIATYRKLLEGEESRISLPLPNFSSLNLRETNLDSLPLVDTH
SKRTLLIKTVETRDGQVINETSQHHDDLE

96 hr membrane fraction/Spot 10/Rab7/Mascot

MTSRKKVLLKVIILGDSGVGKTSLMNQYVNKKFSNQYKATIGADFLTKEVMVDDRLVTMQIWDTAGQE
RFQSLGVAFYRGADCCVLVFDVTAPNTFKTLDSWRDEFLIQASPRDPENFPFVVLGNKIDLENRQVATKRAQA
WCYSKNNIPYFETSAKEAINVEQAFQTIARNALKQETEVELYNEFPEPIKLDKNDRAKASAESCSC

96 hr membrane fraction/Spot 10/Rab7/X!Hunter

MTSRKKVLLKVIILGDSGVGKTSLMNQYVNKKFSNQYKATIGADFLTKEVMVDDRLVTMQIWDTAGQERFQ
SLGVAFYRGADCCVLVFDVTAPNTFKTLDSWRDEFLIQASPRDPENFPFVVLGNKIDLENRQVATKRAQAWC
YSKNNIPYFETSAKEAINVEQAFQTIARNALKQETEVELYNEFPEPIKLDKNDRAKASAESCSC

96 hr membrane fraction/Spot 10/Rab7/X!Tandem P3

MTSRKKVLLKVIILGDSGVGKTSLMNQYVNKKFSNQYKATIGADFLTKEVMVDDRLVTMQIWDTAGQE
RFQSLGVAFYRGADCCVLVFDVTAPNTFKTLDSWRDEFLIQASPRDPENFPFVVLGNKIDLENRQVATKRAQA
WCYSKNNIPYFETSAKEAINVEQAFQTIARNALKQETEVELYNEFPEPIKLDKNDRAKASAESCSC

96 hr membrane fraction/Spot 18/Rab7/Mascot

MTSRKKVLLKVIILGDSGVGKTSLMNQYVNKKFSNQYKATIGADFLTKEVMVDDRLVTMQIWDTAGQE
RFQSLGVAFYRGADCCVLVFDVTAPNTFKTLDSWRDEFLVQASPRDPENFPFVVLGNKVDLENRQVATKRA
QAWCYSKNNIPYFETSAKEAINVEQAFQTIARNALKQETEVELYNEFPEPIKLDKNDRAKASAESCSC

96 hr membrane fraction/Spot 18/Rab7/X!Hunter

MTSRKKVLLKVIILGDSGVGKTSLMNQYVNKKFSNQYKATIGADFLTKEVMVDDRLVTMQIWDTAGQERFQ
SLGVAFYRGADCCVLVFDVTAPNTFKTLDSWRDEFLIQASPRDPENFPFVVLGNKIDLENRQVATKRAQAWC
YSKNNIPYFETSAKEAINVEQAFQTIARNALKQETEVELYNEFPEPIKLDKNDRAKASAESCSC

96 hr membrane fraction/Spot 18/Rab7/X!Tandem P3

MTSRKKVLLKVIILGDSGVGKTSLMNQYVNKKFSNQYKATIGADFLTKEVMVDDRLVTMQIWDTAGQERFQ
SLGVAFYRGADCCVLVFDVTAPNTFKTLDSWRDEFLIQASPRDPENFPFVVLGNKIDLENRQVATKRAQAWC
YSKNNIPYFETSAKEAINVEQAFQTIARNALKQETEV

96 hr membrane fraction/Spot 20/Vimentin/Mascot

MSTRSVSSSSYRRMFGGPGTASRPSSSRSYVTTSTRTYSLGSALRPSTSRSLYASSPGGVYATRSSAVRLRS
SVPGVRLLQDSVDFSLADAINTEFKNTRTNEKVELQELNDRFANYIDKVRFLEQQNKILLAELEQLKGQGKSRL
GDLYEEEMRELRRQVDQLTNDKARVEVERDNLAEDIMRLREKLQEEMLQREEAENTLQSFRQDVDNASLAR
LDLERKVESLQEEIAFLKKLHEEEIQELQAQIQEQHVQIDVDVSKPDLTAALRDVRQQYESVAAKNLQEAEEWY
KSKFADLSEAANRNNDALRQAKQESTEYRRQVQSLTCEVDALKGTNESLERQMREMEENFAVEAANYQDTI
GRLQDEIQNMKEEMARHLREYQDLLNVKMALDIEIATYRKLLEGEESRISLPLPNFSSLNLRETNLDSLPLVDTH
SKRTFLIKTVETRDGQVINETSQHHDDLE

96 hr membrane fraction/Spot 20/Vimentin/X!Hunter

MSTRSVSSSSYRRMFGGPGTASRPSSSRSYVTTSTRTYSLGSALRPSTSRSLYASSPGGVYATRSSAVRLRS
SVPGVRLLQDSVDFSLADAINTEFKNTRTNEKVELQELNDRFANYIDKVRFLEQQNKILLAELEQLKGQGKSRL
GDLYEEEMRELRRQVDQLTNDKARVEVERDNLAEDIMRLREKLQEEMLQREEAENTLQSFRQDVDNASLAR
LDLERKVESLQEEIAFLKKLHEEEIQELQAQIQEQHVQIDVDVSKPDLTAALRDVRQQYESVAAKNLQEAEEWY
KSKFADLSEAANRNNDALRQAKQESTEYRRQVQSLTCEVDALKGTNESLERQMREMEENFAVEAANYQDTI
GRLQDEIQNMKEEMARHLREYQDLLNVKMALDIEIATYRKLLEGEESRISLPLPNFSSLNLRETNLDSLPLVDTH
SKRTFLIKTVETRDGQVINETSQHHDDLE

96 hr membrane fraction/Spot 20/Vimentin/X!Tandem P3

MSTRSVSSSSYRRMFGGPGTASRPSSSRSYVTTSTRTYSLGSALRPSTSRSLYASSPGGVYATRSSAVRLRS
SVPGVRLLQDSVDFSLADAINTEFKNTRTNEKVELQELNDRFANYIDKVRFLEQQNKILLAELEQLKGQGKSRL
GDLYEEEMRELRRQVDQLTNDKARVEVERDNLAEDIMRLREKLQEEMLQREEAENTLQSFRQDVDNASLAR
LDLERKVESLQEEIAFLKKLHEEEIQELQAQIQEQHVQIDVDVSKPDLTAALRDVRQQYESVAAKNLQEAEEWY
KSKFADLSEAANRNNDALRQAKQESTEYRRQVQSLTCEVDALKGTNESLERQMREMEENFAVEAANYQDTI
GRLQDEIQNMKEEMARHLREYQDLLNVKMALDIEIATYRKLLEGEESRISLPLPNFSSLNLRETNLDSLPLVDTH
SKRTLLIKTVETRDGQVINETSQHHDDLE

96 hr membrane fraction/Spot 28/Hsp60/Mascot

MLRLPTVFRQMRPVSRVLAPHLTRAYAKDVKFGADARALMLQGVDLLADAVAVTMGPKGRTVIIEQS
WGSPKVTKDGVTVAKSIDLKDKYKNIGAKLVQDVANNTNEEAGDGTTTATVLARSIAKEGFEKISKGANPVEI
RRGVMLAVDAVIAELKKQSKPVTTPEEIAQVATISANGDKEIGNIISDAMKKVGRKGVITVKDGKTLNDELEIIE
GMKFDRGYISPYFINTSKGQKCEFQDAYVLLSEKKISSIQSIVPALEIANAHRKPLVIIAEDVDGEALSTLVLNRLK
VGLQVVAVKAPGFGDNRKNQLKDMAIATGGAVFGEEGLTLNLEDVQPHDLGKVGEVIVTKDDAMLLKGKG
DKAQIEKRIQEIIEQLDVTTSEYEKEKLNERLAKLSDGVAVLKVGGTSDVEVNEKKDRVTDALNATRAAVEEGIV
LGGGCALLRCIPALDSLTPANEDQKIGIEIIKRTLKIPAMTIAKNAGVEGSLIVEKIMQSSSEVGYDAMAGDFVN
MVEKGIIDPTKVVRTALLDAAGVASLLTTAEVVVTEIPKEEKDPGMGAMGGMGGGMGGGMF

96 hr membrane fraction/Spot 28/Hsp60/X!Hunter

MLRLPTVFRQMRPVSRVLAPHLTRAYAKDVKFGADARALMLQGVDLLADAVAVTMGPKGRTVIIEQS
WGSPKVTKDGVTVAKSIDLKDKYKNIGAKLVQDVANNTNEEAGDGTTTATVLARSIAKEGFEKISKGANPVEI
RRGVMLAVDAVIAELKKQSKPVTTPEEIAQVATISANGDKEIGNIISDAMKKVGRKGVITVKDGKTLNDELEIIE
GMKFDRGYISPYFINTSKGQKCEFQDAYVLLSEKKISSIQSIVPALEIANAHRKPLVIIAEDVDGEALSTLVLNRLK
VGLQVVAVKAPGFGDNRKNQLKDMAIATGGAVFGEEGLTLNLEDVQPHDLGKVGEVIVTKDDAMLLKGKG
DKAQIEKRIQEIIEQLDVTTSEYEKEKLNERLAKLSDGVAVLKVGGTSDVEVNEKKDRVTDALNATRAAVEEGIV
LGGGCALLRCIPALDSLTPANEDQKIGIEIIKRTLKIPAMTIAKNAGVEGSLIVEKIMQSSSEVGYDAMAGDFVN
MVEKGIIDPTKVVRTALLDAAGVASLLTTAEVVVTEIPKEEKDPGMGAMGGMGGGMGGGMF

96 hr membrane fraction/Spot 28/Hsp60/X!Tandem P3

MLRLPTVFRQMRPVSRVLAPHLTRAYAKDVKFGADARALMLQGVDLLADAVAVTMGPKGRTVIIEQSWGS
PKVTKDGVTVAKSIDLKDKYKNIGAKLVQDVANNTNEEAGDGTTTATVLARSIAKEGFEKISKGANPVEIRRGV
MLAVDAVIAELKKQSKPVTTPEEIAQVATISANGDKEIGNIISDAMKKVGRKGVITVKDGKTLNDELEIIEGMKF
DRGYISPYFINTSKGQKCEFQDAYVLLSEKKISSIQSIVPALEIANAHRKPLVIIAEDVDGEALSTLVLNRLKVGLQ
VVAVKAPGFGDNRKNQLKDMAIATGGAVFGEEGLTLNLEDVQPHDLGKVGEVIVTKDDAMLLKGKGDKAQI
EKRIQEIIEQLDVTTSEYEKEKLNERLAKLSDGVAVLKVGGTSDVEVNEKKDRVTDALNATRAAVEEGIVLGGG
CALLRCIPALDSLTPANEDQKIGIEIIKRTLKIPAMTIAKNAGVEGSLIVEKIMQSSSEVGYDAMAGDFVNMVEK
GIIDPTKVVRTALLDAAGVASLLTTAEVVVTEIPKEEKDPGMGAMGGMGGGMGGGMF

96 hr membrane fraction/Spot 97/Enoyl CoA Hydratase 1/Mascot

MAAGIVASRRLRDLLTRRLTGSNYPGLSISLRLTGSSAQEEASGVALGEAPDHSYESLRVTSAQKHVLHVQ
LNRPNKRNAMNKVFWREMVECFNKISRDADCRAVVISGAGKMFTAGIDLMDMASDILQPKGDDVARISW
YLRDIITRYQETFNVIERCPKPVIAAVHGGCIGGGVDLVTACDIRYCAQDAFFQVKEVDVGLAADVGTLQRLPK
VIGNQSLVNELAFTARKMMADEALGSGLVSRVFPDKEVMLDAALALAAEISSKSPVAVQSTKVNLLYSRDHSV
AESLNYVASWNMSMLQTQDLVKSVQATTENKELKTVTFSKL

96 hr membrane fraction/Spot 97/Enoyl CoA Hydratase 1/X!Hunter

MAAGIVASRRLRDLLTRRLTGSNYPGLSISLRLTGSSAQEEASGVALGEAPDHSYESLRVTSAQKHVLHVQLNR
PNKRNAMNKVFWREMVECFNKISRDADCRAVVISGAGKMFTAGIDLMDMASDILQPKGDDVARISWYLR
DIITRYQETFNVIERCPKPVIAAVHGGCIGGGVDLVTACDIRYCAQDAFFQVKEVDVGLAADVGTLQRLPKVIG
NQSLVNELAFTARKMMADEALGSGLVSRVFPDKEVMLDAALALAAEISSKSPVAVQSTKVNLLYSRDHSVAE
SLNYVASWNMSMLQTQDLVKSVQATTENKELKTVTFSKL

96 hr membrane fraction/Spot 97/Enoyl CoA Hydratase 1/X!Tandem P3

MAAGIVASRRLRDLLTRRLTGSNYPGLSISLRLTGSSAQEEASGVALGEAPDHSYESLRVTSAQKHVLHVQLNR
PNKRNAMNKVFWREMVECFNKISRDADCRAVVISGAGKMFTAGIDLMDMASDILQPKGDDVARISWYLR
DIITRYQETFNVIERCPKPVIAAVHGGCIGGGVDLVTACDIRYCAQDAFFQVKEVDVGLAADVGTLQRLPKVIG
NQSLVNELAFTARKMMADEALGSGLVSRVFPDKEVMLDAALALAAEISSKSPVAVQSTKVNLLYSRDHSVAE
SLNYVASWNMSMLQTQDLVKSVQATTENKELKTVTFSKL

96 hr soluble fraction/Spot 122/Aldehyde dehydrogenase 2/Mascot

MLRAAARFGPRLGRRLLSAAATQAVPAPNQQPEVFCNQIFINNEWHDAVSRKTFPTVNPSTGEVICQV
AEGDKEDVDKAVKAARAAFQLGSPWRRMDASHRGRLLNRLADLIERDRTYLAALETLDNGKPYVISYLVDLD
MVLKCLRYYAGWADKYHGKTIPIDGDFFSYTRHEPVGVCGQIIPWNFPLLMQAWKLGPALATGNVVVMKV
AEQTPLTALYVANLIKEAGFPPGVVNIVPGFGPTAGAAIASHEDVDKVAFTGSTEIGRVIQVAAGSSNLKRVTL
ELGGKSPNIIMSDADMDWAVEQAHFALFFNQGQCCCAGSRTFVQEDIYDEFVERSVARAKSRVVGNPFDSK
TEQGPQVDETQFKKILGYINTGKQEGAKLLCGGGIAADRGYFIQPTVFGDVQDGMTIAKEEIFGPVMQILKFK
TIEEVVGRANNSTYGLAAAVFTKDLDKANYLSQALQAGTVWVNCYDVFGAQSPFGGYKMSGSGRELGEYGL
QAYTEVKTVTVKVPQKNS

96 hr soluble fraction/Spot 122/Aldehyde dehydrogenase 2/X!Hunter

MLRAAARFGPRLGRRLLSAAATQAVPAPNQQPEVFCNQIFINNEWHDAVSRKTFPTVNPSTGEVICQV
AEGDKEDVDKAVKAARAAFQLGSPWRRMDASHRGRLLNRLADLIERDRTYLAALETLDNGKPYVISYLVDLD
MVLKCLRYYAGWADKYHGKTIPIDGDFFSYTRHEPVGVCGQIIPWNFPLLMQAWKLGPALATGNVVVMKV
AEQTPLTALYVANLIKEAGFPPGVVNIVPGFGPTAGAAIASHEDVDKVAFTGSTEIGRVIQVAAGSSNLKRVTL
ELGGKSPNIIMSDADMDWAVEQAHFALFFNQGQCCCAGSRTFVQEDIYDEFVERSVARAKSRVVGNPFDSK
TEQGPQVDETQFKKILGYINTGKQEGAKLLCGGGIAADRGYFIQPTVFGDVQDGMTIAKEEIFGPVMQILKFK
TIEEVVGRANNSTYGLAAAVFTKDLDKANYLSQALQAGTVWVNCYDVFGAQSPFGGYKMSGSGRELGEYGL
QAYTEVKTVTVKVPQKNS

96 hr soluble fraction/Spot 122/Aldehyde dehydrogenase 2/X!Tandem P3

MLRAAARFGPRLGRRLLSAAATQAVPAPNQQPEVFCNQIFINNEWHDAVSRKTFPTVNPSTGEVICQV
AEGDKEDVDKAVKAARAAFQLGSPWRRMDASHRGRLLNRLADLIERDRTYLAALETLDNGKPYVISYLVDLD
MVLKCLRYYAGWADKYHGKTIPIDGDFFSYTRHEPVGVCGQIIPWNFPLLMQAWKLGPALATGNVVVMKV
AEQTPLTALYVANLIKEAGFPPGVVNIVPGFGPTAGAAIASHEDVDKVAFTGSTEIGRVIQVAAGSSNLKRVTL
ELGGKSPNIIMSDADMDWAVEQAHFALFFNQGQCCCAGSRTFVQEDIYDEFVERSVARAKSRVVGNPFDSK
TEQGPQVDETQFKKILGYINTGKQEGAKLLCGGGIAADRGYFIQPTVFGDVQDGMTIAKEEIFGPVMQILKFK
TIEEVVGRANNSTYGLAAAVFTKDLDKANYLSQALQAGTVWVNCYDVFGAQSPFGGYKMSGSGRELGEYGL
QAYTEVKTVTVKVPQKNS

Securinine soluble fraction/Spot 1/Hsp70/Mascot

LRSCCDSPLPFSRVTPVVPRLPRANLCGCRHRRVEFPASGRTELFSRIQCSVSSPQSQSRADREQGTGMA
KAAAIGIDLGTTYSCVGVFQHGKVEIIANDQGNRTTPSYVAFTDTERLIGDAAKNQVALNPQNTVFDAKRLIG
RKFGDPVVQSDMKHWPFQVINDGDKPKVQVSYKGDTKAFYPEEISSMVLTKMKEIAEAYLGYPVTNAVITVP
AYFNDSQRQATKDAGVIAGLNVLRIINEPTAAAIAYGLDRTGKGERNVLIFDLGGGTFDVSILTIDDGIFEVKAT
AGDTHLGGEDFDNRLVNHFVEEFKRKHKKDISQNKRAVRRLRTACERAKRTLSSSTQASLEIDSLFEGIDFYTSI
TRARFEELCSDLFRSTLEPVEKALRDAKLDKAQIHDLVLVGGSTRIPKVQKLLQDFFNGRDLNKSINPDEAVAYG
AAVQAAILMGDKSENVQDLLLLDVAPLSLGLETAGGVMTALIKRNSTIPTKQTQIFTTYSDNQPGVLIQVYEGE
RAMTKDNNLLGRFELSGIPPAPRGVPQIEVTFDIDANGILNVTATDKSTGKANKITITNDKGRLSKEEIESMVQE
AEKYKAEDEVQRERVSAKNALESYAFNMKSAVEDEGLKGKISEADKKKVLDKCQEVISWLDANTLAEKDEFEH
KRKELEQVCNPIISGLYQGAGGPGPGGFGAQGPKGGSGSGPTIEEVD

Securinine soluble fraction/Spot 1/Hsp70/X!Hunter

MAKAAAIGIDLGTTYSCVGVFQHGKVEIIANDQGNRTTPSYVAFTDTERLIGDAAKNQVALNPQNTVFDAKR
LIGRKFGDPVVQSDMKHWPFQVINDGDKPKVQVSYKGETKAFYPEEISSMVLTKMKEIAEAYLGYPVTNAVIT
VPAYFNDSQRQATKDAGVIAGLNVLRIINEPTAAAIAYGLDRTGKGERNVLIFDLGGGTFDVSILTIDDGIFEVK
ATAGDTHLGGEDFDNRLVNHFVEEFKRKHKKDISQNKRAVRRLRTACERAKRTLSSSTQASLEIDSLFEGIDFYT
SITRARFEELCSDLFRSTLEPVEKALRDAKLDKAQIHDLVLVGGSTRIPKVQKLLQDFFNGRDLNKSINPDEAVA
YGAAVQAAILMGDKSENVQDLLLLDVAPLSLGLETAGGVMTALIKRNSTIPTKQTQIFTTYSDNQPGVLIQVYE
GERAMTKDNNLLGRFELSGIPPAPRGVPQIEVTFDIDANGILNVTATDKSTGKANKITITNDKGRLSKEEIERM
VQEAEKYKAEDEVQRERVSAKNALESYAFNMKSAVEDEGLKGKISEADKKKVLDKCQEVISWLDANTLAEKD
EFEHKRKELEQVCNPIISGLYQGAGGPGPGGFGAQGPKGGSGSGPTIEEVD

Securinine soluble fraction/Spot 1/Hsp70/X!Tandem P3

MAKAAAIGIDLGTTYSCVGVFQHGKVEIIANDQGNRTTPSYVAFTDTERLIGDAAKNQVALNPQNTVFD
AKRLIGRKFGDPVVQSDMKHWPFQVINDSQRQATKDAGVIAGLNVLRIINEPTAAAIAYGLDRTGKGERNVLI
FDLGGGTFDVSILTIDDGIFEVKATAGDTHLGGEDFDNRLVNHFVEEFKRKHKKDISQNKRAVRRLRTACERAK
RTLSSSTQASLEIDSLFEGIDFYTSITRARFEELCSDLFRSTLEPVEKALRDAKLDKAQIHDLVLVGGSTRIPKVQKL
LQDFFDGRDLNKSINPDEAVAYGAAVQAAILMGDKSENVQDLLLLDVAPLSLGLETAGGVMTALIKRNSTIPT
KQTQIFTTYSDNQPGVLIQVYEGERAMTKDNNLLGRFELSGIPPAPRGVPQIEVTFDIDANGILNVTATDKSTG
NANKITITNDKGRLSKEEIERMVQEAEKYKAEDEVQRERVSAKNALESYAFNMKSAVEDEGLKGKISEADKKK
VLDKCQEVISWLDANTLAEKDEFEHKRKELEQVCNPIISGLYQGAGGPGPGGFGAQGPKGGSGSGPTIEEVD

Securinine soluble fraction/Spot 3/Hsp70/Mascot

LRSCCDSPLPFSRVTPVVPRLPRANLCGCRHRRVEFPASGRTELFSRIQCSVSSPQSQSRADREQGTGMA
KAAAIGIDLGTTYSCVGVFQHGKVEIIANDQGNRTTPSYVAFTDTERLIGDAAKNQVALNPQNTVFDAKRLIG
RKFGDPVVQSDMKHWPFQVINDGDKPKVQVSYKGDTKAFYPEEISSMVLTKMKEIAEAYLGYPVTNAVITVP
AYFNDSQRQATKDAGVIAGLNVLRIINEPTAAAIAYGLDRTGKGERNVLIFDLGGGTFDVSILTIDDGIFEVKAT
AGDTHLGGEDFDNRLVNHFVEEFKRKHKKDISQNKRAVRRLRTACERAKRTLSSSTQASLEIDSLFEGIDFYTSI
TRARFEELCSDLFRSTLEPVEKALRDAKLDKAQIHDLVLVGGSTRIPKVQKLLQDFFNGRDLNKSINPDEAVAYG
AAVQAAILMGDKSENVQDLLLLDVAPLSLGLETAGGVMTALIKRNSTIPTKQTQIFTTYSDNQPGVLIQVYEGE
RAMTKDNNLLGRFELSGIPPAPRGVPQIEVTFDIDANGILNVTATDKSTGKANKITITNDKGRLSKEEIESMVQE
AEKYKAEDEVQRERVSAKNALESYAFNMKSAVEDEGLKGKISEADKKKVLDKCQEVISWLDANTLAEKDEFEH
KRKELEQVCNPIISGLYQGAGGPGPGGFGAQGPKGGSGSGPTIEEVD

Securinine soluble fraction/Spot 3/Hsp70/X!Hunter

MAKAAAIGIDLGTTYSCVGVFQHGKVEIIANDQGNRTTPSYVAFTDTERLIGDAAKNQVALNPQNTVFDAKR
LIGRKFGDPVVQSDMKHWPFQVINDGDKPKVQVSYKGETKAFYPEEISSMVLTKMKEIAEAYLGYPVTNAVIT
VPAYFNDSQRQATKDAGVIAGLNVLRIINEPTAAAIAYGLDRTGKGERNVLIFDLGGGTFDVSILTIDDGIFEVK
ATAGDTHLGGEDFDNRLVNHFVEEFKRKHKKDISQNKRAVRRLRTACERAKRTLSSSTQASLEIDSLFEGIDFYT
SITRARFEELCSDLFRSTLEPVEKALRDAKLDKAQIHDLVLVGGSTRIPKVQKLLQDFFNGRDLNKSINPDEAVA
YGAAVQAAILMGDKSENVQDLLLLDVAPLSLGLETAGGVMTALIKRNSTIPTKQTQIFTTYSDNQPGVLIQVYE
GERAMTKDNNLLGRFELSGIPPAPRGVPQIEVTFDIDANGILNVTATDKSTGKANKITITNDKGRLSKEEIERM
VQEAEKYKAEDEVQRERVSAKNALESYAFNMKSAVEDEGLKGKISEADKKKVLDKCQEVISWLDANTLAEKD
EFEHKRKELEQVCNPIISGLYQGAGGPGPGGFGAQGPKGGSGSGPTIEEVD

Securinine soluble fraction/Spot 3/Hsp70/X!Tandem P3

MAKAAAIGIDLGTTYSCVGVFQHGKVEIIANDQGNRTTPSYVAFTDTERLIGDAAKNQVALNPQNTVFDAKR
LIGRKFGDPVVQSDMKHWPFQVINDGDKPKVQVSYKGETKAFYPEEISSMVLTKMKEIAEAYLGYPVTNAVIT
VPAYFNDSQRQATKDAGVIAGLNVLRIINEPTAAAIAYGLDRTGKGERNVLIFDLGGGTFDVSILTIDDGIFEVK
ATAGDTHLGGEDFDNRLVNHFVEEFKRKHKKDISQNKRAVRRLRTACERAKRTLSSSTQASLEIDSLFEGIDFYT
SITRARFEELCSDLFRSTLEPVEKALRDAKLDKAQIHDLVLVGGSTRIPKVQKLLQDFFNGRDLNKSINPDEAVA
YGAAVQAAILMGDKSENVQDLLLLDVAPLSLGLETAGGVMTALIKRNSTIPTKQTQIFTTYSDNQPGVLIQVYE
GERAMTKDNNLLGRFELSGIPPAPRGVPQIEVTFDIDANGILNVTATDKSTGKANKITITNDKGRLSKEEIERM
VQEAEKYKAEDEVQRERVSAKNALESYAFNMKSAVEDEGLKGKISEADKKKVLDKCQEVISWLDANTLAEKD
EFEHKRKELEQVCNPIISGLYQGAGGPGPGGFGAQGPKGGSGSGPTIEEVD

Securinine soluble fraction/Spot 4/Fatty acid binding protein 5/Mascot

MATVQQLEGRWRLVDSKGFDEYMKELGVGIALRKMGAMAKPDCIITCDGKNLTIKTESTLKTTQFSCTL
GEKFEETTADGRKTQTVCNFTDGALVQHQEWDGKESTITRKLKDGKLVVECVMNNVTCTRIYEKVE

Securinine soluble fraction/Spot 4/Fatty acid binding protein 5/X!Hunter

MATVQQLEGRWRLVDSKGFDEYMKELGVGIALRKMGAMAKPDCIITCDGKNLTIKTESTLKTTQFSCTLGEK
FEETTADGRKTQTVCNFTDGALVQHQEWDGKESTITRKLKDGKLVVECVMNNVTCTRIYEKVE

Securinine soluble fraction/Spot 4/Fatty acid binding protein 5/X!Tandem P3

MATVQQLEGRWRLVDSKGFDEYMKELGVGIALRKMGAMAKPDCIITCDGKNLTIKTESTLKTTQFSCTLGEK
FEETTADGRKTQTVCNFTDGALVQHQEWDGKESTITRKLKDGKLVVECVMNNVTCTRIYEKVE

Securinine soluble fraction/Spot 5/L-plastin/Mascot

MARGSVSDEEMMELREAFAKVDTDGNGYISFNELNDLFKAACLPLPGYRVREITENLMATGDLDQDGRI
SFDEFIKIFHGLKSTDVAKTFRKAINKKEGICAIGGTSEQSSVGTQHSYSEEEKYAFVNWINKALENDPDCRHVIP
MNPNTNDLFNAVGDGIVLCKMINLSVPDTIDERTINKKKLTPFTIQENLNLALNSASAIGCHVVNIGAEDLKEG
KPYLVLGLLWQVIKIGLFADIELSRNEALIALLREGESLEDLMKLSPEELLLRWANYHLENAGCNKIGNFSTDIKD
SKAYYHLLEQVAPKGDEEGVPAVVIDMSGLREKDDIQRAECMLQQAERLGCRQFVTATDVVRGNPKLNLAFI
ANLFNRYPALHKPENQDIDWGALEGETREERTFRNWMNSLGVNPRVNHLYSDLSDALVIFQLYEKIKVPVD
WNRVNKPPYPKLGGNMKKLENCNYAVELGKNQAKFSLVGIGGQDLNEGNRTLTLALIWQLMRRYTLNILEEI
GGGQKVNDDIIVNWVNETLREAEKSSSISSFKDPKISTSLPVLDLIDAIQPGSINYDLLKTENLNDDEKLNNAKY
AISMARKIGARVYALPEDLVEVNPKMVMTVFACLMGKGMKRV

Securinine soluble fraction/Spot 5/L-plastin/X!Hunter

MARGSVSDEEMMELREAFAKVDTDGNGYISFNELNDLFKAACLPLPGYRVREITENLMATGDLDQDGRISFD
EFIKIFHGLKSTDVAKTFRKAINKKEGICAIGGTSEQSSVGTQHSYSEEEKYAFVNWINKALENDPDCRHVIPMN
PNTNDLFNAVGDGIVLCKMINLSVPDTIDERTINKKKLTPFTIQENLNLALNSASAIGCHVVNIGAEDLKEGKPY
LVLGLLWQVIKIGLFADIELSRNEALIALLREGESLEDLMKLSPEELLLRWANYHLENAGCNKIGNFSTDIKDSKA
YYHLLEQVAPKGDEEGVPAVVIDMSGLREKDDIQRAECMLQQAERLGCRQFVTATDVVRGNPKLNLAFIANL
FNRYPALHKPENQDIDWGALEGETREERTFRNWMNSLGVNPRVNHLYSDLSDALVIFQLYEKIKVPVDWNR
VNKPPYPKLGGNMKKLENCNYAVELGKNQAKFSLVGIGGQDLNEGNRTLTLALIWQLMRRYTLNILEEIGGG
QKVNDDIIVNWVNETLREAEKSSSISSFKDPKISTSLPVLDLIDAIQPGSINYDLLKTENLNDDEKLNNAKYAISM
ARKIGARVYALPEDLVEVNPKMVMTVFACLMGKGMKRV

Securinine soluble fraction/Spot 5/L-plastin/X!Tandem P3

MARGSVSDEEMMELREAFAKVDTDGNGYISFNELNDLFKAACLPLPGYRVREITENLMATGDLDQDGRISFD
EFIKIFHGLKSTDVAKTFRKAINKKEGICAIGGTSEQSSVGTQHSYSEEEKYAFVNWINKALENDPDCRHVIPMN
PNTNDLFNAVGDGIVLCKMINLSVPDTIDERTINKKKLTPFTIQENLNLALNSASAIGCHVVNIGAEDLKEGKPY
LVLGLLWQVIKIGLFADIELSRNEALIALLREGESLEDLMKLSPEELLLRWANYHLENAGCNKIGNFSTDIKDSKA
YYHLLEQVAPKGDEEGVPAVVIDMSGLREKDDIQRAECMLQQAERLGCRQFVTATDVVRGNPKLNLAFIANL
FNRYPALHKPENQDIDWGALEGETREERTFRNWMNSLGVNPRVNHLYSDLSDALVIFQLYEKIKVPVDWNR
VNKPPYPKLGGNMKKLENCNYAVELGKNQAKFSLVGIGGQDLNEGNRTLTLALIWQLMRRYTLNILEEIGGG
QKVNDDIIVNWVNETLREAEKSSSISSFKDPKISTSLPVLDLIDAIQPGSINYDLLKTENLNDDEKLNNAKYAISM
ARKIGARVYALPEDLVEVNPKMVMTVFACLMGKGMKRV

Securinine soluble fraction/Spot 7/S100 Ca^{2+} binding protein A4/Mascot
MACPLEKALDVMVSTFHKYSGKEGDKFKLNKSELKELLTRELPSFLGKRTDEAAFQKLMSNLDSNRDNEV
DFQEYCVFLSCIAMMCNEFFEGFPDKQPRKK

Securinine soluble fraction/Spot 7/S100 Ca^{2+} binding protein A4/X!Hunter
MACPLEKALDVMVSTFHKYSGKEGDKFKLNKSELKELLTRELPSFLGKRTDEAAFQKLMSNLDSNRDNEV

DFQEYCVFLSCIAMMCNEFFEGFPDKQPRKK

not found by P3

Securinine soluble fraction/Spot 9/Hsp70/Mascot

MAKAAAIGIDLGTTYSCVGVFQHGKVEIIANDQGNRTTPSYVAFTDTERLIGDAAKNQVALNPQNTVFD
AKRLIGRKFGDPVVQSDMKHWPFQVINDGDKPKVQVSYKGETKAFYPEEISSMVLTKMKEIAEAYLGYPVTN
AVITVPAYFNDSQRQATKDAGVIAGLNVLRIINEPTAAAIAYGLDRTGKGERNVLIFDLGGGTFDVSILTIDDGIF
EVKATAGDTHLGGEDFDNRLVNHFVEEFKRKHKKDISQNKRAVRRLRTACERAKRTLSSSTQASLEIDSLFEGI
DFYTSITRARFEELCSDLFRSTLEPVEKALRDAKLDKAQIHDLVLVGGSTRIPKVQKLLQDFFNGRDLNKSINPDE
AVAYGAAVQAAILMGDKSENVQDLLLLDVAPLSLGLETAGGVMTALIKRNSTIPTKQTQIFTTYSDNQPGVLI
QVYEGERAMTKDNNLLGRFELSGIPPAPRGVPQIEVTFDIDANGILNVTATDKSTGKANKITITNDKGRLSKEEI
ERMVQEAEKYKAEDEVQRERVSAKNALESYAFNMKSAVEDEGLKGKISEADKKKVLDKCQEVISWLDANTLA
EKDEFEHKRKELEQVCNPIISGLYQGAGGPGPGGFGAQGPKGGSGSGPTIEEVD

Securinine soluble fraction/Spot 9/Hsp70/X!Hunter

MSKGPAVGIDLGTTYSCVGVFQHGKVEIIANDQGNRTTPSYVAFTDTERLIGDAAKNQVAMNPTNTVFDAK
RLIGRRFDDAVVQSDMKHWPFMVVNDAGRPKVQVEYKGETKSFYPEEVSSMVLTKMKEIAEAYLGKTVTNA
VVTVPAYFNDSQRQATKDAGTIAGLNVLRIINEPTAAAIAYGLDKKVGAERNVLIFDLGGGTFDVSILTIEDGIFE
VKSTAGDTHLGGEDFDNRMVNHFIAEFKRKHKKDISENKRAVRRLRTACERAKRTLSSSTQASIEIDSLYEGIDF
YTSITRARFEELNADLFRGTLDPVEKALRDAKLDKSQIHDIVLVGGSTRIPKIQKLLQDFFNGKELNKSINPDEAV
AYGAAVQAAILSGDKSENVQDLLLLDVTPLSLGIETAGGVMTVLIKRNTTIPTKQTQTFTTYSDNQPGVLIQVY
EGERAMTKDNNLLGKFELTGIPPAPRGVPQIEVTFDIDANGILNVSAVDKSTGKENKITITNDKGRLSKEDIER
MVQEAEKYKAEDEKQRDKVSSKNSLESYAFNMKATVEDEKLQGKINDEDKQKILDKCNEIINWLDKNQTAEK
EEFEHQQKELEKVCNPIITKLYQSAGGMPGGMPGGFPGGGAPPSGGASSGPTIEEVD

Securinine soluble fraction/Spot 9/Hsp70/X!Tandem P3

MAKAAAIGIDLGTTYSCVGVFQHGKVEIIANDQGNRTTPSYVAFTDTERLIGDAAKNQVALNPQNTVFDAKR
LIGRKFGDPVVQSDMKHWPFQVINDGDKPKVQVSYKGETKAFYPEEISSMVLTKMKEIAEAYLGYPVTNAVIT
VPAYFNDSQRQATKDAGVIAGLNVLRIINEPTAAAIAYGLDRTGKGERNVLIFDLGGGTFDVSILTIDDGIFEVK
ATAGDTHLGGEDFDNRLVNHFVEEFKRKHKKDISQNKRAVRRLRTACERAKRTLSSSTQASLEIDSLFEGIDFYT
SITRARFEELCSDLFRSTLEPVEKALRDAKLDKAQIHDLVLVGGSTRIPKVQKLLQDFFNGRDLNKSINPDEAVA
YGAAVQAAILMGDKSENVQDLLLLDVAPLSLGLETAGGVMTALIKRNSTIPTKQTQIFTTYSDNQPGVLIQVYE
GERAMTKDNNLLGRFELSGIPPAPRGVPQIEVTFDIDANGILNVTATDKSTGKANKITITNDKGRLSKEEIERM
VQEAEKYKAEDEVQRERVSAKNALESYAFNMKSAVEDEGLKGKISEADKKKVLDKCQEVISWLDANTLAEKD
EFEHKRKELEQVCNPIISGLYQGAGGPGPGGFGAQGPKGGSGSGPTIEEVD

Securinine soluble fraction/Spot 10/L-plastin/Mascot

MARGSVSDEEMMELREAFAKVDTDGNGYISFNELNDLFKAACLPLPGYRVREITENLMATGDLDQDGRI
SFDEFIKIFHGLKSTDVAKTFRKAINKKEGICAIGGTSEQSSVGTQHSYSEEEKYAFVNWINKALENDPDCRHVIP
MNPNTNDLFNAVGDGIVLCKMINLSVPDTIDERTINKKKLTPFTIQENLNLALNSASAIGCHVVNIGAEDLKEG
KPYLVLGLLWQVIKIGLFADIELSRNEALIALLREGESLEDLMKLSPEELLLRWANYHLENAGCNKIGNFSTDIKD
SKAYYHLLEQVAPKGDEEGVPAVVIDMSGLREKDDIQRAECMLQQAERLGCRQFVTATDVVRGNPKLNLAFI
ANLFNRYPALHKPENQDIDWGALEGETREERTFRNWMNSLGVNPRVNHLYSDLSDALVIFQLYEKIKVPVD
WNRVNKPPYPKLGGNMKKLENCNYAVELGKNQAKFSLVGIGGQDLNEGNRTLTLALIWQLMRRYTLNILEEI
GGGQKVNDDIIVNWVNETLREAEKSSSISSFKDPKISTSLPVLDLIDAIQPGSINYDLLKTENLNDDEKLNNAKY
AISMARKIGARVYALPEDLVEVNPKMVMTVFACLMGKGMKRV

Securinine soluble fraction/Spot 10/L-plastin/X!Hunter

MARGSVSDEEMMELREAFAKVDTDGNGYISFNELNDLFKAACLPLPGYRVREITENLMATGDLDQDGRISFD
EFIKIFHGLKSTDVAKTFRKAINKKEGICAIGGTSEQSSVGTQHSYSEEEKYAFVNWINKALENDPDCRHVIPMN
PNTNDLFNAVGDGIVLCKMINLSVPDTIDERTINKKKLTPFTIQENLNLALNSASAIGCHVVNIGAEDLKEGKPY
LVLGLLWQVIKIGLFADIELSRNEALIALLREGESLEDLMKLSPEELLLRWANYHLENAGCNKIGNFSTDIKDSKA
YYHLLEQVAPKGDEEGVPAVVIDMSGLREKDDIQRAECMLQQAERLGCRQFVTATDVVRGNPKLNLAFIANL
FNRYPALHKPENQDIDWGALEGETREERTFRNWMNSLGVNPRVNHLYSDLSDALVIFQLYEKIKVPVDWNR
VNKPPYPKLGGNMKKLENCNYAVELGKNQAKFSLVGIGGQDLNEGNRTLTLALIWQLMRRYTLNILEEIGGG
QKVNDDIIVNWVNETLREAEKSSSISSFKDPKISTSLPVLDLIDAIQPGSINYDLLKTENLNDDEKLNNAKYAISM
ARKIGARVYALPEDLVEVNPKMVMTVFACLMGKGMKRV

Securinine soluble fraction/Spot 10/L-plastin/X!Tandem P3

MARGSVSDEEMMELREAFAKVDTDGNGYISFNELNDLFKAACLPLPGYRVREITENLMATGDLDQDGRISFD
EFIKIFHGLKSTDVAKTFRKAINKKEGICAIGGTSEQSSVGTQHSYSEEEKYAFVNWINKALENDPDCRHVIPMN
PNTNDLFNAVGDGIVLCKMINLSVPDTIDERTINKKKLTPFTIQENLNLALNSASAIGCHVVNIGAEDLKEGKPY
LVLGLLWQVIKIGLFADIELSRNEALIALLREGESLEDLMKLSPEELLLRWANYHLENAGCNKIGNFSTDIKDSKA
YYHLLEQVAPKGDEEGVPAVVIDMSGLREKDDIQRAECMLQQAERLGCRQFVTATDVVRGNPKLNLAFIANL
FNRYPALHKPENQDIDWGALEGETREERTFRNWMNSLGVNPRVNHLYSDLSDALVIFQLYEKIKVPVDWNR
VNKPPYPKLGGNMKKLENCNYAVELGKNQAKFSLVGIGGQDLNEGNRTLTLALIWQLMRRYTLNILEEIGGG
QKVNDDIIVNWVNETLREAEKSSSISSFKDPKISTSLPVLDLIDAIQPGSINYDLLKTENLNDDEKLNNAKYAISM
ARKIGARVYALPEDLVEVNPKMVMTVFACLMGKGMKRV

Securinine soluble fraction/Spot 11/Thioredoxin 1/Mascot

MVKQIESKTAFQEALDAAGDKLVVVDFSATWCGPCKMIKPFFHSLSEKYSNVIFLEVDVDDCQDVASECE
VKCMPTFQFFKKGQKVGEFSGANKEKLEATINELV

Securinine soluble fraction/Spot 11/Thioredoxin 1/X!Hunter

MVKQIESKTAFQEALDAAGDKLVVVDFSATWCGPCKMIKPFFHSLSEKYSNVIFLEVDVDDCQDVASECE
VKCMPTFQFFKKGQKVGEFSGANKEKLEATINELV

Securinine soluble fraction/Spot 11/Thioredoxin 1/X!Tandem P3

MVKQIESKTAFQEALDAAGDKLVVVDFSATWCGPCKMIKPFFHSLSEKYSNVIFLEVDVDDCQDVASECE
VKCMPTFQFFKKGQKVGEFSGANKEKLEATINELV

Securinine soluble fraction/Spot 12/Hsp70/Mascot

MSKGPAVGIDLGTTYSCVGVFQHGKVEIIANDQGNRTTPSYVAFTDTERLIGDAAKNQVAMNPTNTVF
DAKRLIGRRFDDAVVQSDMKHWPFMVVNDAGRPKVQVEYKGETKSFYPEEVSSMVLTKMKEIAEAYLGKTV
TNAVVTVPAYFNDSQRQATKDAGTIAGLNVLRIINEPTAAAIAYGLDKKVGAERNVLIFDLGGGTFDVSILTIED
GIFEVKSTAGDTHLGGEDFDNRMVNHFIAEFKRKHKKDISENKRAVRRLRTACERAKRTLSSSTQASIEIDSLYE
GIDFYTSITRARFEELNADLFRGTLDPVEKALRDAKLDKSQIHDIVLVGGSTRIPKIQKLLQDFFNGKELNKSINP
DEAVAYGAAVQAAILSGDKSENVQDLLLLDVTPLSLGIETAGGVMTVLIKRNTTIPTKQTQTFTTYSDNQPGVL
IQVYEGERAMTKDNNLLGKFELTGIPPAPRGVPQIEVTFDIDANGILNVSAVDKSTGKENKITITNDKGRLSKED
IERMVQEAEKYKAEDEKQRDKVSSKNSLESYAFNMKATVEDEKLQGKINDEDKQKILDKCNEIINWLDKNQT
AEKEEFEHQQKELEKVCNPIITKLYQSAGGMPGGMPGGFPGGGAPPSGGASSGPTIEEVD

Securinine soluble fraction/Spot 12/Hsp70/X!Hunter

MSKGPAVGIDLGTTYSCVGVFQHGKVEIIANDQGNRTTPSYVAFTDTERLIGDAAKNQVAMNPTNTVFDAK
RLIGRRFDDAVVQSDMKHWPFMVVNDAGRPKVQVEYKGETKSFYPEEVSSMVLTKMKEIAEAYLGKTVTNA
VVTVPAYFNDSQRQATKDAGTIAGLNVLRIINEPTAAAIAYGLDKKVGAERNVLIFDLGGGTFDVSILTIEDGIFE
VKSTAGDTHLGGEDFDNRMVNHFIAEFKRKHKKDISENKRAVRRLRTACERAKRTLSSSTQASIEIDSLYEGIDF
YTSITRARFEELNADLFRGTLDPVEKALRDAKLDKSQIHDIVLVGGSTRIPKIQKLLQDFFNGKELNKSINPDEAV
AYGAAVQAAILSGDKSENVQDLLLLDVTPLSLGIETAGGVMTVLIKRNTTIPTKQTQTFTTYSDNQPGVLIQVY
EGERAMTKDNNLLGKFELTGIPPAPRGVPQIEVTFDIDANGILNVSAVDKSTGKENKITITNDKGRLSKEDIER
MVQEAEKYKAEDEKQRDKVSSKNSLESYAFNMKATVEDEKLQGKINDEDKQKILDKCNEIINWLDKNQTAEK
EEFEHQQKELEKVCNPIITKLYQSAGGMPGGMPGGFPGGGAPPSGGASSGPTIEEVD

Securinine soluble fraction/Spot 12/Hsp70/X!Tandem P3

MSKGPAVGIDLGTTYSCVGVFQHGKVEIIANDQGNRTTPSYVAFTDTERLIGDAAKNQVAMNPTNTVFDAK
RLIGRRFDDAVVQSDMKHWPFMVVNDAGRPKVQVEYKGETKSFYPEEVSSMVLTKMKEIAEAYLGKTVTNA
VVTVPAYFNDSQRQATKDAGTIAGLNVLRIINEPTAAAIAYGLDKKVGAERNVLIFDLGGGTFDVSILTIEDGIFE
VKSTAGDTHLGGEDFDNRMVNHFIAEFKRKHKKDISENKRAVRRLRTACERAKRTLSSSTQASIEIDSLYEGIDF
YTSITRARFEELNADLFRGTLDPVEKALRDAKLDKSQIHDIVLVGGSTRIPKIQKLLQDFFNGKELNKSINPDEAV
AYGAAVQAAILSGDKSENVQDLLLLDVTPLSLGIETAGGVMTVLIKRNTTIPTKQTQTFTTYSDNQPGVLIQVY
EGERAMTKDNNLLGKFELTGIPPAPRGVPQIEVTFDIDANGILNVSAVDKSTGKENKITITNDKGRLSKEDIER
MVQEAEKYKAEDEKQRDKVSSKNSLESYAFNMKATVEDEKLQGKINDEDKQKILDKCNEIINWLDKNQTAEK
EEFEHQQKELEKVCNPIITKLYQSAGGMPGGMPGGFPGGGAPPSGGASSGPTIEEVD

Securinine soluble fraction/Spot 13/L-plastin/Mascot

MARGSVSDEEMMELREAFAKVDTDGNGYISFNELNDLFKAACLPLPGYRVREITENLMATGDLDQDGRI
SFDEFIKIFHGLKSTDVAKTFRKAINKKEGICAIGGTSEQSSVGTQHSYSEEEKYAFVNWINKALENDPDCRHVIP
MNPNTNDLFNAVGDGIVLCKMINLSVPDTIDERTINKKKLTPFTIQENLNLALNSASAIGCHVVNIGAEDLKEG
KPYLVLGLLWQVIKIGLFADIELSRNEALIALLREGESLEDLMKLSPEELLLRWANYHLENAGCNKIGNFSTDIKD
SKAYYHLLEQVAPKGDEEGVPAVVIDMSGLREKDDIQRAECMLQQAERLGCRQFVTATDVVRGNPKLNLAFI
ANLFNRYPALHKPENQDIDWGALEGETREERTFRNWMNSLGVNPRVNHLYSDLSDALVIFQLYEKIKVPVD
WNRVNKPPYPKLGGNMKKLENCNYAVELGKNQAKFSLVGIGGQDLNEGNRTLTLALIWQLMRRYTLNILEEI
GGGQKVNDDIIVNWVNETLREAEKSSSISSFKDPKISTSLPVLDLIDAIQPGSINYDLLKTENLNDDEKLNNAKY
AISMARKIGARVYALPEDLVEVNPKMVMTVFACLMGKGMKRV

Securinine soluble fraction/Spot 13/L-plastin/X!Hunter

MARGSVSDEEMMELREAFAKVDTDGNGYISFNELNDLFKAACLPLPGYRVREITENLMATGDLDQDGRISFD
EFIKIFHGLKSTDVAKTFRKAINKKEGICAIGGTSEQSSVGTQHSYSEEEKYAFVNWINKALENDPDCRHVIPMN
PNTNDLFNAVGDGIVLCKMINLSVPDTIDERTINKKKLTPFTIQENLNLALNSASAIGCHVVNIGAEDLKEGKPY
LVLGLLWQVIKIGLFADIELSRNEALIALLREGESLEDLMKLSPEELLLRWANYHLENAGCNKIGNFSTDIKDSKA
YYHLLEQVAPKGDEEGVPAVVIDMSGLREKDDIQRAECMLQQAERLGCRQFVTATDVVRGNPKLNLAFIANL
FNRYPALHKPENQDIDWGALEGETREERTFRNWMNSLGVNPRVNHLYSDLSDALVIFQLYEKIKVPVDWNR
VNKPPYPKLGGNMKKLENCNYAVELGKNQAKFSLVGIGGQDLNEGNRTLTLALIWQLMRRYTLNILEEIGGG
QKVNDDIIVNWVNETLREAEKSSSISSFKDPKISTSLPVLDLIDAIQPGSINYDLLKTENLNDDEKLNNAKYAISM
ARKIGARVYALPEDLVEVNPKMVMTVFACLMGKGMKRV

Securinine soluble fraction/Spot 13/L-plastin/X!Tandem P3

MARGSVSDEEMMELREAFAKVDTDGNGYISFNELNDLFKAACLPLPGYRVREITENLMATGDLDQDGRISFD
EFIKIFHGLKSTDVAKTFRKAINKKEGICAIGGTSEQSSVGTQHSYSEEEKYAFVNWINKALENDPDCRHVIPMN
PNTNDLFNAVGDGIVLCKMINLSVPDTIDERTINKKKLTPFTIQENLNLALNSASAIGCHVVNIGAEDLKEGKPY
LVLGLLWQVIKIGLFADIELSRNEALIALLREGESLEDLMKLSPEELLLRWANYHLENAGCNKIGNFSTDIKDSKA
YYHLLEQVAPKGDEEGVPAVVIDMSGLREKDDIQRAECMLQQAERLGCRQFVTATDVVRGNPKLNLAFIANL
FNRYPALHKPENQDIDWGALEGETREERTFRNWMNSLGVNPRVNHLYSDLSDALVIFQLYEKIKVPVDWNR
VNKPPYPKLGGNMKKLENCNYAVELGKNQAKFSLVGIGGQDLNEGNRTLTLALIWQLMRRYTLNILEEIGGG
QKVNDDIIVNWVNETLREAEKSSSISSFKDPKISTSLPVLDLIDAIQPGSINYDLLKTENLNDDEKLNNAKYAISM
ARKIGARVYALPEDLVEVNPKMVMTVFACLMGKGMKRV

Securinine soluble fraction/Spot 18/Hsp70/Mascot

MSKGPAVGIDLGTTYSCVGVFQHGKVEIIANDQGNRTTPSYVAFTDTERLIGDAAKNQVAMNPTNTVF
DAKRLIGRRFDDAVVQSDMKHWPFMVVNDAGRPKVQVEYKGETKSFYPEEVSSMVLTKMKEIAEAYLGKTV
TNAVVTVPAYFNDSQRQATKDAGTIAGLNVLRIINEPTAAAIAYGLDKKVGAERNVLIFDLGGGTFDVSILTIED
GIFEVKSTAGDTHLGGEDFDNRMVNHFIAEFKRKHKKDISENKRAVRRLRTACERAKRTLSSSTQASIEIDSLYE
GIDFYTSITRARFEELNADLFRGTLDPVEKALRDAKLDKSQIHDIVLVGGSTRIPKIQKLLQDFFNGKELNKSINP
DEAVAYGAAVQAAILSGDKSENVQDLLLLDVTPLSLGIETAGGVMTVLIKRNTTIPTKQTQTFTTYSDNQPGVL
IQVYEGERAMTKDNNLLGKFELTGIPPAPRGVPQIEVTFDIDANGILNVSAVDKSTGKENKITITNDKGRLSKED
IERMVQEAEKYKAEDEKQRDKVSSKNSLESYAFNMKATVEDEKLQGKINDEDKQKILDKCNEIINWLDKNQT
AEKEEFEHQQKELEKVCNPIITKLYQSAGGMPGGMPGGFPGGGAPPSGGASSGPTIEEVD

Securinine soluble fraction/Spot 18/Hsp70/X!Hunter

MSKGPAVGIDLGTTYSCVGVFQHGKVEIIANDQGNRTTPSYVAFTDTERLIGDAAKNQVAMNPTNTVFDAK
RLIGRRFDDAVVQSDMKHWPFMVVNDAGRPKVQVEYKGETKSFYPEEVSSMVLTKMKEIAEAYLGKTVTNA
VVTVPAYFNDSQRQATKDAGTIAGLNVLRIINEPTAAAIAYGLDKKVGAERNVLIFDLGGGTFDVSILTIEDGIFE
VKSTAGDTHLGGEDFDNRMVNHFIAEFKRKHKKDISENKRAVRRLRTACERAKRTLSSSTQASIEIDSLYEGIDF
YTSITRARFEELNADLFRGTLDPVEKALRDAKLDKSQIHDIVLVGGSTRIPKIQKLLQDFFNGKELNKSINPDEAV
AYGAAVQAAILSGDKSENVQDLLLLDVTPLSLGIETAGGVMTVLIKRNTTIPTKQTQTFTTYSDNQPGVLIQVY
EGERAMTKDNNLLGKFELTGIPPAPRGVPQIEVTFDIDANGILNVSAVDKSTGKENKITITNDKGRLSKEDIER
MVQEAEKYKAEDEKQRDKVSSKNSLESYAFNMKATVEDEKLQGKINDEDKQKILDKCNEIINWLDKNQTAEK
EEFEHQQKELEKVCNPIITKLYQSAGGMPGGMPGGFPGGGAPPSGGASSGPTIEEVD

Securinine soluble fraction/Spot 18/Hsp70/X!Tandem P3

MSKGPAVGIDLGTTYSCVGVFQHGKVEIIANDQGNRTTPSYVAFTDTERLIGDAAKNQVAMNPTNTVFDAK
RLIGRRFDDAVVQSDMKHWPFMVVNDAGRPKVQVEYKGETKSFYPEEVSSMVLTKMKEIAEAYLGKTVTNA
VVTVPAYFNDSQRQATKDAGTIAGLNVLRIINEPTAAAIAYGLDKKVGAERNVLIFDLGGGTFDVSILTIEDGIFE
VKSTAGDTHLGGEDFDNRMVNHFIAEFKRKHKKDISENKRAVRRLRTACERAKRTLSSSTQASIEIDSLYEGIDF
YTSITRARFEELNADLFRGTLDPVEKALRDAKLDKSQIHDIVLVGGSTRIPKIQKLLQDFFNGKELNKSINPDEAV
AYGAAVQAAILSGDKSENVQDLLLLDVTPLSLGIETAGGVMTVLIKRNTTIPTKQTQTFTTYSDNQPGVLIQVY
EGERAMTKDNNLLGKFELTGIPPAPRGVPQIEVTFDIDANGILNVSAVDKSTGKENKITITNDKGRLSKEDIER
MVQEAEKYKAEDEKQRDKVSSKNSLESYAFNMKATVEDEKLQGKINDEDKQKILDKCNEIINWLDKNQTAEK
EEFEHQQKELEKVCNPIITKLYQSAGGMPGGMPGGFPGGGAPPSGGASSGPTIEEVD

Securinine soluble fraction/Spot 19/Hsp70/Mascot

MSKGPAVGIDLGTTYSCVGVFQHGKVEIIANDQGNRTTPSYVAFTDTERLIGDAAKNQVAMNPTNTVF
DAKRLIGRRFDDAVVQSDMKHWPFMVVNDAGRPKVQVEYKGETKSFYPEEVSSMVLTKMKEIAEAYLGKTV
TNAVVTVPAYFNDSQRQATKDAGTIAGLNVLRIINEPTAAAIAYGLDKKVGAERNVLIFDLGGGTFDVSILTIED
GIFEVKSTAGDTHLGGEDFDNRMVNHFIAEFKRKHKKDISENKRAVRRLRTACERAKRTLSSSTQASIEIDSLYE
GIDFYTSITRARFEELNADLFRGTLDPVEKALRDAKLDKSQIHDIVLVGGSTRIPKIQKLLQDFFNGKELNKSINP
DEAVAYGAAVQAAILSGDKSENVQDLLLLDVTPLSLGIETAGGVMTVLIKRNTTIPTKQTQTFTTYSDNQPGVL
IQVYEGERAMTKDNNLLGKFELTGIPPAPRGVPQIEVTFDIDANGILNVSAVDKSTGKENKITITNDKGRLSKED
IERMVQEAEKYKAEDEKQRDKVSSKNSLESYAFNMKATVEDEKLQGKINDEDKQKILDKCNEIINWLDKNQT
AEKEEFEHQQKELEKVCNPIITKLYQSAGGMPGGMPGGFPGGGAPPSGGASSGPTIEEVD

Securinine soluble fraction/Spot 19/Hsp70/X!Hunter

MSKGPAVGIDLGTTYSCVGVFQHGKVEIIANDQGNRTTPSYVAFTDTERLIGDAAKNQVAMNPTNTVFDAK
RLIGRRFDDAVVQSDMKHWPFMVVNDAGRPKVQVEYKGETKSFYPEEVSSMVLTKMKEIAEAYLGKTVTNA
VVTVPAYFNDSQRQATKDAGTIAGLNVLRIINEPTAAAIAYGLDKKVGAERNVLIFDLGGGTFDVSILTIEDGIFE
VKSTAGDTHLGGEDFDNRMVNHFIAEFKRKHKKDISENKRAVRRLRTACERAKRTLSSSTQASIEIDSLYEGIDF
YTSITRARFEELNADLFRGTLDPVEKALRDAKLDKSQIHDIVLVGGSTRIPKIQKLLQDFFNGKELNKSINPDEAV
AYGAAVQAAILSGDKSENVQDLLLLDVTPLSLGIETAGGVMTVLIKRNTTIPTKQTQTFTTYSDNQPGVLIQVY
EGERAMTKDNNLLGKFELTGIPPAPRGVPQIEVTFDIDANGILNVSAVDKSTGKENKITITNDKGRLSKEDIER
MVQEAEKYKAEDEKQRDKVSSKNSLESYAFNMKATVEDEKLQGKINDEDKQKILDKCNEIINWLDKNQTAEK
EEFEHQQKELEKVCNPIITKLYQSAGGMPGGMPGGFPGGGAPPSGGASSGPTIEEVD

Securinine soluble fraction/Spot 19/Hsp70/X!Tandem P3

MSKGPAVGIDLGTTYSCVGVFQHGKVEIIANDQGNRTTPSYVAFTDTERLIGDAAKNQVAMNPTNTVFDAK
RLIGRRFDDAVVQSDMKHWPFMVVNDAGRPKVQVEYKGETKSFYPEEVSSMVLTKMKEIAEAYLGKTVTNA
VVTVPAYFNDSQRQATKDAGTIAGLNVLRIINEPTAAAIAYGLDKKVGAERNVLIFDLGGGTFDVSILTIEDGIFE
VKSTAGDTHLGGEDFDNRMVNHFIAEFKRKHKKDISENKRAVRRLRTACERAKRTLSSSTQASIEIDSLYEGIDF
YTSITRARFEELNADLFRGTLDPVEKALRDAKLDKSQIHDIVLVGGSTRIPKIQKLLQDFFNGKELNKSINPDEAV
AYGAAVQAAILSGDKSENVQDLLLLDVTPLSLGIETAGGVMTVLIKRNTTIPTKQTQTFTTYSDNQPGVLIQVY
EGERAMTKDNNLLGKFELTGIPPAPRGVPQIEVTFDIDANGILNVSAVDKSTGKENKITITNDKGRLSKEDIER
MVQEAEKYKAEDEKQRDKVSSKNSLESYAFNMKATVEDEKLQGKINDEDKQKILDKCNEIINWLDKNQTAEK
EEFEHQQKELEKVCNPIITKLYQSAGGMPGGMPGGFPGGGAPPSGGASSGPTIEEVD

Securinine soluble fraction/Spot 23/L-plastin/Mascot

MARGSVSDEEMMELREAFAKVDTDGNGYISFNELNDLFKAACLPLPGYRVREITENLMATGDLDQDGRI
SFDEFIKIFHGLKSTDVAKTFRKAINKKEGICAIGGTSEQSSVGTQHSYSEEEKYAFVNWINKALENDPDCRHVIP
MNPNTNDLFNAVGDGIVLCKMINLSVPDTIDERTINKKKLTPFTIQENLNLALNSASAIGCHVVNIGAEDLKEG
KPYLVLGLLWQVIKIGLFADIELSRNEALIALLREGESLEDLMKLSPEELLLRWANYHLENAGCNKIGNFSTDIKD
SKAYYHLLEQVAPKGDEEGVPAVVIDMSGLREKDDIQRAECMLQQAERLGCRQFVTATDVVRGNPKLNLAFI
ANLFNRYPALHKPENQDIDWGALEGETREERTFRNWMNSLGVNPRVNHLYSDLSDALVIFQLYEKIKVPVD
WNRVNKPPYPKLGGNMKKLENCNYAVELGKNQAKFSLVGIGGQDLNEGNRTLTLALIWQLMRRYTLNILEEI
GGGQKVNDDIIVNWVNETLREAEKSSSISSFKDPKISTSLPVLDLIDAIQPGSINYDLLKTENLNDDEKLNNAKY
AISMARKIGARVYALPEDLVEVNPKMVMTVFACLMGKGMKRV

Securinine soluble fraction/Spot 23/L-plastin/X!Hunter

MARGSVSDEEMMELREAFAKVDTDGNGYISFNELNDLFKAACLPLPGYRVREITENLMATGDLDQDGRISFD
EFIKIFHGLKSTDVAKTFRKAINKKEGICAIGGTSEQSSVGTQHSYSEEEKYAFVNWINKALENDPDCRHVIPMN
PNTNDLFNAVGDGIVLCKMINLSVPDTIDERTINKKKLTPFTIQENLNLALNSASAIGCHVVNIGAEDLKEGKPY
LVLGLLWQVIKIGLFADIELSRNEALIALLREGESLEDLMKLSPEELLLRWANYHLENAGCNKIGNFSTDIKDSKA
YYHLLEQVAPKGDEEGVPAVVIDMSGLREKDDIQRAECMLQQAERLGCRQFVTATDVVRGNPKLNLAFIANL
FNRYPALHKPENQDIDWGALEGETREERTFRNWMNSLGVNPRVNHLYSDLSDALVIFQLYEKIKVPVDWNR
VNKPPYPKLGGNMKKLENCNYAVELGKNQAKFSLVGIGGQDLNEGNRTLTLALIWQLMRRYTLNILEEIGGG
QKVNDDIIVNWVNETLREAEKSSSISSFKDPKISTSLPVLDLIDAIQPGSINYDLLKTENLNDDEKLNNAKYAISM
ARKIGARVYALPEDLVEVNPKMVMTVFACLMGKGMKRV

Securinine soluble fraction/Spot 23/L-plastin/X!Tandem P3

MARGSVSDEEMMELREAFAKVDTDGNGYISFNELNDLFKAACLPLPGYRVREITENLMATGDLDQDGRISFD
EFIKIFHGLKSTDVAKTFRKAINKKEGICAIGGTSEQSSVGTQHSYSEEEKYAFVNWINKALENDPDCRHVIPMN
PNTNDLFNAVGDGIVLCKMINLSVPDTIDERTINKKKLTPFTIQENLNLALNSASAIGCHVVNIGAEDLKEGKPY
LVLGLLWQVIKIGLFADIELSRNEALIALLREGESLEDLMKLSPEELLLRWANYHLENAGCNKIGNFSTDIKDSKA
YYHLLEQVAPKGDEEGVPAVVIDMSGLREKDDIQRAECMLQQAERLGCRQFVTATDVVRGNPKLNLAFIANL
FNRYPALHKPENQDIDWGALEGETREERTFRNWMNSLGVNPRVNHLYSDLSDALVIFQLYEKIKVPVDWNR
VNKPPYPKLGGNMKKLENCNYAVELGKNQAKFSLVGIGGQDLNEGNRTLTLALIWQLMRRYTLNILEEIGGG
QKVNDDIIVNWVNETLREAEKSSSISSFKDPKISTSLPVLDLIDAIQPGSINYDLLKTENLNDDEKLNNAKYAISM
ARKIGARVYALPEDLVEVNPKMVMTVFACLMGKGMKRV

Securinine soluble fraction/Spot 27/SERPIN B1/Mascot

MEQLSSANTRFALDLFLALSENNPAGNIFISPFSISSAMAMVFLGTRGNTAAQLSKTFHFNTVEEVHSRFQ
SLNADINKRGASYILKLANRLYGEKTYNFLPEFLVSTQKTYGADLASVDFQHASEDARKTINQWVKGQTEGKIP
ELLASGMVDNMTKLVLVNAIYFKGNWKDKFMKEATTNAPFRLNKKDRKTVKMMYQKKKFAYGYIEDLKCRV
LELPYQGEELSMVILLPDDIEDESTGLKKIEEQLTLEKLHEWTKPENLDFIEVNVSLPRFKLEESYTLNSDLARLGV
QDLFNSSKADLSGMSGARDIFISKIVHKSFVEVNEEGTEAAAATAGIATFCMLMPEENFTADHPFLFFIRHNSS
GSILFLGRFSSP

Securinine soluble fraction/Spot 27/SERPIN B1/X!Hunter

MEQLSSANTRFALDLFLALSENNPAGNIFISPFSISSAMAMVFLGTRGNTAAQLSKTFHFNTVEEVHSRFQSLN
ADINKRGASYILKLANRLYGEKTYNFLPEFLVSTQKTYGADLASVDFQHASEDARKTINQWVKGQTEGKIPELL
ASGMVDNMTKLVLVNAIYFKGNWKDKFMKEATTNAPFRLNKKDRKTVKMMYQKKKFAYGYIEDLKCRVLEL
PYQGEELSMVILLPDDIEDESTGLKKIEEQLTLEKLHEWTKPENLDFIEVNVSLPRFKLEESYTLNSDLARLGVQD
LFNSSKADLSGMSGARDIFISKIVHKSFVEVNEEGTEAAAATAGIATFCMLMPEENFTADHPFLFFIRHNSSGSI
LFLGRFSSP

Securinine soluble fraction/Spot 27/SERPIN B1/X!Tandem P3

MEQLSSANTRFALDLFLALSENNPAGNIFISPFSISSAMAMVFLGTRGNTAAQLSKTFHFNTVEEVHSRFQSLN
ADINKRGASYILKLANRLYGEKTYNFLPEFLVSTQKTYGADLASVDFQHASEDARKTINQWVKGQTEGKIPELL
ASGMVDNMTKLVLVNAIYFKGNWKDKFMKEATTNAPFRLNKKDRKTVKMMYQKKKFAYGYIEDLKCRVLEL
PYQGEELSMVILLPDDIEDESTGLKKIEEQLTLEKLHEWTKPENLDFIEVNVSLPRFKLEESYTLNSDLARLGVQD
LFNSSKADLSGMSGARDIFISKIVHKSFVEVNEEGTEAAAATAGIATFCMLMPEENFTADHPFLFFIRHNSSGSI
LFLGRFSSP

Securinine soluble fraction/Spot 73/Hsp90/Mascot

MPEEVHHGEEEVETFAFQAEIAQLMSLIINTFYSNKEIFLRELISNASDALDKIRYESLTDPSKLDSGKELKIDI
IPNPQERTLTLVDTGIGMTKADLINNLGTIAKSGTKAFMEALQAGADISMIGQFGVGFYSAYLVAEKVVVITKH
NDDEQYAWESSAGGSFTVRADHGEPIGRGTKVILHLKEDQTEYLEERRVKEVVKKHSQFIGYPITLYLEKEREKE
ISDDEAEEEKGEKEEEDKDDEEKPKIEDVGSDEEDDSGKDKKKKTKKIKEKYIDQEELNKTKPIWTRNPDDITQE
EYGEFYKSLTNDWEDHLAVKHFSVEGQLEFRALLFIPRRAPFDLFENKKKKNNIKLYVRRVFIMDSCDELIPEYL
NFIRGVVDSEDLPLNISREMLQQSKILKAIRKNIVKKCLELFSELAEDKENYKKFYEAFSKNLKLGIHEDSTNRRRL
SELLRYHTSQSGDEMTSLSEYVSRMKETQKSIYYITGESKEQVANSAFVERVRKRGFEVVYMTEPIDEYCVQQL
KEFDGKSLVSVTKEGLELPEDEEEKKKMEESKAKFENLCKLMKEILDKKVEKVTISNRLVSSPCCIVTSTYGWTA
NMERIMKAQALRDNSTMGYMMAKKHLEINPDHPIVETLRQKAEADKNDKAVKDLVVLLFETALLSSGFSLED
PQTHSNRIYRMIKLGLGIDEDEVAAEEPNAAVPDEIPLSRAMRMRLAWKKSIRLGVHSWKTCALV

Securinine soluble fraction/Spot 73/Hsp90/X!Hunter

MPEEVHHGEEEVETFAFQAEIAQLMSLIINTFYSNKEIFLRELISNASDALDKIRYESLTDPSKLDSGKELKIDIIPN
PQERTLTLVDTGIGMTKADLINNLGTIAKSGTKAFMEALQAGADISMIGQFGVGFYSAYLVAEKVVVITKHND
DEQYAWESSAGGSFTVRADHGEPIGRGTKVILHLKEDQTEYLEERRVKEVVKKHSQFIGYPITLYLEKEREKEIS
DDEAEEEKGEKEEEDKDDEEKPKIEDVGSDEEDDSGKDKKKKTKKIKEKYIDQEELNKTKPIWTRNPDDITQEE
YGEFYKSLTNDWEDHLAVKHFSVEGQLEFRALLFIPRRAPFDLFENKKKKNNIKLYVRRVFIMDSCDELIPEYLN
FIRGVVDSEDLPLNISREMLQQSKILKVIRKNIVKKCLELFSELAEDKENYKKFYEAFSKNLKLGIHEDSTNRRRLS
ELLRYHTSQSGDEMTSLSEYVSRMKETQKSIYYITGESKEQVANSAFVERVRKRGFEVVYMTEPIDEYCVQQLK
EFDGKSLVSVTKEGLELPEDEEEKKKMEESKAKFENLCKLMKEILDKKVEKVTISNRLVSSPCCIVTSTYGWTAN
MERIMKAQALRDNSTMGYMMAKKHLEINPDHPIVETLRQKAEADKNDKAVKDLVVLLFETALLSSGFSLEDP
QTHSNRIYRMIKLGLGIDEDEVAAEEPNAAVPDEIPPLEGDEDASRMEEVD

Securinine soluble fraction/Spot 73/Hsp90/X!Tandem P3

MPEEVHHGEEEVETFAFQAEIAQLMSLIINTFYSNKEIFLRELISNASDALDKIRYESLTDPSKLDSGKELKIDIIPN
PQERTLTLVDTGIGMTKADLINNLGTIAKSGTKAFMEALQAGADISMIGQFGVGFYSAYLVAEKVVVITKHND
DEQYAWESSAGGSFTVRADHGEPIGRGTKVILHLKEDQTEYLEERRVKEVVKKHSQFIGYPITLYLEKEREKEIS
DDEAEEEKGEKEEEDKDDEEKPKIEDVGSDEEDDSGKDKKKKTKKIKEKYIDQEELNKTKPIWTRNPDDITQEE
YGEFYKSLTNDWEDHLAVKHFSVEGQLEFRALLFIPRRAPFDLFENKKKKNNIKLYVRRVFIMDSCDELIPEYLN
FIRGVVDSEDLPLNISREMLQQSKILKVIRKNIVKKCLELFSELAEDKENYKKFYEAFSKNLKLGIHEDSTNRRRLS
ELLRYHTSQSGDEMTSLSEYVSRMKETQKSIYYITGESKEQVANSAFVERVRKRGFEVVYMTEPIDEYCVQQLK
EFDGKSLVSVTKEGLELPEDEEEKKKMEESKAKFENLCKLMKEILDKKVEKVTISNRLVSSPCCIVTSTYGWTAN
MERIMKAQALRDNSTMGYMMAKKHLEINPDHPIVETLRQKAEADKNDKAVKDLVVLLFETALLSSGFSLEDP
QTHSNRIYRMIKLGLGIDEDEVAAEEPNAAVPDEIPPLEGDEDASRMEEVD

Securinine soluble fraction/Spot 83/Actin/Mascot

MDDDIAALVVDNGSGMCKAGFAGDDAPRAVFPSIVGRPRHQGVMVGMGQKDSYVGDEAQSKRGILT
LKYPIEHGIVTNWDDMEKIWHHTFYNELRVAPEEHPVLLTEAPLNPKANREKMTQIMFETFNTPAMYVAIQA
MLSLYASGRTTGIVMDSGDGVTHTVPIYEGYALPHAILRLDLAGRDLTDYLMKILTERGYSFTTTAEREIVRDIKE
KLCYVALDFEQEMATAASSSSLEKSYELPDGQVITIGNERFRCPEALFQPSFLGMESCGIHETTFNSIMKCDVDI
RKDLYDNTVLSGGTTMYPGIADRMQKEITALAPSTMKIKIIAPPERKYSVWIGGSILASLSTFQQMWISKQEYD
ESGPSIVHRKCF

Securinine soluble fraction/Spot 83/Actin/X!Hunter

MEEEIAALVIDNGSGMCKAGFAGDDAPRAVFPSIVGRPRHQGVMVGMGQKDSYVGDEAQSKRGILTLKYPI
EHGIVTNWDDMEKIWHHTFYNELRVAPEEHPVLLTEAPLNPKANREKMTQIMFETFNTPAMYVAIQAVLSL
YASGRTTGIVMDSGDGVTHTVPIYEGYALPHAILRLDLAGRDLTDYLMKILTERGYSFTTTAEREIVRDIKEKLCY
VALDFEQEMATAASSSSLEKSYELPDGQVITIGNERFRCPEALFQPSFLGMESCGIHETTFNSIMKCDVDIRKDL
YANTVLSGGTTMYPGIADRMQKEITALAPSTMKIKIIAPPERKYSVWIGGSILASLSTFQQMWISKQEYDESGP
SIVHRKCF

Securinine soluble fraction/Spot 83/Actin/X!Tandem P3

MEEEIAALVIDNGSGMCKAGFAGDDAPRAVFPSIVGRPRHQGVMVGMGQKDSYVGDEAQSKRGILTLKYPI
EHGIVTNWDDMEKIWHHTFYNELRVAPEEHPVLLTEAPLNPKANREKMTQIMFETFNTPAMYVAIQAVLSL
YASGRTTGIVMDSGDGVTHTVPIYEGYALPHAILRLDLAGRDLTDYLMKILTERGYSFTTTAEREIVRDIKEKLCY
VALDFEQEMATAASSSSLEKSYELPDGQVITIGNERFRCPEALFQPSFLGMESCGIHETTFNSIMKCDVDIRKDL
YANTVLSGGTTMYPGIADRMQKEITALAPSTMKIKIIAPPERKYSVWIGGSILASLSTFQQMWISKQEYDESGP
SIVHRKCF

Securinine soluble fraction/Spot 89/Hsp60/Mascot

MLRLPTVFRQMRPVSRVLAPHLTRAYAKDVKFGADARALMLQGVDLLADAVAVTMGPKGRTVIIEQS
WGSPKVTKDGVTVAKSIDLKDKYKNIGAKLVQDVANNTNEEAGDGTTTATVLARSIAKEGFEKISKGANPVEI
RRGVMLAVDAVIAELKKQSKPVTTPEEIAQVATISANGDKEIGNIISDAMKKVGRKGVITVKDGKTLNDELEIIE
GMKFDRGYISPYFINTSKGQKCEFQDAYVLLSEKKISSIQSIVPALEIANAHRKPLVIIAEDVDGEALSTLVLNRLK
VGLQVVAVKAPGFGDNRKNQLKDMAIATGGAVFGEEGLTLNLEDVQPHDLGKVGEVIVTKDDAMLLKGKG
DKAQIEKRIQEIIEQLDVTTSEYEKEKLNERLAKLSDGVAVLKVGGTSDVEVNEKKDRVTDALNATRAAVEEGIV
LGGGCALLRCIPALDSLTPANEDQKIGIEIIKRTLKIPAMTIAKNAGVEGSLIVEKIMQSSSEVGYDAMAGDFVN
MVEKGIIDPTKVVRTALLDAAGVASLLTTAEVVVTEIPKEEKDPGMGAMGGMGGGMGGGMF

Securinine soluble fraction/Spot 89/Hsp60/X!Hunter

MLRLPTVFRQMRPVSRVLAPHLTRAYAKDVKFGADARALMLQGVDLLADAVAVTMGPKGRTVIIEQS
WGSPKVTKDGVTVAKSIDLKDKYKNIGAKLVQDVANNTNEEAGDGTTTATVLARSIAKEGFEKISKGANPVEI
RRGVMLAVDAVIAELKKQSKPVTTPEEIAQVATISANGDKEIGNIISDAMKKVGRKGVITVKDGKTLNDELEIIE
GMKFDRGYISPYFINTSKGQKCEFQDAYVLLSEKKISSIQSIVPALEIANAHRKPLVIIAEDVDGEALSTLVLNRLK
VGLQVVAVKAPGFGDNRKNQLKDMAIATGGAVFGEEGLTLNLEDVQPHDLGKVGEVIVTKDDAMLLKGKG
DKAQIEKRIQEIIEQLDVTTSEYEKEKLNERLAKLSDGVAVLKVGGTSDVEVNEKKDRVTDALNATRAAVEEGIV
LGGGCALLRCIPALDSLTPANEDQKIGIEIIKRTLKIPAMTIAKNAGVEGSLIVEKIMQSSSEVGYDAMAGDFVN
MVEKGIIDPTKVVRTALLDAAGVASLLTTAEVVVTEIPKEEKDPGMGAMGGMGGGMGGGMF

Securinine soluble fraction/Spot 89/Hsp60/X!Tandem P3

MLRLPTVFRQMRPVSRVLAPHLTRAYAKDVKFGADARALMLQGVDLLADAVAVTMGPKGRTVIIEQSWGS
PKVTKDGVTVAKSIDLKDKYKNIGAKLVQDVANNTNEEAGDGTTTATVLARSIAKEGFEKISKGANPVEIRRGV
MLAVDAVIAELKKQSKPVTTPEEIAQVATISANGDKEIGNIISDAMKKVGRKGVITVKDGKTLNDELEIIEGMKF
DRGYISPYFINTSKGQKCEFQDAYVLLSEKKISSIQSIVPALEIANAHRKPLVIIAEDVDGEALSTLVLNRLKVGLQ
VVAVKAPGFGDNRKNQLKDMAIATGGAVFGEEGLTLNLEDVQPHDLGKVGEVIVTKDDAMLLKGKGDKAQI
EKRIQEIIEQLDVTTSEYEKEKLNERLAKLSDGVAVLKVGGTSDVEVNEKKDRVTDALNATRAAVEEGIVLGGG
CALLRCIPALDSLTPANEDQKIGIEIIKRTLKIPAMTIAKNAGVEGSLIVEKIMQSSSEVGYDAMAGDFVNMVEK
GIIDPTKVVRTALLDAAGVASLLTTAEVVVTEIPKEEKDPGMGAMGGMGGGMGGGMF

Securinine soluble fraction/Spot 96/Inosine 5’ monophosphate dehydrogenase/Mascot

MADYLISGGTSYVPDDGLTAQQLFNCGDGLTYNDFLILPGYIDFTADQVDLTSALTKKITLKTPLVSSPMD
TVTEAGMAIAMALTGGIGFIHHNCTPEFQANEVRKVKKYEQGFITDPVVLSPKDRVRDVFEAKARHGFCGIPI
TDTGRMGSRLVGIISSRDIDFLKEEEHDCFLEEIMTKREDLVVAPAGITLKEANEILQRSKKGKLPIVNEDDELVA
IIARTDLKKNRDYPLASKDAKKQLLCGAAIGTHEDDKYRLDLLAQAGVDVVVLDSSQGNSIFQINMIKYIKDKYP
NLQVIGGNVVTAAQAKNLIDAGVDALRVGMGSGSICITQEVLACGRPQATAVYKVSEYARRFGVPVIADGGI
QNVGHIAKALALGASTVMMGSLLAATTEAPGEYFFSDGIRLKKYRGMGSLDAMDKHLSSQNRYFSEADKIKV
AQGVSGAVQDKGSIHKFVPYLIAGIQHSCQDIGAKSLTQVRAMMYSGELKFEKRTSSAQVEGGVHSLHSYEK
RLF

Securinine soluble fraction/Spot 96/Inosine 5’ monophosphate dehydrogenase/X!Hunter

MADYLISGGTSYVPDDGLTAQQLFNCGDGLTYNDFLILPGYIDFTADQVDLTSALTKKITLKTPLVSSPMDTVT
EAGMAIAMALTGGIGFIHHNCTPEFQANEVRKVKKYEQGFITDPVVLSPKDRVRDVFEAKARHGFCGIPITDT
GRMGSRLVGIISSRDIDFLKEEEHDCFLEEIMTKREDLVVAPAGITLKEANEILQRSKKGKLPIVNEDDELVAIIAR
TDLKKNRDYPLASKDAKKQLLCGAAIGTHEDDKYRLDLLAQAGVDVVVLDSSQGNSIFQINMIKYIKDKYPNL
QVIGGNVVTAAQAKNLIDAGVDALRVGMGSGSICITQEVLACGRPQATAVYKVSEYARRFGVPVIADGGIQN
VGHIAKALALGASTVMMGSLLAATTEAPGEYFFSDGIRLKKYRGMGSLDAMDKHLSSQNRYFSEADKIKVAQ
GVSGAVQDKGSIHKFVPYLIAGIQHSCQDIGAKSLTQVRAMMYSGELKFEKRTSSAQVEGGVHSLHSYEKRLF

Securinine soluble fraction/Spot 96/Inosine 5’ monophosphate dehydrogenase/X!Tandem P3

MADYLISGGTSYVPDDGLTAQQLFNCGDGLTYNDFLILPGYIDFTADQVDLTSALTKKITLKTPLVSSPMDTVT
EAGMAIAMALTGGIGFIHHNCTPEFQANEVRKVKKYEQGFITDPVVLSPKDRVRDVFEAKARHGFCGIPITDT
GRMGSRLVGIISSRDIDFLKEEEHDCFLEEIMTKREDLVVAPAGITLKEANEILQRSKKGKLPIVNEDDELVAIIAR
TDLKKNRDYPLASKDAKKQLLCGAAIGTHEDDKYRLDLLAQAGVDVVVLDSSQGNSIFQINMIKYIKDKYPNL
QVIGGNVVTAAQAKNLIDAGVDALRVGMGSGSICITQEVLACGRPQATAVYKVSEYARRFGVPVIADGGIQN
VGHIAKALALGASTVMMGSLLAATTEAPGEYFFSDGIRLKKYRGMGSLDAMDKHLSSQNRYFSEADKIKVAQ
GVSGAVQDKGSIHKFVPYLIAGIQHSCQDIGAKSLTQVRAMMYSGELKFEKRTSSAQVEGGVHSLHSYEKRLF

Securinine membrane fraction/Spot 6/Hsp70/Mascot

MSKGPAVGIDLGTTYSCVGVFQHGKVEIIANDQGNRTTPSYVAFTDTERLIGDAAKNQVAMNPTNTVF
DAKRLIGRRFDDAVVQSDMKHWPFMVVNDAGRPKVQVEYKGETKSFYPEEVSSMVLTKMKEIAEAYLGKTV
TNAVVTVPAYFNDSQRQATKDAGTIAGLNVLRIINEPTAAAIAYGLDKKVGAERNVLIFDLGGGTFDVSILTIED
GIFEVKSTAGDTHLGGEDFDNRMVNHFIAEFKRKHKKDISENKRAVRRLRTACERAKRTLSSSTQASIEIDSLYE
GIDFYTSITRARFEELNADLFRGTLDPVEKALRDAKLDKSQIHDIVLVGGSTRIPKIQKLLQDFFNGKELNKSINP
DEAVAYGAAVQAAILSGDKSENVQDLLLLDVTPLSLGIETAGGVMTVLIKRNTTIPTKQTQTFTTYSDNQPGVL
IQVYEGERAMTKDNNLLGKFELTGIPPAPRGVPQIEVTFDIDANGILNVSAVDKSTGKENKITITNDKGRLSKED
IERMVQEAEKYKAEDEKQRDKVSSKNSLESYAFNMKATVEDEKLQGKINDEDKQKILDKCNEIINWLDKNQT
AEKEEFEHQQKELEKVCNPIITKLYQSAGGMPGGMPGGFPGGGAPPSGGASSGPTIEEVD

Securinine membrane fraction/Spot 6/Hsp70/X!Hunter

MSKGPAVGIDLGTTYSCVGVFQHGKVEIIANDQGNRTTPSYVAFTDTERLIGDAAKNQVAMNPTNTVFDAK
RLIGRRFDDAVVQSDMKHWPFMVVNDAGRPKVQVEYKGETKSFYPEEVSSMVLTKMKEIAEAYLGKTVTNA
VVTVPAYFNDSQRQATKDAGTIAGLNVLRIINEPTAAAIAYGLDKKVGAERNVLIFDLGGGTFDVSILTIEDGIFE
VKSTAGDTHLGGEDFDNRMVNHFIAEFKRKHKKDISENKRAVRRLRTACERAKRTLSSSTQASIEIDSLYEGIDF
YTSITRARFEELNADLFRGTLDPVEKALRDAKLDKSQIHDIVLVGGSTRIPKIQKLLQDFFNGKELNKSINPDEAV
AYGAAVQAAILSGDKSENVQDLLLLDVTPLSLGIETAGGVMTVLIKRNTTIPTKQTQTFTTYSDNQPGVLIQVY
EGERAMTKDNNLLGKFELTGIPPAPRGVPQIEVTFDIDANGILNVSAVDKSTGKENKITITNDKGRLSKEDIER
MVQEAEKYKAEDEKQRDKVSSKNSLESYAFNMKATVEDEKLQGKINDEDKQKILDKCNEIINWLDKNQTAEK
EEFEHQQKELEKVCNPIITKLYQSAGGMPGGMPGGFPGGGAPPSGGASSGPTIEEVD

Securinine membrane fraction/Spot 6/Hsp70/X!Tandem P3

MSKGPAVGIDLGTTYSCVGVFQHGKVEIIANDQGNRTTPSYVAFTDTERLIGDAAKNQVAMNPTNTVFDAK
RLIGRRFDDAVVQSDMKHWPFMVVNDAGRPKVQVEYKGETKSFYPEEVSSMVLTKMKEIAEAYLGKTVTNA
VVTVPAYFNDSQRQATKDAGTIAGLNVLRIINEPTAAAIAYGLDKKVGAERNVLIFDLGGGTFDVSILTIEDGIFE
VKSTAGDTHLGGEDFDNRMVNHFIAEFKRKHKKDISENKRAVRRLRTACERAKRTLSSSTQASIEIDSLYEGIDF
YTSITRARFEELNADLFRGTLDPVEKALRDAKLDKSQIHDIVLVGGSTRIPKIQKLLQDFFNGKELNKSINPDEAV
AYGAAVQAAILSGDKSENVQDLLLLDVTPLSLGIETAGGVMTVLIKRNTTIPTKQTQTFTTYSDNQPGVLIQVY
EGERAMTKDNNLLGKFELTGIPPAPRGVPQIEVTFDIDANGILNVSAVDKSTGKENKITITNDKGRLSKEDIER
MVQEAEKYKAEDEKQRDKVSSKNSLESYAFNMKATVEDEKLQGKINDEDKQKILDKCNEIINWLDKNQTAEK
EEFEHQQKELEKVCNPIITKLYQSAGGMPGGMPGGFPGGGAPPSGGASSGPTIEEVD

Securinine membrane fraction/Spot 52/Actin/Mascot

MDDDIAALVVDNGSGMCKAGFAGDDAPRAVFPSIVGRPRHQGVMVGMGQKDSYVGDEAQSKRGILT
LKYPIEHGIVTNWDDMEKIWHHTFYNELRVAPEEHPVLLTEAPLNPKANREKMTQIMFETFNTPAMYVAIQA
VLSLYASGRTTGIVMDSGDGVTHTVPIYEGYALPHAILRLDLAGRDLTDYLMKILTERGYSFTTTAEREIVRDIKE
KLCYVALDFEQEMATAASSSSLEKSYELPDGQVITIGNERFRCPEALFQPSFLGMESCGIHETTFNSIMKCDVDI
RKDLYANTVLSGGTTMYPGIADRMQKEITALAPSTMKIKIIAPPERKYSVWIGGSILASLSTFQQMWISKQEYD
ESGPSIVHRKCF

Securinine membrane fraction/Spot 52/Actin/X!Hunter

MEEEIAALVIDNGSGMCKAGFAGDDAPRAVFPSIVGRPRHQGVMVGMGQKDSYVGDEAQSKRGILTLKYPI
EHGIVTNWDDMEKIWHHTFYNELRVAPEEHPVLLTEAPLNPKANREKMTQIMFETFNTPAMYVAIQAVLSL
YASGRTTGIVMDSGDGVTHTVPIYEGYALPHAILRLDLAGRDLTDYLMKILTERGYSFTTTAEREIVRDIKEKLCY
VALDFEQEMATAASSSSLEKSYELPDGQVITIGNERFRCPEALFQPSFLGMESCGIHETTFNSIMKCDVDIRKDL
YANTVLSGGTTMYPGIADRMQKEITALAPSTMKIKIIAPPERKYSVWIGGSILASLSTFQQMWISKQEYDESGP
SIVHRKCF

Securinine membrane fraction/Spot 52/Actin/X!Tandem P3

MDDDIAALVVDNGSGMCKAGFAGDDAPRAVFPSIVGRPRHQGVMVGMGQKDSYVGDEAQSKRGILT
LKYPIEHGIVTNWDDMEKIWHHTFYNELRVAPEEHPVLLTEAPLNPKANREKMTQIMFETFNTPAMYVAIQA
VLSLYASGRTTGIVMDSGDGVTHTVPIYEGYALPHAILRLDLAGRDLTDYLMKILTERGYSFTTTAEREIVR
DIKEKLCYVALDFEQEMATAASSSSLEKSYELPDGQVITIGNERFRCPEALFQPSFLGMESCGIHETTFN
SIMKCDVDIRKDLYANTVLSGGTTMYPGIADRMQKEITALAPSTMKIKIIAPPERKYSVWIGGSILASLS
TFQQMWISKQEYDESGPSIVHRKCF

LPS membrane fraction/Spot 8/ATP synthase subunit β/Mascot
AVIGAVVDVQFDEGLPPILNALEVQGRETRLVLEVAQHLGESTVRTIAMDGTEGLVRGQKVLDSGAPIKIPVG
PETLGRIMNVIGEPIDERGPIKTKQFAPIHAEAPEFMEMSVEQEILVTGIKVVDLLAPYAKGGKIGLFGGAGVG
KTVLIMELINNVAKAHGGYSVFAGVGERTREGNDLYHEMIESGVINLKDATSKVALVYGQMNEPPGARARV
ALTGLTVAEYFRDQEGQDVLLFIDNIFRFTQAGSEVSALLGRIPSAVGYQPTLATDMGTMQERITTTKKGSITS
VQAIYVPADDLTDPAPATTFAHLDATTVLSRAIAELGIYPAVDPLDSTSRIMDPNIVGSEHYDVARGVQKILQD
YKSLQDIIAILGMDELSEEDKLTVSRARKIQRFLSQPFQVAEVFTGHMGKLVPLKETIKGFQQILAGEYDHLPEQ
AFYM

LPS membrane fraction/Spot 8/ATP synthase subunit β/X!Hunter
MLGFVGRVAAAPASGALRRLTPSASLPPAQLLLRAAPTAVHPVRDYAAQTSPSPKAGAATGRIVAVIGAV
VDVQFDEGLPPILNALEVQGRETRLVLEVAQHLGESTVRTIAMDGTEGLVRGQKVLDSGAPIKIPVGPETLGRI
MNVIGEPIDERGPIKTKQFAPIHAEAPEFMEMSVEQEILVTGIKVVDLLAPYAKGGKIGLFGGAGVGKTVLIME
LINNVAKAHGGYSVFAGVGERTREGNDLYHEMIESGVINLKDATSKVALVYGQMNEPPGARARVALTGLTVA
EYFRDQEGQDVLLFIDNIFRFTQAGSEVSALLGRIPSAVGYQPTLATDMGTMQERITTTKKGSITSVQAIYVPA
DDLTDPAPATTFAHLDATTVLSRAIAELGIYPAVDPLDSTSRIMDPNIVGSEHYDVARGVQKILQDYKSLQDIIAI
LGMDELSEEDKLTVSRARKIQRFLSQPFQVAEVFTGHMGKLVPLKETIKGFQQILAGEYDHLPEQAFYMVGPI
EEAVAKADKLAEEHSS

LPS membrane fraction/Spot 8/ATP synthase subunit β/X! Tandem P3
MLGFVGRVAAAPASGALRRLTPSASLPPAQLLLRAAPTAVHPVRDYAAQTSPSPKAGAATGRIVAVIGAV
VDVQFDEGLPPILNALEVQGRETRLVLEVAQHLGESTVRTIAMDGTEGLVRGQKVLDSGAPIKIPVGPETLGRI
MNVIGEPIDERGPIKTKQFAPIHAEAPEFMEMSVEQEILVTGIKVVDLLAPYAKGGKIGLFGGAGVGKTVLIME
LINNVAKAHGGYSVFAGVGERTREGNDLYHEMIESGVINLKDATSKVALVYGQMNEPPGARARVALTGLTVA
EYFRDQEGQDVLLFIDNIFRFTQAGSEVSALLGRIPSAVGYQPTLATDMGTMQERITTTKKGSITSVQAIYVPA
DDLTDPAPATTFAHLDATTVLSRAIAELGIYPAVDPLDSTSRIMDPNIVGSEHYDVARGVQKILQDYKSLQDIIAI
LGMDELSEEDKLTVSRARKIQRFLSQPFQVAEVFTGHMGKLVPLKETIKGFQQILAGEYDHLPEQAFYMVGPI
EEAVAKADKLAEEHSS

MPL membrane fraction/Spot 8/Rab2A/Mascot

MAYAYLFKYIIIGDTGVGKSCLLLQFTDKRFQPVHDLTIGVEFGARMITIDGKQIKLQIWDTAGQESFRSIT
RSYYRGAAGALLVYDITRRDTFNHLTTWLEDARQHSNSNMVIMLIGNKSDLESRREVKKEEGEAFAREHGLIF
METSAKTASNVEEAFINTAKEIYEKIQEGVFDINNEANGIKIGPQHAATNATHAGNQGGQQAGGGCC

MPL membrane fraction/Spot 8/Rab2A/X!Hunter

MAYAYLFKYIIIGDTGVGKSCLLLQFTDKRFQPVHDLTIGVEFGARMITIDGKQIKLQIWDTAGQESFRSITRSYY
RGAAGALLVYDITRRDTFNHLTTWLEDARQHSNSNMVIMLIGNKSDLESRREVKKEEGEAFAREHGLIFMETS
AKTASNVEEAFINTAKEIYEKIQEGVFDINNEANGIKIGPQHAATNATHAGNQGGQQAGGGCC

MPL membrane fraction/Spot 8/Rab2A/X!Tandem P3

MAYAYLFKYIIIGDTGVGKSCLLLQFTDKRFQPVHDLTIGVEFGARMITIDGKQIKLQIWDTAGQESFRSITRSYY
RGAAGALLVYDITRRDTFNHLTTWLEDARQHSNSNMVIMLIGNKSDLESRREVKKEEGEAFAREHGLIFMETS
AKTASNVEEAFINTAKEIYEKIQEGVFDINNEANGIKIGPQHAATNATHAGNQGGQQAGGGCC

MPL membrane fraction/Spot 42/F1 ATP synthase mitochondrial F1 complex β precursor/Mascot

MLGFVGRVAAAPASGALRRLTPSASLPPAQLLLRAAPTAVHPVRDYAAQTSPSPKAGAATGRIVAVIGAV
VDVQFDEGLPPILNALEVQGRETRLVLEVAQHLGESTVRTIAMDGTEGLVRGQKVLDSGAPIKIPVGPETLGRI
MNVIGEPIDERGPIKTKQFAPIHAEAPEFMEMSVEQEILVTGIKVVDLLAPYAKGGKIGLFGGAGVGKTVLIME
LINNVAKAHGGYSVFAGVGERTREGNDLYHEMIESGVINLKDATSKVALVYGQMNEPPGARARVALTGLTVA
EYFRDQEGQDVLLFIDNIFRFTQAGSEVSALLGRIPSAVGYQPTLATDMGTMQERITTTKKGSITSVQAIYVPA
DDLTDPAPATTFAHLDATTVLSRAIAELGIYPAVDPLDSTSRIMDPNIVGSEHYDVARGVQKILQDYKSLQDIIAI
LGMDELSEEDKLTVSRARKIQRFLSQPFQVAEVFTGHMGKLVPLKETIKGFQQILAGEYDHLPEQAFYMVGPI
EEAVAKADKLAEEHSS

MPL membrane fraction/Spot 42/F1 ATP synthase mitochondrial F1 complex β precursor/X!Hunter

MLGFVGRVAAAPASGALRRLTPSASLPPAQLLLRAAPTAVHPVRDYAAQTSPSPKAGAATGRIVAVIGAVVD
VQFDEGLPPILNALEVQGRETRLVLEVAQHLGESTVRTIAMDGTEGLVRGQKVLDSGAPIKIPVGPETLGRIM
NVIGEPIDERGPIKTKQFAPIHAEAPEFMEMSVEQEILVTGIKVVDLLAPYAKGGKIGLFGGAGVGKTVLIMELI
NNVAKAHGGYSVFAGVGERTREGNDLYHEMIESGVINLKDATSKVALVYGQMNEPPGARARVALTGLTVAE
YFRDQEGQDVLLFIDNIFRFTQAGSEVSALLGRIPSAVGYQPTLATDMGTMQERITTTKKGSITSVQAIYVPAD
DLTDPAPATTFAHLDATTVLSRAIAELGIYPAVDPLDSTSRIMDPNIVGSEHYDVARGVQKILQDYKSLQDIIAIL
GMDELSEEDKLTVSRARKIQRFLSQPFQVAEVFTGHMGKLVPLKETIKGFQQILAGEYDHLPEQAFYMVGPIE
EAVAKADKLAEEHSS

MPL membrane fraction/Spot 42/F1 ATP synthase mitochondrial F1 complex β precursor/X!Tandem P3

MLGFVGRVAAAPASGALRRLTPSASLPPAQLLLRAAPTAVHPVRDYAAQTSPSPKAGAATGRIVAVIGAVVD
VQFDEGLPPILNALEVQGRETRLVLEVAQHLGESTVRTIAMDGTEGLVRGQKVLDSGAPIKIPVGPETLGRIM
NVIGEPIDERGPIKTKQFAPIHAEAPEFMEMSVEQEILVTGIKVVDLLAPYAKGGKIGLFGGAGVGKTVLIMELI
NNVAKAHGGYSVFAGVGERTREGNDLYHEMIESGVINLKDATSKVALVYGQMNEPPGARARVALTGLTVAE
YFRDQEGQDVLLFIDNIFRFTQAGSEVSALLGRIPSAVGYQPTLATDMGTMQERITTTKKGSITSVQAIYVPAD
DLTDPAPATTFAHLDATTVLSRAIAELGIYPAVDPLDSTSRIMDPNIVGSEHYDVARGVQKILQDYKSLQDIIAIL
GMDELSEEDKLTVSRARKIQRFLSQPFQVAEVFTGHMGKLVPLKETIKGFQQILAGEYDHLPEQAFYMVGPIE
EAVAKADKLAEEHSS

MPL membrane fraction/Spot 57/Tropomyosin 3 isoform 2/Mascot

MAGITTIEAVKRKIQVLQQQADDAEERAERLQREVEGERRAREQAEAEVASLNRRIQLVEEELDRAQERL
ATALQKLEEAEKAADEEKMELQEIQLKEAKHIAEEADRKYEEVARKLVIIEGDLERTEERAELAESRCREMDEQI
RLMDQNLKCLSAAEEKYSQKEDKYEEEIKILTDKLKEAETRAEFAERSVAKLEKTIDDLEDKLKCTKEEHLCTQR
MLDQTLLDLNEM

MPL membrane fraction/Spot 57/Tropomyosin 3 isoform 2/X!Hunter

MAGITTIEAVKRKIQVLQQQADDAEERAERLQREVEGERRAREQAEAEVASLNRRIQLVEEELDRAQERLATA
LQKLEEAEKAADESERGMKVIENRALKDEEKMELQEIQLKEAKHIAEEADRKYEEVARKLVIIEGDLERTEERAE
LAESRCREMDEQIRLMDQNLKCLSAAEEKYSQKEDKYEEEIKILTDKLKEAETRAEFAERSVAKLEKTIDDLEDKL
KCTKEEHLCTQRMLDQTLLDLNEM

MPL membrane fraction/Spot 57/Tropomyosin 3 isoform 2/X!Tandem P3

MAGITTIEAVKRKIQVLQQQADDAEERAERLQREVEGERRAREQAEAEVASLNRRIQLVEEELDRAQERLATA
LQKLEEAEKAADESERGMKVIENRALKDEEKMELQEIQLKEAKHIAEEADRKYEEVARKLVIIEGDLERTEERAE
LAESRCREMDEQIRLMDQNLKCLSAAEEKYSQKEDKYEEEIKILTDKLKEAETRAEFAERSVAKLEKTIDDLEDKL
KCTKEEHLCTQRMLDQTLLDLNEM

MPL membrane fraction/Spot 61/Guanine nucleotide binding protein β polypeptide 2-like 1/Mascot

MTEQMTLRGTLKGHNGWVTQIATTPQFPDMILSASRDKTIIMWKLTRDETNYGIPQRALRGHSHFVSD
VVISSDGQFALSGSWDGTLRLWDLTTGTTTRRFVGHTKDVLSVAFSSDNRQIVSGSRDKTIKLWNTLGVCKYT
VQDESHSEWVSCVRFSPNSSNPIIVSCGWDKLVKVWNLANCKLKTNHIGHTGYLNTVTVSPDGSLCASGGKD
GQAMLWDLNEGKHLYTLDGGDIINALCFSPNRYWLCAATGPSIKIWDLEGKIIVDELKQEVISTSSKAEPPQCT
SLAWSADGQTLFAGYTDNLVRVWQVTIGTR

MPL membrane fraction/Spot 61/Guanine nucleotide binding protein β polypeptide 2-like 1/X!Hunter

MTEQMTLRGTLKGHNGWVTQIATTPQFPDMILSASRDKTIIMWKLTRDETNYGIPQRALRGHSHFVSDVVIS
SDGQFALSGSWDGTLRLWDLTTGTTTRRFVGHTKDVLSVAFSSDNRQIVSGSRDKTIKLWNTLGVCKYTVQD
ESHSEWVSCVRFSPNSSNPIIVSCGWDKLVKVWNLANCKLKTNHIGHTGYLNTVTVSPDGSLCASGGKDGQA
MLWDLNEGKHLYTLDGGDIINALCFSPNRYWLCAATGPSIKIWDLEGKIIVDELKQEVISTSSKAEPPQCTSLA
WSADGQTLFAGYTDNLVRVWQVTIGTR

MPL membrane fraction/Spot 61/Guanine nucleotide binding protein β polypeptide 2-like 1/X!Tandem P3

MTEQMTLRGTLKGHNGWVTQIATTPQFPDMILSASRDKTIIMWKLTRDETNYGIPQRALRGHSHFVSDVVIS
SDGQFALSGSWDGTLRLWDLTTGTTTRRFVGHTKDVLSVAFSSDNRQIVSGSRDKTIKLWNTLGVCKYTVQD
ESHSEWVSCVRFSPNSSNPIIVSCGWDKLVKVWNLANCKLKTNHIGHTGYLNTVTVSPDGSLCASGGKDGQA
MLWDLNEGKHLYTLDGGDIINALCFSPNRYWLCAATGPSIKIWDLEGKIIVDELKQEVISTSSKAEPPQCTSLA
WSADGQTLFAGYTDNLVRVWQVTIGTR

MPL membrane fraction/Spot 97/p64 Cl^- ion channel/Mascot

MVLWLKGVTFNVTTVDTKRRTETVQKLCPGGQLPFLLYGTEVHTDTNKIEEFLEAVLCPPRYPKLAALNPE
SNTAGLDIFAKFSAYIKNSNPALNDNLEKGLLKALKVLDNYLTSPLPEEVDETSAEDEGVSQRKFLDGNELTLAD
CNLLPKLHIVQVVCKKYRGFTIPEAFRGVHRYLSNAYAREEFASTCPDDEEIELAYEQVAKALK

MPL membrane fraction/Spot 97/p64 Cl^- ion channel/X!Hunter

MAEEQPQVELFVKAGSDGAKIGNCPFSQRLFMVLWLKGVTFNVTTVDTKRRTETVQKLCPGGQLPFLLYGTE
VHTDTNKIEEFLEAVLCPPRYPKLAALNPESNTAGLDIFAKFSAYIKNSNPALNDNLEKGLLKALKVLDNYLTSPL
PEEVDETSAEDEGVSQRKFLDGNELTLADCNLLPKLHIVQVVCKKYRGFTIPEAFRGVHRYLSNAYAREEFASTC
PDDEEIELAYEQVAKALK

MPL membrane fraction/Spot 97/p64 Cl^- ion channel/X!Tandem P3

MAEEQPQVELFVKAGSDGAKIGNCPFSQRLFMVLWLKGVTFNVTTVDTKRRTETVQKLCPGGQLPFLLYGTE
VHTDTNKIEEFLEAVLCPPRYPKLAALNPESNTAGLDIFAKFSAYIKNSNPALNDNLEKGLLKALKVLDNYLTSPL
PEEVDETSAEDEGVSQRKFLDGNELTLADCNLLPKLHIVQVVCKKYRGFTIPEAFRGVHRYLSNAYAREEFASTC
PDDEEIELAYEQVAKALK

MPL membrane fraction/Spot 100/Prohibitin/Mascot

MAAKVFESIGKFGLALAVAGGVVNSALYNVDAGHRAVIFDRFRGVQDIVVGEGTHFLIPWVQKPIIFDCR
SRPRNVPVITGSKDLQNVNITLRILFRPVASQLPRIFTSIGEDYDERVLPSITTEILKSVVARFDAGELITQRELVSR
QVSDDLTERAATFGLILDDVSLTHLTFGKEFTEAVEAKQVAQQEAERARFVVEKAEQQKKAAIISAEGDSKAAE
LIANSLATAGDGLIELRKLEAAEDIAYQLSRSRNITYLPAGQSVLLQLPQ

MPL membrane fraction/Spot 100/Prohibitin/X!Hunter

MAAKVFESIGKFGLALAVAGGVVNSALYNVDAGHRAVIFDRFRGVQDIVVGEGTHFLIPWVQKPIIFDCRSRP
RNVPVITGSKDLQNVNITLRILFRPVASQLPRIFTSIGEDYDERVLPSITTEILKSVVARFDAGELITQRELVSRQVS
DDLTERAATFGLILDDVSLTHLTFGKEFTEAVEAKQVAQQEAERARFVVEKAEQQKKAAIISAEGDSKAAELIA
NSLATAGDGLIELRKLEAAEDIAYQLSRSRNITYLPAGQSVLLQLPQ

MPL membrane fraction/Spot 100/Prohibitin/X!Tandem P3

MAAKVFESIGKFGLALAVAGGVVNSALYNVDAGHRAVIFDRFRGVQDIVVGEGTHFLIPWVQKPIIFDCR
SRPRNVPVITGSKDLQNVNITLRILFRPVASQLPRIFTSIGEDYDERVLPSITTEILKSVVARFDAGELITQRELVSR
QVSDDLTERAATFGLILDDVSLTHLTFGKEFTEAVEAKQVAQQEAERARFVVEKAEQQKKAAIISAEGDSKAAE
LIANSLATAGDGLIELRKLEAAEDIAYQLSRSRNITYLPAGQSVLLQLPQ

MPL membrane fraction/Spot 110/ F1 ATP synthase mitochondrial F1 complex β precursor/Mascot

MLGFVGRVAAAPASGALRRLTPSASLPPAQLLLRAAPTAVHPVRDYAAQTSPSPKAGAATGRIVAVIGAV
VDVQFDEGLPPILNALEVQGRETRLVLEVAQHLGESTVRTIAMDGTEGLVRGQKVLDSGAPIKIPVGPETLGRI
MNVIGEPIDERGPIKTKQFAPIHAEAPEFMEMSVEQEILVTGIKVVDLLAPYAKGGKIGLFGGAGVGKTVLIME
LINNVAKAHGGYSVFAGVGERTREGNDLYHEMIESGVINLKDATSKVALVYGQMNEPPGARARVALTGLTVA
EYFRDQEGQDVLLFIDNIFRFTQAGSEVSALLGRIPSAVGYQPTLATDMGTMQERITTTKKGSITSVQAIYVPA
DDLTDPAPATTFAHLDATTVLSRAIAELGIYPAVDPLDSTSRIMDPNIVGSEHYDVARGVQKILQDYKSLQDIIAI
LGMDELSEEDKLTVSRARKIQRFLSQPFQVAEVFTGHMGKLVPLKETIKGFQQILAGEYDHLPEQAFYMVGPI
EEAVAKADKLAEEHSS

MPL membrane fraction/Spot 110/ F1 ATP synthase mitochondrial F1 complex β precursor/X!Hunter

MLGFVGRVAAAPASGALRRLTPSASLPPAQLLLRAAPTAVHPVRDYAAQTSPSPKAGAATGRIVAVIGAVVD
VQFDEGLPPILNALEVQGRETRLVLEVAQHLGESTVRTIAMDGTEGLVRGQKVLDSGAPIKIPVGPETLGRIM
NVIGEPIDERGPIKTKQFAPIHAEAPEFMEMSVEQEILVTGIKVVDLLAPYAKGGKIGLFGGAGVGKTVLIMELI
NNVAKAHGGYSVFAGVGERTREGNDLYHEMIESGVINLKDATSKVALVYGQMNEPPGARARVALTGLTVAE
YFRDQEGQDVLLFIDNIFRFTQAGSEVSALLGRIPSAVGYQPTLATDMGTMQERITTTKKGSITSVQAIYVPAD
DLTDPAPATTFAHLDATTVLSRAIAELGIYPAVDPLDSTSRIMDPNIVGSEHYDVARGVQKILQDYKSLQDIIAIL
GMDELSEEDKLTVSRARKIQRFLSQPFQVAEVFTGHMGKLVPLKETIKGFQQILAGEYDHLPEQAFYMVGPIE
EAVAKADKLAEEHSS

MPL membrane fraction/Spot 110/ F1 ATP synthase mitochondrial F1 complex β precursor/X!Tandem P3

MLGFVGRVAAAPASGALRRLTPSASLPPAQLLLRAAPTAVHPVRDYAAQTSPSPKAGAATGRIVAVIGAVVD
VQFDEGLPPILNALEVQGRETRLVLEVAQHLGESTVRTIAMDGTEGLVRGQKVLDSGAPIKIPVGPETLGRIM
NVIGEPIDERGPIKTKQFAPIHAEAPEFMEMSVEQEILVTGIKVVDLLAPYAKGGKIGLFGGAGVGKTVLIMELI
NNVAKAHGGYSVFAGVGERTREGNDLYHEMIESGVINLKDATSKVALVYGQMNEPPGARARVALTGLTVAE
YFRDQEGQDVLLFIDNIFRFTQAGSEVSALLGRIPSAVGYQPTLATDMGTMQERITTTKKGSITSVQAIYVPAD
DLTDPAPATTFAHLDATTVLSRAIAELGIYPAVDPLDSTSRIMDPNIVGSEHYDVARGVQKILQDYKSLQDIIAIL
GMDELSEEDKLTVSRARKIQRFLSQPFQVAEVFTGHMGKLVPLKETIKGFQQILAGEYDHLPEQAFYMVGPIE
EAVAKADKLAEEHSS

96 hr +/- Securinine soluble fraction 3-11NL/Spot 13/Chaperonin containing TCP1/Mascot

MAAVKTLNPKAEVARAQAALAVNISAARGLQDVLRTNLGPKGTMKMLVSGAGDIKLTKDGNVLLHEM
GLHPRIITEGFEAAKEKALQFLEEVKVSREMDRETLIDVARTSLRTKVHAELADVLTEAVVDSILAIKKQDEPIDLF
MIEIMEMKHKSETDTSLIRGLVLDHGARHPDMKKRVEDAYILTCNVSLEYEKTEVNSGFFYKSAEEREKLVKAE
RKFIEDRVKKIIELKRKVCGDSDKGFVVINQKGIDPFSLDALSKEGIVALRRAKRRNMERLTLACGGVALNSFDD
LSPDCLGHAGLVYEYTLGEEKFTFIEKCNNPRSVTLLIKGPNKHTLTQIKDAVRDGLRAVKNAIDDGCVVPGAG
AVEVAMAEALIKHKPSVKGRAQLGVQAFADALLIIPKVLAQNSGFDLQETLVKIQAEHSESGQLVGVDLNTGE
PMVAAEVGVWDNYCVKKQLLHSCTVIATNILLVDEIMRAGMSSLKG

96 hr +/- Securinine soluble fraction 3-11NL/Spot 13/Chaperonin containing TCP1/X!Hunter

MAAVKTLNPKAEVARAQAALAVNISAARGLQDVLRTNLGPKGTMKMLVSGAGDIKLTKDGNVLLHEM
QIQHPTASLIAKVATAQDDITGDGTTSNVLIIGELLKQADLYISEGLHPRIITEGFEAAKEKALQFLEEVKVSREM
DRETLIDVARTSLRTKVHAELADVLTEAVVDSILAIKKQDEPIDLFMIEIMEMKHKSETDTSLIRGLVLDHGARH
PDMKKRVEDAYILTCNVSLEYEKTEVNSGFFYKSAEEREKLVKAERKFIEDRVKKIIELKRKVCGDSDKGFVVINQ
KGIDPFSLDALSKEGIVALRRAKRRNMERLTLACGGVALNSFDDLSPDCLGHAGLVYEYTLGEEKFTFIEKCNNP
RSVTLLIKGPNKHTLTQIKDAVRDGLRAVKNAIDDGCVVPGAGAVEVAMAEALIKHKPSVKGRAQLGVQAFA
DALLIIPKVLAQNSGFDLQETLVKIQAEHSESGQLVGVDLNTGEPMVAAEVGVWDNYCVKKQLLHSCTVIAT
NILLVDEIMRAGMSSLKG

96 hr +/- Securinine soluble fraction 3-11NL/Spot 13/Chaperonin containing TCP1/X!Tandem P3

MAAVKTLNPKAEVARAQAALAVNISAARGLQDVLRTNLGPKGTMKMLVSGAGDIKLTKDGNVLLHEMQIQ
HPTASLIAKVATAQDDITGDGTTSNVLIIGELLKQADLYISEGLHPRIITEGFEAAKEKALQFLEEVKVSREMDRE
TLIDVARTSLRTKVHAELADVLTEAVVDSILAIKKQDEPIDLFMIEIMEMKHKSETDTSLIRGLVLDHGARHPDM
KKRVEDAYILTCNVSLEYEKTEVNSGFFYKSAEEREKLVKAERKFIEDRVKKIIELKRKVCGDSDKGFVVINQKGID
PFSLDALSKEGIVALRRAKRRNMERLTLACGGVALNSFDDLSPDCLGHAGLVYEYTLGEEKFTFIEKCNNPRSVT
LLIKGPNKHTLTQIKDAVRDGLRAVKNAIDDGCVVPGAGAVEVAMAEALIKHKPSVKGRAQLGVQAFADALLI
IPKVLAQNSGFDLQETLVKIQAEHSESGQLVGVDLNTGEPMVAAEVGVWDNYCVKKQLLHSCTVIATNILLVD
EIMRAGMSSLKG

96 hr +/- Securinine soluble fraction 3-11NL/Spot 55/Eukaryotic elongation initiation factor 5a/Mascot

MADDLDFETGDAGASATFPMQCSALRKNGFVVLKGRPCKIVEMSTSKTGKHGHAKVHLVGIDIFTGKKYEDICPSTHNMDVPNIKRNDFQLIGIQDGYLSLLQDSGEVREDLRLPEGDLGKEIEQKYDCGEEILITVLSAMTEEAAVAIKAMAK

96 hr +/- Securinine soluble fraction 3-11NL/Spot 55/Eukaryotic elongation initiation factor 5a/X!Hunter

MADDLDFETGDAGASATFPMQCSALRKNGFVVLKGRPCKIVEMSTSKTGKHGHAKVHLVGIDIFTGKKYEDICPSTHNMDVPNIKRNDFQLIGIQDGYLSLLQDSGEVREDLRLPEGDLGKEIEQKYDCGEEILITVLSAMTEEAAVAIKAMAK

not found by P3

96 hr +/- Securinine soluble fraction 3-11NL/Spot 57/Eukaryotic translation elongation factor 2/Mascot

MVNFTVDQIRAIMDKKANIRNMSVIAHVDHGKSTLTDSLVCKAGIIASARAGETRFTDTRKDEQERCITIKSTAISLFY
ELSENDLNFIKQSKDGAGFLINLIDSPGHVDFSSEVTAALRVTDGALVVVDCVSGVCVQTETVLRQAIAERIKPVLMMNK
MDRALLELQLEPEELYQTFQRIVENVNVIISTYGEGESGPMGNIMIDPVLGTVGFGSGLHGWAFTLKQFAEMYVAKFAAK
GEGQLGPAERAKKVEDMMKKLWGDRYFDPANGKFSKSATSPEGKKLPRTFCQLILDPIFKVFDAIMNFKKEETAKLIEKLD
IKLDSEDKDKEGKPLLKAVMRRWLPAGDALLQMITIHLPSPVTAQKYRCELLYEGPPDDEAAMGIKSCDPKGPLMMYISK
MVPTSDKGRFYAFGRVFSGLVSTGLKVRIMGPNYTPGKKEDLYLKPIQRTILMMGRYVEPIEDVPCGNIVGLVGVDQFLV
KTGTITTFEHAHNMRVMKFSVSPVVRVAVEAKNPADLPKLVEGLKRLAKSDPMVQCIIEESGEHIIAGAGELHLEICLKDLE
EDHACIPIKKSDPVVSYRETVSEESNVLCLSKSPNKHNRLYMKARPFPDGLAEDIDKGEVSARQELKQRARYLAEKYEWDV
AEARKIWCFGPDGTGPNILTDITKGVQYLNEIKDSVVAGFQWATKEGALCEENMRGVRFDVHDVTLHADAIHRGGGQII
PTARRCLYASVLTAQPRLMEPIYLVEIQCPEQVVGGIYGVLNRKRGHVFEESQVAGTPMFVVKAYLPVNESFGFTADLRSN
TGGQAFPQCVFDHWQILPGDPFDNSSRPSQVVAETRKRKGLKEGIPALDNFLDKL

96 hr +/- Securinine soluble fraction 3-11NL/Spot 57/Eukaryotic translation elongation factor 2/X!Hunter

MVNFTVDQIRAIMDKKANIRNMSVIAHVDHGKSTLTDSLVCKAGIIASARAGETRFTDTRKDEQERCITIKSTAISLFY
ELSENDLNFIKQSKDGAGFLINLIDSPGHVDFSSEVTAALRVTDGALVVVDCVSGVCVQTETVLRQAIAERIKPVLMMNK
MDRALLELQLEPEELYQTFQRIVENVNVIISTYGEGESGPMGNIMIDPVLGTVGFGSGLHGWAFTLKQFAEMYVAKFAAK
GEGQLGPAERAKKVEDMMKKLWGDRYFDPANGKFSKSATSPEGKKLPRTFCQLILDPIFKVFDAIMNFKKEETAKLIEKLD
IKLDSEDKDKEGKPLLKAVMRRWLPAGDALLQMITIHLPSPVTAQKYRCELLYEGPPDDEAAMGIKSCDPKGPLMMYISK
MVPTSDKGRFYAFGRVFSGLVSTGLKVRIMGPNYTPGKKEDLYLKPIQRTILMMGRYVEPIEDVPCGNIVGLVGVDQFLV
KTGTITTFEHAHNMRVMKFSVSPVVRVAVEAKNPADLPKLVEGLKRLAKSDPMVQCIIEESGEHIIAGAGELHLEICLKDLE
EDHACIPIKKSDPVVSYRETVSEESNVLCLSKSPNKHNRLYMKARPFPDGLAEDIDKGEVSARQELKQRARYLAEKYEWDV
AEARKIWCFGPDGTGPNILTDITKGVQYLNEIKDSVVAGFQWATKEGALCEENMRGVRFDVHDVTLHADAIHRGGGQII
PTARRCLYASVLTAQPRLMEPIYLVEIQCPEQVVGGIYGVLNRKRGHVFEESQVAGTPMFVVKAYLPVNESFGFTADLRSN
TGGQAFPQCVFDHWQILPGDPFDNSSRPSQVVAETRKRKGLKEGIPALDNFLDKL

96 hr +/- Securinine soluble fraction 3-11NL/Spot 57/Eukaryotic translation elongation factor 2/X!Tandem P3

MVNFTVDQIRAIMDKKANIRNMSVIAHVDHGKSTLTDSLVCKAGIIASARAGETRFTDTRKDEQERCITIKSTAISLFY
ELSENDLNFIKQSKDGAGFLINLIDSPGHVDFSSEVTAALRVTDGALVVVDCVSGVCVQTETVLRQAIAERIKPVLMMNK
MDRALLELQLEPEELYQTFQRIVENVNVIISTYGEGESGPMGNIMIDPVLGTVGFGSGLHGWAFTLKQFAEMYVAKFAAK
GEGQLGPAERAKKVEDMMKKLWGDRYFDPANGKFSKSATSPEGKKLPRTFCQLILDPIFKVFDAIMNFKKEETAKLIEKLD
IKLDSEDKDKEGKPLLKAVMRRWLPAGDALLQMITIHLPSPVTAQKYRCELLYEGPPDDEAAMGIKSCDPKGPLMMYISK
MVPTSDKGRFYAFGRVFSGLVSTGLKVRIMGPNYTPGKKEDLYLKPIQRTILMMGRYVEPIEDVPCGNIVGLVGVDQFLV
KTGTITTFEHAHNMRVMKFSVSPVVRVAVEAKNPADLPKLVEGLKRLAKSDPMVQCIIEESGEHIIAGAGELHLEICLKDLE
EDHACIPIKKSDPVVSYRETVSEESNVLCLSKSPNKHNRLYMKARPFPDGLAEDIDKGEVSARQELKQRARYLAEKYEWDV
AEARKIWCFGPDGTGPNILTDITKGVQYLNEIKDSVVAGFQWATKEGALCEENMRGVRFDVHDVTLHADAIHRGGGQII
PTARRCLYASVLTAQPRLMEPIYLVEIQCPEQVVGGIYGVLNRKRGHVFEESQVAGTPMFVVKAYLPVNESFGFTADLRSN
TGGQAFPQCVFDHWQILPGDPFDNSSRPSQVVAETRKRKGLKEGIPALDNFLDKL

96 hr +/- Securinine soluble fraction 3-11NL/Spot 82/Hsp60/Mascot

MLRLPTVFRQMRPVSRVLAPHLTRAYAKDVKFGADARALMLQGVDLLADAVAVTMGPKGRTVIIEQS
WGSPKVTKDGVTVAKSIDLKDKYKNIGAKLVQDVANNTNEEAGDGTTTATVLARSIAKEGFEKISKGANPVEI
RRGVMLAVDAVIAELKKQSKPVTTPEEIAQVATISANGDKEIGNIISDAMKKVGRKGVITVKDGKTLNDELEIIE
GMKFDRGYISPYFINTSKGQKCEFQDAYVLLSEKKISSIQSIVPALEIANAHRKPLVIIAEDVDGEALSTLVLNRLK
VGLQVVAVKAPGFGDNRKNQLKDMAIATGGAVFGEEGLTLNLEDVQPHDLGKVGEVIVTKDDAMLLKGKG
DKAQIEKRIQEIIEQLDVTTSEYEKEKLNERLAKLSDGVAVLKVGGTSDVEVNEKKDRVTDALNATRAAVEEGIV
LGGGCALLRCIPALDSLTPANEDQKIGIEIIKRTLKIPAMTIAKNAGVEGSLIVEKIMQSSSEVGYDAMAGDFVN
MVEKGIIDPTKVVRTALLDAAGVASLLTTAEVVVTEIPKEEKDPGMGAMGGMGGGMGGGMF

96 hr +/- Securinine soluble fraction 3-11NL/Spot 82/Hsp60/X!Hunter

MLRLPTVFRQMRPVSRVLAPHLTRAYAKDVKFGADARALMLQGVDLLADAVAVTMGPKGRTVIIEQS
WGSPKVTKDGVTVAKSIDLKDKYKNIGAKLVQDVANNTNEEAGDGTTTATVLARSIAKEGFEKISKGANPVEI
RRGVMLAVDAVIAELKKQSKPVTTPEEIAQVATISANGDKEIGNIISDAMKKVGRKGVITVKDGKTLNDELEIIE
GMKFDRGYISPYFINTSKGQKCEFQDAYVLLSEKKISSIQSIVPALEIANAHRKPLVIIAEDVDGEALSTLVLNRLK
VGLQVVAVKAPGFGDNRKNQLKDMAIATGGAVFGEEGLTLNLEDVQPHDLGKVGEVIVTKDDAMLLKGKG
DKAQIEKRIQEIIEQLDVTTSEYEKEKLNERLAKLSDGVAVLKVGGTSDVEVNEKKDRVTDALNATRAAVEEGIV
LGGGCALLRCIPALDSLTPANEDQKIGIEIIKRTLKIPAMTIAKNAGVEGSLIVEKIMQSSSEVGYDAMAGDFVN
MVEKGIIDPTKVVRTALLDAAGVASLLTTAEVVVTEIPKEEKDPGMGAMGGMGGGMGGGMF

96 hr +/- Securinine soluble fraction 3-11NL/Spot 82/Hsp60/X!Tandem P3

MLRLPTVFRQMRPVSRVLAPHLTRAYAKDVKFGADARALMLQGVDLLADAVAVTMGPKGRTVIIEQS
WGSPKVTKDGVTVAKSIDLKDKYKNIGAKLVQDVANNTNEEAGDGTTTATVLARSIAKEGFEKISKGANPVEI
RRGVMLAVDAVIAELKKQSKPVTTPEEIAQVATISANGDKEIGNIISDAMKKVGRKGVITVKDGKTLNDELEIIE
GMKFDRGYISPYFINTSKGQKCEFQDAYVLLSEKKISSIQSIVPALEIANAHRKPLVIIAEDVDGEALSTLVLNRLK
VGLQVVAVKAPGFGDNRKNQLKDMAIATGGAVFGEEGLTLNLEDVQPHDLGKVGEVIVTKDDAMLLKGKG
DKAQIEKRIQEIIEQLDVTTSEYEKEKLNERLAKLSDGVAVLKVGGTSDVEVNEKKDRVTDALNATRAAVEEGIV
LGGGCALLRCIPALDSLTPANEDQKIGIEIIKRTLKIPAMTIAKNAGVEGSLIVEKIMQSSSEVGYDAMAGDFVN
MVEKGIIDPTKVVRTALLDAAGVASLLTTAEVVVTEIPKEEKDPGMGAMGGMGGGMGGGMF

96 hr +/- Securinine soluble fraction 3-11NL/Spot 92/Calmodulin/Mascot

MADQLTEEQIAEFKEAFSLFDKDGDGTITTKELGTVMRSLGQNPTEAELQDMINEVDADDLPGNGTIDF
PEFLTMMARKMKDTDSEEEIREAFRVFDKDGNGYISAAELRHVMTNLGEKLTDEEVDEMIREADIDGDGQV
NYEEFVQMMTAK

96 hr +/- Securinine soluble fraction 3-11NL/Spot 92/Calmodulin/X!Hunter

MADQLTEEQIAEFKEAFSLFDKDGDGTITTKELGTVMRSLGQNPTEAELQDMINEVDADGNGTIDFPEFLTM
MARKMKDTDSEEEIREAFRVFDKDGNGYISAAELRHVMTNLGEKLTDEEVDEMIREADIDGDGQVNYEEFV
QMMTAK

96 hr +/- Securinine soluble fraction 3-11NL/Spot 92/Calmodulin/X!Tandem P3

MADQLTEEQIAEFKEAFSLFDKDGDGTITTKELGTVMRSLGQNPTEAELQDMINEVDADGNGTIDFPEFL
TMMARKMKDTDSEEEIREAFRVFDKDGNGYISAAELRHVMTNLGEKLTDEEVDEMIREADIDGDGQVNYEE
FVQMMTAK

96 hr +/- Securinine soluble fraction 3-11NL/Spot 121/Staphylococcal nuclease domain containing protein 1/Mascot

MASSAQSGGSSGGPAVPTVQRGIIKMVLSGCAIIVRGQPRGGPPPERQINLSNIRAGNLARRAAATQPDAKDTPDE
PWAFPAREFLRKKLIGKEVCFTIENKTPQGREYGMIYLGKDTNGENIAESLVAEGLATRREGMRANNPEQNRLSECEEQA
KAAKKGMWSEGNGSHTIRDLKYTIENPRHFVDSHHQKPVNAIIEHVRDGSVVRALLLPDYYLVTVMLSGIKCPTFRREAD
GSETPEPFAAEAKFFTESRLLQRDVQIILESCHNQNILGTILHPNGNITELLLKEGFARCVDWSIAVYTRGAEKLRAAERFAK
ERRLRIWRDYVAPTANLDQKDKQFVAKVMQVLNADAIVVKLNSGDYKTIHLSSIRPPRLEGENTQDKNKKLRPLYDIPYM
FEAREFLRKKLIGKKVNVTVDYIRPASPATETVPAFSERTCATVTIGGINIAEALVSKGLATVIRYRQDDDQRSSHYDELLAAE
ARAIKNGKGLHSKKEVPIHRVADISGDTQKAKQFLPFLQRAGRSEAVVEYVFSGSRLKLYLPKETCLITFLLAGIECPRGARN
LPGLVQEGEPFSEEATLFTKELVLQREVEVEVESMDKAGNFIGWLHIDGANLSVLLVEHALSKVHFTAERSSYYKSLLSAEE
AAKQKKEKVWAHYEEQPVEEVMPVLEEKERSASYKPVFVTEITDDLHFYVQDVETGTQLEKLMENMRNDIASHPPVEGS
YAPRRGEFCIAKFVDGEWYRARVEKVESPAKIHVFYIDYGNREVLPSTRLGTLSPAFSTRVLPAQATEYAFAFIQVPQDDDA
RTDAVDSVVRDIQNTQCLLNVEHLSAGCPHVTLQFADSKGDVGLGLVKEGLVMVEVRKEKQFQKVITEYLNAQESAKSA
RLNLWRYGDFRADDADEFGYSR

96 hr +/- Securinine soluble fraction 3-11NL/Spot 121/Staphylococcal nuclease domain containing protein 1/X!Hunter

MASSAQSGGSSGGPAVPTVQRGIIKMVLSGCAIIVRGQPRGGPPPERQINLSNIRAGNLARRAAATQPDAKDTPDE
PWAFPAREFLRKKLIGKEVCFTIENKTPQGREYGMIYLGKDTNGENIAESLVAEGLATRREGMRANNPEQNRLSECEEQA
KAAKKGMWSEGNGSHTIRDLKYTIENPRHFVDSHHQKPVNAIIEHVRDGSVVRALLLPDYYLVTVMLSGIKCPTFRREAD
GSETPEPFAAEAKFFTESRLLQRDVQIILESCHNQNILGTILHPNGNITELLLKEGFARCVDWSIAVYTRGAEKLRAAERFAK
ERRLRIWRDYVAPTANLDQKDKQFVAKVMQVLNADAIVVKLNSGDYKTIHLSSIRPPRLEGENTQDKNKKLRPLYDIPYM
FEAREFLRKKLIGKKVNVTVDYIRPASPATETVPAFSERTCATVTIGGINIAEALVSKGLATVIRYRQDDDQRSSHYDELLAAE
ARAIKNGKGLHSKKEVPIHRVADISGDTQKAKQFLPFLQRAGRSEAVVEYVFSGSRLKLYLPKETCLITFLLAGIECPRGARN
LPGLVQEGEPFSEEATLFTKELVLQREVEVEVESMDKAGNFIGWLHIDGANLSVLLVEHALSKVHFTAERSSYYKSLLSAEE
AAKQKKEKVWAHYEEQPVEEVMPVLEEKERSASYKPVFVTEITDDLHFYVQDVETGTQLEKLMENMRNDIASHPPVEGS
YAPRRGEFCIAKFVDGEWYRARVEKVESPAKIHVFYIDYGNREVLPSTRLGTLSPAFSTRVLPAQATEYAFAFIQVPQDDDA
RTDAVDSVVRDIQNTQCLLNVEHLSAGCPHVTLQFADSKGDVGLGLVKEGLVMVEVRKEKQFQKVITEYLNAQESAKSA
RLNLWRYGDFRADDADEFGYSR

96 hr +/- Securinine soluble fraction 3-11NL/Spot 121/Staphylococcal nuclease domain containing protein 1/X!Tandem P3

MASSAQSGGSSGGPAVPTVQRGIIKMVLSGCAIIVRGQPRGGPPPERQINLSNIRAGNLARRAAATQPDAKDTPDEPWA
FPAREFLRKKLIGKEVCFTIENKTPQGREYGMIYLGKDTNGENIAESLVAEGLATRREGMRANNPEQNRLSECEEQAKAAK
KGMWSEGNGSHTIRDLKYTIENPRHFVDSHHQKPVNAIIEHVRDGSVVRALLLPDYYLVTVMLSGIKCPTFRREADGSETP
EPFAAEAKFFTESRLLQRDVQIILESCHNQNILGTILHPNGNITELLLKEGFARCVDWSIAVYTRGAEKLRAAERFAKERRLRI
WRDYVAPTANLDQKDKQFVAKVMQVLNADAIVVKLNSGDYKTIHLSSIRPPRLEGENTQDKNKKLRPLYDIPYMFEAREF
LRKKLIGKKVNVTVDYIRPASPATETVPAFSERTCATVTIGGINIAEALVSKGLATVIRYRQDDDQRSSHYDELLAAEARAIKN
GKGLHSKKEVPIHRVADISGDTQKAKQFLPFLQRAGRSEAVVEYVFSGSRLKLYLPKETCLITFLLAGIECPRGARNLPGLVQ
EGEPFSEEATLFTKELVLQREVEVEVESMDKAGNFIGWLHIDGANLSVLLVEHALSKVHFTAERSSYYKSLLSAEEAAKQKK
EKVWAHYEEQPVEEVMPVLEEKERSASYKPVFVTEITDDLHFYVQDVETGTQLEKLMENMRNDIASHPPVEGSYAPRRG
EFCIAKFVDGEWYRARVEKVESPAKIHVFYIDYGNREVLPSTRLGTLSPAFSTRVLPAQATEYAFAFIQVPQDDDARTDAV
DSVVRDIQNTQCLLNVEHLSAGCPHVTLQFADSKGDVGLGLVKEGLVMVEVRKEKQFQKVITEYLNAQESAKSARLNLW
RYGDFRADDADEFGYSR

96 hr +/- Securinine soluble fraction 3-11NL/Spot 125/Glutamate dehydrogenase 1/Mascot

MYRYLGEALLLSRAGPAALGSASADSAALLGWARGQPAAAPQPGLALAARRHYSEAVADREDDPNFFK
MVEGFFDRGASIVEDKLVEDLRTRESEEQKRNRVRGILRIIKPCNHVLSLSFPIRRDDGSWEVIEGYRAQHSQH
RTPCKGGIRYSTDVSVDEVKALASLMTYKCAVVDVPFGGAKAGVKINPKNYTDNELEKITRRFTMELAKKGFIG
PGIDVPAPDMSTGEREMSWIADTYASTIGHYDINAHACVTGKPISQGGIHGRISATGRGVFHGIENFINEASY
MSILGMTPGFGDKTFVVQGFGNVGLHSMRYLHRFGAKCIAVGESDGSIWNPDGIDPKELEDFKLQHGSILGF
PKAKPYEGSILEADCDILIPAASEKQLTKSNAPRVKAKIIAEGANGPTTPEADKIFLERNIMVIPDLYLNAGGVTV
SYFEWLKNLNHVSYGRLTFKYERDSNYHLLMSVQESLERKFGKHGGTIPIVPTAEFQDRISGASEKDIVHSGLAY
TMERSARQIMRTAMKYNLGLDLRTAAYVNAIEKVFKVYNEAGVTFT

96 hr +/- Securinine soluble fraction 3-11NL/Spot 125/Glutamate dehydrogenase 1/X!Hunter

MYRYLGEALLLSRAGPAALGSASADSAALLGWARGQPAAAPQPGLALAARRHYSEAVADREDDPNFFKMVE
GFFDRGASIVEDKLVEDLRTRESEEQKRNRVRGILRIIKPCNHVLSLSFPIRRDDGSWEVIEGYRAQHSQHRTPC
KGGIRYSTDVSVDEVKALASLMTYKCAVVDVPFGGAKAGVKINPKNYTDNELEKITRRFTMELAKKGFIGPGID
VPAPDMSTGEREMSWIADTYASTIGHYDINAHACVTGKPISQGGIHGRISATGRGVFHGIENFINEASYMSIL
GMTPGFGDKTFVVQGFGNVGLHSMRYLHRFGAKCIAVGESDGSIWNPDGIDPKELEDFKLQHGSILGFPKAK
PYEGSILEADCDILIPAASEKQLTKSNAPRVKAKIIAEGANGPTTPEADKIFLERNIMVIPDLYLNAGGVTVSYFE
WLKNLNHVSYGRLTFKYERDSNYHLLMSVQESLERKFGKHGGTIPIVPTAEFQDRISGASEKDIVHSGLAYTME
RSARQIMRTAMKYNLGLDLRTAAYVNAIEKVFKVYNEAGVTFT

96 hr +/- Securinine soluble fraction 3-11NL/Spot 125/Glutamate dehydrogenase 1/X!Tandem P3

MYRYLGEALLLSRAGPAALGSASADSAALLGWARGQPAAAPQPGLALAARRHYSEAVADREDDPNFFKMVE
GFFDRGASIVEDKLVEDLRTRESEEQKRNRVRGILRIIKPCNHVLSLSFPIRRDDGSWEVIEGYRAQHSQHRTPC
KGGIRYSTDVSVDEVKALASLMTYKCAVVDVPFGGAKAGVKINPKNYTDNELEKITRRFTMELAKKGFIGPGID
VPAPDMSTGEREMSWIADTYASTIGHYDINAHACVTGKPISQGGIHGRISATGRGVFHGIENFINEASYMSIL
GMTPGFGDKTFVVQGFGNVGLHSMRYLHRFGAKCIAVGESDGSIWNPDGIDPKELEDFKLQHGSILGFPKAK
PYEGSILEADCDILIPAASEKQLTKSNAPRVKAKIIAEGANGPTTPEADKIFLERNIMVIPDLYLNAGGVTVSYFE
WLKNLNHVSYGRLTFKYERDSNYHLLMSVQESLERKFGKHGGTIPIVPTAEFQDRISGASEKDIVHSGLAYTME
RSARQIMRTAMKYNLGLDLRTAAYVNAIEKVFKVYNEAGVTFT

96 hr +/- Securinine soluble fraction 3-11NL/Spot 200/Proteasome activator subunit 1 isoform 1/Mascot

MAMLRVQPEAQAKVDVFREDLCTKTENLLGSYFPKKISELDAFLKEPALNEANLSNLKAPLDIPVPDPVKEKEKEERKKQQEKEDKDEKKKGEDEDKGPPCGPVNCNEKIVVLLQRLKPEIKDVIEQLNLVTTWLQLQIPRIEDGNNFGVAVQEKVFELMTSLHTKLEGFHTQISKYFSERGDAVTKAAKQPHVGDYRQLVHELDEAEYRDIRLMVMEIRNAYAVLYDIILKNFEKLKKPRGETKGMIY

96 hr +/- Securinine soluble fraction 3-11NL/Spot 200/Proteasome activator subunit 1 isoform 1/X!Hunter

MAMLRVQPEAQAKVDVFREDLCTKTENLLGSYFPKKISELDAFLKEPALNEANLSNLKAPLDIPVPDPVKEKEKEERKKQQEKEDKDEKKKGEDEDKGPPCGPVNCNEKIVVLLQRLKPEIKDVIEQLNLVTTWLQLQIPRIEDGNNFGVAVQEKVFELMTSLHTKLEGFHTQISKYFSERGDAVTKAAKQPHVGDYRQLVHELDEAEYRDIRLMVMEIRNAYAVLYDIILKNFEKLKKPRGETKGMIY

96 hr +/- Securinine soluble fraction 3-11NL/Spot 200/Proteasome activator subunit 1 isoform 1/X!Tandem P3

MAMLRVQPEAQAKVDVFREDLCTKTENLLGSYFPKKISELDAFLKEPALNEANLSNLKAPLDIPVPDPVKEKEKEERKKQQEKEDKDEKKKGEDEDKGPPCGPVNCNEKIVVLLQRLKPEIKDVIEQLNLVTTWLQLQIPRIEDGNNFGVAVQEKVFELMTSLHTKLEGFHTQISKYFSERGDAVTKAAKQPHVGDYRQLVHELDEAEYRDIRLMVMEIRNAYAVLYDIILKNFEKLKKPRGETKGMIY

96 hr +/- Securinine soluble fraction 3-11NL/Spot 205/Vinculin isoform VCL/Mascot

MPVFHTRTIESILEPVAQQISHLVIMHEEGEVDGKAIPDLTAPVAAVQAAVSNLVRVGKETVQTTEDQILKRDMPPAFIKVE
NACTKLVQAAQMLQSDPYSVPARDYLIDGSRGILSGTSDLLLTFDEAEVRKIIRVCKGILEYLTVAEVVETMEDLVTYTKNLGPGM
TKMAKMIDERQQELTHQEHRVMLVNSMNTVKELLPVLISAMKIFVTTKNSKNQGIEEALKNRNFTVEKMSAEINEIIRVLQLTS
WDEDAWASKDTEAMKRALASIDSKLNQAKGWLRDPSASPGDAGEQAIRQILDEAGKVGELCAGKERREILGTCKMLGQMTD
QVADLRARGQGSSPVAMQKAQQVSQGLDVLTAKVENAARKLEAMTNSKQSIAKKIDAAQNWLADPNGGPEGEEQIRGALAE
ARKIAELCDDPKERDDILRSLGEISALTSKLADLRRQGKGDSPEARALAKQVATALQNLQTKTNRAVANSRPAKAAVHLEGKIEQ
AQRWIDNPTVDDRGVGQAAIRGLVAEGHRLANVMMGPYRQDLLAKCDRVDQLTAQLADLAARGEGESPQARALASQLQDS
LKDLKARMQEAMTQEVSDVFSDTTTPIKLLAVAATAPPDAPNREEVFDERAANFENHSGKLGATAEKAAAVGTANKSTVEGIQ
ASVKTARELTPQVVSAARILLRNPGNQAAYEHFETMKNQWIDNVEKMTGLVDEAIDTKSLLDASEEAIKKDLDKCKVAMANIQP
QMLVAGATSIARRANRILLVAKREVENSEDPKFREAVKAASDELSKTISPMVMDAKAVAGNISDPGLQKSFLDSGYRILGAVAKV
REAFQPQEPDFPPPPPDLEQLRLTDELAPPKPPLPEGEVPPPRPPPPEEKDEEFPEQKAGEVINQPMMMAARQLHDEARKWSS
KGNDIIAAAKRMALLMAEMSRLVRGGSGTKRALIQCAKDIAKASDEVTRLAKEVAKQCTDKRIRTNLLQVCERIPTISTQLKILSTV
KATMLGRTNISDEESEQATEMLVHNAQNLMQSVKETVREAEAASIKIRTDAGFTLRWVRKTPWYQ

96 hr +/- Securinine soluble fraction 3-11NL/Spot 205/Vinculin isoform VCL/X!Hunter

MPVFHTRTIESILEPVAQQISHLVIMHEEGEVDGKAIPDLTAPVAAVQAAVSNLVRVGKETVQTTEDQILKRDMPPAFIKVENAC
TKLVQAAQMLQSDPYSVPARDYLIDGSRGILSGTSDLLLTFDEAEVRKIIRVCKGILEYLTVAEVVETMEDLVTYTKNLGPGMTKM
AKMIDERQQELTHQEHRVMLVNSMNTVKELLPVLISAMKIFVTTKNSKNQGIEEALKNRNFTVEKMSAEINEIIRVLQLTSWDE
DAWASKDTEAMKRALASIDSKLNQAKGWLRDPSASPGDAGEQAIRQILDEAGKVGELCAGKERREILGTCKMLGQMTDQVA
DLRARGQGSSPVAMQKAQQVSQGLDVLTAKVENAARKLEAMTNSKQSIAKKIDAAQNWLADPNGGPEGEEQIRGALAEARKI
AELCDDPKERDDILRSLGEISALTSKLADLRRQGKGDSPEARALAKQVATALQNLQTKTNRAVANSRPAKAAVHLEGKIEQAQR
WIDNPTVDDRGVGQAAIRGLVAEGHRLANVMMGPYRQDLLAKCDRVDQLTAQLADLAARGEGESPQARALASQLQDSLKDL
KARMQEAMTQEVSDVFSDTTTPIKLLAVAATAPPDAPNREEVFDERAANFENHSGKLGATAEKAAAVGTANKSTVEGIQASVK
TARELTPQVVSAARILLRNPGNQAAYEHFETMKNQWIDNVEKMTGLVDEAIDTKSLLDASEEAIKKDLDKCKVAMANIQPQML
VAGATSIARRANRILLVAKREVENSEDPKFREAVKAASDELSKTISPMVMDAKAVAGNISDPGLQKSFLDSGYRILGAVAKVREAF
QPQEPDFPPPPPDLEQLRLTDELAPPKPPLPEGEVPPPRPPPPEEKDEEFPEQKAGEVINQPMMMAARQLHDEARKWSSKPGI
PAAEVGIGVVAEADAADAAGFPVPPDMEDDYEPELLLMPSNQPVNQPILAAAQSLHREATKWSSKGNDIIAAAKRMALLMAE
MSRLVRGGSGTKRALIQCAKDIAKASDEVTRLAKEVAKQCTDKRIRTNLLQVCERIPTISTQLKILSTVKATMLGRTNISDEESEQA
TEMLVHNAQNLMQSVKETVREAEAASIKIRTDAGFTLRWVRKTPWYQ

96 hr +/- Securinine soluble fraction 3-11NL/Spot 205/Vinculin isoform VCL/X!Tandem P3

MPVFHTRTIESILEPVAQQISHLVIMHEEGEVDGKAIPDLTAPVAAVQAAVSNLVRVGKETVQTTEDQILKRDMPPAFIKVENAC
TKLVQAAQMLQSDPYSVPARDYLIDGSRGILSGTSDLLLTFDEAEVRKIIRVCKGILEYLTVAEVVETMEDLVTYTKNLGPGMTKM
AKMIDERQQELTHQEHRVMLVNSMNTVKELLPVLISAMKIFVTTKNSKNQGIEEALKNRNFTVEKMSAEINEIIRVLQLTSWDE
DAWASKDTEAMKRALASIDSKLNQAKGWLRDPSASPGDAGEQAIRQILDEAGKVGELCAGKERREILGTCKMLGQMTDQVA
DLRARGQGSSPVAMQKAQQVSQGLDVLTAKVENAARKLEAMTNSKQSIAKKIDAAQNWLADPNGGPEGEEQIRGALAEARKI
AELCDDPKERDDILRSLGEISALTSKLADLRRQGKGDSPEARALAKQVATALQNLQTKTNRAVANSRPAKAAVHLEGKIEQAQR
WIDNPTVDDRGVGQAAIRGLVAEGHRLANVMMGPYRQDLLAKCDRVDQLTAQLADLAARGEGESPQARALASQLQDSLKDL
KARMQEAMTQEVSDVFSDTTTPIKLLAVAATAPPDAPNREEVFDERAANFENHSGKLGATAEKAAAVGTANKSTVEGIQASVK
TARELTPQVVSAARILLRNPGNQAAYEHFETMKNQWIDNVEKMTGLVDEAIDTKSLLDASEEAIKKDLDKCKVAMANIQPQML
VAGATSIARRANRILLVAKREVENSEDPKFREAVKAASDELSKTISPMVMDAKAVAGNISDPGLQKSFLDSGYRILGAVAKVREAF
QPQEPDFPPPPPDLEQLRLTDELAPPKPPLPEGEVPPPRPPPPEEKDEEFPEQKAGEVINQPMMMAARQLHDEARKWSSKPGI
PAAEVGIGVVAEADAADAAGFPVPPDMEDDYEPELLLMPSNQPVNQPILAAAQSLHREATKWSSKGNDIIAAAKRMALLMAE
MSRLVRGGSGTKRALIQCAKDIAKASDEVTRLAKEVAKQCTDKRIRTNLLQVCERIPTISTQLKILSTVKATMLGRTNISDEESEQA
TEMLVHNAQNLMQSVKETVREAEAASIKIRTDAGFTLRWVRKTPWYQ

96 hr +/- Securinine soluble fraction 4-7/Spot 30/Myosin light chain 6 alkali smooth muscle and nonmuscle isoform 1/Mascot

MCDFTEDQTAEFKEAFQLFDRTGDGKILYSQCGDVMRALGQNPTNAEVLKVLGNPKSDEMNVKVLDFE
HFLPMLQTVAKNKDQGTYEDYVEGLRVFDKEGNGTVMGAEIRHVLVTLGEKMTEEEVEMLVAGHEDSNGCI
NYEAFVRHILSG

96 hr +/- Securinine soluble fraction 4-7/Spot 30/Myosin light chain 6 alkali smooth muscle and nonmuscle isoform 1/X!Hunter

MCDFTEDQTAEFKEAFQLFDRTGDGKILYSQCGDVMRALGQNPTNAEVLKVLGNPKSDEMNVKVLDFEHFL
PMLQTVAKNKDQGTYEDYVEGLRVFDKEGNGTVMGAEIRHVLVTLGEKMTEEEVEMLVAGHEDSNGCINY
EAFVRHILSG

96 hr +/- Securinine soluble fraction 4-7/Spot 30/Myosin light chain 6 alkali smooth muscle and nonmuscle isoform 1/X!Tandem P3

MCDFTEDQTAEFKEAFQLFDRTGDGKILYSQCGDVMRALGQNPTNAEVLKVLGNPKSDEMNVKVLDFE
HFLPMLQTVAKNKDQGTYEDYVEGLRVFDKEGNGTVMGAEIRHVLVTLGEKMTEEEVEMLVAGHEDSNGCI
NYEAFVRHILSG

96 hr +/- Securinine soluble fraction 4-7/Spot 38/Peptididylprolyl isoform a/Mascot

MVNPTVFFDIAVDGEPLGRVSFELFADKVPKTAENFRALSTGEKGFGYKGSCFHRIIPGFMCQGGDFTRH
NGTGGKSIYGEKFEDENFILKHTGPGILSMANAGPNTNGSQFFICTAKTEWLDGKHVVFGKVKEGMNIVEAM
ERFGSRNGKTSKKITIADCGQLE

96 hr +/- Securinine soluble fraction 4-7/Spot 38/Peptididylprolyl isoform a/X!Hunter

MVNPTVFFDIAVDGEPLGRVSFELFADKVPKTAENFRALSTGEKGFGYKGSCFHRIIPGFMCQGGDFTRHNG
TGGKSIYGEKFEDENFILKHTGPGILSMANAGPNTNGSQFFICTAKTEWLDGKHVVFGKVKEGMNIVEAMER
FGSRNGKTSKKITIADCGQLE

96 hr +/- Securinine soluble fraction 4-7/Spot 38/Peptididylprolyl isoform a/X!Tandem P3

MVNPTVFFDIAVDGEPLGRVSFELFADKVPKTAENFRALSTGEKGFGYKGSCFHRIIPGFMCQGGDFTRH
NGTGGKSIYGEKFEDENFILKHTGPGILSMANAGPNTNGSQFFICTAKTEWLDGKHVVFGKVKEGMNIVEAM
ERFGSRNGKTSKKITIADCGQLE

96 hr +/- Securinine soluble fraction 4-7/Spot 45/L-plastin/Mascot

MARGSVSDEEMMELREAFAKVDTDGNGYISFNELNDLFKAACLPLPGYRVREITENLMATGDLDQDGRI
SFDEFIKIFHGLKSTDVAKTFRKAINKKEGICAIGGTSEQSSVGTQHSYSEEEKYAFVNWINKALENDPDCRHVIP
MNPNTNDLFNAVGDGIVLCKMINLSVPDTIDERTINKKKLTPFTIQENLNLALNSASAIGCHVVNIGAEDLKEG
KPYLVLGLLWQVIKIGLFADIELSRNEALIALLREGESLEDLMKLSPEELLLRWANYHLENAGCNKIGNFSTDIKD
SKAYYHLLEQVAPKGDEEGVPAVVIDMSGLREKDDIQRAECMLQQAERLGCRQFVTATDVVRGNPKLNLAFI
ANLFNRYPALHKPENQDIDWGALEGETREERTFRNWMNSLGVNPRVNHLYSDLSDALVIFQLYEKIKVPVD
WNRVNKPPYPKLGGNMKKLENCNYAVELGKNQAKFSLVGIGGQDLNEGNRTLTLALIWQLMRRYTLNILEEI
GGGQKVNDDIIVNWVNETLREAEKSSSISSFKDPKISTSLPVLDLIDAIQPGSINYDLLKTENLNDDEKLNNAKY
AISMARKIGARVYALPEDLVEVNPKMVMTVFACLMGKGMKRV

96 hr +/- Securinine soluble fraction 4-7/Spot 45/L-plastin/X!Hunter

MARGSVSDEEMMELREAFAKVDTDGNGYISFNELNDLFKAACLPLPGYRVREITENLMATGDLDQDGRISFD
EFIKIFHGLKSTDVAKTFRKAINKKEGICAIGGTSEQSSVGTQHSYSEEEKYAFVNWINKALENDPDCRHVIPMN
PNTNDLFNAVGDGIVLCKMINLSVPDTIDERTINKKKLTPFTIQENLNLALNSASAIGCHVVNIGAEDLKEGKPY
LVLGLLWQVIKIGLFADIELSRNEALIALLREGESLEDLMKLSPEELLLRWANYHLENAGCNKIGNFSTDIKDSKA
YYHLLEQVAPKGDEEGVPAVVIDMSGLREKDDIQRAECMLQQAERLGCRQFVTATDVVRGNPKLNLAFIANL
FNRYPALHKPENQDIDWGALEGETREERTFRNWMNSLGVNPRVNHLYSDLSDALVIFQLYEKIKVPVDWNR
VNKPPYPKLGGNMKKLENCNYAVELGKNQAKFSLVGIGGQDLNEGNRTLTLALIWQLMRRYTLNILEEIGGG
QKVNDDIIVNWVNETLREAEKSSSISSFKDPKISTSLPVLDLIDAIQPGSINYDLLKTENLNDDEKLNNAKYAISM
ARKIGARVYALPEDLVEVNPKMVMTVFACLMGKGMKRV

96 hr +/- Securinine soluble fraction 4-7/Spot 45/L-plastin/X!Tandem P3

MARGSVSDEEMMELREAFAKVDTDGNGYISFNELNDLFKAACLPLPGYRVREITENLMATGDLDQDGRISFD
EFIKIFHGLKSTDVAKTFRKAINKKEGICAIGGTSEQSSVGTQHSYSEEEKYAFVNWINKALENDPDCRHVIPMN
PNTNDLFNAVGDGIVLCKMINLSVPDTIDERTINKKKLTPFTIQENLNLALNSASAIGCHVVNIGAEDLKEGKPY
LVLGLLWQVIKIGLFADIELSRNEALIALLREGESLEDLMKLSPEELLLRWANYHLENAGCNKIGNFSTDIKDSKA
YYHLLEQVAPKGDEEGVPAVVIDMSGLREKDDIQRAECMLQQAERLGCRQFVTATDVVRGNPKLNLAFIANL
FNRYPALHKPENQDIDWGALEGETREERTFRNWMNSLGVNPRVNHLYSDLSDALVIFQLYEKIKVPVDWNR
VNKPPYPKLGGNMKKLENCNYAVELGKNQAKFSLVGIGGQDLNEGNRTLTLALIWQLMRRYTLNILEEIGGG
QKVNDDIIVNWVNETLREAEKSSSISSFKDPKISTSLPVLDLIDAIQPGSINYDLLKTENLNDDEKLNNAKYAISM
ARKIGARVYALPEDLVEVNPKMVMTVFACLMGKGMKRV

96 hr +/- Securinine soluble fraction 4-7/Spot 63/S100 Ca^{2+} binding protein A11/Mascot
MAKISSPTETERCIESLIAVFQKYAGKDGYNYTLSKTEFLSFMNTELAAFTKNQKDPGVLDRMMKKLDTN
SDGQLDFSEFLNLIGGLAMACHDSFLKAVPSQKRT

96 hr +/- Securinine soluble fraction 4-7/Spot 63/S100 Ca^{2+} binding protein A11/X!Hunter
MAKISSPTETERCIESLIAVFQKYAGKDGYNYTLSKTEFLSFMNTELAAFTKNQKDPGVLDRMMKKLDTNSDG
QLDFSEFLNLIGGLAMACHDSFLKAVPSQKRT

96 hr +/- Securinine soluble fraction 4-7/Spot 63/S100 Ca^{2+} binding protein A11/X!Tandem P3
MAKISSPTETERCIESLIAVFQKYAGKDGYNYTLSKTEFLSFMNTELAAFTKNQKDPGVLDRMMKKLDTNSDG
QLDFSEFLNLIGGLAMACHDSFLKAVPSQKRT

96 hr +/- Securinine soluble fraction/Spot 67/Programmed cell death 6 interacting protein/Mascot

MATFISMQLKKTSEVDLAKPLVKFIQQTYPSGGEEQAQYCRAAEELSKLRRAAVGRPLDKHEGALETLLRYYDQICSIE
PKFPFSENQICLTFTWKDAFDKGSLFGGSVKLALASLGYEKSCVLFNCAALASQIAAEQNLDNDEGLKIAAKHYQFASGAFL
HIKETVLSALSREPTVDISPDTVGTLSLIMLAQAQEVFFLKATRDKMKDAIIAKLANQAADYFGDAFKQCQYKDTLPKYFYF
QEVFPVLAAKHCIMQANAEYHQSILAKQQKKFGEEIARLQHAAELIKTVASRYDEYVNVKDFSDKINRALAAAKKDNDFIY
HDRVPDLKDLDPIGKATLVKSTPVNVPISQKFTDLFEKMVPVSVQQSLAAYNQRKADLINRSIAQMREATTLANGVLASL
NLPAAIEDVSGDTVPQSILTKSRSVIEQGGIQTVDQLIKELPELLQRNREILDESLRLLDEEEATDNDLRAKFKERWQRTPSN
ELYKPLRAEGTNFRTVLDKAVQADGQVKECYQSHRDTIVLLCKPEPELNAAIPSANPAKTMQGSEVVNVLKSLLSNLDEVK
KEREGLENDLKSVNFDMTSKFLTALAQDGVINEEALSVTELDRVYGGLTTKVQESLKKQEGLLKNIQVSHQEFSKMKQSN
NEANLREEVLKNLATAYDNFVELVANLKEGTKFYNELTEILVRFQNKCSDIVFARKTERDELLKDLQQSIAREPSAPSIPTPAY
QSSPAGGHAPTPPTPAPRTMPPTKPQPPARPPPPVLPANRAPSATAPSPVGAGTAAPAPSQTPGSAPPPQAQGPPYPTY
PGYPGYCQMPMPMGYNPYAYGQYNMPYPPVYHQSPGQAPYPGPQQPSYPFPQPPQQSYYPQQ

96 hr +/- Securinine soluble fraction/Spot 67/Programmed cell death 6 interacting protein/X!Hunter

MATFISVQLKKTSEVDLAKPLVKFIQQTYPSGGEEQAQYCRAAEELSKLRRAAVGRPLDKHEGALETLLRYYDQICSIEPKFP
FSENQICLTFTWKDAFDKGSLFGGSVKLALASLGYEKSCVLFNCAALASQIAAEQNLDNDEGLKIAAKHYQFASGAFLHIKE
TVLSALSREPTVDISPDTVGTLSLIMLAQAQEVFFLKATRDKMKDAIIAKLANQAADYFGDAFKQCQYKDTLPKEVFPVLA
AKHCIMQANAEYHQSILAKQQKKFGEEIARLQHAAELIKTVASRYDEYVNVKDFSDKINRALAAAKKDNDFIYHDRVPDLK
DLDPIGKATLVKSTPVNVPISQKFTDLFEKMVPVSVQQSLAAYNQRKADLVNRSIAQMREATTLANGVLASLNLPAAIEDV
SGDTVPQSILTKSRSVIEQGGIQTVDQLIKELPELLQRNREILDESLRLLDEEEATDNDLRAKFKERWQRTPSNELYKPLRAE
GTNFRTVLDKAVQADGQVKECYQSHRDTIVLLCKPEPELNAAIPSANPAKTMQGSEVVNVLKSLLSNLDEVKKEREGLEN
DLKSVNFDMTSKFLTALAQDGVINEEALSVTELDRVYGGLTTKVQESLKKQEGLLKNIQVSHQEFSKMKQSNNEANLREE
VLKNLATAYDNFVELVANLKEGTKFYNELTEILVRFQNKCSDIVFARKTERDELLKDLQQSIAREPSAPSIPTPAYQSSPAGG
HAPTPPTPAPRTMPPTKPQPPARPPPPVLPANRAPSATAPSPVGAGTAAPAPSQTPGSAPPPQAQGPPYPTYPGYPGYC
QMPMPMGYNPYAYGQYNMPYPPVYHQSPGQAPYPGPQQPSYPFPQPPQQSYYPQQ

96 hr +/- Securinine soluble fraction/Spot 67/Programmed cell death 6 interacting protein/X!Tandem P3

MATFISVQLKKTSEVDLAKPLVKFIQQTYPSGGEEQAQYCRAAEELSKLRRAAVGRPLDKHEGALETLLRYYDQICSIEPKFP
FSENQICLTFTWKDAFDKGSLFGGSVKLALASLGYEKSCVLFNCAALASQIAAEQNLDNDEGLKIAAKHYQFASGAFLHIKE
TVLSALSREPTVDISPDTVGTLSLIMLAQAQEVFFLKATRDKMKDAIIAKLANQAADYFGDAFKQCQYKDTLPKEVFPVLA
AKHCIMQANAEYHQSILAKQQKKFGEEIARLQHAAELIKTVASRYDEYVNVKDFSDKINRALAAAKKDNDFIYHDRVPDLK
DLDPIGKATLVKSTPVNVPISQKFTDLFEKMVPVSVQQSLAAYNQRKADLVNRSIAQMREATTLANGVLASLNLPAAIEDV
SGDTVPQSILTKSRSVIEQGGIQTVDQLIKELPELLQRNREILDESLRLLDEEEATDNDLRAKFKERWQRTPSNELYKPLRAE
GTNFRTVLDKAVQADGQVKECYQSHRDTIVLLCKPEPELNAAIPSANPAKTMQGSEVVNVLKSLLSNLDEVKKEREGLEN
DLKSVNFDMTSKFLTALAQDGVINEEALSVTELDRVYGGLTTKVQESLKKQEGLLKNIQVSHQEFSKMKQSNNEANLREE
VLKNLATAYDNFVELVANLKEGTKFYNELTEILVRFQNKCSDIVFARKTERDELLKDLQQSIAREPSAPSIPTPAYQSSPAGG
HAPTPPTPAPRTMPPTKPQPPARPPPPVLPANRAPSATAPSPVGAGTAAPAPSQTPGSAPPPQAQGPPYPTYPGYPGYC
QMPMPMGYNPYAYGQYNMPYPPVYHQSPGQAPYPGPQQPSYPFPQPPQQSYYPQQ

96 hr +/- Securinine soluble fraction 4-7/Spot 77/Tropomyosin 3 isoform 2/Mascot

MAGITTIEAVKRKIQVLQQQADDAEERAERLQREVEGERRARQAEAEVASLNRRIQLVEEELDRAQERL
ATALQKLEEAEKAADESERGMKVIENRALKDEEKMELQEIQLKEAKHIAEEADRKYEEVARKLVIIEGDLERTEE
RAELAESRCREMDEQIRLMDQNLKCLSAAEEKYSQKEDKYEEEIKILTDKLKEAETRAEFAERSVAKLEKTIDDLE
DKLKCTKEEHLCTQRMLDQTLLDLNEM

96 hr +/- Securinine soluble fraction 4-7/Spot 77/Tropomyosin 3 isoform 2/X!Hunter

MAGITTIEAVKRKIQVLQQQADDAEERAERLQREVEGERRARQAEAEVASLNRRIQLVEEELDRAQERL
ATALQKLEEAEKAADESERGMKVIENRALKDEEKMELQEIQLKEAKHIAEEADRKYEEVARKLVIIEGDLERTEE
RAELAESRCREMDEQIRLMDQNLKCLSAAEEKYSQKEDKYEEEIKILTDKLKEAETRAEFAERSVAKLEKTIDDLE
DELYAQKLKYKAISEELDHALNDMTSI

96 hr +/- Securinine soluble fraction 4-7/Spot 77/Tropomyosin 3 isoform 2/X!Tandem P3

MAGITTIEAVKRKIQVLQQQADDAEERAERLQREVEGERRARQAEAEVASLNRRIQLVEEELDRAQERL
ATALQKLEEAEKAADEKKMELQEIQLKEAKHIAEEADRKYEEVARKLVIIEGDLERTEERAELAESRCRE
MDEQIRLMDQNLKCLSAAEEKYSQKEDKYEEEIKILTDKLKEAETRAEFAERSVAKLEKTIDDLEDKLKC
TKEEHLCTQRMLDQTLLDLNEM

96 hr +/- Securinine soluble fraction 4-7/Spot 117/Hsp60/Mascot

MLRLPTVFRQMRPVSRVLAPHLTRAYAKDVKFGADARALMLQGVDLLADAVAVTMGPKGRTVIIEQS
WGSPKVTKDGVTVAKSIDLKDKYKNIGAKLVQDVANNTNEEAGDGTTTATVLARSIAKEGFEKISKGANPVEI
RRGVMLAVDAVIAELKKQSKPVTTPEEIAQVATISANGDKEIGNIISDAMKKVGRKGVITVKDGKTLNDELEIIE
GMKFDRGYISPYFINTSKGQKCEFQDAYVLLSEKKISSIQSIVPALEIANAHRKPLVIIAEDVDGEALSTLVLNRLK
VGLQVVAVKAPGFGDNRKNQLKDMAIATGGAVFGEEGLTLNLEDVQPHDLGKVGEVIVTKDDAMLLKGKG
DKAQIEKRIQEIIEQLDVTTSEYEKEKLNERLAKLSDGVAVLKVGGTSDVEVNEKKDRVTDALNATRAAVEEGIV
LGGGCALLRCIPALDSLTPANEDQKIGIEIIKRTLKIPAMTIAKNAGVEGSLIVEKIMQSSSEVGYDAMAGDFVN
MVEKGIIDPTKVVRTALLDAAGVASLLTTAEVVVTEIPKEEKDPGMGAMGGMGGGMGGGMF

96 hr +/- Securinine soluble fraction 4-7/Spot 117/Hsp60/X!Hunter

MLRLPTVFRQMRPVSRVLAPHLTRAYAKDVKFGADARALMLQGVDLLADAVAVTMGPKGRTVIIEQS
WGSPKVTKDGVTVAKSIDLKDKYKNIGAKLVQDVANNTNEEAGDGTTTATVLARSIAKEGFEKISKGANPVEI
RRGVMLAVDAVIAELKKQSKPVTTPEEIAQVATISANGDKEIGNIISDAMKKVGRKGVITVKDGKTLNDELEIIE
GMKFDRGYISPYFINTSKGQKCEFQDAYVLLSEKKISSIQSIVPALEIANAHRKPLVIIAEDVDGEALSTLVLNRLK
VGLQVVAVKAPGFGDNRKNQLKDMAIATGGAVFGEEGLTLNLEDVQPHDLGKVGEVIVTKDDAMLLKGKG
DKAQIEKRIQEIIEQLDVTTSEYEKEKLNERLAKLSDGVAVLKVGGTSDVEVNEKKDRVTDALNATRAAVEEGIV
LGGGCALLRCIPALDSLTPANEDQKIGIEIIKRTLKIPAMTIAKNAGVEGSLIVEKIMQSSSEVGYDAMAGDFVN
MVEKGIIDPTKVVRTALLDAAGVASLLTTAEVVVTEIPKEEKDPGMGAMGGMGGGMGGGMF

96 hr +/- Securinine soluble fraction 4-7/Spot 117/Hsp60/X!Tandem P3

MLRLPTVFRQMRPVSRVLAPHLTRAYAKDVKFGADARALMLQGVDLLADAVAVTMGPKGRTVIIEQS
WGSPKVTKDGVTVAKSIDLKDKYKNIGAKLVQDVANNTNEEAGDGTTTATVLARSIAKEGFEKISKGANPVEI
RRGVMLAVDAVIAELKKQSKPVTTPEEIAQVATISANGDKEIGNIISDAMKKVGRKGVITVKDGKTLNDELEIIE
GMKFDRGYISPYFINTSKGQKCEFQDAYVLLSEKKISSIQSIVPALEIANAHRKPLVIIAEDVDGEALSTLVLNRLK
VGLQVVAVKAPGFGDNRKNQLKDMAIATGGAVFGEEGLTLNLEDVQPHDLGKVGEVIVTKDDAMLLKGKG
DKAQIEKRIQEIIEQLDVTTSEYEKEKLNERLAKLSDGVAVLKVGGTSDVEVNEKKDRVTDALNATRAAVEEGIV
LGGGCALLRCIPALDSLTPANEDQKIGIEIIKRTLKIPAMTIAKNAGVEGSLIVEKIMQSSSEVGYDAMAGDFVN
MVEKGIIDPTKVVRTALLDAAGVASLLTTAEVVVTEIPKEEKDPGMGAMGGMGGGMGGGMF

96 hr +/- Securinine soluble fraction 4-7/Spot 192/Vinculin isoform VCL/Mascot

MPVFHTRTIESILEPVAQQISHLVIMHEEGEVDGKAIPDLTAPVAAVQAAVSNLVRVGKETVQTTEDQILKRDMPPAFIKVE
NACTKLVQAAQMLQSDPYSVPARDYLIDGSRGILSGTSDLLLTFDEAEVRKIIRVCKGILEYLTVAEVVETMEDLVTYTKNLGPGM
TKMAKMIDERQQELTHQEHRVMLVNSMNTVKELLPVLISAMKIFVTTKNSKNQGIEEALKNRNFTVEKMSAEINEIIRVLQLTS
WDEDAWASKDTEAMKRALASIDSKLNQAKGWLRDPSASPGDAGEQAIRQILDEAGKVGELCAGKERREILGTCKMLGQMTD
QVADLRARGQGSSPVAMQKAQQVSQGLDVLTAKVENAARKLEAMTNSKQSIAKKIDAAQNWLADPNGGPEGEEQIRGALAE
ARKIAELCDDPKERDDILRSLGEISALTSKLADLRRQGKGDSPEARALAKQVATALQNLQTKTNRAVANSRPAKAAVHLEGKIEQ
AQRWIDNPTVDDRGVGQAAIRGLVAEGHRLANVMMGPYRQDLLAKCDRVDQLTAQLADLAARGEGESPQARALASQLQDS
LKDLKARMQEAMTQEVSDVFSDTTTPIKLLAVAATAPPDAPNREEVFDERAANFENHSGKLGATAEKAAAVGTANKSTVEGIQ
ASVKTARELTPQVVSAARILLRNPGNQAAYEHFETMKNQWIDNVEKMTGLVDEAIDTKSLLDASEEAIKKDLDKCKVAMANIQP
QMLVAGATSIARRANRILLVAKREVENSEDPKFREAVKAASDELSKTISPMVMDAKAVAGNISDPGLQKSFLDSGYRILGAVAKV
REAFQPQEPDFPPPPPDLEQLRLTDELAPPKPPLPEGEVPPPRPPPPEEKDEEFPEQKAGEVINQPMMMAARQLHDEARKWSS
KGNDIIAAAKRMALLMAEMSRLVRGGSGTKRALIQCAKDIAKASDEVTRLAKEVAKQCTDKRIRTNLLQVCERIPTISTQLKILSTV
KATMLGRTNISDEESEQATEMLVHNAQNLMQSVKETVREAEAASIKIRTDAGFTLRWVRKTPWYQ

96 hr +/- Securinine soluble fraction 4-7/Spot 192/Vinculin isoform VCL/X!Hunter

MPVFHTRTIESILEPVAQQISHLVIMHEEGEVDGKAIPDLTAPVAAVQAAVSNLVRVGKETVQTTEDQILKRDMPPAFIKVENAC
TKLVQAAQMLQSDPYSVPARDYLIDGSRGILSGTSDLLLTFDEAEVRKIIRVCKGILEYLTVAEVVETMEDLVTYTKNLGPGMTKM
AKMIDERQQELTHQEHRVMLVNSMNTVKELLPVLISAMKIFVTTKNSKNQGIEEALKNRNFTVEKMSAEINEIIRVLQLTSWDE
DAWASKDTEAMKRALASIDSKLNQAKGWLRDPSASPGDAGEQAIRQILDEAGKVGELCAGKERREILGTCKMLGQMTDQVA
DLRARGQGSSPVAMQKAQQVSQGLDVLTAKVENAARKLEAMTNSKQSIAKKIDAAQNWLADPNGGPEGEEQIRGALAEARKI
AELCDDPKERDDILRSLGEISALTSKLADLRRQGKGDSPEARALAKQVATALQNLQTKTNRAVANSRPAKAAVHLEGKIEQAQR
WIDNPTVDDRGVGQAAIRGLVAEGHRLANVMMGPYRQDLLAKCDRVDQLTAQLADLAARGEGESPQARALASQLQDSLKDL
KARMQEAMTQEVSDVFSDTTTPIKLLAVAATAPPDAPNREEVFDERAANFENHSGKLGATAEKAAAVGTANKSTVEGIQASVK
TARELTPQVVSAARILLRNPGNQAAYEHFETMKNQWIDNVEKMTGLVDEAIDTKSLLDASEEAIKKDLDKCKVAMANIQPQML
VAGATSIARRANRILLVAKREVENSEDPKFREAVKAASDELSKTISPMVMDAKAVAGNISDPGLQKSFLDSGYRILGAVAKVREAF
QPQEPDFPPPPPDLEQLRLTDELAPPKPPLPEGEVPPPRPPPPEEKDEEFPEQKAGEVINQPMMMAARQLHDEARKWSSKPGI
PAAEVGIGVVAEADAADAAGFPVPPDMEDDYEPELLLMPSNQPVNQPILAAAQSLHREATKWSSKGNDIIAAAKRMALLMAE
MSRLVRGGSGTKRALIQCAKDIAKASDEVTRLAKEVAKQCTDKRIRTNLLQVCERIPTISTQLKILSTVKATMLGRTNISDEESEQA
TEMLVHNAQNLMQSVKETVREAEAASIKIRTDAGFTLRWVRKTPWYQ

96 hr +/- Securinine soluble fraction 4-7/Spot 192/Vinculin isoform VCL/X!Tandem P3

MPVFHTRTIESILEPVAQQISHLVIMHEEGEVDGKAIPDLTAPVAAVQAAVSNLVRVGKETVQTTEDQILKRDMPPAFIKVENAC
TKLVQAAQMLQSDPYSVPARDYLIDGSRGILSGTSDLLLTFDEAEVRKIIRVCKGILEYLTVAEVVETMEDLVTYTKNLGPGMTKM
AKMIDERQQELTHQEHRVMLVNSMNTVKELLPVLISAMKIFVTTKNSKNQGIEEALKNRNFTVEKMSAEINEIIRVLQLTSWDE
DAWASKDTEAMKRALASIDSKLNQAKGWLRDPSASPGDAGEQAIRQILDEAGKVGELCAGKERREILGTCKMLGQMTDQVA
DLRARGQGSSPVAMQKAQQVSQGLDVLTAKVENAARKLEAMTNSKQSIAKKIDAAQNWLADPNGGPEGEEQIRGALAEARKI
AELCDDPKERDDILRSLGEISALTSKLADLRRQGKGDSPEARALAKQVATALQNLQTKTNRAVANSRPAKAAVHLEGKIEQAQR
WIDNPTVDDRGVGQAAIRGLVAEGHRLANVMMGPYRQDLLAKCDRVDQLTAQLADLAARGEGESPQARALASQLQDSLKDL
KARMQEAMTQEVSDVFSDTTTPIKLLAVAATAPPDAPNREEVFDERAANFENHSGKLGATAEKAAAVGTANKSTVEGIQASVK
TARELTPQVVSAARILLRNPGNQAAYEHFETMKNQWIDNVEKMTGLVDEAIDTKSLLDASEEAIKKDLDKCKVAMANIQPQML
VAGATSIARRANRILLVAKREVENSEDPKFREAVKAASDELSKTISPMVMDAKAVAGNISDPGLQKSFLDSGYRILGAVAKVREAF
QPQEPDFPPPPPDLEQLRLTDELAPPKPPLPEGEVPPPRPPPPEEKDEEFPEQKAGEVINQPMMMAARQLHDEARKWSSKPGI
PAAEVGIGVVAEADAADAAGFPVPPDMEDDYEPELLLMPSNQPVNQPILAAAQSLHREATKWSSKGNDIIAAAKRMALLMAE
MSRLVRGGSGTKRALIQCAKDIAKASDEVTRLAKEVAKQCTDKRIRTNLLQVCERIPTISTQLKILSTVKATMLGRTNISDEESEQA
TEMLVHNAQNLMQSVKETVREAEAASIKIRTDAGFTLRWVRKTPWYQ

96 hr +/- Securinine soluble fraction 4-7/Spot 200/Enolase 1/Mascot

MSILKIHAREIFDSRGNPTVEVDLFTSKGLFRAAVPSGASTGIYEALELRDNDKTRYMGKGVSKAVEHINK
TIAPALVSKKLNVTEQEKIDKLMIEMDGTENKSKFGANAILGVSLAVCKAGAVEKGVPLYRHIADLAGNSEVILP
VPAFNVINGGSHAGNKLAMQEFMILPVGAANFREAMRIGAEVYHNLKNVIKEKYGKDATNVGDEGGFAPNI
LENKEGLELLKTAIGKAGYTDKVVIGMDVAASEFFRSGKYDLDFKSPDDPSRYISPDQLADLYKSFIKDYPVVSIE
DPFDQDDWGAWQKFTASAGIQVVGDDLTVTNPKRIAKAVNEKSCNCLLLKVNQIGSVTESLQACKLAQANG
WGVMVSHRSGETEDTFIADLVVGLCTGQIKTGAPCRSERLAKYNQLLRIEEELGSKAKFAGRNFRNPLAK

96 hr +/- Securinine soluble fraction 4-7/Spot 200/Enolase 1/X!Hunter

MSILKIHAREIFDSRGNPTVEVDLFTSKGLFRAAVPSGASTGIYEALELRDNDKTRYMGKGVSKAVEHINK
TIAPALVSKKLNVTEQEKIDKLMIEMDGTENKSKFGANAILGVSLAVCKAGAVEKGVPLYRHIADLAGNSEVILP
VPAFNVINGGSHAGNKLAMQEFMILPVGAANFREAMRIGAEVYHNLKNVIKEKYGKDATNVGDEGGFAPNI
LENKEGLELLKTAIGKAGYTDKVVIGMDVAASEFFRSGKYDLDFKSPDDPSRYISPDQLADLYKSFIKDYPVVSIE
DPFDQDDWGAWQKFTASAGIQVVGDDLTVTNPKRIAKAVNEKSCNCLLLKVNQIGSVTESLQACKLAQANG
WGVMVSHRSGETEDTFIADLVVGLCTGQIKTGAPCRSERLAKYNQLLRIEEELGSKAKFAGRNFRNPLAK

96 hr +/- Securinine soluble fraction 4-7/Spot 200/Enolase 1/X!Tandem P3

MSILKIHAREIFDSRGNPTVEVDLFTSKGLFRAAVPSGASTGIYEALELRDNDKTRYMGKGVSKAVEHINK
TIAPALVSKKLNVTEQEKIDKLMIEMDGTENKSKFGANAILGVSLAVCKAGAVEKGVPLYRHIADLAGNSEVILP
VPAFNVINGGSHAGNKLAMQEFMILPVGAANFREAMRIGAEVYHNLKNVIKEKYGKDATNVGDEGGFAPNI
LENKEGLELLKTAIGKAGYTDKVVIGMDVAASEFFRSGKYDLDFKSPDDPSRYISPDQLADLYKSFIKDYPVVSIE
DPFDQDDWGAWQKFTASAGIQVVGDDLTVTNPKRIAKAVNEKSCNCLLLKVNQIGSVTESLQACKLAQANG
WGVMVSHRSGETEDTFIADLVVGLCTGQIKTGAPCRSERLAKYNQLLRIEEELGSKAKFAGRNFRNPLAK

96 hr +/- Securinine soluble fraction 4-7/Spot 273/Glycogen phosphorylase/Mascot

MGEPLTDQEKRRQISIRGIVGVENVAELKKSFNRHLHFTLVKDRNVATTRDYYFALAHTVRDHLVGRWIR
TQQHYYDKCPKRVYYLSLEFYMGRTLQNTMINLGLQNACDEAIYQLGLDIEELEEIEEDAGLGNGGLGRLAAC
FLDSMATLGLAAYGYGIRYEYGIFNQKIRDGWQVEEADDWLRYGNPWEKSRPEFMLPVHFYGKVEHTNTGT
KWIDTQVILALPYDTPEPGYMNNTVNTMRLWSARAPNDFNLRDFNVGDYIQAVLDRNLAENISRVLYPNDN
FFEGKELRLKQEYFVVAATLQDIIRRFKASKFGSTRGAGTVFDAFPDQVAIQLNDTHPALAIPELMRIFVDIEKLP
WSKAWELNQKTFAYTNHTVLPEALERWPVDLVEKLLPRHLEIIYEINQKHLDRIVALFPKDVDRLRRMSLIEEE
GSKRINMAHLCIVGSHAVNGVAKIHSDIVKTKVFKDFSELEPDKFQNKTNGITPRRWLLLCNPGLAELIAEKIGE
DYVKDLSQLTKLHSFLGDDVFLRELAKVKQENKLKFSQFLETEYKVKINPSSMFDVQVKRIHEYKRQLLNCLHVI
TMYNRIKKDPKKLFVPRTVIIGGKAAPGYHMAKMIIKLITSVADVVNNDPMVGSKLKVIFLENYRVSLAEKVIP
ATDLSEQISTAGTEASGTGNMKFMLNGALTIGTMDGANVEMAEEAGEENLFIFGMSIDDVAALDKKGYEAK
EYYEALPELKLVIDQIDNGFFSPKQPDLFKDIINMLFYHDRFKVFADYEAYVKCQDKVSQLYMNPKAWNTMVL
KNIAASGKFSSDRTIKEYAQNIWNVEPSDLKISLSNESNKVNGN

96 hr +/- Securinine soluble fraction 4-7/Spot 273/Glycogen phosphorylase/X!Hunter

MAKPLTDQEKRRQISIRGIVGVENVAELKKSFNRHLHFTLVKDRNVATTRDYYFALAHTVRDHLVGRWIRTQ
QHYYDKCPKRVYYLSLEFYMGRTLQNTMINLGLQNACDEAIYQLGLDIEELEEIEEDAGLGNGGLGRLAACFLD
SMATLGLAAYGYGIRYEYGIFNQKIRDGWQVEEADDWLRYGNPWEKSRPEFMLPVHFYGKVEHTNTGTKW
IDTQVVLALPYDTPVPGYMNNTVNTMRLWSARAPNDFNLRDFNVGDYIQAVLDRNLAENISRVLYPNDNFF
EGKELRLKQEYFVVAATLQDIIRRFKASKFGSTRGAGTVFDAFPDQVAIQLNDTHPALAIPELMRIFVDIEKLPW
SKAWELTQKTFAYTNHTVLPEALERWPVDLVEKLLPRHLEIIYEINQKHLDRIVALFPKDVDRLRRMSLIEEEGS
KRINMAHLCIVGSHAVNGVAKIHSDIVKTKVFKDFSELEPDKFQNKTNGITPRRWLLLCNPGLAELIAEKIGEDY
VKDLSQLTKLHSFLGDDVFLRELAKVKQENKLKFSQFLETEYKVKINPSSMFDVQVKRIHEYKRQLLNCLHVITM
YNRIKKDPKKLFVPRTVIIGGKAAPGYHMAKMIIKLITSVADVVNNDPMVGSKLKVIFLENYRVSLAEKVIPATD
LSEQISTAGTEASGTGNMKFMLNGALTIGTMDGANVEMAEEAGEENLFIFGMRIDDVAALDKKGYEAKEYY
EALPELKLVIDQIDNGFFSPKQPDLFKDIINMLFYHDRFKVFADYEAYVKCQDKVSQLYMNPKAWNTMVLKNI
AASGKFSSDRTIKEYAQNIWNVEPSDLKISLSNESNKVNGN

96 hr +/- Securinine soluble fraction 4-7/Spot 273/Glycogen phosphorylase/X!Tandem P3

MAKPLTDQEKRRQISIRGIVGVENVAELKKSFNRHLHFTLVKDRNVATTRDYYFALAHTVRDHLVGRWIRTQ
QHYYDKCPKRVYYLSLEFYMGRTLQNTMINLGLQNACDEAIYQLGLDIEELEEIEEDAGLGNGGLGRLAACFLD
SMATLGLAAYGYGIRYEYGIFNQKIRDGWQVEEADDWLRYGNPWEKSRPEFMLPVHFYGKVEHTNTGTKW
IDTQVVLALPYDTPVPGYMNNTVNTMRLWSARAPNDFNLRDFNVGDYIQAVLDRNLAENISRVLYPNDNFF
EGKELRLKQEYFVVAATLQDIIRRFKASKFGSTRGAGTVFDAFPDQVAIQLNDTHPALAIPELMRIFVDIEKLPW
SKAWELTQKTFAYTNHTVLPEALERWPVDLVEKLLPRHLEIIYEINQKHLDRIVALFPKDVDRLRRMSLIEEEGS
KRINMAHLCIVGSHAVNGVAKIHSDIVKTKVFKDFSELEPDKFQNKTNGITPRRWLLLCNPGLAELIAEKIGEDY
VKDLSQLTKLHSFLGDDVFLRELAKVKQENKLKFSQFLETEYKVKINPSSMFDVQVKRIHEYKRQLLNCLHVITM
YNRIKKDPKKLFVPRTVIIGGKAAPGYHMAKMIIKLITSVADVVNNDPMVGSKLKVIFLENYRVSLAEKVIPATD
LSEQISTAGTEASGTGNMKFMLNGALTIGTMDGANVEMAEEAGEENLFIFGMRIDDVAALDKKGYEAKEYY
EALPELKLVIDQIDNGFFSPKQPDLFKDIINMLFYHDRFKVFADYEAYVKCQDKVSQLYMNPKAWNTMVLKNI
AASGKFSSDRTIKEYAQNIWNVEPSDLKISLSNESNKVNGN

96 hr +/- Securinine membrane fraction 3-11NL/Spot 3/MHC class I histocompatability antigen HLA alpha chain precursor/Mascot

MAPRTLLLLLSGALALTQTWARSHSMRYFYTTMSRPGAGEPRFISVGYVDDTQFVRFDSDDASPREEPR
APWMEREGPKYWDRNTQICKAQAQTERENLRIALRYYNQSEGGSHTMQVMYGCDVGPDGPFLRGYEQHA
YDGKDYIALNEDLRSWTAADMAAQITKRKWEAARRAEQRRVYLEGEFVEWLRRYLENGKETLQRADPPKTH
MTHHPISDHEATLRCWALGFYPAEITLTWQRDGEDQTQDTELVETRPAGDGTFQKWAAVVVPSGEEQRYT
CHVQHEGLPEPLTLRWEPSSQPTVPIVGIVAGLVLLVAVVTGAVVAAVMWRKKSSDRKGGSYSQAASSNSA
QGSDVSLTA

not found by X!Hunter

96 hr +/- Securinine membrane fraction 3-11NL/Spot 3/MHC class I histocompatability antigen HLA alpha chain precursor/X!Tandem P3

MLVMAPRTVLLLLSAALALTETWAGSHSMRYFDTAMSRPGRGEPRFISVGYVDDTQFVRFDSDAASPREEPR
APWIEQEGPEYWDRNTQIFKTNTQTDRESLRNLRGYYNQSEAGSHTLQSMYGCDVGPDGRLLRGHNQYAY
DGKDYIALNEDLRSWTAADTAAQITQRKWEAARVAEQDRAYLEGTCVEWLRRYLENGKDTLERADPPKTHV
THHPISDHEATLRCWALGFYPAEITLTWQRDGEDQTQDTELVETRPAGDRTFQKWAAVVVPSGEEQRYTCH
VQHEGLPKPLTLRWEPSSQSTVPIVGIVAGLAVLAVVVIGAVVAAVMCRRKSSGGKGGSYSQAACSDSAQGS
DVSLTA

96 hr +/- Securinine membrane fraction 3-11NL/Spot 12/Vimentin (predicted cleavage product due to apoptosis)/Mascot

MSTRSVSSSSYRRMFGGPGTASRPSSSRSYVTTSTRTYSLGSALRPSTSRSLYASSPGGVYATRSSAVRLRS
SVPGVRLLQDSVDFSLADAINTEFKNTRTNEKVELQELNDRFANYIDKVRFLEQQNKILLAELEQLKGQGKSRL
GDLYEEEMRELRRQVDQLTNDKARVEVERDNLAEDIMRLREKLQEEMLQREEAENTLQSFRQDVDNASLAR
LDLERKVESLQEEIAFLKKLHEEEIQELQAQIQEQHVQIDVDVSKPDLTAALRDVRQQYESVAAKNLQEAEEWY
KSKFADLSEAANRNNDALRQAKQESTEYRRQVQSLTCEVDALKGTNESLERQMREMEENFAVEAANYQDTI
GRLQDEIQNMKEEMARHLREYQDLLNVKMALDIEIATYRKLLEGEESRISLPLPNFSSLNLRETNLDSLPLVDTH
SKRTFLIKTVETRDGQVINETSQHHDDLE

96 hr +/- Securinine membrane fraction 3-11NL/Spot 12/Vimentin (predicted cleavage product due to apoptosis)/X!Hunter

MSTRSVSSSSYRRMFGGPGTASRPSSSRSYVTTSTRTYSLGSALRPSTSRSLYASSPGGVYATRSSAVRLRSSVP
GVRLLQDSVDFSLADAINTEFKNTRTNEKVELQELNDRFANYIDKVRFLEQQNKILLAELEQLKGQGKSRLGDL
YEEEMRELRRQVDQLTNDKARVEVERDNLAEDIMRLREKLQEEMLQREEAENTLQSFRQDVDNASLARLDLE
RKVESLQEEIAFLKKLHEEEIQELQAQIQEQHVQIDVDVSKPDLTAALRDVRQQYESVAAKNLQEAEEWYKSKF
ADLSEAANRNNDALRQAKQESTEYRRQVQSLTCEVDALKGTNESLERQMREMEENFAVEAANYQDTIGRLQ
DEIQNMKEEMARHLREYQDLLNVKMALDIEIATYRKLLEGEESRISLPLPNFSSLNLRETNLDSLPLVDTHSKRT
LLIKTVETRDGQVINETSQHHDDLE

96 hr +/- Securinine membrane fraction 3-11NL/Spot 12/Vimentin (predicted cleavage product due to apoptosis)/X!Tandem P3

MSTRSVSSSSYRRMFGGPGTASRPSSSRSYVTTSTRTYSLGSALRPSTSRSLYASSPGGVYATRSSAVRLRSSVP
GVRLLQDSVDFSLADAINTEFKNTRTNEKVELQELNDRFANYIDKVRFLEQQNKILLAELEQLKGQGKSRLGDL
YEEEMRELRRQVDQLTNDKARVEVERDNLAEDIMRLREKLQEEMLQREEAENTLQSFRQDVDNASLARLDLE
RKVESLQEEIAFLKKLHEEEIQELQAQIQEQHVQIDVDVSKPDLTAALRDVRQQYESVAAKNLQEAEEWYKSKF
ADLSEAANRNNDALRQAKQESTEYRRQVQSLTCEVDALKGTNESLERQMREMEENFAVEAANYQDTIGRLQ
DEIQNMKEEMARHLREYQDLLNVKMALDIEIATYRKLLEGEESRISLPLPNFSSLNLRETNLDSLPLVDTHSKRT
LLIKTVETRDGQVINETSQHHDDLE

96 hr +/- Securinine membrane fraction 3-11NL/Spot 35/Pyruvate kinase/Mascot

MSKPHSEAGTAFIQTQQLHAAMADTFLEHMCRLDIDSPPITARNTGIICTIGPASRSVETLKEMIKSGMN
VARLNFSHGTHEYHAETIKNVRTATESFASDPILYRPVAVALDTKGPEIRTGLIKGSGTAEVELKKGATLKITLDN
AYMEKCDENILWLDYKNICKVVEVGSKIYVDDGLISLQVKQKGADFLVTEVENGGSLGSKKGVNLPGAAVDLP
AVSEKDIQDLKFGVEQDVDMVFASFIRKASDVHEVRKVLGEKGKNIKIISKIENHEGVRRFDEILEASDGIMVAR
GDLGIEIPAEKVFLAQKMMIGRCNRAGKPVICATQMLESMIKKPPPTRAEGSDVANAVLDGADCIMLSGETA
KGDYPLEAVRMQHLIAREAEAAIYHLQLFEELRRLAPITSDPTEATAVGAVEASFKCCSGAIIVLTKSGRSAHQV
ARYRPRAPIIAVTRNPQTARQAHLYRGIFPVLCKDPVQEAWAEDVDLRVNFAMNVGKARGFFKKGDVVIVLT
GWRPGSGFTNTMRVVPVP

96 hr +/- Securinine membrane fraction 3-11NL/Spot 35/Pyruvate kinase/X!Hunter

MSKPHSEAGTAFIQTQQLHAAMADTFLEHMCRLDIDSPPITARNTGIICTIGPASRSVETLKEMIKSGMN
VARLNFSHGTHEYHAETIKNVRTATESFASDPILYRPVAVALDTKGPEIRTGLIKGSGTAEVELKKGATLKITLDN
AYMEKCDENILWLDYKNICKVVEVGSKIYVDDGLISLQVKQKGADFLVTEVENGGSLGSKKGVNLPGAAVDLP
AVSEKDIQDLKFGVEQDVDMVFASFIRKASDVHEVRKVLGEKGKNIKIISKIENHEGVRRFDEILEASDGIMVAR
GDLGIEIPAEKVFLAQKMMIGRCNRAGKPVICATQMLESMIKKPRPTRAEGSDVANAVLDGADCIMLSGETA
KGDYPLEAVRMQHLIAREAEAAIYHLQLFEELRRLAPITSDPTEATAVGAVEASFKCCSGAIIVLTKSGRSAHQV
ARYRPRAPIIAVTRNPQTARQAHLYRGIFPVLCKDPVQEAWAEDVDLRVNFAMNVGKARGFFKKGDVVIVLT
GWRPGSGFTNTMRVVPVP

96 hr +/- Securinine membrane fraction 3-11NL/Spot 35/Pyruvate kinase/X!Tandem P3

MSKPHSEAGTAFIQTQQLHAAMADTFLEHMCRLDIDSPPITARNTGIICTIGPASRSVETLKEMIKSGMN
VARLNFSHGTHEYHAETIKNVRTATESFASDPILYRPVAVALDTKGPEIRTGLIKGSGTAEVELKKGATLKITLDN
AYMEKCDENILWLDYKNICKVVEVGSKIYVDDGLISLQVKQKGADFLVTEVENGGSLGSKKGVNLPGAAVDLP
AVSEKDIQDLKFGVEQDVDMVFASFIRKASDVHEVRKVLGEKGKNIKIISKIENHEGVRRFDEILEASDGIMVAR
GDLGIEIPAEKVFLAQKMMIGRCNRAGKPVICATQMLESMIKKPRPTRAEGSDVANAVLDGADCIMLSGETA
KGDYPLEAVRMQHLIAREAEAAIYHLQLFEELRRLAPITSDPTEATAVGAVEASFKCCSGAIIVLTKSGRSAHQV
ARYRPRAPIIAVTRNPQTARQAHLYRGIFPVLCKDPVQEAWAEDVDLRVNFAMNVGKARGFFKKGDVVIVLT
GWRPGSGFTNTMRVVPVP

96 hr +/- Securinine membrane fraction 3-11NL/Spot 36/Hsp60 (cleavage product due to apoptosis)/Mascot

MLRLPTVFRQMRPVSRVLAPHLTRAYAKDVKFGADARALMLQGVDLLADAVAVTMGPKGRTVIIEQS
WGSPKVTKDGVTVAKSIDLKDKYKNIGAKLVQDVANNTNEEAGDGTTTATVLARSIAKEGFEKISKGANPVEI
RRGVMLAVDAVIAELKKQSKPVTTPEEIAQVATISANGDKEIGNIISDAMKKVGRKGVITVKDGKTLNDELEIIE
GMKFDRGYISPYFINTSKGQKCEFQDAYVLLSEKKISSIQSIVPALEIANAHRKPLVIIAEDVDGEALSTLVLNRLK
VGLQVVAVKAPGFGDNRKNQLKDMAIATGGAVFGEEGLTLNLEDVQPHDLGKVGEVIVTKDDAMLLKGKG
DKAQIEKRIQEIIEQLDVTTSEYEKEKLNERLAKLSDGVAVLKVGGTSDVEVNEKKDRVTDALNATRAAVEEGIV
LGGGCALLRCIPALDSLTPANEDQKIGIEIIKRTLKIPAMTIAKNAGVEGSLIVEKIMQSSSEVGYDAMAGDFVN
MVEKGIIDPTKVVRTALLDAAGVASLLTTAEVVVTEIPKEEKDPGMGAMGGMGGGMGGGMF

96 hr +/- Securinine membrane fraction 3-11NL/Spot 36/Hsp60 (cleavage product due to apoptosis)/X!Hunter

MLRLPTVFRQMRPVSRVLAPHLTRAYAKDVKFGADARALMLQGVDLLADAVAVTMGPKGRTVIIEQS
WGSPKVTKDGVTVAKSIDLKDKYKNIGAKLVQDVANNTNEEAGDGTTTATVLARSIAKEGFEKISKGANPVEI
RRGVMLAVDAVIAELKKQSKPVTTPEEIAQVATISANGDKEIGNIISDAMKKVGRKGVITVKDGKTLNDELEIIE
GMKFDRGYISPYFINTSKGQKCEFQDAYVLLSEKKISSIQSIVPALEIANAHRKPLVIIAEDVDGEALSTLVLNRLK
VGLQVVAVKAPGFGDNRKNQLKDMAIATGGAVFGEEGLTLNLEDVQPHDLGKVGEVIVTKDDAMLLKGKG
DKAQIEKRIQEIIEQLDVTTSEYEKEKLNERLAKLSDGVAVLKVGGTSDVEVNEKKDRVTDALNATRAAVEEGIV
LGGGCALLRCIPALDSLTPANEDQKIGIEIIKRTLKIPAMTIAKNAGVEGSLIVEKIMQSSSEVGYDAMAGDFVN
MVEKGIIDPTKVVRTALLDAAGVASLLTTAEVVVTEIPKEEKDPGMGAMGGMGGGMGGGMF

96 hr +/- Securinine membrane fraction 3-11NL/Spot 36/Hsp60 (cleavage product due to apoptosis)/X!Tandem P3

MLRLPTVFRQMRPVSRVLAPHLTRAYAKDVKFGADARALMLQGVDLLADAVAVTMGPKGRTVIIEQS
WGSPKVTKDGVTVAKSIDLKDKYKNIGAKLVQDVANNTNEEAGDGTTTATVLARSIAKEGFEKISKGANPVEI
RRGVMLAVDAVIAELKKQSKPVTTPEEIAQVATISANGDKEIGNIISDAMKKVGRKGVITVKDGKTLNDELEIIE
GMKFDRGYISPYFINTSKGQKCEFQDAYVLLSEKKISSIQSIVPALEIANAHRKPLVIIAEDVDGEALSTLVLNRLK
VGLQVVAVKAPGFGDNRKNQLKDMAIATGGAVFGEEGLTLNLEDVQPHDLGKVGEVIVTKDDAMLLKGKG
DKAQIEKRIQEIIEQLDVTTSEYEKEKLNERLAKLSDGVAVLKVGGTSDVEVNEKKDRVTDALNATRAAVEEGIV
LGGGCALLRCIPALDSLTPANEDQKIGIEIIKRTLKIPAMTIAKNAGVEGSLIVEKIMQSSSEVGYDAMAGDFVN
MVEKGIIDPTKVVRTALLDAAGVASLLTTAEVVVTEIPKEEKDPGMGAMGGMGGGMGGGMF

96 hr +/- Securinine membrane fraction 3-11NL/Spot 44/PCNA/Mascot

MFEARLVQGSILKKVLEALKDLINEACWDISSSGVNLQSMDSSHVSLVQLTLRSEGFDTYRCDRNLAMGV
NLTSMSKILKCAGNEDIITLRAEDNADTLALVFEAPNQEKVSDYEMKLMDLDVEQLGIPEQEYSCVVKMPSGE
FARICRDLSHIGDAVVISCAKDGVKFSASGELGNGNIKLSQTSNVDKEEEAVTIEMNEPVQLTFALRYLNFFTKA
TPLSSTVTLSMSADVPLVVEYKIADMGHLKYYLAPKIEDEEGS

96 hr +/- Securinine membrane fraction 3-11NL/Spot 44/PCNA/X!Hunter

MFEARLVQGSILKKVLEALKDLINEACWDISSSGVNLQSMDSSHVSLVQLTLRSEGFDTYRCDRNLAMGVNLT
SMSKILKCAGNEDIITLRAEDNADTLALVFEAPNQEKVSDYEMKLMDLDVEQLGIPEQEYSCVVKMPSGEFAR
ICRDLSHIGDAVVISCAKDGVKFSASGELGNGNIKLSQTSNVDKEEEAVTIEMNEPVQLTFALRYLNFFTKATPL
SSTVTLSMSADVPLVVEYKIADMGHLKYYLAPKIEDEEGS

96 hr +/- Securinine membrane fraction 3-11NL/Spot 44/PCNA/X!Tandem P3

MFEARLVQGSILKKVLEALKDLINEACWDISSSGVNLQSMDSSHVSLVQLTLRSEGFDTYRCDRNLAMGVNLT
SMSKILKCAGNEDIITLRAEDNADTLALVFEAPNQEKVSDYEMKLMDLDVEQLGIPEQEYSCVVKMPSGEFAR
ICRDLSHIGDAVVISCAKDGVKFSASGELGNGNIKLSQTSNVDKEEEAVTIEMNEPVQLTFALRYLNFFTKATPL
SSTVTLSMSADVPLVVEYKIADMGHLKYYLAPKIEDEEGS

96 hr +/- Securinine membrane fraction 3-11NL/Spot 56/Hsp70/Mascot

MAKAAAIGIDLGTTYSCVGVFQHGKVEIIANDQGNRTTPSYVAFTDTERLIGDAAKNQVALNPQNTVFD
AKRLIGRKFGDPVVQSDMKHWPFQVINDGDKPKVQVSYKGETKAFYPEEISSMVLTKMKEIAEAYLGYPVTN
AVITVPAYFNDSQRQATKDAGVIAGLNVLRIINEPTAAAIAYGLDRTGKGERNVLIFDLGGGTFDVSILTIDDGIF
EVKATAGDTHLGGEDFDNRLVNHFVEEFKRKHKKDISQNKRAVRRLRTACERAKRTLSSSTQASLEIDSLFEGI
DFYTSITRARFEELCSDLFRSTLEPVEKALRDAKLDKAQIHDLVLVGGSTRIPKVQKLLQDFFNGRDLNKSINPDE
AVAYGAAVQAAILMGDKSENVQDLLLLDVAPLSLGLETAGGVMTALIKRNSTIPTKQTQIFTTYSDNQPGVLI
QVYEGERAMTKDNNLLGRFELSGIPPAPRGVPQIEVTFDIDANGILNVTATDKSTGKANKITITNDKGRLSKEEI
ERMVQEAEKYKAEDEVQRERVSAKNALESYAFNMKSAVEDEGLKGKISEADKKKVLDKCQEVISWLDANTLA
EKDEFEHKRKELEQVCNPIISGLYQGAGGPGPGGFGAQGPKGGSGSGPTIEEVD

96 hr +/- Securinine membrane fraction 3-11NL/Spot 56/Hsp70/X!Hunter

MAKAAAIGIDLGTTYSCVGVFQHGKVEIIANDQGNRTTPSYVAFTDTERLIGDAAKNQVALNPQNTVFDAKR
LIGRKFGDPVVQSDMKHWPFQVINDGDKPKVQVSYKGETKAFYPEEISSMVLTKMKEIAEAYLGYPVTNAVIT
VPAYFNDSQRQATKDAGVIAGLNVLRIINEPTAAAIAYGLDRTGKGERNVLIFDLGGGTFDVSILTIDDGIFEVK
ATAGDTHLGGEDFDNRLVNHFVEEFKRKHKKDISQNKRAVRRLRTACERAKRTLSSSTQASLEIDSLFEGIDFYT
SITRARFEELCSDLFRSTLEPVEKALRDAKLDKAQIHDLVLVGGSTRIPKVQKLLQDFFNGRDLNKSINPDEAVA
YGAAVQAAILMGDKSENVQDLLLLDVAPLSLGLETAGGVMTALIKRNSTIPTKQTQIFTTYSDNQPGVLIQVYE
GERAMTKDNNLLGRFELSGIPPAPRGVPQIEVTFDIDANGILNVTATDKSTGKANKITITNDKGRLSKEEIERM
VQEAEKYKAEDEVQRERVSAKNALESYAFNMKSAVEDEGLKGKISEADKKKVLDKCQEVISWLDANTLAEKD
EFEHKRKELEQVCNPIISGLYQGAGGPGPGGFGAQGPKGGSGSGPTIEEVD

96 hr +/- Securinine membrane fraction 3-11NL/Spot 56/Hsp70/X!Tandem P3

MAKAAAIGIDLGTTYSCVGVFQHGKVEIIANDQGNRTTPSYVAFTDTERLIGDAAKNQVALNPQNTVFDAKR
LIGRKFGDPVVQSDMKHWPFQVINDGDKPKVQVSYKGETKAFYPEEISSMVLTKMKEIAEAYLGYPVTNAVIT
VPAYFNDSQRQATKDAGVIAGLNVLRIINEPTAAAIAYGLDRTGKGERNVLIFDLGGGTFDVSILTIDDGIFEVK
ATAGDTHLGGEDFDNRLVNHFVEEFKRKHKKDISQNKRAVRRLRTACERAKRTLSSSTQASLEIDSLFEGIDFYT
SITRARFEELCSDLFRSTLEPVEKALRDAKLDKAQIHDLVLVGGSTRIPKVQKLLQDFFNGRDLNKSINPDEAVA
YGAAVQAAILMGDKSENVQDLLLLDVAPLSLGLETAGGVMTALIKRNSTIPTKQTQIFTTYSDNQPGVLIQVYE
GERAMTKDNNLLGRFELSGIPPAPRGVPQIEVTFDIDANGILNVTATDKSTGKANKITITNDKGRLSKEEIERM
VQEAEKYKAEDEVQRERVSAKNALESYAFNMKSAVEDEGLKGKISEADKKKVLDKCQEVISWLDANTLAEKD
EFEHKRKELEQVCNPIISGLYQGAGGPGPGGFGAQGPKGGSGSGPTIEEVD

96 hr +/- Securinine membrane fraction 3-11NL/Spot 92/Pyruvate kinase/Mascot

MSKPHSEAGTAFIQTQQLHAAMADTFLEHMCRLDIDSPPITARNTGIICTIGPASRSVETLKEMIKSGMN
VARLNFSHGTHEYHAETIKNVRTATESFASDPILYRPVAVALDTKGPEIRTGLIKGSGTAEVELKKGATLKITLDN
AYMEKCDENILWLDYKNICKVVEVGSKIYVDDGLISLQVKQKGADFLVTEVENGGSLGSKKGVNLPGAAVDLP
AVSEKDIQDLKFGVEQDVDMVFASFIRKASDVHEVRKVLGEKGKNIKIISKIENHEGVRRFDEILEASDGIMVAR
GDLGIEIPAEKVFLAQKMMIGRCNRAGKPVICATQMLESMIKKPPPTRAEGSDVANAVLDGADCIMLSGETA
KGDYPLEAVRMQHLIAREAEAAIYHLQLFEELRRLAPITSDPTEATAVGAVEASFKCCSGAIIVLTKSGRSAHQV
ARYRPRAPIIAVTRNPQTARQAHLYRGIFPVLCKDPVQEAWAEDVDLRVNFAMNVGKARGFFKKGDVVIVLT
GWRPGSGFTNTMRVVPVP

96 hr +/- Securinine membrane fraction 3-11NL/Spot 92/Pyruvate kinase/X!Hunter

MSKPHSEAGTAFIQTQQLHAAMADTFLEHMCRLDIDSPPITARNTGIICTIGPASRSVETLKEMIKSGMNVAR
LNFSHGTHEYHAETIKNVRTATESFASDPILYRPVAVALDTKGPEIRTGLIKGSGTAEVELKKGATLKITLDNAYM
EKCDENILWLDYKNICKVVEVGSKIYVDDGLISLQVKQKGADFLVTEVENGGSLGSKKGVNLPGAAVDLPAVS
EKDIQDLKFGVEQDVDMVFASFIRKASDVHEVRKVLGEKGKNIKIISKIENHEGVRRFDEILEASDGIMVARGD
LGIEIPAEKVFLAQKMMIGRCNRAGKPVICATQMLESMIKKPRPTRAEGSDVANAVLDGADCIMLSGETAKG
DYPLEAVRMQHLIAREAEAAIYHLQLFEELRRLAPITSDPTEATAVGAVEASFKCCSGAIIVLTKSGRSAHQVAR
YRPRAPIIAVTRNPQTARQAHLYRGIFPVLCKDPVQEAWAEDVDLRVNFAMNVGKARGFFKKGDVVIVLTG
WRPGSGFTNTMRVVPVP

96 hr +/- Securinine membrane fraction 3-11NL/Spot 92/Pyruvate kinase/X!Tandem P3

MSKPHSEAGTAFIQTQQLHAAMADTFLEHMCRLDIDSPPITARNTGIICTIGPASRSVETLKEMIKSGMNVAR
LNFSHGTHEYHAETIKNVRTATESFASDPILYRPVAVALDTKGPEIRTGLIKGSGTAEVELKKGATLKITLDNAYM
EKCDENILWLDYKNICKVVEVGSKIYVDDGLISLQVKQKGADFLVTEVENGGSLGSKKGVNLPGAAVDLPAVS
EKDIQDLKFGVEQDVDMVFASFIRKASDVHEVRKVLGEKGKNIKIISKIENHEGVRRFDEILEASDGIMVARGD
LGIEIPAEKVFLAQKMMIGRCNRAGKPVICATQMLESMIKKPRPTRAEGSDVANAVLDGADCIMLSGETAKG
DYPLEAVRMQHLIAREAEAAIYHLQLFEELRRLAPITSDPTEATAVGAVEASFKCCSGAIIVLTKSGRSAHQVAR
YRPRAPIIAVTRNPQTARQAHLYRGIFPVLCKDPVQEAWAEDVDLRVNFAMNVGKARGFFKKGDVVIVLTG
WRPGSGFTNTMRVVPVP

96 hr +/- Securinine membrane fraction/Spot 94/β2 microglobin/Mascot
LALLSLSGLEAIQRTPKIQVYSRHPAENGKSNFLNCYVSGFHPSDIEVDLLKNGERIEKVEHSDLSFSKDWSF
YLLYYTEFTPTEKDEYACRVNHVTLSQPKIVKWDRDM

96 hr +/- Securinine membrane fraction/Spot 94/β2 microglobin/X!Hunter
MSRSVALAVLALLSLSGLEAIQRTPKIQVYSRHPAENGKSNFLNCYVSGFHPSDIEVDLLKNGERIEKVEHS
DLSFSKDWSFYLLYYTEFTPTEKDEYACRVNHVTLSQPKIVKWDRDM

96 hr +/- Securinine membrane fraction/Spot 94/β2 microglobin/X!Tandem P3
MSRSVALAVLALLSLSGLEAIQRTPKIQVYSRHPAENGKSNFLNCYVSGFHPSDIEVDLLKNGERIEKVEHSDLSF
SKDWSFYLLYYTEFTPTEKDEYACRVNHVTLSQPKIVKWDRDM

96 hr +/- Securinine membrane fraction 3-11NL/Spot 116/N-ethylmaleimide-sensitive factor attachment protein, alpha/Mascot

MDNSGKEAEAMALLAEAERKVKNSQSFFSGLFGGSSKIEEACEIYARAANMFKMAKNWSAAGNAFCQ AAQLHLQLQSKHDAATCFVDAGNAFKKADPQEAINCLMRAIEIYTDMGRFTIAAKHHISIAEIYETELVDIEKAI AHYEQSADYYKGEESNSSANKCLLKVAGYAALLEQYQKAIDIYEQVGTNAMDSPLLKYSAKDYFFKAALCHFCI DMLNAKLAVQKYEELFPAFSDSRECKLMKKLLEAHEEQNVDSYTESVKEYDSISRLDQWLTTMLLRIKKTIQGD EEDLR

96 hr +/- Securinine membrane fraction 3-11NL/Spot 116/N-ethylmaleimide-sensitive factor attachment protein, alpha/X!Hunter

MDNSGKEAEAMALLAEAERKVKNSQSFFSGLFGGSSKIEEACEIYARAANMFKMAKNWSAAGNAFCQAAQ LHLQLQSKHDAATCFVDAGNAFKKADPQEAINCLMRAIEIYTDMGRFTIAAKHHISIAEIYETELVDIEKAIAHY EQSADYYKGEESNSSANKCLLKVAGYAALLEQYQKAIDIYEQVGTNAMDSPLLKYSAKDYFFKAALCHFCIDML NAKLAVQKYEELFPAFSDSRECKLMKKLLEAHEEQNVDSYTESVKEYDSISRLDQWLTTMLLRIKKTIQGDEED LR

96 hr +/- Securinine membrane fraction 3-11NL/Spot 116/N-ethylmaleimide-sensitive factor attachment protein, alpha/X!Tandem P3

MDNSGKEAEAMALLAEAERKVKNSQSFFSGLFGGSSKIEEACEIYARAANMFKMAKNWSAAGNAFCQAAQ LHLQLQSKHDAATCFVDAGNAFKKADPQEAINCLMRAIEIYTDMGRFTIAAKHHISIAEIYETELVDIEKAIAHY EQSADYYKGEESNSSANKCLLKVAGYAALLEQYQKAIDIYEQVGTNAMDSPLLKYSAKDYFFKAALCHFCIDML NAKLAVQKYEELFPAFSDSRECKLMKKLLEAHEEQNVDSYTESVKEYDSISRLDQWLTTMLLRIKKTIQGDEED LR

96 hr +/- Securinine membrane fraction/Spot 160/MHC class I antigen/Mascot

MARGDQAVMAPRTLLLLLSGALALTQTWAGSHSMRYFFTSVSRPGRGEPRFIAVGYVDDTQFVRFDSD
AASQRMEPRAPWIEQEGPEYWDQETRNVKAQSQTDRVDLGTLRGYYNQSEAGSHTIQIMYGCDVGSDGRF
LRGYRQDAYDGKDYIALNEDLRSWTAADMAAQITKRKWEAAHEAEQLRAYLDGTCVEWLRRYLENGKETLQ
RTDPPKTHMTHHPISDHEATLRCWALGFYPAEITLTWQRDGEDQTQDTELVETRPAGDGTFQKWAAVVVP
SGEEQRYTCHVQHEGLPKPLTLRWELSSQPTIPIVGIIAGLVLLGAVITGAVVAAVMWRRKSSDRKGGSYTQA
AM

96 hr +/- Securinine membrane fraction/Spot 160/MHC class I antigen/X!Hunter

MAVMAPRTLLLLLSGALALTHTWAGSHSMRYFSTSVSRPGSGEPRFIAVGYVDDTQFVRFDSDAASQR
MEPRAPWIEQERPEYWDQETRNVKAQSQTDRVDLGTLRGYYNQSEAGSHTIQIMYGCDVGSDGRFLRGYE
QHAYDGKDYIALNEDLRSWTAADMAAQITQRKWEAARWAEQLRAYLEGTCVEWLRRYLENGKETLQRTDP
PKTHMTHHPISDHEATLRCWALGFYPAEITLTWQRDGEDQTQDTELVETRPAGDGTFQKWAAVVVPSGEE
QRYTCHVQHEGLPKPLTLRWELSSQPTIPIVGIIAGLVLLGAVITGAVVAAVMWRRKSSDRKGGSYTQAASSD
SAQGSDVSLTACKV

96 hr +/- Securinine membrane fraction/Spot 160/MHC class I antigen/X!Tandem P3

MAVMAPRTLLLLLSGALALTQTWAGSHSMRYFFTSVSRPGRGEPRFIAVGYVDDTQFVRFDSDAASQKMEP
RAPWIEQEGPEYWDQETRNMKAHSQTDRANLGTLRGYYNQSEDGSHTIQIMYGCDVGPDGRFLRGYRQD
AYDGKDYIALNEDLRSWTAADMAAQITKRKWEAVHAAEQRRVYLEGRCVDGLRRYLENGKETLQRTDPPKT
HMTHHPISDHEATLRCWALGFYPAEITLTWQRDGEDQTQDTELVETRPAGDGTFQKWAAVVVPSGEEQRY
TCHVQHEGLPKPLTLRWELSSQPTIPIVGIIAGLVLLGAVITGAVVAAVMWRRKSSDRKGGSYTQAASSDSAQ
GSDVSLTACKV

96 hr +/- Securinine membrane fraction/Spot 201/tubulin/Mascot

MREIVHIQAGQCGNQIGAKFWEVISDEHGIDPTGTYHGDSDLQLDRISVYYNEATGGKYVPRAILVDLEP
GTMDSVRSGPFGQIFRPDNFVFGQSGAGNNWAKGHYTEGAELVDSVLDVVRKEAESCDCLQGFQLTHSLG
GGTGSGMGTLLISKIREEYPDRIMNTFSVVPSPKVSDTVVEPYNATLSVHQLVENTDETYCIDNEALYDICFRTL
KLTTPTYGDLNHLVSATMSGVTTCLRFPGQLNADLRKLAVNMVPFPRLHFFMPGFAPLTSRGSQQYRALTVP
ELTQQVFDAKDMMAACDPRHGRYLTVAAVFRGRMSMKEVDEQMLNVQNKNSSYFVEWIPNNVKTAVCD
IPPRGLKMAVTFIGNSTAIQELFKRISEQFTAMFRRKAFLHWYTGEGMDEMEFTEAESNMNDLVSEYQQYQ
DATAEEEEDFGEEAEEEA

96 hr +/- Securinine membrane fraction/Spot 201/tubulin/X!Hunter

MRECISIHVGQAGVQIGNACWELYCLEHGIQPDGQMPSDKTIGGGDDSFNTFFSETGAGKHVPRAVFVDLE
PTVIDEVRTGTYRQLFHPEQLITGKEDAANNYARGHYTIGKEIIDLVLDRIRKLADQCTGLQGFLVFHSFGGGTG
SGFTSLLMERLSVDYGKKSKLEFSIYPAPQVSTAVVEPYNSILTTHTTLEHSDCAFMVDNEAIYDICRRNLDIERP
TYTNLNRLISQIVSSITASLRFDGALNVDLTEFQTNLVPYPRIHFPLATYAPVISAEKAYHEQLSVAEITNACFEPA
NQMVKCDPRHGKYMACCLLYRGDVVPKDVNAAIATIKTKRSIQFVDWCPTGFKVGINYQPPTVVPGGDLAK
VQRAVCMLSNTTAIAEAWARLDHKFDLMYAKRAFVHWYVGEGMEEGEFSEAREDMAALEKDYEEVGVDS
VEGEGEEEGEEY

96 hr +/- Securinine membrane fraction/Spot 201/tubulin/X!Tandem P3

MRECISIHVGQAGVQIGNACWELYCLEHGIQPDGQMPSDKTIGGGDDSFNTFFSETGAGKHVPRAVFVDLE
PTVIDEVRTGTYRQLFHPEQLITGKEDAANNYARGHYTIGKEIIDLVLDRIRKLADQCTGLQGFLVFHSFGGGTG
SGFTSLLMERLSVDYGKKSKLEFSIYPAPQVSTAVVEPYNSILTTHTTLEHSDCAFMVDNEAIYDICRRNLDIERP
TYTNLNRLISQIVSSITASLRFDGALNVDLTEFQTNLVPYPRIHFPLATYAPVISAEKAYHEQLSVAEITNACFEPA
NQMVKCDPRHGKYMACCLLYRGDVVPKDVNAAIATIKTKRSIQFVDWCPTGFKVGINYQPPTVVPGGDLAK
VQRAVCMLSNTTAIAEAWARLDHKFDLMYAKRAFVHWYVGEGMEEGEFSEAREDMAALEKDYEEVGVDS
VEGEGEEEGEEY

96 hr +/- Securinine membrane fraction/Spot 216/MHC class I histocompatibility antigen HLA alpha chain precursor/Mascot

MAPRTLLLLLSGALALTQTWARSHSMRYFYTTMSRPGAGEPRFISVGYVDDTQFVRFDSDDASPREEPR
APWMEREGPKYWDRNTQICKAQAQTERENLRIALRYYNQSEGGSHTMQVMYGCDVGPDGPFLRGYEQHA
YDGKDYIALNEDLRSWTAADMAAQITKRKWEAARRAEQRRVYLEGEFVEWLRRYLENGKETLQRADPPKTH
MTHHPISDHEATLRCWALGFYPAEITLTWQRDGEDQTQDTELVETRPAGDGTFQKWAAVVVPSGEEQRYT
CHVQHEGLPEPLTLRWEPSSQPTVPIVGIVAGLVLLVAVVTGAVVAAVMWRKKSSDRKGGSYSQAASSNSA
QGSDVSLTA

96 hr +/- Securinine membrane fraction/Spot 216/MHC class I histocompatibility antigen HLA alpha chain precursor/X!Hunter

MAVMAPRTLLLLLSGALALTQTWARSHSMRYFYTTMSRPGAGEPRFISVGYVDDTQFVRFDSDDASPREEPR
APWMEREGPKYWDRNTQICKAQAQTERENLRIALRYYNQSEGGSHTMQVMYGCDVGPDGPFLRGYEQHA
YDGKDYIALNEDLRSWTAADMAAQITKRKWEAARRAEQRRVYLEGEFVEWLRRYLENGKETLQRADPPKTH
MTHHPISDHEATLRCWALGFYPAEITLTWQRDGEDQTQDTELVETRPAGDGTFQKWAAVVVPSGEEQRYT
CHVQHEGLPEPLTLRWEPSSQPTVPIVGIVAGLVLLVAVVTGAVVAAVMWRKKSSDRKGGSYSQAASSNSA
QGSDVSLTA

96 hr +/- Securinine membrane fraction/Spot 216/MHC class I histocompatibility antigen HLA alpha chain precursor/X!Tandem P3

MAVMAPRTLLLLLSGALALTQTWAGSHSMRYFFTSVSRPGRGEPRFIAVGYVDDTQFVRFDSDAASQKMEP
RAPWIEQEGPEYWDQETRNMKAHSQTDRANLGTLRGYYNQSEDGSHTIQIMYGCDVGPDGRFLRGYRQD
AYDGKDYIALNEDLRSWTAADMAAQITKRKWEAVHAAEQRRVYLEGRCVDGLRRYLENGKETLQRTDPPKT
HMTHHPISDHEATLRCWALGFYPAEITLTWQRDGEDQTQDTELVETRPAGDGTFQKWAAVVVPSGEEQRY
TCHVQHEGLPKPLTLRWELSSQPTIPIVGIIAGLVLLGAVITGAVVAAVMWRRKSSDRKGGSYTQAASSDSAQ
GSDVSLTACKV

96 hr +/- Securinine membrane fraction 3-11NL/Spot 354/SPFH domain family member 2 isoform 1/Mascot

MAQLGAVVAVASSFFCASLFSAVHKIEEGHIGVYYRGGALLTSTSGPGFHLMLPFITSYKSVQTTLQTDEV
KNVPCGTSGGVMIYFDRIEVVNFLVPNAVYDIVKNYTADYDKALIFNKIHHELNQFCSVHTLQEVYIELFDQIDE
NLKLALQQDLTSMAPGLVIQAVRVTKPNIPEAIRRNYELMESEKTKLLIAAQKQKVVEKEAETERKKALIEAEKV
AQVAEITYGQKVMEKETEKKISEIEDAAFLARKAKADAECYTAMKIAEANKLKLTPEYLQLMKYKAIASNSKIY
FGKDIPNMFMDSAGSVSKQFEGLADKLSFGLEDEPLETATKEN

96 hr +/- Securinine membrane fraction 3-11NL/Spot 354/SPFH domain family member 2 isoform 1/X!Hunter

MAQLGAVVAVASSFFCASLFSAVHKIEEGHIGVYYRGGALLTSTSGPGFHLMLPFITSYKSVQTTLQTDEV
KNVPCGTSGGVMIYFDRIEVVNFLVPNAVYDIVKNYTADYDKALIFNKIHHELNQFCSVHTLQEVYIELFDQIDE
NLKLALQQDLTSMAPGLVIQAVRVTKPNIPEAIRRNYELMESEKTKLLIAAQKQKVVEKEAETERKKALIEAEKV
AQVAEITYGQKVMEKETEKKISEIEDAAFLAREKAKADAECYTAMKIAEANKLKLTPEYLQLMKYKAIASNSKIY
FGKDIPNMFMDSAGSVSKQFEGLADKLSFGLEDEPLETATKEN

96 hr +/- Securinine membrane fraction 3-11NL/Spot 354/SPFH domain family member 2 isoform 1/X!Tandem P3

MAQLGAVVAVASSFFCASLFSAVHKIEEGHIGVYYRGGALLTSTSGPGFHLMLPFITSYKSVQTTLQTDEV
KNVPCGTSGGVMIYFDRIEVVNFLVPNAVYDIVKNYTADYDKALIFNKIHHELNQFCSVHTLQEVYIELFDQIDE
NLKLALQQDLTSMAPGLVIQAVRVTKPNIPEAIRRNYELMESEKTKLLIAAQKQKVVEKEAETERKKALIEAEKV
AQVAEITYGQKVMEKETEKKISEIEDAAFLAREKAKADAECYTAMKIAEANKLKLTPEYLQLMKYKAIASNSKIY
FGKDIPNMFMDSAGSVSKQFEGLADKLSFGLEDEPLETATKEN

96 hr +/- Securinine membrane fraction 4-7/Spot 11/Hsp70/Mascot

MSKGPAVGIDLGTTYSCVGVFQHGKVEIIANDQGNRTTPSYVAFTDTERLIGDAAKNQVAMNPTNTVF
DAKRLIGRRFDDAVVQSDMKHWPFMVVNDAGRPKVQVEYKGETKSFYPEEVSSMVLTKMKEIAEAYLGKTV
TNAVVTVPAYFNDSQRQATKDAGTIAGLNVLRIINEPTAAAIAYGLDKKVGAERNVLIFDLGGGTFDVSILTIED
GIFEVKSTAGDTHLGGEDFDNRMVNHFIAEFKRKHKKDISENKRAVRRLRTACERAKRTLSSSTQASIEIDSLYE
GIDFYTSITRARFEELNADLFRGTLDPVEKALRDAKLDKSQIHDIVLVGGSTRIPKIQKLLQDFFNGKELNKSINP
DEAVAYGAAVQAAILSGDKSENVQDLLLLDVTPLSLGIETAGGVMTVLIKRNTTIPTKQTQTFTTYSDNQPGVL
IQVYEGERAMTKDNNLLGKFELTGIPPAPRGVPQIEVTFDIDANGILNVSAVDKSTGKENKITITNDKGRLSKED
IERMVQEAEKYKAEDEKQRDKVSSKNSLESYAFNMKATVEDEKLQGKINDEDKQKILDKCNEIINWLDKNQT
AEKEEFEHQQKELEKVCNPIITKLYQSAGGMPGGMPGGFPGGGAPPSGGASSGPTIEEVD

96 hr +/- Securinine membrane fraction 4-7/Spot 11/Hsp70/X!Hunter

MSKGPAVGIDLGTTYSCVGVFQHGKVEIIANDQGNRTTPSYVAFTDTERLIGDAAKNQVAMNPTNTVFDAK
RLIGRRFDDAVVQSDMKHWPFMVVNDAGRPKVQVEYKGETKSFYPEEVSSMVLTKMKEIAEAYLGKTVTNA
VVTVPAYFNDSQRQATKDAGTIAGLNVLRIINEPTAAAIAYGLDKKVGAERNVLIFDLGGGTFDVSILTIEDGIFE
VKSTAGDTHLGGEDFDNRMVNHFIAEFKRKHKKDISENKRAVRRLRTACERAKRTLSSSTQASIEIDSLYEGIDF
YTSITRARFEELNADLFRGTLDPVEKALRDAKLDKSQIHDIVLVGGSTRIPKIQKLLQDFFNGKELNKSINPDEAV
AYGAAVQAAILSGDKSENVQDLLLLDVTPLSLGIETAGGVMTVLIKRNTTIPTKQTQTFTTYSDNQPGVLIQVY
EGERAMTKDNNLLGKFELTGIPPAPRGVPQIEVTFDIDANGILNVSAVDKSTGKENKITITNDKGRLSKEDIER
MVQEAEKYKAEDEKQRDKVSSKNSLESYAFNMKATVEDEKLQGKINDEDKQKILDKCNEIINWLDKNQTAEK
EEFEHQQKELEKVCNPIITKLYQSAGGMPGGMPGGFPGGGAPPSGGASSGPTIEEVD

96 hr +/- Securinine membrane fraction 4-7/Spot 11/Hsp70/X!Tandem P3

MSKGPAVGIDLGTTYSCVGVFQHGKVEIIANDQGNRTTPSYVAFTDTERLIGDAAKNQVAMNPTNTVFDAK
RLIGRRFDDAVVQSDMKHWPFMVVNDAGRPKVQVEYKGETKSFYPEEVSSMVLTKMKEIAEAYLGKTVTNA
VVTVPAYFNDSQRQATKDAGTIAGLNVLRIINEPTAAAIAYGLDKKVGAERNVLIFDLGGGTFDVSILTIEDGIFE
VKSTAGDTHLGGEDFDNRMVNHFIAEFKRKHKKDISENKRAVRRLRTACERAKRTLSSSTQASIEIDSLYEGIDF
YTSITRARFEELNADLFRGTLDPVEKALRDAKLDKSQIHDIVLVGGSTRIPKIQKLLQDFFNGKELNKSINPDEAV
AYGAAVQAAILSGDKSENVQDLLLLDVTPLSLGIETAGGVMTVLIKRNTTIPTKQTQTFTTYSDNQPGVLIQVY
EGERAMTKDNNLLGKFELTGIPPAPRGVPQIEVTFDIDANGILNVSAVDKSTGKENKITITNDKGRLSKEDIER
MVQEAEKYKAEDEKQRDKVSSKNSLESYAFNMKATVEDEKLQGKINDEDKQKILDKCNEIINWLDKNQTAEK
EEFEHQQKELEKVCNPIITKLYQSAGGMPGGMPGGFPGGGAPPSGGASSGPTIEEVD

96 hr +/- Securinine membrane fraction 4-7/Spot 12/Hsp60/Mascot

MLRLPTVFRQMRPVSRVLAPHLTRAYAKDVKFGADARALMLQGVDLLADAVAVTMGPKGRTVIIEQS
WGSPKVTKDGVTVAKSIDLKDKYKNIGAKLVQDVANNTNEEAGDGTTTATVLARSIAKEGFEKISKGANPVEI
RRGVMLAVDAVIAELKKQSKPVTTPEEIAQVATISANGDKEIGNIISDAMKKVGRKGVITVKDGKTLNDELEIIE
GMKFDRGYISPYFINTSKGQKCEFQDAYVLLSEKKISSIQSIVPALEIANAHRKPLVIIAEDVDGEALSTLVLNRLK
VGLQVVAVKAPGFGDNRKNQLKDMAIATGGAVFGEEGLTLNLEDVQPHDLGKVGEVIVTKDDAMLLKGKG
DKAQIEKRIQEIIEQLDVTTSEYEKEKLNERLAKLSDGVAVLKVGGTSDVEVNEKKDRVTDALNATRAAVEEGIV
LGGGCALLRCIPALDSLTPANEDQKIGIEIIKRTLKIPAMTIAKNAGVEGSLIVEKIMQSSSEVGYDAMAGDFVN
MVEKGIIDPTKVVRTALLDAAGVASLLTTAEVVVTEIPKEEKDPGMGAMGGMGGGMGGGMF

96 hr +/- Securinine membrane fraction 4-7/Spot 12/Hsp60/X!Hunter

MLRLPTVFRQMRPVSRVLAPHLTRAYAKDVKFGADARALMLQGVDLLADAVAVTMGPKGRTVIIEQSWGS
PKVTKDGVTVAKSIDLKDKYKNIGAKLVQDVANNTNEEAGDGTTTATVLARSIAKEGFEKISKGANPVEIRRGV
MLAVDAVIAELKKQSKPVTTPEEIAQVATISANGDKEIGNIISDAMKKVGRKGVITVKDGKTLNDELEIIEGMKF
DRGYISPYFINTSKGQKCEFQDAYVLLSEKKISSIQSIVPALEIANAHRKPLVIIAEDVDGEALSTLVLNRLKVGLQ
VVAVKAPGFGDNRKNQLKDMAIATGGAVFGEEGLTLNLEDVQPHDLGKVGEVIVTKDDAMLLKGKGDKAQI
EKRIQEIIEQLDVTTSEYEKEKLNERLAKLSDGVAVLKVGGTSDVEVNEKKDRVTDALNATRAAVEEGIVLGGG
CALLRCIPALDSLTPANEDQKIGIEIIKRTLKIPAMTIAKNAGVEGSLIVEKIMQSSSEVGYDAMAGDFVNMVEK
GIIDPTKVVRTALLDAAGVASLLTTAEVVVTEIPKEEKDPGMGAMGGMGGGMGGGMF

96 hr +/- Securinine membrane fraction 4-7/Spot 12/Hsp60/X!Tandem P3

MARGSVSDEEMMELREAFAKVDTDGNGYISFNELNDLFKAACLPLPGYRVREITENLMATGDLDQDGRISFD
EFIKIFHGLKSTDVAKTFRKAINKKEGICAIGGTSEQSSVGTQHSYSEEEKYAFVNWINKALENDPDCRHVIPMN
PNTNDLFNAVGDGIVLCKMINLSVPDTIDERTINKKKLTPFTIQENLNLALNSASAIGCHVVNIGAEDLKEGKPY
LVLGLLWQVIKIGLFADIELSRNEALIALLREGESLEDLMKLSPEELLLRWANYHLENAGCNKIGNFSTDIKDSKA
YYHLLEQVAPKGDEEGVPAVVIDMSGLREKDDIQRAECMLQQAERLGCRQFVTATDVVRGNPKLNLAFIANL
FNRYPALHKPENQDIDWGALEGETREERTFRNWMNSLGVNPRVNHLYSDLSDALVIFQLYEKIKVPVDWNR
VNKPPYPKLGGNMKKLENCNYAVELGKNQAKFSLVGIGGQDLNEGNRTLTLALIWQLMRRYTLNILEEIGGG
QKVNDDIIVNWVNETLREAEKSSSISSFKDPKISTSLPVLDLIDAIQPGSINYDLLKTENLNDDEKLNNAKYAISM
ARKIGARVYALPEDLVEVNPKMVMTVFACLMGKGMKRV

96 hr +/- Securinine membrane fraction 4-7/Spot 27/Calreticulin/Mascot

MLLSVPLLLGLLGLAVAEPAVYFKEQFLDGDGWTSRWIESKHKSDFGKFVLSSGKFYGDEEKDKGLQTSQ
DARFYALSASFEPFSNKGQTLVVQFTVKHEQNIDCGGGYVKLFPNSLDQTDMHGDSEYNIMFGPDICGPGTK
KVHVIFNYKGKNVLINKDIRCKDDEFTHLYTLIVRPDNTYEVKIDNSQVESGSLEDDWDFLPPKKIKDPDASKPE
DWDERAKIDDPTDSKPEDWDKPEHIPDPDAKKPEDWDEEMDGEWEPPVIQNPEYKGEWKPRQIDNPDYK
GTWIHPEIDNPEYSPDPSIYAYDNFGVLGLDLWQVKSGTIFDNFLITNDEAYAEEFGNETWGVTKAAEKQMK
DKQDEEQRLKEEEEDKKRKEEEEAEDKEDDEDKDEDEEDEEDKEEDEEEDVPGQAKDEL

96 hr +/- Securinine membrane fraction 4-7/Spot 27/Calreticulin/X!Hunter

MLLSVPLLLGLLGLAVAEPAVYFKEQFLDGDGWTSRWIESKHKSDFGKFVLSSGKFYGDEEKDKGLQTSQDAR
FYALSASFEPFSNKGQTLVVQFTVKHEQNIDCGGGYVKLFPNSLDQTDMHGDSEYNIMFGPDICGPGTKKVH
VIFNYKGKNVLINKDIRCKDDEFTHLYTLIVRPDNTYEVKIDNSQVESGSLEDDWDFLPPKKIKDPDASKPEDW
DERAKIDDPTDSKPEDWDKPEHIPDPDAKKPEDWDEEMDGEWEPPVIQNPEYKGEWKPRQIDNPDYKGT
WIHPEIDNPEYSPDPSIYAYDNFGVLGLDLWQVKSGTIFDNFLITNDEAYAEEFGNETWGVTKAAEKQMKDK
QDEEQRLKEEEEDKKRKEEEEAEDKEDDEDKDEDEEDEEDKEEDEEEDVPGQAKDEL

96 hr +/- Securinine membrane fraction 4-7/Spot 27/Calreticulin/X!Tandem P3

MLLSVPLLLGLLGLAVAEPAVYFKEQFLDGDGWTSRWIESKHKSDFGKFVLSSGKFYGDEEKDKGLQTSQDAR
FYALSASFEPFSNKGQTLVVQFTVKHEQNIDCGGGYVKLFPNSLDQTDMHGDSEYNIMFGPDICGPGTKKVH
VIFNYKGKNVLINKDIRCKDDEFTHLYTLIVRPDNTYEVKIDNSQVESGSLEDDWDFLPPKKIKDPDASKPEDW
DERAKIDDPTDSKPEDWDKPEHIPDPDAKKPEDWDEEMDGEWEPPVIQNPEYKGEWKPRQIDNPDYKGT
WIHPEIDNPEYSPDPSIYAYDNFGVLGLDLWQVKSGTIFDNFLITNDEAYAEEFGNETWGVTKAAEKQMKDK
QDEEQRLKEEEEDKKRKEEEEAEDKEDDEDKDEDEEDEEDKEEDEEEDVPGQAKDEL

96 hr +/- Securinine membrane fraction/Spot 39/Hsp60/Mascot

MLRLPTVFRQMRPVSRVLAPHLTRAYAKDVKFGADARALMLQGVDLLADAVAVTMGPKGRTVIIEQS
WGSPKVTKDGVTVAKSIDLKDKYKNIGAKLVQDVANNTNEEAGDGTTTATVLARSIAKEGFEKISKGANPVEI
RRGVMLAVDAVIAELKKQSKPVTTPEEIAQVATISANGDKEIGNIISDAMKKVGRKGVITVKDGKTLNDELEIIE
GMKFDRGYISPYFINTSKGQKCEFQDAYVLLSEKKISSIQSIVPALEIANAHRKPLVIIAEDVDGEALSTLVLNRLK
VGLQVVAVKAPGFGDNRKNQLKDMAIATGGAVFGEEGLTLNLEDVQPHDLGKVGEVIVTKDDAMLLKGKG
DKAQIEKRIQEIIEQLDVTTSEYEKEKLNERLAKLSDGVAVLKVGGTSDVEVNEKKDRVTDALNATRAAVEEGIV
LGGGCALLRCIPALDSLTPANEDQKIGIEIIKRTLKIPAMTIAKNAGVEGSLIVEKIMQSSSEVGYDAMAGDFVN
MVEKGIIDPTKVVRTALLDAAGVASLLTTAEVVVTEIPKEEKDPGMGAMGGMGGGMGGGMF

96 hr +/- Securinine membrane fraction/Spot 39/Hsp60/X!Hunter

MLRLPTVFRQMRPVSRVLAPHLTRAYAKDVKFGADARALMLQGVDLLADAVAVTMGPKGRTVIIEQSWGS
PKVTKDGVTVAKSIDLKDKYKNIGAKLVQDVANNTNEEAGDGTTTATVLARSIAKEGFEKISKGANPVEIRRGV
MLAVDAVIAELKKQSKPVTTPEEIAQVATISANGDKEIGNIISDAMKKVGRKGVITVKDGKTLNDELEIIEGMKF
DRGYISPYFINTSKGQKCEFQDAYVLLSEKKISSIQSIVPALEIANAHRKPLVIIAEDVDGEALSTLVLNRLKVGLQ
VVAVKAPGFGDNRKNQLKDMAIATGGAVFGEEGLTLNLEDVQPHDLGKVGEVIVTKDDAMLLKGKGDKAQI
EKRIQEIIEQLDVTTSEYEKEKLNERLAKLSDGVAVLKVGGTSDVEVNEKKDRVTDALNATRAAVEEGIVLGGG
CALLRCIPALDSLTPANEDQKIGIEIIKRTLKIPAMTIAKNAGVEGSLIVEKIMQSSSEVGYDAMAGDFVNMVEK
GIIDPTKVVRTALLDAAGVASLLTTAEVVVTEIPKEEKDPGMGAMGGMGGGMGGGMF

96 hr +/- Securinine membrane fraction/Spot 39/Hsp60/X!Tandem P3

MLRLPTVFRQMRPVSRVLAPHLTRAYAKDVKFGADARALMLQGVDLLADAVAVTMGPKGRTVIIEQSWGS
PKVTKDGVTVAKSIDLKDKYKNIGAKLVQDVANNTNEEAGDGTTTATVLARSIAKEGFEKISKGANPVEIRRGV
MLAVDAVIAELKKQSKPVTTPEEIAQVATISANGDKEIGNIISDAMKKVGRKGVITVKDGKTLNDELEIIEGMKF
DRGYISPYFINTSKGQKCEFQDAYVLLSEKKISSIQSIVPALEIANAHRKPLVIIAEDVDGEALSTLVLNRLKVGLQ
VVAVKAPGFGDNRKNQLKDMAIATGGAVFGEEGLTLNLEDVQPHDLGKVGEVIVTKDDAMLLKGKGDKAQI
EKRIQEIIEQLDVTTSEYEKEKLNERLAKLSDGVAVLKVGGTSDVEVNEKKDRVTDALNATRAAVEEGIVLGGG
CALLRCIPALDSLTPANEDQKIGIEIIKRTLKIPAMTIAKNAGVEGSLIVEKIMQSSSEVGYDAMAGDFVNMVEK
GIIDPTKVVRTALLDAAGVASLLTTAEVVVTEIPKEEKDPGMGAMGGMGGGMGGGMF

96 hr +/- Securinine membrane fraction 4-7/Spot 86/β-galactoside binding lectin precursor/Mascot

MACGLVASNLNLKPGECLRVRGEVAPDAKSFVLNLGKDSNNLCLHFNPRFNAHGDANTIVCNSKDGGAWGTEQREAVFPFQPGSVAEVCITFDQANLTVKLPDGYEFKFPNRLNLEAINYMAADGDFKIKCVAFD

96 hr +/- Securinine membrane fraction 4-7/Spot 86/β-galactoside binding lectin precursor/X!Hunter

MACGLVASNLNLKPGECLRVRGEVAPDAKSFVLNLGKDSNNLCLHFNPRFNAHGDANTIVCNSKDGGAWGTEQREAVFPFQPGSVAEVCITFDQANLTVKLPDGYEFKFPNRLNLEAINYMAADGDFKIKCVAFD

96 hr +/- Securinine membrane fraction 4-7/Spot 86/β-galactoside binding lectin precursor/X!Tandem P3

MACGLVASNLNLKPGECLRVRGEVAPDAKSFVLNLGKDSNNLCLHFNPRFNAHGDANTIVCNSKDGGAWGTEQREAVFPFQPGSVAEVCITFDQANLTVKLPDGYEFKFPNRLNLEAINYMAADGDFKIKCVAFD

96 hr +/- Securinine membrane fraction 4-7/Spot 106/NADH CoQ reductase/Mascot

MLRIPVRKALVGLSKSPKGCVRTTATAASNLIEVFVDGQSVMVEPGTTVLQACEKVGMQIPRFCYHERLS
VAGNCRMCLVEIEKAPKVVAACAMPVMKGWNILTNSEKSKKAREGVMEFLLANHPLDCPICDQGGECDLQ
DQSMMFGNDRSRFLEGKRAVEDKNIGPLVKTIMTRCIQCTRCIRFASEIAGVDDLGTTGRGNDMQVGTYIEK
MFMSELSGNIIDICPVGALTSKPYAFTAQPWETRKTESIDVMDAVGSNIVVSTRTGEVMRILPRMHEDINEE
WISDKTRFAYDGLKRQRLTEPMVRNEKGLLTYTSWEDALSRVAGMLQSFQGKDVAAIAGGLVDAEALVALK
DLLNRVDSDTLCTEEVFPTAGAGTDLRSNYLLNTTIAGVEEADVVLLVGTNPRFEAPLFNARIRKSWLHNDLKV
ALIGSPVDLTYTYDHLGDSPKILQDIASGSHPFSQVLKEAKKPMVVLGSSALQRNDGAAILAAVSSIAQKIRMTS
GVTGDWKVMNILHRIASQVAALDLGYKPGVEAIRKNPPKVLFLLGADGGCITRQDLPKDCFIIYQGHHGDVG
APIADVILPGAAYTEKSATYVNTEGRAQQTKVAVTPPGLAREDWKIIRALSEIAGMTLPYDTLDQVRNRLEEVS
PNLVRYDDIEGANYFQQANELSKLVNQQLLADPLVPPQLTIKDFYMTDSISRASQTMAKCVKAVTEGAQAVE
EPSIC

96 hr +/- Securinine membrane fraction 4-7/Spot 106/NADH CoQ reductase/X!Hunter

MLRIPVRKALVGLSKSPKGCVRTTATAASNLIEVFVDGQSVMVEPGTTVLQACEKVGMQIPRFCYHERLSVAG
NCRMCLVEIEKAPKVVAACAMPVMKGWNILTNSEKSKKAREGVMEFLLANHPLDCPICDQGGECDLQDQS
MMFGNDRSRFLEGKRAVEDKNIGPLVKTIMTRCIQCTRCIRFASEIAGVDDLGTTGRGNDMQVGTYIEKMF
MSELSGNIIDICPVGALTSKPYAFTARPWETRKTESIDVMDAVGSNIVVSTRTGEVMRILPRMHEDINEEWISD
KTRFAYDGLKRQRLTEPMVRNEKGLLTYTSWEDALSRVAGMLQSFQGKDVAAIAGGLVDAEALVALKDLLNR
VDSDTLCTEEVFPTAGAGTDLRSNYLLNTTIAGVEEADVVLLVGTNPRFEAPLFNARIRKSWLHNDLKVALIGS
PVDLTYTYDHLGDSPKILQDIASGSHPFSQVLKEAKKPMVVLGSSALQRNDGAAILAAVSSIAQKIRMTSGVTG
DWKVMNILHRIASQVAALDLGYKPGVEAIRKNPPKVLFLLGADGGCITRQDLPKDCFIIYQGHHGDVGAPIAD
VILPGAAYTEKSATYVNTEGRAQQTKVAVTPPGLAREDWKIIRALSEIAGMTLPYDTLDQVRNRLEEVSPNLVR
YDDIEGANYFQQANELSKLVNQQLLADPLVPPQLTIKDFYMTDSISRASQTMAKCVKAVTEGAQAVEEPSIC

96 hr +/- Securinine membrane fraction 4-7/Spot 106/NADH CoQ reductase/X!Tandem P3

MLRIPVRKALVGLSKSPKGCVRTTATAASNLIEVFVDGQSVMVEPGTTVLQACEKVGMQIPRFCYHERLS
VAGNCRMCLVEIEKAPKVVAACAMPVMKGWNILTNSEKSKKAREGVMEFLLANHPLDCPICDQGGECDLQ
DQSMMFGNDRSRFLEGKRAVEDKNIGPLVKTIMTRCIQCTRCIRFASEIAGVDDLGTTGRGNDMQVGTYIEK
MFMSELSGNIIDICPVGALTSKPYAFTARPWETRKTESIDVMDAVGSNIVVSTRTGEVMRILPRMHEDINEEW
ISDKTRFAYDGLKRQRLTEPMVRNEKGLLTYTSWEDALSRVAGMLQSFQGKDVAAIAGGLVDAEALVALKDL
LNRVDSDTLCTEEVFPTAGAGTDLRSNYLLNTTIAGVEEADVVLLVGTNPRFEAPLFNARIRKSWLHNDLKVAL
IGSPVDLTYTYDHLGDSPKILQDIASGSHPFSQVLKEAKKPMVVLGSSALQRNDGAAILAAVSSIAQKIRMTSG
VTGDWKVMNILHRIASQVAALDLGYKPGVEAIRKNPPKVLFLLGADGGCITRQDLPKDCFIIYQGHHGDVGA
PIADVILPGAAYTEKSATYVNTEGRAQQTKVAVTPPGLAREDWKIIRALSEIAGMTLPYDTLDQVRNRLEEVSP
NLVRYDDIEGANYFQQANELSKLVNQQLLADPLVPPQLTIKDFYMTDSISRASQTMAKCVKAVTEGAQAVEE
PSIC

APPENDIX B

NORMALIZED SPOT VOLUME DATA

NOTE: The following appendix contains the log normalized spot volume data for spots exported from Progenesis. The data has been formatted into appropriate biological replcate and test condition (control or experimental) and an indication as to whether the spot passed or failed offline analysis as described above. Pass of fail will be located either just below the first column or immediately to the right of the spot number. Each column contains data from all technical replicates within that particular condition and biological replicate.

48 hr soluble

Spot 2 Fail

Controlrep1	Controlrep2	Controlrep3	Infectrep1	Infectrep2	Infectrep3
90960.16995	45210.5623	27885.89427	219950.3411	60735.5312	502831.2781
62293.88601	68760.07381	2958.590976	201415.2359	67796.07804	56778.977
42995.97562	56437.92142	35756.53715	107493.8266	89449.08211	6924.042562
30642.6021	52357.98149	37877.83517	163930.0785	97159.24597	28266.74068
67031.60052	26526.70511	32538.45558	208101.9567	52622.6031	46080.15945
36405.0286		272344.085			

Spot 5 Fail

Controlrep1	Controlrep2	Controlrep3	Infectrep1	Infectrep2	Infectrep3
81011.57189	115464.2805	88316.42096	164084.3333	112818.5967	567451.1148
80996.52678	177536.3659	101405.9555	284117.7733	148346.39	148337.6811
69486.31716	51013.26775	55038.89511	149984.8383	75773.85948	41878.21267
54464.88897	32577.64965	22493.04316	118522.3557	77018.2131	52795.51906
82229.02421	49366.31192	66098.4762	185119.8256	104664.7512	93476.4172
208705.5693		788345.5372			

Spot 10 Pass

Controlrep1	Controlrep2	Controlrep3	Infectrep1	Infectrep2	Infectrep3
6576.810794	28597.92923	18068.99493	14993.15517	26378.57239	31171.44427
14838.83843	17807.18539	10573.85031	47131.08419	19150.8043	15933.00304
26349.93897	12182.67881	10734.88909	24291.35437	19267.40302	12288.0206
9065.472913	7661.773033	6359.659178	36378.87354	10816.93439	5589.794142
7583.784012	12414.06968	5768.55886	33428.20633	18596.89762	5868.480033
15370.41641		51146.84645			

Spot 12 Fail

Controlrep1	Controlrep2	Controlrep3	Infectrep1	Infectrep2	Infectrep3
662857.1781	1165093.826	1066759.868	810030.2295	2093247.372	1442119.58
921174.709	1077719.888	1572876.557	1286950.695	1694136.63	1692749.803
864864.5408	688184.1961	1281533.394	877216.8121	1080341.505	2401889.04
517825.195	619471.7499	949609.2319	1235268.71	1879285.047	2202727.398
919987.0885	651046.2115	1109778.074	1687304.777	1011270.821	1566448.321
794241.6162		1834762.737			

Spot 13 Fail

Controlrep1	Controlrep2	Controlrep3	Infectrep1	Infectrep2	Infectrep3
116570.7059	237879.1927	54436.65123	261328.4319	440401.7502	98939.28082
201399.1677	110602.6651	74734.3193	365179.3619	285237.2276	116819.6807
192690.2619	100624.5974	152111.7547	416982.2738	180634.1786	152042.1266
102465.4739	99634.84532	415378.673	170945.3503	220209.6364	415889.0269
215942.9879	98743.32543	102757.1198	308441.5649	147601.7539	71791.07792
112487.2666		230897.5978			

96 hr soluble

Spot 2 Pass

Controlrep1	Controlrep2	Controlrep3	Infectrep1	Infectrep2	Infectrep3
611587.5259	325124.4428	565481.264	2031615.209	1221698.812	1866484.055
276312.6549	232718.8176	543136.8167	851526.4511	796546.0302	2388767.574
334817.9191	384021.4955	527127.4206	1116637.904	1277799.604	2391435.995
305594.5708	268861.0828	397614.8593	1682843.337	1112198.365	817849.0592
728119.0239	315524.5588	404965.254	4198160.951	1545471.642	1292233.404
255306.6622	258472.8291	317984.5377	926010.9715	1551942.983	1601058.204

Spot 5 Pass

Controlrep1	Controlrep2	Controlrep3	Infectrep1	Infectrep2	Infectrep3
280304.9268	306197.5465	625318.8236	1092222.052	1764853.205	1275113.411
471402.0895	727856.2743	543046.0899	1244075.476	2187108.286	1264469.058
239830.652	346349.1804	308129.2279	919450.6142	1729786.328	962406.5609
398354.9362	433413.0539	511103.5062	829729.3719	1576322.486	1255515.614
346710.6423	298274.338	438511.1937	763778.4151	1481004.226	983159.7285
483555.0759	167414.7918	568954.2984	722303.6965	882026.3423	1418783.963

Spot 9 Pass

Controlrep1	Controlrep2	Controlrep3	Infectrep1	Infectrep2	Infectrep3
231363.8488	195044.208	389821.7999	763045.0016	601725.6212	1018482.706
127809.498	198864.2092	411709.4589	303927.1427	432038.1901	1038211.101
211916.3871	149708.7999	499386.1619	462571.2876	580839.9743	1217546.956
133679.8059	119820.1158	264652.6052	560828.6184	597778.3135	575126.2479
278544.7697	101334.948	153301.4982	745275.3778	411023.9895	194386.9659
183947.153	140823.2087	110110.6874	401838.7109	396653.228	236568.3484

Spot 12 Fail

Controlrep1	Controlrep2	Controlrep3	Infectrep1	Infectrep2	Infectrep3
30973.58017	36720.25651	142113.296	37117.03441	232748.8545	386213.8193
7587.313338	56562.5869	95755.94145	22114.98755	314733.4095	258857.1562
25791.48407	89360.77424	135215.8198	78722.04499	415794.8276	393410.7434
2527.140132	96371.8224	160080.344	47935.4774	225297.8748	257755.6015
9480.098452	93141.5575	256067.2268	42795.65269	279372.0138	358223.8196
7467.852439	81757.72798	144098.3144	56888.6829	273321.5111	229443.2138

Spot 13 Fail

Controlrep1	Controlrep2	Controlrep3	Infectrep1	Infectrep2	Infectrep3
68929.11847	93123.38785	1465237.997	337412.6856	732965.6947	1288738.418
107220.5271	74248.30387	58718.38533	370657.8796	800644.533	597147.4681
101103.0762	116874.898	70475.83957	382906.195	592214.0398	544641.8596
156327.9221	187990.1488	115369.9268	331178.2498	432559.1144	246887.0355
106196.4947	61163.53265	74416.82734	92516.9016	474941.8703	249813.3961
127935.9991	78861.74867	106541.7577	229801.0207	352513.8523	305860.8074

Spot 14 Pass

Controlrep1	Controlrep2	Controlrep3	Infectrep1	Infectrep2	Infectrep3
359427.4097	519382.9257	715881.1561	837921.6701	539688.468	3757318.129
328378.398	431108.7407	435385.8095	1117138.372	420249.6378	2103993.316
568479.2482	535838.4745	171939.8292	2187248.765	510582.705	503818.9664
295811.6544	353199.5429	246427.0851	493641.683	930239.5147	370221.0528
394888.5056	508429.0288	126475.1797	819511.2896	1201013.508	328462.7044
359309.224	350266.3407	253794.8384	857819.2399	778358.5687	389585.3349

Spot 16 Fail

Controlrep1	Controlrep2	Controlrep3	Infectrep1	Infectrep2	Infectrep3
21215.95076	73583.36245	143238.8257	61657.97491	224926.4368	282275.5982
36378.69148	90704.3798	139095.749	76553.04699	406378.4796	332885.3814
64634.45658	117627.4978	186798.8223	98220.29324	532380.9481	453675.7919
19663.03494	155466.5063	153975.2904	53054.31935	330370.3297	149273.1018
35489.07153	114865.6303	217466.2725	55223.95131	396644.166	420284.4545
37338.16149	156035.5671	198856.7292	60351.02041	417411.8391	350036.8861

Spot 17 Fail

Controlrep1	Controlrep2	Controlrep3	Infectrep1	Infectrep2	Infectrep3
47225.8805	54871.63743	27431.87682	17223.69313	11512.52628	9616.25173
31284.22783	35026.50747	6713.396722	6861.2047	7816.429197	7667.590238
38671.76328	38944.68588	19706.97876	17037.77238	17839.08011	6246.898165
23229.2362	76382.6474	20206.68994	18962.27284	12876.40463	4891.875418
49315.08644	110820.6819	21915.10313	38019.38466	25239.39456	5556.062085
79144.68142	116994.6819	41107.53313	58280.66609	71687.43478	14778.71087

Spot 18 Fail

Controlrep1	Controlrep2	Controlrep3	Infectrep1	Infectrep2	Infectrep3
660996.3351	455483.7887	297018.4608	243060.9163	167872.4883	116727.0299
322184.3806	649233.9622	219257.0602	134073.2502	182924.6404	81178.0794
657290.2594	582304.2454	305794.9928	279998.3772	244235.7902	123783.23
510091.7389	1025382.367	308705.4761	288939.6574	392719.1152	141578.6133
528665.885	1422866.974	305455.0888	302796.4139	446665.4124	142512.6806
943314.2843	550143.8698	371348.219	615187.3882	180558.0139	177083.1354

Spot 29 Fail

Controlrep1	Controlrep2	Controlrep3	Infectrep1	Infectrep2	Infectrep3
917077.124	634434.9147	386197.2816	324754.132	117003.061	191266.4775
452953.8869	739307.9531	109583.679	96390.42757	124314.1834	131379.9935
839985.6226	667768.9895	187687.3843	282406.3664	131003.3792	92698.27989
426473.4455	535025.2297	505247.2057	164899.188	425573.1175	404027.5523
505808.8649	734806.5811	242409.6066	443455.8208	465897.504	239410.7945
339111.0593	407253.6125	397255.0276	145772.6963	288064.3143	324578.1084

Spot 46 Fail

Controlrep1	Controlrep2	Controlrep3	Infectrep1	Infectrep2	Infectrep3
295546.3931	87741.62322	65304.63189	469914.2528	304957.773	132962.8075
258173.4581	100243.4567	167237.5318	397932.2162	299316.0561	361096.0101
326359.5137	113101.4293	150904.7393	535423.6894	361014.0047	332815.8459
339623.0091	93270.13331	264354.4133	459821.0945	226383.7382	324320.2505
327356.2853	86478.01424	167474.7624	419594.8272	233575.5983	213141.1626
367033.6333	218512.8722	188984.4162	462963.5557	360295.7955	278896.6716

Spot 48 Pass

Controlrep1	Controlrep2	Controlrep3	Infectrep1	Infectrep2	Infectrep3
232531.4386	244001.5224	252086.6153	352317.0249	322549.2956	244441.8207
105250.2786	194467.3878	180660.9905	176398.6001	340127.0261	191371.9467
159286.0062	175300.7773	189811.3436	327660.3016	252757.1755	240648.6461
212564.3283	267093.7667	182504.3993	502689.0967	552895.7363	312530.5377
377039.9437	303084.3927	144281.6656	514285.5109	704963.9129	219262.4168
144607.3976	112729.4853	261940.8347	328351.8892	253256.3219	474989.6442

Spot 50 Fail

Controlrep1	Controlrep2	Controlrep3	Infectrep1	Infectrep2	Infectrep3
244422.899	207378.8433	171752.7998	250199.9783	101431.6955	52471.31418
181125.7068	337914.2425	107064.9796	134371.9957	198650.1111	105957.4282
144313.6442	268003.5341	211085.8377	140040.4197	143510.5997	88539.44645
230034.7093	341345.1943	246283.7965	158035.8527	115574.0893	149038.8538
196696.6501	489477.0065	288203.1121	172879.3605	196307.0814	173914.5861
309235.7205	222211.6791	233491.9812	208612.6781	81495.40933	158661.5066

Spot 53 Fail

Controlrep1	Controlrep2	Controlrep3	Infectrep1	Infectrep2	Infectrep3
228377.2914	460043.5576	355875.1045	133611.5869	307628.3447	256845.3051
202550.7436	447388.9422	271340.55	123389.3261	308923.5105	241359.4824
306171.063	395664.5243	244972.3498	153570.0456	218321.8957	177335.904
292452.2193	408974.0565	377962.3855	115986.3097	256854.6208	214601.7021
250308.512	706418.4175	241340.9129	86898.61866	460221.8118	143000.676
360746.747	540598.8001	370783.541	124318.101	342883.8887	208304.2038

Spot 60 Pass

Controlrep1	Controlrep2	Controlrep3	Infectrep1	Infectrep2	Infectrep3
497488.4839	898231.7594	479057.1789	746357.5002	1337990.526	682065.9166
254908.1887	361674.7365	550667.7836	665694.3124	509387.1535	830393.6892
332250.8142	387799.5591	867675.2809	801651.1243	624754.2073	1256457.442
390922.7869	411585.5497	378720.2559	869251.9034	658851.7487	432966.7266
415495.905	406247.4659	807772.0087	1001630.476	577987.1857	1103357.657
462715.0944	554712.6494	706957.9279	917559.5739	855233.2556	1026146.241

Spot 63 Pass

Controlrep1	Controlrep2	Controlrep3	Infectrep1	Infectrep2	Infectrep3
368583.5605	590553.0568	376065.9782	504331.4537	814838.513	516646.5943
331198.3507	547259.4716	434356.7898	424902.5456	708600.5259	586398.4135
400347.4194	420467.1643	438408.5	553063.5431	605096.5943	632820.5643
270522.2235	298718.8332	472611.0186	623356.8755	647671.997	874899.0137
548903.4876	312482.0516	166759.7949	711104.2466	678126.4599	298992.2875
304821.8032	386187.7975	453551.6255	651816.1072	836857.1624	877630.2038

Spot 69 Pass

Controlrep1	Controlrep2	Controlrep3	Infectrep1	Infectrep2	Infectrep3
126923.4235	98821.57291	89526.52428	172576.0851	150043.3366	44582.62557
106081.2456	100593.8566	193087.8041	176074.5846	146732.8481	144059.9888
99685.67516	233644.9522	267397.009	268397.6099	328577.9058	233774.6484
111253.4275	132500.5701	141890.9927	238459.8232	276838.5652	236436.1219
137858.9615	139461.3781	199277.2902	257934.2863	331041.2643	312392.8087
137158.1257	143281.1506	225815.3526	251494.694	343881.0463	386831.9632

Spot 70 Fail

Controlrep1	Controlrep2	Controlrep3	Infectrep1	Infectrep2	Infectrep3
42402.1011	72169.78587	150339.1302	115148.3087	112274.9931	185690.1228
20158.70542	69059.5573	119074.7761	83570.12446	133112.3127	174924.4656
40000.12962	75551.27081	115305.2881	91712.26129	165501.7587	133291.9078
66018.29888	149799.5222	141121.4179	159443.1047	181108.073	225963.4725
139896.0644	189181.1813	89467.26786	148519.4074	318364.5523	138775.9771
89496.89516	50371.8461	131101.1778	101394.6247	129992.6545	202570.1733

Spot 82 Fail

Controlrep1	Controlrep2	Controlrep3	Infectrep1	Infectrep2	Infectrep3
123090.6225	117647.4198	95928.50803	203647.3209	204986.1464	162281.9486
107308.3029	77009.4223	84264.6886	163449.1007	143153.6929	129004.2159
129468.681	112312.9762	55653.71433	194299.9262	213119.6832	88393.70909
82300.62	39461.63677	63384.04595	141986.5658	67421.23338	92746.26646
92191.97823	75396.36869	27895.61745	140585.6931	131337.4423	37492.97278
214933.0749	57772.96633	55712.95785	219640.1596	86451.38761	84137.72875

Spot 85 Fail

Controlrep1	Controlrep2	Controlrep3	Infectrep1	Infectrep2	Infectrep3
57242.25933	81760.14165	160007.5836	62538.43864	47767.08163	104162.417
37279.41184	77321.47442	86109.78054	47586.69114	51924.22665	77256.85302
44879.69504	68477.4297	52998.88403	43247.89979	38153.09972	36923.36696
50007.27037	177029.5367	65258.2808	24697.56624	87669.95892	41786.73291
62485.61286	87378.85377	105612.0766	33118.48123	49801.99402	65055.79893
44495.05721	90184.36997	121126.9017	20910.71581	41401.41739	79963.95238

Spot 87 Pass

Controlrep1	Controlrep2	Controlrep3	Infectrep1	Infectrep2	Infectrep3
381002.3997	251022.2891	213154.8927	742866.1035	501496.5119	333794.7151
300344.8284	206057.0227	277617.3643	611973.1649	428642.7762	525784.1407
233763.1228	293547.2908	195909.4985	516690.0087	528870.144	404701.7314
555591.1924	347238.9633	517975.6665	650355.5752	492228.0057	695001.075
468631.7496	282094.0723	307357.2148	497376.3459	481027.7357	336067.5678
303847.6066	220483.3118	371541.3682	278718.6182	345593.058	428657.058

Spot 88 Fail

Controlrep1	Controlrep2	Controlrep3	Infectrep1	Infectrep2	Infectrep3
152769.9791	49420.34612	55630.03462	252961.0962	145832.6865	92608.67278
112800.7611	58587.80548	103595.8356	168340.1255	115228.444	201922.5887
199735.647	66406.76752	70382.68656	300274.0444	154265.1649	131540.7816
156642.5506	63148.77366	139018.6461	219418.6251	90638.67394	164577.1796
109170.1045	83588.6333	114962.7754	145876.1361	138597.0978	130570.1898
182501.6618	135176.1201	110842.0389	221050.1276	176529.0094	148723.5029

Spot 94 Fail

Controlrep1	Controlrep2	Controlrep3	Infectrep1	Infectrep2	Infectrep3
267763.9506	172539.2211	120828.1892	102697.0494	117383.8904	74740.63436
209181.8431	181675.8911	138646.779	98383.36593	97269.55352	102870.4581
215905.8899	142277.2018	92285.36517	101075.923	119009.5554	108272.8927
318949.7704	178526.5817	169730.6985	137305.3194	159183.4308	142499.2337
386879.2313	172418.1746	153565.335	201499.4225	152714.475	163893.7698
368036.6311	154997.2451	179222.0216	178499.1635	166921.7905	187314.3073

Spot 98 Fail

Controlrep1	Controlrep2	Controlrep3	Infectrep1	Infectrep2	Infectrep3
122365.6184	187120.2598	104005.4027	246211.6368	387920.7352	189274.4077
123155.9562	196554.9232	234542.4112	226865.7295	393490.0536	338300.2895
72195.3919	169097.8079	161513.4324	180971.446	271111.3353	213995.2641
227133.5275	165257.4218	182724.8937	252407.5626	296479.0767	208180.8589
179795.0056	113682.9572	229800.821	186692.3898	229555.409	219883.3603
167662.6399	204134.4029	198109.1262	178262.1658	304309.9981	212195.5793

Spot 99 Fail

Controlrep1	Controlrep2	Controlrep3	Infectrep1	Infectrep2	Infectrep3
68861.65701	75150.90644	46270.11418	120912.7731	120647.2187	67802.56009
61879.45687	87556.40648	60087.87261	123615.8521	148842.1782	97007.82316
75959.82184	106930.6534	41464.66575	144839.0559	140806.2286	84125.55148
61724.6146	133186.618	58613.01056	95065.81799	153625.6821	73878.0826
98821.92091	76322.86881	49985.14439	134261.3314	127313.102	67564.83692
107146.7685	80520.04749	92968.92117	125224.4715	130817.1248	102296.0634

Spot 102 Pass

Controlrep1	Controlrep2	Controlrep3	Infectrep1	Infectrep2	Infectrep3
255232.1421	200858.4496	295476.1343	376308.0506	337543.685	411671.7607
239997.4161	214539.0762	225337.1991	348061.1861	331411.102	365652.5513
174533.4385	360170.4305	191508.1771	278898.6978	567390.7234	275699.969
318255.2918	334368.0819	260334.0256	390425.9863	611733.7293	327991.15
295633.5151	342489.1534	242142.0321	386313.1348	645120.0476	308953.3549
291575.688	213983.2425	426601.7661	350099.5547	337889.4521	567880.1327

Spot 119 Fail

Controlrep1	Controlrep2	Controlrep3	Infectrep1	Infectrep2	Infectrep3
137311.5735	88846.84072	93732.79813	242899.3081	190817.3459	158123.6282
119577.5293	128129.2048	72249.50323	231299.7167	285701.3787	175208.0983
124371.9008	135130.5745	94176.99991	259960.5236	297049.5278	194603.3586
230378.8995	194486.385	193415.1039	299499.3896	270112.9194	207517.9999
213513.2513	233368.4719	133697.3675	132985.8501	361699.2579	82383.10428
186983.2595	90081.53982	230173.6568	144036.4712	160117.0463	170745.9403

Spot 126 Pass

Controlrep1	Controlrep2	Controlrep3	Infectrep1	Infectrep2	Infectrep3
325223.1732	256747.0777	356435.9469	476919.9462	403572.7067	505225.5384
258803.4481	279465.7845	319689.0643	452469.5333	418134.9663	450652.2321
201674.6801	340610.0335	189316.0001	341557.0665	473340.3925	271813.0185
346084.4047	354758.6507	289446.5411	467384.6686	534597.0483	345155.4837
341796.0192	399161.9728	283785.1038	361884.348	697569.7104	335411.7527
366215.3519	251187.0399	296796.9918	352774.8023	356284.272	427970.038

Spot 131	Fail				
Controlrep1	Controlrep2	Controlrep3	Infectrep1	Infectrep2	Infectrep3
126690.8549	156235.1337	102026.2186	211489.3293	268386.4899	158619.532
105773.8702	173494.1858	160652.3121	282601.4351	277246.041	205939.8539
111672.9425	216387.5381	118838.1268	321790.1966	300564.8639	223415.531
116322.2396	254552.3074	158293.4945	122569.9868	244047.1874	116970.556
93280.49366	203700.8121	159306.4154	133671.1709	226446.2712	155663.1261
122259.443	239392.2635	123300.6659	152411.1847	268495.1072	125547.6511

Spot 140	Fail				
Controlrep1	Controlrep2	Controlrep3	Infectrep1	Infectrep2	Infectrep3
1505917.401	1536047.635	2266018.82	1191283.665	1152771.521	1811874.514
1464370.969	1850038.134	1775037.241	1299633.764	1323756.171	1745417.613
1218819.961	1784195.213	1365340.349	1168328.306	1277685.692	1289847.098
2635711.511	1826357.367	2108666.069	1485311.23	1076942.115	2012632.287
2237379.278	2050890.363	2217174.274	1339925.347	1189996.536	1569459.641
1878948.182	1283135.504	2483320.003	1064412.261	754764.8798	1872640.722

Spot 144	Pass				
Controlrep1	Controlrep2	Controlrep3	Infectrep1	Infectrep2	Infectrep3
164978.9136	149209.5553	108241.6961	172033.6203	181693.4557	168424.9335
92520.14068	180900.4375	158579.6714	125655.5299	176060.6394	215663.656
209536.8535	121607.6018	144663.4908	253598.7278	145165.0612	190039.5431
106273.42	118533.5371	126027.0353	158821.0835	198457.9335	168903.8885
126429.671	113209.6101	101930.0395	149563.3682	201897.8144	116305.4474
129456.4079	139306.0746	152908.612	198797.2679	227340.8585	228795.4099

Spot 147	Fail				
Controlrep1	Controlrep2	Controlrep3	Infectrep1	Infectrep2	Infectrep3
179748.327	137246.7816	83619.88501	240713.223	228530.2205	112797.5507
212613.4051	117212.3575	108781.0187	313257.438	214210.1322	130736.3811
168364.6125	107876.7367	139540.7399	240006.0942	188800.444	189769.5564
147453.944	161535.6969	108884.5883	200151.6108	182320.4233	120347.251
204524.9952	135091.8115	131350.0782	271315.6529	191977.1593	148502.6878
236312.8053	162973.8514	138800.2484	262116.5045	212442.2005	133147.6373

Spot 148	Fail				
Controlrep1	Controlrep2	Controlrep3	Infectrep1	Infectrep2	Infectrep3
1335869.432	1071094.653	1207061.295	1736100.973	1505439.714	1384524.319
1355575.568	1073296.294	870818.4439	1725749.313	1423295.579	996702.8524
1959000.993	932734.2671	823283.924	2637963.802	1322664.768	1000270.587
1630279.175	730592.3437	1085594.743	2068750.415	1092549.714	1477051.632
1514525.179	1090909.683	806320.7552	2032186.268	1828883.479	1079486.119
1497651.121	836667.9414	1069938.005	1691680.829	1412100.478	1401994.952

Spot 149 Fail

Controlrep1	Controlrep2	Controlrep3	Infectrep1	Infectrep2	Infectrep3
1625055.132	2371500.38	1587113.698	1459299.365	1852402.402	1430232.917
1474190.474	2674130.925	1745189.39	1437269.902	2105415.101	1514634.604
1344025.113	2480571.374	1267676.643	1322361.108	1900621.446	1298447.482
2214913.107	2721483.645	2405690.773	1474041.608	1798922.952	1799816.872
1594349.44	3153890.875	1856090.579	1040531.261	1982792.837	1245472.418
1361046.557	1801748.058	3054599.089	769425.0257	1174147.885	2016914.332

Spot 153 Fail

Controlrep1	Controlrep2	Controlrep3	Infectrep1	Infectrep2	Infectrep3
880544.6597	561905.9268	392752.2763	549134.6438	426043.5133	313232.7406
528737.5462	532757.9148	392308.6642	405818.9979	434260.1803	377870.76
628737.0583	508916.9455	330488.5778	418905.3861	362907.1497	336856.314
763240.1213	401238.0659	425056.9705	574493.7219	371653.888	391081.9541
664790.9966	900844.8966	471772.988	471253.5568	598581.3519	338035.8426
608801.4551	373159.7935	496492.9087	438597.022	275900.3381	400044.4541

96 hr membrane

Spot 1 Fail

Controlrep1	Controlrep2	Controlrep3	96hrinfectrep1	96hrinfectrep2	96hrinfectrp3
58712.95687	42346.10866	35533.36747	423895.2258	324820.3359	142203.3217
180068.8828	22101.41251	118167.3811	589818.5968	458799.1102	195304.447
66493.3702	44424.08716	65205.66568	338412.4793	341166.1433	168815.4059
39675.03791	51010.86695	94910.02082	360922.2366	226903.4671	92595.88566
47854.52142	25602.60392	54434.98477	264897.8848	150947.8816	51831.78211
133640.1509	40924.57749	54905.69384	533994.3079	188879.316	70988.98851

Spot 2 Fail

Controlrep1	Controlrep2	Controlrep3	96hrinfectrep1	96hrinfectrep2	96hrinfectp3
594820.6952	689316.5659	1005154.724	3898308.781	4939791.52	2141226.678
509350.6454	761547.9569	994333.0436	4568380.024	6265670.988	1936549.522
498217.4511	1402346.641	915233.8211	4292134.537	5466397.246	2092858.366
539212.5401	857157.549	1648218.297	3339575.791	4667556.13	1901230.322
495076.8798	923338.7251	1045437.788	3031939.106	3787810.154	1323369.846
796972.4313	1318308.538	1275705.356	5444748.421	4499061.595	1209599.613

Spot 3 Fail

Controlrep1	Controlrep2	Controlrep3	96hrinfectrep1	96hrinfectrep2	96hrinfectp3
895631.7252	190030.9491	171701.9173	2017098.232	715810.4706	231735.0152
550411.9152	172554.2103	171917.9648	1580769.496	1213462.606	202617.8358
345578.5291	269107.1182	275529.6264	1777765.289	1691750.803	293106.9209
147430.4635	178533.6682	194779.8085	1056424.491	924468.8041	274731.9078
443609.8272	241656.7763	82998.13404	2116852.003	872767.2774	80994.85196
206952.6446	214804.3124	508452.6276	1524970.505	841561.6081	932165.0634

Spot 4 Fail

Controlrep1	Controlrep2	Controlrep3	96hrinfectrep1	96hrinfectrep2	96hrinfectrp3
80397.2549	17826.9211	23173.31176	334216.8071	253009.2871	147014.5144
142781.8226	23424.26066	120787.32	458061.4944	310099.9682	140452.5627
112616.7232	77733.94059	43543.80195	301959.5488	288951.0993	206263.2116
49207.07082	28243.99749	93145.52428	278158.4795	176166.2599	90754.64935
35986.49666	29383.94861	66373.24335	197526.2412	185130.5222	63637.94539
66735.1575	88518.37982	67517.79309	295470.6736	205247.6013	51613.08759

Spot 5 Fail

Controlrep1	Controlrep2	Controlrep3	96hrinfectrep1	96hrinfectrep2	96hrinfectrp3
178501.8621	124831.9776	214711.1486	883420.8934	704960.5994	431959.1448
234915.8171	162774.6009	122329.8414	930437.1355	1018149.647	205293.1286
195368.6701	408198.5028	437578.9023	1209087.158	1296481	631287.1627
239044.0722	213049.3763	232148.1283	554583.5543	851503.2897	369706.3265
156830.0232	201344.565	208805.1779	996721.3763	870671.0605	365066.587
298726.2077	223197.5687	184077.4062	566744.5459	966428.0195	187541.7942

Spot 6 Pass

Controlrep1	Controlrep2	Controlrep3	96hrinfectrep1	96hrinfectrep2	96hrinfectrp3
3095207.92	2151852.957	2882944.687	8316022.079	8278885.269	6325595.193
2516068.878	1992986.61	1606923.622	7978026.852	7040813.723	3587819.525
2540655.03	2516346.186	2726445.266	8724130.364	8486948.012	5400028.811
1637578.349	1657907.592	1132318.77	5198569.957	5255089.573	4170746.095
1742674.062	1866521.576	835650.3989	7268538.821	5713376.5	2724505.738
1870301.746	2006424.961	1295999.214	5518385.794	6283910.258	4341897.013

Spot 7 Fail

Controlrep1	Controlrep2	Controlrep3	96hrinfectrep1	96hrinfectrep2	96hrinfectrp3
248753.235	117098.7306	95960.56519	605819.7506	542432.7209	120869.9691
140348.8089	160197.4236	119136.2238	410700.4005	534688.6104	156129.0479
201719.8798	89699.0676	88820.99146	551480.9788	456185.9333	138153.7543
193902.5785	190865.9808	153369.1811	547358.2276	436888.0943	170698.3881
166652.0282	167996.9912	61031.28004	387859.0178	396762.0514	96603.14307
202765.9081	201757.5231	130869.3913	482058.3793	427412.6969	74006.91325

Spot 8 Pass

Controlrep1	Controlrep2	Controlrep3	96hrinfectrep1	96hrinfectrep2	96hrinfectrp3
268062.9775	180001.7211	343671.9429	547381.908	371471.5332	498021.9387
193300.4574	162515.163	189625.2218	562004.6853	387196.7056	450590.3406
145341.0349	353821.2175	260072.5395	538939.0956	474513.4648	440724.8399
58900.58327	73542.33478	175387.4537	224587.7545	218286.1218	509783.0891
184378.2231	65051.10297	165948.9234	502484.2025	212523.9962	470426.9994
90883.26256	101714.5817	115126.9607	313574.8693	273620.2676	477198.403

Spot 9 Pass

Controlrep1	Controlrep2	Controlrep3	96hrinfectrep1	96hrinfectrep2	96hrinfectrp3
152711.066	156043.3368	262264.8321	682294.0515	328454.7966	587321.8722
140274.3312	176726.0978	137994.3301	558963.2871	494017.8233	315824.4968
196410.6614	134951.4459	282014.75	682684.1007	429373.829	679980.1751
160872.1462	125492.8765	269694.4032	167852.2794	267631.5368	467300.3628
84737.39032	145073.1086	199068.3225	372858.149	257912.2426	421712.6168
469780.4134	131833.3752	153058.0582	541352.62	257521.1192	428329.2157

Spot 10 Pass

Controlrep1	Controlrep2	Controlrep3	96hrinfectrep1	96hrinfectrep2	96hrinfectrp3
734856.0804	817301.9936	1312912.801	1655062.225	1901301.29	2261947.07
959205.1362	940510.1533	820276.7314	1884502.18	2413405.359	1535484.281
1015821.265	831658.9337	1016624.685	2212762.309	2323501.581	1889601.448
436752.4543	538870.1704	384805.9008	1312545.885	1606845.195	1203539.059
458495.1774	685905.6152	848374.9874	1855215.003	1866909.691	1406255.602
800538.5194	601077.8548	517018.816	1255150.638	1805324.353	1736381.234

Spot 11 Fail

Controlrep1	Controlrep2	Controlrep3	96hrinfectrep1	96hrinfectrep2	96hrinfectrp3
111752.3248	193743.1473	194655.0746	563820.6032	697197.6186	215341.1473
210640.1773	158212.2885	385104.1553	936687.179	896279.5295	294961.4751
222687.5699	171189.3894	213556.9323	1207932.3	705950.4884	163532.4094
151247.1576	142111.048	294051.4114	148031.7448	528204.145	266440.2442
226537.1253	216314.9851	232509.0969	832228.201	496588.5086	270833.1911
587349.7633	111059.2116	234967.8061	300921.1963	317005.1852	261004.3664

Spot 13 Fail

Controlrep1	Controlrep2	Controlrep3	96hrinfectrep1	96hrinfectrep2	96hrinfectrp3
407729.7168	122714.1034	107824.0654	715766.7082	366094.5245	311019.631
169353.5826	113873.5072	95845.93226	372496.3954	349374.9451	299832.6086
395650.0269	88508.92853	78837.4664	1024636.168	291344.0993	363827.3701
396621.4005	155591.8731	109641.1117	746096.0463	274991.3817	147152.7653
237805.6137	132179.6294	75870.44012	464971.7026	192545.4747	80589.62042
273728.7874	96095.27515	183520.6488	484979.176	160743.9153	190917.6555

Spot 14 Fail

Controlrep1	Controlrep2	Controlrep3	96hrinfectrep1	96hrinfectrep2	96hrinfectrp3
471839.3583	477781.1261	1145476.399	1162358.823	2022480.384	1924171.932
556129.1125	621738.5997	778298.7267	1209571.044	2508558.886	1531886.087
582558.7561	788992.6245	920836.6884	1465269.939	2196099.731	1961380.132
392650.7217	750576.7291	1547939.461	1065516.035	1874198.554	2021064.28
309777.2215	698250.7947	1268966.195	1139212.312	1515581.422	1625442.47
650562.7005	861054.5882	1397976.071	1561363.772	1485230.41	1485269.62

Spot 15 Fail

Controlrep1	Controlrep2	Controlrep3	96hrinfectrep1	96hrinfectrep2	96hrinfectrp3
269324.0875	146985.404	142650.9494	609888.4353	449135.0421	392776.7311
316100.0555	214925.1861	161948.5208	798281.1401	589294.8402	223030.2043
316745.265	148530.9737	165418.6814	790860.4638	344691.6556	517055.1753
354088.1101	242249.4914	229384.7419	789757.1052	391084.8212	301916.3001
211293.3895	219447.7966	240295.3019	531381.7307	328925.2412	272689.6249
337479.2382	205405.9684	317187.4883	662093.9207	281005.2567	359427.7766

Spot 16 Fail

Controlrep1	Controlrep2	Controlrep3	96hrinfectrep1	96hrinfectrep2	96hrinfectrp3
145808.4907	30525.96437	119626.2285	439245.3297	206026.3792	261832.0262
184131.4742	105486.2397	160514.5084	504507.829	361132.1607	258378.9398
152779.0494	109938.1676	134482.2997	338297.605	188331.1071	242179.0762
54960.66824	45712.31807	192724.6147	56153.225	155537.8772	106592.7352
86547.9843	66864.26339	79598.98377	221278.0344	157350.8101	56141.0673
121424.7554	65017.97636	198331.6264	226632.1503	252887.9374	86852.69815

Spot 17 Fail

Controlrep1	Controlrep2	Controlrep3	96hrinfectrep1	96hrinfectrep2	96hrinfectrp3
607779.084	282887.8383	138627.4363	321095.3066	186856.632	160415.9851
823605.8181	543063.7169	268469.002	271074.4208	291706.4692	123809.6107
1123055.015	332288.2068	99704.27129	480652.428	170731.9628	79285.9201
550316.5123	388109.7164	186298.0904	246259.9771	217505.5101	131727.8481
1269520.779	317049.6425	255755.162	556743.0815	206056.8442	206474.8263
464399.2698	183825.2141	262158.976	225845.3133	105802.604	71966.90411

Spot 18 Pass

Controlrep1	Controlrep2	Controlrep3	96hrinfectrep1	96hrinfectrep2	96hrinfectrp3
973436.2016	958793.3785	692943.7924	1788543.221	1105351.939	1146993.578
547271.0556	450553.6755	448234.2858	946873.3182	958807.0212	771307.3748
930437.8274	928350.0591	675677.7552	1226743.411	1628683.208	962202.3258
565401.2504	621428.7879	349095.9028	1312151.086	1445627.13	1254034.669
383890.1952	980649.2639	390028.1669	1159769.135	1703400.067	1096179.227
458906.1433	368918.6988	438120.9079	859063.7773	1224473.318	1246271.932

Spot 20 Pass

Controlrep1	Controlrep2	Controlrep3	96hrinfectrep1	96hrinfectrep2	96hrinfectrp3
542848.8057	588962.1649	1002712.119	1374405.163	1249748.825	1093092.594
939060.6023	698936.5473	736896.6684	1592882.772	1408413.34	762824.1723
688259.3901	978132.8443	1343599.94	1919796.329	1423339.358	1991089.049
314416.3793	422927.6796	814310.4766	939641.8042	1144171.299	1385006.637
720201.7847	609522.1169	832047.6623	1887840.087	1443196.226	1326398.139
316905.3238	665150.3117	584381.073	1175855.388	1606621.128	701752.1438

Spot 22 Fail

Controlrep1	Controlrep2	Controlrep3	96hrinfectrep1	96hrinfectrep2	96hrinfectrp3
122892.8831	69200.88535	68258.45059	355610.5312	149195.0918	96786.46166
279714.8202	105953.4573	133069.9557	657391.8062	365894.5804	218075.087
70941.69683	107621.4128	117720.6936	196002.3737	177556.3913	206680.811
84707.05342	124654.4546	83396.93476	186911.5472	238076.6091	92779.11119
147818.4437	110724.771	101406.3081	249463.2982	199763.8543	93036.94859
378244.1785	57903.85916	105144.8871	594150.2408	112829.3217	62809.05677

Spot 25 Fail

Controlrep1	Controlrep2	Controlrep3	96hrinfectrep1	96hrinfectrep2	96hrinfectrp3
355246.3962	69328.65504	152376.914	457852.6235	262419.0188	182863.9147
89949.35882	96406.04116	69510.87227	221459.4794	172490.3158	130184.2724
83741.35532	30253.471	68101.35337	233873.2848	204012.6324	129566.1268
123614.2532	87396.55828	113798.0005	170024.5673	157859.9491	104677.0816
69087.73204	86886.29172	56081.64984	76400.23023	125353.6197	41645.15291
77466.63109	103337.2695	127028.6602	124713.9857	149645.2443	122446.541

Spot 26 Fail

Controlrep1	Controlrep2	Controlrep3	96hrinfectrep1	96hrinfectrep2	96hrinfectrp3
65492.31704	55765.00425	224772.1788	108721.5585	197342.1018	218299.888
145872.0277	121980.9735	196916.6386	275042.8589	253250.8192	216929.8452
64949.91344	91863.07846	263632.5646	191890.7651	216248.1272	284257.5582
93625.06434	92463.95203	89436.2863	187508.5662	226629.4642	79510.29719
127419.779	55120.10184	106297.8072	167069.5064	125118.001	112160.8608
69400.90204	61282.04276	244633.0421	186815.4181	155802.4588	298619.6404

Spot 28 Pass

Controlrep1	Controlrep2	Controlrep3	96hrinfectrep1	96hrinfectrep2	96hrinfectrp3
1346989.484	1857110.734	1306100.726	2014901.463	2835278.313	2529835.734
1235938.621	2045247.833	1445438.297	2957571.888	2822670.627	2601559.967
1411475.938	2410547.163	1372387.163	3135760.576	3116190.586	2338840.459
1335476.129	1541563.606	2346890.931	2625031.775	2831671.496	2605398.29
1203414.175	1506110.246	1180599.227	2100124.645	2564572.465	1682201.959
1875926.63	1898179.406	1598400.663	3509541.735	2960264.309	1165197.646

Spot 30 Fail

Controlrep1	Controlrep2	Controlrep3	96hrinfectrep1	96hrinfectrep2	96hrinfectrp3
129432.6538	82307.27452	241866.7732	532744.8741	192214.9382	372164.7617
71629.30327	441032.2839	219966.8095	397322.6812	569912.9349	344920.8983
122392.3343	131871.2677	213716.3589	648536.4075	244373.3682	316162.7805
95748.67618	136227.6249	243828.101	307759.0845	287997.4524	267006.8765
34310.80455	89517.3001	235726.5895	256796.6149	145948.9966	214894.1347
191761.6749	169950.2284	1286928.046	469180.7521	184795.7391	783680.93

Spot 32 Fail

Controlrep1	Controlrep2	Controlrep3	96hrinfectrep1	96hrinfectrep2	96hrinfectrp3
913818.4712	1117994.673	2243589.509	3047430.305	3028906.988	1714486.021
1658392.636	1226746.655	2400266.687	3168818.941	2447653.78	1602873.296
1652963.536	898373.2275	3049594.462	3376157.021	2402591.751	1961050.055
1062915.901	1654794.488	1356812.117	2471081.408	3095055.877	2473392.497
2056993.692	1686648.578	1290488.753	2178783.022	3249558.904	1597304.593
2495334.734	1021236.744	1499978.45	3427806.755	2554826.174	2007128.342

Spot 34 Fail

Controlrep1	Controlrep2	Controlrep3	96hrinfectrep1	96hrinfectrep2	96hrinfectrp3
886606.119	241752.2218	189285.9201	647514.7609	196789.0587	152498.4664
540418.4297	468851.1453	305278.7485	310928.6513	400820.4423	330396.241
588100.0218	123900.182	291534.29	297412.1728	136289.5664	283117.1382
372905.4408	347107.5737	318188.5236	237712.7997	180387.5904	151754.2243
256039.0498	414158.1446	352909.4896	127155.3911	216525.7852	185348.3076
339458.9331	518967.5474	480034.5569	232561.004	251338.9207	207103.9614

Spot 36 Fail

Controlrep1	Controlrep2	Controlrep3	96hrinfectrep1	96hrinfectrep2	96hrinfectep3
251555.101	155129.2832	129774.0993	483396.1987	313702.3739	271864.554
452459.8751	160816.6161	249832.874	849357.1621	316814.3641	373147.9372
304054.2038	71281.56183	204164.5604	518462.9214	135446.3504	352299.2191
376733.1195	239660.8953	197895.3267	577538.8333	297300.0432	245542.698
232213.6434	234316.3657	138526.8612	341633.5141	288927.905	182365.8719
421273.8891	182895.0075	177205.424	507255.9251	211565.4647	162918.7866

Spot 38 Fail

Controlrep1	Controlrep2	Controlrep3	96hrinfectrep1	96hrinfectrep2	96hrinfectrp3
271923.4125	402974.858	332057.7933	130690.0573	276312 241826.207	
427845.3911	392269.7032	300366.1457	278847.002	247196.4541	252732.8802
340857.2918	317014.9593	354583.9382	151959.4146	179817.3137	265315.4747
305849.7135	380510.6234	243224.2309	178493.1106	227682.1592	193058.7636
192411.1057	372913.7339	252064.3587	134414.4012	222992.216	261686.7291
212416.0506	403474.367	232767.2447	177025.607	230547.7983	161327.6385

Spot 56 Fail

Controlrep1	Controlrep2	Controlrep3	96hrinfectrep1	96hrinfectrep2	96hrinfectrp3
582505.244	289823.7925	333640.7273	733180.1662	445261.0231	445794.196
368192.1352	347331.7561	254039.6668	569991.5529	586353.6711	389778.0858
407810.4066	372297.405	362018.1624	616073.1493	619216.3727	597319.7459
437247.3199	299463.9362	326138.0254	773572.6302	463603.2352	414838.1424
355804.9222	422286.1254	358780.1131	538272.8588	562325.3836	417677.2974
408774.7616	388081.19	477503.2136	652612.8387	478040.4526	431809.0167

Spot 57 Fail

Controlrep1	Controlrep2	Controlrep3	96hrinfectrep1	96hrinfectrep2	96hrinfectrp3
2852032.919	2743922.545	2255925.301	3887992.491	3452901.379	2642086.426
2576308.219	2809308.093	1943672.016	3071143.548	3594922.936	1697992.384
3162458.379	2848359.85	1588468.626	4684815.439	3371323.198	1492169.308
1267183.147	1395945.144	1586294.154	2222732.745	2812883.759	2329936.027
1962575.266	1785594.16	1978364.508	3901321.349	3301405.096	2579805.37
1695475.503	1973289.999	870095.2615	3132259.24	3757504.669	1420964.863

Spot 60 Fail

Controlrep1	Controlrep2	Controlrep3	96hrinfectrep1	96hrinfectrep2	96hrinfectrp3
4321351.603	3138973.487	2589060.547	6217386.011	4753830.412	4380873.63
2486722.598	2753300.735	6601318.712	3057057.28	4231598.536	10173712.73
3427118.446	2538838.371	8125013.936	4567438.321	4085116.687	11200221.46
2826094.971	3246729.862	4755620.556	4506323.444	4043099.723	6519807.23
2064729.219	2676372.089	5099217.02	2768396.673	3295672.101	7327704.888
2037587.632	2860463.35	5053529.947	3661474.344	3557474.211	6286143.607

Spot 82 Fail

Controlrep1	Controlrep2	Controlrep3	96hrinfectrep1	96hrinfectrep2	96hrinfectrp3
993546.0215	745508.9209	760821.5119	599963.5586	559805.6542	866108.586
908064.5185	758205.3527	842888.177	688903.1257	604020.531	877941.318
903591.2388	677284.9782	870359.2468	569474.8964	494595.4602	887922.9628
728587.0945	887075.4489	961789.26	511784.0809	601272.2979	707896.7849
919966.1341	973655.9835	686911.7773	561397.5987	512210.505	515923.9826
1183979.218	1048966.786	1075261.523	814026.092	619956.8475	811067.549

Spot 84 Fail

Controlrep1	Controlrep2	Controlrep3	96hrinfectrep1	96hrinfectrep2	96hrinfectrp3
191500.2507	148151.1142	128206.7461	116652.0959	123552.3811	167521.9428
193772.6974	170726.2204	135073.811	103889.9891	140320.6456	119348.8973
220624.5453	194977.7775	173933.9859	92578.8131	177895.3493	160918.141
154975.2028	221703.3254	131753.2399	72662.32126	115898.4249	130867.8048
183558.8056	187595.5145	146508.6253	154171.8305	109001.6171	120863.917
210205.6068	231515.1281	161080.8347	168799.9784	151860.5691	146982.1883

Spot 87 Fail

Controlrep1	Controlrep2	Controlrep3	96hrinfectrep1	96hrinfectrep2	96hrinfectrp3
464578.621	241948.2527	354673.2002	296146.3911	162550.6992	362459.7116
444679.4869	279243.449	423061.4343	400320.392	240011.5487	425434.4507
456355.843	230584.0005	524171.6209	366179.5347	183027.676	527910.4982
466770.7965	405646.678	376478.8542	318861.9193	225054.0257	285085.7002
443115.0593	425206.5428	403325.1304	294748.0621	238041.6867	251668.9117
605987.8254	385910.2148	476642.8388	447564.9266	219823.2606	287965.9135

Spot 88 Fail

Controlrep1	Controlrep2	Controlrep3	96hrinfectrep1	96hrinfectrep2	96hrinfectep3
2908991.851	2182090.341	1721698.807	1950180.908	2059666.242	1706215.35
2748849.495	1932767.01	1936529.2	1968865.99	1571513.666	1850494
2715828.063	1245634.342	1517821.027	1816238.963	1254371.124	1465848.88
2569682.263	2211470.917	1621400.193	1853157.932	1420293.88	1111315.212
2128942.761	1928977.982	2120081.3	1484235.683	1313340.399	1291019.214
2383568.969	2263283.556	2277791.059	1691030.62	1557924.608	1372615.366

Spot 90 Fail

Controlrep1	Controlrep2	Controlrep3	96hrinfectrep1	96hrinfectrep2	96hrinfectep3
138383.2839	111080.2599	107255.6359	138365.2042	67477.46305	80908.8415
141520.4212	150772.0941	99605.28867	139570.4173	109642.761	99192.07862
138433.4181	103067.9898	86810.54407	137570.989	88473.30916	77479.81671
228120.8284	153788.623	137292.8823	130847.7741	109341.3435	103388.9055
176200.957	132900.2553	120746.7713	102651.8894	100296.8072	73707.17506
227037.2114	192291.9546	153993.5835	137079.088	144786.3044	108305.3544

Spot 94 Fail

Controlrep1	Controlrep2	Controlrep3	96hrinfectrep1	96hrinfectrep2	96hrinfectep3
1356341.763	1755861.763	996858.651	812497.2294	1205370.539	859735.0273
1451029.919	1545827.697	956801.9603	1095777.057	1040077.273	704210.6164
1495290.902	1570781.504	878204.7414	1262275.113	1086287.335	865992.5781
980053.8154	1966415.019	998530.0601	854811.1891	1478318.895	651203.2594
1119849.774	1415436.324	1181086.406	699041.1409	1066592.056	915205.0116
1205969.59	1863137.29	1797156.36	1062300.179	1378046.891	1598809.875

Spot 97 Pass

Controlrep1	Controlrep2	Controlrep3	96hrinfectrep1	96hrinfectrep2	96hrinfectrp3
1930714.572	1937348.317	1210444.045	1253856.028	1419582.61	1328478.216
2029601.45	1981808.311	1688150.553	1476417.217	1721372.431	1843539.033
2280082.356	1769819.679	1898642.35	1519737.362	1569874.613	2005184.13
2070713.848	2158554.733	1722615.125	1644467.152	1355541.147	1228613.398
1864676.813	2737193.843	1789611.433	1308330.412	1857028.675	1179955.694
2562919.821	2522288.553	2688769.909	1949946.052	1637095.987	1852568.699

Spot 102 Fail

Controlrep1	Controlrep2	Controlrep3	96hrinfectrep1	96hrinfectrep2	96hrinfectep3
10433520.26	9676933.876	9265681.615	6187787.962	6192603.168	9329916.544
8464129.055	10715868.08	11868035.58	6030974.056	7295991.088	10523563.3
9649370.113	9653850.084	9739223.794	7129359.205	6462830.086	8542521.139
7740492.426	10044820.37	12722279.67	6214177.639	7134487.429	10541436.32
6137692.386	8146469.627	9641470.906	5702349.084	5836561.844	8650386.559
7738916.17	10703324.09	8442092.031	6844088.63	7412475.47	5241907.908

Spot 112	Fail				
Controlrep1	Controlrep2	Controlrep3	96hrinfectrep1	96hrinfectrep2	96hrinfectp3
18982524.47	18455303.89	8753400.117	20003680.16	26064830.17	11644802.93
16032891.82	17627498.29	14712475.63	16418966.18	22653638.02	16751883.72
15893213.25	17335001.82	15753998.23	17419674.06	23590745.59	17803946.73
15289184.58	15555983.03	12192212.52	19174100.74	20426651.73	17262966.83
10396621.99	12692231.18	16660187.7	13667773.51	16904617.47	24625603.72
10992490.89	12184808.51	14349929.33	17006152.64	16265675.43	19716290.64

Spot 122	Pass				
Controlrep1	Controlrep2	Controlrep3	96hrinfectrep1	96hrinfectrep2	96hrinfectrp3
657919.684	357094.1928	432516.6	666459.8856	531782.543	707980.5955
427800.5877	363005.0396	604146.0422	492582.0061	619124.4634	774558.3016
644788.2705	367141.2025	383050.5971	692895.6638	562776.4521	526441.9096
495387.1343	529125.6177	470487.9297	689183.9429	665718.723	514610.7627
418380.6816	593203.7761	442636.21	505177.8883	756377.9579	400586.3171
607979.816	648323.8609	602900.2321	657293.2056	789411.2836	595308.8118

Spot 124	Fail				
Controlrep1	Controlrep2	Controlrep3	96hrinfectrep1	96hrinfectrep2	96hrinfectp3
3700157.869	2892347.81	1784055.138	3544323.965	3897477.349	2784361.007
2363394.034	2740719.517	2055344.727	2847952.833	3484279.326	2745227.799
3927478.598	2431621.127	1726279.951	3709077.597	3611792.259	2400395.626
3024330.586	2682534.978	3311982.003	4201145.931	3431296.106	3448305.688
2452151.106	2547007.985	3217809.624	2809804.105	3458954.198	3612272.208
2758651.537	2619886.1	2802144.946	3589877.65	3845079.326	2133024.417

Securinine soluble

Spot 1	Pass				
Controlrep1	Controlrep2	Controlrep3	Securininerep1	Securininerep2	Securininre3
946.411	1213.656	739.236	3934.797	5445.892	3281.352
1313.532	1507.207	1833.398	5359.250	7625.121	3132.581
1010.813	1437.430	1592.190	4157.626	5617.842	2808.325
1078.622	892.516	851.866	4578.637	4277.346	4284.731
1091.130	944.305	958.728	4380.034	4935.139	5881.782
1077.798	1025.602	982.511	4581.984	4013.144	1613.849

Spot 2	Fail				
Controlrep1	Controlrep2	Controlrep3	Securininerep1	Securininerep2	Securininerep3
10.26	21.31	39.72	14.61	91.51	59.66
16.73	5.84	30.86	18.12	67.73	55.92
11.20	6.58	30.17	44.85	41.02	54.22
29.90	18.70	19.15	113.07	52.18	193.11
15.70	57.30	33.27	97.25	55.52	185.25
7.76	22.03	52.96	20.60	67.39	22.40

Spot 3	Fail				
Controlrep1	Controlrep2	Controlrep3	Securininerep1	Securininerep2	Securininerp3
266.644	286.928	228.297	776.888	887.312	738.517
325.876	421.447	422.784	1071.047	1309.467	831.729
328.089	422.860	554.146	872.507	1263.421	881.189
315.304	161.917	210.828	1237.674	869.247	1292.420
372.271	194.018	221.507	1459.749	1409.437	762.713
376.727	231.289	203.121	1382.225	1190.197	381.177

Spot 4	Pass				
Controlrep1	Controlrep2	Controlrep3	Securininerep1	Securininerep2	Securininerp3
529.077	532.601	1152.070	1377.167	3149.369	2057.077
113.937	478.997	907.180	368.870	3056.829	2029.491
626.387	403.692	1014.159	1488.693	2522.212	1683.990
525.404	593.630	887.482	1619.070	2176.508	2572.563
731.861	676.608	1067.421	1515.284	2512.849	2300.469
565.019	680.142	731.894	1551.431	2101.351	2210.744

Spot 5	Pass				
Controlrep1	Controlrep2	Controlrep3	Securininerep1	Securininerep2	Securinineep3
251.139	231.121	106.526	436.702	431.798	613.974
311.232	300.352	131.402	524.356	554.042	541.929
273.854	342.282	245.679	529.137	652.197	509.616
314.592	133.158	95.609	1302.664	713.101	416.977
244.190	80.725	119.637	811.121	671.428	230.207
221.135	228.341	121.361	771.678	1029.821	169.325

Spot 7	Pass				
Controlrep1	Controlrep2	Controlrep3	Securininerep1	Securininerep2	Securininerp3
1390.284	1664.560	2056.900	379.751	781.985	632.574
467.434	1263.709	1967.405	119.611	661.070	452.770
1428.381	1035.535	1549.213	440.816	467.642	586.728
1892.622	1882.620	1075.854	1010.071	506.109	238.957
2074.169	1812.113	1027.272	818.288	500.354	279.261
2106.646	2160.997	1090.019	913.390	527.417	340.469

Spot 8	Pass				
Controlrep1	Controlrep2	Controlrep3	Securininerep1	Securininerep2	Securininep3
50.72	136.79	138.26	34.13	61.40	67.66
52.98	41.83	175.29	28.54	54.39	37.04
83.33	95.83	166.84	45.36	42.16	34.47
247.98	124.01	162.26	70.37	25.70	49.95
237.04	107.85	155.97	81.15	30.22	44.91
303.72	140.01	177.58	69.41	32.59	92.51

Spot 9	Pass				
Controlrep1	Controlrep2	Controlrep3	Securininerep1	Securininerep2	Securininerp3
377.411	373.193	286.919	942.360	1565.045	1024.303
396.462	449.376	781.740	1061.420	1811.800	1113.045
406.467	480.466	487.798	1238.608	2074.399	709.931
463.453	372.993	272.345	1070.478	1098.262	1024.771
326.457	445.347	428.354	923.552	1560.698	1369.568
479.999	511.759	528.696	1449.413	1074.864	553.684

Spot 10	Pass				
Controlrep1	Controlrep2	Controlrep3	Securininerep1	Securininerep2	Securininerp3
294.600	735.545	356.142	1065.281	1413.051	952.741
225.607	481.773	480.394	1072.314	1574.919	755.683
328.092	737.389	710.486	1045.014	1982.612	1057.783
522.947	521.195	364.729	1519.863	1136.993	1731.749
459.288	457.126	276.702	1391.004	1436.757	1009.289
411.421	596.814	335.433	1378.364	1459.061	588.553

Spot 11	Pass				
Controlrep1	Controlrep2	Controlrep3	Securininerep1	Securininerep2	Securininerep3
45.94	41.47	168.26	128.52	399.01	119.64
386.24	74.50	82.27	317.71	249.85	209.84
30.01	18.90	48.51	13.55	329.48	115.27
53.57	47.59	52.51	206.34	226.14	326.75
82.16	107.87	61.36	193.58	194.48	400.66
39.05	40.28	133.14	226.26	172.35	163.24
172.348	163.244				

Spot 12 Pass

Controlrep1	Controlrep2	Controlrep3	Securininerep1	Securininerep2	Securininerp3
707.216	924.491	622.720	2406.060	2739.144	2202.642
915.847	1591.215	1105.560	2945.333	4698.566	2534.017
634.909	1477.520	1233.623	2516.886	4973.804	2147.425
1610.623	1279.197	1411.164	2430.209	2510.987	5118.469
1334.421	1471.228	1702.960	2229.353	2404.907	5172.289
1450.879	1566.010	1351.329	2468.830	2464.780	1600.022

Spot 13 Pass

Controlrep1	Controlrep2	Controlrep3	Securininerep1	Securininerep2	Securininerp3
411.394	788.085	358.567	197.094	228.662	367.157
513.476	931.204	364.924	255.023	315.002	325.713
253.780	394.291	498.796	70.433	172.771	334.133
657.660	327.944	693.661	278.860	200.558	240.285
592.338	460.683	594.424	305.733	187.956	131.571
641.432	475.566	597.033	272.550	142.208	179.149

Spot 14 Fail

Controlrep1	Controlrep2	Controlrep3	Securininerep1	Securininerep2	Securinineep3
55.78	63.97	153.78	180.13	831.67	453.39
135.16	74.91	356.05	104.10	634.09	235.54
118.03	73.80	156.56	394.62	671.59	475.25
197.13	158.06	451.56	346.70	559.58	564.82
152.15	196.09	403.55	320.06	664.78	263.59
156.11	178.02	557.30	333.44	444.30	366.00

Spot 17 Fail

Controlrep1	Controlrep2	Controlrep3	Securininerep1	Securininerep2	Securinierep3
34.96	5.50	26.45	20.32	87.11	79.47
51.56	8.50	27.24	48.97	69.91	65.75
64.65	6.74	31.91	38.99	81.10	108.27
35.75	25.17	69.08	85.40	54.58	56.60
19.14	20.26	49.45	82.92	59.60	81.22
31.45	22.62	70.28	78.55	45.33	109.23

Spot 18 Pass

Controlrep1	Controlrep2	Controlrep3	Securininerep1	Securininerep2	Securininerp3
3621.704	4583.222	3524.319	9643.567	9600.005	10033.137
3869.875	5984.919	3388.374	10236.903	13048.412	10424.357
2996.051	5358.744	4519.367	8392.371	13228.446	11797.611
7092.438	5926.631	6376.804	11974.711	12087.389	15609.746
5717.568	5171.170	5737.803	9446.730	9331.325	11037.049
6306.371	7839.459	5382.338	7782.115	11886.802	8104.616

Spot 19 Pass

Controlrep1	Controlrep2	Controlrep3	Securininerep1	Securininerep2	Securininerp3
1520.877	1841.179	1479.605	3539.609	3403.843	4380.584
1345.119	2196.110	1565.084	3248.203	3612.127	3749.334
985.603	1833.662	2590.204	2706.525	4405.270	5533.338
2257.884	1385.254	3161.451	3669.865	2843.120	8843.382
1975.751	1639.952	1834.784	2766.934	3448.781	4254.723
2243.742	1891.443	2366.028	3469.010	3511.408	3113.114

Spot 23 Pass

Controlrep1	Controlrep2	Controlrep3	Securininerep1	Securininerep2	Securininerp3
1073.861	1719.067	720.012	580.519	748.252	861.544
938.395	1779.114	1048.956	593.677	893.333	781.299
680.576	1260.014	1249.623	242.470	507.398	978.567
1580.122	923.597	1252.163	619.780	392.245	804.003
1376.964	1228.342	992.378	494.648	576.710	522.278
1218.847	1652.636	1140.143	545.992	615.534	390.639

Spot 25 Fail

Controlrep1	Controlrep2	Controlrep3	Securininerep1	Securininerep2	Securininerp3
78.175	992.239	339.797	98.025	522.514	325.864
504.066	926.585	456.467	390.877	456.446	547.050
447.382	835.139	416.628	291.662	398.337	308.314
755.237	1102.168	713.613	380.034	507.948	410.638
474.029	1346.263	806.118	140.916	490.392	235.370
726.919	1357.773	567.258	356.907	634.030	135.647

Spot 27 Pass

Controlrep1	Controlrep2	Controlrep3	Securininerep1	Securininerep2	Securininerp3
72.419	112.193	102.245	307.455	387.607	342.238
98.195	162.076	108.969	218.557	479.503	426.158
198.744	117.098	118.682	502.305	434.635	276.690
186.247	209.513	281.166	260.807	409.427	383.898
161.178	197.697	357.689	173.051	318.449	212.936
141.886	236.354	278.960	211.915	342.531	363.141

Spot 28 Pass

Controlrep1	Controlrep2	Controlrep3	Securininerep1	Securininerep2	Securininerp3
204.718	419.856	268.328	113.965	328.233	261.001
177.151	272.645	723.700	73.424 205.884	180.957	
453.225	254.815	312.651	136.764	190.205	123.985
507.654	546.415	406.079	222.921	263.179	129.109
617.616	588.929	487.339	315.134	275.864	218.952
230.566	625.626	887.344	160.871	247.193	711.577

Spot 42 Fail

Controlrep1	Controlrep2	Controlrep3	Securininerep1	Securininerep2	Securininerp3
338.697	370.250	249.020	729.377	769.372	1181.318
392.587	558.500	896.535	1075.516	1196.057	1637.733
323.547	541.837	790.374	837.155	1414.441	1230.653
1090.614	375.869	1315.203	1261.559	1120.991	1799.196
1316.339	445.395	1495.149	1394.253	831.724	3375.043
1184.861	430.696	1315.135	1363.202	820.467	395.032

Spot 44 Fail

Controlrep1	Controlrep2	Controlrep3	Securininerep1	Securininerep2	Securininerp3
470.307	487.812	415.856	971.481	725.323	1420.750
350.207	629.507	593.950	787.111	826.178	465.674
299.787	1124.586	968.006	602.995	1097.530	1713.987
546.797	395.459	986.593	814.644	640.293	2279.444
606.478	515.192	268.795	764.312	1171.997	1021.533
632.452	638.701	947.932	830.430	1059.882	770.883

Spot 47 Fail

Controlrep1	Controlrep2	Controlrep3	Securininerep1	Securininerep2	Securininerp3
57.185	152.409	149.446	94.610	416.383	171.736
32.229	95.222	122.573	141.270	349.870	147.470
192.758	113.915	170.506	259.600	334.628	80.786
105.370	161.869	78.805	167.415	215.710	262.971
137.315	227.415	110.129	210.288	279.946	190.576
135.665	188.749	141.885	167.558	234.923	174.273

Spot 48 Fail

Controlrep1	Controlrep2	Controlrep3	Securininerep1	Securininerep2	Securininerp3
46.543	161.626	53.143	176.382	331.119	228.067
126.476	210.202	85.419	202.565	411.236	184.357
155.546	218.153	157.825	386.471	372.468	177.952
134.813	179.237	158.457	184.311	397.597	113.075
158.481	126.221	183.439	190.944	323.416	136.315
104.943	186.591	215.331	182.346	308.259	58.178

Spot 49 Fail

Controlrep1	Controlrep2	Controlrep3	Securininerep1	Securininerep2	Securininerp3
114.060	154.027	90.942	73.674	93.073	112.821
156.307	179.837	142.294	120.312	114.590	74.371
99.342	229.603	110.122	113.179	152.996	118.409
291.404	274.430	213.236	102.468	160.608	67.955
204.876	200.243	143.674	156.332	97.716	121.812
398.811	231.212	179.538	231.773	127.260	67.964

Spot 51 Fail

Controlrep1	Controlrep2	Controlrep3	Securininerep1	Securininerep2	Securininerp3
326.990	379.975	138.740	221.264	210.555	247.026
260.508	344.848	115.688	179.893	198.438	168.046
312.366	525.693	209.573	187.220	438.633	139.349
408.281	440.590	239.677	193.868	258.832	148.225
455.121	725.826	334.578	265.713	446.802	137.944
650.964	506.515	350.074	296.687	309.364	131.076

Spot 54 Fail

Controlrep1	Controlrep2	Controlrep3	Securininerep1	Securininerep2	Securininep3
35.58	40.62	21.24	25.16	24.74	21.88
38.75	62.22	25.93	29.71	37.04	27.19
30.96	88.42	56.77	17.30	58.72	68.42
57.21	59.22	74.90	24.15	22.78	52.33
50.92	56.57	32.41	11.89	35.73	22.84
65.33	60.76	37.36	23.47	37.76	20.26

Spot 59 Fail

Controlrep1	Controlrep2	Controlrep3	Securininerep1	Securininerep2	Securininp3
144.24	123.87	83.41	80.84	295.29	206.59
71.62	125.98	184.89	86.21	274.77	220.88
50.72	117.62	226.78	77.75	225.93	124.03
81.55	114.09	108.75	181.94	199.36	183.20
94.82	92.44	120.79	175.60	229.11	126.87
106.52	84.32	110.52	150.96	256.48	103.88

Spot 62 Fail

Controlrep1	Controlrep2	Controlrep3	Securininerep1	Securininerep2	Securininerp3
135.961	161.274	178.030	212.879	478.868	451.277
211.120	303.108	345.187	281.905	956.419	580.783
173.780	373.229	341.171	267.538	603.167	420.611
367.079	186.467	315.209	321.243	211.994	462.176
237.043	372.545	391.393	332.031	411.476	1093.787
375.614	431.392	338.655	372.348	393.227	291.486

Spot 68 Fail

Controlrep1	Controlrep2	Controlrep3	Securininerep1	Securininerep2	Securininerp3
250.698	265.449	114.584	166.241	151.999	193.627
198.417	308.272	173.638	146.393	165.044	202.373
239.672	297.278	211.339	149.903	215.638	190.961
557.860	319.579	291.111	348.889	213.091	174.147
476.298	458.731	325.606	327.884	322.527	168.378
659.676	462.506	274.752	386.524	228.258	88.344

Spot 73 Pass

Controlrep1	Controlrep2	Controlrep3	Securininerep1	Securininerep2	Securininep3
11705.032	12384.993	5700.298	17888.433	15553.849	14068.839
13058.458	15884.342	14430.668	21752.474	19484.937	21079.944
10707.145	17912.219	17232.297	17838.487	22583.426	20693.095
12214.276	6949.650	13696.009	17763.189	10179.769	27790.157
9742.718	8488.627	12609.012	16761.655	13425.192	23346.581
11833.585	10021.264	9300.963	19123.835	15887.821	8875.447

Spot 77 Fail

Controlrep1	Controlrep2	Controlrep3	Securininerep1	Securininerep2	Securininerp3
371.773	867.821	499.523	409.279	639.332	634.352
481.986	678.635	886.061	249.654	461.252	676.391
408.515	654.918	605.659	204.764	413.224	521.525
761.885	872.377	471.017	537.628	430.101	231.152
680.312	958.844	502.036	528.252	463.156	296.176
452.237	1008.997	490.569	475.211	543.423	105.439

Spot 83 Pass

Controlrep1	Controlrep2	Controlrep3	Securininerep1	Securininerep2	Securinineep3
1777.321	1858.102	1615.559	2793.109	2855.782	1947.179
1975.349	3174.452	2256.300	2830.079	4035.807	3054.840
1005.560	2429.597	1995.625	2012.088	2929.461	2520.289
2072.460	1388.369	1729.533	2827.120	2598.548	2612.759
1870.265	1519.082	2367.023	2266.256	2877.568	3506.638
1444.957	1673.317	1344.134	1824.757	3243.917	2492.643

Spot 85 Fail

Controlrep1	Controlrep2	Controlrep3	Securininerep1	Securininerep2	Securininep3
48.53	85.45	65.96	30.17	64.92	111.39
76.94	80.96	104.03	63.68	53.63	73.90
73.72	81.70	85.90	54.68	56.56	74.21
71.61	198.02	121.20	64.09	84.66	104.28
80.13	139.06	123.28	73.22	73.22	79.02
126.79	165.39	134.15	67.09	81.29	61.39

Spot 89 Pass

Controlrep1	Controlrep2	Controlrep3	Securininerep1	Securininerep2	Securininep3
681.405	694.799	920.430	1025.674	1066.472	1422.037
888.161	922.597	1212.001	1308.511	1179.772	1471.815
597.723	890.630	1411.227	958.970	1618.058	1509.176
1044.777	974.493	1143.889	1468.962	1552.132	1994.065
934.392	1038.143	1131.789	1384.006	1621.124	1670.534
1011.123	1309.398	970.526	1488.307	1933.534	1145.129

Spot 91 Fail

Controlrep1	Controlrep2	Controlrep3	Securininerep1	Securininerep2	Securininerp3
449.870	810.663	766.177	261.052	850.621	756.880
693.614	696.545	1537.763	401.454	719.428	970.006
612.415	656.649	1280.918	284.116	632.209	687.399
679.193	1264.362	1037.440	621.036	492.530	806.656
851.162	1124.407	1104.713	584.498	631.278	729.587
773.722	1185.442	798.316	692.640	595.981	539.351

Spot 96 Pass

Controlrep1	Controlrep2	Controlrep3	Securininerep1	Securininerep2	Securininerp3
1143.618	1279.929	831.257	1751.093	1733.570	1823.160
1128.778	763.519	1274.568	1883.267	1206.119	1658.830
726.430	1219.626	1284.928	1336.680	1910.532	1877.665
1387.174	957.493	1505.700	2211.139	1573.015	1839.795
1317.155	892.816	1337.581	2253.168	1373.382	1700.116
1319.126	1340.120	1495.199	2262.688	1192.444	998.389

Spot 99 Fail

Controlrep1	Controlrep2	Controlrep3	Securininerep1	Securininerep2	Securininerp3
259.167	359.793	186.988	254.278	295.266	212.557
339.038	412.224	229.767	340.918	336.994	234.953
210.992	372.545	215.523	220.130	291.538	175.393
498.539	548.531	341.985	233.345	317.498	201.294
552.813	403.329	347.963	277.290	264.027	249.664
431.219	391.329	330.469	187.137	242.877	178.779

Spot 102 Fail

Controlrep1	Controlrep2	Controlrep3	Securininerep1	Securininerep2	Securininerp3
438.467	756.672	512.684	450.172	541.154	465.549
523.886	761.287	604.053	658.540	423.523	351.453
959.871	656.349	526.549	828.947	369.034	352.510
606.868	865.799	451.967	267.574	574.210	405.485
788.040	791.727	463.217	258.468	483.921	608.559
830.797	772.008	568.863	352.990	477.153	565.678

Spot 103 Fail

Controlrep1	Controlrep2	Controlrep3	Securininerep1	Securininerep2	Securininerp3
490.309	897.274	916.179	362.149	800.703	622.567
480.629	873.158	1223.175	256.426	742.057	287.668
509.969	596.997	957.087	343.327	579.011	784.477
597.596	1165.248	665.307	550.541	679.587	431.765
692.778	1022.110	428.155	682.553	618.335	467.396
739.154	1029.635	661.373	680.174	554.446	466.753

Spot 107	Fail				
Controlrep1	Controlrep2	Controlrep3	Securininerep1	Securininerep2	Securininep3
840.636	852.638	1466.457	494.056	1173.020	1250.936
1442.415	723.696	1959.888	698.215	1005.163	1264.040
1132.127	843.999	2044.907	737.058	1055.361	1433.700
1186.491	1643.331	1862.665	939.726	954.158	1064.240
1144.894	1909.413	1609.920	975.365	1028.997	940.209
1017.812	1408.657	1752.627	1083.448	813.715	788.699

Spot 108	Fail				
Controlrep1	Controlrep2	Controlrep3	Securininerep1	Securininerep2	Securinineep3
2829.518	6078.154	3342.379	4248.751	7996.447	5431.265
3350.712	6907.053	4340.805	5144.025	9085.318	6358.454
2663.772	6123.530	4036.697	4893.372	7982.753	6722.252
3971.965	3703.062	4826.982	5253.003	5468.242	6712.586
3505.354	4068.179	4808.573	4442.911	5592.778	6667.890
3376.950	4601.596	4037.274	3666.098	7187.397	4565.953

Spot 110	Fail				
Controlrep1	Controlrep2	Controlrep3	Securininerep1	Securininerep2	Securininerp3
211.147	284.446	340.570	284.658	502.229	676.321
268.164	365.500	475.033	436.314	639.193	779.004
250.799	414.684	611.584	336.612	552.992	706.550
363.243	342.996	544.909	382.634	476.151	866.682
484.292	401.667	542.851	549.637	526.715	904.517
363.702	449.310	499.084	323.890	621.305	465.974

Spot 115	Fail				
Controlrep1	Controlrep2	Controlrep3	Securininerep1	Securininerep2	Securininerp3
162.413	355.918	333.634	118.386	224.819	299.558
341.904	406.622	301.735	270.138	264.007	282.107
292.291	416.218	321.890	192.934	255.955	294.956
421.320	459.729	400.098	233.616	312.247	311.473
216.256	356.568	377.335	152.672	241.291	328.721
217.781	431.041	391.807	105.939	296.772	314.060

Spot 122	Fail				
Controlrep1	Controlrep2	Controlrep3	Securininerep1	Securininerep2	Securininerp3
217.604	194.981	224.259	169.681	234.528	279.746
195.654	308.243	299.778	142.245	308.889	206.661
194.655	330.288	215.042	168.371	330.773	178.195
348.350	369.715	323.122	208.485	211.470	200.068
280.385	379.392	292.737	165.967	218.202	276.366
266.257	379.037	385.041	145.348	208.031	176.719

Spot 130	Fail				
Controlrep1	Controlrep2	Controlrep3	Securininerep1	Securininerep2	Securinineep3
316.479	574.441	279.262	249.759	316.452	321.898
330.567	554.986	226.852	275.427	295.030	350.269
471.038	489.655	289.007	484.307	257.407	333.681
572.943	515.933	342.222	375.699	349.427	255.562
425.508	428.739	382.713	335.456	300.564	218.053
522.326	534.074	332.159	392.568	370.739	214.986

Spot 132	Fail				
Controlrep1	Controlrep2	Controlrep3	Securininerep1	Securininerep2	Securininerp3
276.559	409.165	555.943	392.470	805.143	758.918
363.423	474.768	717.905	635.438	693.283	952.042
365.870	522.078	909.428	592.577	790.384	915.445
464.603	488.858	972.696	725.109	841.897	1317.636
518.961	570.753	1080.086	735.194	938.333	809.937
464.589	525.274	846.934	527.105	912.862	616.085

Spot 141	Fail				
Controlrep1	Controlrep2	Controlrep3	Securininerep1	Securininerep2	Securininerp3
783.087	1812.601	1378.819	591.376	1328.985	1462.976
1097.239	1925.754	1294.094	1032.356	1473.295	1346.837
1437.742	1817.408	1642.192	989.569	1279.304	1224.316
1854.469	1948.997	1559.270	1437.157	1527.036	1279.058
1672.672	1886.881	1753.654	1519.445	1599.861	903.979
1946.321	1901.914	1838.414	1215.926	1645.358	983.695

Securinine membrane

Spot 1	Fail				
Controlrep1	Controlrep2	Controlrep3	Securininerep1	Securininerep2	Securininerp3
185520.611	32448.39555	138379.8369	410744.9543	129594.0729	497304.3975
462302.5619	265761.8377	43316.9143	408488.3057	112880.3378	84324.30309
188317.3873	178340.5477	74022.65148	455044.5692	55369.49417	280170.9259
236125.5565	268104.1314	36856.65063	504782.7209	145809.9543	75009.00722
353428.795	275142.7735	74045.97125	536410.9978	3653663.701	328272.4331
196500.3637	49139.81947		380824.4581	208384.4294	

Spot 6 Pass

Controlrep1	Controlrep2	Controlrep3	Securininerep1	Securininerep2	Securinineep3
694290.2591	632665.1768	1134068.763	1662804.444	846285.9115	2186003.829
1025044.418	894694.5599	1729882.311	2648434.74	1722168.415	2565296.199
803732.5372	1215555.425	698315.6467	2058087.367	2083214.982	1033866.73
1005852.279	682787.2003	1429228.409	1584074.917	1267745.872	2615073.498
603689.7782	1603176.954	446241.2802	1080341.874	3124897.754	851911.5563
1057888.542	680788.5154		1682528.569	700610.0607	

Spot 7 Fail

Controlrep1	Controlrep2	Controlrep3	Securininerep1	Securininerep2	Securininerp3
3476412.597	1901759.393	3919658.859	2109958.471	954301.791	1725074.99
2099713.650	2139702.199	4573739.485	1379266.817	1576148.690	1872363.718
3440913.782	1837220.628	3718204.889	2225669.871	1433620.849	1224762.260
3855119.620	1795155.722	4795386.499	2523517.594	1312208.088	1714348.937
2577234.507	2177055.714	2749119.765	1885506.102	1230133.033	1172805.655
3307405.291	1895547.572		2362315.726	1550317.300	

Spot 8 Fail

Controlrep1	Controlrep2	Controlrep3	Securininerep1	Securininerep2	Securininerp3
180564.567	180711.629	194430.460	78580.444	101240.669	137769.476
345884.901	179807.616	312014.695	135841.194	141376.822	136846.006
232172.773	105866.840	201039.645	221875.500	106836.948	94823.319
379895.205	296336.882	285704.361	126735.273	268776.918	132668.035
327477.052	150526.034	135121.401	129704.988	89491.906	75061.750
373146.372	66192.218		113538.870	170775.973	

Spot 9 Fail

Controlrep1	Controlrep2	Controlrep3	Securininerep1	Securininerep2	Securininerp3
111713.949	104666.834	217080.261	115824.286	47769.647	66526.488
182980.335	251556.994	198411.500	118513.692	287078.538	99433.040
263549.238	128586.471	89853.330	216672.827	44589.284	41005.872
192576.836	74224.612	341523.345	72078.772	41195.604	91570.774
193555.727	188584.314	42829.824	100253.531	133927.263	29049.728
215523.001	67852.923		146171.958	52407.689	

Spot 12 Fail

Controlrep1	Controlrep2	Controlrep3	Securininerep1	Securininerep2	Securininerp3
598767.2298	622198.7972	434034.9199	1722107.258	615577.5951	763258.9069
457746.6342	1029402.68	598420.8606	1389400.504	1250545.932	862141.3778
583240.6218	500338.9677	575199.0529	1709335.302	611586.3883	844233.5867
738293.4543	408392.2778	485492.3765	1031942.755	516780.0123	836804.0206
396840.9441	585707.7934	391015.6135	874100.1032	711929.4146	690995.8589
579636.039	831332.6726		954174.4894	538929.5006	

Spot 13 Fail

Controlrep1	Controlrep2	Controlrep3	Securininerep1	Securininerep2	Securininerp3
284654.070	206077.708	488535.349	287579.501	105507.204	199461.762
328534.304	251154.145	408765.130	294842.707	234786.836	122157.276
524474.724	205795.819	178945.275	442180.893	128671.009	50987.663
433698.028	149760.081	616128.733	213134.916	105267.390	243793.904
377955.164	337305.517	154784.142	229860.782	269079.954	36123.355
400312.886	158451.072		285337.232	159315.321	

Spot 14 Fail

Controlrep1	Controlrep2	Controlrep3	Securininerep1	Securininerep2	Securininerp3
155881.0995	35291.22725	372923.2207	131564.3909	23847.03374	148859.9377
137144.0639	144163.9142	274833.4992	134221.1766	129910.3879	93011.66004
189823.8487	116117.3735	182206.3586	172237.7828	93006.04289	82757.57442
246597.6244	137777.1162	458101.6848	164692.8527	123725.9215	164281.5705
166163.6296	79645.18827	170601.7125	114200.6048	79382.93494	82378.89025
199597.8114	91919.24842		117671.1471	114694.7052	

Spot 18 Fail

Controlrep1	Controlrep2	Controlrep3	Securininerep1	Securininerep2	Securinineep3
1411215.117	1029809.897	1405385.244	1006934.794	453878.1384	781364.7061
956130.2313	993701.5097	1911221.578	708587.9583	892239.2572	800065.4391
1419340.21	1045470.747	1991424.444	1069498.068	877262.4349	700167.9447
1727534.982	1181565.643	1891065.801	1302476.446	779276.4163	876388.527
1497734.196	1007969.747	1341989.839	1158827.615	568434.7314	635467.1047
1257809.477	1156373.28		1026846.834	1134952.373	

Spot 20 Fail

Controlrep1	Controlrep2	Controlrep3	Securininerep1	Securininerep2	Securinineep3
253530.7775	273506.1371	208346.6979	664180.7816	270121.4303	272842.8993
210874.1581	394991.2283	152829.172	610306.4049	523002.503	180533.0359
233781.4131	244702.8201	205203.3376	671637.468	279472.7432	247156.3484
241109.5069	183166.9222	217550.094	271599.0435	219525.0887	325030.2969
172955.2761	173048.7195	158556.1589	403120.2304	222625.5217	226390.8103
301899.7732	189904.6264		468482.9255	109945.5892	

Spot 22 Fail

Controlrep1	Controlrep2	Controlrep3	Securininerep1	Securininerep2	Securininerp3
781236.5233	131512.6443	391679.9588	446256.3966	104810.5477	249458.5705
503109.3554	272446.0044	904252.677	331674.4322	302338.7397	397602.9896
736527.4383	237155.2804	574647.2855	471495.4108	249108.0163	228432.9416
419766.8257	240526.6354	644773.532	390451.7257	237502.7113	290422.7574
446409.1408	352835.2729	432352.7681	360530.4505	228821.1566	176741.1376
630178.3126	123447.7912		482936.3858	112684.4462	

Spot 23 Fail

Controlrep1	Controlrep2	Controlrep3	Securininerep1	Securininerep2	Securininerp3
618456.7943	310479.0411	285094.4669	349029.7956	191818.2518	196529.6786
388604.3632	213475.3942	624643.7679	243581.4691	256392.2273	224353.8045
656571.4404	359429.2908	413643.4642	344573.668	329367.7723	141246.9189
525474.4582	277985.0175	324240.6586	442495.2227	265063.3359	186289.3252
396553.6276	340256.7757	342002.1253	382355.5965	183150.7289	115640.5714
458529.7656	233287.6067		412424.6493	132643.0766	

Spot 25 Fail

Controlrep1	Controlrep2	Controlrep3	Securininerep1	Securininerep2	Securininerp3
207325.7893	194524.2937	152294.8551	432579.0639	242595.7789	172973.5995
132283.2332	400529.5978	108370.6325	357093.8702	536848.8865	156423.2088
175003.3044	218689.4921	222515.5621	378203.1266	320443.985	207615.6052
217971.2163	91645.90303	242377.338	426788.4145	130346.4379	347596.5897
83503.04267	130394.7781	149898.8397	267914.1645	146277.7027	175678.5427
175504.0616	168455.1405		339107.2314	83083.49118	

Spot 30 Fail

Controlrep1	Controlrep2	Controlrep3	Securininerep1	Securininerep2	Securininep3
200172.579	263412.4391	67584.60697	98025.17895	227598.1289	26277.22315
112650.2088	245410.6397	76961.42542	61580.62321	255071.6102	23906.50422
240553.8789	178989.2619	84378.23225	124842.567	161812.3143	48107.57343
103799.3706	125153.8408	90828.60672	44069.26169	131140.0338	54271.572
113433.6756	139338.928	70803.94566	58139.24938	99924.1457	30608.03012
163324.2378	150656.5627		74410.65807	111102.7347	

Spot 31 Fail

Controlrep1	Controlrep2	Controlrep3	Securininerep1	Securininerep2	Securinineep3
154651.3146	239648.3856	232741.6367	233304.3499	241763.7944	547394.019
266162.1053	70784.88343	364303.4232	345661.9428	116231.7627	536687.2476
55155.48301	169171.4278	185943.128	179560.1752	180054.5973	217020.5656
142842.3984	153790.491	105999.1659	227797.1586	189302.655	68029.18763
161213.6726	188749.3415	103788.3167	275680.9193	202218.6592	219738.5904
226351.0627	47389.04324		317829.3103	146031.7594	

Spot 32 Fail

Controlrep1	Controlrep2	Controlrep3	Securininerep1	Securininerep2	Securinineep3
142736.5456	124280.1471	219891.2722	118916.9259	102731.5783	113833.6352
180116.7083	174493.0309	328374.8134	149628.4291	143563.5946	205448.5744
270474.5852	101120.7312	203592.394	231268.1864	104253.6948	127028.066
396469.3502	173043.3238	370046.5445	302237.5063	146870.6255	171835.0107
110451.7405	232488.4339	270300.3963	82567.99928	184612.8501	116956.6965
289146.2108	276616.0126		198407.4859	128870.4079	

Spot 36 Fail

Controlrep1	Controlrep2	Controlrep3	Securininerep1	Securininerep2	Securininerp3
817454.3853	746727.1771	958120.9928	1076582.704	1164878.016	1625853.251
1206154.599	895352.5627	1101495.243	1612442.623	1461577.843	1742897.864
1357047.595	1185527.798	1042992.143	1648260.665	1732305.688	1551682.007
1062119.434	729184.3926	1482454.45	1157296.228	1158070.829	2768604.389
595900.9732	1228014.11	1054294.796	630797.1342	2021985.716	1867135.007
1007892.849	884916.2204		1230434.853	758737.4005	

Spot 40 Fail

Controlrep1	Controlrep2	Controlrep3	Securininerep1	Securininerep2	Securininerp3
176843.349	237681.6256	167272.0288	147816.3363	140267.847	99905.2778
155914.1571	363397.9682	157032.9139	166050.0151	273250.42	100662.1017
117898.0014	197553.7411	237567.6933	99025.74274	132459.7045	172484.8253
215068.5225	359797.4649	221962.4719	84949.67624	243727.3372	83789.46653
241762.4559	247810.5732	126505.3424	155828.5048	189246.5133	74092.70093
188187.8072	246079.8351		94979.11535	296007.8055	

Spot 41 Fail

Controlrep1	Controlrep2	Controlrep3	Securininerep1	Securininerep2	Securinineep3
56854.0209	82879.24647	127837.886	60214.12062	104683.3767	104801.3211
44900.36728	125660.5246	139194.7477	154876.4978	192456.2763	153424.069
45043.35196	65201.70097	45095.70793	87468.96332	101713.3521	105940.4347
81560.7129	117954.875	56061.21252	79940.98949	152639.0651	143119.8353
102821.9046	85338.82707	29053.61973	63143.57723	126219.595	101280.0891
50281.47666	89440.21341		80720.05074	111471.9865	

Spot 43 Fail

Controlrep1	Controlrep2	Controlrep3	Securininerep1	Securininerep2	Securininep3
373566.2481	266797.016	356371.6125	317712.9896	182829.2539	299885.553
543900.0187	370220.7888	752682.6344	468631.6451	365091.8928	424587.943
492192.6486	204755.411	383959.4827	522792.0427	184926.1167	353918.3707
719445.4582	497076.3554	649350.8867	338562.1452	433771.9412	229147.0395
598193.2839	479499.013	454904.3077	276349.8563	377845.4823	298982.0157
766264.0587	461236.2109		406662.3478	478457.7526	

Spot 46 Fail

Controlrep1	Controlrep2	Controlrep3	Securininerep1	Securininerep2	Securininerep3
107859.4017	144296.7401	148936.8962	122421.846	84420.47896	111264.0211
125195.4843	204665.0791	77638.22528	105921.6355	159969.4442	42789.98913
128924.6216	137693.4472	63073.83514	117226.5037	74861.52865	57536.87586
94932.63824	67482.87662	180585.2688	103163.9335	42685.52141	103518.869
102622.603	195433.5942	57739.17999	52601.77579	153528.0506	42087.02263
94315.44558	102639.692		66326.95121	57058.94022	

Spot 49 Fail

Controlrep1	Controlrep2	Controlrep3	Securininerep1	Securininerep2	Securininerep3
680497.8959	438341.5059	593762.236	484197.9809	328598.5103	523724.626
1035320.882	411001.5115	579145.5371	796935.5078	363114.14	392785.9965
1171463.057	744021.275	602240.1859	848872.4548	594787.2086	367375.4198
1039105.66	304100.1201	606548.6046	681344.6739	276652.6996	439135.4169
617858.8388	493630.8334	425875.98	495546.636	421041.4285	316931.9719
1005872.52	486902.8921		680417.4201	329300.3179	

Spot 50 Fail

Controlrep1	Controlrep2	Controlrep3	Securininerep1	Securininerep2	Securininerep3
450149.3239	239036.2767	174425.955	271842.8085	213332.8057	125818.4419
251535.1148	300374.9562	205369.0445	156601.6446	287725.2538	132967.016
441592.4337	162321.4124	229124.6527	271061.6271	143297.0391	104249.1256
527307.3654	341817.6996	292422.6527	333116.4442	390642.2578	161665.0782
293486.3903	403996.8299	163410.2733	216059.7761	386183.4057	92031.58255
339434.6244	262483.5434		248242.6462	258482.8873	

Spot 52 Pass

Controlrep1	Controlrep2	Controlrep3	Securininerep1	Securininerep2	Securininerep3
1548548.658	2129612.052	2021298.898	1450366.557	1015474.394	1574971.282
1791534.091	2701821.951	3451494.743	1711018.206	2068937.688	2229056.763
1770845.059	1824139.384	2443668.83	1714542.067	1457974.269	1336802.336
2010424.843	2007992.374	2196807.015	1606785.326	1582894.822	1590688.225
2474802.339	2074251.924	1861585.278	1926075.053	1187635.887	1187180.852
1802923.122	1432406.241		1628852.375	1883592.413	

LPS membrane

Spot 1 Fail

Controlrep1	Controlrep2	Controlrep3	LPSrep1	LPSrep2	LPSrep3
130119.4504	282111.524	142502.3783	163771.9975	188705.8846	160712.5373
113678.2743	223810.3177	161457.1925	259864.773	97562.05707	91088.53162
228141.8448	259289.659	107151.3146	298907.6702	197946.3634	128702.4179
63557.12042	101426.6775	128405.2295	516354.8724	283210.5319	362751.2404
225806.7346	319159.0463	113668.3198	530308.559	502507.5359	210143.1535
194045.4881	115182.4373	112424.9976	470994.2383	498426.0385	162505.1812

Spot 3 Fail

Controlrep1	Controlrep2	Controlrep3	LPSrep1	LPSrep2	LPSrep3
369315.8246	435940.7608	495702.3601	281215.7497	187065.6947	293930.4127
279440.4112	585315.4694	306625.6477	157089.5461	321863.1468	198540.5499
189433.68	613936.7455	367543.3416	118778.7906	321276.7804	268141.9089
283014.8422	317674.4644	412384.9965	336037.3922	334586.5479	389646.5702
186870.4052	320878.1496	324111.7724	189724.8719	360989.5572	344714.18
319193.8505	244997.0997	399963.2688	308745.9699	222304.9539	430938.6167

Spot 4 Fail

Controlrep1	Controlrep2	Controlrep3	LPSrep1	LPSrep2	LPSrep3
432059.5521	634547.2468	676831.4101	310410.6295	433919.2908	638660.2076
352153.6421	619100.5733	505104.8403	284047.1277	431065.5596	439403.913
222736.6453	747708.0625	434099.7499	168551.2266	501040.0701	413445.3354
409894.2304	588423.4273	589312.9987	347301.056	406582.6871	463440.9426
226814.6343	546302.7773	481821.1088	207113.07	384636.5496	417712.8264
393892.2309	385158.982	543627.0716	305179.0121	300711.4014	513262.7252

Spot 5 Fail

Controlrep1	Controlrep2	Controlrep3	LPSrep1	LPSrep2	LPSrep3
601949.4493	778968.6417	850703.4434	1100912.999	1009513.405	1125581.93
884601.4822	993713.5178	712402.9374	1402215.712	1214267.92	1079830.545
1094268.028	830254.2641	750122.6804	1836251.737	939530.1988	1088271.194
953220.4734	705592.7455	1289874.153	1194275.22	742370.2723	1291762.4
1062304.837	735521.7303	637698.5465	974690.8789	749698.4196	541426.2008
866728.055	647982.691	883517.0948	972124.2384	655695.1454	813789.7391

Spot 6 Fail

Controlrep1	Controlrep2	Controlrep3	LPSrep1	LPSrep2	LPSrep3
453930.1135	420993.0877	336721.3741	248573.622	482920.6254	400448.1209
303674.9844	264878.5514	349886.0826	186689.207	329245.167	339868.5989
356819.2069	466839.4406	404245.7427	201479.5352	487594.7168	364015.9718
457559.0457	367424.581	538098.3856	228844.6057	343213.8817	608629.3238
469560.7178	377264.9525	369507.7388	188705.311	216429.8323	398146.0177
525014.3409	229567.8795	368378.4039	211787.3572	196886.7042	397481.4007

Spot 7 Fail

Controlrep1	Controlrep2	Controlrep3	LPSrep1	LPSrep2	LPSrep3
808438.2137	1741888.829	991176.0765	717241.1713	1123910.153	846115.7137
917757.6103	881048.914	796183.0407	819912.7662	714178.9147	725936.4447
737672.537	1028827.644	1129317.566	559408.6381	636752.2017	877921.2982
671589.5367	778221.3491	861380.2735	767870.5577	632178.0613	789948.5794
638217.9712	1016859.996	788904.857	609632.7405	911057.5225	759122.8022
620639.7991	754979.9131	833611.3282	561795.3281	596226.3235	922128.5499

Spot 8 Pass

Controlrep1	Controlrep2	Controlrep3	LPSrep1	LPSrep2	LPSrep3
2021266.287	1822155.589	1555273.061	1367649.171	1506728.858	1211790.153
1489075.311	1495395.107	1600079.866	1032448.384	1230760.886	1250993.956
1575829.595	1678593.436	1702281.805	981145.1765	1310312.656	1325580.241
1594395.145	1586024.066	1708303.309	1600980.083	1663823.469	1689549.547
1444582.414	1090686.157	1389299.544	1059310.691	982490.6461	1337903.718
1677005.213	1229070.616	1183201.398	1694220.351	1359064.373	1101059.576

Spot 9 Fail

Controlrep1	Controlrep2	Controlrep3	LPSrep1	LPSrep2	LPSrep3
1174179.852	735995.6225	1405110.463	941780.807	772850.1766	910232.4982
1325193.583	714042.6576	984934.3581	1100942.689	808860.6282	1095104.041
1125135.518	991612.6418	1475165.012	1001846.685	1139489.003	1037179.754
1557400.376	1070775.842	968436.038	1155850.099	842143.2602	850141.337
1172741.241	1058402.498	1105729.013	688858.6577	1114979.407	950614.1521
1132708.455	1268976.412	837971.4263	906288.9386	1081090.758	1012160.633

Spot 10 Fail

Controlrep1	Controlrep2	Controlrep3	LPSrep1	LPSrep2	LPSrep3
5465221.974	7464026.453	6624232.883	4914563.746	8018659.937	6080101.258
6011404.063	5244856.673	4924318.281	5462037.099	5804879.737	4590537.323
6323526.864	5697123.1	4603344.37	5514927.075	6240257.5	4050336.735
3354074.356	4188767.745	3637813.579	4730156.662	6420156.622	4809965.664
5034490.517	4576051.349	4111738.119	6036959.18	6617274.819	5179898.612
4062261.729	4284700.517	3340558.905	6344357.505	7301875.313	4585848.931

Spot 25 Fail

Controlrep1	Controlrep2	Controlrep3	LPSrep1	LPSrep2	LPSrep3
104651.3913	160393.0535	186449.3099	98162.75733	104399.5887	153513.1296
105836.7747	235921.8165	117582.2678	118509.2514	183908.7435	161240.6454
111147.9208	148175.5465	118344.4724	134479.573	96508.52629	78056.3663
97599.62806	222857.5149	207262.8266	89749.01709	192546.8227	175489.011
148472.9367	169915.2846	211675.3486	87260.44198	115468.039	188380.2922
141759.6036	335052.1805	204140.3314	102739.9529	183264.6123	148897.6123

MPL membrane

Spot 1 Fail

Controlrep1	Controlrep2	Controlrep3	MPLrep1	MPLrep2	MPLrep3
456269.0754	440078.9026	354255.3855	302922.2188	277198.7767	178603.1097
255591.6912	308416.2918	719353.424	183448.9005	189785.4289	310285.8739
237704.1625	305610.8168	314324.158	149288.2769	199172.7705	114106.3544
194052.4104	204224.5426	284574.3539	138046.7889	123085.1244	58424.79382
235041.1407	288470.6906	506428.5651	169311.5187	190451.9479	133996.6686
205645.3583	230760.512	392777.1975	145209.3252	138308.7231	102427.1465

Spot 2 Fail

Controlrep1	Controlrep2	Controlrep3	MPLrep1	MPLrep2	MPLrep3
265591.4637	349242.4838	203739.9159	153195.4232	175719.1056	64293.10585
166315.3162	227705.182	475617.5872	77612.16521	109958.1102	181465.8654
143731.0836	247017.6364	172154.021	54010.96864	115938.7045	35121.29359
81612.56536	93703.23973	161833.3182	100145.6687	89476.69147	27996.28535
112143.0467	163073.5665	178967.1489	116802.1119	153264.0922	83350.89689
77978.62619	97255.27864	128192.3155	81406.83254	104233.1084	80346.05459

Spot 3 Fail

Controlrep1	Controlrep2	Controlrep3	MPLrep1	MPLrep2	MPLrep3
584951.0715	369493.7647	948080.4652	320279.0076	313574.858	507552.6216
683820.9482	461184.6716	934829.9296	433634.4613	417324.8432	394974.6944
499104.6663	446231.7633	520549.4856	337860.773	420518.265	308958.7717
648993.1725	597383.2687	1069864.71	375655.9579	425421.2363	341527.0657
569105.8337	428793.0081	1308651.558	181521.2836	312340.4736	460270.0865
557976.2278	646920.1578	1052344.774	394044.2995	439980.8628	413812.2975

Spot 8 Pass

Controlrep1	Controlrep2	Controlrep3	MPLrep1	MPLrep2	MPLrep3
299883.9693	224029.1027	257918.1868	160536.8827	77579.62819	85988.24082
242211.258	161743.961	194028.8599	104024.271	67961.86413	69682.967
405705.351	322272.4804	270442.0264	150664.3118	232566.1343	95052.15968
237026.4636	319392.8611	309454.59	224072.0091	243902.7171	177071.866
219593.0746	211822.2299	222313.6197	168027.5969	105314.9027	144217.797
216684.1308	295151.6686	158014.1765	271309.1489	181676.2594	87631.46055

Spot 13 Fail

Controlrep1	Controlrep2	Controlrep3	MPLrep1	MPLrep2	MPLrep3
259162.7399	148197.8452	131566.6838	404129.5022	397909.6905	512546.4176
214888.3127	198455.4688	150252.3511	309982.4334	405443.6184	245683.8321
151627.1466	91103.49121	142629.0141	274618.2402	207313.8187	341935.7738
165154.1539	127076.8072	232711.1251	180718.8468	144252.6188	402816.9834
198134.5757	107431.1333	228545.8838	248309.7748	116093.3647	334642.8218
120870.0592	174442.9796	270439.0567	128786.7073	147598.4065	351776.636

Spot 34 Fail

Controlrep1	Controlrep2	Controlrep3	MPLrep1	MPLrep2	MPLrep3
284015.8948	133143.7755	421648.6388	123177.2733	80632.2999	222010.6545
311151.6708	216086.9211	184093.3699	175173.9381	172770.6611	165059.4847
275555.3465	96725.62401	147500.517	133450.0711	84693.79987	109227.2733
337193.8455	138166.334	210670.0675	165113.7629	116016.2058	129334.1889
345255.9753	138124.447	173610.1969	166125.0306	104613.6009	201306.12
249571.6978	157996.3864	162340.5985	144433.8735	228943.2717	95162.63342

Spot 37 Fail

Controlrep1	Controlrep2	Controlrep3	MPLrep1	MPLrep2	MPLrep3
265813.8948	250790.5294	365176.438	408655.6162	653627.3504	938024.6907
416304.4876	253072.1259	445569.2369	598681.6605	438876.5052	847272.1735
263620.665	241578.8243	398391.6379	336466.3917	632739.7031	1070261.072
367873.5798	457902.3299	444958.9226	338026.6043	466562.1981	493005.6574
331654.0297	329266.0936	339106.0669	298667.2964	352099.1341	401674.6581
160839.749	328162.9754	455662.6442	211818.3255	238939.6414	462542.5438

Spot 42 Pass

Controlrep1	Controlrep2	Controlrep3	MPLrep1	MPLrep2	MPLrep3
102432.8304	171187.8664	228509.1331	191005.3195	185719.9646	279457.2815
114330.609	219146.683	199162.7414	197938.8733	220239.7316	266958.9349
128938.0471	136329.5857	142797.9333	181118.3404	149376.7404	170320.6585
132115.2053	84234.93347	73490.18309	252283.6996	139315.0253	185514.8111
42241.66591	95899.40376	48377.41952	142473.9472	150100.0967	136411.8191
90990.95723	81232.62705	66396.1161	119415.2753	125936.7417	94927.49908

Spot 49 Fail

Controlrep1	Controlrep2	Controlrep3	MPLrep1	MPLrep2	MPLrep3
109688.1769	64709.05156	95721.25264	52130.22194	88021.782	65353.66249
117356.8981	95403.3486	61474.43933	41939.85197	56517.31333	87909.8183
120135.5596	50739.81511	69291.81204	74472.92074	36191.54463	64414.94466
66719.41746	50248.26247	63991.6809	27755.42082	26653.78084	47968.7734
53712.79047	71619.4017	49372.58447	66157.73923	64885.3575	22347.03369
114202.4302	119817.321	65906.72782	92659.42234	41559.29054	43366.83479

Spot 57 Pass

Controlrep1	Controlrep2	Controlrep3	MPLrep1	MPLrep2	MPLrep3
148083.4932	192278.4177	211767.9131	152481.5399	145849.8732	130368.1865
139710.0697	155746.6161	146405.6712	158449.1196	108814.1596	126299.6857
85393.22501	131207.7986	114332.1408	82021.68182	101136.2534	67275.10981
100929.7878	113497.5838	137044.566	61881.80523	89403.75796	72726.2795
114061.7582	134147.0252	126058.8154	72304.60385	91590.115	67271.25073
146372.1967	113753.3344	167655.0298	90814.02077	44587.60047	88124.14745

Spot 61 Pass

Controlrep1	Controlrep2	Controlrep3	MPLrep1	MPLrep2	MPLrep3
173690.8928	154545.6377	128965.3764	116844.5081	103689.4551	102121.0123
121503.7361	75232.1887	129799.3138	105971.7826	73409.77982	125641.0416
134553.2222	129396.7818	171906.4115	116329.7525	106305.3101	136382.586
224940.5607	206028.1308	158244.5934	157289.9131	136855.288	102815.1687
156424.3641	170823.5716	126443.9542	110183.6823	101566.0905	67549.52287
211331.0583	181790.0133	162255.6849	137498.1054	113050.5547	86215.27606

Spot 62 Fail

Controlrep1	Controlrep2	Controlrep3	MPLrep1	MPLrep2	MPLrep3
480536.1975	183046.094	359484.0091	309107.6422	209811.3823	378722.3559
486415.818	201865.0289	279770.5852	283233.4802	186782.345	170673.8264
391001.4867	349342.0986	242398.1849	331301.5886	272390.2959	158263.7158
344308.1975	338867.3824	347077.5581	245384.6489	265086.3651	163946.6245
422440.9701	190697.6212	377387.3527	318086.2839	113101.6727	249752.8472
406918.6664	290916.2058	343526.3348	255565.0284	221772.3295	162848.3351

Spot 64 Fail

Controlrep1	Controlrep2	Controlrep3	MPLrep1	MPLrep2	MPLrep3
478589.6824	310470.9559	430376.1428	351918.0847	163784.3324	207385.8618
434318.4388	363429.6508	443975.7972	296187.5823	216537.4916	257637.4243
294469.5657	338265.801	459084.2933	201837.2567	215405.2257	233299.4076
208263.2602	212148.2722	363182.0974	230756.77	148426.1422	287538.5207
243197.2894	307015.2267	469643.0813	259021.1929	278473.9849	335712.7721
249587.4198	296713.4612	370603.3312	240319.533	299621.0862	249467.6843

Spot 68 Fail

Controlrep1	Controlrep2	Controlrep3	MPLrep1	MPLrep2	MPLrep3
294951.7898	300771.8703	136227.4936	266254.6921	411350.9899	183396.3281
294746.1939	328914.1621	115903.3699	269559.4139	425089.5512	201906.9252
251933.4523	479375.3702	179838.2253	317632.6558	430977.2574	303026.2053
224271.5633	294213.2454	210826.1535	241222.9606	292246.0467	472210.611
202802.9288	245524.9593	144381.3718	278556.3857	470712.3946	408551.9732
270915.6563	168907.272	142946.3875	367047.0788	126064.7635	495410.4896

Spot 70 Fail

Controlrep1	Controlrep2	Controlrep3	MPLrep1	MPLrep2	MPLrep3
271664.0935	282622.8369	290958.5023	231580.2613	167721.4118	165613.772
236713.9387	276993.6734	349595.6799	180382.9671	233942.1562	244306.8636
338608.2044	484852.8606	399091.7505	243068.9162	216940.6768	258773.11
196627.6738	408578.1769	368839.7686	226658.6403	331273.9054	246778.5298
259281.0022	335795.8969	275478.9187	251470.0695	233731.2674	165985.14
226603.4538	354025.9249	281110.1549	137101.9332	303303.6616	224544.1577

Spot 72 Fail

Controlrep1	Controlrep2	Controlrep3	MPLrep1	MPLrep2	MPLrep3
199554.2764	107855.8727	130489.466	128225.867	74262.57977	68259.73349
111486.9913	112933.4094	135605.7032	97965.38735	111036.2417	79431.97196
180490.5597	180221.1215	69479.20628	93457.12609	132050.4507	41571.66818
188919.9367	182832.0902	147188.4735	105132.2519	131069.642	105548.2742
172181.8548	163633.8166	115787.5481	128414.4539	145080.4248	110901.5284
86856.27173	125225.6775	87863.11562	66038.86803	88304.84457	107159.8156

Spot 77 Fail

Controlrep1	Controlrep2	Controlrep3	MPLrep1	MPLrep2	MPLrep3
483808.9236	552282.9962	721444.4417	432474.3265	320731.9007	448086.6951
422202.8071	603051.354	895620.3992	396016.8865	470899.1843	609843.925
557209.2241	419115.9317	542449.2981	502464.3222	244860.5326	273732.023
392795.2657	378779.7816	556184.5351	382808.0507	275754.8628	293391.9666
458034.3128	541679.0808	829789.1935	451607.7864	431887.4034	436534.273
450212.0279	541612.7835	274858.0565	390109.063	440724.9655	233667.3544

Spot 97 Pass

Controlrep1	Controlrep2	Controlrep3	MPLrep1	MPLrep2	MPLrep3
207897.449	190454.3179	200641.6003	128518.2101	119011.7657	112656.93
150944.0825	204285.8208	159361.0313	92058.49992	104179.1683	112723.4932
202708.1694	126951.3192	192984.2017	125653.7337	102650.6693	113234.0688
144045.3486	193550.6246	164656.8726	180148.5566	170971.4387	166613.1938
137368.1006	132144.6134	160834.5465	167475.1218	121309.8058	114286.4461
141074.7182	140603.3629	129947.5508	149853.3211	132008.7957	131321.6885

Spot 100 Pass

Controlrep1	Controlrep2	Controlrep3	MPLrep1	MPLrep2	MPLrep3
939648.1746	638271.0759	1013633.614	768407.9013	675281.824	936190.7168
769599.7507	793096.958	1077180.189	701182.1358	797301.0494	811182.7779
853268.0681	730806.3679	578842.5439	772796.8139	666121.6463	568701.9027
974622.3305	893262.5895	787594.8574	770616.974	651245.9758	293194.968
786579.5965	814409.1318	944690.6566	604187.0847	561626.5059	601025.2401
819528.6421	705703.0871	662404.1272	759119.8644	434363.1011	319264.8688

Spot 102 Fail

Controlrep1	Controlrep2	Controlrep3	MPLrep1	MPLrep2	MPLrep3
941081.9232	744996.4303	1518556.394	733436.5096	497197.8412	995771.9329
961740.5374	1189766.867	1766573.472	689397.4394	774872.4393	1247581.107
983824.3328	902617.0023	877643.8239	772048.1277	622774.0026	498126.4963
934107.9404	769399.0514	906850.7053	924146.4242	748734.3874	647628.8486
794097.3203	1199551.348	1377874.848	777221.927	1027084.077	1111109.077
941944.5149	1121314.739	728260.2611	843061.7263	1209131.032	727096.2403

Spot 109 Fail

Controlrep1	Controlrep2	Controlrep3	MPLrep1	MPLrep2	MPLrep3
489827.0843	226119.2918	753974.3943	352548.021	216379.3176	563664.0735
435639.4133	395468.0432	603187.5638	373724.2543	340305.9848	555326.8113
486293.4372	523330.8001	627001.5398	375736.9421	469432.2748	474012.6622
454848.0066	338668.3025	517700.3235	270934.1063	297373.4329	315466.5516
491808.3535	446504.6713	533095.9389	299579.1674	428482.1992	406739.9318
397998.6195	524357.2151	425910.2959	318281.5138	501116.2054	389311.3049

Spot 110 Pass

Controlrep1	Controlrep2	Controlrep3	MPLrep1	MPLrep2	MPLrep3
441177.5944	361742.4291	350183.7432	299283.1593	309845.1526	320138.8666
327915.6032	424291.9229	368005.6216	228605.649	433524.9419	255013.5265
451342.648	313290.7483	226513.3099	369001.2525	335996.6465	214668.3025
377800.2104	349916.3427	529494.559	277573.0904	267617.5521	447820.8651
311589.1533	312617.1156	330467.9108	205265.5434	263038.4003	214857.7131
320083.5391	200899.8707	232321.0298	210703.7644	183806.2481	156048.6243

Spot 113	Fail				
Controlrep1	Controlrep2	Controlrep3	MPLrep1	MPLrep2	MPLrep3
596888.9367	485526.8558	1164792.637	466805.7781	363250.4186	552883.74
558944.3202	742104.7512	915165.8051	458059.7812	550860.4228	645657.2525
550323.65	638298.7881	568907.5536	430608.5147	481104.294	426533.1134
715455.5166	600285.6726	555845.2493	535844.2812	663171.1772	512813.4767
628145.0939	700122.3278	688291.5231	494660.6736	776004.1205	671902.8659
592799.1843	838198.4242	462916.7716	517364.1538	650127.2721	482541.2917

96 hr infect +/- Securinine 3-11 soluble

Spot 2	Fail		
Controlrep1	Controlrep2	Securininerep1	Securininerep2
5925568.568	3055910.635	342881.7308	865714.2995
5159592.839	2998028.07	215968.252	1079333.986
4867873.498	2415672.785	285355.3464	750118.9091
5724204.589	1772624.589	379314.0144	377401.6664
	2641686.154		594949.191
	2531476.415		580213.1429

Spot 3	Fail		
Controlrep1	Controlrep2	Securininerep1	Securininerep2
546195.386	210300.7537	62655.61201	64706.54675
340121.0054	215168.4966	42174.66969	71033.96937
480431.5441	162123.3838	35333.41193	61344.86368
442640.6546	167874.2534	35658.5424	29886.25889
	191050.3361		36366.47562
	166717.0924		29423.22938

Spot 5	Fail		
Controlrep1	Controlrep2	Securininerep1	Securininerep2
150818.8882	116118.7195	992827.5676	547901.8213
129066.8822	57191.42896	1072466.372	498200.7853
215955.2615	104039.4614	551099.3642	444870.8974
171682.2033	107273.1723	1028341.034	350561.5399
	86566.30544		286733.6735
	108009.4939		377202.8926

Spot 6	Fail		
Controlrep1	Controlrep2	Securininerep1	Securininerep2
1381500.184	612929.7883	148703.759	288183.1543
1114578.876	537755.3505	96312.61898	288639.6224
1472273.927	485520.974	87305.86081	246413.9184
1356791.46	403505.3567	75016.35455	129259.1691
	538127.7448		189437.8411
	569001.1403		197550.5641

Spot 7	Fail		
Controlrep1	Controlrep2	Securininerep1	Securininerep2
120653.821	58109.07185	708049.3251	249121.8505
124547.0308	27780.32461	703503.8907	159653.5739
139489.056	38518.67325	652539.9199	197855.0637
118278.0466	42517.74901	464874.9938	133634.6784
	35466.17936		146423.0092
	50469.86967		134650.5403

Spot 8	Fail		
Controlrep1	Controlrep2	Securininerep1	Securininerep2
47051.07464	52746.566	412668.5005	123276.7924
55545.50894	22902.65413	257588.3806	79631.49692
68616.88684	62560.40889	379687.8703	190293.2447
36980.70782	32209.62459	348520.6601	76139.78272
	35939.46724		99455.84382
	25834.84776		79861.72468

Spot 12	Fail		
Controlrep1	Controlrep2	Securininerep1	Securininerep2
288251.9423	293918.7776	2095065.005	646098.2774
329532.3302	182290.4187	1851183.234	345687.4139
355257.9942	438138.8712	2310383.606	886726.1677
286623.599	230189.5038	2469635.036	473624.022
	443493.7929		917586.1695
	246068.4774		473682.1728

Spot 13	Pass		
Controlrep1	Controlrep2	Securininerep1	Securininerep2
38946.67219	51966.36249	259668.1491	123162.8019
41155.80431	23410.91465	192763.9731	107339.5433
82693.73787	33771.43992	363801.8211	146759.532
34922.9088	50041.5467	240683.9411	133846.0381
	63844.07667		205914.2562
	79487.48179		186216.5103

Spot 17	Fail		
Controlrep1	Controlrep2	Securininerep1	Securininerep2
88676.45659	89226.15175	534277.8979	233673.9266
88270.75443	151942.809	372057.5596	380444.1522
84176.52927	105356.0235	605416.0644	279038.9238
89229.98698	124153.7986	548203.4726	332137.8847
	61272.20784		215016.7912
	147224.4244		319259.065

Spot 18	Fail		
Controlrep1	Controlrep2	Securininerep1	Securininerep2
74532.68263	82776.12377	407151.5617	175374.3571
70528.49456	41092.67992	412223.6944	84286.4403
35501.52938	86891.5912	62559.76242	171302.8821
47687.45431	50963.46562	426092.5133	146462.2302
	48634.94308		136638.615
	56088.36622		166869.5105

Spot 20	Fail		
Controlrep1	Controlrep2	Securininerep1	Securininerep2
28823.25306	14004.59981	118998.5428	83536.77255
18908.37159	14018.44339	86610.40961	61358.56633
57023.81499	11297.7778	94103.03289	71571.65629
21111.82827	14819.13367	81353.56433	47345.24587
	12377.5197		59973.67895
	16519.49515		49087.74879

Spot 21	Fail		
Controlrep1	Controlrep2	Securininerep1	Securininerep2
105675.8017	87612.66368	451351.2559	224220.7221
71966.26103	118271.0264	380584.4621	318521.8757
83743.75672	91810.04304	480510.5675	267552.9605
76452.17222	170745.6719	403212.3216	553154.0184
	81084.07999		121080.7593
	98824.40049		287514.1163

Spot 22	Fail		
Controlrep1	Controlrep2	Securininerep1	Securininerep2
36111.33767	30839.65001	210268.9223	127350.2688
52595.62618	47513.78044	186701.5122	138011.0671
31549.92783	40544.59705	226920.2333	128415.5749
40843.85279	57022.17177	236003.8194	132583.0206
	54707.42806		125540.4013
	85106.18777		154327.9691

Spot 24	Fail		
Controlrep1	Controlrep2	Securininerep1	Securininerep2
102668.6204	151725.2133	920062.021	175086.4779
96859.0543	115120.1179	735085.6908	90572.94303
67232.8169	116721.3852	269717.6113	116828.9996
94712.02674	110835.6904	667459.0634	209888.6232
	144428.2855		229231.885
	113584.3851		312487.7525

Spot 25	Fail		
Controlrep1	Controlrep2	Securininerep1	Securininerep2
63314.34079	50446.83505	134362.5401	249000.8511
47430.50459	40265.14634	124407.8947	181368.4851
56861.98094	45594.65959	15847.68007	210509.9337
89113.5941	31522.15072	122940.4553	179860.3792
	39328.5377		231011.8116
	37296.32366		222075.6916

Spot 27	Fail		
Controlrep1	Controlrep2	Securininerep1	Securininerep2
182070.0997	101914.5181	40062.5502	49455.22357
167238.016	63801.32444	42255.98432	33712.86474
191384.5184	99250.58563	26955.6113	53212.97185
202605.8361	117063.458	39171.26864	42575.18274
	90911.2697		36001.99329
	105208.2393		46458.51486

Spot 29	Fail		
Controlrep1	Controlrep2	Securininerep1	Securininerep2
137040.8527	73683.33072	430143.3831	221868.1111
75249.97912	97312.72814	302782.0036	263702.0248
86304.88797	95194.89587	369882.1466	258729.4746
88313.67516	181837.3065	440451.0231	437732.5593
	74698.84778		226849.6648
	108524.3057		312546.5037

Spot 31	Fail		
Controlrep1	Controlrep2	Securininerep1	Securininerep2
89828.17288	60950.76428	290531.8086	145683.7474
49277.33737	103944.3986	233032.8324	222570.2875
62979.66942	99189.53021	413932.2627	177398.9853
42379.5763	125895.2764	345420.001	308762.9658
	95945.72619		181811.1575
	83622.8715		211125.0181

Spot 33	Fail		
Controlrep1	Controlrep2	Securininerep1	Securininerep2
18287.5433	11387.3614	73335.79536	23976.15292
15681.27739	9419.734759	55015.67097	21459.93304
8017.839393	8676.638373	50540.94048	20231.63374
16905.24134	6407.151559	57289.96322	14044.66967
	7855.413185		17513.6439
	11448.74701		19731.15212

Spot 35	Fail		
Controlrep1	Controlrep2	Securininerep1	Securininerep2
121605.8712	161435.535	882705.8078	256535.1693
165308.4596	105867.8708	785071.435	161508.8111
167512.6879	253416.4431	563614.7507	402865.4371
151227.2729	163073.2786	1206935.596	277945.4053
	305937.4441		511642.8245
	167426.1466		309232.9088

Spot 39	Fail		
Controlrep1	Controlrep2	Securininerep1	Securininerep2
20582.02344	16996.03707	5186.193417	6268.035041
23371.91042	16252.55841	4295.160247	4764.858404
31590.59064	27218.4142	16673.92994	10602.87432
15312.24044	11110.15416	6991.737461	3374.8859
	7805.602047		2389.443489
	21904.87756		6921.652841

Spot 47	Fail		
Controlrep1	Controlrep2	Securininerep1	Securininerep2
187963.619	472961.0401	49205.16773	212586.4567
271719.2131	278751.0157	67827.43405	154452.9279
116831.6216	242031.2435	65516.51347	83149.9065
235192.4478	366991.7534	83229.36541	137796.0593
	463911.409		153359.6302
	361756.5835		128126.7983

Spot 48	Fail		
Controlrep1	Controlrep2	Securininerep1	Securininerep2
65140.03613	109134.3864	167686.3483	288973.352
58483.07234	124669.0592	119434.4132	338869.1506
43974.71182	95924.21081	184124.3877	256706.4715
64041.50601	130711.3351	170050.6927	308365.7072
	130590.4703		333735.4323
	102767.6039		267468.2911

Spot 53	Fail		
Controlrep1	Controlrep2	Securininerep1	Securininerep2
122113.3097	246975.8373	41543.70715	83908.73117
74443.21502	182411.5832	24768.49153	91692.6407
110333.2806	199554.9261	50074.84861	75030.43983
110812.7058	261311.5796	50362.25503	112835.8578
	260359.2746		100690.8201
	285836.2722		122371.5509

Spot 54	Fail		
Controlrep1	Controlrep2	Securininerep1	Securininerep2
127669.2733	145464.8274	476219.4273	234557.3336
165358.9639	142139.3665	594916.2729	216689.2102
75395.04446	200641.0027	369322.2878	323903.9571
111034.5544	171687.9781	537600.2566	319203.6508
	227910.4162		441798.7675
	198240.0277		336482.7053

Spot 55	Pass		
Controlrep1	Controlrep2	Securininerep1	Securininerep2
532703.9369	464341.0889	157556.1571	252955.2147
391861.0593	684345.7316	163751.0854	303496.1454
553144.6156	459295.5003	151970.0091	204103.3504
644799.4549	320147.9092	136272.0334	174088.0935
	364238.3585		200887.8194
	303871.6805		176039.1568

Spot 57	Pass		
Controlrep1	Controlrep2	Securininerep1	Securininerep2
24425.08883	21633.91851	6764.008889	9983.93952
15210.88254	38800.3932	5495.903035	14223.90303
23352.35325	18089.22033	10814.08229	9234.800699
9315.138546	13026.20644	5036.010014	5236.827034
	6849.895548		2595.472099
	17397.48007		7324.86732

Spot 60	Fail		
Controlrep1	Controlrep2	Securininerep1	Securininerep2
12474.44287	6490.914977	44004.02286	22902.53067
6598.668663	5411.139219	23796.99497	13227.87198
18292.67843	4575.277714	17584.29985	15719.71498
12054.3683	4373.338472	27756.50589	7428.268283
	6120.187097		12713.82467
	4967.642673		12007.68988

Spot 61	Fail		
Controlrep1	Controlrep2	Securininerep1	Securininerep2
54630.60254	25716.83905	112943	63403.11901
28017.45202	10888.66415	75102.83795	39981.20877
57459.82635	19510.48213	88182.89776	67978.13663
44341.29674	18522.58647	66994.92236	64659.00768
	22224.44454		84324.15627
	17627.09582		58330.77818

Spot 68	Fail		
Controlrep1	Controlrep2	Securininerep1	Securininerep2
150869.3355	153105.73	615464.4838	247097.0242
147737.2401	115302.1341	571930.949	174209.7765
180537.4696	131207.3047	520919.5542	192806.8575
113801.5614	128355.0699	372210.2137	187747.7263
	159055.1962		225487.6039
	140064.5242		197547.671

Spot 69	Fail		
Controlrep1	Controlrep2	Securininerep1	Securininerep2
488762.7738	361572.6849	125321.2256	243138.2562
393280.4844	282884.5726	89218.01017	209261.1559
446495.668	236690.287	87807.64905	203683.0185
484735.0173	167760.235	113862.8629	86684.11361
	201454.8542		112687.6268
	206634.8455		134420.1118

Spot 71	Fail		
Controlrep1	Controlrep2	Securininerep1	Securininerep2
48302.92216	78002.50982	213017.2006	121339.6263
105241.1162	84093.10162	360000.7867	128621.5607
63993.77694	111702.0848	207207.184	163753.596
78743.45264	169899.5656	372878.3352	286660.8998
	125612.3957		228477.5437
	111272.3062		183698.37

Spot 72	Fail		
Controlrep1	Controlrep2	Securininerep1	Securininerep2
18243.13715	16165.1808	77835.14857	35425.61666
15470.7112	17527.19853	71328.18304	39207.00019
53012.98874	20985.22732	117861.235	37688.5481
12739.87321	36738.40849	81156.29766	35318.27317
	35737.45669		33148.00439
	18212.55571		38677.81916

Spot 74	Fail		
Controlrep1	Controlrep2	Securininerep1	Securininerep2
109004.933	43897.74521	46419.58574	22075.09036
72329.1716	26253.47635	29908.52086	15924.41714
39223.19541	32825.53224	12672.52544	18763.48753
88522.2455	26118.5942	27629.78702	11520.7019
	35386.06327		17478.64427
	33110.07715		17092.35882

Spot 77	Fail		
Controlrep1	Controlrep2	Securininerep1	Securininerep2
82777.36314	105046.6265	407170.6625	180215.2878
94091.89689	88482.42511	421871.3502	141433.6442
93241.77383	139886.3513	375605.3605	219434.7394
127039.4057	165635.1461	503690.4161	203387.7428
	213295.8053		272323.6493
	206481.0314		274977.4463

Spot 82	Pass		
Controlrep1	Controlrep2	Securininerep1	Securininerep2
786207.8935	1009198.779	2711428.304	2159186.689
565153.2905	1129327.887	1755921.309	1927380.865
734807.9793	1049047.903	2055814.254	2254541.969
758549.8923	1034949.406	2388001.235	1799818.401
	1078895.936		1876531.055
	954244.3604		1632237.706

Spot 84	Fail		
Controlrep1	Controlrep2	Securininerep1	Securininerep2
272431.8	214504.0524	75433.29085	104587.1369
156365.742	250689.1277	43236.90853	122377.6391
241138.9854	334097.7698	84411.6193	158161.7453
117828.3733	151834.2346	55740.48308	78605.34448
	190826.7656		117126.2034
	216685.8053		112890.5286

Spot 87	Fail		
Controlrep1	Controlrep2	Securininerep1	Securininerep2
23037.97347	12769.91624	44136.38895	56796.5947
17167.05341	13628.72102	41366.82442	42734.8771
23363.41537	10557.89376	19018.38765	37650.62415
23144.03664	13037.74294	37609.3898	27789.21474
	14625.6098		32275.23519
	9980.170511		19706.05912

Spot 90	Fail		
Controlrep1	Controlrep2	Securininerep1	Securininerep2
42354.63201	65004.36257	17701.57964	43710.03352
54517.24574	159372.1091	23763.77892	55532.43942
49030.41891	64192.97293	13343.1337	46884.27208
79296.10318	91604.96653	15941.77584	57790.47947
	65648.9566		32142.13687
	87397.47941		35115.21746

Spot 92	Pass		
Controlrep1	Controlrep2	Securininerep1	Securininerep2
57924.17889	102301.2282	31524.13415	40342.86175
66221.6823	60578.94069	52609.42893	26415.193
66587.46112	89058.91204	36528.65395	34097.62377
138764.1644	95822.27812	49013.05097	63884.97881
	80164.72228		24274.45777
	147899.7033		50394.56782

Spot 95	Fail		
Controlrep1	Controlrep2	Securininerep1	Securininerep2
122873.6145	86671.72061	159649.8053	268568.2813
113768.1825	61952.87118	157772.0403	195130.0038
71585.231	82045.61058	58979.95836	227866.6598
126615.986	61480.54297	132291.952	201496.6715
	66870.48358		249496.5965
	74134.44847		245220.4407

Spot 98	Fail		
Controlrep1	Controlrep2	Securininerep1	Securininerep2
72021.16676	109952.5443	28767.30119	41129.95751
70952.75174	112060.6851	30655.04307	40168.71602
74863.89679	79017.3712	31898.61736	37986.02196
72061.79736	109724.0393	46321.70241	51904.96338
	95587.76657		53690.80275
	83789.9497		48475.09261

Spot 101	Fail		
Controlrep1	Controlrep2	Securininerep1	Securininerep2
155663.6973	159197.0328	434624.4022	211671.5425
132771.5146	85574.39476	384253.5237	119013.7081
109924.198	89350.98373	210878.4021	119055.1359
146364.0489	61155.75281	352450.6073	141991.2562
	71878.72889		161287.0457
	92829.10043		189390.4926

Spot 121	Fail		
Controlrep1	Controlrep2	Securininerep1	Securininerep2
45104.41802	52933.37907	14836.2465	24039.84676
41536.59194	54237.62878	14555.08348	36299.03372
65655.61609	58083.92393	25606.9072	33833.35352
22879.30181	27830.9248	14170.89419	14133.25302
	34481.45711		24622.51451
	32217.3523		16323.08727

Spot 125	Fail		
Controlrep1	Controlrep2	Securininerep1	Securininerep2
143065.1862	206653.3774	320122.0017	365427.3462
114593.3317	167176.3292	251765.4038	279786.8444
86942.87244	97733.81779	109121.7176	187566.0904
102433.4692	79871.22649	230503.1963	141063.3891
	113242.9449		274967.2526
	84901.58384		177080.1189

Spot 126	Fail		
Controlrep1	Controlrep2	Securininerep1	Securininerep2
79631.43405	67469.91447	195758.7263	128474.7495
55499.37372	73761.41621	128006.9563	138656.7753
126262.2454	65342.43964	215796.7558	131908.1332
126771.3024	56863.35507	215307.5726	126040.8939
	64470.8677		127867.006
	65361.74582		116623.9506

Spot 128	Fail		
Controlrep1	Controlrep2	Securininerep1	Securininerep2
95868.88585	150330.0367	40661.70582	84719.33243
93069.41216	109026.4832	35762.20744	68460.47838
71737.73379	170298.4861	64090.18296	95424.2173
116744.7967	146238.0763	40048.24712	69971.62756
	174271.5455		80430.63207
	149211.2839		77011.02449

Spot 131	Fail		
Controlrep1	Controlrep2	Securininerep1	Securininerep2
704564.9595	360418.5823	1178367.26	894793.3677
478405.6181	368411.1464	856036.5933	861466.4693
554975.3673	333734.0505	762098.874	869164.0436
910437.7305	278379.9749	1162230.157	776715.6968
	320317.1258		845746.0919
	270378.0911		675129.0917

Spot 132	Fail		
Controlrep1	Controlrep2	Securininerep1	Securininerep2
122347.4348	106852.4192	48193.51354	62745.89639
114207.8373	95338.02557	40168.3782	60036.3807
113782.2202	75369.9716	42501.41396	30041.48813
105706.0369	99895.19149	41295.32681	68646.89685
	127495.4694		87998.37851
	66548.63062		48572.11151

Spot 133	Fail		
Controlrep1	Controlrep2	Securininerep1	Securininerep2
87350.70958	80310.89307	35020.36277	42582.43935
61514.00188	118987.0792	27952.89141	62461.96835
98917.0775	125966.4499	54576.07707	58142.80067
39556.47534	66632.81738	24870.06213	38959.28152
	69132.11868		37877.83418
	67218.78687		38440.76476

Spot 144	Fail		
Controlrep1	Controlrep2	Securininerep1	Securininerep2
952325.5167	584258.1838	223332.5345	437429.8922
709529.828	557726.2993	166012.9125	419028.3942
824946.1756	575564.3408	219069.2937	401902.3887
710672.3069	637049.9836	189031.6958	508618.5742
	859371.0353		645599.0633
	561810.0632		431807.9163

Spot 146	Fail		
Controlrep1	Controlrep2	Securininerep1	Securininerep2
635040.1986	705115.9074	244488.7504	504629.026
590612.758	491228.0053	247249.9948	389775.9259
876863.4575	613615.2749	268619.8611	424814.6326
708281.4133	647895.4827	199676.3105	358780.1631
	645134.2131		371077.6094
	589885.892		392061.8164

Spot 148	Fail		
Controlrep1	Controlrep2	Securininerep1	Securininerep2
37328.82506	85961.46966	19530.08481	37963.75901
58921.52498	89152.31144	28742.32016	47629.12721
44090.59603	85901.26457	29532.12557	46844.28649
50354.52103	100406.0392	32175.61927	53952.58223
	96652.07395		45259.06317
	109685.5125		59403.42562

Spot 149	Fail		
Controlrep1	Controlrep2	Securininerep1	Securininerep2
674736.6689	386264.129	286653.1309	305941.4056
533393.2828	256729.532	241588.2232	229360.091
589142.6623	307494.1146	214366.6322	250557.3019
648506.2151	231364.6774	236520.8996	133801.5192
	323950.7866		178163.0081
	302474.0994		186650.2745

Spot 161	Fail		
Controlrep1	Controlrep2	Securininerep1	Securininerep2
32795.43045	32931.07223	60180.87159	83279.03927
24671.46775	29571.96612	55506.96957	73760.53375
44444.9945	33221.64143	52946.42659	90032.68846
33571.76079	39909.29767	48091.5303	64098.41201
	44889.59316		61931.87631
	46426.22484		68168.42009

Spot 196	Fail		
Controlrep1	Controlrep2	Securininerep1	Securininerep2
65939.81987	59947.76032	31092.46244	44221.09328
59365.63531	47290.33841	27014.11383	32013.41745
35570.5603	49883.93806	18794.78774	35742.61374
68924.08905	58614.68442	26376.794	41550.29636
	40857.70067		28119.4394
	23975.56495		17665.01466

Spot 200	Pass		
Controlrep1	Controlrep2	Securininerep1	Securininerep2
195724.5608	161604.8779	108235.2409	128119.2212
200829.9367	104828.722	120059.609	65419.26792
212373.5663	161355.8908	101822.6	89808.11781
174050.7509	150856.0954	78546.72504	111476.9236
	208637.0722		147929.3334
	214982.8754		119103.3846

Spot 205	Pass		
Controlrep1	Controlrep2	Securininerep1	Securininerep2
195174.1823	193618.1255	135596.08	126483.7124
189047.6709	244117.3564	124948.666	156762.2373
167424.3361	125223.9035	112376.5314	69611.52664
289965.6467	274197.7857	208361.1601	147117.6393
	266747.8971		128624.0786
	331238.9126		169300.4297

Spot 258	Fail		
Controlrep1	Controlrep2	Securininerep1	Securininerep2
180691.454	131810.1559	220515.4331	209353.6219
298872.6761	118672.5771	292538.9064	226792.3878
196863.7115	135322.7782	232644.553	282132.5532
248819.1928	164858.3674	267781.1716	311086.3997
	150349.7812		315708.3928
	181901.6255		363432.5319

Spot 267	Fail		
Controlrep1	Controlrep2	Securininerep1	Securininerep2
262595.6987	218615.6516	360735.7902	431919.87
173706.052	214365.6539	209402.587	372453.9568
288250.1451	235423.2989	312972.4848	422508.4277
189900.0004	235716.7498	271651.8792	368688.047
	209266.1676		296063.4837
	236111.9319		281315.9649

Spot 181	Fail		
Controlrep1	Controlrep2	Securininerep1	Securininerep2
111627.2406	92406.59298	60453.40645	81939.95676
89993.81614	105109.6972	64336.53837	87166.83833
111151.599	122488.3749	69580.84691	95156.13782
99609.85227	123964.0388	49745.95595	87463.79657
	117840.3189		79488.15441
	85024.06933		64040.29717

Spot 300	Fail		
Controlrep1	Controlrep2	Securininerep1	Securininerep2
271879.9865	167981.3091	184548.0512	137219.2193
167804.337	208192.0327	125136.7085	176231.1366
230582.4068	157663.7831	126252.6493	122323.4201
222030.2901	155075.7985	130606.5914	115443.6166
	193816.0064		155709.2469
	200934.1591		159576.6869

96 hr infect +/- Securinine 3-11 membrane

Spot 1	Fail		
Controlrep1	Controlrep2	Securininerep1	Securininerep2
474932.6736	38517.64245	23375.65422	16478.43817
357494.6133	65995.06371	32719.96532	8398.849283
275493.7031	41586.30073	29468.26537	15895.90041
264027.5399	83210.84738	35884.44322	13261.3782
311693.8131	74102.03293	36192.32911	25796.97391
361244.7195	64149.3709	42691.34571	11581.32174

Spot 3	Pass		
Controlrep1	Controlrep2	Securininerep1	Securininerep2
72321.17419	33851.20936	9023.093655	4426.284647
35384.73013	23570.26272	3984.63382	1345.222962
22343.97476	33456.54004	5960.092905	1815.531917
46084.46905	27813.61513	2662.944246	4558.794675
17715.83237	19352.4549	6391.436816	2676.404251
29351.30692	26716.93142	13313.63374	5070.339481

Spot 4	Fail		
Controlrep1	Controlrep2	Securininerep1	Securininerep2
152561.5923	156547.5607	490657.397	1104000.14
86433.72851	131758.0165	343990.4758	977810.0623
50891.75409	214914.3861	194628.0626	1463700.512
49685.78112	183864.7879	256036.3288	1139296.315
56252.71021	101086.748	114656.9797	1028086.291
84863.19569	140961.5401	257331.2313	1008648.451

Spot 5	Fail		
Controlrep1	Controlrep2	Securininerep1	Securininerep2
261321.9882	81642.8734	49798.61577	13992.65064
153651.6531	77430.19642	25746.40814	13741.5435
238208.6693	99967.29789	40947.06238	14562.71875
107669.3118	92745.75581	20744.51226	21162.8801
181588.0515	70092.56147	35741.16441	15365.25316
221976.9275	79548.51628	15337.11691	15089.72245

Spot 7	Fail		
Controlrep1	Controlrep2	Securininerep1	Securininerep2
1199359.543	267113.1749	198646.7556	79070.18398
1288989.599	347858.0652	193717.3281	68052.86998
841185.2085	320827.6967	107192.8907	79713.89136
790122.5268	261821.5948	114647.2137	50966.89059
865757.9992	317596.5468	129134.8885	84078.55126
1154265.547	226260.4533	208323.1019	78763.28047

Spot 8	Fail		
Controlrep1	Controlrep2	Securininerep1	Securininerep2
100659.6435	161195.8308	687941.4584	834147.3199
73900.02903	131174.3774	611704.4169	754178.8231
45596.32828	192611.6733	399532.2744	848113.7902
31490.22283	190595.0811	422926.0399	1058859.83
35529.51074	218270.6227	292098.7246	513922.5508
45587.31599	155063.5001	537887.6837	753862.0109

Spot 10	Fail		
Controlrep1	Controlrep2	Securininerep1	Securininerep2
458382.9555	155161.9896	89928.90823	25511.01787
272792.6834	131972.0157	52401.3263	17566.40135
138931.5567	174360.8459	17253.1288	22135.91971
209089.2447	157697.8236	29509.96201	40429.74341
149475.2665	117602.2091	27729.45917	21276.69016
327156.2596	107923.1945	77614.01242	22309.90917

Spot 12	Pass		
Controlrep1	Controlrep2	Securininerep1	Securininerep2
295427.6508	637069.6554	87011.44221	148247.1422
955611.9449	683553.6151	76828.19035	157964.343
569011.7956	813890.099	104539.9573	200597.2209
239083.1617	446498.7411	33354.73805	99659.82441
293348.0535	797960.8521	108719.5039	188687.6071
1095643.431	465781.1656	129944.6865	97505.06017

Spot 14	Fail		
Controlrep1	Controlrep2	Securininerep1	Securininerep2
91456.0427	42876.58976	11725.67164	8322.126227
29116.31781	33875.12949	6189.368857	7870.946564
81627.68352	43633.95877	11172.83432	10684.63456
34342.49822	35653.49726	6411.570271	9603.76955
65005.27169	20358.6719	21231.18097	5588.048678
56687.70682	28527.6201	16038.15314	6232.261902

Spot 16	Fail		
Controlrep1	Controlrep2	Securininerep1	Securininerep2
2094186.332	821667.7347	443107.7426	152293.6406
1218214.542	693950.7075	223576.7959	124177.4852
2096708.525	842179.3104	362963.9798	160403.6092
1332652.001	870715.9742	327295.8663	229982.7028
1948992.362	544386.9399	476930.647	138558.3921
2570885.246	641272.913	564944.7278	158824.8722

Spot 18	Fail		
Controlrep1	Controlrep2	Securininerep1	Securininerep2
81835.7367	91874.86172	467461.7692	339380.6959
44017.18239	75221.41236	311098.7692	345428.5476
44881.26312	107518.1828	284406.492	397790.606
70378.39815	86082.2957	454982.433	357502.8784
85093.05694	135333.9491	82215.56469	420857.67
37463.94825	93232.96829	105306.5673	429225.9921

Spot 23	Fail		
Controlrep1	Controlrep2	Securininerep1	Securininerep2
58224.94714	157259.6541	450989.0874	534471.7354
44902.31657	132557.8228	238500.9172	504692.4204
55875.1765	186313.767	324209.2691	738434.3392
56051.04816	197494.9482	209490.7474	801912.7983
24886.82688	110347.7057	56414.94281	385222.0427
47646.51569	186548.1869	514897.4965	694568.0432

Spot 25	Fail		
Controlrep1	Controlrep2	Securininerep1	Securininerep2
108993.1953	274654.5043	1011968.996	866888.9023
88853.49801	213482.8443	573595.8744	787836.4899
46978.74642	329175.8674	666806.4866	1136197.485
69108.59081	364302.5737	701153.473	1175572.604
130937.7967	208241.0312	262784.8802	687494.4537
181291.2456	306634.6878	883403.0243	922771.9264

Spot 28	Fail		
Controlrep1	Controlrep2	Securininerep1	Securininerep2
58225.8719	86522.47394	335620.1876	478255.7159
61985.47289	120935.0742	240793.5188	462796.5303
54753.01198	59144.35908	189006.4009	224113.9433
55590.08559	65344.05744	254122.1957	258310.6601
117788.0663	106709.6787	311667.0068	528535.7045
60468.35615	113962.8586	149129.064	494391.6449

Spot 32	Fail		
Controlrep1	Controlrep2	Securininerep1	Securininerep2
56116.41122	70621.83753	229998.9137	316252.827
34520.56368	53949.54338	166065.075	320372.6525
75828.95448	79935.6019	189965.9358	380283.3453
53648.50288	101384.8961	209954.129	497097.6783
58916.55865	50875.19863	171775.7409	223900.829
89817.3418	104616.1279	209709.7433	447252.3377

Spot 35	Pass		
Controlrep1	Controlrep2	Securininerep1	Securininerep2
53197.26253	52571.87667	280509.8524	212140.0223
43127.7573	101727.6969	202365.6744	302535.7643
43289.71748	63961.21911	179247.7279	225802.4013
59980.17488	69357.5373	240918.1475	325956.7921
77033.69463	57601.05497	298410.0635	210546.9551
26872.07349	88810.97001	105432.062	332089.3645

Spot 36	Pass		
Controlrep1	Controlrep2	Securininerep1	Securininerep2
266759.9167	209361.0094	76010.94345	57009.00238
347845.0128	265973.894	55769.96914	61676.34851
130234.267	312958.6903	24716.98798	70181.07072
220063.8048	242048.5628	57145.96039	81826.57369
207479.5596	315399.3743	45191.53393	60535.31358
270128.3387	207229.4672	73638.79897	90435.60115

Spot 39	Fail		
Controlrep1	Controlrep2	Securininerep1	Securininerep2
1170729.521	425924.0377	272491.5931	78108.88871
1007830.633	378888.0091	232605.0296	81717.46216
1468066.671	382703.5261	303541.102	93956.28384
477930.8591	401588.0841	306375.3528	147129.0589
363735.69	406003.9023	225058.3276	130744.853
1248611.149	363116.0631	261403.2371	109427.9894

Spot 42	Fail		
Controlrep1	Controlrep2	Securininerep1	Securininerep2
223685.0823	284286.1111	57462.65267	58192.56517
189372.4099	271907.3407	58913.81465	56632.48256
135721.0323	383489.9788	39442.0135	79921.28526
185135.5465	297197.3426	93256.32061	131439.5912
145377.1238	368941.9605	38908.95681	49279.28204
232418.527	236427.9564	45506.33702	94074.20936

Spot 44	Pass		
Controlrep1	Controlrep2	Securininerep1	Securininerep2
86267.42503	21517.45021	148263.9074	143319.7091
62917.3308	32454.83247	150437.4671	168564.7033
43376.60402	27219.54968	138833.6491	174136.9809
51336.97059	29040.60266	140078.3158	134985.9201
43553.63995	24295.94818	98296.10831	164956.0957
83580.2283	15442.0995	241757.9145	106275.4394

Spot 52	Fail		
Controlrep1	Controlrep2	Securininerep1	Securininerep2
44062.18937	55870.02838	156854.4842	181524.5003
30141.50508	58442.09858	111390.2847	187533.4054
34241.51912	66252.7737	83534.66211	265784.4335
32055.30897	76684.21067	53513.73994	214493.4483
28649.16012	41483.16013	101899.81	107173.7482
20368.63674	67138.08192	264263.5434	169742.1272

Spot 53	Fail		
Controlrep1	Controlrep2	Securininerep1	Securininerep2
338323.087	113957.9099	100620.5324	65903.1478
281546.4834	141151.8737	80771.67269	51857.00049
284091.213	112046.5091	61293.96264	80606.13792
464609.8717	149622.9332	63657.09663	82106.9732
366205.7094	158094.4787	104692.9415	66216.99187
448900.3316	80270.64323	80599.91551	22566.85409

Spot 55	Fail		
Controlrep1	Controlrep2	Securininerep1	Securininerep2
51474.82634	131433.5626	304275.9914	429121.5646
23607.03653	136393.381	162241.815	460361.9874
64430.63392	163709.8033	291979.3757	523448.8927
25638.08118	184308.1532	110701.7945	464114.8443
16088.94849	111357.8472	16967.34429	286732.4373
99856.87722	191592.1868	513670.4521	468490.5892

Spot 56	Pass		
Controlrep1	Controlrep2	Securininerep1	Securininerep2
15435.25088	55066.06843	190708.5822	145730.6773
65266.85682	53581.76009	105058.7631	147404.3042
54994.55421	78155.51275	160513.0382	213872.723
24628.11849	59579.60651	201986.0805	186942.4295
14952.34377	64880.79133	45984.07327	150398.3251
48711.62724	60727.90308	214417.7114	234639.8932

Spot 63	Fail		
Controlrep1	Controlrep2	Securininerep1	Securininerep2
90209.60263	69303.61246	39953.37179	30437.00786
155845.0783	61890.57925	47311.64637	22484.04219
197399.0162	64035.41333	23494.06151	19684.34243
215961.8722	66007.67138	31510.21352	44416.68563
81413.27508	69074.31457	38692.55371	25758.24113
68234.18371	68301.84127	38792.55642	30161.45463

Spot 65	Fail		
Controlrep1	Controlrep2	Securininerep1	Securininerep2
219158.5906	127602.2721	60392.27088	41007.26883
266716.6909	114934.2588	79148.31142	35823.71245
207038.7288	106333.6615	68615.86082	38460.38288
264246.7382	125099.5481	53099.90201	59210.79505
254717.5419	127915.8308	79748.28679	60116.77299
392152.2058	100848.3993	107832.6244	44070.94554

Spot 76	Fail		
Controlrep1	Controlrep2	Securininerep1	Securininerep2
2011085.914	1402526.269	333945.2339	716051.8842
2974914.212	1549439.685	544374.4349	724012.1183
1007792.942	1363591.42	241633.9249	645814.9215
1217571.681	1346964.826	337550.5153	632301.2958
1371027.987	1520205.251	296643.7447	743450.5259
1707435.094	1422431.261	344852.7437	658993.2763

Spot 81	Fail		
Controlrep1	Controlrep2	Securininerep1	Securininerep2
125480.5869	312497.6181	522810.2945	540122.0214
231594.1739	316298.8669	1153133.134	505226.4478
118778.4453	161825.0747	593513.8211	365591.2099
222411.1085	255110.0892	841588.2433	472994.8766
183227.0806	134208.7244	584114.9737	291060.111
180416.0626	196207.7869	921561.5733	313411.9592

Spot 84	Fail		
Controlrep1	Controlrep2	Securininerep1	Securininerep2
991404.128	357608.2617	266170.9715	171561.8939
591445.0062	289173.186	117469.2904	141337.3414
704111.9501	401771.9487	185636.9316	195904.0612
504081.4427	397255.6137	146412.1101	212229.1898
672788.7289	311305.9345	237306.4277	164335.0094
638457.6573	321766.7603	145084.751	185925.7349

Spot 92	Pass		
Controlrep1	Controlrep2	Securininerep1	Securininerep2
18827.7185	17375.45947	90824.70234	61063.82505
22008.50788	17833.22144	55053.06129	50256.69434
16832.66121	26180.80301	59789.54442	59299.73276
29486.06825	19403.53519	67371.28455	58418.35986
17081.05445	34826.06553	80868.54225	83443.7707
17961.8246	32230.24791	39055.82647	73321.68564

Spot 94	Pass		
Controlrep1	Controlrep2	Securininerep1	Securininerep2
967545.0689	1857753.549	360180.5403	633164.5377
3368011.258	1981586.053	617521.5227	555852.1924
2653183.722	1745976.031	710025.2666	758742.8721
2110800.733	1722730.834	866639.2775	850173.7601
1038300.514	2017198.364	589666.3731	1000650.997
1196448.142	1472693.479	446796.1001	870337.8773

Spot 95	Fail		
Controlrep1	Controlrep2	Securininerep1	Securininerep2
123946.6348	145312.7039	28842.35856	65822.39483
125130.8829	128482.0353	20679.10783	53499.0015
112668.676	168037.7077	24064.50889	65965.31231
87218.08847	136521.3233	17803.34649	78640.63738
54863.12632	71908.98094	15056.26133	34657.65805
71386.40199	126194.3714	20799.61209	62804.68867

Spot 99	Fail		
Controlrep1	Controlrep2	Securininerep1	Securininerep2
25731.60228	98886.90283	101292.9219	138690.2297
35120.55745	132023.2527	85955.90472	273730.166
43064.52966	128070.5842	112746.0107	659288.2068
28087.24632	98426.27171	121368.2227	274284.3581
41012.06644	134504.6054	175333.3017	252408.9681
11180.95575	140490.9454	114148.6592	232838.2075

Spot 116	Pass		
Controlrep1	Controlrep2	Securininerep1	Securininerep2
200609.761	142075.6384	31642.92385	59202.73311
145544.5732	123731.1144	34710.74946	49820.56434
209605.4015	145573.4853	58997.06768	62202.494
117437.9223	126462.8098	24246.2556	88810.71566
99128.90639	88458.40323	49199.88994	58273.95027
47171.6801	110082.5322	40557.98153	70042.62261

Spot 131	Fail		
Controlrep1	Controlrep2	Securininerep1	Securininerep2
6181.065436	13189.3746	34043.98777	39389.47151
10357.9748	12031.79944	24217.46974	39785.03079
7720.430072	16919.60321	27782.59753	38582.45645
5148.789819	16509.43565	20972.10023	55538.27112
11185.14339	20050.94983	46697.54203	55562.14588
45420.29254	20008.50617	34939.85722	51790.13683

Spot 135	Fail		
Controlrep1	Controlrep2	Securininerep1	Securininerep2
285244.9024	258304.629	113481.1166	70505.59547
292447.9089	267105.4497	93459.84223	70491.87265
361025.927	285638.6597	125809.9598	181374.7243
368316.0009	183050.6563	138830.216	64637.8562
466008.0314	254316.852	178124.5962	142350.9185
119461.6412	187584.1804	123712.4801	65572.43602

Spot 136	Fail		
Controlrep1	Controlrep2	Securininerep1	Securininerep2
60280.89235	126368.427	311359.8834	254565.2553
92042.49207	151682.297	247536.5963	328903.4357
83197.97828	150971.1725	202706.0335	327180.3853
46938.52536	152970.3083	231944.4785	276993.6514
92581.81215	131002.1863	100384.9829	228375.6533
26541.54026	132312.2789	114937.4329	242076.2747

Spot 140	Pass		
Controlrep1	Controlrep2	Securininerep1	Securininerep2
35667.47419	16517.20235	51875.8984	52034.67375
17032.14692	30593.87977	55197.4277	57517.94398
21639.42311	15968.69321	63167.18071	36777.14255
25363.53739	37675.39656	94791.65855	65187.88929
23192.11364	8835.098744	47709.76323	62515.06399
22844.89369	34228.6949	14387.46769	76922.83012

Spot 144	Fail		
Controlrep1	Controlrep2	Securininerep1	Securininerep2
61165.05804	238075.063	597694.0315	390779.7099
62790.43676	228085.7939	335169.2975	381599.0774
38532.47646	272674.0684	379564.7934	418925.4399
94160.07406	322119.7924	297514.5149	464614.1704
63865.4303	199633.9493	115771.6355	322069.659
111854.2171	280215.9139	517605.7438	381494.4958

Spot 160	Pass		
Controlrep1	Controlrep2	Securininerep1	Securininerep2
350191.7211	317029.717	131553.6573	147248.9499
274091.8049	257890.1992	107294.5848	126868.6048
273896.1422	284867.3283	109125.9241	124400.3635
282280.9334	295860.3929	141322.698	152263.4276
310725.9525	329094.2352	144343.5768	165815.6021
379906.4379	314579.9269	154306.5024	156725.7896

Spot 167	Fail		
Controlrep1	Controlrep2	Securininerep1	Securininerep2
31838.89376	79267.58445	55259.14635	161069.6161
21863.00333	76418.19193	67426.99239	184447.8411
22455.51301	67954.08788	59456.2742	146280.8809
67997.90417	44615.1165	81535.56186	134423.2275
14672.7279	83646.53644	25341.47003	179109.1222
18631.14312	64325.94184	60693.58642	137175.3122

Spot 170	Fail		
Controlrep1	Controlrep2	Securininerep1	Securininerep2
78437.38134	48544.54329	193676.1844	80555.72087
52347.61858	32583.76872	131446.6084	94244.5365
69404.29617	96987.99067	116363.5075	137109.6983
102994.4698	30793.2507	214713.9068	112315.9013
74355.45868	52370.07734	203732.7444	134351.0279
24965.45411	51967.58254	44178.86775	126403.3671

Spot 186	Fail		
Controlrep1	Controlrep2	Securininerep1	Securininerep2
169850.7799	571296.9131	518499.7373	875594.3318
199168.7955	549050.938	370797.1033	860116.2431
167527.7698	563817.2319	592656.041	887493.9435
188446.7872	467374.3112	655909.9406	1012159.64
179922.5436	597528.0227	772344.6524	1160831.372
145327.7517	594011.9813	773488.984	1152159.824

Spot 187	Fail		
Controlrep1	Controlrep2	Securininerep1	Securininerep2
125565.9301	197518.3226	292133.1281	370555.2251
74790.93169	145593.2597	207969.7396	338265.7756
85540.71584	287657.8401	248323.5168	540628.3247
69750.17069	261967.7128	194377.1959	506522.7905
67892.76876	168326.4079	221630.9792	322140.7444
104717.2978	213884.8233	233983.349	393936.0504

Spot 196	Fail		
Controlrep1	Controlrep2	Securininerep1	Securininerep2
70490.73669	29017.46587	141478.9755	88409.97829
49408.28431	34363.39694	66132.53225	86815.80486
70844.55442	22074.06848	190395.1912	64784.96635
67895.2723	26340.58245	46430.09532	56748.22555
44259.17819	33941.66956	141914.494	81651.99783
108661.251	23654.88182	187347.104	75594.88452

Spot 200	Fail		
Controlrep1	Controlrep2	Securininerep1	Securininerep2
302992.1456	147879.1195	78467.00996	122324.3813
270504.0943	161082.376	92444.22574	118033.2912
73234.50653	179382.8954	27567.11395	133262.1777
152584.2293	126315.3772	51442.60548	88051.21948
140003.3381	182457.5864	39921.70641	134675.0559
244877.798	161783.0183	69626.06135	83465.77116

Spot 201	Pass		
Controlrep1	Controlrep2	Securininerep1	Securininerep2
47280.54576	70054.163	26342.2721	45765.21885
46398.30941	66126.11467	36206.68886	35195.95296
56841.03269	77434.00496	31188.85635	26033.81744
61840.47103	74554.25001	30459.7392	55298.10109
21276.70732	85060.32154	59881.94543	29233.14892
190053.9494	76612.76713	79396.7804	31207.45666

Spot 202	Fail		
Controlrep1	Controlrep2	Securininerep1	Securininerep2
311399.3522	236191.955	193602.7209	85605.07006
512440.0302	203739.7685	209782.1652	72776.45519
477464.1871	203270.0957	190309.087	65104.50754
476060.3396	230184.4912	451707.4608	95195.64843
506653.3883	193143.6415	247761.169	91091.11062
466360.0482	196463.7337	194596.118	104535.7959

Spot 216	Pass		
Controlrep1	Controlrep2	Securininerep1	Securininerep2
89512.4619	59437.16919	127979.2628	100235.9569
45094.73564	50263.12103	90661.56714	94048.25858
77393.52998	43622.12068	116319.3187	114676.4427
46813.20588	53867.88015	88117.36374	137476.5806
81351.41265	59328.1497	104834.4095	90306.49855
51066.28993	42995.50041	119362.2102	122546.8302

Spot 232	Fail		
Controlrep1	Controlrep2	Securininerep1	Securininerep2
179002.7266	91509.38425	86576.52835	34437.19902
256183.6567	84482.30428	195370.5093	55977.64105
325671.0628	104095.1399	149130.5768	51763.20079
149192.7313	110601.3743	46163.12768	50348.10774
173281.721	94544.5522	144818.1354	41367.98421
152433.0303	116767.7132	97191.32909	74669.17287

Spot 237	Fail		
Controlrep1	Controlrep2	Securininerep1	Securininerep2
80687.16543	137503.4999	313689.2579	240268.7406
63563.09162	151390.0989	112636.3745	256454.0378
32222.64252	173474.7974	112749.6538	276892.7417
59751.5872	92599.08427	170700.9726	113707.5836
65655.33822	148367.6569	141627.9173	233487.1942
78126.66036	117691.1005	131447.0887	160304.8705

Spot 245	Fail		
Controlrep1	Controlrep2	Securininerep1	Securininerep2
256303.7404	602087.4126	660768.5238	907823.1273
365892.4971	392949.8577	782743.834	544712.465
348437.532	356479.4272	782984.0453	466151.3428
326277.6343	512505.7718	828599.0662	740171.1026
301914.6337	228977.9935	766116.0637	372634.5456
350282.5518	440983.0692	1001448.281	660606.1663

Spot 259	Fail		
Controlrep1	Controlrep2	Securininerep1	Securininerep2
80189.90452	55773.40295	37089.15845	30154.0858
48531.65136	52297.54798	24501.10243	31113.6401
122956.035	54672.19082	55539.89074	26740.00059
40816.9295	56107.53656	55403.55197	37360.7295
64688.46936	46163.71584	30664.58155	29988.6083
118599.479	53573.53387	43220.16138	32168.36168

Spot 281	Fail		
Controlrep1	Controlrep2	Securininerep1	Securininerep2
318055.9599	298389.1335	348675.9302	151349.2392
354776.5694	275357.6487	198006.3386	125630.4702
429394.1365	282115.7835	222138.6217	112659.6366
410456.4039	293332.5381	302188.5989	156778.1236
457044.6135	251750.6933	283919.9223	160935.9044
297276.0744	278306.5582	104574.2675	159615.9097

Spot 285	Fail		
Controlrep1	Controlrep2	Securininerep1	Securininerep2
880945.713	826545.7644	643872.621	413887.3884
999742.3598	827027.297	497463.7866	387310.5105
1021109.751	837734.6184	482479.702	503026.7236
949962.616	720821.9537	721935.6654	392720.1457
1003461.76	841225.0971	710150.0873	510364.2138
847851.2569	705531.2315	579518.1409	431092.2407

Spot 287	Fail		
Controlrep1	Controlrep2	Securininerep1	Securininerep2
52106.58397	91896.14664	160855.8917	137090.6532
65016.05526	108027.1978	154040.422	155869.7036
49540.35674	98185.50354	142723.7222	168573.2419
62554.00109	124245.3231	253973.755	171099.2331
88548.54651	167703.7227	75629.85546	197439.3426
86313.3089	130211.4703	60863.14484	151309.2546

Spot 318	Fail		
Controlrep1	Controlrep2	Securininerep1	Securininerep2
351872.0177	181233.702	155936.945	161980.4069
247439.9061	153131.6344	109197.0675	114500.9944
330579.9967	195193.0035	138481.6427	155760.9581
196751.5313	179754.1519	100446.4064	161050.6874
152506.9086	116667.912	91102.70112	102519.3107
178379.4336	161245.5713	107911.19	147435.078

Spot 328	Fail		
Controlrep1	Controlrep2	Securininerep1	Securininerep2
3207464.218	3944970.655	2333882.761	2292995.996
2935584.465	3454299.999	1761031.36	2062322.889
3076358.906	5036530.703	1768433.214	2938774.02
2126723.439	4147236.826	1709564.097	2884908.176
1607625.65	2974872.733	1268443.396	2027723.198
2856708.239	4002147.066	2090725.445	2484088.334

Spot 339	Fail		
Controlrep1	Controlrep2	Securininerep1	Securininerep2
250185.995	261568.6076	154514.3412	169556.1
218878.3154	204722.2509	140291.7324	157889.042
283126.3556	204835.0804	104057.8672	166489.1729
246325.0334	244806.0385	172323.4203	211086.1903
284607.0689	210524.6574	165039.789	177386.5476
312464.2813	240392.7653	147174.0612	177192.92

Spot 348	Fail		
Controlrep1	Controlrep2	Securininerep1	Securininerep2
429800.0173	432750.8397	210027.9395	318735.0507
274172.4788	427976.238	170066.4501	316933.5626
529026.0568	476118.9409	250881.9321	365416.6783
559717.2599	481533.1814	268670.6915	451606.9744
415212.7836	481733.533	256605.9463	415574.1955
634372.4826	530751.8263	361356.4438	460373.3258

Spot 354	Pass		
Controlrep1	Controlrep2	Securininerep1	Securininerep2
197860.3882	187361.5278	75178.98626	133159.0894
153243.7072	178163.2813	125868.8919	136347.4202
196288.7794	204748.693	115230.7476	134803.5384
153156.1573	213282.8906	123254.7155	158065.4575
212257.301	228803.9996	124887.0953	189861.0807
337576.1955	227593.2185	205653.8824	169941.0116

96 hr infect +/- Securinine 4-7 soluble			
Spot 1	Fail		
Controlrep1	Controlrep2	Securininerep1	Securininerep2
1970818.193	1316713.904	126663.9382	374747.4995
1867279.3	706294.8074	93976.06258	222233.1241
2051165.402	2238868.101	89717.60625	574224.062
2917119.682	208458.2815	152468.9058	153853.4022
	1389206.734		306371.3285

Spot 2	Fail		
Controlrep1	Controlrep2	Securininerep1	Securininerep2
126516.1253	66153.6351	9084.572679	21401.30384
76555.52391	25602.0005	7353.085981	7547.742811
103347.806	138822.7792	5215.938867	36934.69876
130667.8937	14039.27328	6942.860868	8709.241031
	71626.8659		13951.26898

Spot 3	Fail		
Controlrep1	Controlrep2	Securininerep1	Securininerep2
483940.9713	219465.994	24725.20399	87873.58564
374481.6924	116148.6265	21830.01807	33032.76202
459896.1248	422068.4701	25840.5117	140252.494
497216.2257	42371.03941	23099.41918	24845.56202
	239474.4706		80356.43038

Spot 4	Fail		
Controlrep1	Controlrep2	Securininerep1	Securininerep2
6901.726904	7155.323751	114232.3091	49171.88515
10150.31857	10026.28179	117054.6467	49511.93697
7519.844511	16512.60256	94806.85208	64902.79138
12754.57869	25134.8007	92869.18792	24003.17895
	8980.540429		41182.15715

Spot 5	Fail		
Controlrep1	Controlrep2	Securininerep1	Securininerep2
11274.89309	10959.3946	166043.199	35709.08318
13667.33551	10210.93328	186775.2493	37308.13881
10182.72502	17810.37101	89939.65391	46005.49348
15366.72512	11437.50878	114931.3195	21890.10408
	18547.37987		25258.30008

Spot 7	Fail		
Controlrep1	Controlrep2	Securininerep1	Securininerep2
39874.24329	17710.335	198424.5175	62473.1032
21181.01347	18323.37208	152503.6041	58178.23208
28396.42211	9201.168271	284014.7427	31808.78381
24401.77958	20240.73509	260021.4886	52442.56595
	18100.97107		39816.41843

Spot 9	Fail		
Controlrep1	Controlrep2	Securininerep1	Securininerep2
50083.65714	29618.29692	421914.7078	196991.762
50062.71199	30828.25853	411391.0109	213160.6313
67703.56433	58961.12449	530379.8348	117943.654
61915.4207	32844.46455	527210.4496	184147.2608
	106768.5508		168172.1342

Sot 13	Fail		
Controlrep1	Controlrep2	Securininerep1	Securininerep2
34079.70498	16235.67693	234442.0038	91779.54663
55180.25651	19117.61637	353900.1362	101967.7989
65670.17118	20103.04428	178378.9952	89342.17696
58792.01431	13248.47983	242608.9961	53660.93024
	11713.3381		65693.12428

Spot 19	Fail		
Controlrep1	Controlrep2	Securininerep1	Securininerep2
255676.2657	210761.0582	1416192.091	429688.4736
224656.0986	170533.8641	1291090.593	314305.758
239262.8912	142851.8824	2068032.524	270229.5664
249283.955	224672.1943	2096114.161	488576.3889
	235683.4006		416874.4571

Spot 26	Fail		
Controlrep1	Controlrep2	Securininerep1	Securininerep2
48281.33298	36080.48194	285298.3917	98034.93877
50916.46801	45690.59188	295599.3491	130463.5687
51373.42063	39268.61547	300241.3378	125345.3243
54630.13888	65440.38239	275492.4427	181621.7996
	69488.67532		181172.2186

Spot 27	Fail		
Controlrep1	Controlrep2	Securininerep1	Securininerep2
61126.79582	36233.55403	372182.2902	103053.103
78947.9929	62087.84315	424763.7544	173592.1147
66777.23708	63110.02622	360323.4267	190802.558
59149.38065	81454.4296	349254.5494	205900.3179
	83538.11845		192977.7416

Spot 30	Pass		
Controlrep1	Controlrep2	Securininerep1	Securininerep2
54576.16966	29432.89304	7499.103908	10792.89967
54604.2804	27404.05556	11258.48725	24670.07023
42200.22526	52410.02578	6350.386005	12889.04961
43655.21755	42613.79143	5817.227448	9334.075406
	40040.80556		12493.88438

Spot 33	Fail		
Controlrep1	Controlrep2	Securininerep1	Securininerep2
90372.96523	105953.1944	527771.6638	262759.528
125143.4649	115696.1997	724296.4778	234335.6281
79263.74784	196274.6558	577652.7888	462175.0003
104396.5878	149557.6424	612402.5248	378905.3452
	156353.2384		456015.544

Spot 35	Fail		
Controlrep1	Controlrep2	Securininerep1	Securininerep2
87938.62734	77563.13202	448109.7226	218567.7261
116031.718	76517.23629	582731.465	198140.109
81779.99932	140927.4096	481638.8608	362225.3457
83626.56348	105139.9277	437611.6739	318453.199
	182999.0046		482632.8296

Spot 38	Pass		
Controlrep1	Controlrep2	Securininerep1	Securininerep2
4538.113157	1742.552669	20627.4559	19924.56211
6059.899537	2986.24428	26274.49836	18265.93996
12289.27832	3444.333638	28546.79637	22096.43848
4072.437008	14518.20373	18089.53265	22221.73278
	7028.096237		32244.72584

Spot 42	Fail		
Controlrep1	Controlrep2	Securininerep1	Securininerep2
24307.43046	14212.22035	136037.8043	58314.69722
25359.76033	15110.38692	108804.257	52937.04231
28450.75661	13631.91791	132620.9224	51263.57524
25208.21599	49839.79293	121042.4319	83845.70088
	29363.33261		71835.50184

Spot 44	Fail		
Controlrep1	Controlrep2	Securininerep1	Securininerep2
22303.98485	22829.49434	3842.361306	9333.095918
26970.63961	54857.08647	4855.946114	17389.51198
15516.08851	34096.66625	1827.799819	12854.82628
31226.60085	23764.83828	4479.796964	6623.783512
	28422.57672		11151.64132

Spot 45	Pass		
Controlrep1	Controlrep2	Securininerep1	Securininerep2
315856.4792	419743.123	53529.94823	146982.6762
466770.3953	321166.6431	79690.83874	102732.2837
291867.175	311051.1517	78326.34026	110543.6271
305469.297	163571.1095	69338.84103	61571.79366
	206548.7516		78938.07232

Spot 48	Fail		
Controlrep1	Controlrep2	Securininerep1	Securininerep2
41775.20983	86581.83164	180917.3989	272341.1151
66321.99544	66764.45669	280224.4559	188322.483
74569.70143	36616.19028	328830.2738	93855.69962
58382.65098	23224.05767	238388.3863	63661.635
	33944.09198		88220.24759

Spot 55	Fail		
Controlrep1	Controlrep2	Securininerep1	Securininerep2
14689.17428	27207.26268	131131.8826	52371.43202
15405.15081	38857.56857	174744.7278	75452.97182
36796.27182	37757.306	142982.4143	83194.09468
27243.71003	34334.90692	136596.8666	64403.39196
	64482.15962		99003.41352

Spot 56	Fail		
Controlrep1	Controlrep2	Securininerep1	Securininerep2
23112.99188	9788.761932	78826.79845	33541.06225
12139.47242	15481.70975	39227.70481	29168.80838
8458.441594	18363.09239	58645.49498	30543.66119
6917.71676	22960.08392	57150.55916	59321.14911
	20399.79276		51124.55758

Spot 59	Fail		
Controlrep1	Controlrep2	Securininerep1	Securininerep2
13820.4639	16474.07186	25627.89418	79888.05528
21408.08826	17212.67379	41034.58213	93566.16858
17809.23783	20611.58124	31310.88457	75549.9173
28306.78248	21650.45652	51975.70587	84662.21727
	22216.50308		78791.22399

Spot 63	Pass		
Controlrep1	Controlrep2	Securininerep1	Securininerep2
9264.790226	8842.93588	36036.60969	33113.91823
34106.05661	9805.975443	44546.82907	40540.68902
4145.555573	12367.50713	36940.7181	40511.67828
4470.373112	16498.80199	47238.09506	32861.7886
	11764.83172		30202.75423

Spot 64	Fail		
Controlrep1	Controlrep2	Securininerep1	Securininerep2
9074.664957	38109.84997	60591.72943	86541.92699
9311.464562	25264.81119	78152.82448	75187.92994
8213.134631	31049.43373	42267.77629	99535.5032
13138.20385	34472.64206	50400.69963	54416.96667
	27484.00345		55301.01089

Spot 67	Pass		
Controlrep1	Controlrep2	Securininerep1	Securininerep2
42817.64637	34647.45188	10108.10512	10755.92374
55744.28794	57229.72424	15382.16828	28572.62436
62178.27614	45039.46463	14991.09638	18564.31767
41152.62115	8406.884617	11314.854	3110.396462
	62668.95941		22897.77335

Spot 76	Fail		
Controlrep1	Controlrep2	Securininerep1	Securininerep2
53543.85039	45673.90185	21050.13007	15513.93986
57404.52684	19696.40397	22354.89998	20453.75055
45769.36561	51619.22651	11246.89516	18661.81834
70624.5516	40618.38297	17950.28884	10584.65523
	40303.89647		12500.80597

Spot 77	Pass		
Controlrep1	Controlrep2	Securininerep1	Securininerep2
79493.75705	74074.74718	203867.1402	214680.5636
72895.01165	72107.23036	154549.0313	243247.8968
41367.18411	79200.73561	66688.62889	226871.3679
39913.27839	53950.80102	238433.361	102896.246
	30405.73827		68186.77574

Spot 78	Fail		
Controlrep1	Controlrep2	Securininerep1	Securininerep2
374373.8475	192966.096	51276.34568	177193.9474
488913.1969	188213.2851	60912.58527	151705.8057
550568.3608	197028.8703	58764.45451	170946.9178
706926.6587	192203.0531	77293.39055	175886.1232
	243971.15		209374.1566

Spot 80	Fail		
Controlrep1	Controlrep2	Securininerep1	Securininerep2
32217.26854	16383.35736	87660.27991	60258.95286
17940.22344	23858.36668	47248.14472	50771.97632
11083.50924	22191.5146	66518.65585	38470.8224
6242.88631	26411.11719	49210.79903	44593.85509
	25440.68577		49128.73249

Spot 81	Fail		
Controlrep1	Controlrep2	Securininerep1	Securininerep2
14776.10106	13547.81027	2192.344163	6239.218064
17663.93799	8260.031726	2503.931187	4959.554292
12598.84016	11392.26243	3517.587151	6113.914651
12833.83305	12162.90035	4562.564463	7370.301411
	7813.005985		3868.708715

Spot 82	Fail		
Controlrep1	Controlrep2	Securininerep1	Securininerep2
79828.98656	72796.18669	19506.48966	33164.71681
54775.44399	67553.59496	13586.33835	26620.62739
79627.80143	48995.1272	15100.12631	25509.93102
44518.14072	110064.5021	6453.365028	46917.01396
	47304.02627		38578.08255

Spot 86	Fail		
Controlrep1	Controlrep2	Securininerep1	Securininerep2
50871.11151	67409.84814	234482.4427	97935.23899
39447.06668	45786.75102	166392.5878	71355.46675
42257.97765	73800.51926	192199.8247	97068.0202
45926.21709	59889.55877	193281.5317	105673.471
	42562.22846		81677.22202

Spot 87	Fail		
Controlrep1	Controlrep2	Securininerep1	Securininerep2
108208.4242	98418.40604	31285.31086	54241.36376
94370.69482	58189.94779	22205.02373	26415.65011
84927.04838	61576.62538	29559.09678	31905.05045
91906.11011	44897.90491	28026.10247	18064.02981
	67634.21988		26735.30994

Spot 91	Fail		
Controlrep1	Controlrep2	Securininerep1	Securininerep2
66706.50758	17545.56346	53900.67202	97239.73211
34747.67393	18799.06651	73792.65031	88782.27077
29721.82356	18992.95818	56670.06713	79047.08873
34944.74911	21815.59753	67941.96958	109072.8991
	12685.48815		42269.47836

Spot 102	Fail		
Controlrep1	Controlrep2	Securininerep1	Securininerep2
61138.82482	57944.99759	217202.1175	98118.03556
45540.42996	29187.14202	141276.5023	52993.6877
41642.89003	47761.34379	148499.0762	82877.42583
40700.96203	39773.42329	152292.7498	68940.7465
	48703.15487		80398.24302

Spot 104	Fail		
Controlrep1	Controlrep2	Securininerep1	Securininerep2
286663.1432	549591.387	926968.8902	1046672.54
416969.3295	671258.8427	1389106.255	1301508.455
397612.7672	430139.1711	1492086.647	816050.0195
430806.7394	403113.0539	1613429.197	757987.3553
	479531.6412		887059.135

Spot 109	Fail		
Controlrep1	Controlrep2	Securininerep1	Securininerep2
225889.745	176521.9538	727125.227	259217.0903
148430.8939	115380.8043	453144.0924	159997.2179
139034.1446	142910.9182	461127.8992	199076.1721
132292.5551	103119.3889	520785.175	218138.2928
	119960.3493		240538.149

Spot 117	Pass		
Controlrep1	Controlrep2	Securininerep1	Securininerep2
31024.37739	56385.10303	14467.21539	13013.05496
39349.85749	69181.04032	13312.90987	20714.90584
50268.4566	34827.79999	33879.74485	8277.342967
44026.17137	28825.54775	27380.77044	11600.05914
	41556.45785		21515.53701

Spot 129	Fail		
Controlrep1	Controlrep2	Securininerep1	Securininerep2
35244.37351	24631.93482	17410.66826	13195.16873
35427.5513	11851.0097	16780.76927	7300.998511
34405.47005	35510.91674	12036.66253	18303.97004
52127.84287	30526.19281	18611.80899	11907.37866
	33720.99223		10791.93517

Spot 134	Fail		
Controlrep1	Controlrep2	Securininerep1	Securininerep2
144547.5705	70756.78774	36121.178	50019.02979
102511.5024	62801.06435	25178.36675	38481.1979
128222.3604	65026.03775	32731.38332	47971.73462
98314.84105	107970.7977	29923.23373	62585.22819
	89475.12735		69218.97602

Spot 156	Fail		
Controlrep1	Controlrep2	Securininerep1	Securininerep2
653904.8475	530747.6699	147902.0158	389667.0649
635590.7676	424531.9663	137289.9203	310940.6784
749300.8948	559003.606	200201.3174	403712.8475
636260.3881	356791.833	162597.1426	273181.2491
	494688.4023		394606.7691

Spot 161	Fail		
Controlrep1	Controlrep2	Securininerep1	Securininerep2
134813.2004	103529.4661	51578.33597	71146.78828
84772.7589	114247.8181	34080.41913	77676.61171
132768.6048	68020.72308	32849.49956	48687.51518
101628.1976	96137.20839	25948.6924	64559.57766
	209611.0348		98867.63324

Spot 162	Fail		
Controlrep1	Controlrep2	Securininerep1	Securininerep2
619841.0946	790401.0661	173877.0537	471767.5597
964028.7277	818663.3184	268019.186	482796.4058
564921.5966	599495.4385	247488.5085	364857.0668
581043.4084	273960.3067	237688.2026	202092.9438
	369506.9347		250878.1738

Spot 163	Fail		
Controlrep1	Controlrep2	Securininerep1	Securininerep2
285030.827	150298.0901	118464.4136	112725.8787
288556.7534	167630.5245	123026.7121	120649.0744
343916.5461	156805.8418	115778.4616	113829.1808
411373.274	148040.0176	126703.2685	97527.86883
	170768.8347		104148.5581

Spot 167	Fail		
Controlrep1	Controlrep2	Securininerep1	Securininerep2
48270.65045	61377.25982	24714.9048	36145.84303
45436.2409	77401.62635	22796.59939	41442.5849
52049.86451	73959.64619	15212.14028	42578.5089
67207.95985	83581.16987	20176.23727	42533.22842
	72652.3025		39452.12695

Spot 171	Fail		
Controlrep1	Controlrep2	Securininerep1	Securininerep2
418945.5495	383463.3709	153220.4635	280857.3344
417280.0931	395455.2234	163106.8417	225188.1566
447518.4101	463190.0709	114362.4246	329402.5582
456317.4157	297342.3807	118347.3037	198070.1533
	186067.7213		124241.006

Spot 192	Pass		
Controlrep1	Controlrep2	Securininerep1	Securininerep2
80976.32943	108941.2968	45658.23692	58079.82178
131141.6995	82718.18677	66935.23156	41644.3571
160098.0519	147745.0514	87090.00739	80919.56971
108417.8334	181539.5367	63232.36381	84248.45603
	152461.8793		68063.16631

Spot 200	Pass		
Controlrep1	Controlrep2	Securininerep1	Securininerep2
43775.73443	42458.54834	20214.41467	27826.42421
51453.22216	42838.56555	22786.13457	27096.60554
77724.87137	34373.70683	32815.72431	22922.74298
58114.74556	88870.94248	27209.98212	47530.86918
	60087.16534		34365.37524

Spot 216	Fail		
Controlrep1	Controlrep2	Securininerep1	Securininerep2
29177.28307	43586.45839	68849.69862	49980.1145
26459.30828	33772.08166	62118.18351	41150.97038
35480.51854	30921.11578	86198.5418	41952.81787
29118.34273	29720.85485	75486.07995	44788.42862
	29906.50282		61950.15257

Spot 218	Fail		
Controlrep1	Controlrep2	Securininerep1	Securininerep2
328276.19	201576.8783	504637.4072	473229.5497
229908.4726	300064.5097	353400.2619	636264.731
232107.7874	150774.1607	319942.9021	348084.4679
421636.9042	112282.129	593109.0721	321353.1256
	132454.0449		331757.2832

Spot 244	Fail		
Controlrep1	Controlrep2	Securininerep1	Securininerep2
89091.50689	85005.90612	31185.74749	64574.55733
106039.3061	84288.68881	28855.91479	60928.55176
102386.1753	64143.05717	31484.23639	50690.9923
87873.28987	62329.48048	32052.78342	61296.33139
	58887.46424		59960.66132

Spot 246	Fail		
Controlrep1	Controlrep2	Securininerep1	Securininerep2
37986.98861	61494.33661	20171.64392	39277.32017
49482.93207	52236.12178	23493.76476	32316.4267
65952.59105	49360.14204	32525.24474	29215.27238
49297.0471	56039.92847	26551.26171	36074.03343
	57074.67125		34144.86279

Spot 256	Fail		
Controlrep1	Controlrep2	Securininerep1	Securininerep2
54962.85509	55565.24039	119769.8409	87714.44628
74168.32081	58776.28948	140513.7937	83486.60005
75196.42183	56084.85824	130758.2086	83973.524
72663.13136	49695.86495	134559.7106	90063.32745
	40565.09063		52223.25722

Spot 273	Pass		
Controlrep1	Controlrep2	Securininerep1	Securininerep2
26884.52971	31547.37846	10460.21117	17593.66385
37451.40513	24649.56211	17357.88922	13485.14491
21639.79322	29870.90243	20448.14054	18053.51636
22783.93304	31330.64687	16568.93376	26077.66908
	19560.64697		8361.337468

Spot 281	Fail		
Controlrep1	Controlrep2	Securininerep1	Securininerep2
35851.1634	34421.60956	16355.58939	30161.00057
46995.09354	31563.20025	21476.84909	31112.80605
41863.88923	41698.0219	15243.55358	33794.75848
39453.51382	38465.84316	14953.37157	24930.31794
	32303.84704		21716.63276

Spot 283	Fail		
Controlrep1	Controlrep2	Securininerep1	Securininerep2
5905897.294	6312915.572	2597531.911	4707310.456
9741312.323	6911057.694	4190330.089	4700867.624
6267405.636	6130333.989	3458706.357	4345421.152
7849220.5	4292087.303	4421207.83	3527484.217
	4856863.512		4049416.342

Spot 286	Fail		
Controlrep1	Controlrep2	Securininerep1	Securininerep2
104332.6288	87146.78216	41470.98314	65181.32327
91086.42229	102727.1092	44115.01019	75297.88572
119418.6976	103207.9549	59861.98739	72135.66256
83388.73758	51732.81621	40565.57172	42940.97457
	86275.08744		73610.45621

Spot 385	Fail		
Controlrep1	Controlrep2	Securininerep1	Securininerep2
599287.3087	680859.0622	523857.7252	487977.163
582563.0355	723250.7702	490041.446	440793.7289
591468.0873	727804.0218	499592.4277	491962.7526
528295.5817	628971.4998	458841.7752	449305.4605
	469835.1122		339258.5128

96 hr infection +/- Securinine 4-7 membrane

Spot 2	Fail		
Controlrep1	Controlrep2	Securininerep1	Securininerep2
32530.05775	54929.60648	153676.8549	410393.5636
22417.86127	79004.79436	158681.6158	608996.9404
143437.2616	84535.42505	74455.03518	522874.6215
46729.76374	35653.50055	283624.9794	217319.7211
23723.88346	18197.50617	73785.52518	90956.38999
	46254.69481		440991.1236

Spot 9	Fail		
Controlrep1	Controlrep2	Securininerep1	Securininerep2
12736.23689	8751.664802	23159.63913	97045.67387
12216.73977	35363.92212	50570.62325	134187.4242
113156.2355	24460.20972	48023.78171	117886.6634
9494.2678	26029.78081	52086.39224	206672.9629
13883.63853	15933.23191	82940.5584	92780.07313
	14194.67879		128669.7432

Spot 11	Pass		
Controlrep1	Controlrep2	Securininerep1	Securininerep2
34194.1068	30186.34934	180012.7865	96708.17004
21792.50907	25838.86797	116749.3705	97045.86535
105026.2069	31769.15245	89037.08733	141069.6406
10755.36009	35215.94237	44245.4556	74961.53961
10406.8145	24495.29244	142500.167	93766.50964
	34128.26677		162689.5126

Spot 12	Pass		
Controlrep1	Controlrep2	Securininerep1	Securininerep2
158891.4607	99200.52235	516516.9333	529597.6158
50737.53953	128994.3801	578751.4053	429991.137
479799.8989	135873.814	529720.7203	470251.5601
64077.97989	197887.0474	412911.1023	697027.9289
59837.50009	181803.2853	320280.7208	622464.87
	161335.8637		696725.8652

Spot 16	Fail		
Controlrep1	Controlrep2	Securininerep1	Securininerep2
662513.6964	145706.333	147122.8716	61760.25832
842254.7702	391896.6951	164771.3146	117867.6664
123116.5233	236593.4838	195721.8315	64656.86395
711884.1404	145155.0379	148947.9046	102256.2153
503195.324	152613.4518	99144.94715	119796.8828
	230286.8151		113348.5701

Spot 18	Fail		
Controlrep1	Controlrep2	Securininerep1	Securininerep2
96247.15601	37956.74344	14259.93777	20128.59355
154532.3513	54213.77054	47058.65638	21100.97646
27479.1833	55473.18041	10278.80201	5145.154746
35935.6349	57302.8826	29517.76066	17905.71402
153171.779	51190.76529	40147.03222	27555.51307
	76251.38651		27516.17

Spot 27	Pass		
Controlrep1	Controlrep2	Securininerep1	Securininerep2
470731.2081	1037595.685	256337.146	192207.3414
496418.7653	786869.0396	167903.6798	344402.2199
519912.7233	897329.9623	493342.7875	246413.3813
404742.7564	358755.6431	162968.5003	188957.6099
834495.7083	805195.7572	227293.2686	157356.611
	217425.013		74002.6236

Spot 30	Fail		
Controlrep1	Controlrep2	Securininerep1	Securininerep2
222679.6685	73760.52531	69611.13003	43602.00781
153630.2413	80271.97747	44950.816	42080.27196
40060.38401	55533.18404	57304.86369	18838.02279
247130.7612	72782.08279	53171.02331	36798.35251
177627.5345	73508.21491	69832.75645	23149.40921
	86932.043		26082.98797

Spot 32	Fail		
Controlrep1	Controlrep2	Securininerep1	Securininerep2
1326214.295	780724.336	672725.7457	223451.4489
1211205.048	582574.1312	448393.4251	214698.6752
389988.5243	466799.4163	536615.9232	153575.7179
1024416.872	493192.6106	296476.4393	161646.5051
1847060.689	683372.0174	473718.0615	256685.0686
	524701.0385		117651.8309

Spot 39	Pass		
Controlrep1	Controlrep2	Securininerep1	Securininerep2
41363.90332	37628.30523	83314.96053	120121.3177
32119.95229	29449.22063	147776.3188	91821.61247
95534.79391	33252.03475	67766.13939	102500.1239
34536.94546	42466.01321	117485.4255	138084.0781
22681.35341	32365.19164	59688.90987	64316.53421
	35148.56251		121847.5881

Spot 43	Fail		
Controlrep1	Controlrep2	Securininerep1	Securininerep2
703791.2087	414645.6167	264708.8208	127354.7938
632017.1235	170193.873	174718.9547	114505.0454
136598.0327	213278.2255	234190.1109	58713.27502
486817.1307	181627.9502	134911.8061	97863.83327
695995.5178	209267.4891	148897.5948	108152.9721
	195689.6102		146284.9771

Spot 86	Pass		
Controlrep1	Controlrep2	Securininerep1	Securininerep2
599013.3365	318356.2439	184555.908	174293.7094
828138.251	775962.8478	318769.4871	369355.2415
143020.0027	803981.9274	297813.0271	370099.8509
704788.2892	405467.5066	129296.5199	265991.0549
693172.9468	490371.0119	209735.2168	269945.1527
	801271.9297		465932.1167

Spot 106	Pass		
Controlrep1	Controlrep2	Securininerep1	Securininerep2
13472.24779	18940.93007	21928.1873	39337.16013
16917.02554	21802.23408	41819.78406	36217.22897
26221.67105	21444.10857	41668.24263	40207.93702
22793.08859	30685.52385	61321.47311	48215.36394
6017.880169	15040.16678	34066.94126	26589.33105
	21558.01585		39415.69687

Spot 123	Fail		
Controlrep1	Controlrep2	Securininerep1	Securininerep2
116184.4704	113302.813	287922.5544	257948.6619
57685.73756	134590.0879	366045.9674	233202.6319
354313.8208	137817.5668	443065.7245	235173.6981
154997.3483	185999.6338	153368.1299	316643.5615
41900.72191	176228.7522	294542.7651	259351.0163
	100657.153		127079.6273

Spot 126	Fail		
Controlrep1	Controlrep2	Securininerep1	Securininerep2
57102.95574	84448.84403	112890.7157	127247.1205
61759.83736	41224.09787	122673.0123	43918.13303
122483.3041	80010.76189	230729.2695	115707.3358
85515.75202	32507.58695	211041.6952	108983.6857
75423.71954	56372.30841	88265.99644	115272.1957
	62249.29431		144327.906

Spot 143	Fail		
Controlrep1	Controlrep2	Securininerep1	Securininerep2
65831.38285	137740.5058	203632.2979	171207.8165
78639.34659	150595.3138	152248.7828	109733.9962
21639.18675	80388.93583	80241.60184	97302.62755
50323.28062	107899.5353	201991.5324	160521.6225
107531.4476	80624.57587	206631.6262	136742.3563
	51778.37742		107455.5888

Spot 146	Fail		
Controlrep1	Controlrep2	Securininerep1	Securininerep2
57643.68736	62709.505	28172.28787	28459.77525
61704.24797	48553.55996	23700.29139	39790.45408
60897.83677	20613.41634	28036.26933	20927.2358
92963.78794	57981.4027	37176.67217	21066.03069
37693.93935	31060.97615	22393.60964	27457.62483
	81652.63787		77889.51455

Spot 151	Fail		
Controlrep1	Controlrep2	Securininerep1	Securininerep2
75969.0471	163400.1557	51743.23012	60541.48475
68101.59953	144195.7998	52670.72965	78620.17455
67821.25583	149924.1081	62290.68579	60723.15762
101394.5865	127370.6295	97937.51431	61506.78346
46751.87624	102443.9771	39266.7732	38306.31535
	103435.3405		76292.59138

Spot 156	Fail		
Controlrep1	Controlrep2	Securininerep1	Securininerep2
187110.6388	137842.1162	281079.5987	303174.6867
167757.1055	209456.0535	297957.63	484566.7084
188598.1516	183809.0439	146078.4614	424555.8167
144330.8267	326276.0486	237393.5514	459800.0378
168796.4722	218024.5263	269051.7316	291910.4647
	293577.6487		512801.302

Spot 198	Fail		
Controlrep1	Controlrep2	Securininerep1	Securininerep2
1678897.943	1983251.403	1108057.412	1064046.476
1632670.859	1805395.422	1311446.796	994094.0113
1084645.813	1857968.593	1072947.477	1102053.83
1463977.769	2174366.952	1214147.118	1485222.561
1250966.042	2182267.212	1323033.739	1317622.64
	2341963.883		1541263.502

APPENDIX C

ALTERNATIVE HITS FROM BIOINFORMATICS SEARCHES

Treatment condition	Spot #	Appx. Observed pI	Appx. Observed MW (Da)	Alternative Identification	Calculated pI	Calculated MW (Da)	Mascot	X!Hunter	P3
48 Hr soluble fraction	10	8.5	25000	desmoplakin isoform I gi|58530840	6.44	331569	X	X	X
				heterogeneous nuclear ribonucleoprotein A2/B1 isoform B1 gi|14043072	8.97	37407	X	X	
				neuropolypeptide h3 gi|4261934	8.81	15954	X		
				phosphatidylethanolamine-binding protein 1 gi|4505621	7.01	21044	X		
				biliverdin reductase B [flavin reductase (NADPH)] gi|4502419	7.13	22105	X		X
				dihydrofolate reductase gi|4503323	6.85	21439	X		
				plakoglobin	5.09	62600		X	
				junction plakoglobin P14923	5.75	81700		X	X
				heterogeneous nuclear ribonucleoprotein A1 P09651	9.17	38700			X
				peroxyredoxin 1 Q06830	8.27	22100			X
				galectin 7 P47929	7	15100			X
				transgelin 2 P37802	8.45	22200			X

96 Hr soluble fraction	2	3.95	10000	SH3 domain binding glutamic acid rich protein like gi|4506925	5.22	12766	X	X	
				H4 histone family member A gi|4504301	11.36	11260	X	X	
	5	7.7	60000	novel protein similar to PBEF gi|55960735	7.71	53360	X		
				pyruvate kinase gi|35505	7.58	57841	X		X
				catalase gi|4557014	6.9	59719	X	X	X
				glutathione disulfide reductase gi:1070445	6.07	51667	X	X	X
				2-phosphopuruvate-hydratase alpha-enolase (enolase 1) gi|693933	7.01	47079	X	X	X
				UTP-glucose-1-phosphate uridylyltransferase gi|2136353	8.15	56930	X	X	X
				GTP binding protein (Ras family) gi|4092054	7	24440	X	X	X
				glutamate dehydrogenase 1 gi|4885281	7.66	61359	X	X	X
				fascin 1 gi|4507115	6.84	54496	X		

96 Hr soluble fraction	9	3.1	10000	fatty acid binding protein 4 gi|4557579	6.59	14710	X	X	X
				profilin 1 gi|4826898	8.44	15045	X	X	X
				cystatin A gi|4885165	5.38	11000	X	X	X
				fatty acid binding protein 5 gi|4557581	6.6	15155	X	X	
				SH3 domain binding glutamic acid-rich protein like gi|4506925	5.22	12766	X	X	X
	14	7.5	8000	S100 Ca2+ binding protein A9 gi|4506773	5.71	13234	X	X	X
				unnamed protein product gi|158261511	4.86	49486	X		
				polyubitquitin gi|2627129	7.13	68448	X		
				ubiquitin and ribosomal protein s27a precursor gi|4506713	9.68	17953	X		
				ubiquitin P62988	6.56	14700		X	X
	48	6.7	35000	aldo-keto reductase family 1, member b1 gi|4502049	6.52	35830	X	X	X
				malate dehydrogenase gi|5174539	6.91	36403	X	X	X
				annexin a2 gi|18645167	7.57	38552	X	X	X
				annexin a1 gi|55959290	5.39	22741	X		X
				lactate dehydrogenase A gi|5031857	8.44	36665	X	X	X
				lactate dehydrogenase b gi|4557032	5.71	36615	X		
				LIM and SH3 protein 1 Q14847	6.61	29700		X	X
				glyceraldehyde-3-phosphate dehydrogenase P04406	8.58	36000		X	X

96 Hr soluble fraction	60	4	60000	chaperonin containing TCP1 gi|48762932	5.42	59583	X	X	X
				ubiquitin specific protease 14 isoform a gi|4827050	5.2	56033	X		X
				HMG-CoA synthase gi|1708239	5.22	57257	X	X	X
				beta actin gi|28336	5.22	41786	X	X	X
				endothelial cell growth factor 1 gi|4503445	5.36	49924	X		
				IRA 1 gi|12006104	5.4	55616	X		X
				thymidine phosphorylase IPI00852987.1	5.36	50400		X	X
				alpha tubulin	4.94	50100		X	
				L-plastin P13796	5.2	70200			X
				NAE1, NEDD8 activating enzyme E1 regulatory subunit Q13564	5.25	60500			X
				splicing factor 3A subunit 3 P12874	5.27	58800			X
	63	5	30000	lactate dehydrogenase B gi|4557032	5.71	36615	X	X	X
				chaperonin gi|31542947	5.7	61016	X	X	X
				beta actin	5.22	41786	X	X	
				F-actin capping protein beta subunit gi|4826659	5.69	30609	X	X	X
				glutathione S-transferase P1-1 chain A gi|2554831	5.43	23327	X		X
				ubiquitin specific protease 14 isoform a gi|4827050	5.2	56033	X	X	X
				BRCA1/BRCA2 containing complex subunit 3 gi|13236583	5.59	36049	X		
				c6.1A gi|7709922	5.67	36781	X		X
				peroxiredoxin 2 isoform a gi|32189392	5.66	21878	X		
				gamma actin P63261	5.31	41800		X	X
				alpha tubulin Q13748	4.98	49900		X	X
				malate dehydrogenase 1 IPI00916861.1	5.65	18700			X

96 Hr soluble fraction	69	4	30000	EF-hand domain family member D2 gi|20149675	5.15	26680	X	X	X
				ribonuclease H2 gi|34329831	5.05	33404	X	X	X
				ribonuclease H1 gi|38455391	5.14	33374	X		X
				JUNB gi|48145799	5.14	33332	X		
				alpha tubulin gi|14389309	4.96	49863	X	X	X
				annexin 5 gi|4502107	4.94	35914	X	X	X
				cathepsin B gi|4503139	5.88	37797	X	X	X
				beta actin gi|28336	5.22	41786	X	X	X
				tubulin folding cofactor B gi|2343185	5.14	27378	X		X
				cytoskeleton associated protein 1 gi|50428925	5.06	27308	X		
				p64 chloride ion channel gi|895845	5.12	23528	X		X
				cathepsin D preprotein gi|4503143	6.1	44524	X	X	X
				S100 Ca2+ binding protein A9 gi|4506773	5.71	13234	X		
				protein expressed in prostate, ovary, testis, and placenta 2 gi|134133226	5.83	121286	X		
				heterogeneous nuclear ribonucleoprotein AB isoform a gi|55956919	6.49	35945	X		
				tyrosine 3/tryptophane 5 monooxygtenase activation protein epsilon polypeptide gi|5803225	4.63	29155	X		
				gamma actin P63261	5.31	41800		X	
				Hsp60 P10809	5.24	61000			X
	87	7.2	60000	enolase 1 gi|4503571	7.01	47139	X	X	X
				visfatin precursor gi|5031977	6.69	55487	X		X
				glutamate dehydrogenase 1 gi|4885281	7.66	61359	X	X	X
				desmoplakin gi|1147813	6.44	331571	X		X
				adenylosuccinase lyase P30566	6.73	54900			X
				pyruvate kinase isozymes M1/M2 P14618	7.95	57900			X
				catalase P04040	6.95	59700			X
				Uridine 5'-monophosphate synthase P11172	6.89	52200			X

96 Hr soluble fraction	102	6.4	60000	enolase 1 gi|4503571	7.01	47139	X	X	X
				septin 6 gi|14424536	6.24	49669	X	X	X
				beta actin gi|28336	5.22	41786	X		
				serpin b3 gi|5902072	6.35	44537	X		X
				annexin 1 gi|4502101	6.57	38690	X		X
				alpha actin gi|4501881	5.23	42024	X		
				plakoglobin gi|4504811	5.75	81693	X		X
				unnamed protein product gi|10432867	5.5	43377	X		
				aminopeptidase like 1 gi|47155554	6.41	55825	X		
				annexin 2 gi|4757756	7.57	38580	X		X
				inosine 5'-monophosphate dehydrogenase 1 gi|34328928	6.25	60437	X		
				SCCA2/SCCA1 fusion protein isoform 1 gi|33317676	5.99	44620	X		
				glucose-6-phosphate dehydrogenase gi|182890	6.62	55168	X		
				adenylosuccinate lyase gi|2134709	6.87	52294	X		
				hypothetical protein LOC345651 gi|63055057	5.39	41976	X		
				histone H4 member A gi|4504301	11.36	11360	X		X
				visfatin precursor gi|5031977	6.69	55487	X		
				aspartyl tRNA synthetase gi|45439306	6.11	57100	X		X
				eukaryotic translation elongation factor 1 alpha 1-like 14 gi|927065	8.54	42797	X		
				glutamate ammonia ligase gi|31831	6.61	42120	X		
				glutamine synthetase gi|19923206	6.43	42037	X		
				RuvB-like 1 gi|4506753	6.02	50196	X		
				desmoplakin 1 gi|1147813	6.44	331571	X		
				gamma actin P63261	5.31	41800		X	X

96 Hr soluble fraction	126	6.4	60000	glucose-6-phosphate dehydrogenase gi|108773793	6.39	59219	X	X	X
				enolase 1 gi|4503571	7.01	47139	X	X	X
				phosphoglycerate dehydrogenase gi|23308577	6.29	56614	X	X	X
				enolase 3 gi|4503573	7.58	46929	X		
				annexin a11 gi|4557317	7.53	54355	X	X	X
				inosine 5'-monophosphate dehydrogenase 2 gi|66933016	6.44	55770	X	X	X
				visfatin precursor gi|5031977	6.69	55487	X		X
				aspartyl tRNA synthetase gi|45439306	6.11	57100	X	X	
				septin 11 gi|8922712	6.36	49367	X	X	X
				nucleoporin 50 kDa protein isoform a1 gi|24497447	8.47	46834	X	X	X
				aminopeptidase like 1 gi|47155554	6.41	55825	X	X	
				septin 6 gi|14424536	6.24	49669	X	X	X
				adenylosuccinate lyase gi|2134709	6.87	52294	X		X
				inosine 5'-monophosphate dehydrogenase 1 gi|34328928	6.25	60437	X		X
				Annexin a2 gi|4757756	7.57	38580	X		
				adenylate cyclase associated protein 1 gi|55859737	8.24	51798	X		
				vacuolar protein sorting factor 4B gi|17865802	6.75	49271	X		
				propionyl CoA carboxylase beta subunit gi|455713	7.14	58166	X		
				pyruvate kinase gi|35505	7.58	57841	X		
				fascin 1 gi|4507115	6.84	54496	X		
				adenylyl cyclase associated protein gi|5453595	8.07	51641	X		

96 Hr soluble fraction	144	4.5	30000	beta actin gi|28336	5.22	41786	X		
				alpha tubulin gi|14389309	4.96	49863	X	X	X
				enolase 1 gi|4503571	7.01	47139	X		X
				CGI-150 protein gi|4929769	8.99	54977	X		
				glyoxylase domain containing protein 4 gi|16198390	5.4	33194	X		X
				F-actin capping protein beta subunit gi|4826659	5.69	30609	X	X	X
				lactate dehydrogenase B gi|4557032	5.71	36615	X	X	X
				glucose-6-phosphate dehydrogenase gi|108773793	6.39	59219	X	X	X
				proteasome activator subunit 2 gi|30410792	5.54	27384	X		
				alpha actin gi|4501881	5.23	42024	X		
				lactate dehydrogenase A gi|5031857	8.44	36665	X	X	
				RuvB-like 1 gi|4506753	6.02	50196	X		
				annexin 5 gi|4502107	4.94	35914	X		X
				gamma actin P63261	5.31	41800		X	X
				elongation factor 1 delta P29692	4.9	71400			X
96 hr membrane fraction	6	8	25000	Rab7 gi|4105819	7.98	23517	X	X	X
				peroxyredoxin 1 gi|4505591	8.27	22100	X	X	X
				ras-related C3 botulinum toxin substrate 2 gi|4506381	7.52	21415	X	X	X
				splicing factor arg/ser rich 7 gi|72534660	11.83	27350	X		
				SDF2 like protein 1 gi|11275389	6.83	23497	X		X

96 hr membrane fraction	8	3.25	50000	laminin binding protein gi|34234	4.84	31774	X		
				ribosomal protein SA gi|9845502	4.79	32833	X	X	X
				laminin receptor like protein LAMRL5 gi|14583014	4.84	32975	X	X	
				ATP synthase H+ transporting mitochondrial F1 complex beta subunit gi|32189394	5.26	56525	X	X	X
				HLA class I histocompatibility antigen A36 alpha chain gi|231370	5.96	40908	X	X	X
				Hsp90 protein 1 beta gi|20149594	4.97	83212	X	X	X
				MHC class I antigen gi|5759080	6.03	40481	X		X
				human leukocyte antigen Cw gi|9931112	6.34	41162	X		
				Hsp90 protein alpha class A member 1 isoform 2 gi|40254816	4.94	84673	X		
				unknown protein (appears to be cleavage product of Hsp90) gi|32486	4.59	35760	X		
				tetratricopeptide repeat domain 1 gi|4507711	4.78	33505	X		
				desmin gi|181540	5.21	53487	X		
				Golgi reassembly stacking protein Q9H8Y8	4.73	47000			X
				XRP2 O75695	5	39500			X

96 hr membrane fraction	9	3.25	50000	ATP synthase H+ transporting mitochondrial F1 complex beta subunit gi|32189394	5.26	56525	X	X	X
				Chaperonin gi|31542947	5.7	61016	X	X	X
				MHC class I antigen gi|1280214	5.77	40597	X	X	X
				alpha actinin 4 gi|2804273	5.27	102204	X	X	X
				thioredoxin domain containing protein 4 gi|37183214	5.13	46897	X	X	X
				Hsp70 protein 5 gi|2506545	5.07	72377	X		X
				BiP protein gi|6470150	5.23	70888	X		
				beta tubulin P07437	4.78	49670		X	
				valosin containing protein P55072	5.14	89100			X
				ribosomal protein SA gi|9845502	4.79	32833			X
	10	8.5	25000	ATP synthase H+ transporting mitochondrial F1 complex alpha subunit gi|4757810	9.16	59714	X	X	
				Mn containing superoxide dismutase gi|30841309	6.87	23658	X	X	X
				guanine nucleotide binding protein beta polypeptide 2 like 1 gi|5174447	7.6	35055	X	X	X
				lung cancer oncogene 7 gi|37724561	8.53	37888	X		
				proliferation inducing gene 21 gi|38570357	8.02	29667	X		
				RAS viral oncogene homolog gi|5454028	6.44	23466	X		
				ATP5A1 gi|34782901	9.1	48765	X	X	X
				peroxiredoxin 1 gi|4505591	8.27	22096	X	X	X
				splicing factor Arg/Ser rich 1 isoform 1 gi|5902076	10.37	27728	X	X	X
				unnamed protein product gi|21749793	9.96	15852	X		
				splicing factor Arg/Ser rich 7 gi|72534660	11.83	27350	X		
				Rab1b Q9H0U4	5.55	22200		X	X
				Rras Q6FH12	6.44	23480			X
				Rab31 Q13636	6.59	21700			X

96 hr membrane fraction	18	9	25000	glyceraldehyde 3 phosphate dehydrogenase gi|31645	8.27	36031	X	X	X
				aging-associated gene 9 protein gi|54303910	8.57	36026	X		
				Mn containing superoxide dismutase gi|30841309	6.87	23658	X	X	X
				heterogenous nuclear ribonucleoprotein A2/B1 isoform A2 gi|4504447	8.67	35984	X	X	X
				peroxiredoxin 1 gi|4505591	8.27	22096	X	X	X
				Rab8A P61006	9.15	23700		X	X
	20	3.25	50000	reticulocalbin 1 gi|4506455	4.86	38866	X	X	X
				ribonuclease/angiogenin inhibitor gi|21361547	4.71	49941	X	X	X
				laminin binding protein gi|34234	4.84	31774	X		
				alpha 2 globin gi|4504345	8.72	15248	X	X	X
				unknown protein (possibly ribosomal protein SA) A6NE09	4.78	32900	X		
				ribosomal protein SA gi|9845502	4.79	32833			X
	28	5	60000	Hsp70 protein 9 gi|12653415	6.03	73682	X	X	x
				L-plastin gi|4504965	5.2	70245	X	X	x
				gamma actin P63261	5.31	41800		X	X
				alpha tubulin P68363	4.94	50100		X	X
				major vault protein Q14764	5.34	99300		X	x

96 hr membrane fraction	97	8	35000	Voltage-dependant anion channel 2 gi|48146045	6.81	31575	X	X	X
				guanine nucleotide binding protein beta polypeptide 2 like 1 gi|5174447	7.6	35055	X	X	X
				lung cancer oncogene 7 gi|37724561	8.53	37888	X		
				voltage-dependant anion channel 1 gi|4507879	8.62	30754	X	X	X
				beta tubulin 5 gi|7106439	4.78	49639	X	X	X
				splicing factor Arg/Ser rich 1 isoform 1 gi|5902076	10.37	27728	X	X	X
				electron transfer flavoprotein alpha polypeptide gi|4503607	8.62	35058	X		X
				annexin A2 isoform 2 gi|4757756	7.57	38580	X		X
				beta tubulin 2 gi|5174735	4.79	49799	X	X	
				voltage-dependant anion selective channel 3 Q9Y277	8.84	30600			X
				splicing factor Arg/Ser rich 10 P62995	11.25	33600			X
				torsin A interacting protein 1 IPI00792065.3	8.22	66300			X

96 hr membrane fraction	122	7.5	50000	Lyn B protein gi|187271	6.1	55997	X	X	X
				ATP synthase H+ transporting mitochondrial F1 complex beta subunit gi|32189394	5.26	56525	X	X	X
				dihydrolipoamide succinyltransferase gi|643589	8.9	48554	X	X	X
				ATP synthase H+ transporting mitochondrial F1 complex alpha subunit gi|4757810	9.16	59714	X	X	X
				aldehyde dehydrogenase (NAD+) gi|435487	5.83	50511	X		X
				alpha tubulin gi|34740335	4.94	50120	X	X	X
				cct3 t-complex protein 1 gamma P49368	6.1	60500	X	X	X
				NAD-dependent malic enzyme P23368	6.58	65400			X
				ATP-dependent helicase 2 subunit 1 P12956	6.23	69800			X
Securinine soluble fraction	1	6	70000	78 kDa glucose regulated protein (GRP78, aka Hsp70 protein 5) pi|386758	5.03	72071	X		
				annexin 6 isoform 1 gi|71773329	5.42	75826	X	X	X
				L-plastin gi|4504965	5.2	70245	X	X	X
				aminopeptidase B gi|10933784	5.51	72577	X		X
				Hsp90 beta gi|9082289	5.07	72828	X	X	X
				gamma actin P63261	5.31	41800		X	X

Securinine soluble fraction	3	5.9	70000	78 kDa glucose regulated protein (GRP78, aka Hsp70 protein 5) pi|386758	5.03	72071	X		
				L-plastin gi|4504965	5.2	70245		X	X
				pyruvate kinase isozymes M1/M2 P14618	7.95	57900		X	
				Hsp90 alpha P07900	4.94	84659		X	
				gamma actin P63261	5.31	41800			X
	4	9	20000	enolase 1 gi|693933	7.01	47079	X	X	X
				beta actin gi|28336	5.22	41786	X	X	X
				catalase P04040	6.95	59624		X	X
				C19orf10 uncharacterized protein Q969H8	6.22	18800			X
	5	5.5	70000	Hsp70 gi|188488	5.48	70009	X	X	X
				glyceraldehyde 3 phosphate dehydrogenase gi|31645	8.27	36031		X	
				Hsp90 beta gi|9082289	5.07	72828		X	
				actin P68032	5.23	42000		X	X
				beta spectrin A1YZ73	5.25	267826			X
	7	6.5	10000	beta actin gi|28336	5.22	41786	X		X
				alpha tubulin gi|34740335	4.94	50120		X	
				glyceraldehyde 3 phosphate dehydrogenase gi|31645	8.27	36031		X	
				desmoplakin P15924	6.44	331600		X	
				nucleoprotein TPR P12270	4.97	267100		X	
				pyruvate kinase isozymes M1/M2 P14618	7.95	57900			X

Securinine soluble fraction	9	6.4	70000	aminopeptidase B gi|10933784	5.51	72577	X	X	X
				beta actin gi|28336	5.22	41786	X	X	
				annexin 6 isoform 1 gi|71773329	5.42	75826	X	X	X
				Ran GTPase activating protein 1 IPI00294879.1	4.63	63541		X	
	10	6.6	70000	Hsp70 gi|188488	5.48	70009	X	X	X
				Hsp90 gi|20149594	4.97	83212	X	X	X
				T-plastin gi|2506254	5.52	70391	X	X	X
				beta actin gi|28336	5.22	41786	X		
				plastin 1 gi|4505897	5.33	70308	X		
				enolase 1 gi|693933	7.01	47079	X		X
				78 kDa glucose regulated protein (GRP78, aka Hsp70 protein 5) pi|386758	5.03	72071	X		
				BiP protein gi|6470150	5.23	70888	X		
				heterogeneous nuclear ribonucleoprotein K isoform A gi|14165437	5.19	50996	X		X
				alpha actin gi|4501881	5.23	42024	X		
				alpha tubulin 6 gi|14389309	4.96	49863	X		
				gamma actin P63261	5.31	41800		X	X
				beta tubulin P07437	4.78	49670		X	X
				pyruvate kinase isozymes M1/M2 P14618	7.95	57900			X
				elongation factor 1 alpha 2 Q05639	9.11	50400			X
				heterogeneous nuclear ribonucleoproteins A2/B1 P22626	8.97	37400			X

Securinine soluble fraction	11	4.9	10000	gamma actin P63261	5.31	41800		X	X
	12	6.1	70000	vacuolar ATPase isoform VA68 gi|6523821	5.35	68232	X	X	X
				annexin 6 isoform 1 gi|71773329	5.42	75826	X	X	X
				78 kDa glucose regulated protein (GRP78, aka Hsp70 protein 5) pi|386758	5.03	72071	X		
				L-plastin gi|4504965	5.2	70245	X		X
				gamma actin P63261	5.31	41800		X	X
	13	5	70000	Hsp90 beta gi|20149594	4.97	83212	X	X	X
				lamin B1 gi|5031877	5.11	66368	X	X	X
				T-plastin gi|2506254	5.52	70391	X	X	
				Hsp90 alpha gi|40254816	4.94	84621	X	X	X
				Hsp70 gi|188488	5.48	70009	X	X	
				heterogeneous nuclear ribonucleoprotein K gi|14165437	5.19	50996	X	X	
				gamma actin P63261	5.31	41800		X	X
				alpha tubulin gi|34740335	4.94	50120		X	
				enolase 1 gi|693933	7.01	47079		X	
	18	5.7	70000	78 kDa glucose regulated protein (GRP78, aka Hsp70 protein 5) pi|386758	5.03	72071	X		
				L-plastin gi|4504965	5.2	70245	X	X	X
				vacuolar ATPase isoform VA68 gi|6523821	5.35	68232	X	X	X

Securinine soluble fraction	19	5.4	70000	L-plastin gi|4504965	5.2	70245	X	X	X
				78 kDa glucose regulated protein (GRP78, aka Hsp70 protein 5) pi|386758	5.03	72071	X		
				vacuolar ATPase isoform VA68 gi|6523821	5.35	68232	X	X	X
				T-plastin gi|2506254	5.52	70391	X		
				Hsp90 beta gi|20149594	4.97	83212	X	X	X
				plastin 1 gi|4505897	5.33	70308	X		
				Hsp90 alpha gi|40254816	4.94	84621	X		
				heterogeneous nuclear ribonucleoprotein K gi|14165437	5.19	50996	X		
				gamma actin P63261	5.31	41800		X	
	23	5.1	70000	T-plastin gi|2506254	5.52	70391	X		

Securinine soluble fraction	27	8	45000	enolase 1 gi|693933	7.01	47079	X	X	X
				septin 2 gi|4758158	6.15	41464	X		X
				Hsp40 gi|7706495	5.81	40489	X	X	
				Hsp90 beta gi|20149594	4.97	83212	X	X	X
				beta tubulin gi|18088719	4.75	49640	X	X	X
				pyruvate kinase gi|35505	7.58	57841	X	X	X
				gamma actin P63261	5.31	41800	X	X	X
				heterogeneous nuclear ribonucleoprotein K gi|14165437	5.19	50996	X	X	X
				Hsp70 gi|5729877	5.37	70854	X		X
				Hsp90 alpha gi|40254816	4.94	84621	X	X	
				actin related protein 2 isoform b gi|5031571	6.29	44732	X	X	X
				galactokinase 1 gi|4503895	6.04	42246	X		
				glyceraldehyde 3 phosphate dehydrogenase gi|31645	8.27	36031	X		
				alpha tubulin gi|34740335	4.94	50120	X		
				heterogeneous nuclear ribonucleoprotein D gi|870743	9.2	30352	X		X
				heterogeneous ribonucleoprotein AB isoform a gi|55956919	6.49	35945	X		X
				alpha actin gi|145309046	5.86	121293	X		
				beta actin P60709	5.29	41700		X	
				Macrophage capping protein IPI00027341	5.88	38517			X

Securinine soluble fraction	73	4.5	90000	tumor necrosis factor type 1 receptor associated protein TRAP 1 gi|1082886	8.43	75295	X		
				78 kDa glucose regulated protein (GRP78, aka Hsp70 protein 5) pi|386758	5.03	72071	X	X	X
				nonlens beta gamma crystallin like protein gi|2072425	5.59	179811	X	X	X
				hsp75 gi|2865466	6.09	73971	X		
	83	6.1	45000	protein expressed in prostate, ovary, testis, and placenta 2 gi|134133226	5.83	121286	X		
				creatine kinase gi|49457530	5.34	42648	X	X	X
				myosin 1 P12882	5.59	223000		X	X
				tropomyosin 1 P09493	4.69	32800		X	
				tropomyosin 2	4.66	32800		X	
				nuclear migration protein nudC Q9Y266	5.27	38200			X
				interleukin enhancer binding factor 2 Q12905	5.19	43100			X

Securinine soluble fraction	89	5.7	60000	Hsp70 gi|4885431	5.48	69982	X	X	X
				ubiquitin specific protease 14 isoform a gi|4827050	5.2	56033	X	X	X
				fatty acid binding protein 5 gi|4557581	6.6	15155	X	X	X
				programmed cell death 5 gi|4759224	5.77	14276	X		X
				enolase 1 gi|693933	7.01	47079	X		
				aminopeptidase B gi|10933784	5.51	72577	X	X	X
				gamma actin P63261	5.31	41800	X	X	
				beta actin P60709	5.29	41700	X		
				nucleolin gi|5596788	4.92	76568	X		
				chaperonin containing TCP 1 gi|48762932	5.42	59583	X		
				alpha tubulin gi|34740335	4.94	50120	X	X	X
				lactate dehydrogenase P00338	8.46	36700			X
				pyruvate kinase isozymes M1/M2 P14618	7.95	57900			X
				profilin 1 P07737	8.47	15000			X

Securinine soluble fraction	96	6.4	55000	glucose 6 phosphate dehydrogenase isoform b gi|108773793	6.39	59219	X	X	
				enolase 1 gi|693933	7.01	47079	X	X	
				beta actin P60709	5.29	41700	X		
				annexin A11 gi|47496593	6.91	54302	X		
				catalase gi|4557014	6.9	59719	X		
				leucine aminopeptidase gi|4335941	7.58	56014	X	X	
				phosphoglycerate dehydrogenase gi|23308577	6.29	56614	X		
				glyceraldehyde 3 phosphate dehydrogenase gi|31645	8.27	36031	X		
				Hsp90 beta gi|20149594	4.97	83212	X		
				alpha actin gi|145309046	5.86	121293	X		
				propionyl CoA carboxylase gi|312812	7.56	58169	X	X	
				fascin 1 gi|4507115	6.84	54496	X		
				eukaryotic translation elongation factor 1 alpha 1 gi|4503471	9.1	50109	X		
				alpha tubulin gi|34740335	4.94	50120	X	X	
				glutamate dehydrogenase gi|119600707	7.06	29769	X	X	
				gamma actin P63261	5.31	41800		X	
				profilin 1 P07737	8.47	15000		X	
Securinine membrane fraction	6	5.7	70000	lamin b2 gi|27436951	5.29	67647	X	X	X
				catecholamine-regulated protein 40 gi|94450030	5.28	38064	X		
				chaperonin gi|31542947	5.7	61016	X		X
				annexin 6 P08133	5.42	81500		X	X

Securinine membrane fraction	52	5.7	45000	ERLIN 2 gi|6005721	5.47	37815	X	X	X
				MHC class I antigen gi|67904939	5.44	34216	X	X	X
				protein expressed in prostate, ovary, testis, and placenta 2 gi|134133226	5.83	121286	X		
				dynein heavy chain 1 gi|119602168	6.05	486304	X	X	X
				nuclear distribution gene C homolog gi|5729953	5.27	24339	X		X
				Hsp90 alpha gi|40254816	4.94	84621	X		
LPS membrane fraction	8	5.7	30000	pyruvate kinase 3 isoform 2 gi|33286420	7.61	58025	X	X	X
				catecholamino-o-methyltransferase gi|47678375	5.26	30050	X		X
				protein phosphatase 1 gi|4506003	5.94	37488	X	X	X
				serine hydroxymethyltransferase gi746436	8.35	53421	X		X
				major vault protein gi|19913410	5.34	99266	X	X	X
				ClpX caseinolytic proteiase X homolog gi|7242140	7.51	69181	X		
				heterogeneous nuclear ribonucleoprotein D gi|870743	9.2	30352	X	X	
				alpha tubulin gi|34740335	4.94	50120	X	X	X
				gamma actin P63261	5.31	41800		X	X
				Hsp70 P11142	5.37	70900		X	
				macropain P25788	5.19	28400			X
				prohibitin P35232	5.57	29800			X

MPL membrane fraction	8	8.5	20000	Cdc42 gi|4757952	6.16	21245	X	X	X
				Rap1A gi|4506413	6.39	20974		X	X
	42	5.7	35000	beta tubulin gi|35959	4.81	49599	X	X	X
				laminin binding protein gi|34234	4.84	31774	X		
				NSF attachment protein gamma gi|4505331	5.3	34724	X	X	X
				SEC13 gi|34335134	5.22	35518	X	X	X
				alpha tubulin gi|34740335	4.94	50120	X	X	
				alpha SNAP gi|3929617	5.23	33246	X	X	X
				heterogeneous nuclear ribonucleoprotein K gi|14165437	5.19	50996	X	X	X
				guanine nucleotide binding protein beta 1 subunit gi|6680045	5.33	37353	X		X
				heterogeneous nuclear ribonucleoprotein U Q00839	5.76	90500		X	
				heme oxygenase 2 Q13748	5.31	36000		X	X
				elongation factor 1 delta P29692	4.9	71400		X	

MPL membrane fraction	57	4.7	25000	oligosaccharyltransferase gi|2662375	5.96	50725	X	X	X
				Hsp70 gi|16507237	5.07	72288	X	X	X
				eukaryotic translation elongation factor 1 beta 2 gi|4503477	4.5	24748	X	X	X
				nucleolin gi|55956788	4.6	76568	X	X	X
				laminin binding protein gi|34234	4.84	31774	X		
				14-3-3 protein epsilon P62258	4.63	29200		X	
				Uncharacterized protein A6NE09	4.78	29200		X	
				guanine nucleotide binding protein G(I)/G(S)/G(T) subunit beta 2 P62879	5.6	37300		X	
	61	7.6	35000	ATP synthase H+ transporting mitochondrial F1 complex gi|4757810	9.16	59714	X	X	X
				Tob3 gi|13752411	9.38	65115	X		
				heterogeneous nuclear ribonucleoprotein H1 gi|5031753	5.89	49198	X	X	X
				glyceraldehyde 3 phosphate dehydrogenase gi|31645	8.27	36031	X	X	X
				voltage dependent ion channel VDAC2 gi|346412	7.5	31575	X	X	X
				prostaglandin E synthase 2 isoform 1 gi|13376617	9.22	41971	X		X
				proteasome 26S nonATPase subunit 8 gi|4506233	6.85	29986	X	X	
				ATPase family AAA domain containing protein 3A Q9NVI7	9.08	66200		X	X
				beta tubulin P07437	4.78	49600		X	X
				DEAD-box protein 5 P17844	9.06	69100			X
				ubiquinol cytochrome c reductase complex core protein 2 P22695	7.74	48400			X
				torsin family protein C9orf167 Q9NXH8	9.98	46900			X

MPL membrane fraction	97	5.2	30000	enolase 1 gi|693933	7.01	47079	X	X	X
				prohibitin gi|4505773	5.57	29786	X	X	X
				ATP synthase H+ transporting mitochondrial F1 complex gi|4757810	9.16	59714	X	X	X
				heterogeneous nuclear ribonucleoprotein R gi|5031755	8.23	70899	X		X
				alpha tubulin gi|37492	5.02	50126	X	X	X
				ribosomal protein L5 gi|14591909	9.73	34341	X		X
				uncharacterized protein IPI00893541.1	6.79	13500			X
									X
				cytochrome c1 heme protein P08574	6.49	35400			X
	100	5.2	30000	ATP synthase H+ transporting mitochondrial F1 complex gi|4757810	9.16	59714	X	X	X
				pyruvate kinase isozymes M1/M2 P14618	7.95	57900		X	X
				alpha tubulin gi|37492	5.02	50126		X	
				major vault protein gi|19913410	5.34	99266		X	X
				proteasome subunit alpha type 3 P25788	5.19	28400		X	X
				uncharacterized protein A6NE09	4.78	32909		X	
				cytochrome c1 heme protein P08574	6.49	35400		X	

MPL membrane fraction	110	4.5	35000	beta tubulin P07437	4.78	49600	X	X	X
				alpha SNAP gi|3929617	5.23	33225	X	X	X
				human elongation factor 1 delta gi|38522	4.95	31202	X		
				alpha tubulin gi|37492	5.02	50126	X	X	X
				ribosomal protein SA gi|119584991	8.37	19625	X		
				eukaryotic translation initiation factor 2 subunit 1 alpha gi|4758256	5.02	36089	X	X	X
				splicing factor Arg/Ser rich 2 gi|62898065	11.86	25487	X	X	
				oligosaccharyltransferase gi|2662375	5.96	50725	X		X
				ATP synthase H+ transporting mitochondrial F1 complex gi|4757810	9.16	59714		X	X
				unknown protein IPI00646779.2	4.8	50090		X	
96 hr infect +/- 50 uM Securinine 3-11 soluble	13	8	60000	brain carboxylesterase hBr1 gi|6009626	6.02	46815	X	X	X
				carboxylesterase gi|458470	6.05	62358	X		
				cholesterol acyltransferase gi|8248931	6.15	62552	X		
				ATP citrate pro-S lyase gi|28935	6.42	121342	X	X	X
				T-complex protein subunit beta P40227	6.25	62600		X	X
				pyruvate kinase isozymes M1/M2 P14618	7.95	57900		X	X
				cononin like protein p57 P31146	6.25	51000		X	

96 hr infect +/- 50 uM Securinine 3-11 soluble	55			N/A					
	57	9	120000	methylenetetrahydrofolate gi|13699868	6.75	101467	X	X	X
				EBNA 2 coactivator mutant gi|62088600	7.36	107366	X		
				staphylococcal nuclease domain containing 1 gi|77404397	7.36	101934	X	X	X
				eukaryotic translation initiation factor 5A-1 P63241	5.08	20200		X	
	82	5.5	70000	ubiquitin specific protease 14 isoform a gi|4827050	5.2	56033	X	X	X
				transformation upregulated nuclear protein gi|460789	5.13	51040	X		
				heterogeneous nuclear ribonucleoprotein K gi|14165437	5.19	50996	X	X	X
				L-plastin gi|4504965	5.21	55683	X	X	X
				prolyl 4-hydroxylase beta subunit gi|20070125	4.76	57081	X	X	X
				gamma actin P63261	5.31	41800		X	X
	92	4	30000	nucleoplasmin gi|825671	4.71	30919	X		
				nuclophosmin P06748	4.64	28400	X	X	

96 hr infect +/- 50 uM Securinine 3-11 soluble	121	9	120000	methylenetetrahydrofolate gi|13699868	6.75	101467	X	X	X
				eukaryotic translation elongation factor 2 gi|4503483	6.41	95277	X	X	X
				staphylococcal nuclease domain containing 1 gi|77404397	7.36	101934		X	X
	125	9	60000	enolase 1 gi|693933	7.01	47079	X	X	X
				phosphogluconate dehydrogenase gi|40068518	6.8	53106	X	X	X
				similar to pre-B cell enhancing factor gi|55960735	7.71	53360	X	X	X
				pyruvate kinase isozymes M1/M2 P14618	7.95	57900	X		X
				enolase 3 gi|4503573	7.58	46929	X		
				adenylyl cyclase associated protein 1 IPI00008274.7	7.81	91210		X	X
				MPP1 Q00013	6.91	52300			X
	201	7	40000	endoplasmic reticulum protein 29 isoform 1 gi|5803013	6.77	28975	X	X	X
				F-actin capping protein gi|4826659	5.69	30609	X	X	X
				cathepsin D preproprotein gi|4503143	6.1	44524	X	X	X
				glutathione S transferase omega 1 gi|4758484	6.24	27548	X		X
				6-phosphogluconolactonase gi|6912586	5.7	27530	X	X	
				chloride intracellular channel protein 1 O00299	5.09	26900			X
				14-3-3 protein zeta/delta P63104	4.73	27700			X

96 hr infect +/- 50 uM Securinine 3-11 soluble	205	8	120000	nuclolin gi|55956788	4.6	76568	X	X	
				filamin 1 P21333	5.7	276400		X	
96 hr infect +/- 50 uM Securinine 3-11 membrane	3	4.5	45000	lamin B2 gi|27436951	5.29	67647	X		X
				nuclolin gi|55956788	4.6	76568	X		X
				tropomodulin 3 gi|6934244	5.08	39556	X		X
				stem-cell growth factor precursor gi|4506803	5.06	35672	X		
				beta actin P60709	5.29	41700			X
	12	3.5	45000	prolyl 4-hydroxylase gi|20070125	4.76	57081	X	X	X
				Hsp90 beta gi|20149594	4.97	83212	X	X	X
				oligosaccharyltransferase gi|2662375	5.96	50725	X	X	X
				desmin gi|23506465	5.21	53531	X		
				calreticulin P27797	4.29	48100		X	
	35	8	55000	ATP synthase H+ transporting mitochondrial F1 complex gi|4757810	9.16	59714	X	X	X
				glutamate dehydrogenase 1 gi|4885281	7.66	61359	X	X	X
				CGI-51 protein gi|4929571	6.85	52127	X		X
				glucose-6-phosphate dehydrogenase gi|26224790	6.91	54789	X	X	X
				ATP citrate synthase P53396	6.95	119700		X	

96 hr infect +/- 50 uM Securinine 3-11 membrane	36	5	50000	lamin B1 gi|5031877	5.11	66368	X	X	X
				beta tubulin P07437	4.78	49600	X	X	X
				ATP synthase H+ transporting mitochondrial F1 complex gi|4757810	9.16	59714	X	X	X
				vimentin gi|47115317	5.09	53547	X	X	X
				75 kDa subunit NADH dehydrogenase gi|38079	5.8	79523	X		
				EPB41L3 gi|111185506	7	34313	X		
				alpha actin gi|4501881	5.23	42024	X		
				beta actin gi|28336		41786	X		X
				MHC class I antigen gi|47559183	5.43	31569	X		
				IQ motif containing GTPase activating protein 1 gi|4506787	6.08	189134	X		
				EBNA 2 coactivator gi|62088600	7.36	107366	X		X
				SNAP 1 Q7KZF4	6.77	101900	X		X
	44	3.5	45000	Hsp90 beta gi|20149594	4.97	83212	X	X	X
				calreticulin gi|4757900	4.29	48112	X	X	
				MHC class I antigen gi|47559183	5.43	31569		X	
	56	6	70000	lamin B2 gi|27436951	5.29	67647	X		X
				ATPase H+ transporting lysosomal 70 kDa V1 subunit A isoform 1 gi|19913424	5.35	68260	X	X	X
				alpha tubulin gi|37492	5.02	50126	X		
				ERO1 like gi|7657069	5.48	54358	X	X	X

96 hr infect +/- 50 uM Securinine 3-11 membrane	92	9	60000	hexokinase 1 gi|15991827	6.18	102136	X	X	X
				inosine monophosphate dehydrogenase 2 gi|66933016	6.44	55770	X	X	X
				nucleoporin 54 kDa gi|26051237	6.53	55401	X		X
				CGI-51 protein gi|4929571	6.85	52127	X	X	X
				alpha tubulin gi|37492	5.02	50126	X		X
				glucose-6-phosphate dehydrogenase gi|26224790	6.91	54789	X	X	
				carboxylesterase gi|458470	6.05	62358	X		X
				oligosaccharyltransferase gi|2662375	5.96	50725	X	X	X
				3-phosphoglycerate dehydrogenase O43175	6.31	56600			X
				mannosyl-oligosaccharide glucosidase Q13724	8.97	91900			X
	94	7.5	10000	H4 histone A gi|4504301	11.36	11360	X	X	
				leucine rich repeat containing 15 gi|71680364	6.24	64325	X		
				desmoglein 1 Q02413	4.77	113700		X	X
				pyruvate kinase isozymes M1/M2 P14618	7.95	57900		X	
				betaglobin P68871	6.81	16000		X	X
				glyceraldehyde-3-phosphate dehydrogenase P04406	8.58	36000		X	
				calmodulin like protein 5 Q9NZT1	4.34	15900		X	

96 hr infect +/- 50 uM Securinine 3-11 membrane	116	5.5	40000	beta tubulin P07437	4.78	49600	X	X	X
				ATP synthase H+ transporting mitochondrial F1 complex gi|4757810	9.16	59714	X	X	
				protein disulfide isomerase related protein 5 gi|1710246	6.79	46170	X		X
				alpha tubulin gi|37492	5.02	50126	X	X	X
				gamma actin P63261	5.31	41800		X	
				NAD dependen malic enzyme P23368	6.58	65400			X
	160	6.5	45000	26S proteasome subunit p40.5 gi|3618343	5.53	42918	X		X
				SPFH domain family member 2 isoform 1 gi|6005721	5.47	37815	X		
				enolase 1 gi|693933	7.01	47079	X		X
				beta tubulin P07437	4.78	49600	X	X	X
				glycosylastion aa 86 gi|456694	5.89	40379	X		
				COP9 complex subunit 4 gi|5410300	5.57	46169	X		
				heterogeneous nuclear ribonucleoprotein U gi|32358	5.6	88890	X		X
				alpha tubulin gi|37492	5.02	50126	X		
				gamma actin P63261	5.31	41800		X	
				ERLIN 2 O94905	5.47	37800			X
	201	6	60000	ATP synthase H+ transporting mitochondrial F1 complex gi|4757810	9.16	59714	X	X	X
				nuclear RNA helicase gi|1905998	5.59	49046	X		
				HLA-B associated transcript 1 gi|4758112	5.44	48960	X		
				DEAD box polypeptide 39 gi|21040371	5.46	49094	X		X
				RuvB-like 2 Q9Y230	5.49	51100		X	X
				Hsp90 beta gi|20149594	4.97	83212		X	

96 hr infect +/- 50 uM Securinine 3-11 membrane	216	7	45000	beta tubulin P07437	4.78	49600	X	X	X
				ribosomal protein P0 gi|4506667	5.72	34252	X	X	X
				BLOCK 23 gi|20853684	5.41	34343	X		
				heterogeneous nuclear ribonucleoprotein C gi|13937888	4.99	33578	X		
				isocitrate dehydrogenase 3 gi|5031777	6.49	39566	X		
				gamma actin P63261	5.31	41800		X	X
	354	6.5	45000	MHC class I antigen gi|47559183	5.43	31569	X	X	X
				vesicle amine transport protein 1 gi|18379349	5.88	41893	X		
				glycosylastion aa 86 gi|456694	5.89	40379	X		
				flotillin 2 gi|94538362	5.19	47035	X	X	X
				beta actin gi|4501885	5.29	41710	X	X	X
				beta tubulin P07437	4.78	49600	X	X	X
				ERLIN 2 O94905	5.47	37800		X	X
				synaptic vesicle membrane protein VAT1 homolog Q99536	5.88	41900		X	X
				major vault protein Q14764	5.34	99300		X	

96 hr infect +/- 50 uM Securinine 4-7 soluble	30	4.5	10000	vimentin P08670	5.06	53600		X	
	38	6.75	10000	catalase P04040	6.95	59700		X	
	45	5.25	70000	lamin B1 gi|5031877	5.11	66368	X	X	X
				T-plastin gi|2506254	5.52	70391	X		
				Hsp90 beta gi|20149594	4.97	83212		X	
				Hsp70 P11142	5.37	47800			X
	63	6.2	5000	cofilin 1 P23528	8.26	18500		X	X
				beta actin gi|4501885	5.29	41710		X	
				Enhancer of rudimentary homolog P84090	5.62	12300		X	X
				lactate dehydrogenase A P00338	8.46	36700		X	
				glycyl-tRNA synthetase P41250	6.61	83100		X	
				S100 Ca^{2+} binding protein A4 P26447	5.88	11700		X	

96 hr infect +/- 50 uM Securinine 4-7 soluble	67	6.75	90000	minichromosome maintenance protein 7 isoform 1 gi|33469968	6.08	81257	X	X	X
				FLNA protein gi|15779184	5.93	88534	X	X	X
				carboxylesterase gi|458470	6.05	62358	X	X	X
				egasyn gi5823472	6.15	62408	X		
				acyl coenzyme A: cholesterol acyltransferase gi|8248931	6.15	62552	X		
				minichromosome maintenance 4 gi|33469917	6.28	96516	X	X	X
				eukaryotic translation elongation factor 2 gi|4503483	6.41	95277	X	X	X
				glyceraldehyde-3-phosphate dehydrogenase gi|31645	8.27	36031	X		X
				aconitase 1 gi|8659555	6.23	98337	X		
				moesin gi|4505257	6.08	67778	X	X	X
				PKM2 protein gi|33875497	8.85	61398	X		
				actin-binding protein homolog ABP-278 gi|3282771	5.47	278018	X		
				iron-responsive element binding protein 1 P21399	6.23	98300		X	X
				alpha actin P68032	5.23	42000		X	
				pyruvate kinase isozymes M1/M2 P14618	7.95	57900			X
				dipeptidyl peptidase 9 Q86TI2	6.01	48600			X

96 hr infect +/- 50 uM Securinine 4-7 soluble	77	4.75	35000	tropomyosin gi|825723	4.77	26560	X		
				tropomyosin 1 gi|29792232	5	32602	X		
				tropomyosin 4 gi|14010354	4.8	16662	X		
				tropomyosin 2 gi|6573280	4.7	29923	X		
				tyrosine3/tryptophane 5-monooxygenase activation prototein zeta polypeptide gi|4507953	4.73	27728	X	X	X
				tyrosine3/tryptophane 5-monooxygenase activation prototein epsilon polypeptide gi|5803225	4.63	29155	X	X	
	117	5.5	60000	alpha actin P68032	5.23	42000		X	
	192	6.3	110000	ubiquitin activating enzyme E1 P22314	5.49	117800		X	

96 hr infect +/- 50 uM Securinine 4-7 soluble	200	6.3	55000	Synaptotagmin binding cytoplasminc RNA interacting protein variant gi|33874520	5.85	46714	X	X	X
				enolase 3 gi|4503573	7.58	46929	X		
				alpha tubulin gi|37492	5.02	50126	X	X	X
				proliferation associated 2G4 gi|5453842	6.13	43785	X	X	X
				vesicle amine transport protein 1 gi|18379349	5.88	41893	X	X	X
				gamma tubulin gi|31543831	5.75	51138	X		X
				cathepsin D preproprotein gi|4503143	6.1	44524	X	X	X
				26S proteasome subunit 9 gi|2150046	6.08	47418	X	X	X
				tumor susceptibility gene 101 gi|5454140	6.06	43916	X		X
				enolase 2 gi|5803011	4.91	47239	X		
				TRAF associated factor 4 gi|4580013	5.82	46932	X		
				human Rab GDI gi|285975	5.94	50632	X	X	
				autoantigen La gi|10835067	5.94	46808	X		
				eukaryotic translation elongation factor 1 gamma gi|4503481	6.27	50087	X		
				eukaryotic translation elongation factor 1 alpha gi|4503471	9.1	50109	X	X	X
				annexin 7 isoform 1 gi|4502111	6.25	50284	X		
				mitochondrial processing peptidase beta subunit gi|3342006	6.15	54133	X	X	X
				5'-nucleotidase cytosolic II-like 1 protein gi|38570156	5.94	51812	X		X
				heterogeneous nuclear ribonuclear protein R gi|5031755	8.23	70899	X		
				alanyl tRNA synthetase domain containing 1 gi|13376886	5.57	58716	X		
				BSCv gi|9836652	5.78	47715	X		

96 hr infect +/- 50 uM Securinine 4-7 soluble	273	6.9	100000	lactate dehydrogenase gi|4557032	5.71	36615	X	X	X
				apg-1 gi|4579911	5.65	94446	X		
				MEG3 gi|14248495	5.77	82607	X		
				minichromosome maintenance deficient 5 gi|13177775	8.71	82261	X	X	X
				smooth muscle cell associated protein 1 gi|29725607	5.8	103011	X		
				eukaryotic translation elongation factor 2 gi|4503483	6.41	95277	X	X	X
				talin gi|4235275	5.75	269661	X		X
				myosin heavy polypeptide gi|12667788	5.5	226392	X	X	X
				P1 Cdc21 gi|940536	8.39	102982	X		
				pyruvate kinase isozymes M1/M2 P14618	7.95	57900	X	X	X
				AHNAK nucleoprotein isoform 1 gi|61743954	5.8	628699	X		X
				gelsolin isoform a precursor gi|4504165	5.9	85644	X		
				alpha actin P68032	5.23	42000	X		
				FAM129B niban like protein 1 Q96TA1	5.81	82600		X	X
				Hsp70 protein 4 O95757	5.63	94500		X	X
				gamma actin P63261	5.31	41800		X	
				heterogeneous nuclear ribonucleoprotein U Q00839	5.76	90500			X
				enolase 1 P06733	6.99	47100			X
				STAT 1 P42224	5.74	87300			X

96 hr infect +/- 50 uM Securinine 4-7 membrane	11	5.9	70000	GRP78 Hsp70 protein 5 gi|2506545	5.07	72071	X		
				vATPase VA68 type gi|6523821	5.35	68204	X	X	X
				alpha tubulin gi|37492	5.02	50126	X	X	X
				alpha actinin 4 gi|2804273	5.27	102204	X	X	X
				glucosidase II gi|2274968	5.71	106833	X		X
				75 kDa NADH dehydrogenase precursor gi|38079	5.8	79523	X	X	X
				gamma actin P63261	5.31	41800		X	X
				chaperonin P10809	5.24	61000			X
	12	5.6	60000	lamin B1 gi|5031877	5.11	66368	X	X	X
				L-plastin gi|4504965	5.2	70245	X	X	X
				alpha tubulin gi|37492	5.02	50126	X	X	X
				alpha actinin 4 gi|2804273	5.27	102204	X	X	X
				gamma actin P63261	5.31	41800		X	X
				USP14 P54578	5.2	63600			X
	27	4.75	40000	Hsp90 beta P14625	4.73	92400		X	
	39	5.6	60000	lamin B1 gi|5031877	5.11	66368	X	X	X
				L-plastin gi|4504965	5.2	70245	X	X	X
				beta actin P60709	5.29	41700		X	
				Hsp70 P11142	5.37	70900		X	
				alpha tubulin gi|37492	5.02	50126		X	
				beta tubulin P07437	4.78	49600		X	
				Hsp90 alpha P07900	4.94	84600			X
				USP14 P54578	5.2	63600			X

96 hr infect +/- 50 uM Securinine 4-7 membrane	86	5	10000	Histone H2B gi|1568551	10.31	13928	X	X	
				cytochrome c oxidase subunit Va gi|18999392	6.3	16752	X		
				RPLP0 P05388	5.72	34300	X	X	
				26S proteasome nonATPase regulatory subunit 11 O00231	6.09	47100		X	
	106	5.9	80000	Hsp70 (mortalin) gi|12653415	6.03	73682	X		
				P1 Cdc21 gi|940536	8.39	102982	X	X	X
				cytochrome P450 reductase gi|247307	5.41	76657	X	X	X
				Hsp90 beta P14625	4.73	92400	X	X	X
				alpha tubulin gi|37492	5.02	50126	X	X	X
				annexin 6 gi|71773329	5.42	75826	X		X
				tumor rejection antigen 1 gi|62088648	5.08	65912	X		
				Hsp70 gi|5729877	5.37	70854	X	X	X
				hydroxysteroid (17-beta) dehydrogenase 4 gi|4504505	8.96	79636	X	X	
				alpha actin P68032	5.23	42000		X	
				N-ethylmaleimide sensitive factor B4DFA2	6.52	82594			X
				gamma actin P63261	5.31	41800			X